ABSTRACT

Title of Document: ROLE AND REGULATION OF AUTOPHAGY DURING DEVELOPMENTAL CELL DEATH IN *DROSOPHILA MELANOGASTER*

Christina Kary McPhee, Doctor of Philosophy, 2010

Directed By: Dr. Stephen M. Mount
Associate Professor
Department of Cell Biology and Molecular Genetics
University of Maryland

Two prominent morphological forms of programmed cell death occur during development, apoptosis and autophagic cell death. Improper regulation of cell death can lead to a variety of diseases, including cancer. Autophagy is required for survival in response to starvation, but has also been associated with cell death. It is unclear how autophagy is regulated under specific cell contexts in multi-cellular organisms, and what may distinguish autophagy function during cell survival versus cell death. Autophagic cell death is characterized by cells that die in synchrony, with autophagic vacuoles in the cytoplasm, and phagocytosis of the dying cells is not observed. However, little is known about this form of cell death. Autophagic cell death is observed during mammalian development, during regression of the corpus luteum and involution of the mammary and prostate glands. Autophagic cell death is also observed during development of the fruitfly *Drosophila melanogaster*, during larval

salivary gland cell death. *Drosophila* is an excellent genetic model system to study developmental cell death *in vivo*.

Cells use two main catabolic processes to degrade and recycle cellular contents, the ubiquitin/proteasome system (UPS) and autophagy. Here I investigate the role of the UPS and autophagy in developmental cell death using *Drosophila* larval salivary glands as an *in vivo* model. Proteasome inhibitors are being used in anti-cancer therapies; however the cellular effects of proteasome inhibition have not been studied *in vivo*. Here I demonstrate that the UPS is impaired during developmental cell death *in vivo*. Taking a proteomics approach to identify proteins enriched in salivary glands during developmental cell death and in response to proteasome impairment, I identify several novel genes required for salivary gland cell death, including Cop9 signalsome subunit 6 and the engulfment receptor Draper. Here I show that the engulfment receptor Draper is required for salivary gland degradation. This is the first example of an engulfment factor that is autonomously required for self-clearance. Surprisingly, I find that Draper is cell-autonomously required for autophagy during cell death, but not for starvation-induced autophagy. Draper is the first factor to be identified that genetically distinguishes autophagy that is associated with cell death from cell survival.

ROLE AND REGULATION OF AUTOPHAGY DURING DEVELOPMENTAL CELL DEATH IN *DROSOPHILA MELANOGASTER*.

By

Christina Kary McPhee

Dissertation submitted to the Faculty of the Graduate School of the
University of Maryland, College Park, in partial fulfillment
of the requirements for the degree of
Doctor of Philosophy
2010

Advisory Committee:
Professor Stephen M. Mount, Chair
Professor Eric H. Baehrecke
Professor Eric S. Haag
Professor Zhongchi Liu
Professor Leslie Pick

Dedication

This work is dedicated to my family; to my mother, Carla Iris, for instilling in me her love of reading and writing; to my father, Dan Kary, for teaching me to persevere, and in everything I do, to produce work to be proud of; to my grandmother, Ruth Kary, for opening my eyes to the natural world, to Ron Iris, for teaching me to solve problems creatively, and helping me with my science projects; to Michelle Mazur-Kary, for her encouragement and expert advice; to Susan Johnson-Manicke, for keeping me smiling; and most of all to my husband, Chris McPhee, for convincing me that I could accomplish this goal, and for supporting me every step of the way.

Acknowledgements

I would like to thank my advisor, Eric Baehrecke, for seeing potential in me. Thank you for teaching me how to approach experiments, to test the critical questions. Thank you for always greeting me with a smile, no matter the situation. Thank you for teaching me to accept failure and to continue with optimism. Thank you for guiding me to success—I am indebted to you. Thank you also to my committee members, Steve Mount, Leslie Pick, Eric Haag, and Zhongchi Liu, for challenging me and for providing me with valuable critique and insight. Thanks especially to Steve Mount, for your mentorship, and for encouraging me to apply to graduate school in the first place.

Thank you to those who have collaborated with me on my projects, to Jahda Hill and Yakup Batlevi who assisted in the isolation of the *Drosophila* salivary gland samples that were analyzed using proteomics. Thank you to Brian Balgley and Cheng Lee who carried out proteomics analyses that provided the bases for my projects. Special thanks goes to Marc Freeman and Mary Logan for your encouragement and advice, and especially for their generosity in providing DNA constructs and transgenic flies that were critical to my investigation of Draper.

I would like to thank Baehrecke lab members, past and present. Special thanks to Deb Berry, for your steadfast friendship, for your outstanding mentorship, for your constant encouragement, for never hesitating to help me, both in the lab, in Maryland, and from afar, after the lab moved. I simply can never repay you for everything that you have done. Thanks also to Michelle Beaucher, for always being there with great

advice about science and grad school, and for being quick to laugh and listen, and for your great friendship. Thank you to Jahda Hill, for always being a phone call or an email away when I wanted to talk about an experiment or a problem, or just to have a good laugh. Thanks to Kirsten Tracy, for your friendship and helping me to get through my last few years of grad school. Thanks also to Nellie Moshkovich, Lauren Lane, and Marie Kobayashi for your friendship and for all of the great fun that we had in lab together. Thanks to Yakup Batlevi and Sudeshna Dutta for helping me survive the lab move, and to Rachel Simin for doing an outstanding job of getting the lab up and running after the move. Thanks to Charles Nelson, for bringing so much energy into the lab, to Bhupendra Shravage, for figuring out and teaching me how to get salivary gland cell clones, as this was critical to my project, to Gautam Das for your friendliness and advice, and to Tina Fortier for your efforts in managing the lab. Thanks also to Alya Raphael, Samantha Tangchaiburana, and Noriko Aita.

Thank you to my friends and family for all of the support you have provided, to my parents Carla Iris, Ron Iris, Dan Kary, Michelle Mazur-Kary, and also to Susan Johnson-Manicke and Bob Manicke. Thank you to my siblings, Nicole Kary, Daniel Kary, Andrew Kary, and Luke Iris for your steadfast companionship and support. Thank you to my aunt, Rebecca Kary, for encouraging me to pursue graduate school, to my uncle, Tim Kary, for suggesting to me to pursue a career in biomedical science, and to my uncle, Mark Kary, for encouragement as well. Thank you also to my friends, especially to Holly Mortensen, for her long-lasting and steadfast companionship, and to Laura McNamee, for her immediate welcome to UMass, and great friendship.

Most of all I would like to thank my husband, Chris McPhee, for everything that you have done to help me to accomplish this goal. Thank you for believing in me, for convincing me that I was capable of earning an advanced degree. Thank you for your unwavering support and encouragement throughout the entire process, beginning to end. Thank you especially for moving to Massachusetts with me, for your sacrifice and enduring love.

Table of Contents

List of Tables

List of Figures

List of Appendices

Chapter 1

Introduction

Abstract

Two prominent morphological forms of programmed cell death occur during development, apoptosis and autophagic cell death. While much is known about apoptosis, little is known about the genetic regulation and execution of autophagic cell death. Improper regulation of cell death can lead to a variety of diseases, including cancer. Cells use two main catabolic processes to degrade and recycle cellular contents, the ubiquitin/proteasome system (UPS) and macroautophagy (autophagy). Studies suggest that the proteasome is impaired during cell death; however this has not been tested under physiological conditions or *in vivo*. Proteasome inhibitors are being used in anti-cancer therapies, however little is known about the cellular effects of proteasome inhibitors, and *in vivo* studies are lacking. Autophagy is critical to survival of starvation, but has also been associated with cell death. Autophagy is induced in *Drosophila* in response to starvation, and also during developmental cell death in response to the steroid hormone ecdysone. *Drosophila* is well-suited to *in vivo* studies of the UPS and autophagy, and their relationship to cell survival, growth, and death in the context of a developing organism.

Programmed Cell Death

Programmed cell death is a conserved, genetically regulated process that plays important roles throughout the lives of metazoans (Danial and Korsmeyer, 2004; Lockshin and Williams, 1965). Cell death functions in the formation and shaping of structures during development, and in tissue homeostasis during adulthood (Baehrecke, 2002). Cell death is critical to defense against foreign, damaged, or abnormally proliferating cells. Improper regulation of cell death is associated with a wide range of pathological conditions. Whereas accelerated cell death can lead to neurodegeneration and immune suppression, cell death suppression can lead to autoimmunity and cancer (Thompson, 1995).

In 1973, Schweichel & Merker described three prominent types of programmed cell death that occur in developing mammals and are distinguished by dying cell morphology and use of the lysosome (Clarke, 1990; Schweichel and Merker, 1973). Type I cell death, or apoptosis, occurs in cells that die in isolation from one another, and is characterized by the condensation of nuclei and cytoplasm, DNA fragmentation, and phagocytosis by a secondary cell where the lysosome of the engulfing cell degrades the dead cell (Kerr et al., 1972). In type II, or autophagic cell death, cells die in groups, and cell destruction occurs with little or no phagocytosis. Type II cell death is characterized by the presence of autophagosomes that degrade cytoplasmic contents of the dying cell. The third and least common type, non-lysosomal cell death, is characterized by the lack of known lysosomal activity in the dying cell.

Type II cell death is observed at several stages during mammalian development, including regression of the corpus luteum, involution of mammary and prostate glands, and regression of Mullerian duct structures during male genital development (Clarke, 1990). Type II cell death has also been observed during insect development, for example in dying flight muscle cells of the Hawkmoth *Manduca sexta* after which the term programmed cell death was originally coined (Lockshin and Williams, 1965). *Drosophila* larval salivary glands that die during metamorphosis also exhibit Type II morphology; autophagosomes are present in the cytoplasm, and phagocytosis is not observed (Lee and Baehrecke, 2001; Martin and Baehrecke, 2004). Although genetic evidence indicates that autophagy contributes to cell death in some *in vivo* contexts (Berry and Baehrecke, 2007; Hou et al., 2008; Mohseni et al., 2009; Nezis et al., 2009), little is known about how autophagy may contribute to cell death.

The conserved program of apoptotic cell death

Caspases, a conserved family of cysteine proteases, comprise the core apoptotic cell death machinery (Cryns and Yuan, 1998). Synthesized as inactive zymogens, caspases become activated upon proteolytic cleavage and cleave cellular substrates, leading to cell death. Caspases and their regulators were first discovered in the nematode *C. elegans,* and are conserved in mammals. In *C. elegans*, the caspase Ced-3 is activated by Ced-4, the mammalian APAF-1 homolog (Ellis and Horvitz, 1986; Zou et al., 1997). Ced-9, the anti-apoptotic Bcl-2 family homolog, binds to Ced-4 and inhibits activation of Ced-3 (Hengartner and Horvitz, 1994; Vaux et al.,

1992). EGL-1, a pro-apoptotic member of the Bcl-2 family, activates apoptosis through inhibition of Ced-9 (Conradt and Horvitz, 1998; del Peso et al., 1998).

The core apoptotic machinery and regulators are conserved in *Drosophila* (Abrams, 1999; Aravind et al., 2001). Seven caspases are encoded by the *Drosophila* genome, including apical caspases Dronc, Dream/Strica, and Dredd, and effector caspases Dcp-1, Drice, Decay, and Daydream (Chen et al., 1998; Dorstyn et al., 1999a; Dorstyn et al., 1999b; Fraser and Evan, 1997; Inohara et al., 1997; Song et al., 1997; Vernooy et al., 2000). Activation of Dronc requires Dark, the Ced-4/APAf-1 homolog (Kanuka et al., 1999; Muro et al., 2002; Muro et al., 2004; Rodriguez et al., 1999; Yan et al., 2006; Zhou et al., 1999). Dronc and effector caspases are inhibited by inhibitors of apopotosis (IAPs) (Hay et al., 1995). Caspase activation depends upon the expression of the Rpr, Hid, Grim, and Sickle proteins, which disrupt DIAP-caspase interactions (Chen et al., 1996; Christich et al., 2002; Grether et al., 1995; Srinivasula et al., 2002; White et al., 1994; Wing et al., 2002). While caspases are thought to be critical determinants of cell death, other degradation mechanisms have been implicated in cell death as well.

The Ubiquitin Proteasome System

Eukaryotic cells use two main types of catabolic process to degrade cellular components, the ubiquitin proteasome system (UPS) to degrade short-lived proteins, and autophagy, which is generally thought to be used to degrade long-lived proteins. The UPS is the best-characterized non-lysosomal eukaryotic system to degrade cellular proteins (Hershko and Ciechanover, 1998). The UPS plays a key role in fundamental cellular processes, including the cell cycle, transcription, and antigen

processing. Recent studies have also suggested a role for the UPS in coordinating cell death, and multiple components of the proteasome system are associated with cancer and are potential targets for cancer therapy.

Proteins to be degraded by the UPS are targeted to the proteasome, an ATP-dependent 26S multisubunit protease complex (Ciechanover et al., 1980; Hershko et al., 1980; Hough et al., 1986; Rechsteiner et al., 1993) (**Figure 1-1**). Ubiquitin is conjugated to protein substrates to be degraded by the proteasome (Goldknopf and Busch, 1977; Goldstein et al., 1975). Ubiquitin is activated by an E1 enzyme and then transferred to an E2 conjugating enzyme (Ciechanover et al., 1981; Hershko et al., 1983). An E2 then transfers multiple ubiquitin moieties to a protein substrate specifically bound to an E3 ligase (Haas and Rose, 1982; Hershko et al., 1986). A proteasome subunit binds the multi-ubiquitin conjugate (Deveraux et al., 1994). Ubiquitin moeties are released by de-ubiquitinating enzymes (DUBs) to be reused (Hadari et al., 1992; Wilkinson et al., 1995). Following protein degradation, small peptides are released into the cytosol (**Figure 1-1**). In addition to marking cellular proteins to be degraded, ubiquitin protein modification plays important roles in regulating intracellular signaling via distinct types of ubiquitin binding, for example by mono-ubiquitination and different types of poly-ubiquitination (Bennett and Harper, 2008; Haglund and Dikic, 2005; Katzmann et al., 2002; Komander, 2009; Mukhopadhyay and Riezman, 2007).

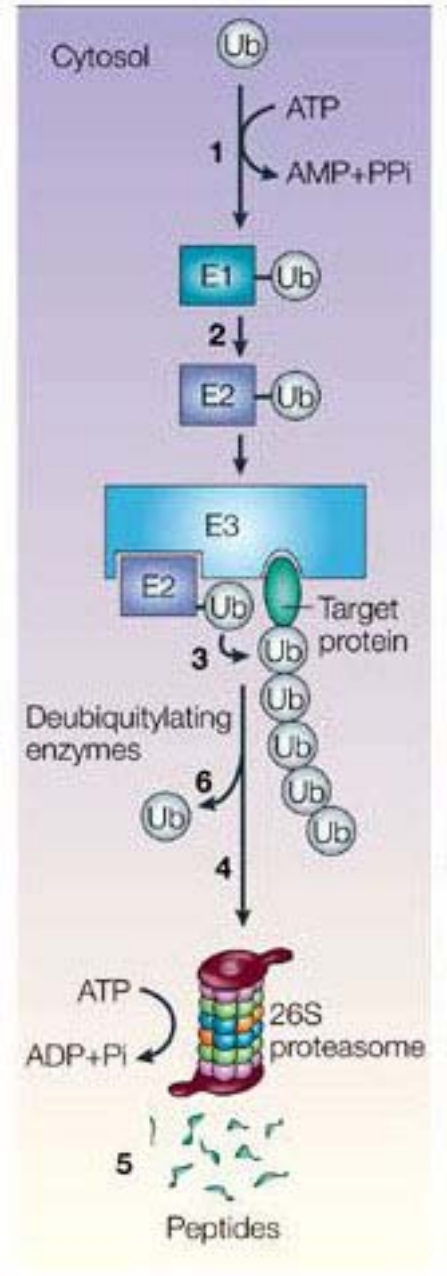

Figure 1-1. Degradation of cellular protein substrates by the proteasome.

Ubiquitin is activated by the ubiquitin activated enzyme, E1 (step 1). Ubiquitin is then transferred to a ubiquitin conjugating enzyme, E2 (step 2). The E2 enzyme and the protein substrate both bind specifically to an E3 ubiquitin protein ligase, and an activated ubiquitin is transferred to the protein substrate (step 3). A poly-ubiquitin

chain that serves as a signal to target the protein substrate to the 26S proteasome is formed by successive conjugation of ubiquitin moieties (step 4). The protein substrate is cleaved into short peptides and released into the cytosol (step 5). Ubiquitin is released by de-ubiquitinating enzymes (DUBs) for re-use (step 6). Adapted from Ciechanover, A. Nature Reviews Molecular Cell Biology 6, 79-87 (Ciechanover, 2005).

The Ubiquitin Proteasome System and its role in cell death

The first studies to suggest a cell death role for the UPS were carried out in the hawkmoth *Manduca Sexta.* Changes in ubiquitination and proteasome composition were shown to occur during hawkmoth development before the onset of cell death in intersegmental muscle cells, which die with type II cell death morphology (Dawson et al., 1995; Jones et al., 1995; Schwartz et al., 1990; Takayanagi et al., 1996). Early studies of the UPS during a cell death showed that p53 and its E3 ubiquitin ligase, Mdm2, are degraded by the UPS (Haupt et al., 1997; Kubbutat et al., 1997). The striking and conserved role of the UPS in regulating cell death by modulating IAPs and caspases is exhibited in *Drosophila*. *Drosophila* DIAP1 deletion mutants undergo massive cell death and die as embryos (Wang et al., 1999). DIAP1-mediated ubiquitination of caspases leads to proteasome degradation of caspases and cell survival (Muro et al., 2002; Wilson et al., 2002). However, pro-apoptotic Reaper, Hid, and Grim disrupt IAP-caspase interactions and stimulate IAP auto-ubiquitination (Ditzel et al., 2003; Wilson et al., 2002). IAPs are thus targeted to the proteasome for degradation, relieving IAP inhibition of caspases and leading to cell death (Ryoo et al., 2002; Wilson et al., 2002; Yoo et al., 2002).

Studies in cell lines suggest that caspase-dependent cleavage of the proteasome may facilitate cell death. Key regulatory proteasome subunits are cleaved during apoptosis following caspase activation in cultivated human cells (Sun et al., 2004). Caspase-dependent cleavage of proteasome subunits results in diminished proteasome function in both human and *Drosophila* cell lines (Adrain et al., 2004). This suggests that caspase-dependent proteasome impairment may be a critical

control point in cell death modulation and may be a conserved mechanism. However, this has not been tested *in vivo*. In addition, while the UPS has been implicated in type II cell death by correlation, this has not been tested empirically.

The Ubiquitin Proteasome System as a target for cancer therapy

Many components of the ubiquitin proteasome system have been associated with cancer and are potential targets for cancer therapies, including ubiquitin ligases, inhibitors of apoptosis, de-ubiquitinating enzymes (DUBs), and the proteasome (Hoeller and Dikic, 2009). Interestingly, while alterations in the proteasome are associated with several human diseases such as cardiac dysfunction and neurodegeneration, defects in the proteasome have not been linked to the development of cancer, suggesting that cancer cells might utilize the proteasome to survive (Hoeller and Dikic, 2009). Recent studies have shown that ectopic proteasome inhibition induces cell death in cell lines (Drexler, 1997; Shinohara et al., 1996), and drug-induced proteasome impairment in tumor cells results in caspase activation and cell death (Henderson et al., 2005).

Several proteasome inhibitors are currently being used in cancer therapies, including a boronic-acid derivative, bortezomib (Velcade, Millennium Pharmaceuticals) that has been successfully used to treat myeloma and lymphoma (Tobinai, 2007). Bortezomib is thought to lead to cell death by down-regulating NF-κB by blocking IκB degradation (Adams, 2004; Ling et al., 2003). There is also evidence that bortezomib treatment leads to endoplasmic-reticulum stress, which in turn is thought to promote cell death (Gu et al., 2008; Meister et al., 2007). However,

little is known about the cellular responses to proteasome impairment, and *in vivo* studies are lacking.

Autophagy

Autophagy is a catabolic process that is ubiquitously implemented by eukaryotic cells. Autophagy is a process to degrade cytoplasmic contents, including macromolecules and organelles (Klionsky, 2005). During autophagy, cytosolic components are sequestered by a double-membrane vesicle, the autophagosome. The autophagosome fuses with the lysosome, and autophagic contents are later degraded by lysosomal hydrolases. Whereas the ubiquitin/proteasome system is used to degrade short-lived proteins specifically targeted for degradation, autophagy is generally thought to be used for the bulk, non-selective degradation of long-lived proteins.

Autophagy is an important cellular response to stress and a survival mechanism during starvation that is conserved in yeast, worms, flies, and mammals (Mizushima, 2007; Xie and Klionsky, 2007). In response to starvation, autophagy functions in the production of amino acids, providing the building blocks for new protein synthesis. Autophagy is also a mechanism for the production of mitochondrial substrates to produce the energy required to survive starvation (Lum et al., 2005). In addition, autophagy is important for the elimination of damaged/unwanted organelles and protein aggregates (Cuervo, 2008; Nedelsky et al., 2008). In animal cells, autophagy also plays a role in cellular remodeling during development and differentiation, and in the elimination of invasive microorganisms. Alterations and deficiencies in autophagy (*atg*) genes are associated with

developmental and cell death defects, sensitivity to starvation and stress, decreased longevity, neurodegeneration, and tumor progression (Cuervo, 2008; Mathew et al., 2007b; Mizushima et al., 2008; Nedelsky et al., 2008).

Genetic regulation of autophagy

The pathways that regulate autophagy are evolutionarily conserved (Meléndez and Neufeld, 2008; Pattingre et al., 2007). The protein kinase Target of Rapamycin (TOR) plays a central role in nutrient sensing and autophagy regulation. When nutrients are readily available, TOR is activated through the Class I phosphatidylinositol-3-kinase (PI3K) signaling pathway. TOR represses autophagy through phosphorylation of Atg13; phosphorylated Atg13 does not bind appreciably to Atg1 (Kamada et al., 2010). Upon starvation, Atg13 is rapidly dephosphorylated, and the binding of dephosphorylated Atg13 to Atg1 leads to Atg1 activation (Kamada et al., 2000; Scott et al., 2007). When nutrients are scarce, TOR becomes inactivated, its repression of Atg13 is relieved, and autophagy is induced. Nucleation of the autophagic membrane requires phosphatidylinositol phosphorylation, which in yeast requires the formation of a complex that includes Atg6/Beclin1, Vps34/Class III PI3K, Atg14 and Vps15 (Kametaka et al., 1998; Kihara et al., 2001; Suzuki et al., 2001). In mammalian cells, additional regulators of the Beclin1/Vps34 complex have been identified, including Ambra1, UVRAG and Bif-1, and the mammalian Atg14 homolog, Barkor (Fimia et al., 2007; Liang et al., 2006; Sun et al., 2008; Takahashi et al., 2007). In addition, 2 distinct Beclin-1 complexes have been described in yeast and mammalian cells that may play distinct roles in membrane trafficking pathways (Itakura et al., 2008; Kametaka et al., 1998; Kihara et al., 2001).

A recent study in yeast demonstrated that the Tor and cAMP-dependent protein kinase (PKA) pathways independently regulate autophagy by affecting Atg13, a key regulator of Atg1 kinase activity (Stephan et al., 2009). They found that although both pathways affect Atg13 phosphorylation, each pathway affects distinct Atg13 phosphorylation sites. Interestingly, this study showed that inhibition of both pathways leads to an increase in autophagy levels compared to inhibition of either pathway alone (Stephan et al., 2009).

Little is known about the origin of the autophagic membrane, and this is a subject of debate (Juhasz and Neufeld, 2006). In yeast, autophagy proteins gather at a punctate structure, the Pre-Autophagosomal Structure (PAS), near the vacuole (the yeast lysosome) (Mizushima, 2007). A recent study suggests that in mammalian cells, nucleation of the autophagic membrane begins in a punctate compartment that is in dynamic equilibrium with the Endoplasmic Reticulum (ER) (Axe et al., 2008). This work is consistent with a previous study suggesting that ER membranes are used to form autophagosomes based on the localization of ER proteins in autophagosomal membranes (Dunn, 1990).

Two ubiquitin-like conjugation systems, conserved from yeast to mammals, function in autophagosome formation (Ohsumi, 2001; Reggiori and Klionsky, 2002). The formation of an Atg12-5-16 complex on the isolation membrane requires the E1-like activating enzyme Atg7 and the E2-like conjugating enzyme Atg10 (Kuma et al., 2002; Mizushima et al., 1999; Mizushima et al., 1998; Shintani et al., 1999; Tanida et al., 1999). This complex disassociates upon formation of the autophagosome. The second conjugation system requires the activity of Atg7 and the E2-like conjugating

enzyme Atg3 (Huang et al., 2000; Kirisako et al., 1999; Lang et al., 1998; Tanida et al., 1999). In this step, cytosolic Atg8 (LC3 in mammals) is modified by the attachment of the phospholipid anchor phosphatidyl-ethanolamine (PE) following its cleavage by the cysteine protease Atg4 (Ichimura et al., 2000; Kabeya et al., 2000; Kirisako et al., 2000). This step results in the localization of Atg8-PE to the isolation membrane, and has been proposed to contribute to elongation of the autophagic membrane (Nakatogawa et al., 2007). Atg8 remains associated with the autophagosome until it is trafficked to the lysosome, when the outer membrane of the autophagosome fuses with the lysosome to form the autolysosome, and Atg4 subsequently releases Atg8 from PE (Ichimura et al., 2000). For these reasons, Atg8/LC3 is a widely used marker of autophagosomes (Klionsky et al., 2008). Upon autophagosome formation, the inner membrane of the autophagosome and its contents are degraded by lysosomal hydrolases, and nutrients are subsequently released into the cytosol for recycling (Xie and Klionsky, 2007).

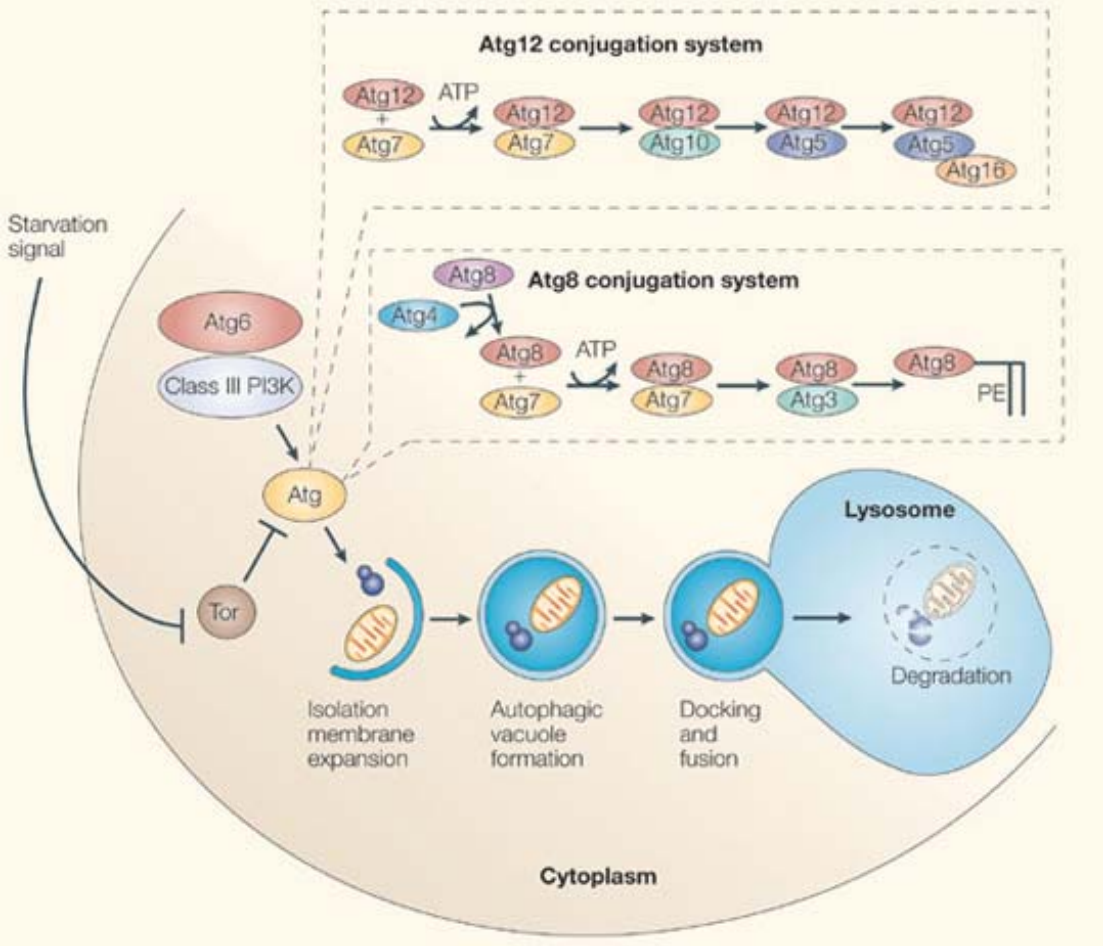

Figure 1-2. Genetic regulation of autophagy.

Autophagy is a catabolic process to degrade cytoplasmic contents. During autophagy, the expansion of the isolation membrane is followed by the formation of a double-membrane autophagic vacuole, which is trafficked to the lysosome, where it docks and fuses, followed by degradation of autophagic contents by lysosomal hydrolases. Autophagy is triggered by starvation through the modulation of Tor signaling. Tor inhibits autophagy by modulating atg genes that are required for autophagic vacuole formation. Class III PI3K, Atg6 (Beclin 1), and the Atg12 and Atg8 ubiquitin-like conjugation systems are required for autophagic vacuole formation. Figure adapted from Baehrecke 2005.

Autophagy in *Drosophila* development

Pioneering genetic screens in the yeast *Saccharomyces cerevisiae* advanced our understanding of autophagy by identifying the genes that are required for this catabolic process (Harding et al., 1995; Harding et al., 1996; Thumm et al., 1994; Tsukada and Ohsumi, 1993). The complexity of multicellular animals presents several interesting questions about autophagy and its relationship to nutrient utilization, cell growth, cell survival and cell death. For example, the ability of animals to respond to nutrient deprivation and adjust metabolic and catabolic processes to maintain homeostasis suggests that the mechanisms that regulate autophagy may differ under specific cellular contexts.

Drosophila melanogaster is an excellent genetic model for animal development. *Drosophila* has a short life cycle, a wide variety of genetic tools available, and mutants and RNAi lines have been systematically generated (http://flybase.org). *atg* genes and their regulators are highly conserved in *Drosophila* (Baehrecke, 2003; Meléndez and Neufeld, 2008), and in many cases, in contrast to mammalian systems, single orthologs to *atg* genes exist in *Drosophila*, allowing for non-redundant genetic studies. Autophagy is induced in many *Drosophila* tissues in response to nutrient restriction; for example, in the fat body of starving larvae, and during the pupal stage upon the cessation of feeding. In addition, autophagy is induced in *Drosophila* in response to the steroid hormone 20-hydroxyecdysone (ecdysone) in both the fat body (Rusten et al., 2004) and in dying larval structures such as the intestine and salivary glands (Lee and Baehrecke, 2001; Lee et al., 2002). Thus, *Drosophila* serves as an excellent model to study autophagy

in vivo, in response to nutrient restriction and also in the context of programmed cell death that occurs during development.

Drosophila atg gene mutant phenotypes suggest a role for autophagy in development (Meléndez and Neufeld, 2008; Neufeld and Baehrecke, 2008). Null mutations in *atg1* are pupal lethal (Scott et al., 2004). Surprisingly, however, mutations in some *atg* genes essential for autophagy are not lethal, even though these flies appear to possess greatly attenuated autophagy. Null *atg7* mutants develop normally whereas strong *atg8* hypomorphic mutations are semi-lethal (Juhász et al., 2007; Nezis et al., 2008; Scott et al., 2007; Simonsen et al., 2008). Both *atg7* and *atg8* mutants are hypersensitive to starvation and oxidative stress, exhibit degenerative neuronal defects, accumulate ubiquitin-positive aggregates in neurons, and have a shortened lifespan (Juhász et al., 2007; Nezis et al., 2008; Scott et al., 2007; Simonsen et al., 2008). This range in phenotypes suggests that some autophagy genes could play specialized roles, while others may be more pleiotropic and should be investigated for phenotypes that are not related to autophagy. The fact that *atg7* null mutations are not lethal suggests a few different possibilities. Some *atg* genes may function redundantly, or it could be that other mechanisms may compensate for macroautophagy deficiencies during *Drosophila* development, such as chaperone-mediated autophagy or micro-autophagy (Cuervo, 2008). Alternatively, given that certain autophagy gene mutations have cell-context-specific effects, there could be factors that determine specificity. Finding such factors will require studies to be carried out in nutritional contexts that are relevant to physiology and development, rather than in cell lines and *Drosophila* is well suited for this type of study.

Autophagy in growth and nutrient utilization

To develop to the proper size, animals require the coordination of cell growth, division and death within individual tissues, and this is influenced by environmental factors including nutrient availability (Conlon and Raff, 1999). *Drosophila* development provides a useful system to investigate the relationship between nutrients, autophagy, growth and development. Fly development lasts approximately 8 days in the laboratory; embryogenesis is 1 day long, the 3 larval feeding stages combine to last 3.5 days, and the transformation to an adult, known as metamorphosis, is 3.5 days long. Like vertebrate animals, fly development is controlled by growth factors and hormones. Insulin and Insulin-like growth factors are secreted when animals are feeding, stimulating protein synthesis, cell growth, and the processes that are required for animal growth (Arsham and Neufeld, 2006). In addition, the steroid ecdysone defines the length of the developmental period in *Drosophila*, as peaks in this steroid regulate larval molting and metamorphosis (King-Jones and Thummel, 2005). Several recent studies have investigated the relationship between growth factor and ecdysone signaling in flies (Colombani et al., 2005; Layalle et al., 2008). Surprisingly, few studies have investigated the relationship between these signaling pathways, autophagy and animal development.

Autophagy plays an important role in nutrient utilization during *Drosophila* larval development, and studies in the *Drosophila* fat body under conditions of starvation have provided important insights into the mechanisms that regulate autophagy. The fly fat body is a nutrient storage and mobilization organ akin to the mammalian liver and autophagy is induced in the fat body in response to amino acid

starvation (Scott et al., 2004). Either null mutations in *TOR*, or repression of TOR by modulation of components of the class I PI3K pathway, lead to the induction of autophagy in the fat body of feeding larvae, and result in the inhibition of growth, a reduction in cell size, and decreased viability (Scott et al., 2004). Conversely, expression of either activated TOR, or activation of components of the PI3K signaling pathway, suppresses starvation-induced autophagy (Scott et al., 2004). However, unlike in mammalian cells, the suppression of starvation-induced autophagy in this context does not require S6K phosphorylation (Scott et al., 2004).

Autophagy is also induced in several *Drosophila* tissues as a normal physiological response to the rise in hormones during metamorphosis. Autophagy and multiple *atg* gene RNA levels are induced following rises in ecdysone that trigger cell death of the larval midgut and salivary glands during metamorphosis (Lee and Baehrecke, 2001; Lee et al., 2002; Lee et al., 2003), suggesting that autophagy, and possibly cell death, play important roles in the maintenance of nutrient homeostasis when developing animals are not feeding. In the fat body, Class I PI3K pathway signaling is down-regulated, and autophagy is induced, following the rise in ecdysone at the end of the third larval stage that triggers metamorphosis (Rusten et al., 2004), indicating that regulation of the PI3K pathway is involved in the induction of autophagy in response to ecdysone as well as starvation. A recent screen for mutants that fail to induce autophagy in the fat body in response to ecdysone identified the *Drosophila* homologue of the AMP-activated protein kinase (AMPK) γ subunit, SNF4Aγ (Lippai et al., 2008). AMPK has been implicated in the regulation of autophagy and cell survival following growth factor withdrawal in mammalian cells

(Liang et al., 2007). In addition, a recent study indicates that AMPK represses TOR and induces autophagy under nutrient-rich conditions in response to calcium signaling in mammals (Hoyer-Hansen et al., 2007). Therefore, these studies suggest a conserved role for AMPK in the regulation of TOR and autophagy.

Studies in the *Drosophila* fat body have also shown that mutations in genes required for endosomal biogenesis are required for autophagy (Rusten et al., 2007). Mutations in *escrt* genes encoding the ESCRT proteins I, II, and III, as well as mutations in *vps4*, the ESCRT complex regulatory ATPase, all lead to an accumulation of autophagosomes in the fat bodies of fed larvae (Lee et al., 2007; Rusten et al., 2007). Furthermore, in *escrt-II* mutant cells, lysosomal associated membrane protein-1 (LAMP-1)-positive structures are distinct from Atg8-positive structures, suggesting a failure in the fusion of autophagosomes and lysosomes. This study also showed that mutations in *fab1*, an endosomal PI3 5-kinase, lead to the accumulation of autolysosomes that fail to degrade their contents, suggesting that *fab1* is required for the maturation, and possibly the acidification, of autophagosomes (Rusten et al., 2007).

The Vps34/Class III PI3K complex is a critical and conserved regulator of autophagy. This complex has been implicated in the regulation of endosomal maturation/lysosomal biogenesis as well as autophagy. It is possible that endosomal maturation/lysosomal biogenesis and autophagy may be co-regulated, although it is also possible that distinct Vps34 complexes regulate these vesicular trafficking pathways. Studies of mammalian cells suggest that amino acids stimulate TOR by activating Vps34/Class III PI3K (Byfield et al., 2005; Nobukuni et al., 2005).

However, some differences in the regulation of autophagy may exist between insect and mammalian systems. In *Drosophila*, whereas *vps34* is required for starvation-induced autophagy in the larval fat body, null mutations in *vps34* do not affect TOR signaling (Juhász et al., 2008). Instead, in Drosophila, starvation results in a TOR/Atg1-dependent recruitment of Vps34 activity to the autophagosomal membrane. It is not clear whether the differences between these results in flies and mammalian cells reflect evolutionary differences, or possibly cell context-specific differences between *in vitro* and *in vivo* studies.

Studies in *Drosophila* have also provided new insights into the relationship between autophagy and growth. Rapamycin treatment induces autophagy (Blommaart et al., 1995), and this revealed the critical regulatory role of TOR on autophagy that has been noted in many studies (Arsham and Neufeld, 2006; Pattingre et al., 2007; Wullschleger et al., 2006). TOR represses autophagy through phosphorylation of Atg13; phosphorylated Atg13 does not bind appreciably to Atg1 (Kamada et al., 2010). Upon starvation, Atg13 is rapidly dephosphorylated, and the binding of dephosphorylated Atg13 by Atg1 leads to Atg1 activation (Kamada et al., 2000; Scott et al., 2007). Scott et al (2007) demonstrated that in the *Drosophila* larval fat body, over-expression of Atg1 inhibits cell growth, and this involves a negative feedback mechanism on TOR. In addition, *atg1* mutant cells have a growth advantage when TOR signaling is reduced (Scott et al., 2007). Thus, there is a reciprocal relationship between autophagy and cell growth. Interestingly, *atg* gene disruption in *Drosophila tor* mutant fat body cells does not restore growth, but enhances the cell size reduction in *tor* mutants, suggesting that in this context,

autophagy is required to supply nutrients in order for cells to grow (Scott et al., 2004). Similarly, null *atg5* or *atg7* mutant mice lack the energy required to survive post-natal nutrient depletion (Komatsu et al., 2005; Kuma et al., 2004).

A recent study in mammalian cells, as well as in *Drosophila*, provided additional mechanistic information regarding the regulation of cell growth and autophagy. Kim et al (2008) found that Rag GTPases activate TOR in response to amino acid signals, and this activation is in parallel to Rheb signaling. Further, expression of constitutively active Rag GTPases in the absence of amino acids activates TOR, suppresses autophagy, and leads to an increase in organ size, whereas expression of dominant negative Rag GTPases leads to a decrease in organ size. Therefore, the reciprocal relationship between autophagy and cell growth involves the activation of Rag GTPases, and this mechanism is conserved (Kim et al., 2008; Sancak et al., 2008).

Autophagy and growth also exhibit a reciprocal relationship in the context of autophagy that occurs during cell death in *Drosophila* larval salivary glands. Growth arrest via regulation of the PI3K pathway is required for the induction of autophagy that occurs during salivary gland degradation (Berry and Baehrecke, 2007). Activation of positive regulators of growth, including Ras, Akt, or the PI3K catalytic subunit Dp110, inhibits autophagy and degradation of salivary glands (Berry and Baehrecke, 2007). Coexpression of the caspase inhibitor p35 with Dp110 enhances the Dp110-induced partial salivary gland degradation phenotype, suggesting that caspases function in parallel to growth arrest in this context. Importantly, expression of Atg1 and activation of autophagy suppresses the persistent phenotype in Dp110-

expressing salivary glands, and *atg* loss of function mutations prevent the destruction of salivary glands (Berry and Baehrecke, 2007). Thus, growth arrest via down-regulation of Class I PI3K is required for the induction of autophagy and salivary gland degradation. Further, the inhibition of salivary gland degradation by positive regulators of cell growth requires the activity of TOR, suggesting that the inhibition of autophagy by cell growth regulators takes place through TOR signaling (Berry and Baehrecke, 2007).

Recent work has elucidated how cell growth arrest is regulated in dying salivary glands. Loss-of-function mutations in the Warts/Hippo pathway, or over-expression of Wts downstream target Yorkie (Yki), the ortholog of mammalian Yes-associated protein (Yap), lead to tissue overgrowth (Edgar, 2006). However, it is not known how these genes influence cell growth and whether this occurs through signaling to the class I PI3K pathway. Significantly, *warts* (*wts*) is required for growth arrest and the induction of autophagy in dying salivary glands (Dutta and Baehrecke, 2008). Mutations in *wts,* as well as knockdown of *wts* pathway components *hpo*, *sav* and *mat*s, prevent salivary gland degradation. Surprisingly, however, over-expression of Yki in salivary glands does not phenocopy *wts* mutations, suggesting that in salivary glands, Wts signals independently of Yki. Significantly, *wts* mutants have altered class I PI3K markers and require the function of TOR and the insulin receptor substrate *chico* to inhibit salivary gland degradation (Dutta and Baehrecke, 2008). Therefore, Wts influences PI3K signaling in salivary glands. These data provide mechanistic information about how cell growth is

regulated during salivary gland cell death. It will be interesting to see whether Wts regulates cell growth in a PI3K-dependent manner in other systems.

Autophagy and Cell Death

Autophagy in mammalian development

Several studies demonstrate a role for autophagy in mammalian development (Cecconi and Levine, 2008). *atg5*, as well as *atg7*, null mutant mice exhibit few developmental defects at birth, but die within 1 day of delivery, and when un-suckled, die earlier than wild-type mice (Komatsu et al., 2005; Kuma et al., 2004). Therefore in this context, autophagy is required to generate the energy necessary to survive nutrient deficiency. Autophagy may also play a role in the context of cell death that occurs during mammalian development. A study utilizing an *in vitro* mouse stem cell model of embryogenesis demonstrated that null *atg* mutant embryonic stem cells are not deficient in the activation of programmed cell death, but fail to generate and display signals that are required for phagocytosis of dying cells (Qu et al., 2007). Significantly, the addition of methylpyruvate was sufficient to rescue *atg* mutant engulfment and clearance defects, indicating that the role of autophagy is to provide the metabolic substrates needed to complete this process. A subsequent study reported similar findings in the context of cell death that occurs in developing chick retina (Mellen et al., 2008). When autophagy was inhibited during retinal development, apoptotic cells accumulated, and this accumulation correlated with a deficiency in phosphatidylserine exposure (Mellen et al., 2008). Thus, these studies suggest that in the context of cell death that occurs during mammalian as well as

amniote vertebrate development, autophagy deficiency is associated with a failure in phagocytic clearance of apoptotic cells. Beyond these studies, little is known about the role of autophagy in developmental cell death in mammalian systems, and the cumbersome nature of mammalian genetics makes such *in vivo* studies difficult.

Autophagy in *Drosophila* cell death

Schweichel & Merker's observations of dying cell morphologies suggested that autophagy is induced in and promotes the death of certain types of dying cells (Schweichel and Merker, 1973). We noted that autophagy and autophagy genes are induced in dying larval salivary gland cells (Lee and Baehrecke, 2001; Lee et al., 2003), suggesting that this process promotes cell death, but it was not until recently that this has been rigorously tested using genetic approaches. The availability of several *in vivo* models for cell death in *Drosophil*a has made it possible to directly test the role of autophagy in cell death. Several *Drosophila* studies demonstrate a positive role for autophagy in cell death. Atg1 over-expression in the *Drosophila* larval fat body is sufficient to induce autophagy and cell death in a caspase-dependent manner (Scott et al., 2007). Mutations in *atg8* or *atg18*, or decreased function of *atg1*, in addition to a number of other *atg* genes, all lead to the incomplete destruction of larval salivary glands, structures that die with Type II morphology (Berry and Baehrecke, 2007). Mutations in *atg2* or *atg18* severely delay larval midgut removal (Denton et al., 2009). Furthermore, knockdown of *atg* genes specifically in salivary gland cells leads to incomplete gland destruction, indicating that the role of autophagy occurring within these dying cells is tissue-autonomous (Berry and Baehrecke, 2007). However, in contrast to the results in the fat body (Scott et al.,

2007), Atg1-overexpression in salivary glands induces cell death in a caspase-independent manner.

The relationship between autophagy and caspases

The relationship between autophagy and caspases may be context-specific. Several studies have suggested a synergistic role for autophagy and caspases in cell death that occurs during oogenesis in several *Drosophila* and other Dipteran species (Mpakou et al., 2006; Nezis et al., 2006a; Nezis et al., 2006b; Velentzas et al., 2007a; Velentzas et al., 2007b; Velentzas et al., 2007c). Two recent studies suggest that there is an epistatic relationship between caspases and autophagy during oogenesis, however their findings differ in important ways **(Figure 1-3)** (Hou et al., 2008; Nezis et al., 2009). Hou et al recently demonstrated that in germaria and midstage egg chambers, starvation-induced autophagy leads to degeneration (Hou et al., 2008). The effector caspase DCP-1 and IAP protein Bruce are required for autophagy induction in these degenerating egg chambers in response to starvation (Hou et al., 2008). Therefore this study suggests that caspases function upstream of starvation-induced autophagy and cell death in the ovary (Hou et al., 2008). In contrast, Nezis et al recently demonstrated that during developmentally-induced cell death that occurs during germarium development and mid-oogenesis, both processed caspase3-like expression and autophagy induction occur, however mutations in autophagy genes result in reduced caspase activation (Nezis et al., 2009). Therefore in this case, developmentally-induced autophagy is required for caspase activation in dying female germline cells (Nezis et al., 2009). Thus the mechanisms underlying the

hierarchical relationship between autophagy and caspases in cells that die during oogenesis remain to be resolved.

Several studies also indicate that caspases and autophagy function in parallel in the destruction of certain tissues during *Drosophila* development (**Figure 1-3**). During the destruction of salivary glands, both autophagy and caspase activation occur, however, expression of the caspase inhibitor p35 only partially prevents salivary gland degradation (Lee and Baehrecke, 2001). In *Drosophila dark* (Apaf-1) mutants, salivary gland degradation is incomplete, but autophagy occurs normally, suggesting a role for this caspase regulator in type II cell death downstream or parallel to autophagy (Akdemir et al., 2006). Significantly, Berry & Baehrecke demonstrate that the combined inhibition of autophagy and caspases enhances the incomplete destruction of salivary glands (Berry and Baehrecke, 2007). However, in contrast, Denton et al find that knockdown of caspases fails to enhance defects in larval midgut destruction in *atg* mutants (Denton et al., 2009). A recent study by Mohseni et al find that the destruction of the *Drosophila* amnioserosa, an extra-embryonic membrane that is eliminated late in embryogenesis, requires both autophagy and caspase activation (Mohseni et al., 2009). It is not clear in this study whether the relationship between caspases and autophagy is either parallel or epistatic, but this finding provides additional support for the hypothesis that caspases and autophagy function cooperatively in the destruction of tissues during cell death. A similar process may occur in some types of mammalian cells, given that mammalian 3-dimensional cultures of MCF-10A mammary cells die with similar characteristics (Debnath et al., 2002; Mills et al., 2004). Studies of MCF-10A

mammary epithelial cell lines, a model for mammary lumen formation, implicate both autophagy and caspases in the elimination of cells during lumen formation (Debnath et al., 2002; Mills et al., 2004). Suppression of either caspase activity or autophagy does not prevent lumen formation, whereas inhibition of both prevents cell elimination (Mills et al., 2004).

Autophagy and cell death: Questions

Although genetic evidence now indicates that autophagy contributes to cell death in some *in vivo* contexts (Berry and Baehrecke, 2007; Hou et al., 2008; Mohseni et al., 2009; Nezis et al., 2009), how autophagy may function in cell death is not completely clear. One possibility is that autophagy is required to generate the metabolic substrates that are required for cell autonomous destruction. It is also possible that autophagy functions to specifically deplete a cell survival factor as has been shown in mammalian cells (Yu et al., 2006a), and with accumulating models in which autophagy functions in physiological cell death, *Drosophila* may provide the best system to discover such a factor. Alternatively, autophagy may deplete critical resources, such as substrates for metabolism and mitochondria, which are required for cell survival, and this may lead to cell death.

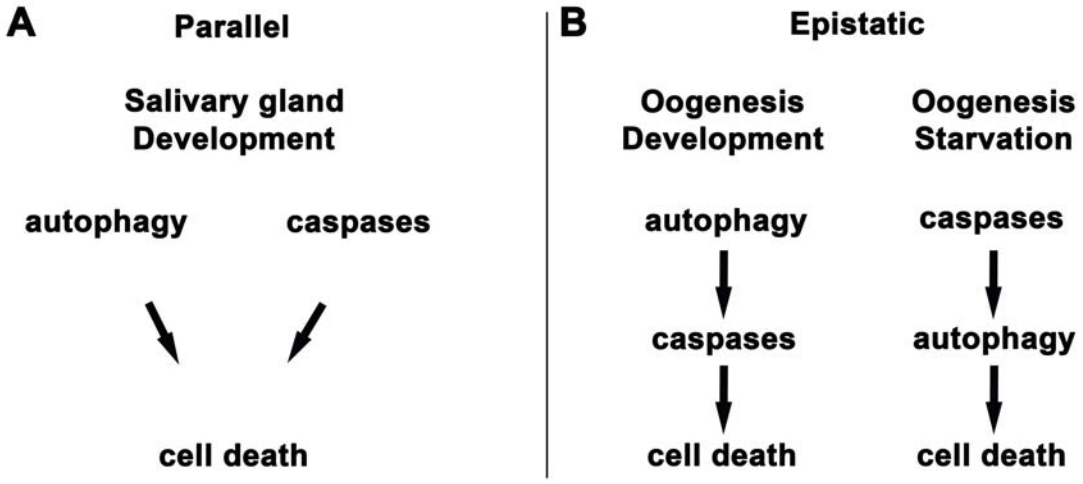

Figure 1-3. The relationship between autophagy and caspases during cell death may be context specific. A: During metamorphosis, *Drosophila* larval salivary glands undergo developmental programmed cell death. During destruction of salivary glands, both autophagy genes and caspases are required for complete degradation, and the combined inhibition of autophagy and caspases enhances this incomplete destruction (Akdemir et al., 2006; Berry and Baehrecke, 2007). In addition, caspases are activated in autophagy mutants and autophagy occurs when caspases are inhibited, indicating that autophagy and caspases function in parallel pathways. **B:** During *Drosophila* oogenesis, starvation-induced autophagy leads to degeneration of egg chambers, and effector caspase DCP-1 and IAP protein Bruce are required for autophagy induction (Hou et al., 2008). During developmentally-induced cell death that occurs during oogenesis, however, mutations in autophagy genes result in reduced caspase activation (Nezis et al., 2009). These studies indicate that autophagy and caspases function in an epistatic regulatory hierarchy.

Autophagy and Disease Models in *Drosophila*

Drosophila provides an ideal model system for studies of genes that have been implicated in human disease. More than 60% of the genes implicated in human disease have orthologs in flies, and studies in fly disease models have identified novel factors that regulate disease (Bernards and Hariharan, 2001; Hariharan and Haber, 2003). Whereas knowledge of a gene associated with a human disorder may initially be limited to a genetic locus, the ease of fly genetics, the ability to generate mutants, knockdown or over-express genes of interest make it possible to identify the function of such genes in flies. In addition, many signaling pathways are highly conserved between flies and humans. Therefore, the use of genetic modifier screens in flies, to look for mutations that enhance or suppress a mutant phenotype, makes it possible to quickly place a gene in the context of a genetic pathway and identify novel factors not previously associated with a disease (Bernards and Hariharan, 2001; Hariharan and Haber, 2003).

Autophagy has been implicated in aging, protein aggregate disorders, neurodegeneration, immunity, and cancer (Mathew et al., 2007; Mizushima et al., 2008; Nedelsky et al., 2008). While there are no cancer models in *Drosophila*, fly *atg7* and *atg8* mutants, like *atg* mutant mice, have a decreased life span and exhibit neurodegenerative defects (Hara et al., 2006; Juhász et al., 2007; Komatsu et al., 2006; Scott et al., 2007; Simonsen et al., 2008). Autophagy is also required for *Drosophila* innate immune responses (Ferrandon et al., 2007). Fly disease models have proven useful in identifying new factors that may regulate disease, and have also

provided mechanistic evidence for how autophagy is regulated in the context of neurodegenerative disorders, immune responses, and aging.

Protein aggregate disorders and the relationship between the UPS and autophagy

The accumulation of protein aggregates in degenerating neurons is associated with many human neurodegenerative diseases (Nedelsky et al., 2008). These protein aggregates are often ubiquitin-positive, suggesting defects in protein degradation by the UPS, and a number of studies have shown that the UPS is impaired in neurodegenerative disorders. However, an increase in the number of autophagosomes in degenerating neurons has also been noted in patients with many polyglutamine diseases, as well as Alzheimer's and Parkinson's. Autophagy gene mutant phenotypes also suggest a role for autophagy in aggregate protein disorders and neurodegeneration. *atg7* conditional knockout mice are impaired in autophagosome formation, and accumulate ubiquitin-positive aggregates (Komatsu et al., 2005). Loss of either *atg5* or *atg7* specifically in neurons leads to the accumulation of ubiquitin-positive aggregates and neurodegeneration in mice (Hara et al., 2006; Komatsu et al., 2006). *Drosophila atg7* and *atg8* null mutants also exhibit the accumulation of ubiquitin-positive aggregates in degenerating neurons (Juhász et al., 2007; Nezis et al., 2008; Simonsen et al., 2007).

Although an increase in the number of autophagosomes is associated with neurodegeneration, whether autophagy functions as a cytoprotective or as a cell death mechanism in this context has been a subject of debate. In both *Drosophila* and mouse models of Huntington disease, TOR inhibition induced autophagy and led to a

decrease in huntingtin protein accumulation and cell death, whereas autophagy inhibition enhanced polyglutamine toxicity (Ravikumar et al., 2004). In a *Drosophila* model of the neurodegenerative disease spinobulbar muscular atrophy (SBMA), polyglutamine expansion led to cell degeneration and *atg* gene-knockdown enhanced this degeneration (Pandey et al., 2007). Conversely, induction of autophagy via rapamycin treatment in this study suppressed cell degeneration (Pandey et al., 2007). Thus, these studies suggest that autophagy plays a cytoprotective role in the context of aggregate protein disorders.

While protein aggregate disorders are characterized by defects in the UPS and autophagy, these two catabolic systems have typically been thought to act independently of one another. However recent studies suggest that there may be a relationship between the UPS and autophagy, and several proteins have been implicated in a possible mechanism linking these processes. In the *Drosophila* model for SBMA mentioned above, genetic impairment of the proteasome led to the induction of autophagy (Pandey et al., 2007). Furthermore, this study demonstrated that the microtubule-associated protein Histone Deacetylase 6 (HDAC6), previously shown to interact with polyubiquitinated proteins (Kawaguchi et al., 2003), is required for autophagy induction upon proteasome impairment (Pandey et al., 2007). In addition, expression of HDAC6 during proteasome impairment was sufficient to rescue cell degeneration in an autophagy-dependent manner.

Other proteins have also been implicated in providing a link between autophagy and the UPS. p62/Sequestosome 1 (SQSTM1) binds both poly-ubiquitin and atg8/LC3, and loss of p62 leads to an increase in huntingtin-induced cell death in

cell lines (Bjorkoy et al., 2005). In autophagy-deficient mice, p62 is required for the formation of ubiquitin-positive protein aggregates (Komatsu et al., 2007). Similarly, the *Drosophila* p62 ortholog Ref2P is required for ubiquitin-positive aggregate formation in *atg8* mutants (Nezis et al., 2008). In addition, autophagy-linked FYVE protein (Alfy) localizes to ubiquitinated protein aggregates and autophagosomes, and mutations in its *Drosophila* homolog, *blue cheese*, lead to an accumulation of ubiquitin-positive aggregates in neurons (Finley et al., 2003; Simonsen et al., 2004). In line with these findings, *Drosophila* null mutations in *vps15,* the Vps34/Class III PI3K regulatory kinase required for autophagy, exhibit ubiquitin- and Ref2P-positive aggregates (Lindmo et al., 2008).

Studies in *Drosophila* also suggest a role for endosomal biogenesis genes in aggregate protein disorders. Mutations in *escrt* genes are linked to several human neurodegenerative disorders, including frontotemporal dementia and amyotrophic lateral sclerosis (Parkinson et al., 2006; Skibinski et al., 2005). In a *Drosophila* model for Huntington disease, reducing the genetic dosage of ESCRT proteins, or expressing a dominant-negative form of the ESCRT regulatory ATPase Vps4, led to the accumulation of autophagosomes and ubiquitin-positive aggregates (Rusten et al., 2007). In ESCRT-depleted HeLa cells, ubiquitin-positive aggregates also contained p62 and Alfy (Filimonenko et al., 2007). Rab5, a gene known to be involved in endocytosis, was also shown to be required for autophagosome formation, and inhibition of Rab5 enhanced polyglutamine toxicity in a *Drosophila* model of Huntington disease (Ravikumar et al., 2008).

Autophagy and aging

Drosophila atg7 and *atg8* mutants have a decreased lifespan and are sensitive to oxidative stress, demonstrating a role for autophagy in aging (Juhász et al., 2007; Simonsen et al., 2008). In *Drosophila*, autophagy gene expression is reduced with age (Simonsen et al., 2008). Conversely, Atg8 over-expression in adult neurons results in an increase in resistance to oxidative stress, a process that has been linked to aging (Terlecky et al., 2006), and the extension of lifespan (Simonsen et al., 2008). Further, *atg7* conditional knockout mice accumulate peroxisomes in their livers and exhibit oxidative stress, demonstrating a direct role for autophagy in peroxisomal degradation in mammals (Iwata et al., 2006).

Evidence in mice suggests that the relationship between autophagy and aging involves chaperone-mediated autophagy (CMA) (Paglin et al., 2001; Zhang and Cuervo, 2008). CMA is a selective degradation process in which soluble proteins are delivered directly to the lysosome (Cuervo, 2008). Like macroautophagy, CMA is activated in response to oxidative stress (Kiffin et al., 2004; Massey et al., 2006). In addition, LAMP2A, a receptor required for CMA, decreases with age due to a loss in LAMP2A protein stability (Cuervo and Dice, 2000; Kiffin et al., 2007). Furthermore, inducing the expression of LAMP2A in the livers of transgenic mice increases the levels of CMA, and these mice accumulate fewer damaged proteins in their livers (Zhang and Cuervo, 2008). CMA has not been investigated in *Drosophila*, and it would be useful to apply the strength of fly genetics to this important catabolic process.

Autophagy and immunity

Evidence suggests that autophagy plays important roles in mammalian innate and adaptive immunity in the elimination of pathogens, and antigen processing and presentation (Mizushima et al., 2008; Vyas et al., 2008). Autophagy is important during T-cell selection to generate self-tolerance, and autophagy deficiency leads to multi-organ inflammation (Nedjic et al., 2008). Furthermore, mutations in *atg16* have been linked to inflammatory bowel disease in humans and mice (Cadwell et al., 2008; Saitoh et al., 2008). Autophagy is also important as a host-defense mechanism to clear intracellular pathogens (Andrade et al., 2006; Gutierrez et al., 2004; Ling et al., 2006; Nakagawa et al., 2004; Ogawa et al., 2005), and some invading pathogens and viruses utilize or inhibit the autophagic machinery to evade host-defense mechanisms (Huang and Klionsky, 2007; Jounai et al., 2007; Kirkegaard et al., 2004). During *M. tuberculosis* infection, autophagy is induced, and this induction requires the immunity-related GTPase family member IRGM (Gutierrez et al., 2004; Singh et al., 2006). However, mechanistic evidence demonstrating how autophagy is regulated in the context of immune signaling has been lacking.

Drosophila lack adaptive immunity, but can mount innate immune responses. Recent *in vivo* studies in *Drosophila* have helped to elucidate the mechanism of autophagy induction during pathogenic infection. Yano et al found that *Drosophila* resistance to the gram-positive bacteria *L. monocytogenes* requires the pattern-recognition receptor PGRP-LE, a member of a family of receptors that recognize bacterial peptidoglycans, induce antimicrobial peptide (AMP) genes, and activate the innate immune signaling IMD and Toll pathways (Yano et al., 2008). Significantly,

Yano et al showed that autophagy in blood cells is necessary to inhibit the intracellular growth of *L. monocytogenes*, and to survive infection. Further, the PGRP-LE receptor is required for the induction of autophagy following *L. monocytogenes* infection (Yano et al., 2008). However, autophagy induction in this case is independent of the Toll and IMD immune signaling pathways, suggesting the possibility that the PGRP-LE receptor may signal through an unknown factor to induce autophagy (Yano et al., 2008).

Another recent *Drosophila* study has provided new information about the crosstalk between autophagy and innate immune signaling pathways. A screen for genes required for *Drosophila* innate immune responses to bacterial infection identified the gene immune response-deficient 1 (*ird1*), the *Drosophila* homolog of the Vps34/Class III PI3K regulator, *vps15* (Wu et al., 2007). AMP genes are induced during starvation (Zinke et al., 2002), but *ird1* mutants fail to express AMP genes upon infection (Wu et al., 2007). Furthermore, *ird1* mutants cannot activate the IMD pathway, demonstrating that *ird1/vps15* is an important regulator of the innate immune response (Wu et al., 2007). In addition, this study showed that if wild-type flies are starved during bacterial infection, the expression of AMP genes is suppressed, and these flies exhibit decreased survival upon infection, suggesting that autophagy plays an important role in modulating nutrient sensing and immune signaling (Wu et al., 2007). This result provides insight into studies suggesting that in human and mouse populations, malnutrition leads to an increased susceptibility to infections (Chan et al., 1996; Chandra, 1996; Faggioni et al., 2000).

Summary

Here I investigate the role of the ubiquitin/proteasome system and autophagy in *Drosophila* salivary gland cell death. *Drosophila* larval salivary gland cells die in synchrony during development with type II morphology; autophagic vacuoles are present in the cytoplasm, and phagocytosis is not observed (Lee and Baehrecke, 2001). The onset of salivary gland cell death is triggered by a pulse of the steroid 20-hydroxyecdysone (ecdysone), which begins to rise in titer 10 hours after puparium formation (APF) and peaks 12 hours APF (Baehrecke, 2000). This ecdysone pulse is followed by DNA fragmentation and caspase activation between 12 and 14 hours APF, and the appearance of autophagic vacuoles in the cytoplasm by 14 hours APF (Jiang et al., 1997; Lee and Baehrecke, 2001; Martin and Baehrecke, 2004). Note the timing of salivary gland cell death events (**Figure 1-4**). As mentioned above, a similar process may occur in mammalian cells, given that mammalian 3-D cultures of MCF-10A mammary cells die with similar characteristics (Debnath et al., 2002; Mills et al., 2004), and similar morphology is observed during several types of mammalian developmental cell death (Clarke, 1990).

The salivary gland model is an excellent system to functionally test questions about the role of catabolic mechanisms during type II cell death, given the conservation of cell death mechanisms, the wide range of genetic tools, and the ability to study cell death *in vivo* in *Drosophila* (Hay et al., 2004; Rubin, 2000). *Drosophila* is well-suited to *in vivo* studies of the ubiquitin proteasome system and autophagy, and their relationship to cell survival, growth, and death in the context of a developing multi-cellular organism. While changes in the proteasome system have

been correlated with cell death in cells that die with Type II morphology in the Hawkmoth, this has not been tested empirically. In addition, while recent studies suggest that ectopic proteasome impairment leads to cell death, and proteasome inhibitors are being used in anti-cancer therapies, little is known about the *in vivo* effects of proteasome inhibition. The availability of *Drosophila* temperature-sensitive proteasome mutants, and tools to monitor the function of the proteasome, make it possible to study proteasome function and the effects of ectopic proteasome impairment *in vivo*.

Drosophila research has produced many new discoveries about the role and regulation of autophagy during development, aging, innate immunity, and in the context of diseases such as protein aggregate disorders and neurodegeneration. Autophagy is induced in *Drosophila* upon starvation in tissues such as the fat body, muscle, and ovaries. Autophagy is also induced in response to the steroid hormone ecdysone during metamorphosis in tissues such as the fat body, intestine, and salivary glands. This allows studies to be carried out in different cell types and in response to different stimuli. Autophagy regulation may differ in the contexts of nutrient deprivation compared to ecdysone induction, in the context of cell survival versus cell death, or in response to different pathogens. Thus, there may be a cell-context specific component to the proper regulation of autophagy, and it is possible that as-yet undiscovered regulators that influence the induction of autophagy in response to different stimuli, and/or in specific cell-types, may exist, and flies are well-suited to such discoveries.

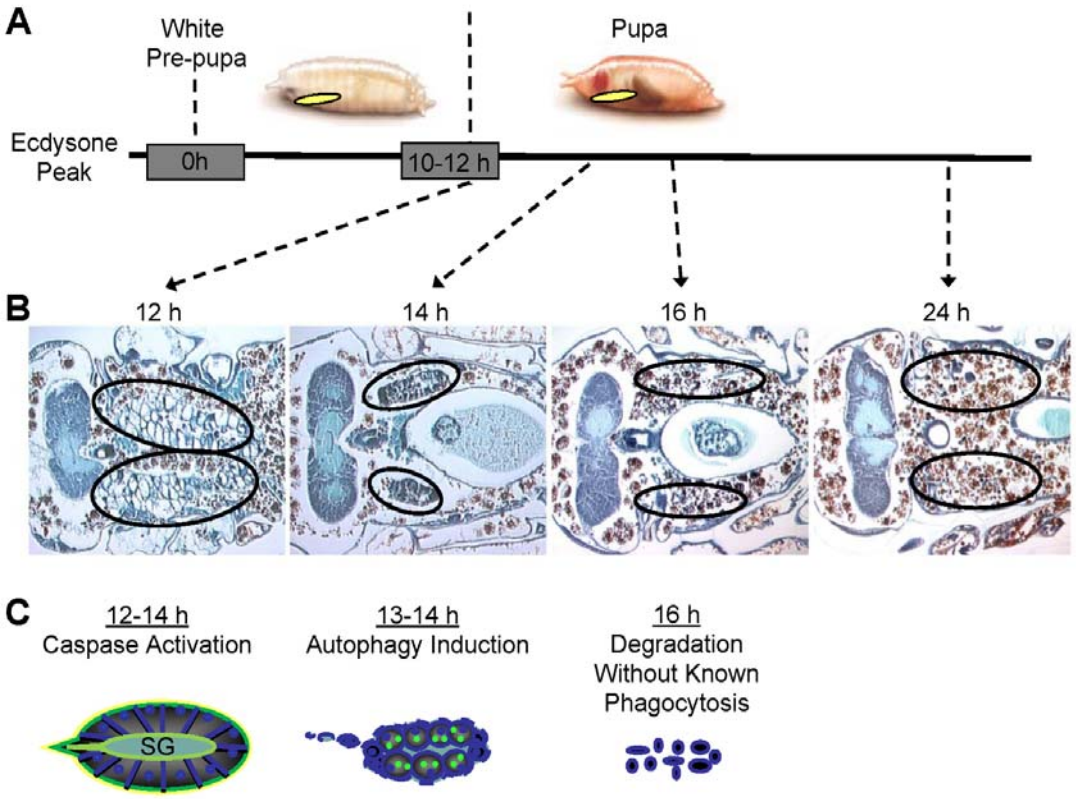

Figure 1-4. Timing of *Drosophila* salivary gland cell death. A. The formation of the white pre-pupa is triggered by a rise in titer of the steroid hormone hydroxyecdysone (ecdysone), designated 0 hours (0h). The pre-pupal to pupal transition is triggered by an ecdysone pulse that occurs 10-12 h APF. B. Histological sections depicting wild-type salivary gland degradation: at 12 h APF, salivary glands (circled) are large and vacuolated; by 14h APF, salivary glands (circled) become condensed; by 16 h APF, salivary glands are completely degraded (circled). Genetic mutants are screened for defects in salivary gland cell death 24 h APF. C. Caspase activation and DNA fragmentation occur in salivary gland cells between 12 and 14 h APF; autophagic vacuoles can be detected in the cytoplasm by 14 h APF; by 16 hours APF, salivary gland cells are degraded without known phagocytosis.

Chapter 2

Identification of proteins required for autophagic cell death using proteomics

Abstract

Much is known about the mechanisms that regulate apoptosis, but autophagic cell death remains poorly understood. Studies in cell lines suggest that the proteasome is impaired during cell death (Adrain et al., 2004; Sun et al., 2004), but this has not been tested *in vivo*. Proteasome inhibitors lead to cell death in cell lines (Drexler, 1997; Shinohara et al., 1996) and are currently being used in anti-cancer therapies (Hoeller and Dikic, 2009; Tobinai, 2007). However little is known about *in vivo* cellular responses to proteasome impairment. Shotgun proteomic analyses of purified dying larval salivary glands identified proteins that are enriched during autophagic programmed cell death in wild-type dying salivary glands, and this resulted in the identification of many proteins associated with the ubiquitin/proteasome system (UPS). Here we show that the UPS is impaired during wild-type salivary gland cell death, and that ectopic proteasome impairment leads to the onset of early salivary gland cell death *in vivo*. Surprisingly, we find that the expression of caspase inhibitor p35 during proteasome impairment does not suppress early gland degradation. We

used proteomics to identify factors following proteasome impairment and compared these factors to proteins indentified during wild-type salivary gland cell death, and screened top candidates for defects in salivary gland cell death. We find that several novel factors, including *lysozyme E*, *trol*, and the Cop9 signalsome component *csn6*, are required for salivary gland cell death.

Introduction

Programmed cell death is critical to animal development and homeostasis, and dysregulation of cell death can lead to disorders such as autoimmunity and cancer (Danial and Korsmeyer, 2004; Lockshin and Williams, 1965; Thompson, 1995). There are two main morphological forms of programmed cell death that occur during development, apoptosis, and autophagic cell death (Clarke, 1990; Schweichel and Merker, 1973). Autophagic cell death is characterized by the induction of autophagy in dying cells that are removed without known phagocytosis (Clarke, 1990). Macroautophagy (autophagy) is a catabolic process to degrade cytoplasmic contents including damaged/unwanted proteins and organelles (Klionsky, 2005). Contents to be degraded are engulfed by a double-membrane autophagosome and trafficked to the lysosome, where they are degraded by lysosomal hydrolases. Autophagy is required for survival in response to nutrient restriction, but has also been associated with cell death (Levine and Klionsky, 2004). Although genetic evidence indicates that autophagy contributes to cell death in several *in vivo* contexts (Berry and Baehrecke, 2007; Denton et al., 2009; Hou et al., 2008; Mohseni et al., 2009; Nezis et al., 2009),

how autophagy is regulated during and contributes to cell death remains poorly understood.

Eukaryotic cells use two main catabolic processes to degrade cellular components, autophagy and the ubiquitin proteasome system (UPS). Proteins to be degraded by the UPS are poly-ubiquitinated and targeted to the proteasome, an ATP-dependent 26S multisubunit protease complex (Ciechanover, 2005). The UPS plays a key role in multiple cellular processes, including cell cycle regulation (Schwartz and Ciechanover, 1999) and antigen processing (Wang and Maldonado, 2006), and studies have suggested a role for the UPS in coordinating cell death (Drexler, 1998). Several studies in cell lines suggest that caspase-dependent proteasome impairment may facilitate cell death (Adrain et al., 2004; Sun et al., 2004); however this has not been tested under physiological conditions *in vivo*. Changes in ubiquitination and proteasome composition have been shown to occur during hawkmoth development in dying intersegmental muscle cells (Dawson et al., 1995; Jones et al., 1995; Schwartz et al., 1990; Takayanagi et al., 1996). Interestingly, these cells die with autophagic cell death morphology, suggesting a possible role for the UPS in autophagic cell death, but this has not been tested empirically.

Several studies have shown that ectopic proteasome impairment induces cell death in cell lines (Drexler, 1997; Shinohara et al., 1996), and drug-induced proteasome impairment in tumor cells results in caspase activation and cell death (Henderson et al., 2005). In addition, proteasome inhibitors are being used in cancer therapies (Hoeller and Dikic, 2009). The reversible proteasome inhibitor Bortezomib (Velcade, Millennium Parmaceuticals) has been successfully used to treat myeloma

and lymphoma (Tobinai, 2007). Evidence in cell lines suggests that proteasome inhibitors lead to cell death by down-regulating NF-κB (Adams, 2004; Ling et al., 2003), and/or by inducing endoplasmic-reticulum stress (Gu et al., 2008; Meister et al., 2007). However, little is known about the effects of proteasome inhibitors on cellular processes, and how proteasome inhibition leads to cell death has not been tested *in vivo*.

Mass Spectrometry (MS)-based proteomics has been successfully used to analyze protein populations isolated from a variety of cells and tissues (Aebersold and Mann, 2003). During *Drosophila* development, larval salivary glands undergo programmed cell death requiring autophagy (*atg*) genes (Berry and Baehrecke, 2007). A previous analyses of purified dying salivary glands in wild-type *Drosophila* by shotgun high-throughput MS-based proteomics (Chen et al., 2003) led to the identification of proteins that function in a number of different processes during salivary gland cell death, including, among others, apoptosis and autophagy (Martin et al., 2007). This proteomics approach resulted in the identification of several proteins not detected in a whole-genome microarray of dying salivary glands (Lee et al., 2003), including the serine/threonine kinase Warts (Wts). Through functional analyses, *wts* mutants were shown to have a defect in autophagy induction and salivary gland degradation (Dutta and Baehrecke, 2008; Martin et al., 2007).

Recent developments in high-throughput MS-based proteomic technologies have led to dramatic improvements in quantification techniques and sensitivity, allowing for the identification of rare proteins (Domon and Aebersold, 2006; Fang et al., 2009). In light of these developments, we conducted a new proteomic analysis of

wild-type dying salivary glands in *Drosophila* to identify proteins not detected by previous methods, and not previously known to be involved in *Drosophila* autophagic programmed cell death. We found that among many groups of proteins identified, a number of UPS components are present in wild-type dying salivary glands, suggesting a role for the UPS in salivary gland cell death.

Here we show that the UPS is impaired during wild-type salivary gland cell death, and that ectopic proteasome impairment leads to the onset of early salivary gland cell death and DNA degradation. Surprisingly, we find that the expression of caspase inhibitor p35 during proteasome impairment does not suppress early salivary gland degradation. This suggests the involvement of other factors, in addition to caspases, in the cellular response to proteasome impairment that leads to ectopic cell death. To identify novel factors that function in the response to proteasome impairment during autophagic cell death, we conducted a proteomic analysis of salivary glands following ectopic proteasome impairment. To ensure physiological relevance, we compared the factors identified following proteasome impairment to those identified during wild-type salivary gland cell death and screened top candidates identified in both datasets for defects in salivary gland cell death. Here we demonstrate that several novel factors, *lysozyme e*, *trol*, and the Cop9 signalsome component *csn6*, are required for salivary gland cell death.

Results

Identification of proteins enriched during autophagic cell death in *Drosophila* salivary glands.

During *Drosophila* development, autophagic programmed cell death of larval salivary glands is triggered by a rise in the steroid hormone 20-hydroxyecdysone (ecdysone) 12 hours after puparium formation (APF), and salivary gland material is cleared without known phagocytosis (Lee and Baehrecke, 2001; Martin and Baehrecke, 2004). Caspases are activated and autophagy genes are induced in response to this rise in ecdysone (Lee and Baehrecke, 2001; Lee et al., 2003; Martin and Baehrecke, 2004), and these processes function in an additive manner to bring about the death and destruction of salivary glands (Berry and Baehrecke, 2007).

To identify new proteins required for salivary gland cell death, we isolated soluble proteins from purified salivary glands before (6 hours APF), during (12 hours APF), and after (13 hours APF) the onset of salivary gland cell death (**Table 2-1**). Salivary gland proteins were analyzed using shotgun high-throughput MS-based proteomics (Chen et al., 2003). At least 3 independent biological samples for each timepoint were isolated. Proteins were fully trypsinized, and peptides were separated by two-dimensional chromatography; first into 15 fractions by capillary isoelectric focusing (CIEF), and further resolved by capillary reversed phase liquid chromatography (nano-RPLC). Two runs of each protein sample were carried out. Fractions were analyzed by ESI-tandem-MS using a ThermoFinnigan LTQ linear ion trap mass spectrometer (San Jose, CA). Following MS analysis, peaklists were generated using extract_msn, and searches to identify MS/MS peptide spectra were

carried out using the Open Mass Sepctrometry Search Algorithm (OMSSA) (Geer et al., 2004) (NCBI). For each dataset, protein and peptide hits were generated assuming a false positive rate of 5%, and proteins present in the samples were identified based upon peptide sequences detected. We identified an average of 12,487 distinct peptides that mapped to 4,157 distinct proteins in the 6h samples with greater than 95% confidence (**Table 2-2**). Similarly, we identified an average of 11,530 distinct peptides in the 12h samples, which mapped to 3,566 distinct proteins, and an average of 13,012 distinct peptides that mapped to an average of 4,184 distinct proteins in the 13h samples, with greater than 95% confidence (**Table 2-2**).

Proteins previously shown to be involved in salivary gland programmed cell death were identified using this proteomic approach, including the ecdysone receptor component Usp, the ecdysone response protein Eip93F (E93), the nuclear receptor competence factor βFtz-f1, the caspase protease Ice, and several autophagy proteins (**Table 2-3 and Appendix 1**). This is consistent with DNA microarray studies, a previous proteomics study (Lee et al., 2003; Martin et al., 2007), and genetic studies identifying genes required for salivary gland cell death (Berry and Baehrecke, 2007; Lee et al., 2000; Martin and Baehrecke, 2004; Yao et al., 1993). These data support the hypothesis that proteins required for salivary gland cell death can be identified using this proteomics approach.

Table 2-1. Experiments to identify proteins present in salivary glands during developmental cell death by proteomics.

Experiment	Genotype	Temperature	Time-point	# Independent Samples
Wild-type	Canton-S	25ºC	6h	4
	Canton-S	25ºC	12h	3
	Canton-S	25ºC	13h	3
Proteasome Control	Control: UAS-Dts7^{2c}/+	28ºC	6h	3
Proteasome Impairment	*fkh*-GAL4/+; UAS-Dts7^{2c}/+	28ºC	6h	4

Wild-type (Canton-S) pupae were staged to 6h, 12h, and 13h after puparium formation at 25ºC. Control (UAS-Dts7^{2c}/+) and proteasome impairment (fkh-GAL4/+; UAS-Dts7^{2c}/+) pupae were temperature shifted from permissive (25ºC) to restrictive (28ºC) temperature at puparium formation (0h) and staged to 6h after puparium formation.

Table 2-2. Range and average number of distinct peptides (dpep) and distinct proteins (dpro) identified in salivary glands by proteomics.

Sample	Range: dpep	Average: dpep	Range: dpro	Average: dpro
Wild-type 6h	12,119-12,429	12,487	4,083-4,255	4,157
Wild-type 12h	9,733-12,846	11,530	3,221-3,836	3,566
Wild-type13.5h	11,362-11,895	13,012	3,502-3,919	3,880
Proteasome Control	6,453-16,578	12,601	3,603-5,027	4,184
Proteasome Impairment	9,462-15,610	12,094	3,265-4,625	3,922

Proteins from purified salivary glands were analyzed using shotgun high-throughput mass-spec (MS)-based proteomics (Chen et al. 2003).

Table 2-3. Proteins identified by proteomics that are known to function in salivary gland cell death.

Category	Symbol	Notes	6h AVE	12h AVE	13h AVE
Ecdysone Response					
	Usp	Ecdysone receptor	0.0012	0	0
	Eip93F	E93	0	0	0.00271
	βFtz-f1	Nuclear receptor competence factor	0.00219	0.00212	0.00091
Apoptosis					
	Ice	Caspase	0.01138	0.00726	0.00444
Autophagy					
	Atg1		0.00557	0.00218	0.00364
	Atg2		0	0.00039	0.00040
	Atg4		0.02736	0.00175	0.00184
	Atg5		0.00225	0	0.00447
	Atg9		0	0	0.00269
	Atg18		0	0.00264	0.00856

Protein names are based on Flybase annotation (http://flybase.org/). The values for peptides mapped to the genes listed are indicated. Protein quantities were determined using the spectral counting method in which spectral counts (spectral peptide matches) for each protein were summed and normalized across runs based on the total spectral counts obtained for each run.

Ubiquitin/proteasome system components are enriched in dying *Drosophila* salivary glands.

We sought to identify groups of proteins that were enriched in the proteomics data that suggested the involvement of a cellular component or genetic pathway that might function in salivary gland cell death. We identified groups of proteins that increased in detection values between 6h and 13h APF, as indicated by positive ratio2 values (**Appendix 2**). Among the many categories of proteins identified as being enriched in wild-type dying salivary glands, we noted the presence of number of proteasome components and ubiquitination regulators, suggesting a possible role for the ubiquitin/proteasome system in salivary gland cell death (**Table 2-4**). In addition, we used the Ingenuity Pathway Analysis ™ and this approach also identified the protein ubiquitination pathway. This was intriguing, as several studies have shown a correlation between changes in ubiquitination and proteasome composition during autophagic cell death that occurs during hawkmoth development (Dawson et al., 1995; Jones et al., 1995; Schwartz et al., 1990; Takayanagi et al., 1996). Several studies in cell lines have indicated that the proteasome is impaired in dying cells (Adrain et al., 2004; Sun et al., 2004). These findings suggest several possibilities. It could be that UPS components are enriched in dying salivary glands because the UPS has increased function during salivary gland cell death. It could also be that the UPS is impaired during salivary gland cell death, and perhaps this could be explained by system overload that might result from the increase in UPS components that occurs in dying salivary glands.

Table 2-4. List of ubiquitin/proteasome system components identified in Wild-type dying salivary glands.

		Wild-type 6h vs 13h	
Symbol	**Notes**	**ratio2**	**p value**
ari-1	ubiquitin-protein ligase activity	1.5	0.7884
ben	ubiquitin protein ligase activity	1	0.8501
CG17331	proteasome core complex	1.1	0.5807
CG1950	ubiquitin thiolesterase activity	1.5	0.4562
CG30382	proteasome core complex	1.2	0.5712
CG3473	ubiquitin protein ligase activity	1.2	0.9195
CG7656	ubiquitin protein ligase activity	1.1	0.9309
CG8184	ubiquitin-protein ligase activiy	Inf	0.2855
CG9086	ubiquitin-protein ligase activiy	5.9	0.0651
crl	ubiquitin-protein ligase activity	Inf	0.2855
Cul-2	ubiquitin protein ligase binding	1.2	0.9108
Cul-2	ubiquitin protein ligase binding	1.2	0.9108
Cul-5	cullin-RING ubiquitin ligase complex	1.5	0.7994
hyd	ubiquitin protein ligase activity	1.1	0.9309
Pros25	proteasome core complex	1.5	0.0136
Pros26.4	proteasome regulatory particle	1.1	0.5846
Pros45	proteasome regulatory particle, base subcomplex	1.3	0.1907
Prosalpha3T	endopeptidase activity	1.2	0.9195
Prosalpha5	proteasome complex	1.1	0.4613
Prosbeta1	proteasome core complex	1.3	0.0064
Prosbeta3	proteasome core complex	1.3	0.1033
Prosbeta7	proteasome core complex	1.1	0.523
Prp19	ubiquitin-protein ligase activiy	7.2	0.02349
Rpn1	proteasome regulatory particle, base subcomplex	1.5	0.0088
Rpn11	proteasome regulatory particle, lid subcomplex	1.1	0.5851
Rpn2	proteasome regulatory particle, base subcomplex	1.4	0.011
Rpn5	proteasome regulatory particle, lid subcomplex	1.5	0.05447
Rpn7	proteasome regulatory particle, lid subcomplex	1.3	0.4598
Rpt4	proteasome regulatory particle, base subcomplex	1	0.7778
Rpt6R	proteasome regulatory particle, base subcomplex	1	0.9667
slmb	ubiquitin-protein ligase activiy	Inf	0.2855
Tbp-1	proteasome regulatory particle	1.6	0.03149
UbcD4	ubiquitin-protein ligase activiy	Inf	0.2855
UbcD6	ubiquitin protein ligase activity	1.2	0.8294
Ubc-E2H	ubiquitin protein ligase activity	1.1	0.9407
Ufd1-like	proteasome complex, base subcomplex	2.4	0.4157

Protein names are based on Flybase annotation (http://flybase.org/). The ratio2 values for peptides mapped to the genes listed are indicated (ratio2=average detection value

experimental sample divided by average detection value control sample). p values were obtained using the Student's t-test followed by multiple testing adjustment using the Benjamini-Hochberg method (Hochberg and Benjamini, 1990). Inf indicates a numerical value divided by 0. –Inf indicates 0 divided by a numerical value.

The ubiquitin/proteasome system is impaired during *Drosophila* salivary gland cell death *in vivo*

Previous studies in cell lines have suggested that proteasome impairment may be part of a normal cell death program (Adrain et al., 2004; Sun et al., 2004), but evidence to support this possibility has never been shown under physiological conditions *in vivo*. To monitor the function of the UPS during *Drosophila* salivary gland cell death, we used transgenic fly lines containing UPS reporter substrates that consist of fusions between GFP and degron sequences targeted for degradation by UPS pathways (Bence et al., 2005; Dantuma et al., 2000; Pandey et al., 2007). These reporters are under the control of the UAS/GAL4 system, allowing spatial and temporal control of their expression (Brand and Perrimon, 1993). In this system, the degron sequence is recognized by UPS pathway components. When the UPS is functioning properly, GFP is targeted to the proteasome to be degraded, but when the UPS is impaired, GFP accumulates.

The UPS reporter (UAS-GFP-CL1) and a stable control line (UAS-Ub-MGFP) were expressed in salivary glands by crossing the reporter lines to a line containing the salivary gland-specific driver *forkhead*-GAL4 (*fkh*-GAL4). To monitor UPS function in salivary glands, glands were dissected and examined by fluorescence microscopy to assay for GFP at stages before (6 hours APF), during (12 hours APF), and after the onset of cell death (13.5 hours APF). All of the positive control Ub-M-GFP pupae possess fluorescence in salivary glands at 6, 12, and 13.5 hours APF (**Fig. 2-1a, top panels)**. Pupae expressing the GFP-CL1 UPS reporter exhibit low fluorescence in salivary glands at 6 and 12 hours APF (**Fig. 2-1a, bottom panels**),

however GFP fluorescence increases dramatically in these salivary glands by 13.5 hours APF (**Fig. 2-2a, bottom panels**), suggesting that the UPS is impaired in dying salivary glands. If the UPS is impaired in salivary glands, we would expect ubiquitinated proteins to accumulate. We analyzed wild-type salivary gland protein extracts by western blot with an Ubiquitin antibody and found that indeed, ubiquitinated proteins increase between 6h and 13.5 hours APF (**Fig. 2-2b**). These results suggest that the UPS is impaired during salivary gland cell death, and that UPS impairment is a physiologically relevant component of autophagic cell death.

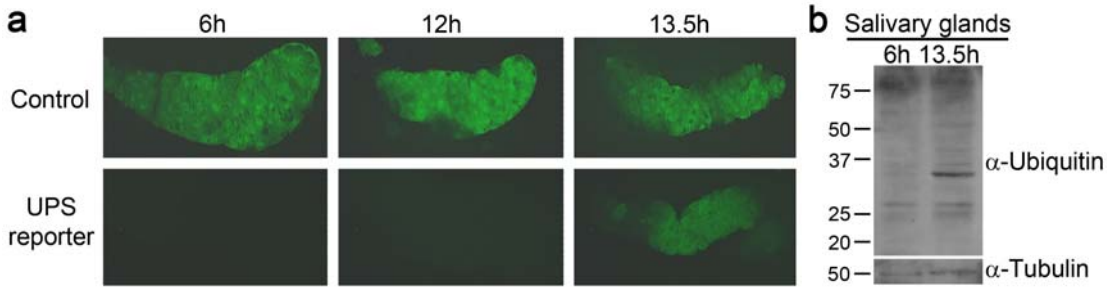

Figure 2-1. The ubiquitin/proteasome system is impaired during salivary gland developmental cell death.

a, Control animals (fkh-GAL4/+; UAS-Ub-M-GFP/+), expressing a stable GFP reporter in salivary glands exhibit GFP fluorescence in salivary glands 6h, 12h, and 13.5h after puparium formation, n≥11. Pupae with salivary gland-specific expression of a reporter for ubiquitin/proteasome system impairment (fkh-GAL4/+; UAS-GFP-CL1/+) exhibit low GFP fluorescence in salivary glands at 6h and 12h after puparium formation, but intense GFP fluorescence in salivary glands 13.5 hours after puparium formation, n≥29. **b,** Protein extracts from wild-type Canton-S salivary glands 6h and 13.5h after puparium formation were analyzed by western Blotting with an anti-Ubiquitin antibody.

Ectopic proteasome impairment in salivary glands leads to early gland condensation that is not suppressed by expression of caspase inhibitor p35.

Evidence in cell lines suggests that ectopic proteasome impairment leads to caspase activation and cell death (Henderson et al., 2005). To test whether proteasome impairment leads to early cell death *in vivo*, we expressed a GAL4-inducible, dominant temperature-sensitive mutant allele of the $ß_2$ subunit of the 20S proteasome (UAS-Dts7) (Belote and Fortier, 2002) specifically in salivary glands. To impair proteasome function well before the onset of wild-type salivary gland cell death, animals expressing Dts7 were shifted from permissive to restrictive temperature at puparium formation (0h) to 8h APF. We found that whereas salivary glands in control pupae are intact, salivary glands undergo premature condensation upon ectopic proteasome impairment (**Fig. 2-2a**). To quantify this phenotype, we measured salivary gland material in histological sections and found a significant difference in salivary gland area between control animals and those expressing Dts7 in salivary glands **(Fig. 2-2e)**. Therefore, ectopic proteasome impairment in salivary gland cells leads to the early onset of salivary gland condensation *in vivo.*

To test whether proteasome impairment leads to ectopic cell death *in vivo*, the proteasome was impaired in salivary glands from 0-8 hrs APF, and histological sections were TUNEL stained to assay for DNA fragmentation. We found that while nuclei in the larval midgut of control pupae stain positively for TUNEL at this stage, their salivary gland cells do not (**Fig. 2-2b**). By contrast, the salivary glands cells of pupae expressing UAS-Dts7 contain fragmented DNA as indicated by dark TUNEL-

positive nuclei (**Fig.2-2b**). These data suggest that ectopic proteasome impairment in salivary glands leads to early DNA fragmentation *in vivo*.

DNA fragmentation is a caspase-dependent process in salivary glands (Lee and Baehrecke, 2001). Therefore, we wanted to determine whether the early condensation phenotype observed upon proteasome impairment in salivary glands is caspase dependent by co-expressing the caspase inhibitor p35 with Dts7 in salivary glands. We found that salivary glands of pupae expressing p35 alone are not significantly different in size than other control salivary glands (**Fig. 2-2c,e)**. Surprisingly however, we found that salivary glands of pupae that co-express p35 and Dts7 still undergo significant early condensation (**Fig. 2-2d,e**). These data suggest that although caspases are ectopically activated following proteasome impairment in salivary glands, the early condensation phenotype may be dependent upon other non-caspase-dependent mechanisms.

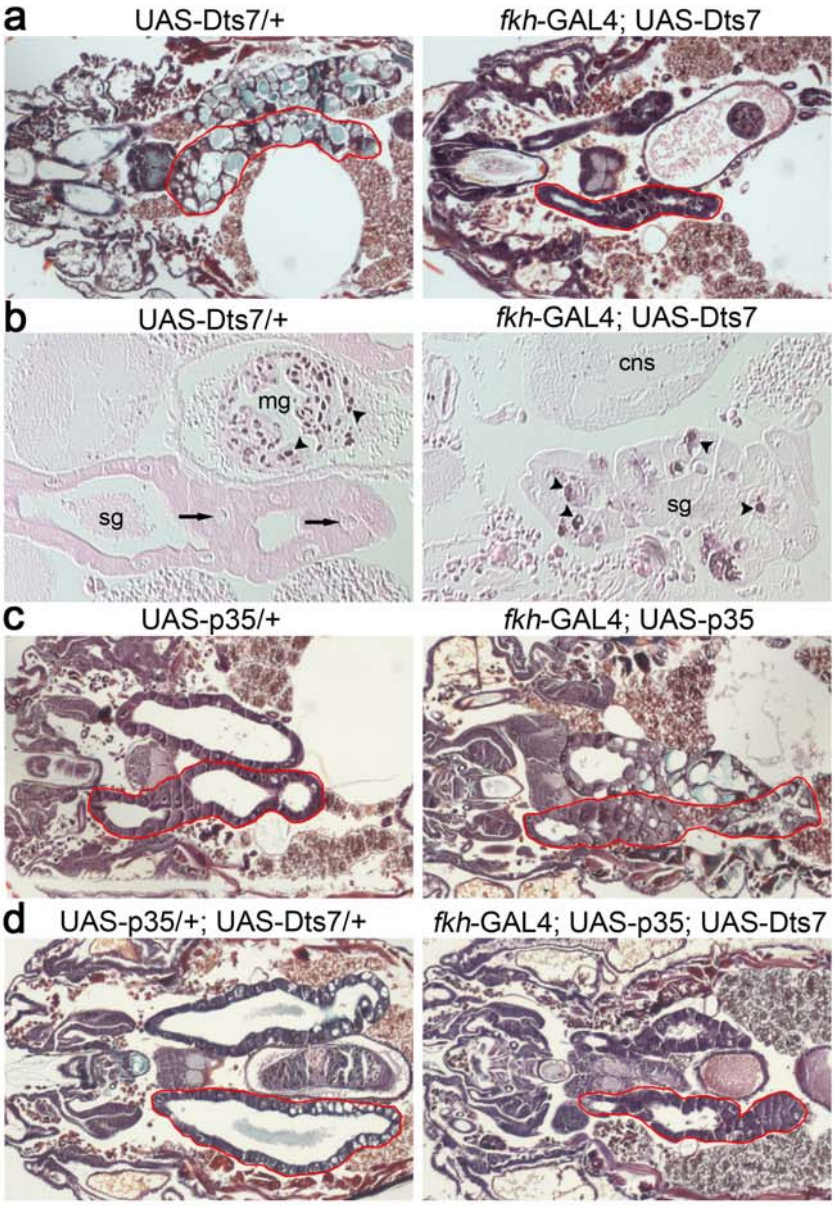
a
UAS-Dts7/+
fkh-GAL4; UAS-Dts7
b
UAS-Dts7/+
fkh-GAL4; UAS-Dts7
mg
sg
cns
sg
c
UAS-p35/+
fkh-GAL4; UAS-p35
d
UAS-p35/+; UAS-Dts7/+
fkh-GAL4; UAS-p35; UAS-Dts7
e
Salivary gland area (μm²)
140,000
120,000
100,000
80,000
60,000
40,000
20,000
0
UAS-Dts7/+
UAS-p35/+
UAS-p35/+; UAS-Dts7/+
fkh-GAL4; UAS-p35
fkh-GAL4; UAS-Dts7
fkh-GAL4; UAS-p35; UAS-Dts7
Control
Experimental

Figure 2-2. Ectopic proteasome impairment leads to early salivary gland cell condensation that is not suppressed by expression of caspase inhibitor p35. Pupae were shifted from permissive (25C) to restrictive (28C) temperature at puparium formation (0h), fixed 8h after puparium formation, and processed for histology. **a,** Control animals (+/UAS-Dts7), n=9, and those with salivary gland-specific expression of $Dts7^{2c}$ to impair proteasome function (fkh-GAL4/+; UAS-Dts7/+), n=13 were analyzed by histology 8h after temperature shift for salivary gland material (outlined in red), which was measured using Zeiss AxioVisionLE software, shown in **e**. **b,** Control animals (+/UAS-Dts7), n=10, and those with salivary gland-specific expression of Dts7 to impair proteasome function (fkh-GAL4/+; UAS-Dts7/+), n=12 were *in situ* TUNEL-labeled to assay for DNA fragmentation. Control UAS-Dts7 salivary glands (sg) do not possess fragmented DNA, as indicated by the light TUNEL-negative salivary gland nuclei (arrows), whereas internal control midgut (mg) nuclei possess fragmented DNA (arrowheads). Salivary glands of experimental animals (fkh-GAL4/+; UAS-Dts7/+) contain fragmented DNA (arrowheads) following UPS impairment. sg, salivary glands; mg, midgut; cns, central nervous system. **c,** Control animals (UAS-p35/+), n=9 and those expressing p35 in the salivary glands (fkh-GAL4/+; UAS-p35/+), n=18, were analyzed for salivary gland material (outlined in red), which was measured using Zeiss AxioVisionLE software, shown in **e**. **d,** Control animals (UAS-p35/+; UAS-Dts7/+), n=12 and those expressing p35 in the salivary glands (fkh-GAL4/+; UAS-p35/+; UAS-Dts7/+), n=15, were analyzed for salivary gland material (outlined in red), which was measured using Zeiss AxioVisionLE software. **e,** For all slides of

genotypes shown in **a**, **b**, and **d**, the largest salivary gland per slide was outlined and the area was measured using Zeiss Axiovision software. Red outlines designate the area measured. Error bars represent standard error.

Identification of proteins that are altered following ectopic proteasome impairment in salivary glands using proteomics

Drugs targeting the proteasome are currently being used in anti-cancer therapies (Hoeller and Dikic, 2009; Tobinai, 2007), however, how cells die in response to proteasome-targeting drugs has not been investigated *in vivo*. Upon finding that the onset of early salivary gland cell condensation following ectopic proteasome impairment is not suppressed by expression of the caspase inhibitor p35, we wondered what other factors might be involved in the cell condensation response. To gain a better understanding of cellular responses to changes in catabolism, we conducted a proteomics study in proteasome-impaired *Drosophila* salivary glands.

To generate proteomics samples under conditions of proteasome impairment, fkh-GAL4/+; UAS-Dts7/+ white pre-pupae were temperature shifted from permissive (25ºC) to restrictive (28ºC) temperature from 0-6h APF. Control +/UAS-Dts7 flies that lacked the GAL4 driver were temperature shifted in the same way. At least 3 independent samples were collected for each genotype and analyzed using high-throughput shotgun proteomics, as described above (**Table 2-1**). In the proteasome impairment samples, an average of 12,601 distinct peptides that mapped to an average of 4,184 distinct proteins were identified assuming a 5% false positive rate, whereas in the control samples, an average of 12,094 distinct peptides that mapped to an average of 3,922 distinct proteins were identified assuming a 5% false positive rate (**Table 2-2**). Proteins identified in the proteasome impairment and control samples by proteomics are listed in **Appendix 3**. An additional fkh-GAL4/+ control was also collected and analyzed by proteomics.

Identification of new genes required for salivary gland cell degradation

We sought to identify physiologically relevant candidates that might function during proteasome impairment-dependent salivary gland condensation. To accomplish this goal, we queried for proteins that increased, as indicated by positive ratio2 values, upon both proteasome impairment and between 6h and 13h after puparium formation in wild-type dying salivary glands (**Appendix 4**). Of these, proteins detected in the proteasome impairment sample with p values ≤ 0.002 and not previously shown to function in salivary gland cell degradation were considered top candidates for genetic analyses. Genes with available transgenic RNAi lines were screened for defects in salivary gland cell degradation **(Table 2-5)**.

To knock down genes specifically in salivary glands, transgenic fly lines containing UAS-RNAi constructs were crossed to those expressing *fkh*-GAL4. Progeny expressing RNAi in salivary glands were staged to 24h after puparium formation; a time that is 8 hours after salivary gland material is cleared in wild-type *Drosophila*. We found that compared to control animals, animals expressing RNAi against *CG1180,* a gene encoding *lysozyme e* in salivary glands, were deficient in salivary gland degradation **(Fig. 2-3a)**. We also found that compared to control animals, those expressing RNAi against the gene *trol* possessed persistent salivary gland fragments (**Fig. 2-3b**). Neither of these genes has previously been shown to function in salivary gland cell death. Thus, our proteomics approach to identify proteins present in salivary glands both during wild-type salivary gland cell degradation and following proteasome impairment successfully led to the identification of two new factors that are required for salivary gland autophagic

programmed cell degradation. Additional top candidates to be screened are discussed in Chapter 4.

Table 2-5. List of proteins screened for function in salivary gland cell death that are enriched both in response to proteasome impairment and during wild-type salivary gland cell degradation.

		Proteasome Impairment		Wild-type 6h vs 13h		
symbol	**Notes**	**ratio2**	**p value**	**ratio2**	**p value**	**Phenotype?**
CG11880	Lysozyme E	Inf	7.48E-06	Inf	0.0664	Y
CG3074	Cysteine-type endopeptidase	4.5	0.0014	3.4	0.0543	N
CG9336		8.9	0.0005	Inf	0.0653	N
CG9917		Inf	0.0009	Inf	0.2856	N
CG9977	Adenoxylhomo-cysteinase	2.3	0.0017	1.1	0.7471	N
Dbi		3.5	0.0008	Inf	0.0008	N
Ect3	Lysosome	10.3	0.0004	28.1	0.0009	N
Trol/ Perlecan	Apical/basal polarity	1.5	0.0019	1.9	0.0088	Y

The proteins listed were identified by proteomics in wild-type dying salivary glands and upon proteasome impairment. Genes encoding these proteins were knocked down in salivary glands by expressing RNAi driven by the salivary gland-specific driver *fkh*-GAL4. Pupae were staged to 24h after puparium formation, processed for histology, and analyzed for the presence of salivary gland material. Names of genes are based on Flybase annotation (http://flybase.org/). The ratio2 values for peptides mapped to the genes listed are indicated (ratio2=average detection value experimental sample/average detection value control sample). p values were obtained using the Student's t-test followed by multiple testing adjustment using the Benjamini-Hochberg method (Hochberg and Benjamini, 1990). Y, gene knockdown leads to salivary gland degradation phenotype; N, no phenotype. Inf indicates a numerical value divided by 0.

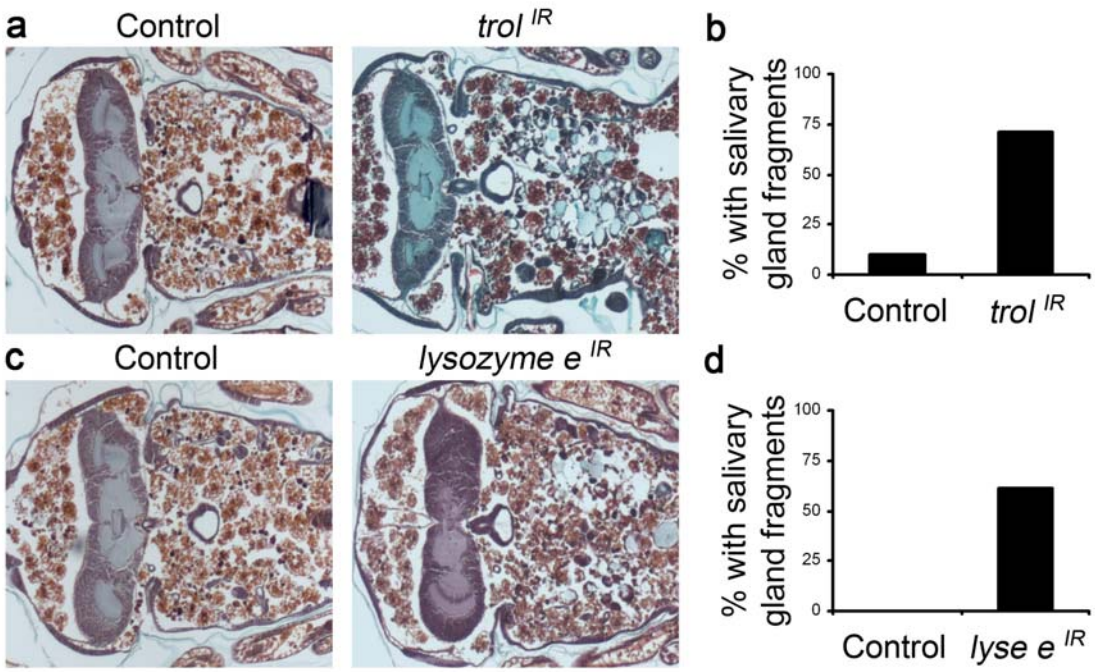

Figure 2-3. The genes *trol* and *lysozyme e* are required for salivary gland cell degradation.

a, Control animals (+/w; +/UAS-*trol*^{IR}), n=10, and those with salivary gland-specific knockdown of *trol* (*fkh*-GAL4/w; UAS-*trol*^{IR}/+), n=17, were analyzed by histology for the presence of salivary glands 24 hours after puparium formation. *trol*^{IR} = VDRC TID # 245498 on II**. b,** quantification of data from **a**. 10 % of control animals and 71 % experimental animals have persistent salivary gland fragments. **c,** Control animals (+/w; +/UAS-*lysozyme e*^{IR}), n=10, and those with salivary gland-specific knockdown of *lysozyme e* (*fkh*-GAL4/w; UAS-*lysozyme e*^{IR}/+), n=23, were analyzed by histology for the presence of salivary glands 24 hours after puparium formation. *lysozyme e*^{IR} = VDRC TID # 22867 on II**. d,** quantification of data from **a**. 0 % of control animals and 61% of experimental animals have persistent salivary gland fragments).

The Cop9 signalsome functions in salivary gland cell degradation

In addition to identifying individual factors that were up-regulated during wild-type salivary gland cell death and following proteasome impairment, we also sought to identify groups of proteins that are either in a common pathway or are members of a cellular component or process, which might suggest a role in regulating salivary gland death. Interestingly, we found that a number of engulfment factors were detected in wild-type dying salivary glands and/or in salivary glands upon proteasome impairment (**Table 2-6**), and this is the subject of Chapter 3. We also found that a number of Cop9 signalsome subunits were detected in both wild-type dying salivary glands and following proteasome impairment (**Table 2-7**). Although the p values for the detection of each individual component were relatively high and therefore did not engender high confidence in the detection of any single subunit, the detection of Cop9 signalsome (CSN) subunits 1b, 3, 4, 5, 6, 7, and 8 following proteasome impairment and/or during wild-type salivary gland cell death suggested a possible role for the CSN in salivary gland death **(Table 2-7)**.

To test the function of the CSN in salivary gland cell death, we expressed RNAi against the genes encoding CSN component CSN6 in salivary glands. Previous studies have shown that the loss or knockdown of one subunit leads to the destabilization and loss of the entire complex (Busch et al., 2007; Serino and Deng, 2003; Su et al., 2009). We found that whereas 10% of control animals contained persistent salivary gland fragments, 100% of those expressing $cns6^{IR}$ in salivary glands contained persistent salivary gland fragments by 24 hours after puparium formation **(Fig. 2-4a-d)**. These data suggest that Cop9 Signalsome component CSN6

is required for salivary gland cell degradation, and demonstrate the successful use of a proteomics approach to identify genes that function in cell degradation.

Table 2-6. Engulfment proteins detected in salivary glands by proteomics

Symbol	Notes	Proteasome Impairment ratio2	Proteasome Impairment p value	Wild-type 6h vs 13h ratio2	Wild-type 6h vs 13h p value
Drpr	Engulfment receptor	Inf	0.0051	-Inf	0.2031
Crq	Engulfment receptor	ND	NA	Inf	0.0019
Crk (Ced-2)	SH3/SH2 adaptor	-Inf	0.2855	-7.88	0.0003
Ced-10 (Rac1)	GTPase, cytoskeltal rarrangement	ND	NA	1.59	0.3128
Ced-12	Cytoskeletal rearrangement	Inf	0.4365	ND	NA
Rab7	GTPase, endosome to lysosome transport	-1.3	0.0706	7.97	0.0007
Rac2	GTPase	1.26	0.4696	-1.43	0.5874
Shibire	Dynamin	1.49	0.2067	-1.83	0.2393
Src42a	Tyrosine Kinase	Inf	0.2069	ND	NA

Protein names are based on Flybase annotation (http://flybase.org/). The ratio2 values for peptides mapped to the genes listed are indicated (ratio2=average detection value experimental sample divided by average detection value control sample). p values were obtained using the Student's t-test followed by multiple testing adjustment using the Benjamini-Hochberg method (Hochberg and Benjamini, 1990). Inf indicates a numerical value divided by 0. –Inf indicates 0 divided by a numerical value. ND denotes not detected; NA, not applicable.

Table 2-7. Cop9 signalsome subunits detected in salivary glands by proteomics.

Symbol	Notes	Proteasome Impairment ratio2	Proteasome Impairment p value	Wild-type 6h vs 13h ratio2	Wild-type 6h vs 13h p value
CSN1b	Signalosome complex subunit 1b	-1.2	0.7530	Inf	0.2855
CSN3	Signalosome complex subunit 3	-1.2	0.9047	2.0	0.4593
CSN4	Signalosome complex subunit 4	1.1	0.8339	-1.6	0.6866
CSN5	Signalosome complex subunit 5	1.6	0.2789	1.8	0.1618
CSN6	Signalosome complex subunit 6	1.8	0.0716	-2.6	0.4925
CSN7	Signalosome complex subunit 7	1.5	0.2554	4.6	0.2600
CSN8	Signalosome complex subunit 8	-2.0	0.1428	ND	ND

Protein names are based on Flybase annotation (http://flybase.org/). The ratio2 values for peptides mapped to the genes listed are indicated (ratio2=average detection value experimental sample divided by average detection value control sample). p values were obtained using the Student's t-test followed by multiple testing adjustment using the Benjamini-Hochberg method (Hochberg and Benjamini, 1990). Inf indicates a numerical value divided by 0. ND denotes not detected; NA, not applicable.

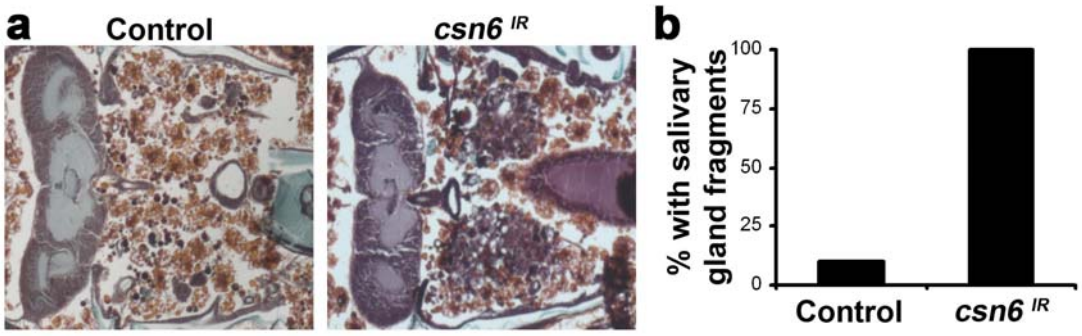

Figure 2-4. RNAi knockdown of *cop9 signalsome subunit 6* prevents salivary gland degradation.

a, Control animals (+/w; +/UAS-$csn6^{IR}$), n=10, and those with salivary gland-specific knockdown of *cns6* (*fkh*-GAL4/w; UAS-$csn6^{IR}$/+), n=22, were analyzed by histology for the presence of salivary glands 24 hours after puparium formation. $csn6^{IR}$ = VDRC TID # 22308 on II**. b,** quantification of data from **a** (1/10 of control animals and 22/22 of experimental animals have persistent salivary gland fragments).

Discussion

Autophagic programmed cell death occurs during insect and mammalian development, yet the mechanisms that contribute to this type of cell death are not well understood. Given new developments in MS-based proteomics that have led to improvements in quantification and sensitivity (Domon and Aebersold, 2006; Fang et al., 2009), we used a shotgun proteomic approach (Chen et al., 2003) to identify proteins enriched during autophagic programmed cell death in purified dying *Drosophila* larval salivary glands. We found that a number of ubiquitin proteasome system (UPS) components are present in dying salivary glands, which suggests a role for the UPS in salivary gland cell death. We tested the function of the UPS in salivary glands and found that the UPS becomes impaired during salivary gland cell death. This is the first i*n vivo* demonstration that the UPS becomes impaired during programmed cell death. While the mechanism of UPS impairment remains unknown, it could be that the UPS is impaired by system overload, given that a number of UPS components are enriched in dying salivary gland samples as detected by proteomics. We also show that ectopic proteasome impairment leads to the onset of early salivary gland condensation, but that expression of the caspase inhibitor p35 during proteasome impairment does not suppress ectopic condensation. This suggests that proteasome impairment-induced gland condensation may require the activity of other non-caspase-dependent processes.

To identify factors that are present in salivary glands upon proteasome impairment, we analyzed the proteins enriched in purified salivary glands after proteasome impairment. We compared factors identified following proteasome

impairment to those identified during wild-type salivary gland cell death to identify physiologically relevant factors that might function in salivary gland cell death. The presence of proteins in dying salivary glands is not evidence that these proteins function in cell death. Therefore we took a genetic approach to screen top candidates for defects in salivary gland cell death by RNAi knockdown. Here we show that the knockdown of *lysozyme e* and *trol* prevent proper salivary gland cell clearance. *lysozyme e* functions in *Drosophila* digestive function (Daffre et al., 1994; Regel et al., 1998) and has been suggested to play a role in host intestinal defense, as it was identified in a genome-wide RNAi screen in *Drosophila* for genes involved in defense responses to intestinal pathogenic bacterial infection (Cronin et al., 2009). However, *lysozyme e* has not previously been shown to function in salivary gland cell death. The gene *trol* has been shown to function in controlling the onset of stem cell proliferation in the developing *Drosophila* nervous system by modulating Fibroblast Growth Factor branchless and Hedgehog signaling, and mutations in *trol* also affect Decapentaplegic and Wingless signaling (Lindner et al., 2007; Park et al., 2003; Voigt et al., 2002). However, *trol* has not been previously shown to function in salivary gland cell death.

To identify additional genes that might function in autophagic cell death, we looked for proteins that were members of a pathway or cellular component that were present during wild-type cell death and also in response to proteasome impairment in salivary glands. We identified a number of Cop9 Signalsome (CSN) components by proteomics and demonstrated that RNAi knockdown of CSN subunit *csn6* prevented salivary gland degradation. The Cop9 signalsome is a conserved multi-subunit protein

complex that functions in the ubiquitin/proteasome pathway (Wei et al., 2008). First discovered in plants, the CSN is essential for *Drosophila* development and functions in a variety of essential cellular processes, including cell cycle control, the DNA-damage response, and circadian rhythm (Chamovitz et al., 1996; Knowles et al., 2009; Kwok et al., 1996; Wei and Deng, 1992; Wei et al., 1994; Wei et al., 2008). Composed of eight subunits, CSN1-CSN8, the CSN contains Nedd8 isopeptidase activity, and functions to remove the ubiquitin-like Nedd8 from proteins (deneddylate) (Karniol et al., 1999; Peng et al., 2001; Serino et al., 1999; Serino et al., 2003; Staub et al., 1996).

The best-characterized function of the CSN is to deneddylate the cullin subunit of cullin-RING ligases (CRL), a superfamily of ubiquitin E3 complexes (Cope et al., 2002; Lyapina et al., 2001; Schwechheimer et al., 2001). The core of CRL complexes is composed of a cullin family member and a small RING protein, RBX1 (Bosu and Kipreos, 2008; Hotton and Callis, 2008). An active CRL is formed through the binding of cullin-RBX1 to a specific substrate-binding molecule that recruits substrates. Neddylation is thought to activate CRLs, whereas deneddylation leads to CRL disassembly. Neddylated CRLs are active but also become auto-ubiquitinated if they are not deneddylated (Bosu and Kipreos, 2008; Gusmaroli et al., 2007; Hotton and Callis, 2008; Wu et al., 2005). CRLs have also been reported to associate with de-ubiquitinating enzymes (Hetfeld et al., 2005; Wee et al., 2005; Zhou et al., 2003). Therefore, the CSN is thought to deactivate CRL complexes through deneddylation, and thus maintain dynamic cycles of CRLs, but also to protect CRLs from poly-ubuquitination and subsequent proteasomal degradation.

Our finding that *csn6* is required for salivary gland degradation demonstrates a role for the CSN in this autophagic cell death, and suggests that proper control of protein neddylation and deneddylation cycles is important to regulate salivary gland destruction. Several studies have demonstrated a role for the CSN in regulating cell death. *Csn5* knockout mice exhibit massive apoptosis (Panattoni et al., 2008; Tomoda et al., 2004). In addition, several cullin-RING ligase components have been shown to negatively regulate the *C. elegans* p53 (CEP-1)-dependent germ cell apoptosis in response to DNA damage (Gao et al., 2008). Cullin-RING ligase complexes may also function in salivary gland cell death, and this will be the subject of future investigations.

Our proteomics analyses led to the discovery of several new genes that are required for salivary gland cell death. These findings exhibit the power of a high-throughput proteomic approach to identify novel factors that function in biological processes. Further, our proteomics data will serve as a foundation for future genetic studies of autophagic programmed cell death and *in vivo* cellular responses to proteasome inhibition by providing a description of proteins enriched during wild-type cell death as well as in response to proteasome impairment.

Acknowledgements

We thank J.P Taylor, P. Meier, the Bloomington Stock Center, and the VDRC for transgenic *Drosophila* lines.

Author Contributions

Jahda H. Hill and Yakup Batlevi assisted in the isolation of the *Drosophila* salivary gland samples that were analyzed using proteomics. The proteomics analyses were carried out by Brian M. Balgley and Cheng S. Lee, University of Maryland, College Park, MD. All experiments were performed by C.K.M., and were designed by C.K.M and E.H.B..

Methods

Proteomics Analysis. To generate the proteomics datasets, at least 3 independent biological samples for each condition were collected. For each independent sample, 80 pairs of salivary glands were dissected per 100µl 8M Urea/40mM Tris-Hcl, Ph8. At least two runs of each replicate were analyzed, using 10µg of sample per run, by high-throughput MS-based proteomics (Chen et al., 2003). Proteins were fully trypsinized, and peptides were separated by two-dimensional chromatography; first into 15 fractions by capillary isoelectric focusing (CIEF), and further resolved by capillary reversed phase liquid chromatography (nano-RPLC). Two runs of each protein sample were carried out. Fractions were analyzed by ESI-tandem-MS using a ThermoFinnigan LTQ linear ion trap mass spectrometer (San Jose, CA). Following MS analysis, peaklists were generated using extract_msn, and searches to identify MS/MS peptide spectra were carried out using the Open Mass Sepctrometry Search Algorithm (OMSSA) (Geer et al., 2004) (NCBI). For each dataset, protein and peptide hits were generated assuming a false positive rate of 5%, and proteins present in the samples were identified based upon peptide sequences detected.

***Drosophila* strains.** The Canton-S strain was used as wild-type. For ectopic proteasome impairment studies, UAS-Dts7^{2c} on III was used (Belote and Fortier, 2002). To monitor proteasome impairment, UAS-M-GFP was used as the positive control, and UAS-GFP-CL1 was used as the experimental stock (Bence et al., 2005; Dantuma et al., 2000; Pandey et al., 2007). For ectopic P35 expression, UAS-p35 was used (Hay et al., 1994).

Histology. Histology was performed as described previously(Muro et al., 2006).

Protein Extracts and Western Blotting. Protein extraction and Western Blotting were performed as described previously (Dutta and Baehrecke, 2008). Primary antibodies used were rabbit anti-Ubiquitin (1:1000), and mouse anti-Beta-Tubulin (1:50) (Developmental Studies Hybridoma Bank).

Microscopy. Imaging was performed on a Zeis Axiophot II microscope.

Chapter 3

Activation of autophagy during cell death requires the engulfment receptor Draper

Abstract

Macroautophagy (autophagy) degrades cytoplasmic components and is required for survival in response to starvation, but has also been associated with cell death (Levine and Klionsky, 2004). It is unclear how autophagy is regulated under specific cell contexts in multi-cellular organisms, and what may distinguish autophagy function during cell survival versus cell death. *Drosophila* larval salivary glands undergo programmed cell death that requires autophagy genes (Berry and Baehrecke, 2007), and engulfment of salivary gland cells by phagocytes does not appear to occur (Martin and Baehrecke, 2004). Here we show that Draper (Drpr), the *Drosophila* orthologue of the *C. elegans* engulfment receptor CED-1, is required for autophagy during cell death. Null mutations in *drpr*, as well as salivary gland-specific knockdown of *drpr*, inhibits salivary gland degradation. *drpr* knockdown prevents the induction of autophagy in dying salivary glands, and Atg1 expression in *drpr* mutants suppresses the failure in salivary gland degradation, suggesting that *drpr* functions upstream of autophagy induction during cell death. Surprisingly, we show that *drpr* is cell-autonomously required for autophagy induction in dying salivary

gland cells, while *drpr* knockdown does not prevent starvation-induced autophagy in the larval fatbody which is associated with survival. This is the first example of an engulfment factor that is autonomously required for self-clearance. Furthermore, Drpr is the first factor to be identified that genetically distinguishes autophagy that is associated with cell death from cell survival.

Introduction

Programmed cell death is a conserved, genetically regulated process that is critical to metazoan development and homeostasis (Danial and Korsmeyer, 2004; Lockshin and Williams, 1965). Improper regulation of cell death can lead to a variety of pathological conditions, including cancer (Thompson, 1995). There are two main types of programmed cell death that occur during development, apoptosis and autophagic cell death (Clarke, 1990; Schweichel and Merker, 1973). Autophagy is a process by which cytoplasmic components are delivered to the lysosome for degradation in eukaryotic cells. Autophagy is an important cellular response to stress that is required for survival in response to starvation (Levine and Klionsky, 2004), and has also been associated with cell death in several *in vivo* contexts (Berry and Baehrecke, 2007; Hou et al., 2008; Mohseni et al., 2009; Nezis et al., 2009). Autophagic cell death is observed during several types of mammalian developmental cell death, including the regression of the corpus luteum and involution of mammary and prostate glands (Clarke, 1990).

Whereas the activation of caspases occurs during both apoptosis and autophagic cell death, what appears to distinguish these two types of cell death is the presence of phagocytosis machinery and the location of the lysosomal system used to

degrade cellular contents. During apoptosis, dying cells are recognized and engulfed by phagocytic cells where the lysosomes of the engulfing cell degrade the dead cell (Kerr et al., 1972). By contrast, autophagic cell death occurs without known phagocytosis. Rather, this type of cell death is characterized by the presence of autophagosomes in the dying cell; autophagic contents are delivered to lysosomes and contents are thought to be degraded within the lysosomes of the dying cell itself.

While autophagy has been associated with cell death, it is not clear how autophagy might function in cell death, and what might determine its function in cell death versus cell survival. *Drosophila* larval salivary gland cell death is induced by a rise in steroid 12 hours after puparium formation, and this tissue is completely degraded by 16 hours after puparium formation (Lee and Baehrecke, 2001). Both caspases and autophagy are induced by this rise in steroid, and function in an additive manner to kill and degrade salivary glands (Berry and Baehrecke, 2007). By contrast, autophagy is induced in response to starvation in the larval fatbody (Scott et al., 2004), and this induction is associated with cell survival.

To identify genes required for autophagic cell death, we queried proteomics and genome-wide microarray data from purified dying *Drosophila* salivary glands (Lee et al., 2003). We found that several factors associated with engulfment were present or induced during salivary gland cell death, including Draper (Drpr), the *Drosophila* orthologue of the *C. elegans* engulfment receptor CED-1 (Freeman et al., 2003; MacDonald et al., 2006). This was intriguing as salivary gland destruction is thought to occur without phagocytosis. Phagocytosis machinery is well conserved from worms to mammals. In *C. elegans*, the CED-1 receptor is expressed in engulfing

cells where it is required for the recognition and phagocytosis of cell corpses (Zhou et al., 2001). CED-1 binding of the adaptor protein CED-6 is required for cell corpse engulfment, and CED-1 mediation of actin-dependent cytoskeletal reorganization requires the Rac1 GTPase and Dynamin (Kinchen et al., 2005; Liu and Hengartner, 1998; Su et al., 2002; Yu et al., 2006b). *C. elegans* engulfment of cell corpses also requires CED-2, CED-5, CED-10, and CED-12, which are orthologs of mammalian Crk, Dock180, and ELMO, respectively (Gumienny et al., 2001; Reddien and Horvitz, 2000; Wu and Horvitz, 1998). The Crk/Dock180/ELMO pathway is partially redundant with the Drpr/Ced-6 pathway and both require Rac1 ((Kinchen et al., 2005; Reddien and Horvitz, 2000).

In *Drosophila*, Drpr and Ced-6 are required for the engulfment of severed axons by glia during axonal pruning (Awasaki et al., 2006; Freeman et al., 2003; Hoopfer et al., 2006; MacDonald et al., 2006; Williams et al., 2006). Like Ced-1, Drpr contains 15 extracellular epidermal growth factor repeats, a single-pass transmembrane domain, and intracellular motifs required for the binding of downstream signaling molecules (Freeman et al., 2003; Ziegenfuss et al., 2008). There are three isoforms of Draper that are produced by alternative splicing, Drpr-I, II, and III (Freeman et al., 2003). Drpr-mediated phagocytosis of severed axons by glia also requires *Drosophila* Shark, a non-receptor tyrosine kinase similar to mammalian Syk, and the Src family kinase Src42A (Ziegenfuss et al., 2008).

Here we show that Drpr is required for autophagy and cell degradation of *Drosophila* larval salivary glands. We find that null mutations in *drpr*, as well as salivary gland-specific *drpr* knockdown, prevent salivary gland clearance.

Knockdown of *drpr* prevents autophagy induction in dying salivary glands, and the expression of Atg1 suppresses the failure in gland degradation in *drpr* null mutants. Surprisingly, we find that *drpr* knockdown in the fatbody does not prevent starvation-induced autophagy. We find that *drpr* is required for autophagy during programmed cell death but not in response to starvation; this is the first demonstration of a cell-context-specific requirement of a gene for the induction of autophagy.

Results

To identify genes that may regulate autophagy in cell-specific contexts, we queried proteomics data in dying salivary glands, as well as genome-wide microarray data from dying salivary glands. Interestingly, several factors that have been implicated in engulfment of apoptotic cells are present in wild-type dying salivary glands (**Table 2-6**). We found that a number of engulfment genes are also induced in dying salivary glands (Lee et al., 2003) **(Table. 3-1)**, while there are no detectable changes in these genes after larval starvation (Zinke et al., 2002). Although many engulfment factors are pleiotropic through their regulation of the cytoskeleton and vesicular transport, the identification of the engulfment receptor *drpr* (Freeman et al., 2003; MacDonald et al., 2006) is intriguing, as salivary gland destruction is thought to be largely independent of phagocytes.

Table 3-1. Engulfment genes are transcribed in dying salivary glands.

Symbol	CG#	Fold change dying salivary glands	Fold change 1h starved	Fold change 4h starved	Fold change 12h starved
draper (Ced-1)	CG2086	2.67	nd	nd	nd
Crk (Ced-2)	CG1587	-4.8	nd	nd	nd
mbc (Ced-5/ dock180)	CG10379	21.14	nd	nd	nd
ced-6	CG11804	12.6	nc	1.5	1.8
ced-10 (Rac1)	CG2248	2.07	nd	nd	nd
ced-12	CG5336	0.14	nc	nc	nc
croquemort (Crq)	CG4280	10.97	nd	nd	nd
rab7	CG5915	2.03	nd	nd	nd
rac2	CG8556	33.63	nd	nd	nd
shark (Syk)	CG18247	1.26	nd	nd	nd
shibire (Dynamin)	CG18102	0.14	nd	nd	nd
simu	CG4820	-2.38	nc	nc	nc
src42a	CG7873	20.01	nd	nd	nd
src64b	CG7524	2.77	nd	nd	nd
btk29a	CG8049	0.83	nd	nd	nd

Engulfment gene transcripts that are detected in dying *Drosophila* salivary glands, and fold change between 6h and 12h after puparium formation (Lee et al., 2003). The majority of these gene transcripts were either not detected (nd) or not changed (nc) in whole larvae in response to starvation for either 1h, 4h, or 12h compared to larvae

raised on normal food (Zinke et al., 2002). CG numbers and names of genes are based on Flybase annotation (http://flybase.org/).

Draper is required for *Drosophila* salivary gland cell death

We tested whether Drpr is present in dying salivary glands. Whereas no Drpr protein is present in $drpr^{\Delta 5}$ null mutants, Drpr-I, II and/or III isoforms are present at low levels in salivary gland protein extracts at 6 hours after puparium formation, and increase dramatically in conjunction with the rise in steroid that triggers cell death 12 hours after puparium formation (**Figure 3-1a**). Drpr I protein levels remain high through 14 hours after puparium formation, while the Drpr II/III isoforms decrease at this stage (**Figure3-1a**). We tested whether $drpr^{\Delta 5}$ null mutants have a defect in salivary gland cell death, and found that 98% of $drpr^{\Delta 5}$ null mutants have persistent salivary gland fragments compared to 0% of control animals at 24 hours after puparium formation (**Figure 3-1b, c**).

The presence of Drpr protein in salivary glands suggested the possibility that Drpr could function directly within salivary gland cells to mediate their degradation. As a known engulfment factor, Drpr could also function in phagocytic blood cells to mediate salivary gland clearance, and this could explain the defect in clearance observed in whole animal $drpr^{\Delta 5}$ null mutants. We tested this possibility by driving an upstream activating sequence (UAS)-regulated double-stranded inverse repeat construct designed to target *drpr* ($drpr^{IR}$) with the blood cell-specific *hml*-GAL4 driver and assaying for the persistence of salivary glands. We found that whereas hml-GAL4 is clearly expressed in blood cells but not salivary glands, *drpr* knockdown in blood cells does not lead to a defect in salivary gland clearance (**Figure 3-2a-c**). By contrast, expression of $drpr^{IR}$ in salivary glands with the salivary gland-specific *fkh*-GAL4 driver resulted in the persistence of salivary gland fragments

in 89% of pupae compared to 0% of control animals 24 hours after puparium formation (**Figure 3-1c-d**). These data indicate that *drpr* functions in a tissue-autonomous manner during salivary gland degradation.

We explored the role of Drpr isoforms in salivary gland cell death. Knockdown of *drpr-I* in salivary glands prevents tissue clearance in 80% of these animals compared to 0% of controls (**Figure 3-1e, f**), suggesting that the defect in salivary gland cell death is due *drpr-I* function. In addition, salivary-gland-specific expression of Drpr-I in $drpr^{\Delta 5}$ null mutant animals is sufficient to rescue the salivary gland persistence phenotype; 78% of Drpr-I $drpr^{\Delta 5}$ pupae that lack the GAL4 driver have persistent salivary gland fragments, while only 10% of $drpr^{\Delta 5}$ pupae expressing Drpr-I have persistent gland fragments (**Figure 3-1g, h**). Taken together, these results indicate that *drpr-I* is required for salivary gland cell death.

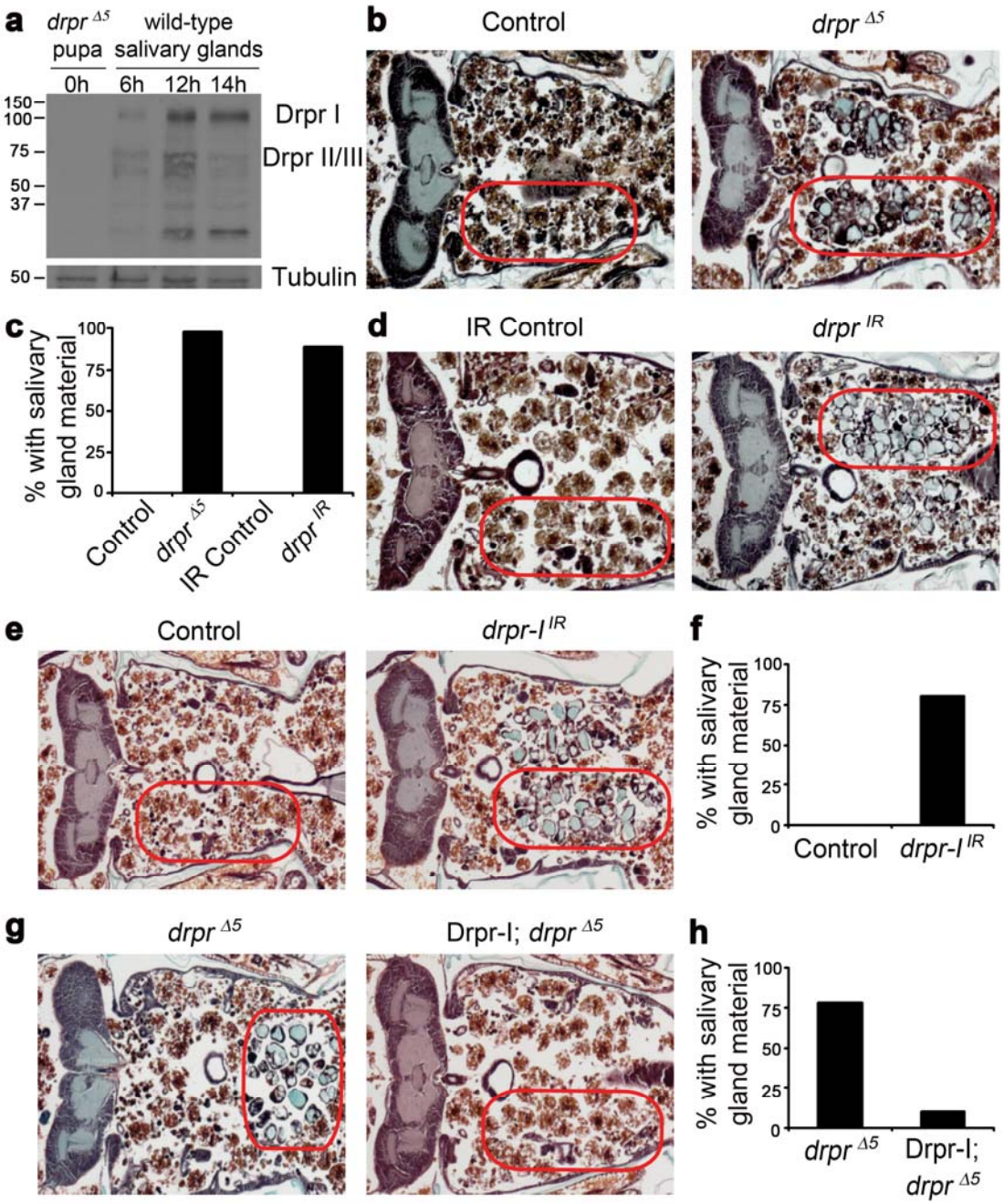

Figure 3-1. Draper is required for *Drosophila* salivary gland cell death

a, Protein extracts from *drpr* null (*w*; $drpr^{\Delta 5}/drpr^{\Delta 5}$) pupae at puparium formation (0h) and wild-type (Canton-S) salivary glands 6h, 12h, and 14h after puparium formation, were analyzed by Western Blotting with anti-Drpr antibody. **b,** Control animals (+/*w*; +/$drpr^{\Delta 5}$), n=12, and *drpr* null mutants (*w*; $drpr^{\Delta 5}/drpr^{\Delta 5}$), n=47, were analyzed by

histology for the presence of salivary gland material (red circles) 24h after puparium formation. **c,** quantification of data from **b** and **d**. **d,** Control animals (+/*w*; +/UAS-*drpr*^{IR}), n=11, and those with salivary gland-specific knockdown of *drpr* (*fkh*-GAL4/*w*; UAS-*drpr*^{IR}/+), n=19, were analyzed by histology for the presence of salivary gland material (red circles) 24h after puparium formation. **e,** Control animals (+/*w*; +/UAS-*drpr-I*^{IR}), n=9, and those with salivary gland-specific knockdown of *drpr-I* (*fkh*-GAL4/*w*; UAS-*drpr-I*^{IR}/+), n=20, were analyzed by histology for the presence of salivary gland material (red circles) 24h after puparium formation. **f,** quantification of data from **e**. **g,** *drpr* null animals (+/*w*; +/UAS-Drpr-I; *drpr*$^{\Delta 5}$/*drpr*$^{\Delta 5}$), n=9, and those with salivary gland-specific expression of Drpr-I (*fkh*-GAL4/*w*; UAS-Drpr-I/+; *drpr*$^{\Delta 5}$/*drpr*$^{\Delta 5}$), n=20, were analyzed by histology for the presence of salivary gland material (red circles) 24h after puparium formation. **h,** quantification of data from **g**.

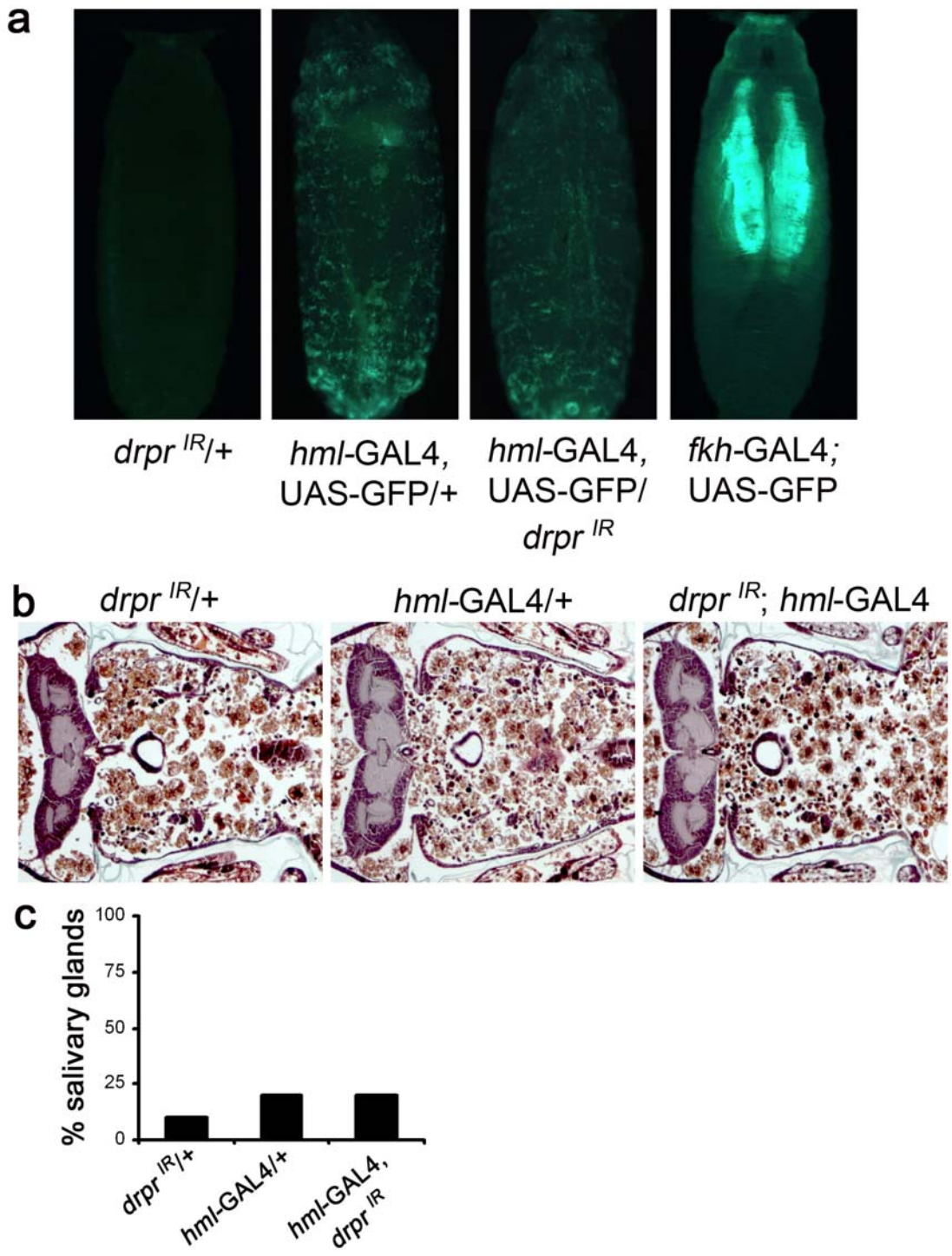

Figure 3-2. Knockdown of *draper* in blood cells does not affect salivary gland cell death.

a, IR control animals (+/*w*; +/UAS-*drpr*^{IR}), those with blood-cell-specific expression of GFP (+/*w*; *hml*-GAL4, +/UAS-GFP), those with blood cell-specific GFP expression and *drpr* knockdown (*w*; *hml*-GAL4, UAS-GFP/UAS-*drpr*^{IR}), and those with salivary gland-specific expression of GFP (*fkh*-GAL4; UAS-GFP) were imaged for GFP as white pre-pupae. b, IR control animals (+/*w*; +/UAS-*drpr*^{IR}), n=10, GAL4 control animals (+/*w*; +/*hml*-GAL4, UAS-GFP), n=10 and those with blood cell-specific knockdown of *drpr* (*w*; *hml*-GAL4, UAS-GFP/UAS-*drpr*^{IR}), n=20, were analyzed by histology for the presence of salivary glands 24h after puparium formation. c, quantification of data from b.

Draper functions downstream or parallel to caspases in dying salivary glands

Drpr is localized to the luminal side and apical region of salivary gland cells before the onset of cell death (**Figure 3-3a**) where it co-localizes with the apical protein crumbs (data not shown). At 14 hours after puparium formation, Drpr localization changes from apical to cytoplasmic (**Figure 3-3a**). This prompted us to investigate whether Drpr might play a role in regulating an intracellular cell death process. Caspases and autophagy have been shown to function in an additive manner in the degradation of salivary glands, and inhibition of genes in either pathway leads to partial persistence of salivary glands (Berry and Baehrecke, 2007). Expression of the caspase inhibitor p35 alone leads to the persistence of condensed salivary gland cell fragments in 94% of pupae, and salivary gland fragments in 6% of pupae (**Figure 3-3b, c**). Control homozygous $drpr^{\Delta 5}$ mutant pupae that contain the p35 transgene but lack the salivary gland GAL4 driver have persistent vacuolated salivary gland cell fragments in 80% of animals. However 100% of experimental $drpr^{\Delta 5}$ pupae that also express p35 in salivary glands contain larger amounts of persistent salivary gland material, including multi-cell gland fragments (**Figure 3-3b, c**). Therefore the salivary gland persistence phenotype in $drpr^{\Delta 5}$ is enhanced by the expression of p35, indicating that Drpr functions in an additive manner with caspases. To further test the relationship between Drpr and caspases, we tested whether *drpr* knockdown in salivary glands affects degradation of nuclear Lamin, a known caspase substrate in this tissue (Martin and Baehrecke, 2004). Clones of salivary gland cells that express $drpr^{IR}$ and GFP possess strong Lamin staining 6 hours after puparium formation, and both control and $drpr^{IR}$-expressing cells contain decreased Lamin staining 14 hours

after puparium formation (**Figure 3-3d**). Taken together, these results suggest that Drpr does not influence caspase activity, and functions downstream or parallel to caspases in dying salivary glands.

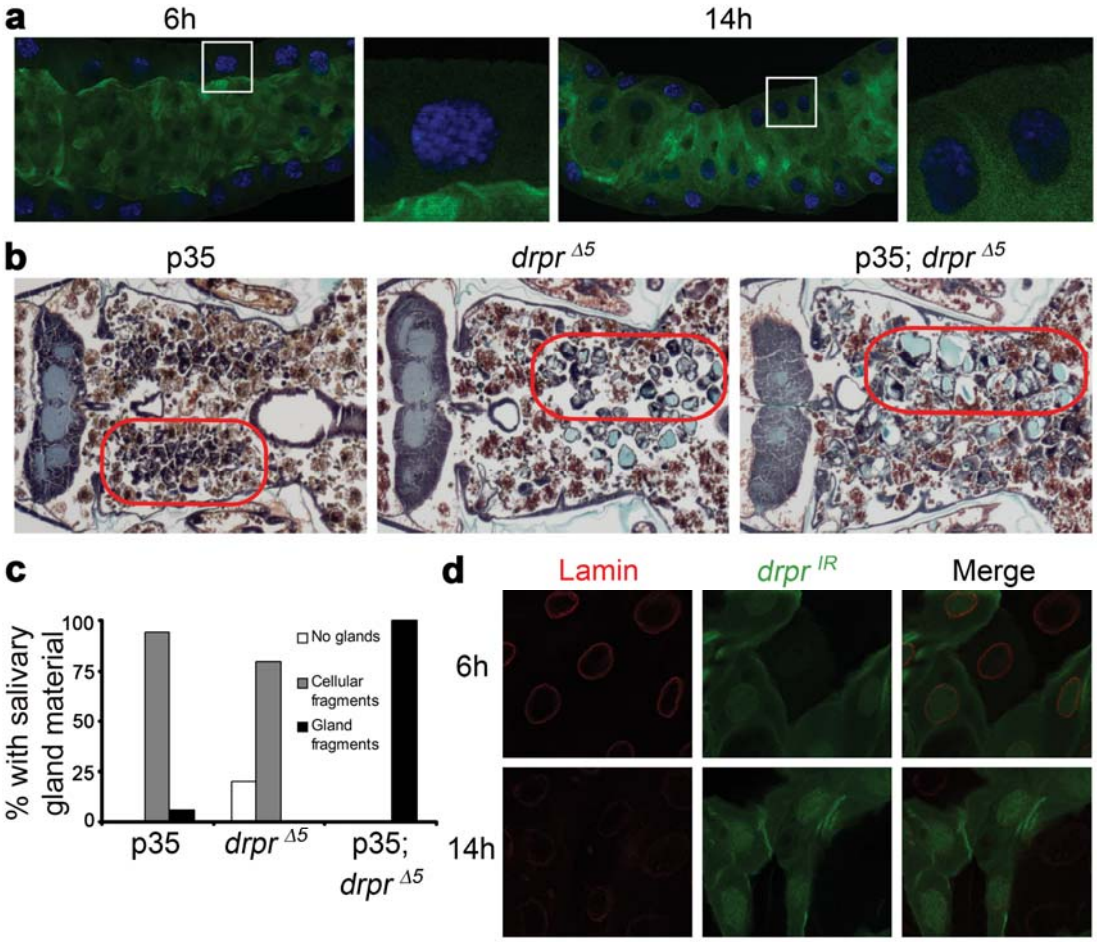

Figure 3-3. Draper localizes to the cytoplasm and functions downstream or in parallel to caspases during salivary gland cell death.

a, Salivary glands from wild-type (Canton-S) pupae were stained with anti-Drpr antibody (green) at 6h and14h after puparium formation. Nuclei were stained with DAPI (blue). Boxes outline adjacent enlarged areas. **b,** Animals with salivary gland-specific expression of p35 (*fkh*-GAL4/+; UAS-p35/+), n=18, *drpr* null animals (+/*w*; +/UAS-p35; $drpr^{\Delta 5}/drpr^{\Delta 5}$), n=10, and *drpr* null animals with salivary gland-specific expression of p35 (*fkh*-GAL4/*w*; UAS-p35/+; $drpr^{\Delta 5}/drpr^{\Delta 5}$), n=16, were analyzed by histology for the presence of salivary gland material (red circles) 24h after puparium formation. **c,** quantification of data from **b**. **d,** Salivary glands were dissected from animals expressing $drpr^{IR}$ specifically in GFP-marked clone cells (hsflp/*w*; UAS-

drpr^{IR}/+; *act*<FRT,cd2, FRT>Gal4, UAS-GFP/+) 6h and 14h after puparium formation. Salivary glands were stained with GFP antibody (green) to label cells expressing *drpr* ^{IR}, and Lamin antibody (red).

Draper is required for autophagy in dying salivary glands

We next tested whether the salivary gland phenotype caused by expression of *drpr*^{IR} is enhanced by knockdown of *Atg12*, a gene required for autophagy. We found that 81% of pupae expressing *Atg12*^{IR} in salivary glands have persistence of salivary gland cell fragments, whereas 100% of those expressing *Atg12*^{IR} *drpr-I*^{IR} have gland cell fragments (**Figure 3-4a, b**). These phenotypes are very similar to each other, and unlike expression of p35 in *drpr*$^{\Delta 5}$ (**Figure 3-4b**), co-expression of *Atg12*^{IR}and *drpr-I*^{IR} does not lead to an increase in the amount of salivary gland material that persists, and multi-cell gland fragments are absent. This led us to hypothesize that Drpr could function in the same pathway as autophagy genes. To test this possibility, we knocked down *drpr* in salivary glands expressing the autophagy reporter GFP-LC3. Autophagy induction leads to the association of GFP-LC3 with autophagosomal membranes, which are visible as GFP puncta. We found that whereas autophagy is highly induced in control salivary glands 14 hours after puparium formation, those expressing *drpr*^{IR} contain few GFP-LC3 puncta at the same stage (**Figure 3-4c, d**). Autophagosomes are trafficked to and fuse with lysosomes, where autophagic content is degraded by lysosomal hydrolases. To test whether *drpr* knockdown affects lysosome numbers, we expressed *drpr*^{IR} in salivary glands and assayed for the number of Lysosome Associated Membrane Protein 1 (LAMP1)-GFP puncta. We found that salivary glands expressing *drpr*^{IR} contained more lysosomes than control salivary glands (**Figure 3-4e, f**). Therefore, *drpr* is required for the induction of autophagy, but not lysosomes, in salivary glands. The increase in lysosome numbers in *drpr* knockdown salivary gland cells is consistent with the failure in autophagy

induction, given that lysosome numbers decrease when autophagy and autolysosome formation are abundant.

Expression of Atg1 is sufficient to induce ectopic cell death in several *Drosophila* tissues, including the fatbody and salivary glands (Berry and Baehrecke, 2007; Scott et al., 2007). Therefore, we tested whether expression of Atg1 is sufficient to suppress the $drpr^{\Delta 5}$ null mutant defect in degradation of salivary glands. Whereas 100% of $Atg1^{6A}$ $drpr^{\Delta 5}$ animals that lack the GAL4 driver have persistent salivary gland fragments 24 hours after puparium formation, this phenotype is completely suppressed by the expression of Atg1 in salivary glands (**Figure 3-4g, h**). This suggests that *Atg1* functions downstream of *drpr*.

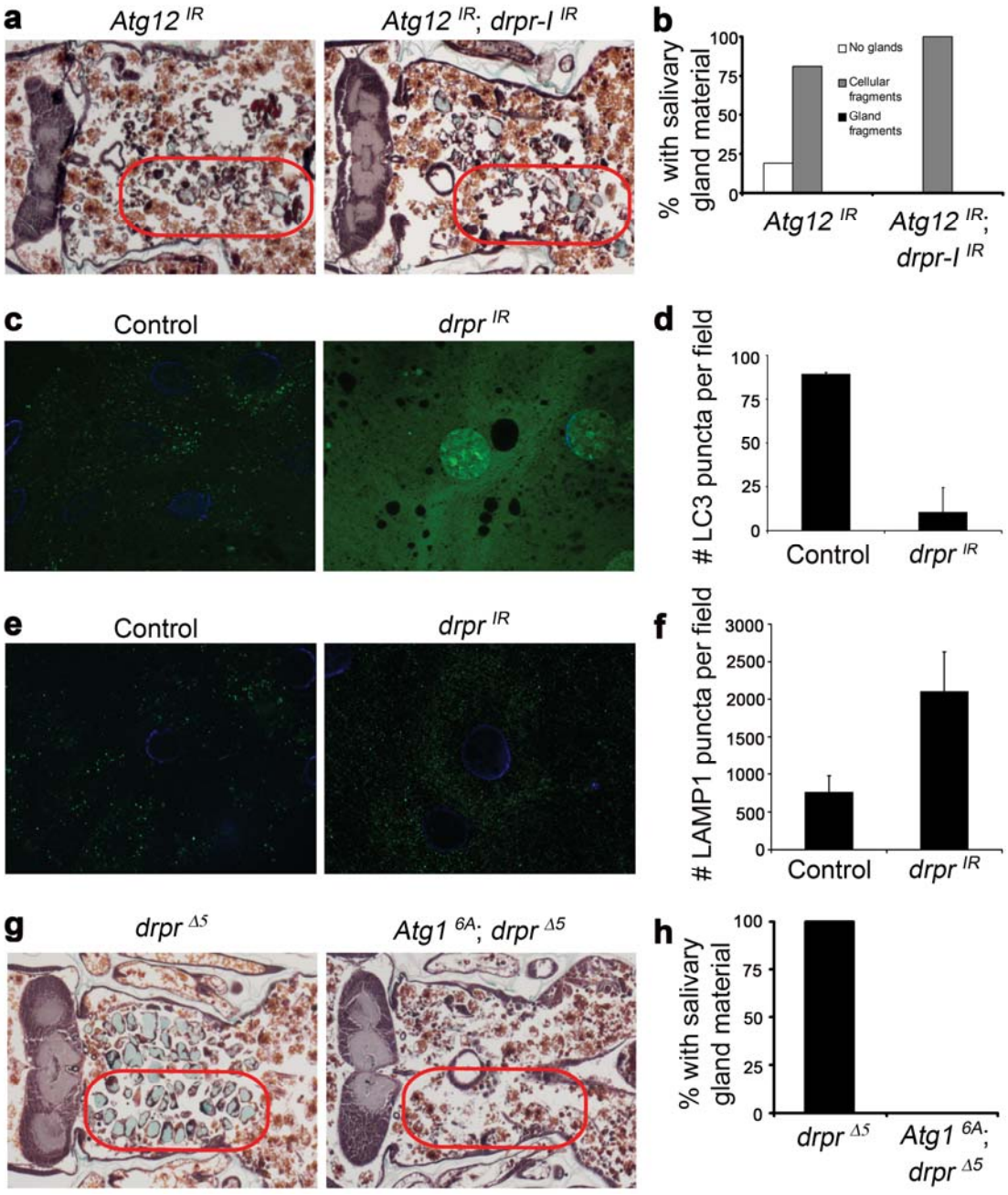

Figure 3-4. Draper is required for the induction of autophagy in dying salivary glands.

a, Animals with salivary gland-specific knockdown of *Atg12* (*fkh*-GAL4/*w*; UAS-*Atg12*^{IR}/+), n=21, and those with salivary gland-specific knockdown of both *Atg12* and *drpr-I* (*fkh*-GAL4/*w*; UAS-*Atg12*^{IR}/+; UAS-*drpr-I*^{IR}/+), n=19, were analyzed by histology for the presence of salivary gland material (red circles) 24h after puparium

formation. **b,** quantification of data from **a**. **c,** GFP-LC3 was expressed in salivary glands of control animals (+/*w*; UAS-GFP-LC3/+; *fkh*-GAL4/+) and those with salivary gland-specific knockdown of *drpr* (*w*; UAS-$drpr^{IR}$/UAS-GFP-LC3; *fkh*-GAL4/+). Salivary glands were dissected 6h and 14h after puparium formation, imaged for GFP-LC3, and LC3 puncta were quantified using Zeiss Automeasure software. **d,** quantification of data from **c**. Error bars represent standard error; n ≥ 10. **e,** LAMP-GFP was expressed in control animals (*tub*-LAMP-GFP/*w*; +/*fkh*-GAL4) and those with salivary gland-specific knockdown of *drpr* (*tub*-LAMP-GFP/*w*; UAS-$drpr^{IR}$/+; *fkh*-GAL4/+). Salivary glands were dissected 14h after puparium formation, imaged for LAMP-GFP, and LAMP puncta were quantified using Zeiss Automeasure software. **f,** quantification of data from **e.** Error bars represent standard error; n ≥ 10. **g,** *drpr* mutant animals (+/*w*; +/UAS-$Atg1^{6A}$; $drpr^{\Delta 5}/drpr^{\Delta 5}$), n=10, and those with salivary gland-specific expression of $Atg1^{6A}$ (*fkh*-GAL4/*w*; UAS-$Atg1^{6A}$/+; $drpr^{\Delta 5}/drpr^{\Delta 5}$), n=16, were analyzed by histology for the presence of salivary gland material (red circles) 24h after puparium formation. **h,** quantification of data from **g**.

Draper is cell-autonomously required for autophagy in dying salivary glands, but not in response to starvation in the larval fatbody

The question of whether autophagy plays dual roles in cell survival versus cell death has been controversial, and raises the possibility that different factors may regulate autophagy in different cell contexts. We analyzed whether Drpr protein is present in the larval fatbody, since *drpr* RNA was not detected in microarray analyses of starving larvae (Zinke et al., 2002). We found that Drpr is expressed in larval fatbody, but the levels and localization of Drpr do not change in response to starvation (**Figure 3-5a, b**). Since *drpr* is required for autophagy during salivary gland cell death, we wondered whether *drpr* is required for starvation-induced autophagy in the *Drosophila* larval fatbody. We starved third instar larvae expressing GFP-Atg8a (fly homologue of LC3 in mammals) in all cells and $drpr^{IR}$ specifically in dsRed-marked cell clones, and assayed for the induction of autophagy. Surprisingly, we found that GFP-Atg8a puncta form in both $drpr^{IR}$-expressing cells, as well as neighboring control cells (**Figure 3-5c**). Therefore, unlike in dying salivary glands, *drpr* is not required for starvation-induced autophagy in the *Drosophila* fatbody. One possibility is that *drpr* mediates a tissue-wide autophagic response, as we had not tested whether *drpr* functions in a cell autonomous manner in dying salivary glands. To test the cell-autonomous requirement of *drpr* for autophagy, salivary glands of animals expressing GFP-Atg8a in all cells, and $drpr^{IR}$ specifically in dsRed-marked clone cells, were assayed for GFP-Atg8a puncta. Strikingly, we found that cells expressing $drpr^{IR}$ contain diffuse GFP-Atg8a, whereas neighboring control cells

contain numerous GFP-atg8a puncta (**Figure 3-5d**). Thus, *drpr* functions upstream of autophagy in dying salivary glands and this is a cell-autonomous effect.

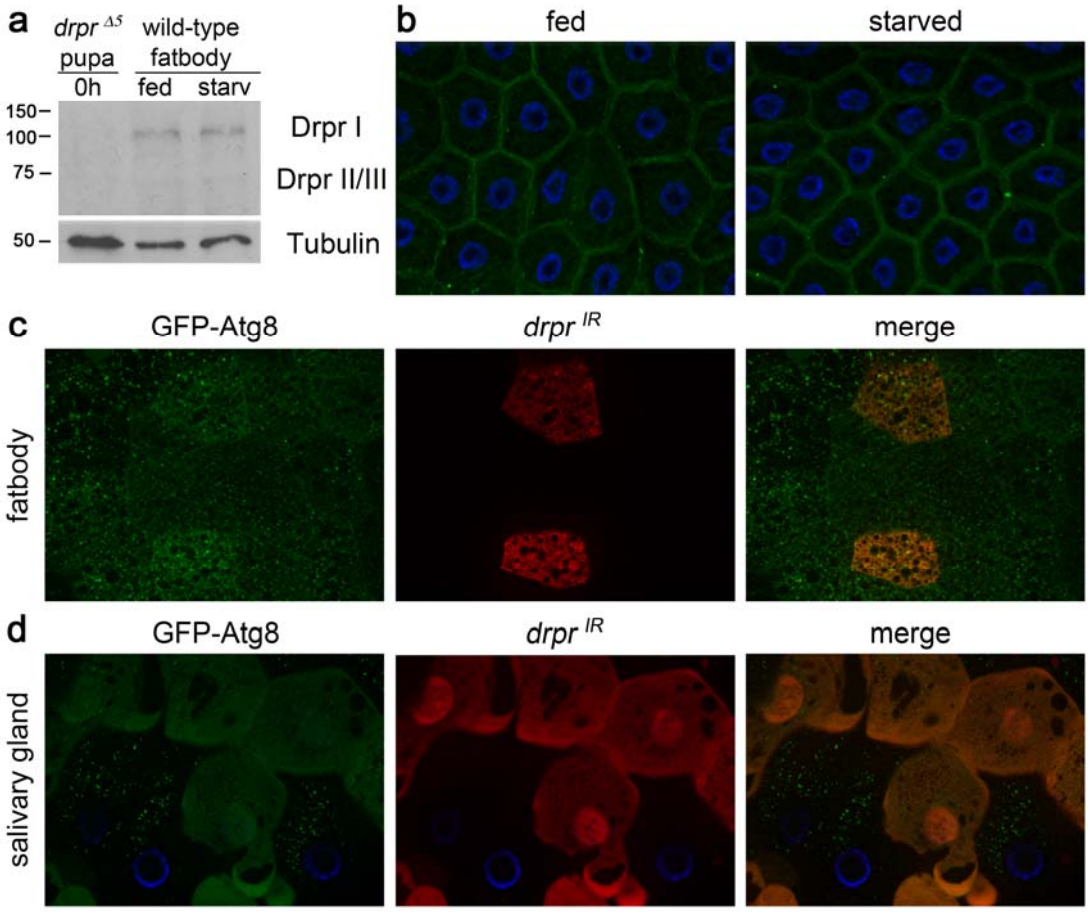

Figure 3-5. Draper is cell-autonomously required for autophagy in dying salivary glands, but not in response to starvation in the larval fatbody.

a, Protein extracts from *drpr* null (*w*; $drpr^{\Delta 5}/drpr^{\Delta 5}$) pupae at puparium formation (0h) and from the fatbodies of Wild-type (Canton-S) third instar larvae were analyzed by Western Blotting with anti-Drpr antibody. Third instar larvae were either fed or starved 4h. **b,** Wild-type (Canton-S) third instar larvae were either fed or starved 4h, and fatbodies were dissected, stained with anti-Drpr antibody, and imaged for Drpr (green). Nuclei were stained with DAPI (blue). **c,** Third instar larvae expressing GFP-Atg8 in all cells, and $drpr^{IR}$ specifically in dsRed-marked clone cells (hsflp/*w*; UAS-$drpr^{IR}$/+; hsGFPAtg8b, *act*<FRT,cd2, FRT>Gal4, UAS-dsRed/+), were starved 4h.

Larval fatbodies were dissected and imaged for GFPAtg8 (green) and dsRed (red). **d,** Salivary glands of animals expressing GFP-Atg8 in all cells, and *drpr*^{IR} specifically in dsRed-marked clone cells (hsflp/*w*; UAS-*drpr*^{IR}/+; hsGFPAtg8b, *act*<FRT,cd2, FRT>Gal4, UAS-dsRed/+) were dissected 14h after puparium formation. Salivary glands were imaged for GFPAtg8 (green) and dsRed (red). Nuclei were stained with Höescht (blue). **e,** Salivary glands of animals expressing GFP-Atg8 in all cells, and Drpr-II specifically in dsRed-marked clone cells (hsflp/*w*; UAS-Drpr-II/+; hsGFPAtg8b, *act*<FRT,cd2, FRT>Gal4, UAS-dsRed/+) were dissected 14h after puparium formation. Salivary glands were imaged for GFPAtg8 (green) and dsRed (red). Nuclei were stained with Höescht (blue).

Discussion

Autophagy has long been considered to be a survival process, but recent studies have shown that autophagy functions in cell death in certain *in vivo* contexts (Berry and Baehrecke, 2007; Hou et al., 2008; Mohseni et al., 2009; Nezis et al., 2009). Programmed cell death is required for animal development and adult tissue homeostasis, and a wide range of pathological conditions result from improper cell death regulation, including autoimmunity and cancer (Thompson, 1995). Several morphological forms of cell death that occur during mammalian development have been described, including apoptosis and autophagic cell death (Clarke, 1990; Schweichel and Merker, 1973). Autophagic cell death is characterized by the presence of autophagosomes in dying cells that are not known to be engulfed by phagocytes.

How autophagy might function in survival in some contexts and cell death in others is unknown. Autophagy is induced in *Drosophila* in response to starvation in the fat body where it promotes cell survival, while autophagy is induced by the steroid hormone ecdysone in salivary glands where it promotes cell death. This allows studies to be carried out in different cell types and in response to different stimuli. *Drosophila* larval salivary glands die with autophagic cell death morphology and autophagy is required for salivary gland cell degradation (Berry and Baehrecke, 2007). We queried proteomics and genome-wide microarray data from purified dying salivary glands and noted the presence of engulfment factors in these dying cells (**Table 2-6**) (Lee et al., 2003). Intriguingly, we also noted that there were no

detectable changes in engulfment genes after *Drosophila* larval starvation (Zinke et al., 2002).

Little is known about how autophagy induction leads to different outcomes in different contexts. It is possible that autophagy functions to deplete specific survival factors during cell death. Alternatively, different levels of autophagy could also be induced during different contexts, and extensive autophagy and depletion of cell resources could kill a cell. Here we report that the engulfment receptor Drpr is cell-autonomously required for autophagy induction in dying salivary glands, but not in response to starvation in the larval fatbody. Thus, our findings suggest that distinct signaling mechanisms regulate autophagy in response to nutrient deprivation compared to ecdysone induction. How Drpr is induced during ecdysone-regulated cell death is unknown. It could be that Drpr is induced by ecdysone. A recent study has identified *Drosophila pretaporter* as a ligand for Drpr in the context of engulfment of apoptotic cells (Kuraishi et al., 2009). It will be interesting to determine whether *pretaporter* functions as a Drpr ligand in dying salivary glands, and whether *pretaporter* and/or Drpr might be induced in salivary glands in response to ecdysone.

Our work suggests that Drpr is required for the induction of autophagy in a cell death-specific context. However, how Drpr might signal to induce autophagy remains to be determined. Like CED-1, Drpr contains a YXXL immunoreceptor tyrosine-based activation motif (ITAM) in its intracellular domain (Freeman et al., 2003; Zhou et al., 2001; Ziegenfuss et al., 2008). CED-1 and Dpr-mediated phagocytosis require binding of the adaptor protein Ced-6 to its NPXY motif (Awasaki et al., 2006; Ellis et al., 1991; Liu and Hengartner, 1998; Su et al., 2002).

The Src family kinase Src42A is required for the interaction of the non-receptor tyrosine kinase Shark with Drpr (Ziegenfuss et al., 2008). The interactions of Drpr with Src42A and Shark are required for Drpr-dependent phagocytosis, and are remarkably similar to mammalian immunoreceptor signaling requiring phosphorylation of an ITAM motif by a Src family kinase and the binding of a non-receptor tyrosine kinase (Fodor et al., 2006; Monroe, 2006; Underhill and Goodridge, 2007; Ziegenfuss et al., 2008). It could be that similar signaling events are required for Drpr-dependent induction of autophagy. If that is the case, we would expect the requirement of a src family kinase such as Src42A, Src64b, or Btk29a, and a non-receptor tyrosine kinase such as Shark, Fak, or Abl. The engulfment receptor six-microns-under (Simu) has been shown to act upstream of Drpr in *Drosophila* apoptotic cell engulfment (Kurant et al., 2008). It will be intriguing to see whether these signaling molecules are required for Drpr-dependent induction of autophagy in dying salivary glands.

We found that salivary gland-specific expression of an activated form of Atg1 a drpr null mutant background was sufficient to rescue the salivary gland degradation phenotype. This suggests that Atg1 functions downstream of Drpr. There are two known mechanisms by which autophagy induction is regulated. The target of Rapamycin (TOR) represses autophagy through phosphorylation of Atg13, and phosphorylated Atg13 does not bind to Atg1 (Kamada et al., 2010). In response to starvation, however, TOR is inactivated and its repression of Atg13 is relieved. Atg13 is rapidly dephosphorylated and binds to Atg1, leading to Atg1 activation (Kamada et al., 2000; Scott et al., 2007). In addition, a complex including Atg6/Beclin1,

Vps34/Class III PI3K, Atg14 and Vps15 is required for recruitment of PI(3)P to the autophagic membrane (Juhász et al., 2008; Kametaka et al., 1998; Kihara et al., 2001; Suzuki et al., 2001). In *Drosophila*, starvation results in a TOR/Atg1-dependent recruitment of Vps34 activity to the autophagosomal membrane (Juhász et al., 2008). It is possible that Drpr signaling might affect autophagy via negative regulation of TOR and thus affect the activation of Atg13 and Vps34 recruitment. It could also be that Drpr signaling might affect activation of Atg13 or the Atg6/Vps34 complex directly. Testing these questions will be important to understanding how Drpr affects the induction of autophagy in dying salivary glands.

Our findings indicate that Drpr is autonomously required for the clearance of cells that are not removed by phagocytosis. Although autophagy has been associated with engulfment in studies of TLR4- and CD46-mediated clearance of pathogens (Joubert et al., 2009; Sanjuan et al., 2007), this is the first example of an "engulfment factor" regulating cell-autonomous clearance. Caspase activation occurs during both apoptosis and autophagic cell death. The main difference between these two types of cell death is the location of phagocytosis machinery and the lysosomal system used to degrade cellular contents. During apoptosis, dying cells are recognized and engulfed by phagocytic cells where the lysosomes of the engulfing cell degrade the dead cell (Kerr et al., 1972). Autophagic cell death, however, occurs without known phagocytosis. Rather, this type of cell death is characterized by the presence of autophagosomes in the dying cell; autophagic contents are delivered to lysosomes and contents are thought to be degraded within the lysosomes of the dying cell itself. It could be that the processes that take place in two separate cells during apoptotic cell

death—phagocytic uptake and degradation of a dead cell—take place in a single cell during autophagic cell death.

Given recent interest in manipulation of autophagy for therapies, it is possible that factors such as Drpr could be used as biomarkers to distinguish autophagy leading to cell death versus cell survival. Drugs targeting autophagy have been suggested for disease therapies. Mono-allelic loss of the human Atg6 homolog Beclin1 is prevalent in human cancers. This suggests that autophagy is a tumor-suppressive mechanism, although autophagy also occurs in tumor cells as a survival mechanism. Autophagy inhibitors have been proposed for anti-cancer therapies to prevent the survival of tumor cells (Chen and Karantza-Wadsworth, 2009). However Mathew et al demonstrated that autophagic degradation of p62 protects cells from cellular damage that can lead to tumor formation (Mathew et al., 2009). White and colleagues have therefore proposed the use of autophagy enhancers in cancer prevention (Mathew et al., 2007a). Autophagy enhancers have also been proposed for the treatment of neurodegenerative diseases (Sarkar and Rubinsztein, 2008). Understanding how autophagy might be regulated differently in different contexts, and what specific regulators are responsible, will be critical for taking the right therapeutic strategies.

Acknowledgements

We thank H. Kramer, T.P. Neufeld, T.E. Rusten, H. Stenmark, the Bloomington Stock Center, the VDRC, and the Developmental Studies Hybridoma Bank for flies and antibodies.

Author Contributions

All the experiments were performed by C.K.M., and were designed by C.K.M and E.H.B.. Mary Logan and Marc R. Freeman provided critical DNA constructs and transgenic flies.

Methods

***Drosophila* strains.** The Canton-S strain was used as the wild-type control. For loss of function studies, drprΔ5 null mutants were used (Freeman et al., 2003). For RNAi studies, the following fly strains were used: pWiz-drpr-RNA-IR (MacDonald et al., 2006), pWiz-drpr-I-RNA-IR (Logan & Freeman, in preparation), UAS-Atg12-RNA-IR (Pandey et al., 2007). For ectopic expression studies, UAS-Drpr-I and UAS-Drpr-II (Logan & Freeman, in preparation), UAS-p35 (Hay et al., 1994), and UAS-Atg16A (Scott et al., 2007) were used. UAS-GFP-LC3 (Rusten et al., 2004), hs-GFP-Atg8a (Scott et al., 2004) and tub-LAMP1-GFP (Rusten et al., 2004) were used as markers of autophagy and lysosomes.

Transgenic strains. To generate the UAS-Drpr-I strain, full length *drpr-I* cDNA (GH24127) was inserted into the XhoI site of the pUAST transformation vector

(Brand and Perrimon, 1993). The *pWiz-drpr-I-IR* RNAi construct was made by amplifying a 1041 nucleotide sequence unique to Drpr-I (nucleotides 1331-2371 from GH 24127) and inserting this fragment into the NheI and XbaI sites of the pWIZ transformation vector (Lee and Carthew, 2003). The same sequence was then inserted in the XhoI and EcoRI sites in the 3' to 5' direction to generate the final *pWiz-drpr-I-IR* RNAi construct. Constructs were sequenced and used to generate transgenic *Drosophila* (BestGene, Inc.).

Protein Extracts and Western Blotting. Protein extraction and Western Blotting were performed as described previously (Dutta and Baehrecke, 2008). Primary antibodies used were rabbit anti-Drpr (1:1000) (Freeman et al., 2003), and mouse anti-Beta-Tubulin (1:50) (Developmental Studies Hybridoma Bank).

Histology. Histology was performed as described previously (Berry and Baehrecke, 2007; Muro et al., 2006).

Immunolabeling and Microscopy. Dissection, fixation, and antibody labeling of *Drosophila* tissues was performed as described previously (Martin and Baehrecke, 2004). Imaging was performed on a Zeis Axiophot II microscope. Primary antibodies were used at the following concentrations: rabbit anti-Drpr (1:500) (Freeman et al., 2003), and mouse anti-Lamin DMO (1:10) (Hybridoma Bank). For LC3 and LAMP1 quantification, salivary glands were imaged without fixation on a Zeiss Axiophot II microscope and GFP puncta were quantified using Zeiss Automeasure software.

Induction of cell clones. To induce RNAi-expressing clones in *Drosophila* tissues, an overnight egg lay was obtained at 25°C, and following the egg lay, embryos were heat shocked at 37°C for 15 min. To induce expression of hsGFPAtg8, larvae were

heat shocked at 37°C for 30 minutes, and then recovered at 25°C until the time of dissection.

Starvation of larvae. Third instar larvae were either allowed to remain in the food (fed) or removed from food and placed on moist petri dishes for 4 hours (starved).

Chapter 4: Summary and Future Directions:

The Role of Catabolic Processes in Autophagic cell death

Programmed cell death is required for proper metazoan development and homeostasis, and improper regulation of cell death can lead to diseases such as autoimmunity and cancer. There are two main types of developmental cell death that occur during development, apoptosis and autophagic cell death. Little is known about the mechanisms that regulate autophagic cell death. The two main catabolic processes used by cells to degrade cytoplasmic contents are the ubiquitin/proteasome system and autophagy. While changes in the UPS have been correlated with autophagic cell death, this has not been tested empirically. Proteasome inhibitors are being used in anti-cancer therapies; however the cellular effects of proteasome impairment have not been studied *in vivo*. In addition, while autophagy has been shown to be required for cell death in several *in vivo* contexts, how autophagy functions in some contexts to promote survival in response to stress, and in other contexts to contribute to programmed cell death, is unknown. Using a *Drosophila* model to study autophagic cell death *in vivo*, we have shown that two main cellular catabolic processes, the UPS and autophagy, are very important for the proper execution of programmed cell death. These findings have advanced our understanding of autophagic cell death, and also provide several new starting points for future investigations.

The role of the Ubiquitin Proteasome System in salivary gland cell death

We sought to identify previously unknown factors and pathways that might be involved in autophagic cell death. To do this, we took a shot-gun proteomics approach (Chen et al., 2003) to identify proteins present in purified dying salivary glands, a *Drosophila* model for autophagic cell death that occurs during development. We found that a number of ubiquitin/proteasome system (UPS) components were present in dying salivary glands. We tested the function of the UPS during wild-type salivary gland cell death and found that the UPS becomes impaired in dying salivary glands. However, how the UPS becomes impaired during salivary gland cell death is still unknown. Studies in cell lines have suggested that the proteasome is impaired in a caspase-dependent manner (Adrain et al., 2004; Sun et al., 2004). This is an important question to test in the context of salivary gland cell death. To test this, we will co-express the caspase inhibitor p35 and the reporter for UPS function, GFP-CL1. We will test whether p35 expression prevents GFP-CL1 accumulation. We will also test whether caspase mutants such as those with mutations in *dronc* (*Drosophila* Caspase-9 homolog) or *ark* (APAF-1 homolog) prevent proteasome impairment.

Studies show that ectopic proteasome impairment leads to cell death (Drexler, 1997; Henderson et al., 2005; Shinohara et al., 1996), and proteasome inhibitors are being used in anti-cancer therapies to kill tumor cells (Hoeller and Dikic, 2009; Tobinai, 2007). However, little is known about the *in vivo* affects of proteasome impairment. We tested the effects of ectopic proteasome inhibition *in vivo* in *Drosophila* salivary glands. We found that ectopic proteasome impairment leads to

the induction of early salivary gland degradation and DNA fragmentation, which suggests that proteasome impairment leads to caspase activation. Unexpectedly, we found that expression of the caspase inhibitor p35 fails to suppress ectopic salivary gland degradation during proteasome impairment.

In order to gain insight into the cellular effects of ectopic proteasome impairment, we conducted a proteomic analysis of salivary glands following ectopic proteasome impairment. To ensure physiological relevance of candidates to screen, we compared proteins present upon ectopic proteasome impairment to those present in wild-type dying salivary glands. We screened top candidates that were identified as proteins that were increased both upon proteasome impairment and in wild-type dying salivary glands with the lowest p values. To screen genes for function in salivary gland cell death, we expressed RNAi against these genes specifically in salivary glands and tested for a failure in proper salivary gland degradation. We found that knockdown of *lysoszyme e* and *trol* prevented proper salivary gland cell clearance. These genes were not previously known to function in salivary gland cell death, demonstrating the power and validity of our proteomics approach.

To identify additional proteins that might function in salivary gland cell death and in response to proteasome impairment, we have generated a list of the next top candidates to be screened. These candidates were chosen based upon their identification as having positive ratio2 values, indicating proteins that increased in detection value, in both wild-type 6h to 13h salivary glands, and upon proteasome impairment in salivary glands. These candidates have the p values ≤ 0.005 in one or both datasets, have not yet been screened, and are not known to function in salivary

gland cell death (**Table 4-1**). This list provides a starting point for discovery of additional genes required for autophagic cell death. We will begin by expressing RNAi targeting these genes specifically in salivary glands and testing whether RNAi expression leads to a defect in salivary gland degradation. If we find phenotypes, we will then test whether gene knockdown affects autophagy and/or caspase activation.

Table 4-1. List of proteins detected by proteomics in salivary glands that are top candidates to be screened for function in salivary gland cell death.

		Proteasome Impairment		Wild-type 6h to 13h	
symbol	Notes	ratio2	p value	ratio2	p value
Act57B	cytoskeleton organization	1.4	0.0050	1.4	0.0255
Act79B	cytoskeleton organization	1.5	0.0044	1.2	0.1714
Act87E	cytoskeleton organization	1.4	0.0052	1.	0.0314
alpha-Adaptin	AP-2 complex subunit alpha	1.5	0.2535	4.5	0.0006
Argk	arginine kinase activity	1.3	0.0033	1.7	0.0195
CG10126	calcium ion binding	3.3	8.51E-05	1.2	0.7184
CG10433	defense response	Inf	0.2051	Inf	0.0019
CG11334	translation regulator	1.6	0.0558	4.1	0.0002
CG11876	pyruvate dehydrogenase	1.3	0.0004	1.3	0.1900
CG12163	cysteine-type endopeptidase	1.8	0.0341	3.1	0.0035
CG14109	unknown	Inf	0.0024	1.6	0.5281
CG1600	response to hypoxia	1.6	0.2664	9.7	8.38E-06
CG1681	glutathione transferase activity	16.9	0.0001	Inf	0.2855
CG17746	serine/threonine phosphatase	Inf	0.2032	Inf	0.0019
CG1950	ubiquitin thiolesterase activity	1.7	0.0004	1.5	0.4562
Cg25C	extracellular matrix	1.6	0.0049	1.8	0.0025
CG3011	mitochondrion	1.6	0.0014	1.7	0.0504
CG3164	ATP-binding cassette (ABC) transporter	Inf	0.4365	Inf	0.0017
CG31673	glyoxylate reductase (NADP)	2.8	0.0041	Inf	2.49E-05
CG33138	carbohydrate metabolic process	2.9	0.0041	3.0	0.0149
CG3415	oxidation/reduction	1.7	0.0006	1.3	0.1129
CG3987	mesoderm development	4.0	0.0551	Inf	0.0012
CG4572	dsRNA transport	4.9	0.0026	1.4	0.4289
CG5171	trehalose-phosphatase activity	2.2	0.0041	5.8	0.0006
CG5174		1.3	0.0029	1.0	0.8415
CG6287	oxidation/reduction	1.1	0.1165	1.6	0.0006
CG7470	proline biosynthetic process	3.1	0.0531	12.9	0.0042
CG8306		1.6	0.2368	3.9	0.0038

CG9027	oxidation/reduction	1.6	0.6998	Inf	0.0029
CG9629	oxidation/reduction	2.2	0.0032	6.3	0.0077
Chc	sperm individualization	1.3	0.0402	2.2	0.0006
CPTI	mitochondrion	1.7	0.4314	Inf	0.0013
Cyp12c1	electron transport	15.2	0.0004	Inf	0.2855
dro2		Inf	0.0014	Inf	0.0653
Drs	aspartate-tRNA ligase activity	2.3	0.0033	1.1	0.8893
fau	Protein anoxia up-regulated	2.3	0.0176	8.4	0.0024
Gapdh1	glycolysis	1.2	0.0029	1.1	0.4115
Glt	basement membrane	1.6	0.0023	1.4	0.0272
Glycogenin	mesoderm development	1.0	0.9282	3.8	6.37E-05
GlyP	Glycogen phosphorylase	1.0	0.7930	2.1	0.0004
Gpdh	glycerol-3-phosphate metabolism	1.0	0.6614	1.2	0.0024
Gs2	glutamate-ammonia ligase	1.8	0.0115	15.0	1.65E-07
Hf	innate immune response	Inf	0.0031	Inf	0.0963
Hsp23	actin binding	3.8	9.57E-05	1.2	0.0323
Idh	glyoxylate cycle	1.4	0.0008	1.6	0.0003
lectin-28C	galactose binding	Inf	0.0030	Inf	0.0229
Lsp1alpha	Larval serum protein 1 alpha chain	1.1	0.5014	3.6	1.44E-05
Lsp1beta	Larval serum protein 1 beta chain	1.0	0.7955	2.7	0.0002
Map205	microtubule binding	6.8	0.0078	Inf	1.15E-09
Men	cytokinesis	1.7	0.0086	1.6	0.0018
Mf	muscle thick filament assembly	1.5	0.0135	3.3	0.0029
Mlc1	microfilament motor activity	1.0	0.8311	4.9	0.0017
Ost48	N-linked glycosylation	1.0	0.5577	1.8	0.0019
Pax	cytoskeletal anchoring at plasma membrane	1.5	0.0082	1.7	0.0004
Pcd	tetrahydrobiopterin biosynthesis	1.9	0.0047	1.7	0.2783
Pepck	gluconeogenesis	4.1	0.0050	5.7	0.0209
Pgi	gluconeogenesis	1.0	0.5569	1.8	0.0036
Prm	myofibril assembly	1.1	0.4507	3.2	0.0002
Reg-2	phosphoglycolate phosphatase	1.4	0.3359	4.6	0.0038
RpL34a	cytosolic large ribosomal subunit	1.1	0.3514	2.4	0.0037
RpL7A	structural constituent of ribosome	1.2	0.1162	1.5	0.0014
sals	actin filament polymerization	1.6	0.5964	Inf	0.0003
Sodh-1	oxidation/reduction	1.4	0.0009	1.17	0.5085

Syx5	neurotransmitter secretion	1.1	0.8863	Inf	0.0019
Tango9	transport and golgi organization	Inf	0.4365	Inf	2.25E-05
Thor	starvation response, growth regulation	Inf	0.4365	Inf	1.72E-05
tmod	cytoskeleton organization	1.4	0.1843	3.3	0.0045
TpnC47D	Troponin C, isoform 2	1.1	0.8062	3.2	0.0011
Vago		Inf	0.0033	9.0	0.0128
Vha100-2	ATP synthesis coupled proton transport	2.3	0.1222	11.3	0.0011
Vha16-3	ATP synthesis coupled proton transport	3.0	0.3845	Inf	0.0017
VhaAC39	proton transport	1.4	0.1762	34.5	0.0001
Zasp66	mesoderm development	1.1	0.6507	2.4	0.0021

List of proteins to be screened based on the following criteria: 1) positive ratio2 values following proteasome impairment and during wild-type salivary gland cell death between 6h and 13h APF; 2) p values ≤ 0.005 in one or both datasets. Names of genes are based on Flybase annotation (http://flybase.org/). The ratio2 values for peptides mapped to the proteins listed are indicated (ratio2=average detection value experimental samples/ average detection value control samples). p values were obtained using the Student's t-test followed by multiple testing adjustment using the Benjamini-Hochberg method (Hochberg and Benjamini, 1990). Inf indicates a numerical value divided by 0.

The Cop9 signalsome functions in salivary gland cell degradation

To identify additional genes that might function in salivary gland cell death, we sought to identify proteins present in the salivary gland proteomics datasets that suggested the involvement of a cellular component or genetic pathway. We identified two groups of genes that successfully led to the identification of genes required for salivary gland cell death, namely a group of engulfment genes, as well as a number of Cop9 signalsome (CSN) components. As discussed in more detail below, we identified the engulfment gene Draper as being required for salivary gland cell degradation. In addition, we found that RNAi knockdown of the CSN subunit *csn6* prevented salivary gland cell degradation. This suggests that the CSN functions in salivary gland degradation, given that CSN6 is an integral part of the CSN complex.

The CSN complex functions to de-neddylate and deactivate the cullin-RING ligase families of ubiquitin E3 complexes (Cope et al., 2002; Lyapina et al., 2001; Schwechheimer et al., 2001; Wei et al., 2008). Thus, our finding that *cns6* knockdown prevents proper salivary gland degradation suggests that de-neddylation could be important for the regulation of proper salivary gland clearance. In addition, this result suggests the possibility that cullin-RING ubiquitin ligase (CRL) complexes could function in salivary gland cell death, given that the CSN is known to deneddylated CRL complexes. Indeed, we found that several E3 ubiquitin protein ligases, as well as specific cullin-RING ligase components, are present in both wild-type dying salivary glands and following proteasome impairment, including the cullins Cul-2, Cul-4, Cul-5, and the SCF ubiquitin ligase components skpA and slmb

(**Table 4-2**). Thus, these genes are prime candidates to be tested for function in salivary gland cell death and serve as a new avenue for investigation of genes that might play a role in regulating autophagic cell death. To test the involvement of these genes in salivary gland degradation, we will start by knocking down these genes specifically in salivary glands using available RNAi strains and crossing these strains to the salivary gland-specific driver *fkh*-GAL4. If we find a phenotype with any of these genes, we will test for alterations in caspase activation or autophagy induction upon RNAi expression or in available mutants. We will also use tagged versions of these cullin ring ligase complex components and do pull-down experiments to identify potential cullin ring ligase complex target proteins. We will then test whether these potential target proteins become neddylated upon *csn6* knockdown. We will also test whether knockdown of these potential CSN target proteins prevents salivary gland cell death, caspase activation, or autophagy induction.

Some evidence suggests that the CSN may regulate proteasome proteolytic function by direct interaction with the 26S proteasome (Huang et al., 2005). A recent report found that *csn8* knockdown led to a decrease in CSN deneddylation activity and an increase in proteasomal proteolytic function (Su et al., 2009). Given these findings, it is possible that the proteasome could be regulated by the Cop9 signalsome during salivary gland cell death. This is an important question to test, as the mechanism of UPS impairment that occurs during salivary gland cell death is unknown. We will test this by knocking down *csn6* in salivary glands and co-expressing the UPS reporter UAS-GFP-CL1. We will test for a failure in UPS impairment during *csn6* knockdown. We will also test whether there is a defect in the

accumulation of ubiquitinated proteins in salivary glands during *csn6* knockdown by probing salivary gland extracts with Ubiquitin antibody.

Additional groups of proteins present in dying salivary glands

In addition to the engulfment genes and CSN components, we also noted many additional groups of proteins that are present in both wild-type dying salivary glands and following proteasome impairment. These groups include cysteine-type endopeptidases and metalloendopeptidases (**Table 4-3**), protein kinases (**Table 4-4**), DNA-and RNA-interacting proteins (**Table 4-5**), actin binding proteins (**Table 4-6**), lysosomal and mitochondrial proteins (**Table 4-7**), GTPases (**Table 4-8**), and calcium ion binding proteins (**Table 4-9**). Each of these groups of proteins is interesting and together these data provide starting points for future investigations to identify new genes that function in salivary gland cell death.

Table 4-2. List of ubiquitin ligases and SCF ubiquitin ligase complex components detected by proteomics.

			Proteasome Impairment		Wild-type 6h to 13h	
Category	**Symbol**	**Notes**	**ratio2**	**p value**	**ratio2**	**pvalue**
Ubiquitin protein ligases						
	Prp19	nuclear mRNA splicing	1.5	0.7158	7.1	0.0234
	Hyd	female gonad development	Inf	0.4365	1.1	0.9309
	CG9086	protein ubiquitination	1.8	0.1447	5.9	0.0651
	Ubc-E2H		1.2	0.7406	1.1	0.9407
	CG3473		2.8	0.0161	1.2	0.9195
Cullin-RING ubiquitin ligase complex						
	Cul-2	cullin-RING ubiquitin ligase complex	-1.7	0.7181	1.2	0.9108
	Cul-4	cullin-RING ubiquitin ligase complex	Inf	1.05E-05	-1.8	0.6219
	Cul-5	cullin-RING ubiquitin ligase complex	Inf	0.43658	1.5	0.7994
	skpA	SCF ubiquitin ligase complex	-1.0	0.92742	1.6	0.1076
	Slmb	SCF ubiquitin ligase complex	Inf	0.4365	Inf	0.2855

Protein names are based on Flybase annotation (http://flybase.org/). The ratio2 values for peptides mapped to the genes listed are indicated (ratio2=average detection value experimental sample divided by average detection value control sample). p values were obtained using the Student's t-test followed by multiple testing adjustment using the Benjamini-Hochberg method (Hochberg and Benjamini, 1990). Inf indicates a numerical value divided by 0.

Table 4-3. List of endopeptidases up-regulated following proteasome impairment and during wild-type salivary gland cell death.

			Proteasome Impairment		Wild-type 6h vs 13h	
Category	**Symbol**	**Notes**	**ratio2**	**p value**	**ratio2**	**p value**
Cysteine-type endopeptidases						
	CG3074	immune response	4.5	0.0013	3.4	0.0542
	CG1440		1.3	0.0746	1.5	0.1506
	CG10992		1.1	0.5613	1.6	0.0162
	CG12163		1.8	0.0341	3.1	0.0035
	CG11459		1.9	0.2460	Inf	0.2855
Metalloendopeptidases						
	Tok	wing vein morphogenesis	Inf	0.4365	Inf	0.2855
	CG2025		1.6	0.3031	1.5	0.2578
	Mmp1		Inf	0.0002	1.4	0.5690

Protein names are based on Flybase annotation (http://flybase.org/). The ratio2 values for peptides mapped to the genes listed are indicated (ratio2=average detection value experimental sample divided by average detection value control sample). p values were obtained using the Student's t-test followed by multiple testing adjustment using the Benjamini-Hochberg method (Hochberg and Benjamini, 1990). Inf indicates a numerical value divided by 0.

Table 4-4. List of protein kinases up-regulated following proteasome impairment and during wild-type salivary gland cell death.

			Proteasome Impairment		Wild-type 6h to 13h	
Category	**Symbol**	**Notes**	**ratio2**	**p value**	**ratio2**	**pvalue**
Protein kinases						
	aux		Inf	0.2044	1.2	0.8994
	CkIIalpha	protein kinase CK2 complex	1.1	0.4950	1.1	0.4446
	sds22	protein phosphatase type 1 regulator	1.6	0.2737	1.7	0.1170
	Pp2A-29B	pp2A regulator	1.0	0.5401	1.5	0.0808
	CaMKII		1.3	0.8238	5.9	0.0719
	Phk-3	response to bacterium	1.4	0.3317	1.2	0.9206
	fray		1.1	0.5976	1.9	0.4220
	SNF4Ag		Inf	0.2035	1.1	0.9309
	Pp1-13C	protein phosphatase type 1 complex	1.1	0.6610	1.7	0.3161
	Tws	protein phosphatase type 2A complex	1.5	0.1861	1.0	0.9806
	Flw	protein phosphatase type 1 complex	1.1	0.6874	3.5	0.19599
	CG17746		Inf	0.2032	Inf	0.00191
	Alph	response to oxidative stress	1.4	0.4829	4.9	0.04607
	snRNP70K	nuclear mRNA splicing	1.8	0.4896	Inf	0.28559

Protein names are based on Flybase annotation (http://flybase.org/). The ratio2 values for peptides mapped to the genes listed are indicated (ratio2=average detection value experimental sample divided by average detection value control sample). p values were obtained using the Student's t-test followed by multiple testing adjustment using the Benjamini-Hochberg method (Hochberg and Benjamini, 1990). Inf indicates a numerical value divided by 0.

Table 4-5. List of DNA- and RNA-interacting proteins up-regulated following proteasome impairment and during wild-type salivary gland cell death.

			Proteasome Impairment		Wild-type 6h to 13h	
Category	**Symbol**	**Notes**	**ratio2**	**p value**	**ratio2**	**p value**
Transcription						
	Hira	transcription corepressor	1.2	0.1339	1.5	0.5072
	nvy	transcription factor	1.9	0.4267	Inf	0.2855
	CG5690	transcription regulator	1.7	0.5494	2.3	0.5865
	simj	transcription repressor	Inf	0.083	Inf	0.2855
DNA binding						
	CG6905	spliceosomal complex	Inf	0.096	1.1	0.9309
	PDCD-5	apoptosis	1.17	0.6443	4.6	0.4138
	Stat92E	disc morphogenesis	1.8	0.6180	Inf	0.0780
	His3.3B	chromatin assembly	3.8	0.0154	1.2	0.5995
	RPA2	DNA replication factor	1.6	0.6171	1.2	0.9108
	ph-p	gene silencing	Inf	0.0995	1.4	0.8089
	baf	karyosome formation	1.7	0.2192	1.2	0.7667
	Osa	Wnt receptor signaling	1.7	0.6610	Inf	0.2855
	scf	DNA topoisomerase	1.1	0.5766	1.9	0.1096
	Top1	DNA topoisomerase	1.0	0.8929	1.4	0.5953
Nuclear splicing						
	snf	mRNA splicing	Inf	0.4365	Inf	0.2855
	snRNP70K	mRNA splicing	1.8	0.4896	Inf	0.2855
	SmG	mRNA splicing	Inf	0.0855	Inf	0.0653
	snRNP2	mRNA splicing	1.4	0.0575	1.0	0.9021
	CG10418	mRNA splicing	1.1	0.8680	1.6	0.1879
	CG7564	U1 snRNP	4.4	0.0418	Inf	0.0653
	CG2021	U6 snRNP	3.9	0.0436	1.6	0.1449
	hoip	mRNA splicing	1.0	0.9096	1.1	0.7238
	xl6	mRNA splicing	1.1	0.9236	Inf	0.2855
mRNA binding						

Imp	mRNA binding	2.7	0.0110	1.8	0.0731
lark	mRNA binding	1.49	0.3040	1.6	0.3851
Srp14	mRNA binding	1.3	0.1187	1.1	0.9141
Fmr1	mRNA binding	1.1	0.6617	1.8	0.2235

Protein names are based on Flybase annotation (http://flybase.org/). The ratio2 values for peptides mapped to the genes listed are indicated (ratio2=average detection value experimental sample divided by average detection value control sample). p values were obtained using the Student's t-test followed by multiple testing adjustment using the Benjamini-Hochberg method (Hochberg and Benjamini, 1990). Inf indicates a numerical value divided by 0.

Table 4-6. List of actin-binding proteins up-regulated following proteasome impairment and during wild-type salivary gland cell death.

			Proteasome Impairment		Wild-type 6h to 13h	
Category	**Symbol**	**Notes**	**ratio2**	**pvalue**	**ratio2**	**p value**
Actin binding						
	Bif	negative regulation of axon extension	1.2	0.8601	1.7	0.2889
	Cpa	actin filament organization	1.2	0.2076	1.1	0.6948
	CG31352	cytoskeleton organization	1.91	0.0378	1.1	0.7963
	Tsr	actin filament depolymerization	1.1	0.3504	1.0	0.6515
	SCAR	cytoskeleton organization	1.3	0.3298	1.2	0.8994
	Hsp23	response to heat	3.8	9.57E-05	1.2	0.0323
	p16-ARC	phagocytosis	1.0	0.6927	2.6	0.2373
	Tm2	muscle thin filament tropomyosin	1.1	0.640	1.9	0.0984
	Arc-p34	Arp2/3 protein complex	1.6	0.3480	1.1	0.9471
	Tm1	pole plasm oskar mRNA localization	1.0	0.9119	1.4	0.1081
	Capt	actin polymerization or depolymerization	1.1	0.0636	1.2	0.3197
	Tmod	cytoskeleton organization	1.4	0.1843	3.3	0.0045
	CG5023	actomyosin structure organization	1.2	0.0951	2.8	0.0226
	Cpb	F-actin capping protein complex	1.2	0.1612	1.5	0.5266
	Mical	axon guidance	2.3	0.1941	55.2	0.0077
	Myo61F	mesoderm development	Inf	0.4365	3.5	0.2832
	unc-115		1.9	0.0378	1.4	0.6303
	Sals	actin filament polymerization	1.6	0.5964	Inf	0.0003

Protein names are based on Flybase annotation (http://flybase.org/). The ratio2 values for peptides mapped to the genes listed are indicated (ratio2=average detection value experimental sample divided by average detection value control sample). p values were obtained using the Student's t-test followed by multiple testing adjustment using the Benjamini-Hochberg method (Hochberg and Benjamini, 1990). Inf indicates a numerical value divided by 0.

Table 4-7. List of lysosomal and mitochondrial proteins up-regulated following proteasome impairment and during wild-type salivary gland cell death.

			Proteasome Impairment		Wild-type 6h vs 13h	
Category	**Symbol**	**Notes**	**ratio2**	**p value**	**ratio2**	**p value**
Lysosome						
	Ect3	lysosome	10.3	0.0004	28.1	0.0009
	Gal	lysosome	2.6	0.0205	2.2	0.1840
	Ppt1	lysosome	Inf	0.0100	2.3	0.4386
Mitochondria						
	aralar1	mitochondrial envelope	1.3	0.3119	Inf	0.2855
	Tim8	mitochondrial inner membrane	1.0	0.8312	1.8	0.3002
	CG7280	mito intermembrane space	1.6	0.6781	2.3	0.2993
	mRpL24	mito large ribosomal subunit	3.0	0.2738	Inf	0.2855
	Oat	mitochondrial matrix	1.5	0.0104	1.1	0.8715
	CG6638	mitochondrial matrix	1.2	0.6146	2.9	0.1397
	ND23	mitochondrial electron transport	1.2	0.0418	1.1	0.8966
	CG3683	mitochondrial electron transport	1.3	0.3110	1.8	0.0835
	CG12203	mitochondrial electron transport	1.1	0.5496	1.2	0.3837
	CG14235	mitochondrial respiratory chain	1.2	0.2446	2.6	0.0056
	Cyp12c1	oxidation reduction	15.2	0.0004	Inf	0.2855
	CPTI		1.7	0.4314	Inf	0.0013
	CG12262	fatty acid beta-oxidation	1.2	0.1126	1.2	0.1387
	L2G0255	tricarboxylic acid cycle	1.4	0.1239	1.1	0.6307
	Prx5037	cell redox homeostasis	1.1	0.6444	1.4	0.4242
	CG3011	L-serine biosynthetic process	1.6	0.0014	1.7	0.0504
	Pepck	gluconeogenesis	4.1	0.0050	5.6	0.0209

Protein names are based on Flybase annotation (http://flybase.org/). The ratio2 values for peptides mapped to the genes listed are indicated (ratio2=average detection value experimental sample divided by average detection value control sample). p values were obtained using the Student's t-test followed by multiple testing adjustment using the Benjamini-Hochberg method (Hochberg and Benjamini, 1990). Inf indicates a numerical value divided by 0.

Table 4-8. List of GTPases/GTP binding proteins up-regulated following proteasome impairment and during wild-type salivary gland cell death.

			Proteasome Impairment		Wild-type 6h vs 13h	
Category	**Symbol**	**Notes**	**Ratio2**	**p value**	**Ratio2**	**p value**
GTPases/GTP binding						
	CG31048		1.1	0.8088	Inf	0.1347
	Rab-RP4	cell adhesion	1.9	0.4312	Inf	0.2855
	Rab14		1.1	0.3135	2.5	0.0103
	Chrw	nervous system development	1.1	0.6444	2.2	0.0159
	Rab-RP3		1.1	0.6444	2.2	0.0159
	Rbcn-3B	heterotrimeric G-protein complex	1.1	0.9075	1.5	0.3839
	Rab39		1.1	0.5065	2.2	0.0159
	Rheb	imaginal disc growth	1.4	0.3748	Inf	0.0715
	Rab3	neurotransmitter secretion	1.1	0.6444	2.2	0.0159
	Rala	dorsal closure	1.2	0.7702	Inf	0.2855
	Rab30		1.1	0.6444	2.2	0.0159
	Rho1	gastrulation	1.0	0.8181	1.2	0.1214
	Ras85D	determination of anterior/posterior axis	1.2	0.7498	Inf	0.0624
	Rac1	phagocytosis	1.3	0.4295	1.6	0.3128
	R	ovarian follicle cell stalk formation	1.6	0.1413	4.4	0.0090
	Rab35	cytokinesis	1.1	0.6444	2.3	0.0086
	Gbeta13F	actin filament organization	1.2	0.5697	1.7	0.0295
	RabX4		1.1	0.6444	2.2	0.0159
	Cdc42	dorsal closure	1.2	0.7191	2.23	0.0380

Protein names are based on Flybase annotation (http://flybase.org/). The ratio2 values for peptides mapped to the genes listed are indicated (ratio2=average detection value experimental sample divided by average detection value control sample). p values were obtained using the Student's t-test followed by multiple testing adjustment using

the Benjamini-Hochberg method (Hochberg and Benjamini, 1990). Inf indicates a numerical value divided by 0.

Table 4-9. List of calcium ion binding proteins up-regulated following proteasome impairment and during wild-type salivary gland cell death.

			Proteasome Impairment		Wild-type 6h vs 13h	
Category	**Symbol**	**Notes**	**ratio2**	**p value**	**ratio2**	**p value**
Calcium binding						
	BM-40-SPARC	cell adhesion	1.3	0.6954	2.7	0.3896
	CanB2	calcineurin complex	1.0	0.9414	4.06	0.0375
	Mp20	cell adhesion	1.5	0.0607	1.8	0.0354
	CG9906	protein folding	1.1	0.4960	1.3	0.5086
	CG1924	protein folding	1.1	0.5739	1.8	0.1280
	CG10126		3.3	8.51E-05	1.2	0.7184
	Glt	basement membrane	1.6	0.0023	1.4	0.0272
	TpnC47D		1.1	0.8062	3.2	0.0011
	TpnC73F		1.2	0.4774	5.5	0.0059
	aralar1	mitochondrial transport	1.3	0.3119	Inf	0.2855
	CalpB	proteolysis	1.2	0.6749	9.4	0.0215
	Scp2	sarcoplasmic reticulum	Inf	0.4365	Inf	0.2855

Protein names are based on Flybase annotation (http://flybase.org/). The ratio2 values for peptides mapped to the genes listed are indicated (ratio2=average detection value experimental sample divided by average detection value control sample). p values were obtained using the Student's t-test followed by multiple testing adjustment using the Benjamini-Hochberg method (Hochberg and Benjamini, 1990). Inf indicates a numerical value divided by 0.

The role of engulfment genes in salivary gland cell degradation

We identified several engulfment factors in proteomics and genome-wide microarray data from purified dying salivary glands (Lee et al., 2003). This was surprising, as salivary gland clearance is not known to involve phagocytosis. Interestingly, no detectable changes were found in these engulfment genes following larval starvation (Zinke et al., 2002). We tested the requirement for the phagocytosis receptor Draper (Drpr), the *Drosophila* orthologue of *C. elegans* CED-1(Freeman et al., 2003). We found that null mutations in *drpr*, as well as salivary gland-specific knockdown of *drpr*, led to defective salivary gland degradation. This is the first demonstration of the involvement of an engulfment factor in a self-degradative cell death mechanism.

Autophagy is required for salivary gland cell death (Berry and Baehrecke, 2007), and we found that *drpr* knockdown prevented the induction of autophagy in dying salivary glands. We found that Atg1 expression in *drpr* mutants suppressed the failure in salivary gland degradation, suggesting that Atg1 functions downstream of Drpr in salivary gland cell death. Surprisingly, we found that *drpr* knockdown is cell-autonomously required for the induction of autophagy in salivary gland cells; however *drpr* knockdown does not prevent the induction of autophagy in the larval fatbody of starved larvae. Autophagy induced in the larval fatbody in response to starvation is associated with tissue and organism survival (Scott et al., 2004), whereas autophagy induced in salivary glands in response to a rise in the hormone ecdysone is associated with cell death (Berry and Baehrecke, 2007; Lee and Baehrecke, 2001).

This is the first example of a factor that is required for autophagy associated with cell death, but not for autophagy associated with cell survival in response to starvation.

How Drpr functions in a pathway with autophagy genes remains unknown, and a number of outstanding questions remain to be answered that will serve as the basis for future studies. It is unknown how Drpr is activated in dying salivary glands. Given what we know, it could be that Drpr is activated in response to ecdysone, since a rise in ecdysone titer triggers the onset of salivary gland cell death. We will test this hypothesis by probing for Drpr protein levels in available ecdysone-regulated gene mutants including *ßFTZ-F1*, *BR-C*, *E74A*, and *E93* mutants. A recent report identified *pretaporter* as the *Drosophila* ligand for Drpr in the phagocytosis of apoptotic cells (Kuraishi et al., 2009). We checked microarray data from our lab and found that *pretaporter* gene RNA increases 92.5 fold between 6h and 14h after puparium formation (Clough, Lee and Baehrecke, unpublished). We have obtained *pretaporter* mutants and will test the requirement of this gene for salivary gland degradation and autophagy induction in salivary glands.

The precise role of Drpr in the activation of autophagy during cell death remains unknown. We identified the presence of several engulfment factors in dying salivary glands by proteomics and microarray studies. In addition to Drpr, the engulfment receptors Croquemort (Crq) and Six-microns-under (Simu) function in *Drosophila* cell corpse engulfment (Franc et al., 1999; Kurant et al., 2008). Previous Baehrecke lab studies have shown that Crq is localized to the cytoplasm in *Drosophila* salivary glands (Lee and Baehrecke, 2001). Furthermore, Simu functions upstream of Drpr in cell corpse engulfment (Kurant et al., 2008). Studies in *C.elegans*

have shown that CED-1-dependent cell corpse engulfment requires the adaptor protein CED-6, the GTPase Rac1 (CED-10), and Dynamin (Kinchen et al., 2005; Liu and Hengartner, 1998; Su et al., 2002; Yu et al., 2006b). In addition, *C. elegans* engulfing cell cytoskeletal rearrangement requires CED-2 (Crk), CED-5 (mbc/Dock180), and CED-12 (ELMO), as well as Rac1 (Gumienny et al., 2001; Reddien and Horvitz, 2000; Wu and Horvitz, 1998). In *Drosophila*, Drpr and Ced-6 are required for the engulfment of severed axons by glia during axonal pruning (Awasaki et al., 2006; Freeman et al., 2003; Hoopfer et al., 2006; MacDonald et al., 2006; Williams et al., 2006).

We therefore screened for the requirement of these engulfment genes in salivary gland cell death. *simu* mutants, as well as animals expressing RNAi in salivary glands against *crq*, *rab7*, *rac1*, *rac2*, *crk*, *ced-12*, and *mbc* all exhibited salivary gland degradation phenotypes, suggesting that these genes may function in salivary gland cell death (**Figure 4-1**). Although *ced-6* knockdown did not result in a salivary gland degradation phenotype, we recently tested *ced-6* excision mutants (Kuraishi et al., 2009) and found that ced-6 mutants/deficiency do have persistent salivary gland fragments. I next plan to test whether knockdown of the engulfment genes with salivary gland degradation phenotypes also affect autophagy induction in dying salivary glands. As many of these downstream engulfment factors may be pleiotropic, we will also test whether knockdown of these genes in salivary glands affects caspase activation.

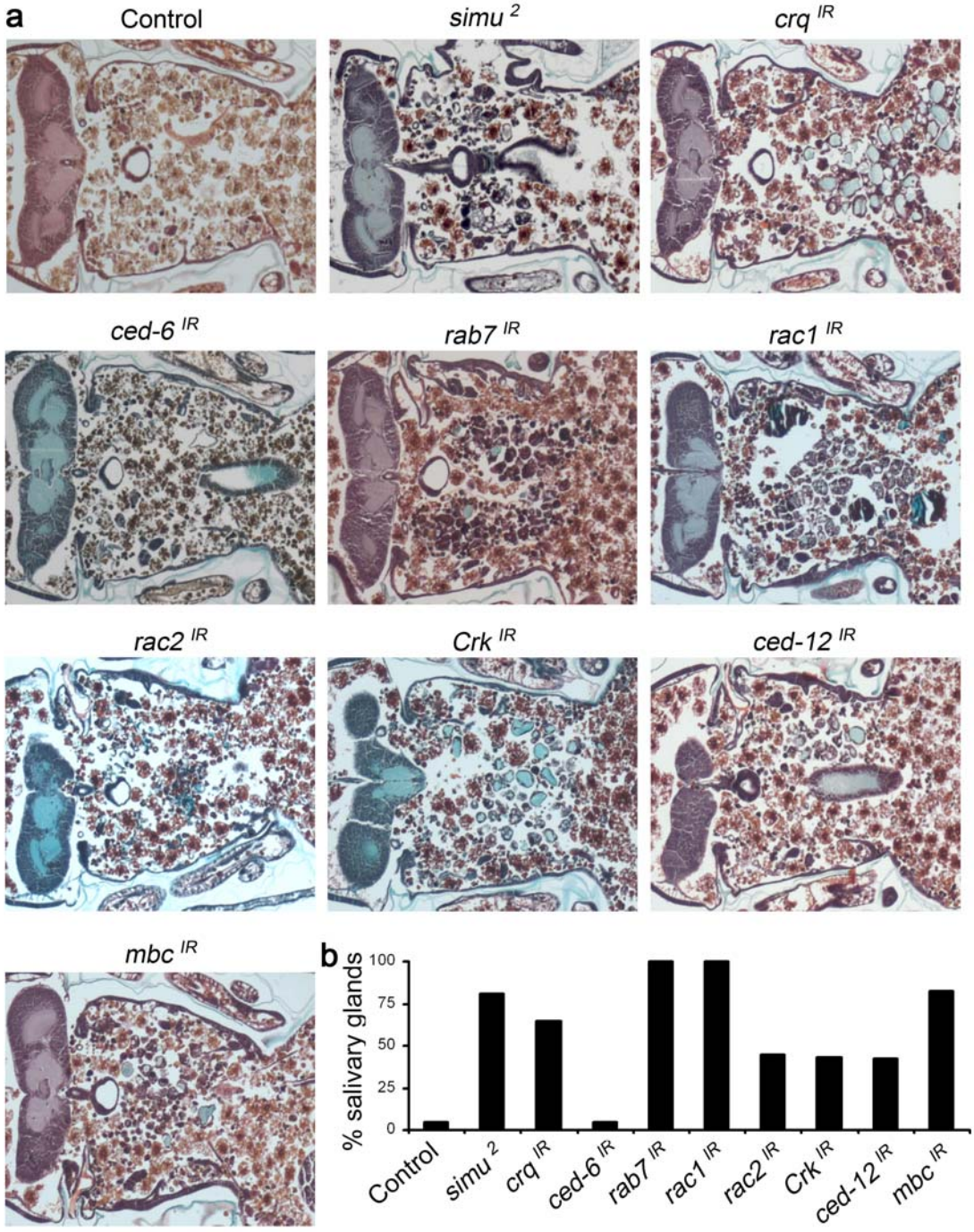

Figure 4-1. Engulfment gene screen.

a, Control animals (+/w^{1118}), n=20, *simu* homozygous mutants ($simu^2/simu^2$), n=11 and those with salivary gland-specific knockdown of the following genes: *crq* (*fkh*-

GAL4/*w*; UAS-*crq*^{IR}/+), n=20, *ced-6* (*fkh*-GAL4/*w*; UAS-*ced-6*^{IR}/+), n=22, *rab7* (*fkh*-GAL4/*w*; UAS-*rab7*^{IR}/+), n=20, *rac1* (*fkh*-GAL4/*w*; UAS-*rac1*^{IR}/+), n=19, *rac2* (*fkh*-GAL4/*w*; UAS-*rac2*^{IR}/+), n=20, *crk* (*fkh*-GAL4/*w*; UAS-*crk*^{IR}/+), n=14, *ced-12* (*fkh*-GAL4/*w*; UAS-*ced-12*^{IR}/+), n=19, *and mbc* (*fkh*-GAL4/*w*; UAS-*mbc*^{IR}/+), n=17, were analyzed by histology for the presence of salivary glands 24h after puparium formation. **b,** quantification of data from **a.**

Drpr-mediated phagocytosis of severed axons by glia requires the Src family kinase Src42a and the non-receptor tyrosine kinase Shark via interactions that are similar to mammalian ITAM signaling (Ziegenfuss et al., 2008). It could be that these genes or a similar signaling mechanism requiring phosphorylation of an ITAM motif by a Src family kinase and the binding of a non-receptor tyrosine kinase might also be required for salivary gland cell death and Drpr-dependent induction of autophagy in salivary glands. There are three Src family kinases in *Drosophila*, Src42A, Src64B, and btk29A. We expressed RNAi against all three of these genes specifically in salivary glands and obtained strong phenotypes with both *src42a-RNAi* and *src64b*-RNAi expression (**Figure 4-2**). Therefore it may be that Src signaling is required for salivary gland cell death.

We wondered whether *shark* might be required for salivary gland degradation. To test this, we expressed RNAi against *shark* in salivary glands and this did not prevent salivary gland destruction (data not shown), even though expression of this shark-RNAi prevents glial uptake of severed axons (Ziegenfuss et al., 2008). There are other non-receptor kinases in *Drosophila* that might function downstream of Drpr in salivary gland cell death, including Focal Adhesion protein 56D (Fak) and Abl Tyrosine Kinase (Abl). We expressed RNAi against these genes in salivary glands and whereas the expression of *abl*-RNAi did not affect salivary gland degradation, all pupae expressing *fak*-RNAi in salivary glands (n=20) exhibited a defect in salivary gland degradation. Therefore my preliminary data indicate that in salivary glands, Drpr activity requires the SH2-domain containing protein Fak.

These data provide a starting point for future investigations of the role of Drpr-mediated signaling in salivary gland cell death, and in the induction of autophagy in dying salivary glands. We will test whether RNAi knockdown of *src42a*, *src64b*, and *fak* in salivary glands prevents autophagy induction. We will also test whether knockdown of these genes affects caspase activation. To test whether Drpr and Fak physically interact, we will express tagged versions of these genes in pull-down assays. We will also express available Drpr ITAM motif mutants to test whether the ITAM motif is required for Drpr-Fak binding.

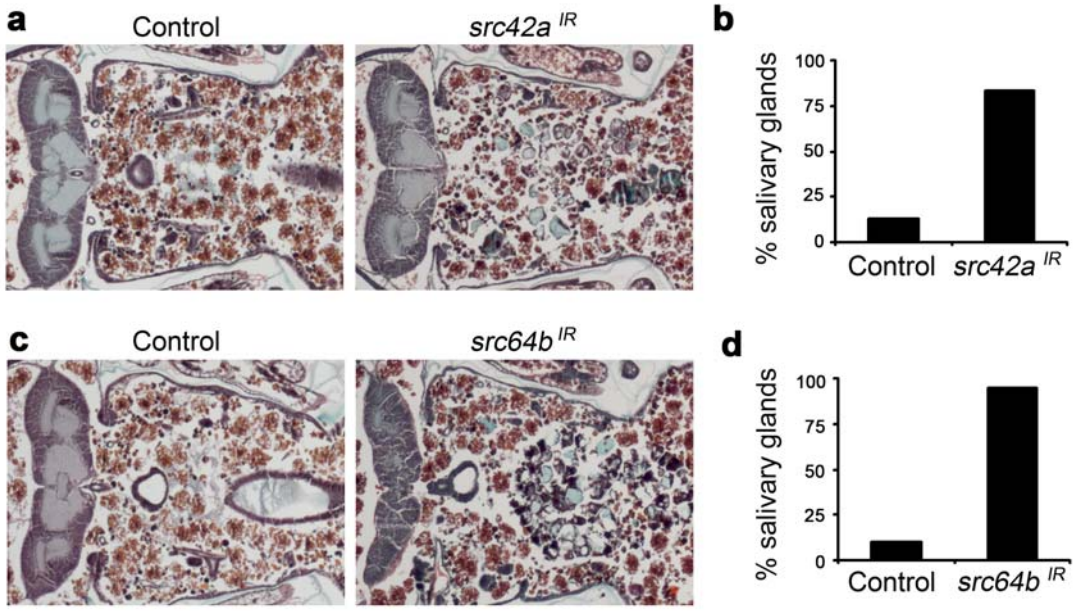

Figure 4-2. Knockdown of *src* genes prevents salivary gland degradation.

a, Control animals (+/*w*; +/UAS-*src42a*^{IR}), n=8, and those with salivary gland-specific knockdown of *src42a* (*fkh*-GAL4/*w*; UAS-*src42a*^{IR}/+), n=18, were analyzed by histology for the presence of salivary glands 24h after puparium formation. **b,** quantification of data from **a. c,** Control animals (+/*w*; +/UAS-*src64b*^{IR}), n=10, and those with salivary gland-specific knockdown of *src64b* (*fkh*-GAL4/*w*; UAS-*src64b*^{IR}/+), n=19, were analyzed by histology for the presence of salivary glands 24h after puparium formation. **d,** quantification of data from **b.**

Alternative splicing generates three Drpr isoforms, Drpr-I, II, and III, each containing different extracellular and intracellular sequences (Freeman et al., 2003)(Logan and Freeman, in preparation). We showed that Drpr-I is required for salivary gland degradation. Splice variants II and III have fewer EGF repeats than variant I; splice variant II contains an alternatively spiced 11 amino acid exon in the intracellular domain; splice variant III is identical to variant II, except that it includes an alternative exon that includes a stop codon (Freeman et al., 2003)(Freeman et al Neuron 2003). Drpr-II/III isoforms are up-regulated in dying salivary glands 12 hours after puparium formation, and decline by 14 hours after puparium formation even though Drpr I levels remain elevated (**Figure 3-1a**). Recent evidence indicates that the additional amino acids found in Drpr-II interrupt the Drpr ITAM motif to produce a putative immunoreceptor tyrosine-based inhibitory motif (ITIM) (Barrow and Trowsdale, 2006)(Logan & Freeman, in preparation). Logan and Freeman found that Drpr-II inhibits Drpr-I activity by recruiting the phosphatase Corkscrew (Csw) that de-phosphorylates and de-activates Drpr-I (Logan & Freeman, in preparation).

We tested whether expression of Drpr-II is sufficient to inhibit salivary gland degradation, and found that 91% of pupae that express Drpr-II in salivary glands exhibited a defect in gland clearance (**Figure 4-3a,b**). This result suggests that Drpr-II expression in salivary glands inhibits proper gland destruction, and this could be due to Drpr-II inhibition of Drpr-I. If Drpr-II inhibits the activity of Drpr-I in salivary glands, then we would expect Drpr-II mis-expression to inhibit Drpr-I and autophagy. We tested whether expression of Drpr-II in ds-Red-marked salivary gland clone cells inhibits autophagy, and found that GFP-Atg8a is diffuse with reduced GFP puncta in

Drpr-II expressing cells (**Figure 4-3c**). These data suggest that Drpr-II may act to inhibit Drpr-I-dependent salivary gland autophagy induction and degradation. It could be that Drpr-II inhibits Drpr-I activity through a similar mechanism as in glial degradation of severed axons, through the activity of the phosphatase Csw, and we will test whether this is the case in salivary glands.

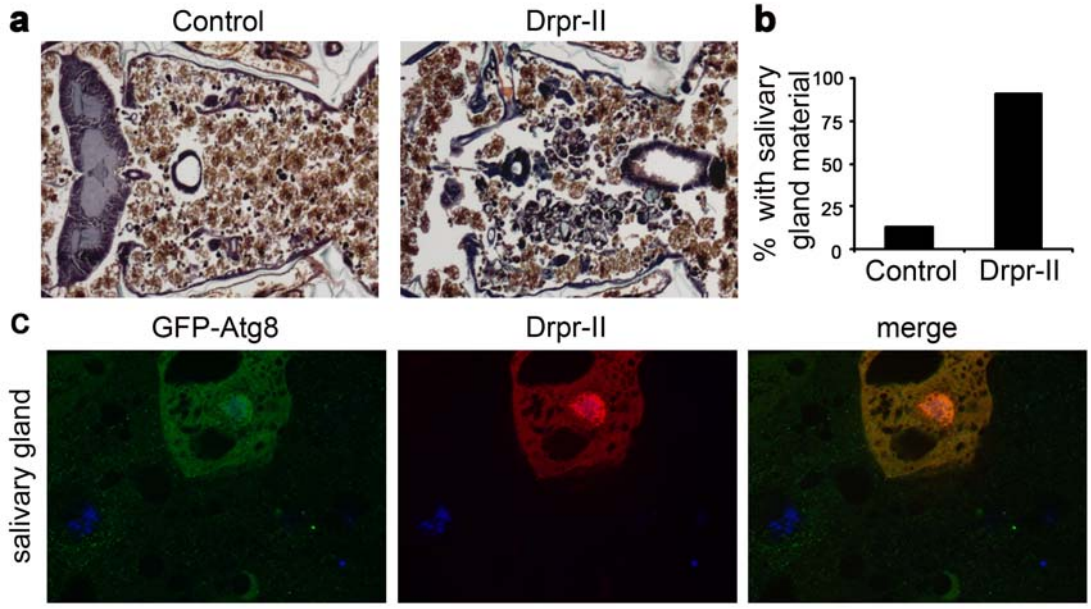

Figure 4-3. Mis-expression of Drpr-II isoform prevents salivary gland degradation and the cell-autonomous induction of autophagy in salivary glands. **a,** Control animals (+/*w*; +/UAS-Drpr-II), n=15, and those with salivary gland-specific expression of Drpr-II (*fkh*-GAL4/*w*; UAS-Drpr-II/+), n=22, were analyzed by histology for the presence of salivary glands 24h after puparium formation. **b,** quantification of data from **a**. **c,** Salivary glands of animals expressing GFP-Atg8 in all cells, and Drpr-II specifically in dsRed-marked clone cells (hsflp/*w*; UAS-Drpr-II/+; hsGFPAtg8b, *act*<FRT,cd2, FRT>Gal4, UAS-dsRed/+) were dissected 14h after puparium formation. Salivary glands were imaged for GFPAtg8 (green) and dsRed (red). Nuclei were stained with Höescht (blue).

We demonstrated that Drpr is required for autophagy induction in dying salivary glands, and that Atg1 functions downstream of Drpr. It is still unclear, however, how Drpr signaling affects autophagy induction. There are two known mechanisms which function to regulate autophagy. During nutrient availability, TOR represses autophagy via Atg13 phosphorylation; upon starvation, TOR repression of autophagy is relieved, leading to Atg13 dephosphorylation and Atg1 activation (Kamada et al., 2010; Scott et al., 2007). In addition, the Atg6/Vps34 complex is required for autophagy, and Vps34 is required for the production of PI(3) phosphate (PI(3)P) at the autophagic membrane. In *Drosophila*, Vps34 is also regulated by TOR-dependent signaling (Juhász et al., 2008).

Drpr may function to repress TOR activity and thus allow for the induction of autophagy. Phosphorylated S6 Kinase and phosphorylated Akt have been used as a read-out for TOR activity in *Drosophila* (Juhász et al., 2008). To test whether Drpr affects Tor signaling, we could probe for Drpr, phospho-S6K, S6K, and phospho-Akt using in western blots of salivary gland extracts of *drpr*-/- null mutants compared to *drpr*+/- controls. We would expect to see changes in phospho-Akt and phospho-S6K in *drpr* mutants compared to controls if Drpr affects Tor signaling. Ideally, we would test the phosphorylation status of Atg13 in drpr null mutants compared to drpr+/- controls using a phospho-specific antibody in western blots of salivary gland extracts, but such an antibody does not exist at this time.

It is also possible that Drpr signaling might not affect TOR signaling but might directly affect Atg13 or the Atg6/Vps34 complexes. If Drpr affects Atg13 but not TOR, then we would expect that disruption of Drpr signaling would affect Atg13

phosphorylation status but not S6K or Akt phosphorylation status. We could test this by assaying for Atg13 phosphorylation in salivary gland extracts of *drpr* null mutants compared to *drpr*+/- Controls and probe extracts with anti-phospho-specific-Atg13 antibody. If this hypothesis is correct, then we would expect to find that Atg13 would be phosphorylated (and inactive) in *drpr* null mutants but de-phosphorylated (and active) in controls.

Alternatively, Drpr might affect Vps34 directly. Vps34 generates the monophosphorylated lipid PtdIns3P, which recruits PX (Phox homology) and FYVE domain-containing proteins to membranes (Backer, 2008; Lindmo and Stenmark, 2006). Vps34 activity has been successfully monitored using a reporter for PI(3)P, GFP-2X-FYVE, which was shown to change localization from perinuclear to cytoplasmic upon starvation in a Vps34-dependent manner in the *Drosophila* fatbody (Juhász et al., 2008). To test whether Drpr affects Vps34 activity, we could monitor GFP-2X-FYVE localization in drpr null mutant salivary glands compared to Control drpr+/- salivary glands. We would expect that the localization of GFP-2X-FYVE would not change from perinuclear to cytoplasmic in drpr mutants. One of the problems with this experiment is that PI(3)P regulates all vesicular traffic and we do not know how to distinguish between PI(3)P in different types of vesicles. However if we do see an autophagy- and also a Drpr-dependent change in PI(3)P localization, then this would provide a starting point for further investigation of this question using this assay.

Finally, a study in mammalian cells suggests an additional hypothesis for a possible mechanism of Drpr-dependent signaling to autophagy. In Yeast, the

Atg1/Atg13 protein kinase complex includes Atg17 (Cheong et al., 2005). An Atg17 orthologue has not been reported in flies or mammals. However, the mammalian FAK-interacting protein FIP200 is required for autophagosome formation in mammalian cells, and has been suggested to play a role analogous to that of Atg17 as it functions with ULK-1, the mammalian Atg1 ortholog (Hara et al., 2008). This study found that in FIP200-deficient cells, both the stability and phosphorylation of ULK1/Atg1 were impaired, suggesting that FIP200 functions upstream of ULK1/Atg1 (Hara et al., 2008). I found that a protein-protein BLAST of FIP200 identified the *Drosophila* protein CG1347 as the closest-related fly homolog to FIP200. I searched salivary gland microarray data and found that *CG1347* is induced 14-fold between 6h and 12h in dying salivary glands, and *fak* is induced 15-fold between 6h and 14h (Clough, Lee, and Baehrecke unpublished). In light of my finding that expression of *fak*-RNAi in salivary glands prevents salivary gland degradation (data not shown), it is possible that a mechanism involving Drpr, Fak, and CG1347 may affect autophagy induction in salivary glands. I will test the requirement of *CG1347* in salivary gland cell death by expressing RNAi against this gene in salivary glands. I will also test the requirement of this gene for autophagy induction during salivary gland cell death, and whether this gene functions upstream of Atg1 in salivary glands. If I find positive results, then I will test whether *CG1347* functions in parallel to or in the same pathway as *drpr* and/or *fak* during salivary gland cell death.

Revised model for autophagic cell death

Based upon my research, I propose a revised model for autophagic cell death regulation (**Figure 4-4**). Previous work in the Baehrecke lab has shown that autophagic cell death of *Drosophila* larval salivary glands is induced by steroid signaling, which induces many genes including caspase and autophagy regulators (Lee and Baehrecke, 2001; Lee et al., 2003). Caspases function in salivary gland cell death, and autophagy genes are also required for degradation (Berry and Baehrecke, 2007; Martin and Baehrecke, 2004). Autophagy and caspases function in parallel during this type of cell death, as the combined inhibition of autophagy and caspases enhances the incomplete destruction of salivary glands when either caspases or autophagy are inhibited alone (Berry and Baehrecke, 2007). Growth arrest via down-regulation of the PI3K pathway is required for autophagy induction in salivary glands (Berry and Baehrecke, 2007). Furthermore, Warts (Wts) influences PI3K signaling and is required for the induction of autophagy and salivary gland cell death (Dutta and Baehrecke, 2008).

My studies indicate that the engulfment receptor Drpr is required for the induction of autophagy and salivary gland cell degradation. How Drpr is activated and signals to influence autophagy induction is unknown. Drpr may be activated by steroid signaling and/or may be induced by a ligand. My data indicate that other engulfment factors are also required for salivary gland degradation, but it is not known whether these factors are also required for autophagy induction. Drpr could regulate TOR signaling directly. Alternatively, Drpr might directly influence Atg

genes, and this may require other engulfment factors. How Drpr is induced, and how Drpr signals to influence autophagy, is the subject of ongoing investigations.

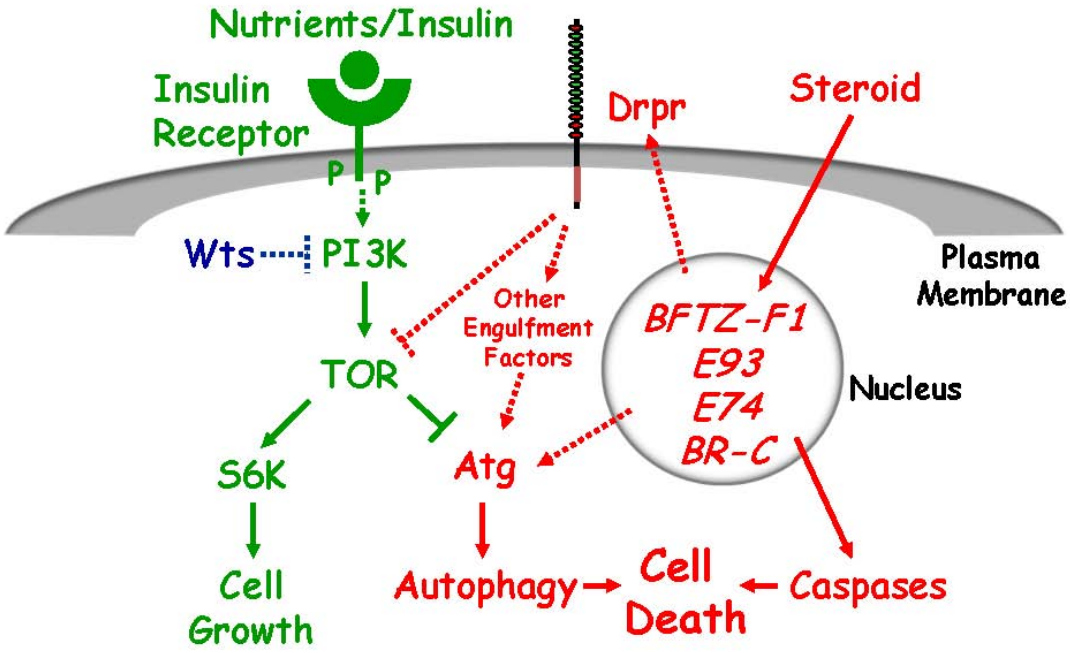

Figure 4-4. A model for autophagic cell death in salivary glands

This model provides a relationship between steroid signaling, nutrient availability, cell growth, engulfment genes, and cell death in salivary glands. Steroid signaling modulates cell death by influencing the transcription of many genes including regulators of caspases and autophagy. Nutrient availability regulates cell growth and autophagy via Target of Rapamycin (TOR). Wts also regulates cell growth and autophagy by modulating the PI3K pathway. The engulfment receptor Drpr is required for cell death and the induction of autophagy. Drpr may be regulated in response to steroid signaling in dying salivary glands, or may be induced by a ligand. How Drpr regulates autophagy in salivary glands is unknown. Drpr could influence autophagy by regulating TOR. Alternatively, Drpr could regulate Autophagy (Atg) proteins directly or through a signaling cascade involving other engulfment factors.

A model for apoptotic versus autophagic cell death

Here I have demonstrated that engulfment genes are required for the cell autonomous degradation of *Drosophila* larval salivary glands *in vivo*. I propose that the events that take place in a single cell during autophagic cell death could be a fusion of the events that take place in two cells during apoptosis. During apoptotic cell death, caspases are activated in the dying cell. The nucleus and cytoplasm of this dying cell become condensed, and this cell displays "eat-me" ligands that are recognized by a secondary phagocytic cell. The phagocyte recognizes and binds to "eat-me" ligands via engulfment receptors present on the engulfing cell. The dead cell is engulfed and eventually degraded by the lysosomal system within the phagocyte. During autophagic cell death, caspases are also activated within the dying cell. However, the autophagy and lysosomal machinery within the dying cell itself are required for degradation of the dying cell. This type of cell death occurs without known phagocytosis by a secondary cell; rather, engulfment receptors present in the dying cell are required for the induction of autophagy and subsequent cell degradation. Therefore, the main difference between these two types of cell death is the location of the lysosomal and engulfment machinery that are required to degrade the contents of the dying cell.

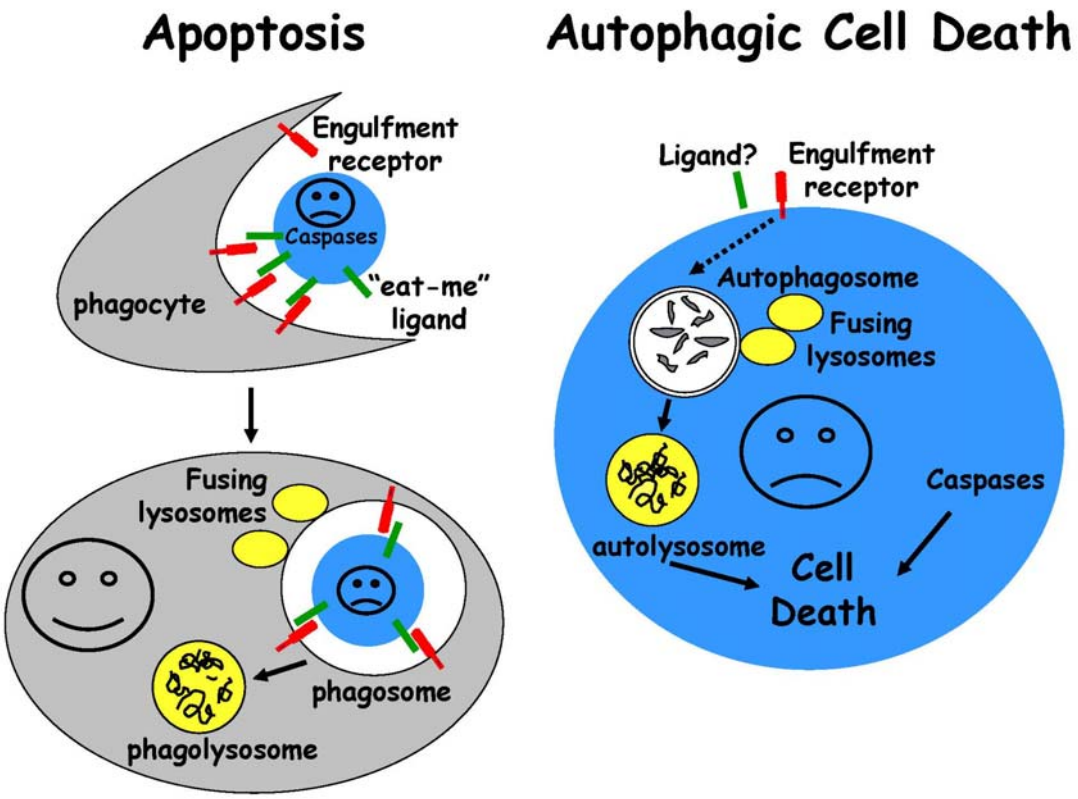

Figure 4-5. A model for apoptotic versus autophagic cell death.

During apoptosis, caspases are activated and the nucleus and cytoplasm become condensed. Engulfment receptors on a secondary phagocyte recognize "eat-me" ligands presented on the surface of the apoptotic cell. The dead cell is engulfed by the phagocyte and internalized into the phagosome. Lysosomes of the engulfing cell deliver lysosomal hydrolases to the phagosome, and the dead cell is degraded in the phagolysosome of the engulfing cell. During autophagic cell death, caspases are activated but cell destruction is not known to involve phagocytosis by a secondary cell. Engulfment genes present within the dying cell itself are required for autophagy induction. It is unknown whether engulfment receptors are activated by a ligand during autophagic cell death. Lysosomes fuse with autophagosomes to form autolysosomes, where contents are degraded. Thus the main difference between these

two morphological forms of cell death is the location of the phagocytosis machinery and the lysosomal system used to degrade cellular contents.

Appendices

Appendix 1: List of proteins identified in Wild-type *Drosophila* salivary glands by proteomics 6h, 12h, and 13h after puparium formation.

Protein names and FBgn numbers are based on Flybase annotation (http://flybase.org/). The values for peptides mapped to the genes listed are indicated. Protein quantities were determined using the spectral counting method in which spectral counts (spectral peptide matches) for each protein were summed and normalized across runs based on the total spectral counts obtained for each run.

Symbol	FBgn	6h AVE	12h AVE	13h AVE
128up	FBgn0010339	0.066191	0.048288	0.043507
14-3-3epsilon	FBgn0020238	0.462569	0.371323	0.47237
14-3-3zeta	FBgn0004907	0.691078	0.47563	0.518494
26-29-p	FBgn0250848	0.115894	0.065037	0.067989
825-Oak	FBgn0052208	0	0.009672	0
a	FBgn0000008	0.000928	0.000542	0
Aac11	FBgn0027885	0.026001	0.010579	0.01998
Aats-ala	FBgn0027094	0.123929	0.079474	0.068264
Aats-arg	FBgn0027093	0.054783	0.032078	0.027713
Aats-asn	FBgn0086443	0.08095	0.045175	0.044867
Aats-asp	FBgn0002069	0.200084	0.144135	0.132551
Aats-gln	FBgn0027090	0.036528	0.04583	0.047445
Aats-glupro	FBgn0005674	0.040311	0.041851	0.033569
Aats-gly	FBgn0027088	0.214828	0.154228	0.117486
Aats-his	FBgn0027087	0.030949	0.019767	0.023029
Aats-ile	FBgn0027086	0.040722	0.031396	0.02683
Aats-leu	FBgn0027085	0	0	0.00087
Aats-lys	FBgn0027084	0.11008	0.061806	0.066345
Aats-thr	FBgn0027081	0.154146	0.091194	0.114437
Aats-trp	FBgn0010803	0.292688	0.128174	0.078475
Aats-tyr	FBgn0027080	0.105259	0.054438	0.042382
Aats-val	FBgn0027079	0.039333	0.032158	0.029939
ab	FBgn0259750	0.00067	0	0
Abi	FBgn0020510	0.00128	0.003684	0.004051
Abl	FBgn0000017	0.000508	0.001076	0

AcCoAS	FBgn0012034	0.017915	0.017492	0.030451
Acer	FBgn0016122	0.009753	0.001143	0.002689
Acon	FBgn0010100	0.298008	0.098922	0.161918
Acox57D-p	FBgn0034628	0	0	0.001117
Acp62F	FBgn0020509	0	0.012525	0.006551
Acph-1	FBgn0000032	0.00941	0.037418	0.034167
Act42A	FBgn0000043	2.781777	3.75264	2.975351
Act57B	FBgn0000044	2.459391	3.163034	3.2852
Act5C	FBgn0000042	3.075786	4.214029	3.310572
Act79B	FBgn0000045	1.598198	2.130262	2.094357
Act87E	FBgn0000046	2.410966	3.022153	3.211995
Act88F	FBgn0000047	2.185765	2.307599	2.36169
Actn	FBgn0000667	0.230928	0.314706	0.362739
ade2	FBgn0000052	0.002712	0.002732	0.008797
ade3	FBgn0000053	0.012663	0.011214	0.049967
ade5	FBgn0020513	0.062751	0.06801	0.156363
Adgf-A	FBgn0036752	0.001126	0.011054	0.010827
Adh	FBgn0000055	1.044687	1.598486	1.368144
Adk1	FBgn0022709	0	0.003145	0.02256
Adk2	FBgn0022708	0.126205	0.169235	0.21544
Adk3	FBgn0042094	0.042781	0.031634	0.028893
Ag5r	FBgn0015010	0.345804	0.033403	0.095581
AGO1	FBgn0026611	0.001438	0	0.003995
AGO2	FBgn0087035	0.016321	0.00184	0.005057
Ahcy13	FBgn0014455	0.206793	0.129541	0.177145
Ahcy89E	FBgn0015011	0.009576	0.007034	0.004291
AIF	FBgn0031392	0.000819	0	0
Akap200	FBgn0027932	0.131439	0.101655	0.117096
Akt1	FBgn0010379	0.007363	0.0092	0.00806
alc	FBgn0260972	0	0.003385	0.003438
Ald	FBgn0000064	1.304932	1.850448	1.583974
Aldh-III	FBgn0010548	0.032492	0.034638	0.041773
alien	FBgn0013746	0.001374	0	0.002711
ALiX	FBgn0086346	0.027876	0.014986	0.02105
alph	FBgn0086361	0.001644	0.010587	0.008336
alpha4GT2	FBgn0039378	0	0.002338	0
alpha-Adaptin	FBgn0015567	0.001951	0.00336	0.012054
alpha-Cat	FBgn0010215	0.001344	0	0
alphaCop	FBgn0025725	0.260867	0.410814	0.348454
alpha-Est2	FBgn0015570	0.002194	0.007977	0.024208
alpha-Est7	FBgn0015575	0.022146	0.029211	0.057119
alpha-Man-I	FBgn0259170	0	0.004557	0.001172
alphaPS4	FBgn0034005	0.002021	0.0027	0.000745
alpha-Spec	FBgn0250789	0.103421	0.09179	0.091812
alphaTub67C	FBgn0087040	0.044681	0.027824	0.041431
alphaTub84B	FBgn0003884	1.042825	1.59214	1.196756

alphaTub84D	FBgn0003885	1.042825	1.59214	1.196756
alphaTub85E	FBgn0003886	0.580113	0.881919	0.658924
alt	FBgn0038535	0.032285	0.052932	0.045791
Aly	FBgn0010774	0.011462	0.006459	0.010727
Ama	FBgn0000071	0.122971	0.026691	0.038227
Amun	FBgn0030328	0.046757	0.003168	0.002188
Amy-d	FBgn0000078	0.038773	0	0
ana1	FBgn0039206	0.00226	0.001368	0
Ance	FBgn0012037	0.082731	0.007598	0.01209
Ance-4	FBgn0033366	0.004974	0.004686	0.00122
Ank	FBgn0011747	0.008873	0.007294	0.004734
Ank2	FBgn0085445	0	0	0.000766
AnnIX	FBgn0000083	0.288704	0.181736	0.177159
AnnX	FBgn0000084	0.113732	0.093968	0.089667
Ant2	FBgn0025111	0.105096	0.057723	0.078911
Anxb11	FBgn0030749	0.05782	0.093941	0.13111
Aos1	FBgn0029512	0.044235	0.016826	0.020748
AP-1gamma	FBgn0030089	0.008103	0.015731	0.015652
AP-1sigma	FBgn0039132	0	0.004744	0
AP-47	FBgn0024833	0.059205	0.052652	0.061421
AP-50	FBgn0024832	0.021116	0.005	0.02216
APC4	FBgn0052707	0.000804	0.000961	0.00292
ApepP	FBgn0026150	0.065793	0.032141	0.024139
aPKC	FBgn0022131	0.002364	0.001188	0.001986
APP-BP1	FBgn0261112	0.001155	0	0.001438
Aprt	FBgn0000109	0.006748	0.007914	0
Arc42	FBgn0038742	0.0258	0.005395	0.008458
Arc-p20	FBgn0031781	0.010941	0.00872	0.004484
Arc-p34	FBgn0032859	0.014153	0.011579	0.013982
Ard1	FBgn0036064	0.081305	0.012691	0.016704
Arf102F	FBgn0013749	0.227257	0.298131	0.358858
Arf72A	FBgn0000115	0.033048	0.039367	0.078822
Arf79F	FBgn0010348	0.340669	0.525316	0.675613
Arf84F	FBgn0004908	0.003314	0	0
arg	FBgn0023535	0.00313	0.007362	0.020793
Argk	FBgn0000116	1.010286	1.275723	1.387779
ari-1	FBgn0017418	0.001204	0	0.001864
arm	FBgn0000117	0.004433	0	0
Arp11	FBgn0031050	0.001613	0.004545	0.003184
Arp14D	FBgn0011742	0.029082	0.014454	0.013949
Arp53D	FBgn0011743	0.059819	0.139342	0.066837
Arp66B	FBgn0011744	0.096049	0.049152	0.046538
Arp87C	FBgn0011745	0.141781	0.048438	0.053955
Arpc3A	FBgn0038369	0.01944	0	0.012669
Art1	FBgn0037834	0.004888	0.013669	0.015254
Art3	FBgn0038306	0	0.002105	0.002539

Art4	FBgn0037770	0	0	0.002271
Art8	FBgn0032329	0.001826	0	0
As	FBgn0061469	0	0.001531	0.001237
asf1	FBgn0029094	0.003774	0.004577	0.003456
ash2	FBgn0000139	0	0	0.002536
asp	FBgn0000140	0	0.000381	0
asparagine-synthetase	FBgn0041607	0.013134	0.005251	0.004789
Atac1	FBgn0031876	0.007486	0.002023	0.002124
Ate1	FBgn0025720	0.00126	0	0.001556
Atg18	FBgn0035850	0	0.002647	0.008568
Atg2	FBgn0044452	0	0.000398	0.000402
Atg4	FBgn0031298	0.027368	0.001752	0.00184
Atg5	FBgn0029943	0.002251	0	0.004474
Atg8a	FBgn0052672	0.053948	0.032461	0.044213
Atg9	FBgn0034110	0	0	0.002695
atl	FBgn0039213	0.03435	0.030957	0.055689
atms	FBgn0010750	0	0.001339	0.0014
Atox1	FBgn0052446	0.198861	0.208815	0.138455
ATP7	FBgn0030343	0.0005	0	0
Atpalpha	FBgn0002921	0.016246	0.032831	0.040034
ATPCL	FBgn0020236	0.222681	0.108395	0.187255
ATPsyn-b	FBgn0019644	0.167337	0.044081	0.141274
ATPsyn-beta	FBgn0010217	0.825138	0.928476	1.115798
ATPsyn-Cf6	FBgn0016119	0.226049	0.131545	0.205287
ATPsyn-d	FBgn0016120	0.348008	0.285394	0.418865
ATPsyn-gamma	FBgn0020235	0.359014	0.175422	0.23825
AttA	FBgn0012042	0.008148	0	0
AttB	FBgn0041581	0.008372	0	0
Aut1	FBgn0036813	0.00557	0.002182	0.003647
aux	FBgn0037218	0.000912	0	0.001139
awd	FBgn0000150	1.898877	1.691522	1.328554
B52	FBgn0004587	0.104788	0.09022	0.076937
baf	FBgn0031977	0.109372	0.047	0.141863
bai	FBgn0045866	0.156801	0.173684	0.213667
Bap	FBgn0010380	0.030189	0.044936	0.062517
Bap170	FBgn0042085	0.001897	0	0
Bap60	FBgn0025463	0.006764	0.001398	0.003806
bchs	FBgn0043362	0.000236	0	0
BEAF-32	FBgn0015602	0.002209	0.006092	0.00695
bel	FBgn0000171	0.101041	0.082948	0.078239
ben	FBgn0000173	0.134096	0.123123	0.142097
Bet1	FBgn0260857	0	0.008528	0
Bet3	FBgn0260859	0.07007	0.01802	0.013961
betaCop	FBgn0008635	0.181713	0.234549	0.236477
beta'Cop	FBgn0025724	0.141779	0.276084	0.265695

betaggt-I	FBgn0015000	0.004665	0	0
betaggt-II	FBgn0028970	0.005923	0	0.005521
beta-Spec	FBgn0250788	0.034734	0.04301	0.04699
betaTub56D	FBgn0003887	1.926209	3.097866	2.513356
betaTub60D	FBgn0003888	0.755714	1.168588	1.012664
betaTub85D	FBgn0003889	1.070154	1.558541	1.34996
betaTub97EF	FBgn0003890	0.481381	0.679789	0.551715
bic	FBgn0000181	0.214039	0.345252	0.33791
BicD	FBgn0000183	0.015247	0.010127	0.006207
bif	FBgn0014133	0.001097	0.001573	0.002575
bip1	FBgn0026263	0	0	0.002237
Bj1	FBgn0002638	0.088625	0.033893	0.03294
bl	FBgn0015907	0.044655	0.015179	0.023239
blue	FBgn0041161	0.003493	0	0
blw	FBgn0011211	0.620994	0.485882	0.529313
BM-40-SPARC	FBgn0026562	0.011416	0.002369	0.007454
bnb	FBgn0001090	0.085535	0	0
boca	FBgn0004132	0.16602	0.150583	0.150989
bocksbeutel	FBgn0037719	0.006135	0.004367	0.006141
bor	FBgn0040237	0.012457	0	0
bou	FBgn0261284	0.004063	0.004999	0.005076
br	FBgn0000210	0.010917	0.011825	0.006292
brm	FBgn0000212	0.000875	0	0
bsf	FBgn0032679	0.002899	0.00102	0.000536
Bsg	FBgn0011219	0.006839	0.042511	0.056272
bsk	FBgn0000229	0.014258	0	0.005268
bt	FBgn0005666	0.010727	0.041147	0.085064
btz	FBgn0045862	0	0.001779	0
bun	FBgn0259176	0.000502	0	0
bur	FBgn0000239	0.014822	0.007312	0.024468
Bx42	FBgn0004856	0	0.003186	0
c11.1	FBgn0040236	0.00043	0.00246	0.001071
CaBP1	FBgn0025678	0.285217	0.21298	0.236343
Cad96Ca	FBgn0022800	0.000806	0	0
Caf1	FBgn0015610	0.074613	0.048197	0.059157
CAH1	FBgn0027844	0.004565	0.005426	0.012949
CalpA	FBgn0012051	0.000752	0.000899	0.003499
CalpB	FBgn0025866	0.000673	0.001884	0.006232
cals	FBgn0039928	0.000637	0	0
Cam	FBgn0000253	0.282645	0.232966	0.74585
CaMKII	FBgn0004624	0.001175	0.005575	0.018565
CanA1	FBgn0010015	0.000973	0.002316	0.001573
CanB	FBgn0010014	0.003587	0	0.028156
CanB2	FBgn0015614	0.010915	0.00587	0.03927
CAP	FBgn0033504	0.003488	0	0.001857
Ca-P60A	FBgn0004551	0.084942	0.077548	0.095303

Cap-D3	FBgn0051989	0	0.001062	0
capt	FBgn0261458	0.208664	0.370993	0.264422
car	FBgn0000257	0	0.001167	0
Cas	FBgn0022213	0.017386	0.005322	0.00472
Cat	FBgn0000261	0.358573	0.360643	0.364349
Catsup	FBgn0002022	0.005926	0.003881	0.004267
caz	FBgn0011571	0.006124	0.004367	0.003016
CBP	FBgn0026144	0.002696	0	0
Cbp20	FBgn0022943	0.011935	0	0.012726
Cbp53E	FBgn0004580	0	0	0.00243
Cby	FBgn0067317	0	0	0.00605
Ccp84Aa	FBgn0004783	0.010089	0	0.005871
Ccp84Ab	FBgn0004782	0.009359	0	0
Ccp84Ad	FBgn0004780	0.030111	0	0.006048
Ccp84Ae	FBgn0004779	0.002994	0.060398	0.038902
Ccp84Ag	FBgn0004777	0.019026	0.014342	0.016954
CCS	FBgn0010531	0.050365	0.014971	0.011983
Cctgamma	FBgn0015019	0.1467	0.087378	0.097231
CD98hc	FBgn0037533	0.009011	0.020433	0.040197
Cda4	FBgn0052499	0.005475	0	0
CDase	FBgn0039774	0	0	0.001074
cdc2	FBgn0004106	0.002053	0	0
Cdc37	FBgn0011573	0.05151	0.036198	0.02506
Cdc42	FBgn0010341	0.017123	0.02678	0.046725
cdi	FBgn0004876	0.000499	0	0
Cdk5	FBgn0013762	0.002074	0.011771	0.004094
Cdlc2	FBgn0026141	0.417651	0.550544	0.544059
CdsA	FBgn0010350	0	0.001611	0.005887
CecA1	FBgn0000276	0	0	0.023915
CecA2	FBgn0000277	0	0	0.023915
CecC	FBgn0000279	0	0	0.023915
Cenp-C	FBgn0086697	0	0	0.00067
cg	FBgn0000289	0.002422	0	0
CG10005	FBgn0037972	0.005317	0	0
CG10069	FBgn0034611	0	0.001272	0.001331
CG10077	FBgn0035720	0.002993	0.00091	0.002067
CG10083	FBgn0036372	0.034269	0.014007	0.010483
CG10096	FBgn0038032	0	0.003303	0.008315
CG10098	FBgn0037472	0.21424	0.125212	0.112249
CG10103	FBgn0035715	0.015196	0.00524	0.012382
CG10126	FBgn0038088	0.055831	0.058642	0.070311
CG10131	FBgn0033949	0.004149	0.002433	0.005722
CG10133	FBgn0036366	0.004574	0	0
CG10140	FBgn0036363	0.008959	0	0
CG10154	FBgn0036361	0.00842	0	0
CG10166	FBgn0032799	0.123126	0.060324	0.123585

CG10175	FBgn0039084	0.014592	0.00113	0
CG10184	FBgn0039094	0.044151	0.083068	0.136574
CG10188	FBgn0032796	0	0	0.00079
CG10194	FBgn0032790	0.005249	0	0
CG10217	FBgn0039113	0.001329	0.001203	0.001944
CG10221	FBgn0028475	0.003978	0.003037	0.002763
CG10225	FBgn0039110	0.021817	0.010406	0.01031
CG10237	FBgn0032783	0	0.090934	0.080994
CG10277	FBgn0037442	0	0	0.002245
CG10289	FBgn0035688	0.006386	0.003237	0.001367
CG10306	FBgn0034654	0.094687	0.084032	0.123501
CG10333	FBgn0032690	0	0	0.00118
CG10340	FBgn0022344	0.009711	0.005347	0.011691
CG10343	FBgn0032703	0.006673	0.008143	0.008106
CG10347	FBgn0030342	0.004557	0.00172	0
CG10353	FBgn0030349	0	0.00069	0
CG10359	FBgn0035452	0	0.003185	0.003771
CG10399	FBgn0031877	0.016461	0.004535	0.007452
CG1041	FBgn0037440	0.079418	0.027512	0.031398
CG10413	FBgn0032689	0.001748	0.000765	0.001993
CG10414	FBgn0032691	0	0	0.000973
CG10418	FBgn0036277	0.040799	0.039091	0.05435
CG10420	FBgn0039296	0.011422	0	0.009137
CG10424	FBgn0036848	0.012877	0.007284	0.013571
CG10425	FBgn0039304	0.001815	0.00297	0.00279
CG10433	FBgn0034638	0	0	0.019245
CG10463	FBgn0032819	0	0	0.001252
CG10467	FBgn0035679	0.142631	0.038752	0.044511
CG10470	FBgn0032746	0.008093	0	0
CG10512	FBgn0037057	0.085639	0.106979	0.106112
CG10516	FBgn0036549	0.002405	0	0.002203
CG10527	FBgn0034583	0.186035	0.232608	0.28834
CG10535	FBgn0037926	0.001517	0	0.001395
CG10555	FBgn0030034	0.001331	0	0
CG10559	FBgn0039323	0	0.00247	0
CG10565	FBgn0037051	0.008879	0.001153	0
CG10576	FBgn0035630	0.493486	0.451545	0.419299
CG10585	FBgn0037044	0.001351	0	0
CG10590	FBgn0035622	0.001052	0.025732	0.033087
CG10602	FBgn0032721	0.104304	0.037991	0.064235
CG10616	FBgn0036286	0.002163	0.012272	0.021728
CG10621	FBgn0032726	0	0	0.00232
CG10623	FBgn0032727	0.112248	0.043878	0.053525
CG10625	FBgn0035612	0.001206	0	0
CG10627	FBgn0036298	0.070774	0.014859	0.017145
CG10635	FBgn0035603	0.0326	0.019858	0.009819

CG10638	FBgn0036290	0.186375	0.10134	0.101532
CG10639	FBgn0032729	0.026972	0.010135	0.006212
CG10641	FBgn0032731	0	0.012629	0.005546
CG10650	FBgn0046302	0.01202	0	0
CG10657	FBgn0036289	0	0	0.00641
CG10664	FBgn0032833	0.010075	0.034072	0.026284
CG10672	FBgn0035588	0.007804	0.006893	0.013911
CG10673	FBgn0035590	0.00278	0.00665	0.019495
CG10688	FBgn0036300	0.055518	0.058273	0.072963
CG10710	FBgn0036377	0	0.001016	0
CG10721	FBgn0032846	0.001292	0	0
CG10754	FBgn0036314	0	0	0.004559
CG10777	FBgn0029979	0.003245	0.001576	0.003109
CG10802	FBgn0029664	0.011763	0.003997	0.001728
CG10830	FBgn0038839	0.008958	0	0.005279
CG10834	FBgn0032972	0.006241	0	0
CG10853	FBgn0035478	1.009118	1.69619	1.03455
CG10877	FBgn0038804	0.001412	0	0
CG10881	FBgn0038796	0.057665	0.046033	0.05948
CG10882	FBgn0031408	0.158096	0.251357	0.219554
CG1091	FBgn0037470	0.001199	0.004877	0.004181
CG10932	FBgn0029969	0.297561	0.121906	0.173488
CG10943	FBgn0036320	0	0	0.013039
CG10958	FBgn0030004	0.000821	0.001939	0.002036
CG10960	FBgn0036316	0	0.003058	0.003211
CG10962	FBgn0030073	0.014746	0.023435	0.064386
CG10973	FBgn0036306	0.003226	0	0
CG10990	FBgn0030520	0.024541	0.012652	0.045083
CG10992	FBgn0030521	0.258453	0.402907	0.371688
CG11009	FBgn0036318	0.02499	0.014908	0.02028
CG11015	FBgn0031830	0.143346	0.13252	0.118136
CG1104	FBgn0037467	0.091616	0.114303	0.087937
CG1105	FBgn0037465	0.001445	0.014968	0.024728
CG11050	FBgn0031836	0.001572	0	0
CG11069	FBgn0039244	0	0	0.001247
CG11070	FBgn0028467	0.001443	0	0
CG11089	FBgn0039241	0.271433	0.264041	0.380378
CG11092	FBgn0027537	0	0.002963	0.003844
CG11134	FBgn0030518	0.046235	0.03911	0.067412
CG11148	FBgn0039936	0.001945	0	0.003438
CG1115	FBgn0037299	0.00576	0.011508	0.011449
CG11151	FBgn0030519	0.35397	0.249279	0.418181
CG11178	FBgn0030499	0	0.008468	0.012756
CG11188	FBgn0031851	0	0.002045	0.018589
CG11241	FBgn0037186	0.001619	0	0
CG11242	FBgn0034451	0.02039	0.010721	0.007221

CG11255	FBgn0036337	0.0427	0.037382	0.062587
CG11266	FBgn0031883	0	0.001254	0
CG11267	FBgn0036334	0.548263	0.222286	0.251863
CG11284	FBgn0030056	0.002439	0	0.006939
CG11309	FBgn0037070	0.00174	0.011216	0.016766
CG11313	FBgn0039798	0.03369	0	0
CG11334	FBgn0039849	0.019717	0.062522	0.083509
CG11347	FBgn0035542	0	0.001861	0
CG11367	FBgn0037185	0	0.002756	0
CG11377	FBgn0031217	0.001665	0.005843	0.002616
CG11378	FBgn0040364	0.009842	0.002308	0.010267
CG11384	FBgn0040363	0	0.00245	0.001594
CG1140	FBgn0035298	0.011019	0	0.006381
CG11406	FBgn0034990	0.247714	0.017545	0.019616
CG11409	FBgn0024366	0	0	0.001606
CG11414	FBgn0035024	0.005942	0	0.000872
CG11423	FBgn0034251	0.00379	0.001026	0
CG11444	FBgn0029715	0.03336	0.031782	0.025034
CG11459	FBgn0037396	0	0	0.002251
CG11474	FBgn0034688	0.004206	0.001656	0.012709
CG11490	FBgn0031233	0.001151	0	0.001054
CG11523	FBgn0037156	0.028391	0.004714	0
CG11526	FBgn0035437	0.000672	0	0
CG11570	FBgn0036230	0	0	0.007915
CG11577	FBgn0036847	0.008238	0	0.012911
CG11594	FBgn0035484	0.005576	0	0.012687
CG11710	FBgn0031115	0	0.001945	0
CG11739	FBgn0037239	0.028612	0.004487	0.02468
CG11771	FBgn0039252	0.002512	0	0
CG11779	FBgn0038683	0.007599	0.001569	0.003295
CG11790	FBgn0039265	0.029222	0.027016	0.060588
CG11811	FBgn0036099	0.005346	0	0.011469
CG11854	FBgn0039299	0.002439	0	0
CG11857	FBgn0039303	0.081624	0.120507	0.129525
CG11870	FBgn0037804	0	0.00061	0
CG11874	FBgn0039634	0	0.001087	0.005718
CG11875	FBgn0039301	0	0.002327	0
CG11876	FBgn0039635	0.217954	0.126587	0.251126
CG11880	FBgn0039637	0	0	0.004058
CG11882	FBgn0039642	0.003128	0	0
CG11899	FBgn0014427	0.00226	0.018009	0.045827
CG11900	FBgn0039650	0	0.004023	0
CG11902	FBgn0028647	0	0.001945	0.001513
CG11909	FBgn0039330	0.000928	0	0
CG11943	FBgn0031078	0	0	0.001575
CG11964	FBgn0037644	0	0.001282	0

CG11975	FBgn0037648	0.001794	0	0
CG11980	FBgn0037652	0.096274	0.073278	0.113842
CG11982	FBgn0037653	0.001639	0	0
CG11985	FBgn0040534	0.014449	0	0
CG11999	FBgn0037312	0.200092	0.227566	0.163692
CG12004	FBgn0035236	0	0	0.001877
CG12007	FBgn0037293	0.002394	0	0
CG12024	FBgn0035283	0.022221	0.003615	0.004361
CG12030	FBgn0035147	0.834988	0.955384	0.771677
CG12038	FBgn0035179	0	0	0.002287
CG12063	FBgn0039851	0.001851	0	0
CG12065	FBgn0030052	0.002104	0	0
CG12068	FBgn0039695	0.00182	0.005202	0.002921
CG12079	FBgn0035404	0.117091	0.042369	0.111887
CG12082	FBgn0035402	0.053662	0.024448	0.019903
CG12084	FBgn0043458	0	0	0.004832
CG12093	FBgn0035372	0.0019	0	0
CG12112	FBgn0030048	0.004093	0	0
CG12119	FBgn0030102	0.072548	0.014271	0.019438
CG12130	FBgn0033466	0	0.001331	0.009549
CG12163	FBgn0260462	0.01894	0.034886	0.049243
CG12171	FBgn0037354	0.251031	0.138667	0.155022
CG12173	FBgn0037305	0.007197	0.002909	0.002954
CG12203	FBgn0031021	0.060398	0.040373	0.067425
CG12224	FBgn0037974	0.004118	0.009798	0.028378
CG12237	FBgn0031048	0.003971	0.005695	0
CG12241	FBgn0038304	0	0.000926	0.002663
CG12262	FBgn0035811	0.141514	0.127261	0.152853
CG12264	FBgn0032393	0.003978	0.003118	0
CG12279	FBgn0038080	0.224833	0.204565	0.213363
CG12288	FBgn0032620	0	0.001656	0.001739
CG12301	FBgn0036514	0.000791	0	0
CG12304	FBgn0036515	0.01905	0.007374	0.013648
CG12310	FBgn0036467	0.045193	0	0
CG12321	FBgn0038577	0.026535	0.014877	0.028047
CG12338	FBgn0033543	0	0	0.007314
CG12343	FBgn0033556	0.005397	0.004415	0
CG1236	FBgn0037370	0.158688	0.152113	0.227883
CG12360	FBgn0038111	0.012625	0.001876	0.001416
CG12398	FBgn0030596	0.000956	0	0
CG1240	FBgn0035370	0.085657	0.054859	0.048907
CG12400	FBgn0031505	0.033301	0	0.014602
CG12404	FBgn0032465	0.006979	0.013108	0.009269
CG12413	FBgn0039588	0.000876	0.003104	0.001087
CG12428	FBgn0039543	0	0.001165	0.00489
CG12433	FBgn0030811	0.009191	0	0.008523

CG12455	FBgn0028859	0.000278	0	0
CG12481	FBgn0030542	0.068183	0	0
CG12483	FBgn0040688	0	0	0.008594
CG12512	FBgn0031703	0.005515	0.001214	0
CG12519	FBgn0036872	0.02041	0.016868	0.025531
CG12560	FBgn0031974	0.00231	0	0
CG12582	FBgn0037215	0.001343	0.001099	0.001032
CG12608	FBgn0030630	0.001377	0	0
CG12703	FBgn0031069	0.00091	0	0.002543
CG1271	FBgn0035392	0.001156	0	0
CG12715	FBgn0030443	0.093257	0.066322	0.071651
CG12734	FBgn0035411	0.000451	0	0
CG1275	FBgn0035321	0	0.002964	0.008065
CG12773	FBgn0024365	0	0	0.001058
CG12811	FBgn0037779	0.03422	0	0.004618
CG12848	FBgn0040666	0.006856	0	0
CG12883	FBgn0039538	0.009096	0.004744	0.009596
CG1291	FBgn0035401	0.013958	0.02514	0.032854
CG12926	FBgn0033437	0	0.002379	0.003845
CG13041	FBgn0036605	0.005023	0	0.009706
CG13043	FBgn0036600	0.012389	0	0.008132
CG13044	FBgn0036599	0.079259	0	0
CG13049	FBgn0036592	0.088791	0.069544	0.015991
CG13059	FBgn0036607	0.065243	0	0
CG13060	FBgn0036606	0.004754	0	0.009187
CG13077	FBgn0032810	0	0	0.003485
CG1308	FBgn0035507	0.001071	0	0.000441
CG1309	FBgn0035519	0.005852	0.001374	0.003734
CG13096	FBgn0032050	0.000915	0.001465	0
CG13097	FBgn0032051	0.000941	0	0
CG13117	FBgn0032140	0	0	0.006848
CG13124	FBgn0032156	0	0	0.00236
CG1316	FBgn0035526	0.010417	0.005292	0.01351
CG13189	FBgn0033665	0	0	0.002209
CG1319	FBgn0035529	0.05185	0.018544	0.038781
CG13284	FBgn0032614	0	0	0.002327
CG13295	FBgn0035674	0	0	0.001559
CG13343	FBgn0033882	0	0	0.002675
CG13360	FBgn0025620	0	0.003538	0
CG13364	FBgn0026879	0.223287	0.042819	0.072329
CG13366	FBgn0025633	0.000656	0	0
CG13369	FBgn0025640	0.012807	0.00245	0.013006
CG13393	FBgn0032035	0	0.037109	0.054444
CG1342	FBgn0039795	0.092509	0.001148	0
CG1344	FBgn0027507	0.000944	0	0.003057
CG13457	FBgn0036482	0.000661	0.000781	0.000817

CG1347	FBgn0037363	0.000479	0	0
CG13472	FBgn0036450	0.001469	0	0
CG13492	FBgn0034662	0.000411	0.001251	0.002222
CG13506	FBgn0034723	0.001212	0.003967	0.003001
CG1354	FBgn0030151	0.277396	0.198217	0.18064
CG13551	FBgn0040660	0.350299	0.142303	0.252239
CG13567	FBgn0034963	0	0	0.007935
CG13569	FBgn0034979	0	0.000836	0
CG13630	FBgn0039219	0.00821	0.003983	0.007254
CG13634	FBgn0039224	0	0	0.002605
CG13641	FBgn0039239	0	0	0.005305
CG13674	FBgn0035858	0.010551	0	0
CG13779	FBgn0040954	0.046204	0	0.033788
CG13813	FBgn0036956	0.042752	0.001675	0.007545
CG13822	FBgn0039098	0.047422	0	0
CG13827	FBgn0039068	0.002598	0	0.005165
CG13842	FBgn0039009	0.001585	0	0
CG13887	FBgn0035165	0.129231	0.112609	0.138682
CG13890	FBgn0035169	0.002284	0.016492	0.060842
CG13900	FBgn0035162	0.003163	0.003427	0.003567
CG13907	FBgn0035173	0	0.002136	0.008214
CG13928	FBgn0035246	0	0.002939	0.006913
CG13962	FBgn0032824	0	0.024014	0.054681
CG13991	FBgn0031785	0.000931	0	0
CG13993	FBgn0031776	0	0	0.033985
CG13994	FBgn0031772	0.018759	0.008987	0.00464
CG14000	FBgn0031749	0.00313	0	0.0019
CG14005	FBgn0031739	0.00191	0.002272	0
CG14043	FBgn0031659	0	0	0.004012
CG14062	FBgn0039592	1.33488	0.53871	0.380145
CG14095	FBgn0036870	0	0.004597	0
CG14096	FBgn0036871	0.006743	0	0
CG14103	FBgn0036908	0.00408	0	0.005025
CG14109	FBgn0036364	0	0.019026	0.016742
CG14125	FBgn0036232	0	0.010705	0.021561
CG14126	FBgn0036223	0	0.0033	0
CG1416	FBgn0032961	0.045605	0.056151	0.047975
CG14184	FBgn0036932	0	0.004138	0.005436
CG14207	FBgn0031037	0.391354	0.450692	0.448468
CG14215	FBgn0031052	0	0	0.000357
CG14216	FBgn0031054	0.006255	0.003819	0.005018
CG14220	FBgn0031036	0	0	0.002867
CG14232	FBgn0031061	0.001714	0	0.002507
CG14235	FBgn0031066	0.159822	0.448635	0.45192
CG14285	FBgn0038674	0	0.00485	0.002546
CG14286	FBgn0038673	0.00919	0.003601	0.008674

CG14291	FBgn0038660	0.005818	0.001374	0.001443
CG14362	FBgn0038186	0	0.035199	0.014686
CG1440	FBgn0030038	0.069483	0.101343	0.105476
CG14407	FBgn0030584	0.02057	0.004684	0.015409
CG14434	FBgn0029915	0.010922	0.005336	0
CG14438	FBgn0029899	0	0.000225	0
CG14476	FBgn0027588	0.156117	0.17881	0.218846
CG14526	FBgn0027578	0.009565	0.003199	0.003977
CG14527	FBgn0039613	0.003497	0.002093	0.00108
CG14542	FBgn0039402	0.010444	0	0.010438
CG14544	FBgn0039407	0.007708	0.005497	0.007593
CG1458	FBgn0062442	0.066168	0.035132	0.04521
CG14629	FBgn0040398	0.060865	0.018446	0.030357
CG14630	FBgn0014903	0	0.002858	0.009109
CG14636	FBgn0037217	0	0	0.003094
CG14641	FBgn0037220	0	0.004169	0
CG1468	FBgn0030157	0	0.00834	0.015551
CG14681	FBgn0037820	0	0	0.000961
CG14688	FBgn0037819	0.00425	0.002509	0.014043
CG14696	FBgn0037853	0.001363	0	0
CG14722	FBgn0037943	0.004092	0	0.001519
CG14767	FBgn0040777	0	0.001683	0
CG14782	FBgn0025381	0.006106	0	0.004796
CG14786	FBgn0027794	0	0.001344	0.002286
CG14787	FBgn0027793	0	0	0.006515
CG14812	FBgn0026090	0	0.009978	0.030222
CG14815	FBgn0023516	0	0.001288	0
CG14823	FBgn0035734	0.00467	0	0.009305
CG14841	FBgn0038218	0	0	0.004392
CG1486	FBgn0031174	0.102048	0.091815	0.090083
CG14876	FBgn0038368	0	0.0018	0
CG14894	FBgn0038428	0.010117	0.005477	0.007285
CG14899	FBgn0038438	0.007042	0.026518	0.013136
CG14933	FBgn0040968	0.023871	0	0
CG14935	FBgn0032382	0	0	0.001341
CG14939	FBgn0032378	0	0	0.001863
CG14946	FBgn0032405	0	0	0.002521
CG14971	FBgn0035449	0	0	0.002566
CG14985	FBgn0035482	0.019515	0	0
CG1499	FBgn0039852	0.002939	0	0
CG14990	FBgn0035496	0.010143	0	0.002349
CG14997	FBgn0035515	0.002697	0	0.001655
CG15032	FBgn0030626	0.005172	0.009893	0.00272
CG15080	FBgn0034391	0.00107	0	0
CG15093	FBgn0034390	0.443551	0.147154	0.154018
CG15100	FBgn0034401	0.04662	0.023988	0.028697

CG15111	FBgn0034419	0.001484	0.002428	0.002281
CG15118	FBgn0034418	0.001974	0.004395	0.008557
CG15145	FBgn0032649	0	0.000822	0
CG1516	FBgn0027580	0.137376	0.090591	0.192133
CG15168	FBgn0032732	0	0.009154	0.01385
CG15169	FBgn0032734	0	0	0.002192
CG1518	FBgn0031149	0	0	0.003174
CG15202	FBgn0030271	0.11421	0.137597	0.163572
CG15239	FBgn0029681	0.001263	0.001511	0.01183
CG15283	FBgn0028844	0	0.002657	0
CG15293	FBgn0028526	0.00799	0.004473	0.013523
CG15309	FBgn0030183	0.00535	0	0.006608
CG1532	FBgn0031143	0.100579	0.063789	0.055637
CG15343	FBgn0030029	0.00865	0.013871	0.004594
CG15356	FBgn0031377	0.000609	0	0
CG15369	FBgn0030105	0.655656	0.105912	0.183624
CG15404	FBgn0031512	0.111076	0.375227	0.197742
CG15438	FBgn0025684	0	0.00561	0.005148
CG15445	FBgn0031161	0.00741	0.00301	0.00169
CG15523	FBgn0039727	0	0	0.000645
CG15630	FBgn0031627	0	0	0.001674
CG15715	FBgn0036538	0.079794	0.009672	0
CG15717	FBgn0030451	0.081256	0.068158	0.101613
CG1572	FBgn0030309	0	0	0.007522
CG15725	FBgn0030417	0.000819	0	0
CG15727	FBgn0030410	0.002074	0	0
CG15735	FBgn0030364	0.006661	0.009197	0.012517
CG15743	FBgn0030465	0.010931	0.050908	0.053159
CG1578	FBgn0030336	0.000691	0.000799	0.003926
CG15784	FBgn0029766	0.011438	0.009392	0.00767
CG15814	FBgn0030873	0.0019	0.007749	0.013247
CG1582	FBgn0030246	0.001424	0	0
CG15820	FBgn0035312	0	0.002338	0.003908
CG15828	FBgn0032136	0	0	0.001052
CG15829	FBgn0035743	0.014874	0.024337	0.05317
CG15881	FBgn0036909	0.026935	0.007337	0.017158
CG15891	FBgn0029860	0.004093	0	0
CG1600	FBgn0033188	0.007075	0.049039	0.062114
CG1607	FBgn0039844	0.003649	0	0.003348
CG1622	FBgn0030468	0.003097	0	0
CG1637	FBgn0030245	0.005913	0.003201	0.005847
CG1640	FBgn0030478	0.062355	0.042516	0.077107
CG1648	FBgn0033446	0.026402	0.018134	0.037894
CG1665	FBgn0033451	0.001832	0	0.002224
CG16704	FBgn0031558	0.143157	0.008374	0.020171
CG16712	FBgn0031561	0.434334	0.128743	0.116463

CG16713	FBgn0031560	0.179251	0.009083	0
CG1674	FBgn0039897	0.039288	0.041339	0.072104
CG16758	FBgn0035348	0.0019	0.006807	0.025465
CG1677	FBgn0029941	0	0.001743	0
CG1681	FBgn0030484	0	0	0.006382
CG16817	FBgn0037728	0.092305	0.091798	0.151593
CG16892	FBgn0030122	0.001309	0.001545	0.004206
CG16903	FBgn0040394	0	0	0.0035
CG16908	FBgn0037741	0.031419	0.052222	0.038483
CG16935	FBgn0033883	0.023507	0.010224	0.056656
CG16936	FBgn0027590	0.292571	0.182986	0.24566
CG16940	FBgn0035111	0.001168	0.000713	0.001153
CG16941	FBgn0038464	0.000772	0	0
CG1695	FBgn0031116	0	0.000649	0
CG16979	FBgn0036512	0.011134	0.026676	0.02853
CG16985	FBgn0035355	0.0261	0.004999	0
CG16986	FBgn0035356	0.004233	0	0
CG1702	FBgn0031117	0.008119	0	0.003317
CG17024	FBgn0032437	0.004653	0.003709	0.006765
CG17026	FBgn0036550	0.009307	0.009649	0.01128
CG1703	FBgn0030321	0.080691	0.00859	0.015835
CG17032	FBgn0036547	0.001955	0	0
CG17065	FBgn0031099	0.008868	0.003513	0.004055
CG17109	FBgn0039051	0.008198	0	0
CG17119	FBgn0039045	0.005133	0.002513	0.002361
CG17121	FBgn0039043	0.003415	0	0.00419
CG17122	FBgn0036962	0.003415	0	0
CG17124	FBgn0032297	0	0	0.006075
CG17127	FBgn0032299	0.012355	0	0.009984
CG17134	FBgn0032304	0.003697	0	0
CG17173	FBgn0036447	0.0012	0	0
CG17184	FBgn0037884	0	0	0.002122
CG17186	FBgn0038741	0	0	0.001977
CG17202	FBgn0038043	0.011259	0.027213	0.016681
CG17219	FBgn0031494	0	0	0.006018
CG17224	FBgn0031489	0	0	0.004012
CG17244	FBgn0039031	0.019313	0.004684	0
CG17249	FBgn0035249	0.001292	0	0
CG17255	FBgn0030205	0.009562	0.004075	0.002513
CG17258	FBgn0031496	0.000713	0	0
CG17259	FBgn0031497	0.488774	0.376938	0.340798
CG17271	FBgn0038829	0.241389	0.243692	0.361673
CG17272	FBgn0038830	0.004063	0	0
CG17273	FBgn0027493	0.126274	0.05464	0.066943
CG17278	FBgn0046763	0.007785	0	0
CG17293	FBgn0032030	0	0	0.003797

CG17294	FBgn0032032	0.002442	0.002824	0.002954
CG17323	FBgn0032713	0	0	0.001457
CG17331	FBgn0032596	0.136265	0.169458	0.157836
CG17333	FBgn0030239	0.11076	0.032428	0.065522
CG1737	FBgn0030293	0.001949	0.001058	0.002078
CG17471	FBgn0039924	0.004529	0.001844	0.016208
CG1749	FBgn0030305	0.160926	0.127001	0.127348
CG1753	FBgn0031148	0.008211	0.003338	0.006831
CG17556	FBgn0038462	0.056104	0.050743	0.069469
CG17565	FBgn0038424	0.001455	0	0.004475
CG17593	FBgn0031544	0.003	0.005122	0.01392
CG17597	FBgn0032715	0.148215	0.19243	0.18675
CG17598	FBgn0031194	0.007598	0.00646	0.002314
CG17646	FBgn0031362	0	0.002243	0.002207
CG17660	FBgn0031356	0	0.005113	0.004985
CG17734	FBgn0037890	0.021635	0	0.009868
CG17737	FBgn0035423	0.275737	0.271284	0.337172
CG17746	FBgn0035425	0	0.008646	0
CG17754	FBgn0030114	0	0.005819	0.011119
CG17768	FBgn0032240	0.005342	0.009672	0.006088
CG17838	FBgn0038826	0.045611	0.045817	0.0524
CG17840	FBgn0031611	0.000706	0	0
CG17896	FBgn0023537	0.347693	0.15573	0.157626
CG17904	FBgn0032597	0.01182	0.013522	0.017823
CG17919	FBgn0037433	0.040448	0.003565	0.003744
CG17931	FBgn0038421	0.09878	0.012413	0.035684
CG17996	FBgn0032595	0.005168	0	0
CG18012	FBgn0038552	0.005966	0.009996	0.002194
CG18067	FBgn0034512	0.030226	0.005761	0.031285
CG18081	FBgn0036537	0.103833	0.041657	0.034172
CG18135	FBgn0036837	0.014382	0.039182	0.083604
CG18179	FBgn0036023	0	0.007446	0
CG18249	FBgn0037553	0	0.001798	0
CG18259	FBgn0030956	0.001287	0	0
CG18294	FBgn0036873	0.023256	0.015672	0.032256
CG1832	FBgn0032979	0.002633	0	0
CG18347	FBgn0260743	0.0019	0	0
CG1837	FBgn0030329	0.093478	0.117593	0.153846
CG18417	FBgn0035780	0	0.006977	0.007919
CG18418	FBgn0035568	0.003907	0	0
CG18445	FBgn0033476	0	0	0.002669
CG18477	FBgn0028864	0	0.003104	0.00326
CG18490	FBgn0036149	0	0.002581	0
CG18507	FBgn0028527	0	0	0.005637
CG18508	FBgn0028746	0	0.007275	0
CG18522	FBgn0038347	0.001447	0.001151	0.002485

CG18547	FBgn0037973	0.010605	0.012667	0.017031
CG18591	FBgn0031962	0	0.007661	0.024106
CG18594	FBgn0038973	0	0.071485	0.042066
CG18616	FBgn0260444	0.000981	0	0
CG18811	FBgn0042134	0.018526	0.013113	0.016618
CG18815	FBgn0042138	0.119422	0.055837	0.073319
CG1885	FBgn0030066	0.006636	0	0.006104
CG18858	FBgn0042175	0.019923	0.018484	0.029645
CG1890	FBgn0039869	0.011048	0	0.006848
CG1907	FBgn0039674	0.015362	0.002272	0.013508
CG1910	FBgn0022349	0.1747	0.118509	0.133343
CG1924	FBgn0030377	0.009986	0.009375	0.019567
CG1943	FBgn0037468	0.084965	0.104355	0.113313
CG1950	FBgn0030370	0.007187	0.009362	0.017943
CG1951	FBgn0039623	0.00073	0.000892	0
CG1962	FBgn0032876	0	0	0.000957
CG1968	FBgn0033401	0.001957	0.006234	0.013388
CG1969	FBgn0039690	1.022044	0.698334	0.706771
CG1970	FBgn0039909	0.029721	0.01668	0.030769
CG1983	FBgn0039751	0.005622	0.002835	0.013168
CG2004	FBgn0030060	0.02935	0.041928	0.049041
CG2010	FBgn0039667	0	0	0.001469
CG2016	FBgn0250839	0.030446	0	0.015446
CG2021	FBgn0035271	0.027961	0.00784	0.064187
CG2023	FBgn0037383	0.008097	0.036727	0.032538
CG2025	FBgn0030344	0.003744	0.005109	0.008866
CG2046	FBgn0037378	0.027964	0.021065	0.044417
CG2051	FBgn0037376	0.003525	0	0
CG2064	FBgn0033205	0.100449	0.008729	0.011612
CG2070	FBgn0033203	0.005709	0.004432	0
CG2082	FBgn0027608	0	0	0.003748
CG2107	FBgn0035383	0.002641	0	0.001087
CG2118	FBgn0039877	0.013244	0.001136	0.001193
CG2120	FBgn0030005	0	0.002094	0
CG2145	FBgn0030251	0.036993	0.014913	0.029317
CG2147	FBgn0030025	0.032357	0.03015	0.014161
CG2177	FBgn0039902	0.003034	0.029347	0.008412
CG2200	FBgn0030447	0.11406	0.070777	0.082887
CG2233	FBgn0029990	0.319521	0.171641	0.333586
CG2246	FBgn0039790	0	0.001861	0.008174
CG2254	FBgn0029994	0.001906	0	0.002363
CG2263	FBgn0030007	0.034431	0.026222	0.023593
CG2277	FBgn0035204	0	0	0.001756
CG2444	FBgn0030326	0.194063	0.040771	0.11459
CG2493	FBgn0032864	0.01631	0.004548	0.01293
Cg25C	FBgn0000299	0.018097	0.024591	0.024315

CG2604	FBgn0037298	0.001448	0.002321	0.009537
CG2736	FBgn0035090	0.006022	0.004261	0.026093
CG2767	FBgn0037537	0.27295	0.199396	0.205079
CG2774	FBgn0031534	0.0667	0.035017	0.032462
CG2789	FBgn0031263	0.03985	0.003893	0.022383
CG2807	FBgn0031266	0.00092	0	0.003322
CG2812	FBgn0034931	0.041746	0.010015	0.010823
CG2846	FBgn0014930	0.029261	0.004868	0.015271
CG2862	FBgn0031459	0.272691	0.214224	0.169041
CG2915	FBgn0033241	0.111726	0.10017	0.062396
CG2918	FBgn0023529	0.226527	0.215231	0.248605
CG2924	FBgn0023528	0	0.00436	0.003055
CG2943	FBgn0037530	0.006253	0.004147	0.009046
CG2947	FBgn0029676	0.098113	0.061854	0.065602
CG2950	FBgn0031637	0.002815	0.001528	0.001498
CG2970	FBgn0034936	0.00944	0	0.007852
CG2976	FBgn0031633	0.03397	0.034262	0.033422
CG2990	FBgn0030170	0.000545	0	0
CG30022	FBgn0050022	0.019089	0	0.004314
CG30035	FBgn0050035	0	0	0.001495
CG3004	FBgn0030142	0.001948	0	0
CG30069	FBgn0050069	0.009106	0.019893	0.00786
CG3009	FBgn0029720	0.009515	0	0
CG30103	FBgn0050103	0.002067	0	0.001286
CG30104	FBgn0050104	0.007334	0.045468	0.033177
CG3011	FBgn0029823	0.127862	0.117555	0.200761
CG30115	FBgn0050115	0.003085	0	0.004171
CG30120	FBgn0050120	0	0.005142	0.004724
CG30122	FBgn0050122	0.014102	0.008015	0.008769
CG30152	FBgn0034543	0.009369	0.003416	0.003469
CG30185	FBgn0050185	0.054879	0.028514	0.046195
CG30193	FBgn0050193	0	0	0.001732
CG30197	FBgn0050197	0.012638	0.142145	0.206919
CG30291	FBgn0050291	0.078035	0.088507	0.077206
CG30344	FBgn0050344	0	0.00142	0.0072
CG30349	FBgn0050349	0.001327	0	0
CG30359	FBgn0050359	0.020226	0.025546	0.057321
CG30384	FBgn0050384	0	0.001256	0
CG30392	FBgn0050392	0.002793	0.003229	0.006756
CG30394	FBgn0050394	0	0	0.002513
CG3040	FBgn0029925	0	0	0.003165
CG30410	FBgn0050410	0.072996	0.066399	0.101274
CG30463	FBgn0050463	0.011035	0.073913	0.073333
CG30499	FBgn0050499	0.031293	0.025658	0.030194
CG3056	FBgn0024987	0.001406	0	0
CG3061	FBgn0038195	0	0.001946	0

CG3074	FBgn0034709	0.012854	0.045059	0.048944
CG3077	FBgn0031457	0	0.002209	0.003692
CG31012	FBgn0027598	0.008625	0.009293	0.004441
CG31048	FBgn0051048	0	0.00033	0.001121
CG31054	FBgn0051054	0	0.006006	0
CG31063	FBgn0051063	0.007529	0	0.014859
CG3107	FBgn0033005	0.002363	0	0.001895
CG31075	FBgn0051075	0.744571	0.346795	0.308723
CG31076	FBgn0051076	0	0	0.003965
CG31086	FBgn0051086	0	0.013484	0
CG31088	FBgn0051088	0.004552	0	0
CG31098	FBgn0051098	0	0	0.005134
CG31120	FBgn0051120	0.001138	0	0
CG31122	FBgn0051122	0	0	0.002297
CG31150	FBgn0051150	0.004462	0	0
CG31198	FBgn0051198	0	0.001062	0
CG31213	FBgn0051213	0	0.000483	0
CG31249	FBgn0051249	0.0073	0	0.007839
CG31294	FBgn0051294	0	0.003201	0
CG31300	FBgn0051300	0.004819	0	0
CG31313	FBgn0051313	0.13698	0.02343	0.061283
CG31315	FBgn0051315	0	0.011822	0
CG31343	FBgn0051343	0.001899	0.004785	0.007649
CG31352	FBgn0051352	0.008137	0.009481	0.010486
CG31357	FBgn0051357	0.00525	0.00189	0
CG31472	FBgn0051472	0.034493	0.012259	0.006357
CG31493	FBgn0051493	0	0.016225	0.004892
CG31546	FBgn0051546	0.009338	0.002821	0.002853
CG31548	FBgn0051548	0.116115	0.035323	0.032504
CG31549	FBgn0051549	0.071627	0.02019	0.025634
CG31550	FBgn0051550	0.00199	0	0
CG31551	FBgn0051551	0	0	0.000543
CG31636	FBgn0051636	0	0	0.004833
CG31637	FBgn0051637	0.001255	0	0
CG31639	FBgn0051639	0.101076	0.053945	0.07867
CG3164	FBgn0025683	0	0.016579	0.039057
CG31673	FBgn0051673	0	0.014257	0.025191
CG31674	FBgn0051674	0.009324	0.006682	0.00886
CG31683	FBgn0051683	0.033485	0.015062	0.024102
CG31687	FBgn0051687	0.000871	0	0
CG31688	FBgn0051688	0.001869	0	0
CG31689	FBgn0031449	0	0.001171	0.002749
CG31694	FBgn0051694	0.025506	0.014533	0.037973
CG31698	FBgn0051698	0.478413	0.433661	0.428809
CG31705	FBgn0028490	0.029982	0	0.002479
CG31715	FBgn0051715	0.216029	0.046659	0.064952

CG31716	FBgn0051716	0.000582	0	0
CG31729	FBgn0051729	0	0.000918	0.0009
CG31739	FBgn0051739	0.001699	0	0
CG31751	FBgn0086909	0.016617	0.011871	0.021299
CG31769	FBgn0051769	0	0	0.002432
CG31778	FBgn0051778	0	0.007061	0.020991
CG31780	FBgn0051780	0	0.003104	0.00326
CG31919	FBgn0031674	0.018236	0.022809	0.024566
CG31935	FBgn0051935	0.000666	0.002179	0.003376
CG31974	FBgn0051974	0.00445	0.005963	0.001824
CG31997	FBgn0051997	0	0	0.024687
CG31999	FBgn0051999	0.002887	0	0
CG32068	FBgn0052068	0.023019	0.032997	0.028734
CG32069	FBgn0052069	0	0	0.019752
CG32113	FBgn0052113	0	0.004087	0.001554
CG3214	FBgn0031436	0.027295	0.005072	0.008476
CG32147	FBgn0047178	0.050255	0.044088	0.049423
CG32164	FBgn0042177	0.004541	0.001335	0.003137
CG32165	FBgn0042178	0.004537	0.001334	0.003134
CG32186	FBgn0052186	0	0.000488	0.002361
CG32195	FBgn0052195	0	0	0.001886
CG32210	FBgn0052210	0.001409	0	0.000862
CG32214	FBgn0052214	0.008711	0.010564	0.008536
CG32226	FBgn0052226	0.000461	0	0.00056
CG3223	FBgn0037538	0.014292	0.004199	0.006982
CG32230	FBgn0052230	0.258938	0.047026	0.075501
CG3226	FBgn0029882	0.054247	0.035575	0.024936
CG32264	FBgn0052264	0	0.000714	0
CG32267	FBgn0052267	0.012711	0	0
CG32306	FBgn0052306	0	0.000793	0
CG32335	FBgn0063667	0.005708	0.009176	0.010638
CG32352	FBgn0052352	0	0	0.000769
CG32398	FBgn0052398	0	0.005864	0
CG32412	FBgn0052412	0.001794	0	0
CG32425	FBgn0052425	0.002595	0	0
CG3244	FBgn0031629	0.120242	0.019025	0.022352
CG32441	FBgn0052441	0.002431	0.008776	0.011636
CG3246	FBgn0031538	0	0.001674	0
CG32468	FBgn0052468	0.00198	0	0
CG32473	FBgn0052473	0.001186	0.002108	0.008448
CG32479	FBgn0052479	0.001622	0.000966	0.001937
CG32486	FBgn0052486	0	0	0.001828
CG32495	FBgn0052495	0.111273	0.1402	0.113494
CG32521	FBgn0052521	0.008798	0.002069	0.007032
CG32528	FBgn0052528	0.00725	0.02261	0.023531
CG32536	FBgn0052536	0.002785	0.012401	0.015137

CG32549	FBgn0052549	0.019046	0.008677	0.052678
CG32573	FBgn0052573	0.001589	0	0
CG32579	FBgn0052579	0	0.002046	0
CG32603	FBgn0052603	0.039686	0	0
CG32626	FBgn0052626	0.010789	0.014206	0.023213
CG32631	FBgn0052631	0.001955	0.01429	0.007853
CG32633	FBgn0052633	0	0	0.003289
CG32638	FBgn0052638	0.008965	0.168428	0.112695
CG32662	FBgn0052662	0.002625	0.000617	0
CG32663	FBgn0052663	0.020776	0.012754	0.009087
CG32667	FBgn0052667	0.500711	0.078207	0.049776
CG3267	FBgn0042083	0.021609	0	0.001308
CG32679	FBgn0052679	0.051692	0.003928	0.005943
CG32702	FBgn0052702	0.001063	0	0
CG32703	FBgn0052703	0	0.000813	0.001023
CG32762	FBgn0052762	3.8732	1.278028	0.824649
CG3295	FBgn0034573	0.001401	0	0.003488
CG32972	FBgn0028905	0.000994	0	0
CG3301	FBgn0038878	0.094117	0.058447	0.056854
CG3305	FBgn0032949	0.034042	0.048014	0.060245
CG33052	FBgn0053052	0.003647	0	0.004466
CG33054	FBgn0053054	0.008057	0	0
CG33056	FBgn0053056	0	0.013028	0.124111
CG3308	FBgn0038877	0.005776	0	0
CG33099	FBgn0053099	0.008052	0	0
CG33111	FBgn0053111	0.005954	0.003384	0.003068
CG33123	FBgn0053123	0.035207	0.024843	0.023413
CG33127	FBgn0053127	0	0.003513	0
CG33129	FBgn0053129	0.025008	0.050102	0.08548
CG33138	FBgn0053138	0.021182	0.028864	0.066071
CG33205	FBgn0053205	0.00171	0.006242	0.009677
CG3321	FBgn0038224	0.480405	0	0.062696
CG33214	FBgn0053214	0	0	0.001091
CG3330	FBgn0039511	0.00422	0.002501	0.005881
CG33303	FBgn0053303	0.189752	0.299819	0.25724
CG33307	FBgn0053307	0.02649	0	0.02989
CG33331	FBgn0067628	0.001783	0	0
CG3338	FBgn0031598	0	0	0.001103
CG33487	FBgn0053487	0.011742	0.020388	0.025929
CG3349	FBgn0036459	0.000814	0	0
CG33491	FBgn0053491	0.048617	0.04668	0.019152
CG33493	FBgn0053493	0.052044	0	0
CG33496	FBgn0053496	0.011742	0.020388	0.025929
CG33498	FBgn0053498	0.049019	0.047066	0.014337
CG3353	FBgn0038869	0	0	0.001917
CG3362	FBgn0034988	0.001912	0.002258	0

CG33649	FBgn0064115	0	0.005032	0.00509
CG3376	FBgn0034997	0.000861	0.001017	0.006485
CG33791	FBgn0035240	0	0	0.000588
CG3394	FBgn0034999	0.014816	0.01079	0.036264
CG3397	FBgn0037975	0.015983	0.025341	0.059994
CG3402	FBgn0035148	0.004958	0	0
CG3408	FBgn0036008	0	0	0.005921
CG34126	FBgn0083962	0.000418	0	0.003224
CG34133	FBgn0083969	0.001105	0	0
CG3415	FBgn0030731	0.114208	0.069935	0.157657
CG34408	FBgn0085437	0.000407	0	0
CG34422	FBgn0085451	0.000829	0.000506	0.001662
CG3446	FBgn0029868	0.011935	0	0
CG3473	FBgn0028913	0.008134	0.009539	0.009997
CG3493	FBgn0034854	0.007962	0.016021	0.008134
CG3500	FBgn0034849	0.006226	0	0.00382
CG3501	FBgn0034791	0.08562	0.076582	0.055473
CG3505	FBgn0038250	0.02439	0.014208	0.064849
CG3511	FBgn0035027	0	0.001169	0
CG3523	FBgn0027571	0.176323	0.149499	0.244672
CG3529	FBgn0035995	0.068687	0.046889	0.044936
CG3530	FBgn0028497	0	0	0.001582
CG3532	FBgn0037979	0.011599	0.007548	0.006064
CG3534	FBgn0038463	0.00149	0.004462	0.00218
CG3542	FBgn0031492	0	0.006906	0.006354
CG3560	FBgn0030733	0.208335	0.08501	0.175875
CG3566	FBgn0029854	0.020884	0.014684	0
CG3588	FBgn0025643	0.001145	0	0
CG3590	FBgn0038467	0.019555	0.016725	0.029435
CG3603	FBgn0029648	0.078929	0.008677	0.015282
CG3604	FBgn0031562	0.009305	0	0
CG3605	FBgn0031493	0.003576	0.001956	0.002617
CG3609	FBgn0031418	0.189992	0.099901	0.116291
CG3621	FBgn0025839	0.053831	0.021454	0.04674
CG3652	FBgn0031600	0.00278	0.015339	0.026315
CG3663	FBgn0035044	0.029505	0	0
CG3683	FBgn0035046	0.061992	0.081687	0.107757
CG3689	FBgn0035987	0.029974	0	0.008545
CG3699	FBgn0040349	0.008137	0.017215	0.032285
CG3702	FBgn0031590	0	0	0.002642
CG3704	FBgn0040346	0	0.009124	0.004908
CG3714	FBgn0031589	0.005885	0.001342	0.003804
CG3731	FBgn0038271	0.180042	0.110208	0.168403
CG3740	FBgn0023530	0.004449	0	0
CG3756	FBgn0031657	0.00187	0	0.002938
CG3760	FBgn0022343	0.147749	0.115756	0.096188

CG3773	FBgn0038692	0	0	0.005818
CG3775	FBgn0030425	0	0	0.001155
CG3781	FBgn0029853	0.002759	0.003259	0
CG3800	FBgn0034802	0.494007	0.219184	0.105518
CG3835	FBgn0023507	0.026474	0.002702	0.012158
CG3847	FBgn0029867	0.001639	0	0
CG3860	FBgn0034951	0.00134	0.002193	0.001662
CG3884	FBgn0033786	0.002117	0.01705	0.021795
CG3887	FBgn0031670	0.015552	0.019961	0.076257
CG3902	FBgn0036824	0.294827	0.19109	0.230371
CG3909	FBgn0027524	0.021538	0.024646	0.02729
CG3940	FBgn0037788	0	0	0.012877
CG3961	FBgn0036821	0.001222	0	0.0149
CG3987	FBgn0038292	0	0.008505	0.018627
CG3999	FBgn0037801	0.005169	0.01626	0.029879
CG4004	FBgn0030418	0	0	0.00355
CG4019	FBgn0034885	0.015666	0.038819	0.079456
CG4038	FBgn0011824	0.061193	0.066767	0.123823
CG4041	FBgn0029736	0	0	0.001797
CG4045	FBgn0025629	0.004747	0	0
CG4069	FBgn0036301	0.001198	0	0
CG4091	FBgn0034894	0	0	0.008261
CG4095	FBgn0029890	0.002416	0.001481	0.008767
CG4115	FBgn0038017	0.045593	0.01343	0.019022
CG4140	FBgn0028535	0.011406	0	0
CG4151	FBgn0029770	4.287818	3.099863	1.873434
CG4159	FBgn0038811	0.003007	0	0
CG4164	FBgn0031256	0.102189	0.093011	0.090608
CG4165	FBgn0029763	0.001091	0	0
CG4169	FBgn0250814	0.277333	0.19542	0.269338
CG4198	FBgn0029753	0	0.00151	0.006074
CG4199	FBgn0025628	0.003157	0	0.001449
CG42232	FBgn0250754	0	0	0.003465
CG42348	FBgn0259679	0	0.00097	0
CG42388	FBgn0259734	0	0.007074	0.025301
CG4239	FBgn0030745	0	0	0.006126
CG42533	FBgn0260486	0	0	0.000607
CG4278	FBgn0014092	0.004146	0.007483	0.005412
CG4293	FBgn0024983	0	0	0.003416
CG4297	FBgn0031258	0.001238	0.001639	0
CG4300	FBgn0036272	0.020107	0.016836	0.028399
CG4306	FBgn0036787	0.053921	0.011194	0.003438
CG4332	FBgn0030456	0	0.001325	0
CG4334	FBgn0038312	0	0	0.003218
CG4335	FBgn0038795	0.051203	0.056384	0.061604
CG4338	FBgn0038313	0.002209	0	0

CG4365	FBgn0037024	0.051956	0.02563	0.019442
CG4382	FBgn0032132	0.00105	0	0
CG4389	FBgn0028479	0.15024	0.073135	0.16378
CG4390	FBgn0038771	0.122734	0.12422	0.130266
CG4406	FBgn0023545	0	0	0.00339
CG4408	FBgn0039073	0.028435	0.004679	0.003233
CG4420	FBgn0030753	0.034851	0.018225	0.043436
CG4452	FBgn0035981	0.002109	0.002559	0
CG4538	FBgn0038745	0.005121	0	0
CG4552	FBgn0031304	0.0095	0.006746	0.011368
CG4557	FBgn0029912	0.010946	0.008013	0.00726
CG4572	FBgn0038738	0.019915	0.013258	0.026269
CG4586	FBgn0029924	0	0.001064	0.005914
CG4589	FBgn0019886	0.001212	0	0
CG4593	FBgn0029929	0.048989	0.042596	0.025415
CG4594	FBgn0032161	0.013129	0	0
CG4598	FBgn0032160	0.121523	0.01299	0.04234
CG4612	FBgn0035016	0.006044	0	0.006974
CG4631	FBgn0032590	0.001034	0	0
CG4645	FBgn0030435	0.009073	0.039114	0.016816
CG4658	FBgn0032170	0.002343	0.002785	0.001782
CG4669	FBgn0035598	0	0	0.001238
CG4692	FBgn0035032	0.049775	0	0
CG4702	FBgn0037992	0.004993	0	0
CG4706	FBgn0037862	0.022187	0.006228	0.006113
CG4729	FBgn0036623	0.019565	0.005661	0.010834
CG4747	FBgn0043456	0.083473	0.082113	0.07401
CG4752	FBgn0034733	0.001578	0.000576	0.006761
CG4757	FBgn0027584	0.045064	0	0
CG4764	FBgn0031310	0.076122	0.023387	0.040732
CG4769	FBgn0035600	0.055988	0.008022	0.040105
CG4789	FBgn0030792	0.006708	0.00636	0.005499
CG4802	FBgn0034215	0.03615	0.052832	0.05204
CG4810	FBgn0037994	0.003312	0.005821	0.002459
CG4844	FBgn0061354	0.006472	0	0
CG4848	FBgn0037998	0.001372	0.005873	0.006078
CG4858	FBgn0037011	0	0.012242	0.01012
CG4877	FBgn0036624	0.004003	0	0.003893
CG4907	FBgn0039010	0.000659	0	0
CG4914	FBgn0036436	0.004892	0	0
CG4928	FBgn0027556	0	0.001339	0.001406
CG4933	FBgn0036615	0	0	0.003468
CG4960	FBgn0039371	0.021202	0.050881	0.013023
CG4968	FBgn0032214	0.007032	0.00834	0.019852
CG4972	FBgn0032217	0.002197	0.002611	0.001343
CG4980	FBgn0039558	0.00224	0	0

CG5001	FBgn0031322	0.007788	0	0.014354
CG5010	FBgn0260747	0.055407	0.004236	0.042395
CG5021	FBgn0035944	0.010899	0.03948	0.03996
CG5023	FBgn0038774	0.223645	0.28959	0.589462
CG5028	FBgn0039358	0.067131	0.026358	0.056597
CG5044	FBgn0038326	0.075277	0.007527	0.024581
CG5045	FBgn0032229	0.023409	0	0.006857
CG5075	FBgn0032464	0.076234	0.082374	0.073494
CG5103	FBgn0036784	0.01277	0.001156	0.007253
CG5110	FBgn0032642	0.004882	0	0.025786
CG5111	FBgn0039343	0	0.001625	0.002825
CG5112	FBgn0039341	0.0113	0.001377	0.009
CG5126	FBgn0031320	0.013046	0.001583	0.007351
CG5131	FBgn0032644	0.002155	0	0
CG5149	FBgn0031904	0.016828	0	0
CG5167	FBgn0038038	0.025564	0.071535	0.086284
CG5168	FBgn0032246	0.020026	0.007862	0.017152
CG5171	FBgn0031907	0.040375	0.179169	0.234496
CG5174	FBgn0034345	0.230289	0.362662	0.26604
CG5177	FBgn0031908	0.265472	0.347238	0.538061
CG5189	FBgn0034350	0	0.005761	0.0075
CG5191	FBgn0038803	0.002335	0	0
CG5205	FBgn0038344	0	0.00093	0
CG5214	FBgn0037891	0.089414	0.051706	0.054774
CG5265	FBgn0038486	0.005086	0	0
CG5276	FBgn0037900	0	0.002381	0.011424
CG5287	FBgn0032477	0	0	0.002292
CG5288	FBgn0035950	0.074348	0.184682	0.147508
CG5290	FBgn0036772	0.006167	0	0
CG5325	FBgn0032407	0.02874	0.005017	0.016242
CG5346	FBgn0038981	0.00454	0	0.008299
CG5355	FBgn0032242	0.256993	0.157281	0.150461
CG5362	FBgn0032237	0.433393	0.351014	0.372923
CG5366	FBgn0027568	0.008062	0.009408	0.014861
CG5377	FBgn0038974	0.011749	0	0.00814
CG5381	FBgn0032218	0.00744	0.003959	0
CG5382	FBgn0038950	0.066934	0.164114	0.127967
CG5384	FBgn0032216	0.152116	0.08138	0.11422
CG5389	FBgn0036568	0.158931	0.15816	0.212446
CG5390	FBgn0032213	0.051383	0.009051	0.018162
CG5404	FBgn0038354	0	0.001149	0
CG5412	FBgn0038806	0.004465	0.003576	0
CG5431	FBgn0034888	0.008457	0.019655	0.0171
CG5432	FBgn0039425	0	0.006071	0.006613
CG5446	FBgn0032429	0.049917	0.048199	0.032588
CG5451	FBgn0038666	0.001224	0	0

CG5484	FBgn0039450	0.012479	0.009288	0.023786
CG5510	FBgn0039160	0.014934	0	0.023484
CG5515	FBgn0039163	0.006743	0	0.009274
CG5525	FBgn0032444	0.120618	0.129369	0.098001
CG5537	FBgn0035639	0.009429	0	0.01212
CG5543	FBgn0034908	0.000931	0	0
CG5548	FBgn0030605	0.01571	0	0.016751
CG5554	FBgn0034914	0.134814	0.172485	0.205046
CG5555	FBgn0038686	0.00219	0	0.001357
CG5567	FBgn0036760	0.002493	0.006696	0.004584
CG5577	FBgn0036759	0.001936	0	0.002401
CG5590	FBgn0039537	0.109815	0.014837	0.042212
CG5594	FBgn0025698	0	0	0.001428
CG5599	FBgn0030612	0.015957	0	0
CG5602	FBgn0034922	0.00081	0.000964	0.001012
CG5611	FBgn0039531	0.001871	0	0
CG5613	FBgn0030839	0.001256	0	0
CG5641	FBgn0038046	0	0	0.001902
CG5642	FBgn0036258	0.097648	0.064953	0.108905
CG5656	FBgn0037083	0.012141	0.017096	0.013692
CG5665	FBgn0036977	0	0	0.004136
CG5690	FBgn0035295	0.002174	0.002166	0.005094
CG5703	FBgn0030853	0.057357	0.021035	0.030809
CG5706	FBgn0039175	0.047537	0.050259	0.038848
CG5746	FBgn0039186	0.001334	0	0
CG5757	FBgn0034299	0.003642	0	0
CG5787	FBgn0032454	0.007155	0.003084	0.00333
CG5793	FBgn0038858	0.021473	0.009692	0.014063
CG5804	FBgn0035926	0	0.012169	0.020656
CG5810	FBgn0038866	0	0	0.001767
CG5844	FBgn0038049	0.039447	0	0.012547
CG5849	FBgn0038897	0.00063	0	0
CG5854	FBgn0039130	0.013014	0.002264	0.013404
CG5862	FBgn0038868	0.010528	0.014429	0.021956
CG5869	FBgn0028894	0.125967	0.038267	0.079435
CG5871	FBgn0038870	0.000598	0	0.003696
CG5873	FBgn0038511	0.004868	0	0
CG5885	FBgn0025700	0.034564	0.05697	0.141805
CG5902	FBgn0039136	0.005126	0	0.008065
CG5903	FBgn0038400	0.032678	0	0.003333
CG5919	FBgn0038876	0.007961	0	0
CG5931	FBgn0036548	0.001724	0.002418	0.00337
CG5941	FBgn0029833	0.087716	0.062311	0.06062
CG5946	FBgn0036211	0.003128	0	0.002864
CG5958	FBgn0031913	0.024889	0.072735	0.155692
CG5966	FBgn0029831	0	0.002667	0.004537

CG5976	FBgn0036999	0.006879	0.028196	0.025147
CG5978	FBgn0035916	0	0	0.002326
CG5987	FBgn0039501	0	0.003455	0.003497
CG5991	FBgn0026576	0	0.001611	0.002692
CG6000	FBgn0039145	0.008416	0.009898	0.01531
CG6013	FBgn0038675	0.002924	0.008181	0.004594
CG6015	FBgn0038927	0.002132	0	0
CG6020	FBgn0037001	0.049983	0.004405	0.015799
CG6026	FBgn0038676	0.000404	0	0
CG6055	FBgn0031918	0.034643	0	0
CG6073	FBgn0039417	0.003305	0	0.002041
CG6074	FBgn0039486	0	0	0.002432
CG6083	FBgn0036183	0	0.002237	0
CG6084	FBgn0086254	0.298826	0.204874	0.191503
CG6116	FBgn0032499	0.001182	0	0.001082
CG6129	FBgn0039152	0.001002	0	0
CG6136	FBgn0038332	0	0	0.002864
CG6151	FBgn0036533	0.032664	0.038084	0.053715
CG6153	FBgn0032445	0.002869	0	0.005704
CG6178	FBgn0039156	0	0.006619	0.01261
CG6180	FBgn0032453	0.067596	0.091124	0.078508
CG6188	FBgn0038074	0.079809	0.022768	0.032881
CG6194	FBgn0038325	0.000927	0	0
CG6195	FBgn0038723	0.010726	0	0.005898
CG6206	FBgn0027611	0.061861	0.029563	0.043517
CG6208	FBgn0037789	0	0	0.004253
CG6230	FBgn0027582	0.000508	0.005237	0.002148
CG6236	FBgn0038318	0	0	0.00177
CG6255	FBgn0038708	0.026283	0	0
CG6259	FBgn0036740	0.071454	0.069908	0.045003
CG6287	FBgn0032350	0.130513	0.167065	0.154647
CG6345	FBgn0037816	0.004213	0	0.001297
CG6356	FBgn0039178	0	0.001263	0
CG6357	FBgn0033875	0.017974	0	0
CG6361	FBgn0030925	0.001648	0	0.002001
CG6364	FBgn0039179	0.037792	0.008404	0.025767
CG6385	FBgn0034276	0	0.004791	0.008394
CG6388	FBgn0032430	0.001055	0.001246	0
CG6409	FBgn0036106	0.001682	0	0
CG6410	FBgn0034265	0	0	0.005279
CG6412	FBgn0032646	0.009656	0	0
CG6415	FBgn0032287	0.025459	0.028474	0.064727
CG6418	FBgn0036104	0.001558	0	0
CG6422	FBgn0039261	0.004679	0.00103	0
CG6439	FBgn0038922	0.116675	0.035673	0.065592
CG6448	FBgn0032976	0.000354	0.000436	0

CG6453	FBgn0032643	0.049565	0.048538	0.045004
CG6454	FBgn0039187	0.000928	0	0
CG6455	FBgn0019960	0.067693	0.011191	0.02998
CG6463	FBgn0047038	0.147036	0.011814	0.085038
CG6475	FBgn0038886	0.002474	0	0
CG6488	FBgn0032361	0.0068	0.010879	0.009262
CG6512	FBgn0036702	0.002949	0.001033	0
CG6522	FBgn0034223	0.00101	0	0
CG6523	FBgn0032509	0.129687	0.127402	0.09679
CG6567	FBgn0037842	0.037456	0.006234	0.033055
CG6607	FBgn0039204	0.003004	0.002458	0
CG6617	FBgn0030944	0.020149	0.011055	0.013733
CG6638	FBgn0035911	0.005849	0	0.017727
CG6639	FBgn0032638	0.014088	0.002965	0.003429
CG6643	FBgn0039208	0.008516	0.019264	0.039011
CG6656	FBgn0038912	0.001544	0	0
CG6661	FBgn0036403	0	0.001282	0.001684
CG6673	FBgn0035906	0.034376	0	0
CG6680	FBgn0036968	0.001355	0	0
CG6686	FBgn0032388	0.001745	0	0
CG6687	FBgn0038299	0.001931	0	0
CG6697	FBgn0027526	0.009596	0	0
CG6701	FBgn0033889	0.000494	0	0
CG6707	FBgn0036058	0.014702	0.017473	0.032052
CG6719	FBgn0037893	0.036515	0.012077	0.036214
CG6724	FBgn0032298	0.002924	0.005922	0.00762
CG6726	FBgn0039049	0.023894	0.020824	0.021544
CG6751	FBgn0033562	0.01113	0.003797	0.006312
CG6762	FBgn0030876	0.029084	0.033288	0.016495
CG6766	FBgn0032398	0.006396	0.007674	0.009103
CG6767	FBgn0036030	0.06367	0.059751	0.099205
CG6770	FBgn0032400	0.062115	0.096283	0.047999
CG6776	FBgn0035904	0.089056	0.031239	0.051852
CG6782	FBgn0037912	0.001924	0	0.004772
CG6783	FBgn0037913	0.536562	0.546533	0.587557
CG6812	FBgn0036843	0.026905	0	0
CG6838	FBgn0037182	0.087197	0.077329	0.064403
CG6841	FBgn0036828	0.001979	0	0.001819
CG6852	FBgn0036820	0.125542	0.151313	0.211248
CG6856	FBgn0036819	0.00422	0	0
CG6876	FBgn0036487	0.001642	0	0
CG6891	FBgn0030955	0.204174	0.146882	0.185594
CG6900	FBgn0030958	0.091661	0.04751	0.03245
CG6904	FBgn0038293	0.004306	0.01541	0.045459
CG6905	FBgn0035136	0	0	0.000925
CG6907	FBgn0031711	0.011332	0.005	0.006215

CG6910	FBgn0036262	0.002147	0.002554	0.003324
CG6912	FBgn0038290	0	0	0.001747
CG6950	FBgn0037955	0.018608	0.002976	0.022601
CG6961	FBgn0030959	0.001287	0	0
CG6972	FBgn0039008	0.002067	0	0
CG6983	FBgn0035896	0	0.005543	0.008779
CG6995	FBgn0039229	0.000657	0	0.001297
CG7011	FBgn0036489	0.008756	0.007347	0.014438
CG7048	FBgn0038976	0.052343	0.027813	0.01481
CG7054	FBgn0038972	0	0.005574	0
CG7059	FBgn0038957	0.028385	0.013678	0.005356
CG7077	FBgn0038946	0	0	0.006087
CG7083	FBgn0035877	0	0.002278	0.005334
CG7112	FBgn0035879	0	0.000717	0.00075
CG7115	FBgn0027515	0	0.001421	0.001438
CG7145	FBgn0037138	0.137235	0.005545	0.034148
CG7181	FBgn0037097	0.120264	0	0
CG7182	FBgn0035878	0.008389	0.006794	0.007348
CG7185	FBgn0035872	0.010667	0.004203	0.009266
CG7203	FBgn0031942	0.004295	0	0.005195
CG7207	FBgn0027569	0.012898	0.011054	0.010829
CG7215	FBgn0038571	0.054736	0.018944	0.020556
CG7227	FBgn0031970	0	0	0.00327
CG7255	FBgn0036493	0	0.00094	0.003199
CG7265	FBgn0038272	0.003929	0	0.002566
CG7272	FBgn0036501	0	0.007643	0.03442
CG7277	FBgn0031713	0.001279	0	0
CG7280	FBgn0030966	0.004272	0.002514	0.007232
CG7288	FBgn0030969	0	0	0.002436
CG7298	FBgn0036948	0.015485	0	0
CG7299	FBgn0032282	0.010458	0	0.009569
CG7320	FBgn0036782	0	0.001252	0.008132
CG7322	FBgn0030968	0.165266	0.074805	0.102669
CG7324	FBgn0037074	0.002054	0	0.00169
CG7332	FBgn0030973	0	0	0.002149
CG7349	FBgn0030975	0.016364	0	0.017642
CG7375	FBgn0035853	0.02363	0.00823	0.012502
CG7379	FBgn0038546	0	0	0.00174
CG7402	FBgn0036768	0	0.009414	0.018436
CG7414	FBgn0037135	0.020233	0.013144	0.01607
CG7429	FBgn0031979	0.004674	0	0
CG7430	FBgn0036762	0.295362	0.107276	0.192405
CG7433	FBgn0036927	0.001282	0.001482	0.004953
CG7447	FBgn0035539	0	0	0.001471
CG7456	FBgn0032258	0.007369	0.004817	0.006364
CG7470	FBgn0037146	0.006549	0.04227	0.077257

CG7484	FBgn0036745	0.103374	0.066555	0.06028
CG7504	FBgn0035842	0	0.00123	0.003129
CG7510	FBgn0036741	0.00257	0	0
CG7518	FBgn0038108	0.001394	0	0.000643
CG7519	FBgn0037087	0.031901	0.013811	0.019752
CG7526	FBgn0035798	0.001482	0	0
CG7532	FBgn0028915	0.092899	0.013743	0.020166
CG7546	FBgn0035793	0.010702	0.003586	0.008347
CG7556	FBgn0030990	0.01843	0.021753	0.016406
CG7564	FBgn0036734	0.002966	0	0.002232
CG7580	FBgn0036728	0.048137	0	0.027046
CG7587	FBgn0038523	1.313366	0.358553	0.229922
CG7600	FBgn0064766	0	0.000803	0
CG7603	FBgn0036726	0.009997	0.008179	0.006175
CG7627	FBgn0032026	0	0	0.000952
CG7630	FBgn0040793	0.16137	0.024006	0.082837
CG7634	FBgn0037101	0	0.001244	0
CG7637	FBgn0033548	0.02872	0.108144	0.092102
CG7671	FBgn0038609	0	0	0.004853
CG7675	FBgn0038610	0.015179	0	0
CG7714	FBgn0038645	0.003656	0.003201	0
CG7739	FBgn0036509	0.002039	0	0.005066
CG7766	FBgn0030087	0	0	0.000606
CG7770	FBgn0036918	0.004843	0.027488	0.031006
CG7787	FBgn0032020	0.005105	0.005903	0.041031
CG7789	FBgn0039698	0.025432	0.010482	0.022857
CG7802	FBgn0039704	0.00082	0	0
CG7806	FBgn0032018	0.000419	0	0
CG7813	FBgn0034133	0	0.001015	0
CG7816	FBgn0039714	0.001718	0.006155	0.004244
CG7830	FBgn0032015	0.021064	0.054997	0.064937
CG7834	FBgn0039697	0.340199	0.163044	0.181269
CG7843	FBgn0033062	0.005422	0.005518	0.001676
CG7857	FBgn0026738	0.012464	0.008783	0.010399
CG7860	FBgn0030653	0.066003	0.098752	0.114835
CG7872	FBgn0030658	0.026441	0.027346	0.028346
CG7889	FBgn0031003	0	0	0.003773
CG7906	FBgn0036417	0.095255	0.046555	0.035523
CG7911	FBgn0039735	0.351759	0.182057	0.153387
CG7920	FBgn0039737	0.035222	0.047598	0.023559
CG7924	FBgn0036416	0.168086	0.009127	0.011946
CG7927	FBgn0027549	0.000887	0	0
CG7945	FBgn0036505	0.012382	0.014053	0.006995
CG7946	FBgn0039743	0.003934	0.010421	0.009099
CG7949	FBgn0036107	0.007873	0	0.010838
CG7967	FBgn0035251	0.013604	0	0

CG7993	FBgn0038585	0.003893	0	0
CG7998	FBgn0038587	0.753918	0.535996	0.590955
CG8003	FBgn0036096	0.003029	0	0.004815
CG8031	FBgn0038110	0.127131	0.071753	0.069444
CG8036	FBgn0037607	0.393211	0.469958	0.527996
CG8042	FBgn0027554	0.003645	0.002926	0.001486
CG8066	FBgn0038243	0.047449	0.101884	0.049253
CG8100	FBgn0036410	0.004154	0.001235	0.003892
CG8108	FBgn0027567	0.010804	0.009396	0.007833
CG8121	FBgn0037680	0.002414	0	0
CG8129	FBgn0037684	0	0	0.001613
CG8132	FBgn0037687	0.007969	0.017405	0.008658
CG8136	FBgn0037616	0	0.002263	0
CG8149	FBgn0037700	0.012034	0.002418	0
CG8176	FBgn0037702	0.003991	0	0
CG8184	FBgn0030674	0	0	0.000785
CG8193	FBgn0033367	0.519854	0.049554	0.069693
CG8199	FBgn0037709	0.00741	0.012284	0.012174
CG8207	FBgn0034035	0.055538	0.033047	0.046279
CG8209	FBgn0035830	0.067235	0.077716	0.086357
CG8223	FBgn0037624	0.211276	0.126162	0.107244
CG8234	FBgn0033644	0	0	0.00155
CG8239	FBgn0030683	0.003144	0	0
CG8289	FBgn0030854	0.018911	0.00297	0.002242
CG8306	FBgn0034142	0.005951	0.010036	0.020279
CG8310	FBgn0040377	0.032912	0.011006	0.012244
CG8331	FBgn0033906	0.061045	0.102952	0.071363
CG8336	FBgn0036020	0.001626	0	0.003949
CG8353	FBgn0032002	0.007251	0	0.00708
CG8360	FBgn0032001	0.079157	0.011029	0.027633
CG8368	FBgn0035707	0.000889	0	0
CG8369	FBgn0040532	0.171512	0.007661	0.036474
CG8379	FBgn0037638	0.005489	0	0
CG8414	FBgn0034073	0	0.000724	0
CG8417	FBgn0037744	0.014441	0.007399	0.009219
CG8420	FBgn0037664	0.006923	0	0
CG8444	FBgn0037671	0.003798	0	0
CG8451	FBgn0031998	0	0.0012	0
CG8460	FBgn0031996	0.04382	0.006126	0.0119
CG8475	FBgn0031995	0	0	0.000692
CG8492	FBgn0035813	0	0.001532	0
CG8498	FBgn0031992	0.350321	0.294836	0.213379
CG8507	FBgn0037756	0.015077	0.012329	0.009154
CG8545	FBgn0033741	0.002301	0	0
CG8547	FBgn0033919	0.006394	0.005559	0.005284
CG8549	FBgn0035714	0.008138	0.005813	0.008496

CG8552	FBgn0031990	0.028066	0.038316	0.023245
CG8578	FBgn0030699	0.001573	0.001819	0.003039
CG8602	FBgn0035763	0.001266	0.003646	0.008896
CG8605	FBgn0035762	0.009619	0.008759	0.009932
CG8613	FBgn0033924	0.006786	0.00229	0.005916
CG8628	FBgn0250836	0.00726	0.011879	0
CG8629	FBgn0035742	0	0.008574	0
CG8636	FBgn0029629	0.165726	0.094467	0.100363
CG8671	FBgn0032938	0	0	0.007716
CG8677	FBgn0026577	0	0.001186	0
CG8680	FBgn0031684	0.154152	0.0404	0.112787
CG8683	FBgn0031985	0.001344	0.000445	0.004544
CG8709	FBgn0033269	0.002999	0.002029	0.006152
CG8745	FBgn0036381	0	0	0.003423
CG8774	FBgn0038136	0	0	0.000855
CG8777	FBgn0033376	0	0	0.001881
CG8798	FBgn0036892	0.006889	0	0.000905
CG8831	FBgn0033737	0.001	0.002857	0
CG8858	FBgn0033698	0.000963	0.000775	0.002829
CG8860	FBgn0033691	0.008968	0	0.024865
CG8885	FBgn0031656	0.00243	0	0
CG8891	FBgn0031663	0.044893	0.019239	0.034463
CG8945	FBgn0030815	0.000426	0.000698	0
CG8993	FBgn0035334	0.087985	0.022588	0.060287
CG9007	FBgn0036398	0	0.000229	0
CG9009	FBgn0027601	0.008186	0.006114	0.015315
CG9018	FBgn0035318	0	0.00192	0
CG9021	FBgn0031747	0.011592	0.002357	0
CG9027	FBgn0033631	0	0.005761	0.016121
CG9034	FBgn0040931	0.023871	0	0
CG9063	FBgn0028500	0.001002	0.001025	0.003182
CG9086	FBgn0030809	0.000341	0.001732	0.004042
CG9099	FBgn0030802	0.00643	0.005279	0.027535
CG9119	FBgn0035189	0.283445	0.206157	0.120613
CG9132	FBgn0030791	0.040827	0.058011	0.017178
CG9133	FBgn0035198	0.001959	0.003229	0.005604
CG9135	FBgn0031769	0.020632	0.014182	0.018866
CG9140	FBgn0031771	0.042786	0.00922	0.031206
CG9149	FBgn0035203	0.023954	0.023777	0.041358
CG9172	FBgn0030718	0.005519	0	0.003422
CG9175	FBgn0031779	0.00413	0.003347	0.008551
CG9186	FBgn0035206	0.031889	0.056235	0.05723
CG9205	FBgn0035181	0.006404	0.003501	0.00874
CG9231	FBgn0036887	0	0.005761	0
CG9232	FBgn0031845	0.015762	0	0.010316
CG9248	FBgn0032923	0.00246	0	0.001531

CG9257	FBgn0032916	0.003515	0	0.00218
CG9281	FBgn0030672	0.026276	0.005651	0.004966
CG9286	FBgn0038183	0.002053	0	0
CG9297	FBgn0038181	0.00812	0.02889	0.062213
CG9300	FBgn0036886	0	0	0.001788
CG9302	FBgn0032514	0.0076	0.002872	0.005761
CG9306	FBgn0032511	0.03121	0.020176	0.027967
CG9318	FBgn0032880	0.007403	0.051708	0.052597
CG9330	FBgn0036888	0.008396	0	0.001914
CG9331	FBgn0032889	0.191384	0.068882	0.088188
CG9336	FBgn0032897	0	0.023382	0.019577
CG9338	FBgn0032899	0.008385	0	0.013033
CG9344	FBgn0034564	0.015768	0	0.009573
CG9356	FBgn0037688	0.01462	0.002227	0.008553
CG9360	FBgn0030332	0	0.027673	0.007796
CG9363	FBgn0037697	0	0.003281	0
CG9380	FBgn0035094	0	0.000835	0.001963
CG9391	FBgn0037063	0.015464	0.012448	0.026168
CG9411	FBgn0030569	0.000627	0	0
CG9416	FBgn0034438	0	0	0.001089
CG9425	FBgn0036451	0	0.001138	0
CG9426	FBgn0032485	0.001312	0	0
CG9427	FBgn0037721	0.080573	0	0
CG9466	FBgn0032068	0.003547	0.004	0.004446
CG9468	FBgn0032069	0.001817	0	0
CG9471	FBgn0037749	0.053096	0	0.0059
CG9472	FBgn0036874	0.002513	0	0.00698
CG9485	FBgn0034618	0.000392	0.001413	0.006284
CG9486	FBgn0031791	0	0.003334	0.009073
CG9498	FBgn0031801	0.001438	0.002353	0.003995
CG9510	FBgn0032076	0.027364	0.013544	0.032353
CG9512	FBgn0030593	0	0.001156	0.002719
CG9527	FBgn0031813	0.00117	0	0.006273
CG9536	FBgn0031818	0	0	0.001681
CG9547	FBgn0031824	0.015601	0.010371	0.010093
CG9572	FBgn0031089	0.008375	0	0
CG9577	FBgn0031092	0.144965	0.103311	0.233119
CG9578	FBgn0031094	0.004532	0	0
CG9586	FBgn0032101	0.002932	0	0
CG9588	FBgn0038166	0.002772	0.003385	0
CG9603	FBgn0040529	0.145359	0	0.008498
CG9629	FBgn0036857	0.012121	0.03651	0.063366
CG9662	FBgn0031529	0.045211	0	0.04769
CG9667	FBgn0037550	0.010533	0.006407	0.006216
CG9669	FBgn0036667	0	0.012793	0
CG9673	FBgn0030775	0.002319	0.003823	0.020163

CG9674	FBgn0036663	0.006236	0.003148	0.007098
CG9684	FBgn0037583	0.002224	0	0.004094
CG9689	FBgn0030159	0.015305	0	0
CG9691	FBgn0030160	0.089716	0.026509	0.054785
CG9705	FBgn0036661	0.051627	0.042747	0.044029
CG9706	FBgn0036662	0	0.002744	0.004078
CG9733	FBgn0039759	0.005898	0	0
CG9769	FBgn0037270	0.140847	0.177545	0.196353
CG9775	FBgn0037261	0	0	0.001796
CG9776	FBgn0027866	0	0.000792	0
CG9779	FBgn0037231	0.022012	0.011154	0.015164
CG9782	FBgn0030763	0.002698	0	0
CG9784	FBgn0030761	0.014128	0.004848	0.003111
CG9796	FBgn0038149	0.049808	0.009851	0.009052
CG9804	FBgn0037251	0.008728	0	0
CG9812	FBgn0034860	0.079963	0.02372	0.04737
CG9837	FBgn0037635	0	0	0.011628
CG9853	FBgn0086605	0	0.002943	0.002231
CG9879	FBgn0031444	0.001882	0	0
CG9894	FBgn0031453	0.175944	0.053345	0.111636
CG9906	FBgn0030755	0.021358	0.026802	0.032727
CG9911	FBgn0030734	0.577405	0.523243	0.71023
CG9914	FBgn0030737	0.113276	0.110545	0.144588
CG9920	FBgn0038200	0.03817	0.017084	0.024422
CG9922	FBgn0038196	0.031117	0.030147	0.033724
CG9932	FBgn0032469	0.001147	0	0
CG9934	FBgn0032467	0.000627	0	0.001752
CG9953	FBgn0035726	0.004819	0.002884	0.006387
CG9977	FBgn0035371	0.038484	0.024262	0.035784
Chc	FBgn0000319	0.114835	0.21473	0.24085
Chd1	FBgn0250786	0.000331	0	0
Chd64	FBgn0035499	1.28598	1.470121	1.139804
chic	FBgn0000308	0.725952	1.011314	0.827105
CHIP	FBgn0027052	0.002155	0.002577	0
Chit	FBgn0013763	0.426011	0.093385	0.157128
Chmp1	FBgn0036805	0.015255	0	0
CHOp24	FBgn0029709	0.108268	0.279626	0.269538
CHORD	FBgn0029503	0.015613	0.004923	0.0049
Chro	FBgn0044324	0.010173	0.006423	0.007689
chrw	FBgn0015372	0.019556	0.037838	0.054212
Cht5	FBgn0038180	0.059865	0.004139	0.00666
Cht6	FBgn0030171	0.00068	0	0.000168
cib	FBgn0026084	1.104264	0.911271	1.025045
cin	FBgn0000316	0.000898	0.002137	0.004299
Cip4	FBgn0035533	0.00421	0.002762	0.001199
Cka	FBgn0044323	0.006472	0.003027	0.004233

CkIalpha	FBgn0015024	0.00181	0.002137	0.015321
CkIIalpha	FBgn0000258	0.118092	0.112613	0.146855
CkIIbeta	FBgn0000259	0.034041	0.049335	0.031553
cl	FBgn0000318	0.413994	0.289139	0.412117
Clc	FBgn0024814	0.11961	0.179916	0.140529
Clic	FBgn0030529	0.106241	0.124018	0.102395
CLIP-190	FBgn0020503	0.004118	0.003243	0.003032
clt	FBgn0000326	0	0.001281	0
cni	FBgn0000339	0	0	0.016716
Cnx99A	FBgn0015622	0.077584	0.076788	0.083123
Cog3	FBgn0031536	0.004971	0.008777	0.010646
Cog7	FBgn0051040	0.006604	0.015218	0.017357
coil	FBgn0033265	0	0	0.001193
colt	FBgn0019830	0.013362	0	0.002472
comt	FBgn0000346	0.004116	0.002933	0.005104
Cont	FBgn0037240	0.002945	0	0
Coprox	FBgn0021944	0.014172	0.015314	0.010439
cora	FBgn0010434	0.022387	0.019495	0.012375
CoRest	FBgn0053525	0	0.001096	0
Cortactin	FBgn0025865	0.007714	0.011929	0.006749
CoVa	FBgn0019624	0.265028	0.210885	0.264183
Cp1	FBgn0013770	0.824663	1.23709	1.114653
Cp190	FBgn0000283	0.004657	0.006257	0.005217
cpa	FBgn0034577	0.101463	0.108015	0.101034
cpb	FBgn0011570	0.022929	0.062132	0.030292
Cpr	FBgn0015623	0.025879	0.024814	0.042301
Cpr100A	FBgn0039805	0	0.002988	0
Cpr31A	FBgn0053302	0.003612	0	0
Cpr49Ac	FBgn0033725	0.081435	0.012248	0.017653
Cpr60D	FBgn0050163	0.024201	0	0.008132
Cpr64Ab	FBgn0035511	0.005596	0	0
Cpr64Ad	FBgn0035513	0.076612	0.083432	0.048487
Cpr65Av	FBgn0052405	0.011065	0	0
Cpr65Ax2	FBgn0042118	0.048195	0.014362	0.033182
Cpr78E	FBgn0037114	0.008998	0.005436	0
Cpsf73	FBgn0261065	0.000892	0	0
CPTI	FBgn0027842	0.001554	0.014021	0.021152
Crc	FBgn0005585	1.163533	1.558839	1.409592
CrebB-17A	FBgn0014467	0.001735	0	0
CREG	FBgn0025456	0.124204	0.260247	0.288537
Crk	FBgn0024811	0.053735	0.014584	0.009192
crl	FBgn0015374	0	0	0.0113
CRMP	FBgn0023023	0	0.002568	0.005982
crn	FBgn0000377	0.0026	0	0
croc	FBgn0014143	0	0	0.002978
crq	FBgn0015924	0	0.001576	0.006672

Csat	FBgn0024994	0.001645	0.0358	0.057759
CSN3	FBgn0027055	0.00277	0	0.006412
CSN4	FBgn0027054	0.005541	0	0.002303
CSN5	FBgn0027053	0.012557	0.014214	0.021649
CSN6	FBgn0028837	0.005441	0	0.002218
CSN7	FBgn0028836	0.00224	0.008859	0.008961
CstF-50	FBgn0039867	0	0.002353	0.002839
CstF-64	FBgn0027841	0	0.002283	0.003448
csw	FBgn0000382	0.003886	0	0.000891
CtBP	FBgn0020496	0.040053	0.02823	0.035956
ctp	FBgn0011760	0.461542	0.583465	0.584744
Cul-2	FBgn0032956	0	0	0.001004
Cul-3	FBgn0261268	0	0	0.003223
Cul-4	FBgn0033260	0.001015	0	0
Cwc25	FBgn0031452	0.001195	0	0
Cyp1	FBgn0004432	1.104761	1.082646	0.848201
Cyp12c1	FBgn0036806	0	0	0.001789
Cyp12d1-d	FBgn0053503	0	0	0.001452
Cyp12d1-p	FBgn0050489	0	0	0.001452
Cyp12e1	FBgn0037817	0.021038	0	0
Cyp18a1	FBgn0010383	0.001134	0.001339	0
Cyp28d1	FBgn0031689	0	0	0.003374
cyp33	FBgn0028382	0	0	0.004517
Cyp4ad1	FBgn0033292	0.007116	0.004282	0.008299
Cyp4d1	FBgn0005670	0.002789	0.002813	0.009925
Cyp4d8	FBgn0015033	0	0	0.002025
Cyp4e2	FBgn0014469	0	0.001369	0.00322
Cyp6a21	FBgn0033981	0	0.001429	0.001495
Cyp6d2	FBgn0034756	0	0.003404	0.005897
Cyp6d5	FBgn0038194	0.0012	0	0
Cyp9b2	FBgn0015039	0.001208	0.001426	0.020124
Cyp9f2	FBgn0038037	0	0	0.00146
cype	FBgn0015031	0.10338	0	0
Cypl	FBgn0035141	0	0.004232	0.00428
Cys	FBgn0004629	0.472583	0.143513	0.305294
Cyt-b5	FBgn0033189	0.079394	0.082009	0.128328
Cyt-b5-r	FBgn0000406	0.002777	0.001652	0.007094
Cyt-c-p	FBgn0000409	0.424799	0.384054	0.339218
D1	FBgn0000412	0.077859	0.006937	0.014619
D19A	FBgn0022935	0.000722	0	0
Dak1	FBgn0028833	0.586576	0.444601	0.485378
dalao	FBgn0030093	0.00492	0.002664	0.001607
dally	FBgn0011577	0.002923	0	0
Dbi	FBgn0010387	0	0.085172	0.170298
Dbp73D	FBgn0004556	0.002085	0.003585	0.002525
dco	FBgn0002413	0.001416	0	0.007287

Dcr-2	FBgn0034246	0.003332	0.003034	0.003734
Ddc	FBgn0000422	0.016774	0	0.002966
Ddx1	FBgn0015075	0.001132	0	0
DebB	FBgn0000426	0.041774	0	0.027353
Def	FBgn0010385	0.013209	0	0.008188
Dek	FBgn0026533	0.032071	0.01492	0.017461
deltaCOP	FBgn0028969	0.388332	0.262684	0.210957
Df31	FBgn0022893	0.360022	0.063141	0.168903
Dgp-1	FBgn0027836	0.005207	0.001076	0.001126
dgt4	FBgn0026085	0	0.008866	0
Dhc16F	FBgn0013809	0.000354	0.000182	0.000414
Dhc36C	FBgn0013810	0.001116	0.003363	0.006475
Dhc62B	FBgn0013811	0	0	0.00245
Dhc64C	FBgn0010349	0.005647	0.008729	0.012558
Dhc98D	FBgn0013813	0	0	0.000148
Dhod	FBgn0000447	0	0	0.002315
DhpD	FBgn0261436	0.004064	0.009645	0.015555
Dhpr	FBgn0035964	0.253035	0.078246	0.211952
dia	FBgn0011202	0.000571	0	0.00069
didum	FBgn0261397	0.001596	0.000557	0.000422
DIP2	FBgn0024806	0.003464	0	0
Dip-B	FBgn0000454	0.19412	0.097484	0.115511
Dip-C	FBgn0000455	0.015381	0.009516	0.023852
Dis3	FBgn0039183	0.000634	0	0
dj-1beta	FBgn0039802	0.062027	0.048294	0.059904
dl	FBgn0260632	0	0.000721	0
Dlc90F	FBgn0024432	0.011065	0.098533	0.049385
dlg1	FBgn0001624	0.017091	0.004792	0.005278
Dlic	FBgn0030276	0.023142	0.014247	0.00766
Dmau\CecA1	FBgn0023320	0	0	0.023915
dmt	FBgn0016792	0.00213	0	0
DnaJ-1	FBgn0015657	0.012255	0.013275	0.012652
DNaseII	FBgn0000477	0.037995	0.015809	0.030401
dnc	FBgn0000479	0.003059	0.009598	0.016785
Doa	FBgn0259220	0	0.000866	0.001447
dod	FBgn0015379	0.039429	0.056678	0.050101
dom	FBgn0020306	0	0	0.000295
dor	FBgn0000482	0	0.00271	0.001201
Dp1	FBgn0027835	0.215308	0.164582	0.146408
dpa	FBgn0015929	0.003093	0.001152	0.002263
Dph5	FBgn0024558	0.017407	0	0.010205
DppIII	FBgn0037580	0.242606	0.190613	0.173533
dpr	FBgn0040726	0	0.001962	0
Dpy-30L1	FBgn0032293	0.062564	0.042683	0.056495
dre4	FBgn0002183	0.001323	0	0
Dref	FBgn0015664	0.003446	0.009336	0.01356

drk	FBgn0004638	0.117381	0.013769	0.062115
dro2	FBgn0052279	0	0.010288	0.065588
dro5	FBgn0035434	0.073973	0	0
dro6	FBgn0052268	0.207827	0	0.010463
Droj2	FBgn0038145	0.128858	0.074963	0.086829
Drp1	FBgn0026479	0.033386	0.02823	0.022251
drpr	FBgn0027594	0.002091	0	0
Drs	FBgn0010381	0.055805	0.077038	0.059698
Drs-l	FBgn0052274	0.017677	0	0
dsh	FBgn0000499	0	0.001195	0
Dsor1	FBgn0010269	0.016025	0.004401	0
Dsp1	FBgn0011764	0.020757	0.004434	0.004302
dUTPase	FBgn0250837	0.057494	0.0127	0.025245
Dyb	FBgn0033739	0.000986	0	0
dyn-p25	FBgn0040228	0.002953	0	0
Dys	FBgn0260003	0.001283	0	0.000344
E(bx)	FBgn0000541	0.000233	0	0.000283
e(r)	FBgn0011586	0	0.016756	0
e(y)2	FBgn0000618	0.006038	0	0
Eb1	FBgn0027066	0.145439	0.11074	0.1031
ebi	FBgn0023444	0.005568	0.002093	0.001339
eca	FBgn0069242	0.131697	0.272831	0.31443
Ect3	FBgn0260746	0.015093	0.35574	0.464074
Ect4	FBgn0085402	0.000605	0.002377	0.001162
Edem2	FBgn0032480	0.001539	0	0.002166
Edg84A	FBgn0000552	0	0.129424	0.040622
eEF1delta	FBgn0032198	0.626072	0.625152	0.556553
Ef1alpha100E	FBgn0000557	1.48782	1.561164	1.093393
Ef1alpha48D	FBgn0000556	3.016065	3.94121	2.598671
Ef1beta	FBgn0028737	0.807835	0.85098	0.903366
Ef1gamma	FBgn0029176	0.572428	0.672997	0.594316
Ef2b	FBgn0000559	1.024938	1.154288	0.922774
eff	FBgn0011217	0.117981	0.075878	0.129149
Egfr	FBgn0003731	0	0	0.000571
egl	FBgn0000562	0	0.001005	0
eIF-1A	FBgn0026250	0.147629	0.080212	0.102456
eIF-2alpha	FBgn0004925	0.276513	0.164288	0.175894
eIF2B-alpha	FBgn0039726	0.010251	0	0
eIF2B-beta	FBgn0024996	0.003539	0.004232	0.003419
eIF2B-epsilon	FBgn0023512	0.008872	0.009114	0.005425
eIF-2beta	FBgn0004926	0.065601	0.023759	0.033931
eIF2B-gamma	FBgn0034029	0.022427	0.01149	0.008851
eIF-3p40	FBgn0022023	0.205874	0.170799	0.203317
eIF-3p66	FBgn0040227	0.176255	0.155656	0.135834
eIF3-S10	FBgn0037249	0.09047	0.105416	0.101397
eIF-4a	FBgn0001942	0.855862	0.728103	0.699754

eIF4AIII	FBgn0037573	0.124117	0.026212	0.041112
eIF-4E	FBgn0015218	0.196508	0.108259	0.12999
eIF4E-4	FBgn0035709	0.006312	0.00629	0.029398
eIF4G	FBgn0023213	0.074484	0.053728	0.036676
eIF5	FBgn0030719	0.049427	0.012168	0.012098
eIF-5A	FBgn0034967	0.80411	0.920266	1.061353
eIF5B	FBgn0026259	0.017343	0.015555	0.017714
eIF6	FBgn0034915	0.035069	0.034129	0.034593
Eig71Ea	FBgn0004588	1.498391	0.423704	0.423835
Eig71Eb	FBgn0004589	1.290288	0.508051	0.386204
Eig71Ec	FBgn0004590	1.274443	1.358438	1.140285
Eig71Ed	FBgn0004591	3.400465	1.919753	1.520074
Eig71Ef	FBgn0004593	4.373492	3.140239	1.917939
Eig71Eg	FBgn0004594	0.937773	0.391226	0.43717
Eig71Eh	FBgn0014848	0.320237	0	0
Eig71Ei	FBgn0014849	0.653674	0.072676	0.007385
Eig71Ej	FBgn0014850	0.397693	0.469265	0.676493
Eig71Ek	FBgn0014851	0.683093	1.259931	1.350827
Eip55E	FBgn0000566	0.149056	0.164514	0.135224
Eip63E	FBgn0005640	0	0.001962	0.002053
Eip63F-1	FBgn0004910	0	0	0.007806
Eip71CD	FBgn0000565	0	0.002928	0.003074
Eip93F	FBgn0013948	0	0	0.002715
elav	FBgn0260400	0	0.003084	0.003119
Elf	FBgn0020443	0.189441	0.158527	0.14217
elm	FBgn0037358	0.006148	0.003196	0.003246
Elongin-B	FBgn0023212	0.132013	0.217583	0.151302
Elongin-C	FBgn0023211	0.087628	0.100271	0.065239
Elp3	FBgn0031604	0	0.001349	0.00137
emb	FBgn0020497	0.006523	0.006081	0.012926
emp	FBgn0010435	0	0.002823	0.009359
EndoGI	FBgn0028515	0.191159	0.160485	0.167344
endos	FBgn0061515	0.032608	0.008385	0.022825
Eno	FBgn0000579	0.752302	1.006718	1.140873
ens	FBgn0035500	0.002222	0.008309	0.005141
Eps-15	FBgn0035060	0.001997	0.00081	0
epsilonCOP	FBgn0027496	0.386291	0.369144	0.345081
eRF1	FBgn0036974	0.237747	0.156523	0.165844
ergic53	FBgn0035909	0.084616	0.236108	0.206511
Ero1L	FBgn0261274	0.032098	0.013231	0.026273
Est-6	FBgn0000592	0.005692	0	0
etaTry	FBgn0011554	0	0	0.002887
exba	FBgn0250753	0.054349	0.037171	0.044507
exo84	FBgn0260946	0.001153	0	0
f	FBgn0000630	0	0.000661	0
Faa	FBgn0016013	0.001462	0	0

faf	FBgn0005632	0.001105	0.000895	0.001954
Faf	FBgn0025608	0.001773	0	0.009925
Fancd2	FBgn0038827	0.000819	0.000487	0
Fas1	FBgn0000634	0.00219	0	0.00116
Fas2	FBgn0000635	0.002111	0	0.002245
Fas3	FBgn0000636	0	0.001964	0
Fatp	FBgn0021953	0.002281	0.004602	0.001203
fat-spondin	FBgn0026721	0.015898	0.001616	0.005308
fau	FBgn0020439	0.009865	0.071658	0.127127
fax	FBgn0014163	0.094916	0.04599	0.107074
fbp	FBgn0032820	0.228665	0.262191	0.197363
Fbp1	FBgn0000639	1.712995	3.822756	3.860396
Fbp2	FBgn0000640	0.421883	0.657839	0.634451
Fdh	FBgn0011768	0.280857	0.24477	0.199428
fdl	FBgn0045063	0	0	0.001824
Fer1HCH	FBgn0015222	0.498022	0.19736	0.358663
Fer2LCH	FBgn0015221	0.544539	0.267327	0.301822
ferrochelatase	FBgn0024891	0.039431	0.003815	0.006487
fh	FBgn0030092	0.003278	0	0
Fib	FBgn0003062	0.118302	0.110626	0.128739
Fim	FBgn0024238	0.054877	0.051627	0.067066
Fis1	FBgn0039969	0.006355	0.010182	0.019998
Fit1	FBgn0035498	0.01101	0.010078	0.009467
Fit2	FBgn0036688	0.005439	0	0.001683
FK506-bp1	FBgn0013269	0.071057	0.075953	0.081849
FK506-bp2	FBgn0013954	0.589942	0.894574	0.6113
Fkbp13	FBgn0010470	0.065546	0.079527	0.151913
FKBP59	FBgn0029174	0.096971	0.034724	0.051611
fl(2)d	FBgn0000662	0.001131	0	0
flfl	FBgn0024555	0.001274	0.000755	0.003548
Flo-2	FBgn0024753	0	0	0.00214
flr	FBgn0260049	0.116458	0.113832	0.117454
flw	FBgn0000711	0.001887	0.002182	0.015984
Fmo-2	FBgn0033079	0	0	0.003948
Fmr1	FBgn0028734	0.018516	0.006831	0.020473
fne	FBgn0086675	0	0.004184	0.006348
fon	FBgn0032773	0.131123	0.143584	0.136759
for	FBgn0000721	0.001954	0	0.00181
Fpps	FBgn0025373	0.00972	0	0.003167
fray	FBgn0023083	0.005571	0.004462	0.012491
Fs(2)Ket	FBgn0000986	0.015258	0.004443	0.007536
ftz-f1	FBgn0001078	0.002196	0.002128	0.000913
FucT6	FBgn0030327	0	0	0.001222
fwd	FBgn0004373	0	0.002048	0
fws	FBgn0024689	0.002453	0.008912	0.007672
fz2	FBgn0016797	0	0	0.00109

Gal	FBgn0001089	0.00486	0.005432	0.008813
galectin	FBgn0031213	0.008953	0.001481	0.004645
GalNAc-T1	FBgn0034025	0.087187	0.262004	0.189347
GalNAc-T2	FBgn0030930	0.051959	0.173488	0.171373
Galpha49B	FBgn0004435	0	0.002827	0.002143
gammaCop	FBgn0028968	0.344542	0.413149	0.376504
gammaSnap	FBgn0028552	0.026393	0.013844	0.008848
Gap69C	FBgn0020655	0.067317	0.032677	0.038465
Gapdh1	FBgn0001091	1.209121	1.427458	1.341287
Gapdh2	FBgn0001092	1.684834	1.703164	1.37106
garz	FBgn0033714	0.003372	0.002366	0.002908
Gasp	FBgn0026077	0.07529	0.013553	0
gbb	FBgn0024234	0.00134	0.00766	0.001656
Gbeta13F	FBgn0001105	0.075262	0.1104	0.097455
gce	FBgn0030627	0.000904	0.001448	0
GckIII	FBgn0086736	0.000943	0	0
Gclc	FBgn0040319	0.006006	0	0.00189
Gclm	FBgn0046114	0	0	0.002654
Gdh	FBgn0001098	0.371891	0.134525	0.185916
Gdi	FBgn0004868	0.499968	0.585666	0.468871
Ge-1	FBgn0032340	0.001808	0.001082	0.003369
Gel	FBgn0010225	0.13927	0.061488	0.0881
Gfat2	FBgn0039580	0.021521	0.004383	0.016159
gfzf	FBgn0250732	0.001574	0.000689	0.003027
Gga	FBgn0030141	0.004672	0.006026	0.002283
Ggamma1	FBgn0004921	0	0.024894	0.017193
Gie	FBgn0037551	0.007678	0.013241	0.034589
gig	FBgn0005198	0	0.00108	0.000408
Gip	FBgn0011770	0.111434	0.030714	0.037554
Gl	FBgn0001108	0.006118	0.003913	0.004465
GlcAT-I	FBgn0066114	0	0.031494	0.020807
Gld	FBgn0001112	0.000969	0	0
glo	FBgn0259139	0.008529	0.013857	0.008923
glob1	FBgn0027657	0.340279	0.09072	0.276329
Glt	FBgn0001114	0.097882	0.12722	0.145924
Glycogenin	FBgn0034603	0.078783	0.167001	0.284913
GlyP	FBgn0004507	0.200162	0.224702	0.399311
GM130	FBgn0034697	0.068891	0.073136	0.06796
Gmap	FBgn0027287	0.013064	0.023712	0.01726
Gmd	FBgn0031661	0.00623	0.008761	0.017448
Gmer	FBgn0034794	0.011412	0.00232	0.017258
GNBP3	FBgn0040321	0.027566	0	0.001543
G-oalpha47A	FBgn0001122	0	0	0.002136
Golgin84	FBgn0039188	0.001182	0.003329	0
Gos28	FBgn0044871	0.005313	0.004301	0.005841
Got1	FBgn0001124	0.093036	0.086435	0.113103

Got2	FBgn0001125	0.287392	0.132871	0.185749
Gp150	FBgn0013272	0	0	0.002156
Gp93	FBgn0039562	0.452046	0.930022	0.869444
Gpdh	FBgn0001128	0.395546	0.422179	0.49726
Gr22c	FBgn0045499	0	0.00188	0.001975
Grasp65	FBgn0036919	0.141852	0.174212	0.188448
grh	FBgn0259211	0.000454	0	0
gro	FBgn0001139	0.003701	0	0.003348
growl	FBgn0037245	0.196291	0.104797	0.138186
GS	FBgn0030882	0.251315	0.31165	0.244177
Gs1	FBgn0001142	0.116305	0.152393	0.204241
Gs2	FBgn0001145	0.019402	0.263967	0.238415
G-salpha60A	FBgn0001123	0.001584	0	0
GstD1	FBgn0001149	2.366164	2.333538	1.759573
GstD10	FBgn0042206	0	0.010405	0.010917
GstD2	FBgn0010038	0.009458	0.013742	0.008721
GstD3	FBgn0010039	0.192949	0.132885	0.080829
GstD4	FBgn0010040	0.383012	0.651566	0.479993
GstD5	FBgn0010041	0.006611	0.01023	0.00868
GstD7	FBgn0010043	0.023659	0.00654	0.006753
GstD9	FBgn0038020	0.350067	0.563843	0.562298
GstE6	FBgn0063494	0	0	0.00521
GstE7	FBgn0063493	0.190486	0.116519	0.150764
GstE8	FBgn0063492	0.014634	0	0.008828
GstS1	FBgn0010226	0.077184	0.030235	0.068879
Gtp-bp	FBgn0010391	0.119506	0.073951	0.087971
gw	FBgn0051992	0.004585	0.001259	0.00196
Gyk	FBgn0025592	0.016812	0.001519	0.001596
hay	FBgn0001179	0.000764	0	0
Hcf	FBgn0039904	0.001644	0	0.000502
HDAC6	FBgn0026428	0.000549	0.000635	0.000666
Hel25E	FBgn0014189	0.244572	0.206922	0.207891
heph	FBgn0011224	0.002509	0	0
Herp	FBgn0031950	0	0	0.001626
Hex-A	FBgn0001186	0.062622	0.055007	0.045919
Hex-C	FBgn0001187	0	0	0.005402
Hexo1	FBgn0041630	0.009128	0	0.004781
Hexo2	FBgn0041629	0.00098	0.003474	0.006165
Hf	FBgn0014000	0	0.003365	0.010588
Hip1	FBgn0036309	0	0.000685	0
Hira	FBgn0022786	0.007624	0.014825	0.009963
His1	FBgn0001195	0.082236	0.09527	0.106688
His1:CG31617	FBgn0051617	0.082236	0.09527	0.106688
His2A	FBgn0001196	1.545113	2.111637	1.755072
His2A:CG31618	FBgn0051618	1.545113	2.111637	1.755072
His2Av	FBgn0001197	0.717916	0.896722	0.782228

His2B	FBgn0001198	0.731965	0.719609	0.514659
His2B:CG17949	FBgn0061209	0.731965	0.719609	0.514659
His3	FBgn0001199	0.302154	0.102719	0.276421
His3.3A	FBgn0014857	0.202784	0.11011	0.215056
His3.3B	FBgn0004828	0.202784	0.11011	0.215056
His4	FBgn0001200	1.615582	0.655487	0.799036
His4:CG31611	FBgn0051611	1.615582	0.655487	0.799036
His4r	FBgn0013981	1.615582	0.655487	0.799036
hk	FBgn0001202	0.003027	0	0
hkl	FBgn0086441	0.014325	0.001198	0.002813
Hlc	FBgn0001565	0.001572	0	0
HmgD	FBgn0004362	0.191812	0.019949	0
HmgZ	FBgn0010228	0.446588	0.227318	0.24797
Hml	FBgn0029167	0.013573	0	0
Hmu	FBgn0015737	0.051299	0.104733	0.109238
Hn	FBgn0001208	0.011274	0.017635	0.04307
Ho	FBgn0037933	0	0.002433	0.009788
hoip	FBgn0015393	0.341588	0.316217	0.347239
Hop	FBgn0024352	0.140994	0.081824	0.085373
how	FBgn0017397	0.003012	0	0
HP1b	FBgn0030082	0.003428	0	0
HP1c	FBgn0039019	0.005201	0	0.00637
Hph	FBgn0086689	0.006833	0	0
Hr4	FBgn0023546	0	0	0.000496
Hrb27C	FBgn0004838	0.170041	0.148066	0.106088
Hrb87F	FBgn0004237	0.146755	0.094236	0.109877
Hrb98DE	FBgn0001215	0.068389	0.052727	0.072895
Hrs	FBgn0031450	0.022332	0.01856	0.020125
Hsc70-1	FBgn0001216	0.182803	0.0665	0.108788
Hsc70-2	FBgn0001217	0.091071	0.038568	0.063419
Hsc70-3	FBgn0001218	1.889616	2.451945	2.471659
Hsc70-4	FBgn0001219	1.123074	1.460344	1.219346
Hsc70-5	FBgn0001220	0.068022	0.019445	0.039147
Hsc70Cb	FBgn0026418	0.265438	0.209685	0.216419
Hsp23	FBgn0001224	1.465214	1.773881	1.784819
Hsp26	FBgn0001225	0.114175	0.070312	0.097931
Hsp27	FBgn0001226	0.707208	0.736815	0.584904
Hsp60	FBgn0015245	0.364914	0.196921	0.255732
Hsp60C	FBgn0031728	0.059238	0.034095	0.051263
Hsp67Ba	FBgn0001227	0.0014	0.005021	0.00609
Hsp67Bb	FBgn0001228	0.053552	0.084411	0.055979
Hsp68	FBgn0001230	0.153991	0.068162	0.115751
Hsp70Ab	FBgn0013276	0.135721	0.05949	0.088244
Hsp70Bbb	FBgn0051354	0.134961	0.059583	0.088382
Hsp70Bc	FBgn0013279	0.134961	0.059583	0.088382
Hsp83	FBgn0001233	0.646815	0.584004	0.608974

hts	FBgn0004873	0.078972	0.085184	0.069739
hyd	FBgn0002431	0	0.000258	0
hyx	FBgn0037657	0.002283	0	0
I-2	FBgn0028429	0.021904	0	0.004773
Iap2	FBgn0015247	0.001225	0	0
Ice	FBgn0019972	0.011382	0.007265	0.004444
icln	FBgn0029079	0.008509	0	0
ics	FBgn0028546	0.008696	0.011334	0.019966
Ide	FBgn0001247	0.001233	0.001506	0.000989
Idgf1	FBgn0020416	0.004227	0.005034	0.009945
Idgf2	FBgn0020415	0.046576	0.014787	0.042877
Idgf3	FBgn0020414	0.104157	0.059827	0.088685
Idgf4	FBgn0026415	0.487563	0.158988	0.228788
Idgf5	FBgn0064237	0.00414	0	0
Idh	FBgn0001248	0.360387	0.662048	0.504607
if	FBgn0001250	0.004106	0.002461	0.003128
Ilk	FBgn0028427	0.014116	0.00389	0.010918
Ilp6	FBgn0044047	0.01152	0	0
IM10	FBgn0033835	0.009199	0	0
IM18	FBgn0067903	0.017179	0	0
imd	FBgn0013983	0	0	0.003972
Imp	FBgn0030235	0.017207	0.026187	0.027465
ImpE1	FBgn0001253	0.002409	0.000461	0
ImpE2	FBgn0001254	0.089089	0	0
ImpE3	FBgn0001255	0.003753	0	0
ImpL1	FBgn0001256	0.269152	0.02796	0.039737
ImpL2	FBgn0001257	0	0.002789	0.002833
ImpL3	FBgn0001258	0.147217	0.247927	0.438985
Indy	FBgn0036816	0	0.008899	0.007245
Inos	FBgn0025885	0.024164	0	0.003463
Int6	FBgn0025582	0.122812	0.203696	0.179285
inx2	FBgn0027108	0.001662	0.001962	0.003279
inx3	FBgn0028373	0.00773	0	0.001907
iPLA2-VIA	FBgn0036053	0.000688	0	0
Ir68a	FBgn0036150	0.000976	0	0
Irc	FBgn0038465	0.014366	0.00317	0.005782
ird1	FBgn0260935	0.000454	0	0
Irp-1A	FBgn0024958	0.059867	0.045267	0.053636
Irp-1B	FBgn0024957	0.143825	0.10031	0.169842
Iswi	FBgn0011604	0	0	0.000734
Itp-r83A	FBgn0010051	0.000219	0	0.000597
Jafrac1	FBgn0040309	0.50907	0.632414	0.563137
Jafrac2	FBgn0040308	0.123431	0.096091	0.110032
janA	FBgn0001280	0.031715	0.025816	0.00558
jar	FBgn0011225	0.010093	0.004123	0.002875
jbug	FBgn0028371	0.001721	0	0.000406

jdp	FBgn0027654	0.003127	0	0.008686
Jhe	FBgn0010052	0	0	0.002097
Jheh1	FBgn0010053	0	0	0.002989
Jheh2	FBgn0034405	0.005287	0.001555	0.0075
jigr1	FBgn0039350	0.001854	0	0
Jon25Bi	FBgn0020906	0.003025	0	0
Jon99Cii	FBgn0003356	0.00235	0	0
Jon99Ciii	FBgn0003357	0.00235	0	0
Kap-alpha1	FBgn0024889	0.0055	0	0.010482
Kap-alpha3	FBgn0027338	0.15832	0.074454	0.070531
Karybeta3	FBgn0087013	0.092912	0.094649	0.100496
kat80	FBgn0040207	0.00076	0	0
kay	FBgn0001297	0	0.004827	0.001667
KdelR	FBgn0022268	0	0.031105	0.040292
kdn	FBgn0086133	0.197536	0.06762	0.121143
Khc	FBgn0001308	0.082394	0.060255	0.045297
Klc	FBgn0010235	0.074513	0.055685	0.063795
Klp10A	FBgn0030268	0.007632	0.00182	0
Klp61F	FBgn0004378	0.000584	0	0
ko	FBgn0020294	0.000577	0	0
Kr-h2	FBgn0028419	0.00666	0.011443	0.03097
krz	FBgn0040206	0.003874	0.008252	0.009614
kst	FBgn0004167	0.006284	0.003175	0.005488
kuk	FBgn0038476	0.004317	0	0
l(1)G0156	FBgn0027291	0.17978	0.079703	0.166391
l(1)G0193	FBgn0027280	0.002818	0	0
l(1)G0222	FBgn0028343	0.010364	0.011669	0.003483
l(1)G0230	FBgn0028342	0.412629	0.327713	0.3942
l(1)G0232	FBgn0028341	0.001225	0	0.002417
l(1)G0255	FBgn0028336	0.044221	0.02569	0.039559
l(1)G0289	FBgn0028331	0.000969	0.002305	0.006561
l(1)G0320	FBgn0028327	0.081921	0.093472	0.100454
l(1)G0334	FBgn0028325	0.184106	0.078637	0.17312
l(2)01289	FBgn0010482	0.000799	0.007698	0.028321
l(2)01810	FBgn0010497	0	0	0.00189
l(2)06225	FBgn0010612	0.19015	0.007523	0.047667
l(2)06496	FBgn0010622	0.020255	0.030979	0.025858
l(2)09851	FBgn0022288	0.015672	0.003213	0.004624
l(2)35Bg	FBgn0001977	0.054502	0.027453	0.040108
l(2)35Df	FBgn0001986	0.000574	0	0
l(2)35Di	FBgn0001989	0.02451	0	0
l(2)37Cc	FBgn0002031	0.374356	0.39618	0.352191
l(2)44DEa	FBgn0010609	0.021222	0.01938	0.025543
l(2)efl	FBgn0011296	0.150031	0.336002	0.414427
l(2)gd1	FBgn0250747	0.001495	0	0
l(2)gl	FBgn0002121	0.003692	0.003199	0.003796

l(2)k09913	FBgn0021979	0.009717	0.002279	0.019692
l(2)s5379	FBgn0010704	0.067495	0	0.015096
l(2)tid	FBgn0002174	0.007053	0	0
l(3)01239	FBgn0010741	0.048547	0.027295	0.033738
l(3)03670	FBgn0010808	0.022967	0.017393	0.038281
l(3)04053	FBgn0010830	0	0	0.001288
l(3)82Fd	FBgn0013576	0.014323	0.004226	0.00346
l(3)neo18	FBgn0011455	0.03861	0.007744	0.004066
La	FBgn0011638	0.049796	0.030862	0.024825
Lac	FBgn0010238	0.001735	0	0
Lam	FBgn0002525	0.033023	0.048795	0.058985
LamC	FBgn0010397	0.115061	0.180416	0.13617
LanA	FBgn0002526	0.025134	0.017829	0.018697
LanB1	FBgn0002527	0.016255	0.011967	0.014636
LanB2	FBgn0002528	0.026891	0.021901	0.0196
lap	FBgn0086372	0.009548	0.009579	0.012649
lark	FBgn0011640	0.012744	0.009831	0.022815
larp	FBgn0260724	0.008331	0.0028	0.003378
Lasp	FBgn0063485	0.009028	0.012379	0.010269
LBR	FBgn0034657	0.002481	0	0
Lcp1	FBgn0002531	0.061301	0.024863	0.011635
Lcp2	FBgn0002533	0.146082	0.025652	0.012005
Lcp3	FBgn0002534	0.08451	0.00665	0.015123
Lcp4	FBgn0002535	0.27952	0.026599	0.091877
Lcp65Ab1	FBgn0020644	0.013899	0.085601	0.076206
Lcp65Ab2	FBgn0020643	0.013899	0.085601	0.076206
Lcp65Ac	FBgn0020642	0.043226	0.031974	0.062506
Lcp65Ad	FBgn0020641	0	0.12551	0.106184
Lcp65Af	FBgn0020639	0.018381	0	0
Lcp65Ag1	FBgn0020638	0.070378	0	0
Lcp65Ag2	FBgn0020637	0.070378	0	0
Lcp65Ag3	FBgn0086611	0.070378	0	0
Lcp9	FBgn0025578	0.024464	0.016191	0.008188
ldlCp	FBgn0026634	0.004888	0.004518	0.012723
lds	FBgn0002542	0	0	0.001847
lectin-28C	FBgn0040099	0	0	0.020594
Lectin-galC1	FBgn0016675	0.011112	0	0
Lerp	FBgn0051072	0.00232	0.015366	0.015912
levy	FBgn0034877	0.120074	0.015761	0.050095
Lhr	FBgn0034217	0.02082	0.002156	0
lic	FBgn0261524	0.013495	0.005202	0.012614
lid	FBgn0031759	0.000339	0	0
ligatin	FBgn0041588	0.004726	0	0
lin19	FBgn0015509	0	0	0.001555
Lip4	FBgn0032264	0	0.001659	0.001743
Lis-1	FBgn0015754	0	0.005992	0.002381

Lmpt	FBgn0036672	0.010857	0.015016	0.031944
loco	FBgn0020278	0.001749	0	0
lola	FBgn0005630	0.005591	0.005078	0.003935
lolal	FBgn0022238	0.004767	0	0.017181
lox	FBgn0039848	0.390181	0.093726	0.04386
lqf	FBgn0028582	0.002951	0.004498	0.002576
Lsd-1	FBgn0039114	0	0.015038	0.046448
Lsd-2	FBgn0030608	0.027823	0.02046	0.074892
LSm1	FBgn0261067	0.004419	0	0
LSm3	FBgn0051184	0	0	0.007314
LSm7	FBgn0261068	0.080056	0.033984	0.076702
Lsp1alpha	FBgn0002562	0.572438	1.487486	1.498692
Lsp1beta	FBgn0002563	1.085923	2.139919	2.379482
Lsp1gamma	FBgn0002564	1.071914	3.02413	4.027936
Lsp2	FBgn0002565	1.531129	0.341774	0.362798
lva	FBgn0029688	0.062587	0.077821	0.057005
LysB	FBgn0004425	0.084512	0.051245	0.019066
LysD	FBgn0004427	0.084512	0.051245	0.019066
LysE	FBgn0004428	0.069863	0.051245	0.019066
LysP	FBgn0004429	0	0.063415	0.042306
LysS	FBgn0004430	0.004356	0	0
LysX	FBgn0004431	0.041615	0.045451	0.018797
M(2)21AB	FBgn0005278	0.006011	0.008946	0.007952
Mad	FBgn0011648	0.001369	0	0
Madm	FBgn0027497	0.002885	0	0
mago	FBgn0002736	0.004118	0.009798	0
mal	FBgn0002641	0	0.000954	0
Manf	FBgn0027095	0.45231	0.246822	0.40219
Map205	FBgn0002645	0	0.006884	0.009113
Map60	FBgn0010342	0	0.001693	0.002224
MAPk-Ak2	FBgn0013987	0.009703	0.00686	0.018043
Mapmodulin	FBgn0034282	0.025977	0.021537	0.024539
Marf	FBgn0029870	0.000747	0.000919	0
mats	FBgn0038965	0.008473	0	0
MBD-like	FBgn0027950	0	0	0.002222
MBD-R2	FBgn0038016	0	0.000854	0
mbf1	FBgn0026208	0.030967	0.030578	0
mbo	FBgn0026207	0	0	0.001714
Mbs	FBgn0005536	0.001074	0	0
Mcm3	FBgn0024332	0.002504	0.001218	0
Mcm6	FBgn0025815	0.003018	0.000912	0
Mcm7	FBgn0020633	0.00257	0	0
Mcr	FBgn0020240	0	0.000423	0
Mct1	FBgn0023549	0	0.005752	0.003914
Mdh	FBgn0029155	0.014854	0.002425	0.002244
Mdr49	FBgn0004512	0	0.000572	0.000581

me31B	FBgn0004419	0.047252	0.036762	0.055417
Mec2	FBgn0030993	0	0.002128	0.0126
MED19	FBgn0036761	0.001848	0	0
MED4	FBgn0035754	0.002346	0.002791	0.002931
membrin	FBgn0260856	0.051051	0.023975	0.037617
Men	FBgn0002719	0.136195	0.123997	0.17914
MESK2	FBgn0043070	0	0.007559	0.014847
MESR3	FBgn0032694	0.002162	0	0
MESR6	FBgn0036846	0.021295	0.027784	0.01994
Mf	FBgn0038294	0.238895	0.414536	0.555637
mfas	FBgn0260745	0.107413	0.028144	0.054537
Mgat1	FBgn0034521	0	0	0.001659
mge	FBgn0035473	0.01681	0	0.006199
Mhc	FBgn0086783	0.392268	0.659927	0.934292
Mi-2	FBgn0013591	0.005568	0.001746	0.002466
Mical	FBgn0053208	0.000444	0.004999	0.025852
mip130	FBgn0023509	0.00125	0	0.001221
miple2	FBgn0029002	0.008774	0	0.00942
mit(1)15	FBgn0004643	0.003377	0.0134	0.016669
Mkk4	FBgn0024326	0.002897	0.006463	0.002839
Mlc1	FBgn0002772	0.289934	0.638668	1.239714
Mlc2	FBgn0002773	0.536864	0.880378	1.526024
Mlc-c	FBgn0004687	0.866914	0.952358	1.01417
mle	FBgn0002774	0.000468	0	0
Mlp60A	FBgn0259209	0.250792	0.359681	0.312786
Mlp84B	FBgn0014863	0.067267	0.066076	0.11102
Mmp1	FBgn0035049	0.005768	0	0.008556
Mmp2	FBgn0033438	0	0.000983	0.003467
Mms19	FBgn0037301	0.003424	0	0.005152
mmy	FBgn0259749	0.015657	0	0.008298
Mo25	FBgn0017572	0.101921	0.023172	0.038257
Moca-cyp	FBgn0039581	0.000642	0	0
mod	FBgn0002780	0.121856	0.104509	0.084398
mod(mdg4)	FBgn0002781	0.003348	0.004037	0.002221
Moe	FBgn0011661	0.319228	0.204856	0.217056
mof	FBgn0014340	0.000995	0	0
mop	FBgn0036448	0.004227	0.001202	0.000532
mor	FBgn0002783	0.003277	0.003454	0.009178
Mov34	FBgn0002787	0.317025	0.1872	0.228605
MP1	FBgn0027930	0.058148	0.011269	0.024442
Mp20	FBgn0002789	0.375546	0.401008	0.458553
Mpcp	FBgn0026409	0.090773	0.008092	0.016505
Mpk2	FBgn0015765	0.003308	0.009455	0.002066
MRG15	FBgn0027378	0.001469	0	0
MRP	FBgn0032456	0	0.00093	0.000605
mRpL12	FBgn0011787	0.025429	0.008523	0.029497

mRpL18	FBgn0026741	0.006627	0	0
mRpL20	FBgn0036335	0	0.119452	0.095773
mRpL24	FBgn0031651	0	0	0.003062
mRpL3	FBgn0030686	0.003993	0	0.003325
mRpL33	FBgn0040907	0	0.738666	0.749027
mRpL4	FBgn0001995	0.008314	0	0
mRpL44	FBgn0037330	0.005516	0	0.002255
mRpL50	FBgn0028648	0.003227	0	0
mRpL54	FBgn0034579	0.013826	0	0.009118
mRpL9	FBgn0038319	0	0.002904	0
mRpS14	FBgn0044030	0.004764	0	0
mRpS16	FBgn0033907	0.096751	0	0.024182
mRpS22	FBgn0039555	0.001585	0	0
mRpS23	FBgn0260407	0.00643	0	0
mRpS30	FBgn0030692	0.0033	0	0
mRpS31	FBgn0036557	0	0.001915	0.002493
MSBP	FBgn0030703	0.023111	0.04869	0.068051
msk	FBgn0026252	0.050958	0.020563	0.050303
Msp-300	FBgn0260952	0	0.003898	0
msps	FBgn0027948	0.000602	0.000363	0.000368
Msr-110	FBgn0015766	0	0	0.001226
mst	FBgn0020272	0.001433	0.002595	0.002361
MstProx	FBgn0015770	0	0.001271	0
MTA1-like	FBgn0027951	0.003191	0.001293	0
mtacp1	FBgn0011361	0.076614	0.040054	0.069982
Mtch	FBgn0027786	0.027154	0.01491	0.004777
mtm	FBgn0025742	0.000978	0.001203	0.001515
Mtor	FBgn0013756	0.00387	0.005179	0.001029
Mtp	FBgn0032904	0.011064	0.031055	0.0808
mts	FBgn0004177	0.085216	0.099451	0.125682
mtSSB	FBgn0010438	0.022282	0.011767	0.031726
mub	FBgn0014362	0.017444	0.008049	0.012034
Muc11A	FBgn0052656	0.000637	0	0.002558
Muc14A	FBgn0052580	0	4.44E-05	9.31E-05
Muc55B	FBgn0034294	0.006464	0	0
Mur11Da	FBgn0052644	0.001414	0	0
mus209	FBgn0005655	0.03226	0.014039	0.007369
Mvl	FBgn0011672	0	0	0.002019
Myo31DF	FBgn0086347	0.00143	0.016028	0.011517
Myo61F	FBgn0010246	0.000589	0	0.001676
mys	FBgn0004657	0.000736	0.004614	0.005703
Nacalpha	FBgn0086904	0.214781	0.219374	0.28863
nAcRbeta-21C	FBgn0031261	0	0	0.007493
Nap1	FBgn0015268	0.142664	0.066362	0.072542
Nat1	FBgn0031020	0.0101	0.005195	0.014085
Nc73EF	FBgn0010352	0.051541	0.017954	0.037549

nct	FBgn0039234	0.000896	0.001036	0.001088
ND23	FBgn0017567	0.070919	0.021306	0.081662
ND42	FBgn0019957	0.044182	0.007138	0.033107
ND75	FBgn0017566	0.127855	0.02203	0.045527
Ndae1	FBgn0259111	0	0.002494	0.000853
Neb-cGP	FBgn0083167	0.665728	0.015516	0.047762
nec	FBgn0002930	0.005207	0.00204	0
Nedd4	FBgn0259174	0.002625	0.001706	0.00225
Nedd8	FBgn0032725	0.185276	0.034587	0.094949
nej	FBgn0015624	0	0	0.000237
NELF-B	FBgn0027553	0	0.00168	0
Nelf-E	FBgn0017430	0.010325	0	0
Nep2	FBgn0027570	0.001593	0	0
nero	FBgn0261479	0.014897	0.010621	0.002504
nes	FBgn0026630	0.007825	0	0.001969
Neurochondrin	FBgn0037447	0.015252	0.014047	0.066981
Nhe1	FBgn0026787	0	0	0.001854
NHP2	FBgn0029148	0.015299	0.010738	0.029623
nimB2	FBgn0028543	0.057485	0.003538	0.007672
nimC4	FBgn0260011	0	0.003951	0.006018
ninaG	FBgn0037896	0.00105	0	0
Nipped-A	FBgn0053554	0.000648	0.000262	0.000199
Nipsnap	FBgn0030724	0.279979	0.068334	0.09292
nito	FBgn0027548	0.005575	0.00414	0.003842
NLaz	FBgn0053126	0.194531	0.074812	0.105551
Nle	FBgn0021874	0.001271	0	0
Nlp	FBgn0016685	0.213895	0.177742	0.178206
Nmdmc	FBgn0010222	0.013941	0	0.00879
Nmt	FBgn0020392	0.016046	0.003104	0.004944
Nnp-1	FBgn0022069	0.000888	0	0
Noa36	FBgn0026400	0	0	0.002391
noi	FBgn0014366	0.001212	0.001432	0.002393
nonA	FBgn0004227	0.005276	0.009129	0.011515
nonA-l	FBgn0015520	0	0.001752	0.002928
nop5	FBgn0026196	0.030085	0.006241	0.016289
Nop56	FBgn0038964	0.020872	0.004056	0
Nop60B	FBgn0259937	0.043216	0.024018	0.024978
Nopp140	FBgn0037137	0.003543	0.002171	0
Not1	FBgn0085436	0.004213	0	0
Npc2a	FBgn0031381	0.283328	0.25713	0.329363
Npc2d	FBgn0037782	0	0.004305	0
Npc2f	FBgn0039154	0.004839	0	0
Npc2g	FBgn0039800	0.355085	0.065622	0.058535
Npc2h	FBgn0039801	0.081768	0.027699	0.024665
Nplp2	FBgn0040813	1.015987	0.637887	0.799706
Nrg	FBgn0002968	0.006442	0.003638	0.005688

Nrt	FBgn0004108	0	0	0.002762
nrv1	FBgn0015776	0	0.002331	0.014647
nrv2	FBgn0015777	0.003802	0	0.006058
Nrx-IV	FBgn0013997	0.001432	0	0
ns1	FBgn0038473	0.009129	0.013998	0.005584
ns3	FBgn0028274	0.001028	0	0
ns4	FBgn0032882	0.001061	0	0
Nsf2	FBgn0013998	0.032697	0.016006	0.020121
Ntf-2	FBgn0031145	0.160381	0.198402	0.238696
Ntf-2r	FBgn0032680	0	0.005729	0.05544
NTPase	FBgn0024947	0.016617	0.055369	0.067634
NUCB1	FBgn0052190	0.157224	0.133665	0.181533
nudC	FBgn0021768	0.07999	0.029058	0.025864
Nup133	FBgn0039004	0.001196	0	0.002291
Nup153	FBgn0061200	0	0	0.000791
Nup154	FBgn0021761	0	0	0.001958
Nup160	FBgn0260937	0	0.00051	0.00096
Nup214	FBgn0010660	0.000728	0.002281	0.001145
Nup358	FBgn0039302	0.007041	0.008361	0.007983
Nup58	FBgn0038722	0	0	0.001385
Nup75	FBgn0034310	0	0	0.001802
Nup98	FBgn0039120	0.00042	0.002146	0.000806
Nurf-38	FBgn0016687	0.408319	0.299236	0.268807
nvy	FBgn0005636	0	0	0.001014
Oat	FBgn0022774	0.051582	0.030248	0.058284
Oatp30B	FBgn0032123	0	0.00189	0
Oatp74D	FBgn0036732	0	0.006208	0
Obp56a	FBgn0034468	0.160472	0.005181	0.012186
Obp56d	FBgn0034470	0.300117	0.047039	0.070741
Obp83g	FBgn0046875	0.008323	0	0
Obp99a	FBgn0039678	0.071861	0	0
Obp99b	FBgn0039685	6.319982	1.646999	1.786062
Obp99c	FBgn0039682	0.538496	0.071426	0.145044
Obp99d	FBgn0039684	0	0	0.01757
obst-A	FBgn0031097	0.093883	0.010495	0
obst-B	FBgn0027600	0.003645	0	0
obst-E	FBgn0031737	0.00504	0	0
O-fut1	FBgn0033901	0.006089	0	0
oho23B	FBgn0015521	1.380377	1.26424	1.138083
omd	FBgn0038168	0	0	0.001211
opa1-like	FBgn0261276	0.001307	0.001868	0.004485
Or82a	FBgn0041621	0	0.003805	0.009376
Or85b	FBgn0037590	0	0	0.004343
Orct	FBgn0019952	0	0.003943	0.003576
Orct2	FBgn0086365	0	0.00127	0
osa	FBgn0003013	0	0	0.000639

Osbp	FBgn0020626	0.039189	0.031122	0.019556
Oscillin	FBgn0031717	0.079334	0.095165	0.147614
Oscp	FBgn0016691	0.308012	0.228976	0.311932
Osi12	FBgn0037419	0.002067	0	0
Osi14	FBgn0040279	0.009134	0	0
Osi6	FBgn0027527	0.048461	0	0
Osi7	FBgn0037414	0.0724	0	0
Ost48	FBgn0014868	0.102975	0.166477	0.18343
OstStt3	FBgn0011336	0.005548	0.013299	0.026557
Ote	FBgn0003022	0.001438	0	0
ox	FBgn0011227	0.011007	0	0
p115	FBgn0040087	0.034491	0.049307	0.05799
p16-ARC	FBgn0031437	0.014935	0.026011	0.029436
p24-1	FBgn0030341	0.108974	0.180547	0.205911
p24-2	FBgn0053105	0.116584	0.241523	0.278348
p38b	FBgn0024846	0.020678	0.023736	0.011465
P58IPK	FBgn0037718	0.083408	0.061905	0.079583
pAbp	FBgn0003031	0.737766	0.301182	0.244745
Pabp2	FBgn0005648	0.007345	0.022099	0.012921
Paf-AHalpha	FBgn0025809	0.07011	0.007745	0.017767
Pak	FBgn0014001	0.002035	0	0.001332
Pak3	FBgn0044826	0.003033	0.001839	0.002416
Papss	FBgn0020389	0.044874	0.065415	0.039124
Papst2	FBgn0036695	0	0.00252	0.00382
par-1	FBgn0260934	0	0.000768	0
par-6	FBgn0026192	0.001737	0	0
pasha	FBgn0039861	0.00095	0	0
Past1	FBgn0016693	0.281102	0.217934	0.221023
path	FBgn0036007	0	0.004237	0.012003
Patj	FBgn0067864	0.00236	0.002856	0
Pax	FBgn0041789	0.091814	0.154421	0.141629
Pbgs	FBgn0036271	0.020029	0.00448	0.008297
Pcd	FBgn0024841	0.022323	0.022505	0.033523
pch2	FBgn0051453	0.002887	0	0
Pcl	FBgn0003044	0	0	0.000725
pcm	FBgn0020261	0.002415	0	0
Pcmt	FBgn0086768	0.008133	0	0.004148
pcx	FBgn0003048	0.000358	0.000846	0.002622
PDCD-5	FBgn0036580	0.004585	0.018517	0.015853
Pdi	FBgn0014002	2.800399	3.203748	3.242839
Pdp	FBgn0029958	0.002595	0	0
Pdsw	FBgn0021967	0.04635	0.025103	0.036001
PebIII	FBgn0011695	0	0.005911	0
Pen	FBgn0011823	0.005097	0	0.006131
pen	FBgn0015527	0.00361	0	0
Pep	FBgn0004401	0.069899	0.053214	0.029241

Pepck	FBgn0003067	0.019877	0.041413	0.118903
Peritrophin-15a	FBgn0040959	0.008942	0.007828	0.038791
Pfk	FBgn0003071	0.069618	0.025902	0.0813
Pfrx	FBgn0027621	0.007736	0.00104	0
pgant4	FBgn0051956	0	0.001093	0
pgant5	FBgn0031681	0.013951	0.132939	0.123505
pgant6	FBgn0035375	0.00276	0.042385	0.048668
Pgd	FBgn0004654	0.22078	0.156548	0.206813
Pgi	FBgn0003074	0.221315	0.245983	0.392474
Pgk	FBgn0250906	0.591329	0.533584	0.496483
Pglym78	FBgn0014869	0.599476	0.521963	0.609738
Pglym87	FBgn0011270	0.076241	0.031356	0.123986
Pgm	FBgn0003076	0.085816	0.050721	0.099243
PGRP-SA	FBgn0030310	0.03315	0	0.003711
PGRP-SB2	FBgn0043577	3.050608	0.387655	0.219852
PH4alphaEFB	FBgn0039776	0	0.001309	0
PH4alphaNE1	FBgn0039780	0.013613	0	0
PH4alphaSG1	FBgn0051014	0.071206	0	0
PH4alphaSG2	FBgn0039779	0.06181	0	0
ph-d	FBgn0004860	0.000458	0.001096	0.000886
PHGPx	FBgn0035438	0.25802	0.320373	0.298018
Phk-3	FBgn0035089	0.01015	0	0.012476
Phm	FBgn0019948	0.020107	0.021629	0.022692
ph-p	FBgn0004861	0.000392	0.000937	0.000757
Pi3K21B	FBgn0020622	0.002402	0	0
Pi3K68D	FBgn0015278	0.000323	0	0
Pi3K92E	FBgn0015279	0.000756	0	0
Pi4KIIalpha	FBgn0037339	0	0.001014	0
pic	FBgn0260962	0.007331	0.008641	0.016253
pita	FBgn0034878	0.000979	0	0
Pitslre	FBgn0016696	0	0.000756	0
pix	FBgn0086706	0.123504	0.081689	0.069537
Pka-C1	FBgn0000273	0.023817	0.009831	0.020466
Pka-R1	FBgn0259243	0	0.005812	0.019067
Pka-R2	FBgn0022382	0.020574	0.033465	0.031838
Pkcdelta	FBgn0259680	0	0	0.000607
Pkn	FBgn0020621	0.001736	0.000613	0.001025
Plap	FBgn0024314	0.016641	0.015294	0.016902
plexA	FBgn0025741	0	0.001279	0
Pli	FBgn0025574	0	0	0.002839
Pmm45A	FBgn0033377	0.008339	0	0.008661
pnut	FBgn0013726	0.018553	0.016074	0.007764
pod1	FBgn0029903	0.027307	0.014893	0
poe	FBgn0011230	0.000229	0.00051	0.001041
Pop2	FBgn0036239	0.002126	0	0
porin	FBgn0004363	0.638947	0.355761	0.443378

POSH	FBgn0040294	0.000722	0.000859	0
Pp1-13C	FBgn0003132	0.023045	0.036843	0.04579
Pp1-87B	FBgn0004103	0.052695	0.114332	0.144566
Pp1alpha-96A	FBgn0003134	0.036773	0.100337	0.121063
Pp2A-29B	FBgn0260439	0.139548	0.136349	0.185045
PP2A-B'	FBgn0042693	0.011546	0.001098	0.00808
Pp2B-14D	FBgn0011826	0.024043	0.031483	0.032025
Pp4-19C	FBgn0023177	0.001986	0.002426	0.009438
PpD3	FBgn0005777	0.010267	0.001385	0.011307
PpD6	FBgn0005779	0.007324	0.025858	0.002251
ppl	FBgn0027945	0.049623	0.03973	0.083966
Ppn	FBgn0003137	0.032685	0.009766	0.013126
Ppt1	FBgn0030057	0	0.002372	0.007933
Ppt2	FBgn0032358	0.004235	0	0.004179
PpV	FBgn0003139	0.001998	0.002377	0
pr	FBgn0003141	0.036545	0.06765	0.045946
PR2	FBgn0013955	0.000466	0	0
Prat	FBgn0004901	0	0.001319	0
Prat2	FBgn0041194	0.002586	0.003065	0.009289
primo-1	FBgn0040077	0.021213	0.038215	0.030881
PRL-1	FBgn0024734	0.004622	0.009652	0.031043
Prm	FBgn0003149	0.101964	0.209201	0.300378
prominin-like	FBgn0026189	0	0	0.001672
Pros25	FBgn0086134	0.128579	0.223614	0.167923
Pros26	FBgn0002284	0.210029	0.176392	0.215051
Pros26.4	FBgn0015282	0.135066	0.130933	0.114198
Pros28.1	FBgn0004066	0.248831	0.186796	0.19295
Pros28.1A	FBgn0017557	0.004898	0.012783	0.017197
Pros29	FBgn0261394	0.244387	0.211126	0.21645
Pros35	FBgn0250843	0.313303	0.287855	0.239196
Pros45	FBgn0020369	0.140509	0.168338	0.163636
Pros54	FBgn0015283	0.027823	0.037315	0.03152
Prosalpha1	FBgn0026781	0.170966	0.197405	0.150461
Prosalpha3T	FBgn0261395	0.002412	0.012681	0.003001
Prosalpha5	FBgn0016697	0.215535	0.24316	0.24259
Prosalpha7	FBgn0023175	0.179464	0.202574	0.163384
Prosbeta1	FBgn0010590	0.217163	0.197069	0.212124
Prosbeta2	FBgn0023174	0.175219	0.078841	0.131224
Prosbeta2R1	FBgn0029812	0.029987	0.010448	0.019369
Prosbeta3	FBgn0026380	0.245591	0.231221	0.226213
Prosbeta5	FBgn0029134	0.133876	0.092527	0.093098
Prosbeta7	FBgn0250746	0.121207	0.133412	0.116282
Prp19	FBgn0261119	0.007159	0.016839	0.04548
Prp8	FBgn0033688	0	0.001103	0.002274
Prx2540-1	FBgn0033520	0.22665	0.080307	0.14464
Prx2540-2	FBgn0033518	0.221067	0.073537	0.14464

Prx5	FBgn0038570	0.278871	0.342242	0.302897
Prx5037	FBgn0038519	0.035938	0.034441	0.051991
Prx6005	FBgn0031479	0.008241	0.006488	0.007801
ps	FBgn0026188	0.035198	0.014297	0.036999
Psa	FBgn0261243	0.014625	0.032795	0.03239
Psf2	FBgn0031599	0	0	0.003711
Psi	FBgn0014870	0.006806	0.001127	0
psidin	FBgn0243511	0	0.000786	0
Ptpa	FBgn0016698	0.001532	0	0
Pu	FBgn0003162	0	0	0.002893
pUf68	FBgn0028577	0.006099	0.002736	0.001889
pug	FBgn0020385	0.037472	0.015032	0.052771
pum	FBgn0003165	0.000801	0	0
Pur-alpha	FBgn0022361	0.006794	0.002619	0.005746
Pvr	FBgn0032006	0	0.001139	0.000501
Pxn	FBgn0011828	0.001201	0.000472	0.004932
pyd	FBgn0003177	0	0.004215	0.001107
PyK	FBgn0003178	0.512999	0.481331	0.538881
pzg	FBgn0259785	0.043173	0.043863	0.031094
qkr58E-1	FBgn0022986	0.006719	0	0
qkr58E-2	FBgn0022985	0.013777	0.00413	0.006965
qkr58E-3	FBgn0022984	0	0.002349	0
qm	FBgn0019662	0	0	0.004457
Qm	FBgn0024733	0.689214	0.931615	0.731855
r	FBgn0003189	0.012038	0.006916	0.009992
R	FBgn0004636	0.006605	0.007828	0.03482
r2d2	FBgn0031951	0.002003	0	0
Rab1	FBgn0016700	0.164639	0.36502	0.500694
Rab10	FBgn0015789	0.051106	0.10247	0.123657
Rab11	FBgn0015790	0.050592	0.083626	0.117718
Rab14	FBgn0015791	0.023962	0.047348	0.070567
Rab2	FBgn0014009	0.021142	0.067724	0.118264
Rab26	FBgn0086913	0.013155	0.025453	0.036467
Rab3	FBgn0005586	0.023201	0.04489	0.064315
Rab30	FBgn0031882	0.022889	0.044286	0.06345
Rab35	FBgn0031090	0.048835	0.099035	0.118303
Rab39	FBgn0029959	0.023414	0.045301	0.064905
rab3-GAP	FBgn0027505	0.00152	0.001074	0.001124
Rab5	FBgn0014010	0.005529	0.028843	0.049392
Rab6	FBgn0015797	0.050123	0.166306	0.134141
Rab7	FBgn0015795	0.021627	0.029293	0.110369
Rab8	FBgn0015796	0.063219	0.122523	0.13251
Rab9D	FBgn0067052	0.023917	0.050916	0.05602
Rab9Db	FBgn0030221	0.023917	0.050916	0.05602
Rab9E	FBgn0052673	0.023917	0.050916	0.05602
Rab9Fa	FBgn0052671	0.023917	0.050916	0.05602

Rab-RP3	FBgn0015793	0.023307	0.045095	0.064608
Rab-RP4	FBgn0015794	0	0.008721	0.026006
RabX4	FBgn0051118	0.023963	0.046365	0.066428
Rac1	FBgn0010333	0.026698	0.035589	0.06141
Rac2	FBgn0014011	0.023454	0.024336	0.017036
Rack1	FBgn0020618	1.611378	2.009476	1.489711
Rad23	FBgn0026777	0.063239	0.065436	0.053032
rad50	FBgn0034728	0.000473	0	0
Rae1	FBgn0034646	0.001682	0.010139	0.005444
Rala	FBgn0015286	0	0.003705	0.003763
ran	FBgn0020255	0.596731	0.500961	0.477852
Ranbp9	FBgn0037894	0.003221	0.003858	0.006776
RanGap	FBgn0003346	0.005509	0.009473	0.01322
ras	FBgn0003204	0.057546	0.032475	0.034621
Ras64B	FBgn0003206	0.01821	0.02289	0.020991
Ras85D	FBgn0003205	0	0.005279	0.007987
Rassf	FBgn0039055	0.000757	0	0.000935
Rat1	FBgn0031868	0.005665	0.00082	0.00083
rb	FBgn0003210	0	0	0.00146
Rbcn-3A	FBgn0023458	0.000715	0.000725	0.000351
Rbcn-3B	FBgn0023510	0.002914	0.001485	0.005859
Rbp1	FBgn0260944	0.081112	0.084368	0.038167
Rbp1-like	FBgn0030479	0.066041	0.061305	0.037188
Rbp9	FBgn0010263	0	0.002302	0.002329
Rbsn-5	FBgn0261064	0	0.001426	0
RecQ5	FBgn0027375	0	0	0.001138
ref(2)P	FBgn0003231	0.007163	0.005777	0.005353
REG	FBgn0029133	0.035838	0.010052	0.032767
Reg-2	FBgn0016715	0.023587	0.097515	0.137303
regucalcin	FBgn0030362	1.134491	1.401427	1.349549
Rel	FBgn0014018	0	0.000742	0.000779
Rep	FBgn0026378	0.010414	0.004868	0.004428
Reps	FBgn0032341	0.003159	0.004916	0
rept	FBgn0040075	0.018715	0.010736	0.019248
retm	FBgn0031814	0.002167	0.00113	0.002291
retn	FBgn0004795	0.002687	0.001581	0.006625
Rfabg	FBgn0087002	0.482436	0.102756	0.13762
RfC3	FBgn0032244	0.005536	0	0
rg	FBgn0086911	0.00057	0.000758	0.000893
rhea	FBgn0260442	0.041159	0.072975	0.063708
Rheb	FBgn0041191	0	0.004092	0.016589
rhi	FBgn0004400	0	0	0.002243
Rho1	FBgn0014020	0.265087	0.314672	0.350315
RhoGAP15B	FBgn0030808	0	0	0.000614
RhoGAP18B	FBgn0261461	0	0.001539	0
RhoGAP68F	FBgn0036257	0.002562	0	0.003644

RhoGDI	FBgn0036921	0.172289	0.127368	0.147432
RhoGEF3	FBgn0259743	0.000603	0	0
RhoGEF4	FBgn0035761	0.005977	0.004882	0.004951
RhoL	FBgn0014380	0.010794	0.00379	0.007961
ric8a	FBgn0028292	0	0	0.0021
rig	FBgn0250850	0	0	0.000612
rin	FBgn0015778	0.056597	0.051248	0.037553
r-l	FBgn0003257	0.022014	0.007967	0.010864
Rm62	FBgn0003261	0.047768	0.020952	0.02891
RnrL	FBgn0011703	0.004511	0	0
robo3	FBgn0041097	0	0	0.000699
Roc1a	FBgn0025638	0	0.023031	0.022288
Roe1	FBgn0014877	0.031491	0.006878	0.010638
rok	FBgn0026181	0.002801	0.002154	0
Rop	FBgn0004574	0.021593	0.011952	0.026255
row	FBgn0033998	0.00207	0	0.001288
Rox8	FBgn0005649	0.012564	0.008305	0.013477
RpA-70	FBgn0010173	0.004131	0	0
Rpb10	FBgn0039218	0	0	0.017963
Rpb11	FBgn0032634	0	0	0.013506
Rpb4	FBgn0053520	0.005484	0	0
Rpb7	FBgn0051155	0.007099	0	0
Rpb8	FBgn0037121	0.004093	0.004833	0
Rpd3	FBgn0015805	0.012196	0.008921	0.010769
RpI135	FBgn0003278	0.00054	0.00066	0.001337
RpII140	FBgn0003276	0.000519	0.001246	0.000643
RpII15	FBgn0004855	0.004727	0	0.00584
RpII215	FBgn0003277	0.00033	0.000382	0.000519
RpII33	FBgn0026373	0	0.018676	0
RpL10Ab	FBgn0036213	0.479579	0.359236	0.422488
RpL11	FBgn0013325	0.615102	0.597311	0.455768
RpL12	FBgn0034968	0.560682	0.605531	0.520882
RpL13	FBgn0011272	0.739591	1.051963	0.855174
RpL13A	FBgn0037351	0.112906	0.289546	0.15278
RpL14	FBgn0017579	0.852706	1.314187	1.063299
RpL17	FBgn0029897	0.740727	0.796802	0.870497
RpL18	FBgn0035753	0.350349	0.65568	0.517819
RpL18A	FBgn0010409	0.439284	0.890776	0.510578
RpL19	FBgn0002607	0.594351	0.792144	0.689032
RpL21	FBgn0032987	0.940773	1.604194	1.187097
RpL22	FBgn0015288	0.497829	0.891299	0.487968
RpL23	FBgn0010078	1.357355	2.037738	1.412946
RpL23A	FBgn0026372	0.461821	0.786075	0.773665
RpL24	FBgn0032518	0.547573	1.125754	0.841964
RpL26	FBgn0036825	1.070938	0.737544	0.61889
RpL27	FBgn0039359	0.609079	0.966003	0.675004

RpL27A	FBgn0010410	0.957724	1.268403	1.0636
RpL28	FBgn0035422	0.890874	1.523262	1.076435
RpL29	FBgn0016726	0.312378	0.302416	0.234687
RpL3	FBgn0020910	0.543028	0.982805	0.735949
RpL30	FBgn0086710	0.890599	1.697851	1.158899
RpL31	FBgn0025286	0.407782	0.766024	0.468965
RpL32	FBgn0002626	0.568163	0.630097	0.520213
RpL34a	FBgn0039406	0.088414	0.363972	0.282171
RpL34b	FBgn0037686	0.160918	0.440497	0.357761
RpL35	FBgn0029785	0.207616	0.234216	0.254795
RpL35A	FBgn0037328	0.310561	0.265777	0.163387
RpL36	FBgn0002579	0.322553	0.505723	0.451558
RpL36A	FBgn0031980	0.094885	0.346284	0.139638
RpL37A	FBgn0028696	0.71771	1.534008	1.100851
RpL37a	FBgn0030616	0.077527	0.042498	0.030242
RpL4	FBgn0003279	0.797796	1.343904	1.010862
RpL6	FBgn0039857	0.304225	0.51726	0.575859
RpL7	FBgn0005593	0.372057	0.690506	0.456714
RpL7A	FBgn0014026	0.660124	1.101461	0.956769
RpL8	FBgn0024939	0.806957	1.323283	1.092945
RpL9	FBgn0015756	0.415732	0.797995	0.546087
RpLP0	FBgn0000100	1.068867	1.337374	0.90462
RpLP1	FBgn0002593	1.692389	1.83771	2.208602
RpLP2	FBgn0003274	2.240793	0.804644	0.849631
Rpn1	FBgn0028695	0.087054	0.106802	0.130908
Rpn11	FBgn0028694	0.158775	0.143882	0.163989
Rpn12	FBgn0028693	0.108379	0.082189	0.09029
Rpn2	FBgn0028692	0.077599	0.065445	0.088491
Rpn3	FBgn0261396	0.07503	0.073706	0.095432
Rpn5	FBgn0028690	0.076601	0.087431	0.110972
Rpn7	FBgn0028688	0.064462	0.045879	0.095583
RpS10a	FBgn0027494	0.116779	0.189977	0.098509
RpS10b	FBgn0031035	0.922804	1.005538	0.854641
RpS12	FBgn0260441	1.279516	1.637742	1.681801
RpS13	FBgn0010265	0.428252	0.724827	0.537274
RpS14a	FBgn0004403	1.537615	1.31235	1.604984
RpS14b	FBgn0004404	1.537615	1.31235	1.604984
RpS15Aa	FBgn0010198	0.636732	0.513122	0.388998
RpS15Ab	FBgn0033555	0.401912	0.32907	0.303464
RpS16	FBgn0034743	0.741453	0.892768	0.627443
RpS17	FBgn0005533	1.291355	1.835511	1.619844
RpS18	FBgn0010411	0.894144	1.026248	0.861181
RpS19a	FBgn0010412	1.205974	1.119904	0.948089
RpS20	FBgn0019936	0.45323	0.535687	0.339581
RpS23	FBgn0033912	1.547994	2.696332	1.925909
RpS24	FBgn0034751	0.619898	0.801869	0.664643

RpS25	FBgn0086472	0.69558	0.608813	0.480247
RpS26	FBgn0004413	0.616741	0.793869	0.706748
RpS27	FBgn0039300	0.691048	0.682872	0.57891
RpS27A	FBgn0003942	0.718791	0.965356	0.926894
RpS28b	FBgn0030136	0.809369	1.252895	0.943223
RpS29	FBgn0037752	0.157461	0.180871	0.196174
RpS3	FBgn0002622	0.915884	1.124588	0.855343
RpS30	FBgn0038834	0.395413	0.725964	0.584646
RpS3A	FBgn0017545	0.858658	0.933698	0.793279
RpS4	FBgn0011284	1.148073	1.49886	1.154585
RpS5a	FBgn0002590	0.628956	0.540516	0.376038
RpS5b	FBgn0038277	0.208734	0.210961	0.160551
RpS6	FBgn0004922	0.5527	0.681397	0.614337
RpS7	FBgn0039757	1.218805	1.342209	1.540359
RpS8	FBgn0039713	0.90829	1.134597	0.812953
RpS9	FBgn0010408	0.601748	0.674408	0.443587
Rpt3	FBgn0028686	0.271581	0.230206	0.241592
Rpt3R	FBgn0037742	0.041978	0.007234	0.01264
Rpt4	FBgn0028685	0.128964	0.135159	0.139927
Rpt4R	FBgn0036224	0.029204	0.02243	0.019481
Rpt6R	FBgn0039788	0.084642	0.103133	0.077364
Rrp1	FBgn0004584	0.005741	0.001097	0
Rrp4	FBgn0034879	0.002046	0	0
Rrp40	FBgn0260648	0.002629	0	0
Rrp45	FBgn0030789	0.002992	0.001748	0.002921
Rrp46	FBgn0037815	0	0.004283	0.003233
Rrp6	FBgn0038269	0	0	0.000855
Rtf1	FBgn0034722	0	0	0.000976
rumi	FBgn0086253	0.006453	0	0.007525
rump	FBgn0260010	0.032337	0.046517	0.054901
rut	FBgn0003301	0.000271	0.00032	0.000435
rux	FBgn0003302	0.003628	0	0
ry	FBgn0003308	0	0	0.001833
S6k	FBgn0015806	0.007999	0	0
SA	FBgn0020616	0.000546	0	0
Sac1	FBgn0035195	0.006533	0.012908	0.012413
sals	FBgn0051374	0	0.00154	0.00407
SamDC	FBgn0019932	0	0.004293	0
san	FBgn0024188	0.014436	0	0.006541
santa-maria	FBgn0025697	0	0.002723	0.014156
Sap47	FBgn0013334	0.035269	0.030618	0.042146
Sap-r	FBgn0000416	0.124764	0.192985	0.217167
sar1	FBgn0038947	0.132856	0.129455	0.211189
Sara	FBgn0026369	0.000454	0	0
sbr	FBgn0003321	0.001224	0	0.003642
Sc2	FBgn0035471	0.003957	0.010402	0.023459

SC35	FBgn0040286	0.051461	0.033224	0.01679
Scamp	FBgn0040285	0.002398	0.01517	0.014269
SCAR	FBgn0041781	0.002004	0	0.003197
scat	FBgn0011232	0.000644	0	0.00128
scb	FBgn0003328	0.009193	0.009355	0.006791
scf	FBgn0025682	0.026446	0.026375	0.043504
Sclp	FBgn0030357	0.035361	0.011767	0.072808
ScpX	FBgn0015808	0.119402	0.139187	0.154227
scramb1	FBgn0052056	0.001837	0	0
scramb2	FBgn0035390	0	0	0.004576
scrib	FBgn0261263	0.002426	0.000941	0.000732
Scsalpha	FBgn0004888	0.315852	0.232256	0.299517
scu	FBgn0021765	0.551601	0.496703	0.651472
Sdc	FBgn0010415	0.003046	0.00361	0.009047
SdhA	FBgn0261439	0.070615	0.030321	0.057383
SdhB	FBgn0014028	0.112392	0.024959	0.064177
Sdic	FBgn0261516	0.011108	0	0
sds22	FBgn0028992	0.013814	0.006778	0.028408
sdt	FBgn0243505	0.000689	0	0
sec13	FBgn0024509	0.272671	0.361914	0.348103
sec15	FBgn0038856	0	0.001303	0.000987
Sec16	FBgn0052654	0.014544	0.033737	0.015786
Sec22	FBgn0260855	0.072724	0.167588	0.158089
sec23	FBgn0037357	0.331701	0.35587	0.283852
sec24	FBgn0033460	0.101948	0.079866	0.081452
sec3	FBgn0086475	0.001382	0	0
sec31	FBgn0033339	0.105468	0.120651	0.124183
Sec61alpha	FBgn0086357	0.130546	0.198283	0.176818
Sec61gamma	FBgn0031049	0.008968	0	0.024865
sec63	FBgn0035771	0.012493	0.039466	0.047473
sec71	FBgn0028538	0.000369	0.003163	0.000592
sec8	FBgn0086685	0	0	0.001222
SelD	FBgn0261270	0.139829	0.135745	0.116497
SelR	FBgn0037847	0.014813	0.015614	0.014557
Sema-1b	FBgn0016059	0.001068	0	0
Sema-2a	FBgn0011260	0.00086	0	0
serp	FBgn0260653	0.004533	0	0
serpin-1	FBgn0011710	0.033466	0.029916	0.023364
serpin-2	FBgn0014029	0.018035	0.014196	0.019238
serpin-5	FBgn0026361	0	0	0.001785
sesB	FBgn0003360	0.473879	0.09684	0.175775
Set	FBgn0014879	0.035682	0.02488	0.025469
SF1	FBgn0025571	0.000789	0	0.000978
SF2	FBgn0040284	0.117878	0.06587	0.078509
sgg	FBgn0003371	0.007086	0.002983	0.007347
Sgs1	FBgn0003372	0.003336	0.004193	0.004481

Sgs3	FBgn0003373	0.755759	1.29225	1.093395
Sgs5	FBgn0003375	4.519059	9.295925	6.876612
Sgs7	FBgn0003377	4.661451	18.71617	9.225886
Sgs8	FBgn0003378	5.780866	8.447676	8.745752
Sgt	FBgn0032640	0.12111	0.12342	0.14034
Sgt1	FBgn0260939	0.003775	0	0
Sh3beta	FBgn0035772	0.120209	0.074733	0.099205
SH3PX1	FBgn0040475	0.014454	0.004807	0.010597
Shc	FBgn0015296	0.002011	0	0.004584
shg	FBgn0003391	0.002434	0	0
shi	FBgn0003392	0.015191	0.006466	0.012159
shot	FBgn0013733	0.001257	0	0.003167
shrb	FBgn0086656	0.0897	0.074432	0.075116
simj	FBgn0010762	0.000683	0	0.001073
Sin3A	FBgn0022764	0.000296	0.000711	0.000951
skap	FBgn0037643	0.102596	0.04129	0.097051
skpA	FBgn0025637	0.032928	0.019648	0.049738
sktl	FBgn0016984	0.00077	0	0
sl	FBgn0003416	0.002467	0.000583	0
slgA	FBgn0003423	0.005685	0	0
Slh	FBgn0015816	0.100837	0.085773	0.102995
slik	FBgn0035001	0	0.011316	0.011227
sll	FBgn0038524	0	0.001549	0
sls	FBgn0086906	0.001878	0.005413	0.012288
SmB	FBgn0010083	0.058782	0.008757	0.027728
SmD3	FBgn0023167	0.017822	0.027687	0.024176
SmG	FBgn0030765	0	0.009476	0.095582
Smg5	FBgn0019890	0.002666	0	0
smi35A	FBgn0016930	0.002522	0	0.01074
smid	FBgn0016983	0.006482	0.002926	0.004825
Smn	FBgn0036641	0.002698	0	0
Smox	FBgn0025800	0.001287	0	0
smp-30	FBgn0038257	0.012864	0.023386	0.03197
smt3	FBgn0026170	0.279783	0.29593	0.240989
sn	FBgn0003447	0.052813	0.005771	0.011846
Snap	FBgn0250791	0.147306	0.315001	0.24323
SNF4Agamma	FBgn0025803	0.000943	0	0.001512
sni	FBgn0030026	0.002522	0	0
Snr1	FBgn0011715	0.005015	0.002013	0.003253
snRNP2	FBgn0037434	0.032718	0.047443	0.025621
snRNP69D	FBgn0016940	0.085491	0.079445	0.093137
snRNP70K	FBgn0016978	0.00139	0.001608	0.001688
Snx6	FBgn0032005	0.015935	0.0209	0.01803
Sod	FBgn0003462	0.698712	0.703463	0.59346
Sod2	FBgn0010213	0.19899	0.063157	0.105343
Sodh-1	FBgn0024289	0.105107	0.044871	0.116803

Sodh-2	FBgn0022359	0.194359	0.167267	0.203626
sop	FBgn0004867	0.569735	0.759663	0.582607
Sop2	FBgn0001961	0.027747	0.023046	0.024672
Sox14	FBgn0005612	0	0.005588	0.004663
SP1070	FBgn0031879	0.001084	0	0
spag	FBgn0015544	0.004584	0	0
Spase12	FBgn0040623	0.071195	0.077973	0.085761
Spase18-21	FBgn0026567	0.134367	0.212342	0.247937
Spase22-23	FBgn0039172	0.070827	0.084732	0.098671
Spase25	FBgn0030306	0.281645	0.355489	0.415522
Spat	FBgn0014031	0	0.025093	0.086122
SpdS	FBgn0037723	0.033551	0.043173	0.07193
SPE	FBgn0039102	0.003082	0	0
spict	FBgn0032451	0.001584	0	0.001964
sPLA2	FBgn0033170	0	0.00713	0
Sply	FBgn0010591	0.039379	0.011171	0.007754
Spn	FBgn0010905	0	0.00056	0
Spn1	FBgn0028988	0.001627	0	0
Spn27A	FBgn0028990	0.011419	0	0
Spn28D	FBgn0031973	0	0.001862	0.002816
Spn4	FBgn0028985	0.097954	0.022121	0.055587
Spn43Aa	FBgn0024294	0.141047	0.031297	0.031584
Spn43Ab	FBgn0024293	0.039594	0.003665	0.020518
Spn5	FBgn0028984	0.032666	0	0.00396
spn-F	FBgn0086362	0.001675	0	0
Spp	FBgn0031260	0.024157	0.025919	0.061212
spt4	FBgn0028683	0.031729	0.015022	0
Spt5	FBgn0040273	0.00913	0.00642	0.004893
Spt6	FBgn0028982	0	0	0.000413
Sptr	FBgn0014032	0.042281	0.0105	0.005784
spz	FBgn0003495	0.01746	0.004494	0.00232
sqd	FBgn0086897	0.142146	0.124393	0.151276
sqh	FBgn0003514	0.531281	0.455675	0.459399
sra	FBgn0086370	0.008383	0	0
SRm160	FBgn0036340	0	0.000781	0
Srp14	FBgn0038808	0.056348	0	0.02542
Srp19	FBgn0015298	0.102555	0.122831	0.100989
Srp54	FBgn0024285	0.003549	0.001452	0.002943
Srp54k	FBgn0010747	0.059411	0.036601	0.030117
Srp68	FBgn0035947	0.085944	0.099238	0.074049
Srp72	FBgn0038810	0.168479	0.098896	0.105719
Srp9	FBgn0035827	0.148979	0.144821	0.166622
SRPK	FBgn0026370	0.003221	0.00681	0.006556
Sry-delta	FBgn0003512	0.021281	0	0.00174
Ssadh	FBgn0039349	0.004809	0	0
Ssb-c31a	FBgn0015299	0.022372	0.015618	0.006848

Ssdp	FBgn0011481	0.00137	0	0
SsRbeta	FBgn0011016	0.325179	0.423217	0.332757
Ssrp	FBgn0010278	0.003446	0	0
sta	FBgn0003517	1.285378	1.015374	0.997846
stai	FBgn0051641	0.038357	0.012521	0.049214
Stam	FBgn0027363	0.02139	0.014701	0.020091
stan	FBgn0024836	0.000401	0	0
Stat92E	FBgn0016917	0	0.000979	0.001988
stck	FBgn0020249	0.013002	0.021415	0.015171
Stim	FBgn0045073	0.013226	0.004321	0.006994
stops	FBgn0086704	0	0.00143	0
Strn-Mlck	FBgn0013988	0.003521	0.008781	0.004621
stv	FBgn0086708	0.009114	0	0.002332
Su(fu)	FBgn0005355	0	0.002132	0
su(Hw)	FBgn0003567	0.00262	0	0
su(r)	FBgn0086450	0.005192	0.003334	0.00196
su(s)	FBgn0003575	0.00046	0	0
Su(var)205	FBgn0003607	0.115086	0.071851	0.08978
Su(var)2-10	FBgn0003612	0.002194	0	0
Su(var)3-9	FBgn0003600	0.039002	0.010064	0.010196
sub	FBgn0003545	0.002927	0.002333	0.004614
Sucb	FBgn0029118	0.064	0.01929	0.042107
sun	FBgn0014391	0.41975	0.407244	0.399586
Surf4	FBgn0019925	0.027257	0.037851	0.05875
svr	FBgn0004648	0.00363	0.003638	0.007431
sw	FBgn0003654	0.007699	0.005924	0.006815
swm	FBgn0002044	0.001345	0	0
sxc	FBgn0261403	0	0	0.00119
Sxl	FBgn0003659	0.00171	0.002104	0.002136
Syb	FBgn0003660	0.063292	0.097053	0.098298
Syn1	FBgn0037130	0.00148	0	0
Synd	FBgn0053094	0.019058	0.003478	0.005492
synj	FBgn0034691	0.000636	0	0.00251
Syt1	FBgn0004242	0	0	0.003191
Syx16	FBgn0031106	0	0.002835	0.00214
Syx18	FBgn0039212	0	0.004412	0.003431
Syx5	FBgn0011708	0	0.010141	0.004846
t	FBgn0086367	0	0	0.003909
T3dh	FBgn0017482	0.004392	0.006261	0.016225
tacc	FBgn0026620	0.001032	0.00121	0.001011
Taf11	FBgn0011291	0	0	0.006141
Taf2	FBgn0011836	0.000496	0.000817	0.001418
Taf4	FBgn0010280	0.000676	0	0.001307
Taf6	FBgn0010417	0.002364	0	0
tai	FBgn0041092	0	0.000366	0
Tal	FBgn0023477	0.027209	0.049226	0.109456

Tango13	FBgn0086674	0	0	0.003031
Tango2	FBgn0030503	0	0	0.004253
Tango4	FBgn0030365	0.019118	0.033696	0.024965
Tango5	FBgn0052675	0	0.001883	0.00404
Tango6	FBgn0032728	0	0	0.004477
Tango9	FBgn0260744	0	0.00189	0.007014
Tap42	FBgn0051852	0.001593	0	0
Tbp-1	FBgn0028684	0.106886	0.124096	0.124205
T-cp1	FBgn0003676	0.151892	0.063257	0.08909
Tcp-1eta	FBgn0037632	0.141458	0.089212	0.106638
Tcp-1zeta	FBgn0027329	0.127186	0.10504	0.113868
Tctp	FBgn0037874	0.680035	0.617352	0.526202
TepII	FBgn0041182	0.486123	0.07431	0.063328
TepIII	FBgn0041181	0.000412	0	0
TepIV	FBgn0041180	0.05971	0.001461	0.005212
Tequila	FBgn0023479	0.005749	0.001495	0.005793
tex	FBgn0037569	0	0	0.003761
TFAM	FBgn0038805	0.046896	0.012272	0.006746
TfIIB	FBgn0004915	0	0	0.002401
TfIIFalpha	FBgn0010282	0.008173	0.00302	0
TfIIFbeta	FBgn0010421	0.002202	0	0
TfIIS	FBgn0010422	0.013652	0.002379	0
Tg	FBgn0031975	0.001588	0.006347	0.009608
TH1	FBgn0010416	0.001078	0	0.001303
Thiolase	FBgn0025352	0.191528	0.062832	0.111128
tho2	FBgn0031390	0.000846	0	0
thoc5	FBgn0034939	0	0.002829	0
Thor	FBgn0022073	0	0.347755	0.068077
Tig	FBgn0011722	0.031331	0.027598	0.050073
Tim10	FBgn0027360	0.006629	0	0
Tim8	FBgn0027359	0.088385	0.131467	0.12106
Tim9a	FBgn0030480	0.032323	0.038163	0.034463
Timp	FBgn0025879	0.002904	0.004752	0.026731
Tina-1	FBgn0035083	0.160462	0.014747	0.033191
Tm1	FBgn0003721	0.269502	0.217544	0.339526
Tm2	FBgn0004117	0.467687	0.410207	0.740332
TM9SF4	FBgn0028541	0.012043	0.060244	0.044671
tmod	FBgn0082582	0.02496	0.027512	0.081113
tnc	FBgn0039257	0.002955	0.000269	0
toe	FBgn0036285	0	0	0.001182
Tom20	FBgn0036928	0.007209	0	0.004423
Tom34	FBgn0010812	0.039073	0.007602	0.009113
Tom40	FBgn0016041	0.007078	0	0
Tom70	FBgn0032397	0.001035	0	0
tomosyn	FBgn0030412	0.001631	0	0
Top1	FBgn0004924	0.004834	0.016515	0.005901

Top2	FBgn0003732	0.026269	0.001702	0.002785
tor	FBgn0003733	0.000675	0	0
torp4a	FBgn0025615	0.003625	0	0.004431
TotA	FBgn0028396	0.090475	0.056209	0.162926
Tpi	FBgn0086355	0.469536	0.439418	0.393429
TpnC25D	FBgn0031692	0	0.009832	0.027791
TpnC47D	FBgn0010423	0.101677	0.184949	0.335618
TpnC73F	FBgn0010424	0.067233	0.232793	0.338198
TppII	FBgn0020370	0.160285	0.081439	0.084873
Tps1	FBgn0027560	0.010051	0.030328	0.092999
tral	FBgn0041775	0.031312	0.03018	0.01738
TRAM	FBgn0040340	0.036615	0.0255	0.053707
Trap1	FBgn0026761	0.022822	0.018452	0.018777
Trax	FBgn0038327	0.012694	0	0.021591
trbd	FBgn0037734	0.000801	0	0
Treh	FBgn0003748	0.006533	0.00125	0.003288
trio	FBgn0024277	0	0	0.000333
Trip1	FBgn0015834	0.319743	0.333553	0.281818
Trl	FBgn0013263	0.006724	0	0.002603
Trn	FBgn0024921	0.005004	0.005205	0.004131
trol	FBgn0261451	0.063051	0.103379	0.113475
Trp1	FBgn0011584	0.016249	0.025545	0.042491
Trx-2	FBgn0040070	0.134547	0.090727	0.075525
Trxr-1	FBgn0020653	0.267968	0.184345	0.194896
Trxr-2	FBgn0037170	0.00476	0	0.002332
Ts	FBgn0024920	0.001886	0	0.002356
Tsc1	FBgn0026317	0.000554	0	0
Tsf1	FBgn0022355	0.290685	0.017593	0.013947
Tsf2	FBgn0036299	0.001489	0	0
Tsf3	FBgn0034094	0.032903	0.017237	0.029813
TSG101	FBgn0036666	0.001495	0.001825	0.005554
Tsp42Ee	FBgn0029506	0	0.003159	0.012578
tsr	FBgn0011726	1.131881	1.370085	1.283831
tst	FBgn0039117	0.000509	0.001435	0.001601
tsu	FBgn0033378	0.052073	0.031385	0.021974
tud	FBgn0003891	0.002179	0.000869	0.001258
Tudor-SN	FBgn0035121	0.513878	0.660016	0.48255
TwdlB	FBgn0039436	0.002117	0	0
TwdlL	FBgn0039437	0.002124	0	0
twf	FBgn0038206	0.060254	0.022206	0.017557
twin	FBgn0011725	0.00174	0	0
tws	FBgn0004889	0.009042	0.011413	0.011535
TXBP181-like	FBgn0026326	0	0.00102	0
Txl	FBgn0035631	0.172659	0.159993	0.122299
U2A	FBgn0033210	0.007002	0	0.002843
U2af38	FBgn0017457	0.054979	0.029569	0.035468

U2af50	FBgn0005411	0.001497	0.004189	0.009422
U4-U6-60K	FBgn0036733	0.001126	0.007103	0.003544
Uba1	FBgn0023143	0.166945	0.133107	0.12739
Uba2	FBgn0029113	0.023971	0.026882	0.016568
UbcD4	FBgn0015321	0	0.012376	0
UbcD6	FBgn0004436	0.012173	0.009539	0.013983
Ubc-E2H	FBgn0029996	0.003664	0.004236	0.005755
Ubi-p63E	FBgn0003943	0.718791	0.965356	0.926894
ubl	FBgn0022224	0.067421	0	0.01036
Ubp64E	FBgn0016756	0.002642	0.000479	0.000773
Ubqn	FBgn0031057	0.041528	0.049269	0.045943
Uch	FBgn0010288	0.281264	0.195904	0.274588
Uch-L3	FBgn0011327	0.101076	0.053945	0.07867
Uev1A	FBgn0035601	0.144897	0.085954	0.057869
Ufd1-like	FBgn0036136	0.001916	0.004636	0.004777
UGP	FBgn0035978	0.21854	0.201943	0.198846
Ugt	FBgn0014075	0.05521	0.040559	0.073284
UK114	FBgn0086691	0.210606	0.150096	0.220911
unc-115	FBgn0260463	0.004843	0.009107	0.006348
unc79	FBgn0038693	0	0.001129	0.001886
und	FBgn0025117	0.033313	0.019817	0.022614
unk	FBgn0004395	0.00205	0	0.005281
up	FBgn0004169	0.101591	0.220732	0.331638
Updo	FBgn0033428	0.101051	0.034017	0.041278
Upf1	FBgn0030354	0.00224	0	0.001339
Use1	FBgn0035965	0	0	0.006027
usnp	FBgn0034913	0.03162	0.020944	0.018159
usp	FBgn0003964	0.0012	0	0
Usp7	FBgn0030366	0.010146	0.003725	0.00648
v	FBgn0003965	0.001609	0	0
v(2)k05816	FBgn0042627	0.01644	0.008133	0.008603
Vago	FBgn0030262	0	0.009732	0.01022
vap	FBgn0003969	0	0	0.001262
Vap-33-1	FBgn0029687	0.167308	0.160202	0.193733
vas	FBgn0003970	0.001884	0	0.001821
verm	FBgn0261341	0.08396	0	0
Vha100-1	FBgn0028671	0.002895	0.006419	0.010764
Vha100-2	FBgn0028670	0.002935	0.003816	0.016463
Vha13	FBgn0026753	0.171012	0.006366	0.15691
Vha14	FBgn0010426	0.062515	0.106956	0.108081
Vha16	FBgn0004145	0	0	0.05598
Vha16-3	FBgn0028667	0	0	0.081565
Vha26	FBgn0015324	0.365623	0.423144	0.402257
Vha36	FBgn0022097	0.097262	0.059498	0.033549
Vha44	FBgn0020611	0.017744	0.016203	0.03386
Vha55	FBgn0005671	0.590021	0.888885	0.862412

Vha68-1	FBgn0020368	0.304661	0.293579	0.220619
Vha68-2	FBgn0020367	0.539587	0.547843	0.508234
VhaAC39	FBgn0028665	0.00173	0.024613	0.055845
VhaSFD	FBgn0027779	0.076352	0.07913	0.117951
viaf	FBgn0036237	0.034841	0.030887	0.009723
vib	FBgn0260992	0.178995	0.078932	0.121126
vig	FBgn0024183	0.017945	0.013429	0.016444
vig2	FBgn0046214	0.05911	0.037433	0.025915
vimar	FBgn0022960	0.007305	0	0.002965
Vinc	FBgn0004397	0.098308	0.07039	0.074707
vir-1	FBgn0043841	0.036651	0.05543	0.075569
vkg	FBgn0016075	0.010901	0.012968	0.020297
vls	FBgn0003978	0.008959	0	0
Vps20	FBgn0034744	0.006757	0	0.015082
Vps26	FBgn0014411	0.011115	0.013024	0.006689
Vps28	FBgn0021814	0.002966	0.008181	0.013783
Vps33B	FBgn0039335	0	0	0.002145
Vps35	FBgn0034708	0.032104	0.002394	0.009047
Vps36	FBgn0086785	0.003089	0.001867	0
Vps4	FBgn0027605	0.047503	0.012145	0.019474
Vps45	FBgn0261049	0.001062	0	0.010484
wal	FBgn0010516	0.333913	0.162772	0.280249
WASp	FBgn0024273	0.00246	0.008975	0.014869
wbl	FBgn0004003	0.119429	0.102856	0.141611
wdb	FBgn0027492	0.001164	0	0.003016
wdp	FBgn0034718	0	0.001064	0
wds	FBgn0040066	0.002279	0.002764	0
wkd	FBgn0037917	0.001668	0	0.002075
wmd	FBgn0034876	0.001859	0	0.007339
woc	FBgn0010328	0.002307	0	0.000713
wol	FBgn0261020	0.023805	0.03398	0.028534
wuho	FBgn0029857	0.002866	0.002353	0.010299
wun	FBgn0016078	0	0	0.001996
wupA	FBgn0004028	0.035096	0.037988	0.076441
Wwox	FBgn0031972	0.001491	0	0
xl6	FBgn0028554	0	0.00866	0.00292
XNP	FBgn0039338	0.000628	0	0
yata	FBgn0260990	0.004475	0.004845	0.005434
yellow-c	FBgn0041713	0.026002	0.004989	0
yellow-d	FBgn0041712	0.001749	0.002023	0
yellow-e	FBgn0041711	0.004627	0	0
yellow-f	FBgn0041710	0.00474	0	0.001763
yip2	FBgn0040064	0.188468	0.197468	0.272504
yki	FBgn0034970	0.017338	0.014284	0.014172
Ykt6	FBgn0260858	0.009302	0.011228	0.021029
yps	FBgn0022959	0.030265	0.024433	0.025909

yrt	FBgn0004049	0	0.000988	0.002688
yuri	FBgn0045842	0.002155	0.028549	0.032041
Zasp52	FBgn0083919	0.031526	0.028958	0.02705
Zasp66	FBgn0035917	0.030961	0.041412	0.064781
zetaCOP	FBgn0040512	0.148137	0.155811	0.178189
zip	FBgn0005634	0.370985	0.404081	0.377181
Zn72D	FBgn0017453	0.001389	0	0.000852
zormin	FBgn0052311	0	0.003304	0.003469
Zpr1	FBgn0030096	0.015201	0.004835	0.006922
Zw	FBgn0004057	0.007803	0.006919	0.021797

Appendix 2: List of proteins identified in Wild-type *Drosophila* salivary glands by proteomics 6h vs 13h after puparium formation.

Protein names and FBgn numbers are based on Flybase annotation (http://flybase.org/). The values for peptides mapped to the genes listed are indicated. Protein quantities were determined using the spectral counting method in which spectral counts (spectral peptide matches) for each protein were summed and normalized across runs based on the total spectral counts obtained for each run. The ratio2 values for peptides mapped to the genes listed are indicated (ratio2=average detection value experimental sample divided by average detection value control sample). p values were obtained using the Student's t-test followed by multiple testing adjustment using the Benjamini-Hochberg method (Hochberg and Benjamini, 1990). Inf indicates a numerical value divided by 0. –Inf indicates 0 divided by a numerical value.

Symbol	FBgn	13h AVE	6h AVE	ratio2	p_value
Map205	FBgn0002645	0.00907	0	Inf	1.15E-09
Gs2	FBgn0001145	0.29237	0.01944	15.039187	1.65E-07
CG8193	FBgn0033367	0.06421	0.50521	-7.8675986	3.06E-07
ImpE2	FBgn0001254	0	0.10773	-Inf	2.31E-06

CG1600	FBgn0033188	0.0689	0.00713	9.6660667	8.38E-06
lox	FBgn0039848	0.03476	0.37302	-10.732519	1.01E-05
Lsp1alpha	FBgn0002562	1.89551	0.53303	3.5560909	1.44E-05
CG5885	FBgn0025700	0.10925	0.03133	3.4869303	1.54E-05
Rfabg	FBgn0087002	0.16853	0.46949	-2.7857749	1.67E-05
Osi7	FBgn0037414	0	0.0725	-Inf	1.70E-05
Thor	FBgn0022073	0.06569	0	Inf	1.72E-05
cher	FBgn0014141	0.33296	0.2573	1.2940358	2.00E-05
CG17660	FBgn0031356	0.00434	0	Inf	2.25E-05
Cyp4e2	FBgn0014469	0.00443	0	Inf	2.25E-05
Tango9	FBgn0260744	0.00611	0	Inf	2.25E-05
CG34053	FBgn0054053	0.00226	0.3818	-168.58969	2.42E-05
CG31673	FBgn0051673	0.02797	0	Inf	2.49E-05
TepII	FBgn0041182	0.06991	0.45722	-6.5404796	2.82E-05
verm	FBgn0261341	0.00128	0.08198	-64.120143	3.23E-05
CG17896	FBgn0023537	0.14884	0.36427	-2.4474401	3.33E-05
CG2064	FBgn0033205	0.00485	0.11172	-23.052822	4.53E-05
ergic53	FBgn0035909	0.19959	0.07401	2.6968133	5.03E-05
CG15093	FBgn0034390	0.12128	0.44594	-3.6770883	5.36E-05
Glycogenin	FBgn0034603	0.28686	0.07624	3.7623838	6.37E-05
Dek	FBgn0026533	0.0187	0.03547	-1.8965629	6.77E-05
HmgD	FBgn0004362	0	0.19787	-Inf	7.56E-05
pgant5	FBgn0031681	0.09617	0.01598	6.0163879	8.37E-05
CG10140	FBgn0036363	0	0.00896	-Inf	9.36E-05
CG10154	FBgn0036361	0	0.00843	-Inf	9.36E-05
CG11423	FBgn0034251	0	0.00379	-Inf	9.36E-05
CG15715	FBgn0036538	0	0.06915	-Inf	9.36E-05
CG7896	FBgn0039728	0	0.00191	-Inf	9.36E-05
Idgf5	FBgn0064237	0	0.006	-Inf	9.36E-05
ligatin	FBgn0041588	0	0.00473	-Inf	9.36E-05
Tsf1	FBgn0022355	0.01033	0.29197	-28.274298	0.0001099
CG32603	FBgn0052603	0	0.03973	-Inf	0.0001204
VhaAC39	FBgn0028665	0.05946	0.00173	34.462446	0.0001285
CG17259	FBgn0031497	0.30898	0.48289	-1.5628341	0.000129
CG15369	FBgn0030105	0.15907	0.62451	-3.925986	0.0001512
CG33129	FBgn0053129	0.09587	0.02247	4.2670743	0.0001597
mRpS16	FBgn0033907	0.0124	0.09058	-7.3059836	0.0001862
Aldh	FBgn0012036	0.47506	0.86213	-1.8147764	0.000197
CG11406	FBgn0034990	0.01567	0.25828	-16.478774	0.0002154
CG6357	FBgn0033875	0	0.01518	-Inf	0.0002169
Pcl	FBgn0003044	0.00516	0	Inf	0.0002183
CG5261	FBgn0031912	0.11758	0.03758	3.1285962	0.0002192

Npc2g	FBgn0039800	0.05326	0.27939	-5.2458242	0.0002217
Prm	FBgn0003149	0.30324	0.09591	3.161585	0.0002223
eIF4AIII	FBgn0037573	0.0367	0.12271	-3.3434367	0.0002276
Gasp	FBgn0026077	0.00322	0.05083	-15.783338	0.0002305
Mpcp	FBgn0026409	0.01907	0.09484	-4.9731414	0.0002329
CG9427	FBgn0037721	0	0.10081	-Inf	0.0002382
Ance	FBgn0012037	0.00971	0.07422	-7.6432829	0.0002457
CG13551	FBgn0040660	0.20867	0.7772	-3.7246122	0.00025
Osi6	FBgn0027527	0	0.05049	-Inf	0.0002557
CG32762	FBgn0052762	0.5709	4.08773	-7.1601494	0.0002557
ND75	FBgn0017566	0.04792	0.14351	-2.9948518	0.0002571
Obp56a	FBgn0034468	0.00524	0.17248	-32.898907	0.0002632
Lsp1beta	FBgn0002563	2.89848	1.08934	2.6607712	0.0002686
CG11334	FBgn0039849	0.09755	0.0237	4.1153116	0.0002704
CG5381	FBgn0032218	0	0.00658	-Inf	0.0002729
nero	FBgn0261479	0	0.01494	-Inf	0.0002729
CG4408	FBgn0039073	0.0015	0.02631	-17.503628	0.0002851
Vha68-1	FBgn0020368	0.22129	0.32553	-1.4710092	0.0002875
deltaCOP	FBgn0028969	0.21612	0.39996	-1.8505859	0.0002885
Chit	FBgn0013763	0.14164	0.40332	-2.8474524	0.0003113
Crk	FBgn0024811	0.00797	0.06281	-7.8816559	0.0003166
Spn43Aa	FBgn0024294	0.02241	0.12912	-5.7628893	0.0003461
Eig71Ea	FBgn0004588	0.2921	1.51363	-5.1819298	0.0003608
pAbp	FBgn0003031	0.23018	0.74046	-3.2169164	0.0003659
Aats-trp	FBgn0010803	0.07496	0.29168	-3.8909147	0.0003694
Idh	FBgn0001248	0.52517	0.33462	1.5694717	0.0003819
Cpr49Ac	FBgn0033725	0.02376	0.0745	-3.1361417	0.0003881
CG8605	FBgn0035762	0.00519	0	Inf	0.0003942
CkIalpha	FBgn0015024	0.01115	0	Inf	0.0003942
LysP	FBgn0004429	0.02666	0	Inf	0.0003942
sals	FBgn0051374	0.00402	0	Inf	0.0003942
GlyP	FBgn0004507	0.40646	0.19527	2.0814861	0.0004105
Cys	FBgn0004629	0.13914	0.50131	-3.6028318	0.0004159
Cht5	FBgn0038180	0.00518	0.06245	-12.051471	0.0004277
Lsp2	FBgn0002565	0.42012	1.52837	-3.6379522	0.0004546
Pax	FBgn0041789	0.17424	0.10115	1.7225894	0.000459
Cam	FBgn0000253	1.00079	0.28848	3.4691582	0.0004611
PGRP-SB2	FBgn0043577	0.19275	3.19225	-16.561377	0.0004619
CG8636	FBgn0029629	0.06372	0.15382	-2.4139109	0.0005092
CG5390	FBgn0032213	0.01547	0.08282	-5.3524577	0.0005111
Obp99b	FBgn0039685	1.82126	6.80028	-3.7338395	0.0005351
Eig71Ef	FBgn0004593	1.11362	4.64935	-4.1749911	0.0005388

CG7911	FBgn0039735	0.12446	0.36377	-2.9227577	0.0005463
CG17273	FBgn0027493	0.06151	0.11551	-1.8780209	0.0005529
Fkbp13	FBgn0010470	0.16831	0.06013	2.7991258	0.0005687
CG32663	FBgn0052663	0.00603	0.01881	-3.1206153	0.0006037
CG5171	FBgn0031907	0.25118	0.04348	5.7767697	0.0006069
Chc	FBgn0000319	0.24862	0.11155	2.228799	0.0006268
CG6287	FBgn0032350	0.19744	0.12266	1.6096154	0.0006356
ImpL1	FBgn0001256	0.03864	0.28753	-7.4410712	0.0006442
Rab2	FBgn0014009	0.13158	0.0154	8.546753	0.0006917
Gdh	FBgn0001098	0.18841	0.3643	-1.9335849	0.0006933
Aats-ala	FBgn0027094	0.05622	0.11899	-2.1164095	0.000695
alpha-Adaptin	FBgn0015567	0.01465	0.00327	4.4874579	0.0006952
Nipsnap	FBgn0030724	0.08209	0.27252	-3.3198987	0.0006963
Rab6	FBgn0015797	0.12543	0.04723	2.6558723	0.0006965
Eig71Ed	FBgn0004591	0.85112	3.06346	-3.599333	0.000713
TepIV	FBgn0041180	0.0041	0.0559	-13.618737	0.0007138
CG7145	FBgn0037138	0.03084	0.12922	-4.1900557	0.0007331
Dbi	FBgn0010387	0.18887	0	Inf	0.0007509
CG1342	FBgn0039795	0	0.08951	-Inf	0.0007565
Rab7	FBgn0015795	0.09349	0.01173	7.9696965	0.0007578
CG30463	FBgn0050463	0.05602	0.00912	6.1420635	0.0007963
Ama	FBgn0000071	0.03386	0.12259	-3.6201179	0.0008076
ApepP	FBgn0026150	0.02215	0.06963	-3.1436439	0.0008118
Ag5r	FBgn0015010	0.09566	0.36782	-3.8450548	0.0008458
CG4151	FBgn0029770	1.18936	3.96884	-3.3369397	0.0008487
CG10467	FBgn0035679	0.03938	0.14557	-3.6967675	0.0008616
Acon	FBgn0010100	0.16229	0.32289	-1.989537	0.0008666
CG4306	FBgn0036787	0.00331	0.05401	-16.306526	0.0008724
PH4alphaSG1	FBgn0051014	0	0.0703	-Inf	0.0008745
sesB	FBgn0003360	0.21456	0.49497	-2.306869	0.0008772
CG5355	FBgn0032242	0.15603	0.25265	-1.6192582	0.0009028
bnb	FBgn0001090	0	0.07978	-Inf	0.0009084
PH4alphaSG2	FBgn0039779	0	0.0559	-Inf	0.0009121
CG1969	FBgn0039690	0.52568	1.01895	-1.9383352	0.000931
Ect3	FBgn0260746	0.42312	0.01508	28.065178	0.0009433
CG10627	FBgn0036298	0.01492	0.06951	-4.6574029	0.0009652
Actn	FBgn0000667	0.41404	0.22227	1.8627738	0.0009996
CG5590	FBgn0039537	0.0339	0.10602	-3.1269765	0.001
CG3244	FBgn0031629	0.01943	0.11711	-6.0285173	0.0010031
CG14062	FBgn0039592	0.24289	1.33995	-5.5165819	0.0010446
14-3-3zeta	FBgn0004907	0.35267	0.65788	-1.8654319	0.0010725
Eig71Ei	FBgn0014849	0.00688	0.47521	-69.042559	0.0010906

Vha100-2	FBgn0028670	0.01658	0.00146	11.327475	0.0011237
RpL15	FBgn0028697	0.35862	0.192	1.8678194	0.0011279
TpnC47D	FBgn0010423	0.2801	0.0885	3.1650305	0.00113
ImpL3	FBgn0001258	0.47587	0.14907	3.1921977	0.0012218
CG3987	FBgn0038292	0.01951	0	Inf	0.0012677
Obp56d	FBgn0034470	0.04151	0.29588	-7.1274554	0.0012719
CG33998	FBgn0053998	0.27673	1.06753	-3.8576338	0.0012726
tsu	FBgn0033378	0.00969	0.05215	-5.3798387	0.0012821
Eig71Eb	FBgn0004589	0.29365	1.15836	-3.944678	0.0012991
Sry-delta	FBgn0003512	0.00162	0.02277	-14.044693	0.0012994
CPTI	FBgn0027842	0.02044	0	Inf	0.0013029
Edg84A	FBgn0000552	0.03701	0	Inf	0.0013665
Hsp60	FBgn0015245	0.22193	0.36065	-1.6250938	0.0013825
CG10590	FBgn0035622	0.03289	0.00106	31.001808	0.0013932
Txl	FBgn0035631	0.09549	0.16127	-1.6889597	0.0013983
Neb-cGP	FBgn0083167	0	0.78529	-Inf	0.0014005
CG10932	FBgn0029969	0.14714	0.30885	-2.0991092	0.0014088
CG3603	FBgn0029648	0.01802	0.07415	-4.1141279	0.0014477
RpL7A	FBgn0014026	0.95298	0.64294	1.4822237	0.0014602
Amun	FBgn0030328	0	0.04686	-Inf	0.0014603
CG3800	FBgn0034802	0.08503	0.50405	-5.9278816	0.0015598
TppII	FBgn0020370	0.08687	0.15816	-1.8206252	0.0016236
Myo31DF	FBgn0086347	0.00904	0.00143	6.3417874	0.001653
Eig71Eg	FBgn0004594	0.31254	1.08725	-3.4788079	0.0016597
Mlc1	FBgn0002772	1.5034	0.30879	4.8687145	0.001722
CG3164	FBgn0025683	0.03475	0	Inf	0.0017415
Vha16-3	FBgn0028667	0.06372	0	Inf	0.0017975
CG6455	FBgn0019960	0.02988	0.06562	-2.1959034	0.0018801
Men	FBgn0002719	0.21156	0.13568	1.5593254	0.0018947
CG6439	FBgn0038922	0.05459	0.11243	-2.0595838	0.0019029
CG10433	FBgn0034638	0.02386	0	Inf	0.0019188
CG15814	FBgn0030873	0.00944	0	Inf	0.0019188
CG17746	FBgn0035425	0.00817	0	Inf	0.0019188
CG30344	FBgn0050344	0.00598	0	Inf	0.0019188
crq	FBgn0015924	0.00663	0	Inf	0.0019188
Syx5	FBgn0011708	0.00649	0	Inf	0.0019188
Ost48	FBgn0014868	0.18249	0.10038	1.8179649	0.0019557
CG11899	FBgn0014427	0.04492	0.00224	20.090586	0.0019643
CG7906	FBgn0036417	0.0363	0.10062	-2.7722051	0.0019707
GstE7	FBgn0063493	0.06395	0.14585	-2.2808789	0.0020198
hkl	FBgn0086441	0.00266	0.01639	-6.1581511	0.0020572
mfas	FBgn0260745	0.05565	0.10524	-1.8911797	0.002126

Zasp66	FBgn0035917	0.05644	0.02353	2.3981719	0.0021429
eIF-2alpha	FBgn0004925	0.16164	0.27737	-1.7160046	0.0021434
CG8369	FBgn0040532	0.03999	0.17846	-4.4628961	0.0021952
RpL26	FBgn0036825	0.32458	0.80846	-2.4907841	0.0022166
CG6028	FBgn0038924	0.26445	0.14281	1.8518399	0.002265
yip2	FBgn0040064	0.27879	0.1941	1.4363122	0.0023334
CG10237	FBgn0032783	0.07419	0	Inf	0.0023705
bt	FBgn0005666	0.08434	0.01052	8.0194636	0.0024169
Gpdh	FBgn0001128	0.47707	0.3892	1.225766	0.0024177
Lsp1gamma	FBgn0002564	4.7664	1.04231	4.5729262	0.0024537
fau	FBgn0020439	0.13615	0.01617	8.4206312	0.002488
NTPase	FBgn0024947	0.05754	0.01669	3.4470615	0.002586
Cg25C	FBgn0000299	0.03286	0.01849	1.7765928	0.0025889
Rab1	FBgn0016700	0.52779	0.17701	2.9816919	0.0026557
CG14876	FBgn0038368	0.00407	0.03017	-7.4215037	0.0026822
CG31075	FBgn0051075	0.35887	0.76458	-2.1305455	0.0027723
Nc73EF	FBgn0010352	0.02949	0.04612	-1.5637868	0.0027846
Spase18-21	FBgn0026567	0.2746	0.14226	1.9302082	0.00285
CG4335	FBgn0038795	0.02712	0.00224	12.131248	0.002858
oho23B	FBgn0015521	0.61515	1.39678	-2.2706473	0.0028669
mus209	FBgn0005655	0.00615	0.03001	-4.8780367	0.0028768
Mf	FBgn0038294	0.65075	0.19927	3.2656802	0.0029029
CG10639	FBgn0032729	0.00589	0.02704	-4.5916076	0.0029122
CG16704	FBgn0031558	0.03554	0.1959	-5.5115845	0.0029904
CG13907	FBgn0035173	0.00749	0	Inf	0.0029923
CG1468	FBgn0030157	0.01484	0	Inf	0.0029923
CG2528	FBgn0032969	0.00448	0	Inf	0.0029923
CG9027	FBgn0033631	0.01223	0	Inf	0.0029923
ry	FBgn0003308	0.00229	0	Inf	0.0029923
Kr-h2	FBgn0028419	0.02205	0.0067	3.2926538	0.0030059
CD98hc	FBgn0037533	0.03847	0.00796	4.8301291	0.0030954
Bj1	FBgn0002638	0.03907	0.08831	-2.2602269	0.0030975
Aats-tyr	FBgn0027080	0.03906	0.09244	-2.3662796	0.0031599
CG4557	FBgn0029912	0	0.01096	-Inf	0.0032439
CG16979	FBgn0036512	0.02768	0.00981	2.8219348	0.0032714
CG7402	FBgn0036768	0.01521	0	Inf	0.0032984
bic	FBgn0000181	0.37941	0.21546	1.7608829	0.003333
CG8460	FBgn0031996	0.0111	0.0424	-3.8209451	0.0033897
Vha36	FBgn0022097	0.02612	0.09254	-3.5431119	0.0034292
CG12163	FBgn0260462	0.05249	0.01706	3.0767475	0.0035263
Uev1A	FBgn0035601	0.05013	0.12721	-2.5377423	0.003547
Gp93	FBgn0039562	0.70539	0.42199	1.6715798	0.0035758

Gel	FBgn0010225	0.1019	0.13835	-1.3577222	0.0035994
ImpE1	FBgn0001253	0	0.00242	-Inf	0.0036443
pcm	FBgn0020261	0	0.00242	-Inf	0.0036443
PH4alphaNE1	FBgn0039780	0	0.01366	-Inf	0.0036443
Pgi	FBgn0003074	0.39981	0.22372	1.7871001	0.0036648
Atg4	FBgn0031298	0.00177	0.02088	-11.773593	0.0036719
CG16713	FBgn0031560	0.00889	0.17272	-19.434653	0.0036732
Eno	FBgn0000579	1.3625	0.84263	1.6169605	0.0037122
CG7587	FBgn0038523	0.07097	1.32608	-18.685871	0.0037343
RpL34a	FBgn0039406	0.19132	0.07972	2.3998368	0.0037378
CG17919	FBgn0037433	0.00361	0.0446	-12.362747	0.0037392
Reg-2	FBgn0016715	0.12232	0.02678	4.5669557	0.0038014
dlg1	FBgn0001624	0.00625	0.01689	-2.7028418	0.0038377
CG8306	FBgn0034142	0.02354	0.00599	3.9267876	0.0038467
CG10650	FBgn0046302	0	0.01207	-Inf	0.0038718
Pbgs	FBgn0036271	0.00652	0.02627	-4.0280369	0.0038807
CG31705	FBgn0028490	0.00543	0.03761	-6.9218626	0.0039201
CG18081	FBgn0036537	0.02112	0.08515	-4.0324274	0.0039256
CG30197	FBgn0050197	0.21601	0.01255	17.217978	0.0039313
Rab5	FBgn0014010	0.03765	0.00276	13.656089	0.0040109
Sptr	FBgn0014032	0.00269	0.03051	-11.342707	0.0040896
caz	FBgn0011571	0	0.00819	-Inf	0.0041001
CG17931	FBgn0038421	0.01495	0.09881	-6.6075687	0.0041384
Srp72	FBgn0038810	0.10018	0.21966	-2.1925904	0.0042342
CG7470	FBgn0037146	0.07416	0.00573	12.931663	0.0042614
Cctgamma	FBgn0015019	0.07127	0.13839	-1.9418697	0.0044362
Kap-alpha3	FBgn0027338	0.07985	0.17309	-2.1676775	0.0044396
CG7298	FBgn0036948	0	0.01553	-Inf	0.0044635
CG13822	FBgn0039098	0	0.04758	-Inf	0.0044783
CG8289	FBgn0030854	0	0.01529	-Inf	0.0044783
CG15743	FBgn0030465	0.05484	0.01097	4.9974109	0.004483
wbl	FBgn0004003	0.08022	0.10997	-1.3709633	0.0045027
Hn	FBgn0001208	0.03096	0.00996	3.1101425	0.0045341
tmod	FBgn0082582	0.07721	0.02312	3.3401713	0.0045539
TpnC25D	FBgn0031692	0.02654	0	Inf	0.0045634
CG4692	FBgn0035032	0.02201	0.0917	-4.166811	0.0045681
ran	FBgn0020255	0.43508	0.60585	-1.3925117	0.0045866
Vha100-1	FBgn0028671	0.0099	0.00291	3.3977233	0.0046752
Akap200	FBgn0027932	0.08864	0.13734	-1.5493296	0.0047279
l(2)03709	FBgn0010551	0.08386	0.26338	-3.1405521	0.0047324
CG40160	FBgn0058160	0	0.03273	-Inf	0.004777
CG33493	FBgn0053493	0	0.04605	-Inf	0.0047954

Klp10A	FBgn0030268	0	0.00583	-Inf	0.0047954
CLIP-190	FBgn0020503	0.00086	0.00534	-6.1902152	0.0048561
dro5	FBgn0035434	0	0.08323	-Inf	0.0049253
TM9SF4	FBgn0028541	0.04284	0.01111	3.8549981	0.004958
l(2)01289	FBgn0010482	0.02564	0.0008	32.181456	0.0050737
CG3214	FBgn0031436	0	0.02309	-Inf	0.0050742
CG6422	FBgn0039261	0	0.00469	-Inf	0.0050742
CG5903	FBgn0038400	0.00311	0.03539	-11.393149	0.0051113
Spp	FBgn0031260	0.06519	0.0257	2.5366178	0.005143
sec63	FBgn0035771	0.05496	0.01172	4.6891804	0.0052677
mop	FBgn0036448	0.00038	0.00391	-10.236281	0.0053102
CG8525	FBgn0033735	0.0235	0.00281	8.3750583	0.005329
Mo25	FBgn0017572	0.04485	0.09849	-2.1959878	0.0053594
smi35A	FBgn0016930	0.04855	0.00877	5.5329539	0.0054314
Spn27A	FBgn0028990	0	0.01288	-Inf	0.0054509
CG12082	FBgn0035402	0.01591	0.05231	-3.2873139	0.005516
CG14235	FBgn0031066	0.41318	0.16203	2.5500539	0.0056161
RpL34b	FBgn0037686	0.20601	0.10241	2.0116687	0.0056686
Mov34	FBgn0002787	0.20965	0.32258	-1.53865	0.0057357
Surf4	FBgn0019925	0.06421	0.02726	2.3557655	0.0058002
Ppn	FBgn0003137	0.01031	0.03052	-2.9588335	0.0058055
eIF4G	FBgn0023213	0.03605	0.07135	-1.9794816	0.0058364
TpnC73F	FBgn0010424	0.29581	0.05415	5.4632973	0.0059758
CG6412	FBgn0032646	0	0.01035	-Inf	0.0060215
Fit2	FBgn0036688	0	0.0046	-Inf	0.0060215
l(2)35Di	FBgn0001989	0	0.0197	-Inf	0.0060215
Psi	FBgn0014870	0	0.00498	-Inf	0.0060215
Fbp1	FBgn0000639	4.73879	1.74009	2.7233009	0.0060618
l(2)06225	FBgn0010612	0.0473	0.19013	-4.0195646	0.0061319
CG32667	FBgn0052667	0.04908	0.50941	-10.379098	0.0061722
CG32638	FBgn0052638	0.08925	0.00899	9.9256321	0.0061905
alt	FBgn0038535	0.04987	0.03162	1.577316	0.0062595
MAPk-Ak2	FBgn0013987	0.01696	0.00573	2.9568615	0.0062922
26-29-p	FBgn0250848	0.0651	0.11084	-1.7026405	0.0063749
Sply	FBgn0010591	0.00788	0.03727	-4.7326689	0.0064128
Top2	FBgn0003732	0.00161	0.02239	-13.91553	0.0064561
Prosbeta1	FBgn0010590	0.25345	0.20111	1.2602069	0.0064928
CG5958	FBgn0031913	0.1552	0.02289	6.7802488	0.0065631
Tal	FBgn0023477	0.09828	0.02535	3.8762046	0.0066126
Aats-gly	FBgn0027088	0.12149	0.21286	-1.7521072	0.0066166
CG11267	FBgn0036334	0.30772	0.50595	-1.6441774	0.0067312
Trp1	FBgn0011584	0.04054	0.0122	3.3224083	0.006805

Mlc2	FBgn0002773	1.79304	0.54833	3.2699819	0.0068088
Tina-1	FBgn0035083	0.02687	0.16112	-5.9957315	0.0068254
CG5010	FBgn0260747	0	0.04337	-Inf	0.0069421
ade5	FBgn0020513	0.15147	0.05585	2.7121097	0.0069587
Mhc	FBgn0086783	1.0633	0.39307	2.7051464	0.0070031
Spat	FBgn0014031	0.07592	0	Inf	0.0070405
tral	FBgn0041775	0.01261	0.02947	-2.337877	0.007074
lola	FBgn0005630	0.0016	0.00887	-5.5482129	0.0070926
Eig71Ec	FBgn0004590	0.6373	1.41823	-2.2253786	0.0071139
Rab8	FBgn0015796	0.12848	0.0633	2.0298522	0.0071445
CG9281	FBgn0030672	0.00231	0.02571	-11.130825	0.0072622
Cyp1	FBgn0004432	0.76852	1.07567	-1.3996562	0.0073017
Adk2	FBgn0022708	0.22745	0.14436	1.5755956	0.0073438
sar1	FBgn0038947	0.18981	0.13626	1.39295	0.0073465
Cpr	FBgn0015623	0.04292	0.02407	1.7830385	0.0074591
Pros28.1	FBgn0004066	0.18282	0.25849	-1.4139189	0.0074602
CG11790	FBgn0039265	0.0585	0.02928	1.9980958	0.0075262
D1	FBgn0000412	0.01645	0.07756	-4.7159116	0.0075893
CG1041	FBgn0037440	0.03177	0.0768	-2.417314	0.0076557
RpL6	FBgn0039857	0.57985	0.32051	1.8091641	0.0076558
Lcp65Ag2	FBgn0020637	0	0.07043	-Inf	0.0076793
Lcp65Ag3	FBgn0086611	0	0.07043	-Inf	0.0076793
rhea	FBgn0260442	0.06932	0.04026	1.7216274	0.0076905
CG9629	FBgn0036857	0.06258	0.00986	6.3441433	0.007711
CG11313	FBgn0039798	0	0.03771	-Inf	0.0077382
Mical	FBgn0053208	0.02465	0.00045	55.212767	0.0077962
OstStt3	FBgn0011336	0.01993	0.00473	4.2144429	0.007851
CCS	FBgn0010531	0.00616	0.04589	-7.4511005	0.0078597
CG3267	FBgn0042083	0.00126	0.02058	-16.324209	0.0078637
obst-A	FBgn0031097	0	0.0923	-Inf	0.0079059
pgant6	FBgn0035375	0.05101	0.00278	18.377232	0.0079216
CG2017	FBgn0037391	0	0.01967	-Inf	0.0079918
Dp1	FBgn0027835	0.12375	0.20045	-1.6198185	0.0080044
CG30104	FBgn0050104	0.03131	0.00742	4.2216227	0.0080474
Scamp	FBgn0040285	0.01562	0.00237	6.5841049	0.0081622
CG10373	FBgn0032704	0.0401	0.00692	5.7980759	0.0081637
Spn5	FBgn0028984	0.0021	0.03464	-16.484585	0.0081675
CG13393	FBgn0032035	0.06038	0	Inf	0.008178
CG10638	FBgn0036290	0.08939	0.19402	-2.1704049	0.0084344
CG14786	FBgn0027794	0.00971	0	Inf	0.0084459
CG5276	FBgn0037900	0.01118	0	Inf	0.0084796
CG11975	FBgn0037648	0.0047	0.02828	-6.0117838	0.0086062

Rab35	FBgn0031090	0.11278	0.04887	2.3076572	0.0086834
Dlic	FBgn0030276	0.00585	0.02004	-3.4253544	0.0087149
Rab10	FBgn0015789	0.11112	0.05118	2.1713279	0.0087342
CG1968	FBgn0033401	0.01532	0.00198	7.752891	0.0088077
trol	FBgn0261451	0.1262	0.06615	1.9077558	0.0088082
Rpn1	FBgn0028695	0.12724	0.08629	1.474499	0.0088156
CG8798	FBgn0036892	0.00084	0.00764	-9.0587461	0.0088193
CG7924	FBgn0036416	0.00786	0.1821	-23.16634	0.0089503
eIF5	FBgn0030719	0.00665	0.03899	-5.8675637	0.0089739
CG16712	FBgn0031561	0.11259	0.43577	-3.8705235	0.0090242
CG7830	FBgn0032015	0.06656	0.01688	3.9424784	0.0090649
R	FBgn0004636	0.02927	0.00663	4.4115844	0.009084
ferrochelatase	FBgn0024891	0.01125	0.04163	-3.7016082	0.0091283
Arf72A	FBgn0000115	0.06467	0.02972	2.1761525	0.0091423
CG9691	FBgn0030160	0.05611	0.08129	-1.4488144	0.0095571
Vha16	FBgn0004145	0.05203	0	Inf	0.009754
RpS29	FBgn0037752	0.44619	0.86737	-1.9439415	0.0097917
CG12481	FBgn0030542	0	0.06811	-Inf	0.0098054
CG8223	FBgn0037624	0.12014	0.21654	-1.8023867	0.0099334
boca	FBgn0004132	0.11547	0.15955	-1.3817445	0.009974
Anxb11	FBgn0030749	0.11919	0.04777	2.4950855	0.0099995
Rab14	FBgn0015791	0.05376	0.0214	2.51209	0.0103305
CG33303	FBgn0053303	0.28073	0.1962	1.4308658	0.010686
CG31715	FBgn0051715	0.05728	0.24222	-4.2288067	0.0107179
Hsc70-2	FBgn0001217	0.03546	0.08878	-2.5037669	0.0107431
GalNAc-T2	FBgn0030930	0.18016	0.05251	3.4307759	0.0107469
CG6385	FBgn0034276	0.00754	0	Inf	0.0108869
Rpn2	FBgn0028692	0.1113	0.08037	1.3848871	0.0110528
Clbn	FBgn0259152	0.00327	0.0147	-4.4934165	0.0110745
Vha14	FBgn0010426	0.0923	0.06272	1.4715865	0.0111726
SdhB	FBgn0014028	0.04721	0.10226	-2.1660349	0.0112757
CG3999	FBgn0037801	0.02887	0.00456	6.3373439	0.0112888
RpLP0	FBgn0000100	0.76011	1.08027	-1.421201	0.011296
l(3)82Fd	FBgn0013576	0.00287	0.01609	-5.602326	0.0114738
GalNAc-T1	FBgn0034025	0.19092	0.08638	2.2102743	0.0115464
CREG	FBgn0025456	0.24074	0.11742	2.0501737	0.011613
Synd	FBgn0053094	0.00432	0.01906	-4.4156366	0.011717
eIF-4a	FBgn0001942	0.67695	0.89848	-1.3272382	0.0117248
CG5044	FBgn0038326	0.03117	0.07916	-2.539929	0.0117297
RpL35A	FBgn0037328	0.09791	0.18959	-1.9363141	0.0117986
Moe	FBgn0011661	0.18287	0.29497	-1.6130032	0.0118162
Fer2LCH	FBgn0015221	0.31668	0.53346	-1.6845349	0.0119106

CG3501	FBgn0034791	0.0485	0.08991	-1.8538532	0.0119134
CG10175	FBgn0039084	0	0.01375	-Inf	0.0119545
CG8036	FBgn0037607	0.48841	0.3565	1.370013	0.0119976
RpS5a	FBgn0002590	0.30808	0.53018	-1.7209015	0.0121538
HmgZ	FBgn0010228	0.20541	0.51912	-2.5272541	0.0121553
up	FBgn0004169	0.30941	0.10386	2.9791676	0.0123208
alphaCop	FBgn0025725	0.34538	0.25209	1.3700604	0.012321
eca	FBgn0069242	0.27015	0.12085	2.2353985	0.0123913
p24-2	FBgn0053105	0.23915	0.10698	2.2353985	0.0123913
AnnX	FBgn0000084	0.06426	0.10557	-1.6429838	0.0124582
Vago	FBgn0030262	0.13828	0.0154	8.9801972	0.0128619
Aats-asp	FBgn0002069	0.12099	0.2211	-1.8273497	0.0128619
CG3321	FBgn0038224	0.02007	0.38716	-19.286547	0.0129897
sls	FBgn0086906	0.01183	0.00166	7.1414859	0.013016
Obp99c	FBgn0039682	0.16101	0.57957	-3.5995841	0.0130573
Adh	FBgn0000055	1.71348	1.10705	1.547793	0.0132996
Pros25	FBgn0086134	0.19503	0.12962	1.5046254	0.0136302
Tctp	FBgn0037874	0.43922	0.66312	-1.5097507	0.0136385
CG30359	FBgn0050359	0.06932	0.01796	3.8597592	0.0138121
Chd64	FBgn0035499	0.78818	1.31089	-1.6631783	0.0138271
Hsp70Aa	FBgn0013275	0.06385	0.13348	-2.0906341	0.0139719
Hsp70Bbb	FBgn0051354	0.06395	0.13369	-2.0906341	0.0139719
Hsp70Bc	FBgn0013279	0.06395	0.13369	-2.0906341	0.0139719
CG10347	FBgn0030342	0	0.01124	-Inf	0.0140843
r-l	FBgn0003257	0.0148	0.03705	-2.5035618	0.0142072
CG16817	FBgn0037728	0.12426	0.07241	1.7160321	0.014289
eIF2B-gamma	FBgn0034029	0.0082	0.02701	-3.2930163	0.0143177
CG5177	FBgn0031908	0.61453	0.25451	2.4146036	0.0144221
CG10083	FBgn0036372	0.01009	0.03479	-3.4480529	0.0144326
Nap1	FBgn0015268	0.07347	0.14504	-1.9741541	0.014483
Vha55	FBgn0005671	0.71145	0.60668	1.1726909	0.0145148
Eig71Eh	FBgn0014848	0	0.32575	-Inf	0.0145881
CG9331	FBgn0032889	0.09037	0.20658	-2.2858308	0.0145993
Rab11	FBgn0015790	0.11194	0.0478	2.3421351	0.0146312
mys	FBgn0004657	0.00716	0.00146	4.9194826	0.0146967
jar	FBgn0011225	0	0.008	-Inf	0.0147549
ras	FBgn0003204	0.03996	0.06262	-1.5669896	0.0149017
CG33138	FBgn0053138	0.06796	0.02298	2.9576834	0.0149539
CG5288	FBgn0035950	0.13449	0.06789	1.9810495	0.0149804
nimB2	FBgn0028543	0.0076	0.06352	-8.3603539	0.0150653
CG7430	FBgn0036762	0.21843	0.28924	-1.3241787	0.0151081
Gie	FBgn0037551	0.03363	0.00762	4.4124766	0.0151162

CG6415	FBgn0032287	0.05801	0.02251	2.5766556	0.0152615
bsk	FBgn0000229	0.00241	0.01975	-8.1875584	0.0152756
CG12360	FBgn0038111	0.00132	0.01425	-10.797391	0.0154887
ATPsyn-gamma	FBgn0020235	0.28389	0.35317	-1.2440232	0.0155783
Su(var)3-9	FBgn0003600	0.01317	0.03203	-2.4321868	0.0157288
CG2444	FBgn0030326	0.06002	0.15657	-2.6086135	0.0158423
CHOp24	FBgn0029709	0.27516	0.08791	3.1298863	0.0158872
CG32626	FBgn0052626	0.02195	0.00999	2.1961323	0.0159454
CG1910	FBgn0022349	0.13374	0.21744	-1.6258223	0.015948
chrw	FBgn0015372	0.04375	0.0196	2.2323615	0.0159819
Rab3	FBgn0005586	0.0519	0.02325	2.2323615	0.0159819
Rab30	FBgn0031882	0.0512	0.02294	2.2323615	0.0159819
Rab39	FBgn0029959	0.05238	0.02346	2.2323615	0.0159819
Rab-RP3	FBgn0015793	0.05214	0.02336	2.2323615	0.0159819
RabX4	FBgn0051118	0.05361	0.02401	2.2323615	0.0159819
CdsA	FBgn0010350	0.00722	0	Inf	0.0160184
CG13962	FBgn0032824	0.04244	0	Inf	0.0160184
Nsf2	FBgn0013998	0.01589	0.02947	-1.8542153	0.0160317
p24-1	FBgn0030341	0.20078	0.10518	1.9089912	0.0160673
CG10992	FBgn0030521	0.45298	0.27822	1.6281018	0.0162801
CG13890	FBgn0035169	0.0619	0.00228	27.163604	0.0165158
KdelR	FBgn0022268	0.0503	0	Inf	0.0165959
RabX2	FBgn0030200	0.02734	0	Inf	0.0165959
CG11523	FBgn0037156	0	0.02848	-Inf	0.0169634
CG6904	FBgn0038293	0.03757	0.00603	6.2285403	0.0171567
VhaSFD	FBgn0027779	0.11837	0.06996	1.6919733	0.017193
RpS4	FBgn0011284	0.89784	1.08111	-1.2041203	0.0173894
Int6	FBgn0025582	0.18094	0.12679	1.4271152	0.0174016
dnc	FBgn0000479	0.01858	0.00256	7.2621231	0.0178573
Lerp	FBgn0051072	0.01707	0.00211	8.0756045	0.0179743
Lcp4	FBgn0002535	0.08036	0.3182	-3.9595839	0.018063
CG9330	FBgn0036888	0.00099	0.00667	-6.724592	0.0181806
Rab9D	FBgn0067052	0.05711	0.0239	2.3894589	0.0181821
Rab9Db	FBgn0030221	0.05711	0.0239	2.3894589	0.0181821
Rab9E	FBgn0052673	0.05711	0.0239	2.3894589	0.0181821
Rab9Fa	FBgn0052671	0.05711	0.0239	2.3894589	0.0181821
Cyp12e1	FBgn0037817	0	0.01832	-Inf	0.0184952
CG4848	FBgn0037998	0.00421	0	Inf	0.0186802
T3dh	FBgn0017482	0.02018	0.00263	7.6728476	0.018796
Hsc70Cb	FBgn0026418	0.20687	0.27186	-1.3141081	0.0188465
Nop56	FBgn0038964	0	0.01838	-Inf	0.0188873

vkg	FBgn0016075	0.01741	0.00988	1.7624994	0.019047
Idgf4	FBgn0026415	0.29936	0.47495	-1.5865543	0.0191107
Df31	FBgn0022893	0.16208	0.41175	-2.5403923	0.0192789
CG12811	FBgn0037779	0.00442	0.03437	-7.7752463	0.0192812
CG7532	FBgn0028915	0.02398	0.10077	-4.2030274	0.0193867
EfTuM	FBgn0024556	0.01439	0.06933	-4.8173175	0.0194385
LKR	FBgn0025687	0.00612	0.0205	-3.3520719	0.0194815
CG6751	FBgn0033562	0.00354	0.00983	-2.774324	0.0195021
Argk	FBgn0000116	1.68075	0.98201	1.7115403	0.019551
CG5167	FBgn0038038	0.08686	0.02274	3.8204019	0.019558
CG8031	FBgn0038110	0.05582	0.12316	-2.2064877	0.019562
CG5890	FBgn0039380	0.05712	0	Inf	0.0196357
path	FBgn0036007	0.01149	0	Inf	0.019783
TFAM	FBgn0038805	0.00247	0.04496	-18.18629	0.0198009
Aats-asn	FBgn0086443	0.04354	0.07197	-1.6530255	0.0198212
CG10565	FBgn0037051	0.00139	0.00891	-6.4148701	0.0198884
CG9297	FBgn0038181	0.05735	0.0075	7.6445839	0.0201199
RpS8	FBgn0039713	0.58172	0.84419	-1.4511998	0.0202335
nudC	FBgn0021768	0.01708	0.05666	-3.3175444	0.0204168
CG3523	FBgn0027571	0.25755	0.18258	1.4106351	0.0204443
unc	FBgn0003950	0.00393	0	Inf	0.0205913
Adgf-A	FBgn0036752	0.00807	0.00114	7.1031722	0.0206627
CG1703	FBgn0030321	0.02757	0.09081	-3.2936715	0.0206862
Pepck	FBgn0003067	0.11801	0.02086	5.6568074	0.0209017
GNBP3	FBgn0040321	0.00149	0.02457	-16.523877	0.0209195
His4:CG33881	FBgn0053881	0.48197	1.0059	-2.0870357	0.0209295
CG3887	FBgn0031670	0.0626	0.01562	4.0092539	0.0209722
Arp14D	FBgn0011742	0.01132	0.02759	-2.4369	0.0211339
pyd3	FBgn0037513	0.02681	0.01003	2.6734909	0.0212453
Lsd-2	FBgn0030608	0.07242	0.03481	2.0808629	0.0213731
RpS19a	FBgn0010412	0.59213	1.05263	-1.77771	0.0214074
CG8680	FBgn0031684	0.11643	0.14967	-1.2854513	0.0214581
CG4019	FBgn0034885	0.06727	0.01563	4.3031745	0.0215057
CalpB	FBgn0025866	0.00637	0.00068	9.381449	0.0215208
CG4729	FBgn0036623	0.00967	0.02976	-3.0779827	0.0215393
TfIIFalpha	FBgn0010282	0	0.01066	-Inf	0.0215638
CG3326	FBgn0031519	0.00858	0.00115	7.431442	0.021785
Acph-1	FBgn0000032	0.02367	0.00807	2.9320376	0.0220386
Hsp68	FBgn0001230	0.09042	0.15071	-1.6667071	0.0220586
CG4706	FBgn0037862	0.00483	0.01308	-2.7057572	0.0221926
galectin	FBgn0031213	0.00145	0.00777	-5.3615739	0.0223989
Treh	FBgn0003748	0.00122	0.00656	-5.3615739	0.0223989

Unc-89	FBgn0053519	0.01847	0.00145	12.760253	0.0224613
CG3760	FBgn0022343	0.08325	0.17543	-2.1072402	0.0225604
CG4598	FBgn0032160	0.0456	0.11106	-2.4356589	0.0226165
CG5599	FBgn0030612	0.00352	0.0159	-4.5180672	0.022643
AnnIX	FBgn0000083	0.17377	0.275	-1.5825385	0.0226745
CG5023	FBgn0038774	0.58708	0.21166	2.7736661	0.0226845
Csat	FBgn0024994	0.0642	0.00164	39.126698	0.0227037
Lcp1	FBgn0002531	0.01811	0.06135	-3.3872174	0.0228806
CG1371	FBgn0033482	0.00318	0	Inf	0.0229705
lectin-28C	FBgn0040099	0.01653	0	Inf	0.0229705
Lcp65Ad	FBgn0020641	0.10414	0	Inf	0.0230471
TER94	FBgn0261014	0.35845	0.42864	-1.195822	0.0233882
GstD1	FBgn0001149	1.5833	2.51024	-1.5854471	0.0234867
Prp19	FBgn0261119	0.05158	0.00722	7.1456725	0.023494
Tps1	FBgn0027560	0.0898	0.01033	8.6915595	0.023523
NLaz	FBgn0053126	0.10044	0.20412	-2.032262	0.0235987
CG13044	FBgn0036599	0	0.0795	-Inf	0.0237176
Fbp2	FBgn0000640	0.98874	0.45342	2.1805967	0.0237322
Lcp2	FBgn0002533	0.01869	0.14598	-7.8112377	0.0239853
CG5554	FBgn0034914	0.2406	0.12036	1.9989477	0.0244363
CG2774	FBgn0031534	0.03155	0.07084	-2.2454251	0.0244549
CG7630	FBgn0040793	0.08007	0.16833	-2.1023297	0.0249249
CG9318	FBgn0032880	0.04726	0.00651	7.2604189	0.0250261
Sod2	FBgn0010213	0.10291	0.20926	-2.0334128	0.0254224
Act57B	FBgn0000044	3.11101	2.29292	1.3567908	0.0255132
Hsc70-1	FBgn0001216	0.08998	0.15287	-1.6989661	0.0256706
CG9471	FBgn0037749	0.00344	0.05632	-16.365115	0.0256722
sn	FBgn0003447	0.01798	0.06343	-3.5273087	0.0257065
CG4757	FBgn0027584	0	0.04266	-Inf	0.0259818
vib	FBgn0260992	0.12493	0.24026	-1.9231136	0.0262762
Pp1alpha-96A	FBgn0003134	0.08576	0.0294	2.9168467	0.0264944
eIF-4E	FBgn0015218	0.12055	0.20403	-1.6924022	0.0264991
Sap-r	FBgn0000416	0.17601	0.09909	1.7761866	0.026519
Ef2b	FBgn0000559	0.87251	1.07203	-1.2286662	0.0265929
CG5149	FBgn0031904	0	0.0238	-Inf	0.0266171
Obp99a	FBgn0039678	0	0.06207	-Inf	0.026731
CG3609	FBgn0031418	0.10661	0.19032	-1.7851805	0.0267754
Osbp	FBgn0020626	0.02004	0.0427	-2.1308856	0.0267853
tnc	FBgn0039257	0.00025	0.00364	-14.343479	0.0267853
Inos	FBgn0025885	0.00249	0.0242	-9.7374107	0.0268678
CG18012	FBgn0038552	0.00157	0.00597	-3.7923685	0.0268898
csw	FBgn0000382	0.00083	0.00315	-3.7923685	0.0268898

gro	FBgn0001139	0.00098	0.0037	-3.7923685	0.0268898
Uch-L3	FBgn0011327	0.06848	0.09754	-1.4243416	0.0269334
eRF1	FBgn0036974	0.16456	0.24792	-1.5066132	0.027071
Glt	FBgn0001114	0.14135	0.10361	1.3642628	0.0272804
Bsg	FBgn0011219	0.04771	0.00956	4.9915107	0.0272924
CG13813	FBgn0036956	0.00986	0.04013	-4.0704494	0.0273846
CG6255	FBgn0038708	0	0.02216	-Inf	0.0275866
RpS5b	FBgn0038277	0.11428	0.17074	-1.4940535	0.0275993
Hsc70-5	FBgn0001220	0.03876	0.06698	-1.7282431	0.0278315
Hml	FBgn0029167	0	0.01145	-Inf	0.0278561
SF2	FBgn0040284	0.06666	0.1061	-1.5916242	0.0278605
l(3)neo18	FBgn0011455	0.00392	0.03983	-10.164906	0.0278719
CG31548	FBgn0051548	0.02628	0.11385	-4.33257	0.0279555
Tcp-1eta	FBgn0037632	0.0954	0.13861	-1.4530274	0.0279812
RpL18	FBgn0035753	0.44386	0.32353	1.3719271	0.0280509
RhoGAP68F	FBgn0036257	0.00831	0.0013	6.4111101	0.0281143
pzg	FBgn0259785	0.03087	0.04803	-1.5559042	0.0281959
SmB	FBgn0010083	0.01085	0.03927	-3.6185603	0.0282698
TotA	FBgn0028396	0.16718	0.0859	1.9462762	0.0282999
CG1105	FBgn0037465	0.02074	0.00146	14.192548	0.0285311
CG32679	FBgn0052679	0.0084	0.04939	-5.8818436	0.0289239
FKBP59	FBgn0029174	0.04301	0.08139	-1.89221	0.029019
MSBP	FBgn0030703	0.06525	0.0257	2.5391978	0.0291075
CG31683	FBgn0051683	0.01999	0.03507	-1.7546225	0.0292352
Dak1	FBgn0028833	0.34343	0.5594	-1.6288619	0.0292676
Gbeta13F	FBgn0001105	0.1019	0.06032	1.6892321	0.0295098
Fer1HCH	FBgn0015222	0.34358	0.47833	-1.3921867	0.0295193
Vps35	FBgn0034708	0.00812	0.02876	-3.5433069	0.0297878
Zpr1	FBgn0030096	0.00159	0.01662	-10.419609	0.0297945
Mtp	FBgn0032904	0.07532	0.00879	8.5660633	0.0298119
cype	FBgn0015031	0	0.14659	-Inf	0.0299891
CG7768	FBgn0036415	0.08923	0.16901	-1.8942035	0.0301875
CG9812	FBgn0034860	0.03558	0.07766	-2.1827475	0.030306
CG7033	FBgn0030086	0.13262	0.18913	-1.4260558	0.0305549
CG18135	FBgn0036837	0.07048	0.01355	5.1994027	0.0306208
rad50	FBgn0034728	0.00489	0.00048	10.271475	0.0307529
CG6055	FBgn0031918	0	0.03483	-Inf	0.0309122
l(2)efl	FBgn0011296	0.64169	0.16484	3.8928571	0.0312121
Act87E	FBgn0000046	3.01814	2.2466	1.3434247	0.0314689
Tbp-1	FBgn0028684	0.15782	0.09816	1.607794	0.0314913
bsf	FBgn0032679	0.00052	0.00189	-3.6534694	0.0315419
Bet3	FBgn0260859	0.01578	0.07493	-4.7496382	0.0318397

CG9796	FBgn0038149	0.00931	0.05314	-5.7070038	0.0322188
Hsp23	FBgn0001224	1.93737	1.59294	1.2162228	0.0323062
cora	FBgn0010434	0.01416	0.02416	-1.706369	0.0324291
Cyt-c-p	FBgn0000409	0.20836	0.43046	-2.065906	0.0324941
CG9784	FBgn0030761	0.00282	0.01174	-4.169558	0.0325454
Trxr-1	FBgn0020653	0.19867	0.28409	-1.4299964	0.0326827
didum	FBgn0261397	0.00078	0.00411	-5.2504584	0.0329391
CG31549	FBgn0051549	0.02444	0.06782	-2.7746907	0.033014
CG30410	FBgn0050410	0.10098	0.06146	1.6431366	0.0331555
His4:CG33909	FBgn0053909	0.82435	1.53257	-1.8591149	0.0333408
CG5009	FBgn0027572	0.0259	0.00122	21.291536	0.0335994
Cont	FBgn0037240	0	0.0025	-Inf	0.0336218
Akt1	FBgn0010379	0.00262	0.00839	-3.2062594	0.0342044
bl	FBgn0015907	0.01629	0.04477	-2.7492342	0.0342323
CG6206	FBgn0027611	0.03883	0.05803	-1.4945148	0.0346362
eIF2B-epsilon	FBgn0023512	0.00563	0.01472	-2.6163102	0.034674
NAT1	FBgn0010488	0.0023	0.00915	-3.978157	0.0349017
CG9232	FBgn0031845	0	0.01106	-Inf	0.035009
CG8360	FBgn0032001	0.02503	0.0741	-2.9607768	0.0350643
Mp20	FBgn0002789	0.58243	0.32255	1.8057418	0.0354769
su(r)	FBgn0086450	0.00188	0.00593	-3.1536287	0.0354827
Tom34	FBgn0010812	0.01067	0.0409	-3.8335986	0.035641
CG1354	FBgn0030151	0.1997	0.29809	-1.4927124	0.035727
vig2	FBgn0046214	0.02363	0.05319	-2.2511625	0.0357345
Hsp67Bc	FBgn0001229	0.32454	0.74997	-2.3108588	0.0358185
Rep	FBgn0026378	0.00417	0.01042	-2.4966067	0.0359161
Sec22	FBgn0260855	0.14491	0.06717	2.1574725	0.03655
CG10098	FBgn0037472	0.11144	0.2086	-1.8718137	0.0370326
CG5844	FBgn0038049	0.01232	0.03951	-3.2079033	0.0374535
CG7834	FBgn0039697	0.20298	0.31938	-1.5734411	0.0374585
CanB2	FBgn0015614	0.04438	0.01102	4.0284396	0.037588
Chro	FBgn0044324	0.00636	0.01264	-1.9873271	0.0376154
CG9119	FBgn0035189	0.1384	0.31238	-2.2571242	0.0377583
Ccp84Ae	FBgn0004779	0.02563	0.00302	8.4894022	0.0380175
CG16758	FBgn0035348	0.02192	0.00192	11.410674	0.0380596
Cdc42	FBgn0010341	0.03187	0.01387	2.2973366	0.0380779
Npc2h	FBgn0039801	0.01811	0.06761	-3.7328184	0.038108
Hexo1	FBgn0041630	0.00268	0.00848	-3.1605558	0.0381453
Arf79F	FBgn0010348	0.67642	0.38369	1.7629472	0.0386987
vimar	FBgn0022960	0.00132	0.00617	-4.6869123	0.0387053
CG14985	FBgn0035482	0	0.01617	-Inf	0.0387845
mbf1	FBgn0026208	0	0.02687	-Inf	0.0387845

stv	FBgn0086708	0	0.00755	-Inf	0.0387845
Amy-d	FBgn0000078	0	0.03596	-Inf	0.038826
ATPsyn-beta	FBgn0010217	1.13472	0.86318	1.314578	0.0392267
Spn43Ab	FBgn0024293	0.00927	0.05178	-5.5848706	0.0393985
Vha44	FBgn0020611	0.03261	0.01785	1.8270838	0.0395441
CG8602	FBgn0035763	0.00634	0.00126	5.0178524	0.0396014
CG32789	FBgn0260484	0.05533	0.0915	-1.6539362	0.0398861
Gyk	FBgn0025592	0.00154	0.02364	-15.374014	0.0407443
CG2767	FBgn0037537	0.22833	0.28308	-1.239779	0.0410681
CG12119	FBgn0030102	0.02065	0.06788	-3.2867986	0.0412491
RpS17	FBgn0005533	1.11524	1.29597	-1.1620593	0.0415647
Ntf-2	FBgn0031145	0.26906	0.17387	1.5475072	0.0416822
Oscp	FBgn0016691	0.36946	0.30279	1.2201951	0.0417224
128up	FBgn0010339	0.02844	0.06696	-2.3538696	0.0419983
CG4849	FBgn0039566	0.0045	0.00092	4.9130108	0.0421872
Mdh	FBgn0029155	0.00232	0.0149	-6.4095135	0.0428895
Nmt	FBgn0020392	0.00595	0.02353	-3.9544343	0.0430552
CG6463	FBgn0047038	0.10384	0.16193	-1.559419	0.0433411
ade3	FBgn0000053	0.04702	0.01221	3.8515592	0.0438103
CG16985	FBgn0035355	0	0.03424	-Inf	0.0440172
Arp87C	FBgn0011745	0.05388	0.13555	-2.5155427	0.0441035
und	FBgn0025117	0.01884	0.03156	-1.6746799	0.0442462
CG8310	FBgn0040377	0.00857	0.03287	-3.837299	0.0445119
arg	FBgn0023535	0.01523	0.00316	4.8248954	0.0445472
CalpA	FBgn0012051	0.00366	0.00076	4.8248954	0.0445472
Prosbeta2R1	FBgn0029812	0.01517	0.02802	-1.8475569	0.0447469
B52	FBgn0004587	0.05806	0.10455	-1.8008424	0.0449907
CG5484	FBgn0039450	0.01741	0.0047	3.7012978	0.0451581
RpS27A	FBgn0003942	0.24969	0.3949	-1.581571	0.0452015
Amy-p	FBgn0000079	0	0.03721	-Inf	0.0454556
poly	FBgn0086371	0	0.02186	-Inf	0.0455311
rump	FBgn0260010	0.05389	0.03007	1.7919839	0.0455374
Rbp1-like	FBgn0030479	0.0293	0.05313	-1.8132109	0.0460784
alph	FBgn0086361	0.00824	0.00166	4.9562873	0.0460788
Syb	FBgn0003660	0.0919	0.05951	1.5440969	0.0463662
CG10881	FBgn0038796	0.01921	0.04352	-2.2661775	0.0464546
gw	FBgn0051992	0.00154	0.00564	-3.6585627	0.0468062
CG7181	FBgn0037097	0	0.12057	-Inf	0.0470519
S6k	FBgn0015806	0	0.00803	-Inf	0.0475917
Gs1	FBgn0001142	0.20918	0.11749	1.7804336	0.0477419
CG7224	FBgn0031971	0.13654	0.03247	4.2053511	0.0479034
Lmpt	FBgn0036672	0.02805	0.00724	3.8740727	0.0480139

CG8498	FBgn0031992	0.2101	0.32349	-1.5396433	0.0480337
sta	FBgn0003517	1.10958	1.37607	-1.2401785	0.0482266
CG10616	FBgn0036286	0.01711	0.00219	7.8226564	0.0483075
CG4877	FBgn0036624	0.0006	0.00347	-5.8116931	0.0483504
CG15239	FBgn0029681	0.0062	0.00127	4.8673957	0.0484629
Spt5	FBgn0040273	0.002	0.00972	-4.8521866	0.0486946
svr	FBgn0004648	0.00892	0.00321	2.7795676	0.049157
Dgp-1	FBgn0027836	0.00105	0.00612	-5.8300482	0.0495128
CG17737	FBgn0035423	0.18822	0.30332	-1.6115439	0.049719
Hsp60C	FBgn0031728	0.03477	0.06036	-1.7360064	0.0497652
Spn4	FBgn0028985	0.0651	0.10483	-1.6102635	0.0497966
Pp1-87B	FBgn0004103	0.11014	0.04677	2.3546302	0.0498852
Sec61alpha	FBgn0086357	0.19064	0.14201	1.3424005	0.0501836
Hex-A	FBgn0001186	0.03499	0.0601	-1.7174617	0.0502599
Atpalpha	FBgn0002921	0.03491	0.01278	2.7323294	0.0504063
CG3011	FBgn0029823	0.21931	0.12981	1.6894009	0.0504172
CG9920	FBgn0038200	0.02805	0.07661	-2.7307959	0.0506994
CG17255	FBgn0030205	0.00338	0.01142	-3.378693	0.0509874
RpLP2	FBgn0003274	0.86641	2.07545	-2.3954598	0.0513845
RpS25	FBgn0086472	0.46684	0.65572	-1.40459	0.0516682
CG12428	FBgn0039543	0.0073	0	Inf	0.0517279
CG9894	FBgn0031453	0.09044	0.2112	-2.3353448	0.0518241
SpdS	FBgn0037723	0.08158	0.02727	2.9913317	0.0518268
CG7998	FBgn0038587	0.63115	0.80451	-1.2746706	0.0518681
MP1	FBgn0027930	0.02171	0.05682	-2.6167585	0.051945
CG3223	FBgn0037538	0.00392	0.01138	-2.9034365	0.0520326
Dip-B	FBgn0000454	0.12947	0.18741	-1.4475443	0.0520937
Khc	FBgn0001308	0.04544	0.07806	-1.7178911	0.0521626
CG4603	FBgn0035593	0.01698	0.0319	-1.878822	0.0522058
CG12264	FBgn0032393	0	0.004	-Inf	0.0522641
CG14933	FBgn0040968	0	0.02401	-Inf	0.0522641
CG1499	FBgn0039852	0	0.00222	-Inf	0.0522641
CG31739	FBgn0051739	0	0.00171	-Inf	0.0522641
CG8420	FBgn0037664	0	0.00696	-Inf	0.0522641
CG9034	FBgn0040931	0	0.02401	-Inf	0.0522641
janA	FBgn0001280	0	0.02739	-Inf	0.0522641
mRpS30	FBgn0030692	0	0.00332	-Inf	0.0522641
Nrx-IV	FBgn0013997	0	0.00144	-Inf	0.0522641
qkr58E-1	FBgn0022986	0	0.00467	-Inf	0.0522641
slgA	FBgn0003423	0	0.00271	-Inf	0.0522641
Hsp27	FBgn0001226	0.53102	0.74492	-1.4027974	0.0522999
Sgs8	FBgn0003378	3.83398	5.91192	-1.5419786	0.0523912

CG6639	FBgn0032638	0.00329	0.0129	-3.9181672	0.0525457
Aats-thr	FBgn0027081	0.1124	0.1519	-1.3514136	0.053432
nimC2	FBgn0028939	0.01563	0.00184	8.4895296	0.0534691
qkr58E-2	FBgn0022985	0.00391	0.01535	-3.9260922	0.0537148
CG5325	FBgn0032407	0.01844	0.02883	-1.5633233	0.0538645
ScpX	FBgn0015808	0.19904	0.10658	1.867503	0.0538776
CG3074	FBgn0034709	0.05016	0.01479	3.3912577	0.0542464
Rpn5	FBgn0028690	0.10495	0.0698	1.5035505	0.0544784
Atox1	FBgn0052446	0.14231	0.31161	-2.1896655	0.0547034
Hmu	FBgn0015737	0.11237	0.05837	1.9252526	0.0549514
Neurochondrin	FBgn0037447	0.06058	0.01446	4.1893399	0.055055
RhoGAP92B	FBgn0038747	0.0019	0.00803	-4.2304628	0.0552413
beta'Cop	FBgn0025724	0.25945	0.13387	1.9381384	0.0553571
CG11943	FBgn0031078	0.00334	0.00137	2.442456	0.0555864
Dhc64C	FBgn0010349	0.01162	0.00486	2.3903132	0.0556473
CG2862	FBgn0031459	0.15522	0.27285	-1.7578022	0.05567
rin	FBgn0015778	0.03014	0.06059	-2.0105054	0.0557447
CG10863	FBgn0027552	0.26298	0.2122	1.2393406	0.0558819
RpS15Aa	FBgn0010198	0.3188	0.52603	-1.6500383	0.0560995
CG31313	FBgn0051313	0.05224	0.1783	-3.413394	0.0561095
CG5021	FBgn0035944	0.03837	0.01376	2.7879112	0.0571286
Rbp2	FBgn0010256	0.02343	0.03846	-1.6412546	0.0574546
Prosbeta2	FBgn0023174	0.11862	0.16871	-1.4222991	0.0577824
CG10038	FBgn0038013	0	0.00666	-Inf	0.0578035
CG10133	FBgn0036366	0	0.01303	-Inf	0.0578035
CG12007	FBgn0037293	0	0.004	-Inf	0.0578035
CG32488	FBgn0052488	0	0.00671	-Inf	0.0578035
Patj	FBgn0067864	0	0.00236	-Inf	0.0578035
alphaPS4	FBgn0034005	0	0.00202	-Inf	0.0583192
CG16837	FBgn0035009	0	0.01574	-Inf	0.0583192
CG4165	FBgn0029763	0	0.00182	-Inf	0.0583192
CG7802	FBgn0039704	0	0.0055	-Inf	0.0583192
Dis3	FBgn0039183	0	0.00208	-Inf	0.0583192
Mcm3	FBgn0024332	0	0.0025	-Inf	0.0583192
sns	FBgn0024189	0	0.00138	-Inf	0.0583192
CG10882	FBgn0031408	0.21006	0.15657	1.3416309	0.0583378
LysE	FBgn0004428	0.02145	0.09174	-4.2765216	0.058478
asparagine-synthetase	FBgn0041607	0.00417	0.01206	-2.8913708	0.058689
l(2)k07824	FBgn0022070	0	0.00402	-Inf	0.0586948
Nep3	FBgn0031081	0	0.00259	-Inf	0.0586948
tomosyn	FBgn0030412	0	0.00273	-Inf	0.0586948

CG7519	FBgn0037087	0.00878	0.03197	-3.6428511	0.0588604
LamC	FBgn0010397	0.14553	0.10831	1.3437355	0.0597515
l(2)37Cc	FBgn0002031	0.31284	0.39954	-1.2771302	0.05988
CG10527	FBgn0034583	0.36126	0.25536	1.4147367	0.0606039
RpS3	FBgn0002622	0.6969	0.87523	-1.2558895	0.060656
zetaCOP	FBgn0040512	0.15727	0.12447	1.2635313	0.0610647
CG18003	FBgn0061356	0.05166	0.01355	3.8113754	0.0610871
Gtp-bp	FBgn0010391	0.07475	0.10967	-1.4671101	0.061203
CG10576	FBgn0035630	0.35926	0.48866	-1.3601891	0.0612377
CG12171	FBgn0037354	0.17855	0.24085	-1.3489524	0.0612984
CG31150	FBgn0051150	0	0.00323	-Inf	0.0614884
CG2789	FBgn0031263	0.02137	0.03984	-1.8640458	0.0615139
porin	FBgn0004363	0.48387	0.63089	-1.3038418	0.0619423
LysB	FBgn0004425	0.02145	0.09606	-4.4775811	0.0620804
LysD	FBgn0004427	0.02145	0.09606	-4.4775811	0.0620804
CG7059	FBgn0038957	0.00555	0.0285	-5.1353399	0.0620874
Snap	FBgn0250791	0.25702	0.14561	1.7650982	0.0621106
zip	FBgn0005634	0.32566	0.36829	-1.130903	0.0622011
CG10359	FBgn0035452	0.00311	0	Inf	0.0624487
CG13928	FBgn0035246	0.00584	0	Inf	0.0624487
CG16903	FBgn0040394	0.00255	0	Inf	0.0624487
CG33635	FBgn0053635	0.00719	0	Inf	0.0624487
CG6793	FBgn0036242	0.00254	0	Inf	0.0624487
CG7077	FBgn0038946	0.00577	0	Inf	0.0624487
CG7083	FBgn0035877	0.00327	0	Inf	0.0624487
CRMP	FBgn0023023	0.00493	0	Inf	0.0624487
His1:CG33834	FBgn0053834	0.00559	0	Inf	0.0624487
Oatp58Da	FBgn0050277	0.00227	0	Inf	0.0624487
Orct	FBgn0019952	0.00261	0	Inf	0.0624487
Ras85D	FBgn0003205	0.00757	0	Inf	0.0624487
Rpb11	FBgn0032634	0.01223	0	Inf	0.0624487
Spn28D	FBgn0031973	0.00267	0	Inf	0.0624487
Tsp42Ee	FBgn0029506	0.01255	0	Inf	0.0624487
yrt	FBgn0004049	0.00196	0	Inf	0.0624487
CG17597	FBgn0032715	0.23013	0.13223	1.7404258	0.0625789
RpS20	FBgn0019936	0.29456	0.42945	-1.4579241	0.0627242
santa-maria	FBgn0025697	0.0106	0	Inf	0.0627909
scat	FBgn0011232	0	0.00349	-Inf	0.062883
rok	FBgn0026181	0	0.00238	-Inf	0.063291
CG6643	FBgn0039208	0.03313	0.01022	3.2408327	0.0641369
Pfrx	FBgn0027621	0.00125	0.00773	-6.1685366	0.0647058
RpI135	FBgn0003278	0.00206	0.00053	3.8552577	0.0648009

CG4769	FBgn0035600	0.04029	0.05806	-1.441089	0.0649115
Tg	FBgn0031975	0.0094	0.0016	5.8611731	0.0649486
CG7787	FBgn0032020	0.03059	0.00515	5.9427836	0.0651669
CG9086	FBgn0030809	0.00205	0.00034	5.9427836	0.0651669
CG10743	FBgn0036376	0.00239	0	Inf	0.0653286
CG11570	FBgn0036230	0.0076	0	Inf	0.0653286
CG11913	FBgn0039331	0.00307	0	Inf	0.0653286
CG12004	FBgn0035236	0.00403	0	Inf	0.0653286
CG1428	FBgn0032967	0.00365	0	Inf	0.0653286
CG14630	FBgn0014903	0.00645	0	Inf	0.0653286
CG14787	FBgn0027793	0.00625	0	Inf	0.0653286
CG18507	FBgn0028527	0.00316	0	Inf	0.0653286
CG31126	FBgn0051126	0.01161	0	Inf	0.0653286
CG33977	FBgn0053977	0.0173	0	Inf	0.0653286
CG3702	FBgn0031590	0.00254	0	Inf	0.0653286
CG3940	FBgn0037788	0.00723	0	Inf	0.0653286
CG5804	FBgn0035926	0.01983	0	Inf	0.0653286
CG6034	FBgn0036750	0.00328	0	Inf	0.0653286
CG7564	FBgn0036734	0.00387	0	Inf	0.0653286
CG9336	FBgn0032897	0.01099	0	Inf	0.0653286
CG9380	FBgn0035094	0.00188	0	Inf	0.0653286
CG9512	FBgn0030593	0.00261	0	Inf	0.0653286
Cyp28d1	FBgn0031689	0.00324	0	Inf	0.0653286
Cyp6a9	FBgn0013771	0.00323	0	Inf	0.0653286
dro2	FBgn0052279	0.04646	0	Inf	0.0653286
flfl	FBgn0024555	0.0017	0	Inf	0.0653286
Galpha49B	FBgn0004435	0.00461	0	Inf	0.0653286
Ho	FBgn0037933	0.00549	0	Inf	0.0653286
Indy	FBgn0036816	0.00284	0	Inf	0.0653286
Itp-r83A	FBgn0010051	0.00057	0	Inf	0.0653286
Or82a	FBgn0041621	0.00422	0	Inf	0.0653286
prominin-like	FBgn0026189	0.00161	0	Inf	0.0653286
SmG	FBgn0030765	0.04279	0	Inf	0.0653286
Oscillin	FBgn0031717	0.12743	0.06993	1.8220943	0.0656297
Cbp80	FBgn0022942	0.0046	0	Inf	0.0664825
CG11880	FBgn0039637	0.00402	0	Inf	0.0664825
CG11902	FBgn0028647	0.00126	0	Inf	0.0664825
CG12703	FBgn0031069	0.0024	0	Inf	0.0664825
CG13972	FBgn0039522	0.00357	0	Inf	0.0664825
CG15770	FBgn0029803	0.00533	0	Inf	0.0664825
GstD10	FBgn0042206	0.00762	0	Inf	0.0664825
Parg	FBgn0023216	0.00208	0	Inf	0.0664825

pst	FBgn0035770	0.00245	0	Inf	0.0664825
Sox14	FBgn0005612	0.00239	0	Inf	0.0664825
Nelf-E	FBgn0017430	0	0.03437	-Inf	0.0667064
growl	FBgn0037245	0.12404	0.18423	-1.4852268	0.067202
Lcp65Ac	FBgn0020642	0.06407	0.03743	1.711763	0.0674351
CG3621	FBgn0025839	0	0.04199	-Inf	0.0675642
Arp66B	FBgn0011744	0.04987	0.09736	-1.9520579	0.0676037
RpS27	FBgn0039300	0.52595	0.65824	-1.2515345	0.0681818
CG9603	FBgn0040529	0.00819	0.09236	-11.279403	0.0683751
Spase25	FBgn0030306	0.41315	0.26763	1.5437601	0.0688409
CG30122	FBgn0050122	0.00732	0.01496	-2.0428418	0.0688654
PRL-1	FBgn0024734	0.0271	0.00457	5.9285064	0.0689474
CG4645	FBgn0030435	0.01683	0.00907	1.8553758	0.0690171
CG8709	FBgn0033269	0.00556	0.003	1.8553758	0.0690171
Elf	FBgn0020443	0.13125	0.18498	-1.4093206	0.0696155
CG15100	FBgn0034401	0.02345	0.05487	-2.3392981	0.0696729
CanB	FBgn0010014	0.02227	0.00363	6.1378677	0.0697825
Ge-1	FBgn0032340	0.0028	0.00046	6.1378677	0.0697825
CG17471	FBgn0039924	0.01153	0.00305	3.774707	0.0702174
Nup154	FBgn0021761	0.00171	0.00045	3.774707	0.0702174
PpD3	FBgn0005777	0.0028	0.00988	-3.5259977	0.0707564
CG12715	FBgn0030443	0.06715	0.09752	-1.4524027	0.0711386
Hrb87F	FBgn0004237	0.09705	0.14763	-1.521166	0.0711589
Idgf1	FBgn0020416	0.01553	0.00567	2.7377206	0.0713938
eIF3-S8	FBgn0034258	0.08053	0.11918	-1.4798794	0.071461
Rheb	FBgn0041191	0.01958	0	Inf	0.0715529
CG16935	FBgn0033883	0.05757	0.01788	3.2194426	0.0717521
CG4858	FBgn0037011	0.01241	0.00232	5.3411258	0.071855
Sdc	FBgn0010415	0.00808	0.00151	5.3411258	0.071855
CaMKII	FBgn0004624	0.01392	0.00235	5.9255005	0.0719344
PyK	FBgn0003178	0.65161	0.51769	1.2586845	0.0724264
twf	FBgn0038206	0.02316	0.06443	-2.7816576	0.0725504
CG10602	FBgn0032721	0.05853	0.09759	-1.6672005	0.0728853
Imp	FBgn0030235	0.02781	0.01544	1.8004211	0.073168
CG1416	FBgn0032961	0.03637	0.04976	-1.3680581	0.0736528
Lam	FBgn0002525	0.06137	0.02692	2.2798789	0.0738082
Vps4	FBgn0027605	0.01333	0.04485	-3.3646866	0.0739763
CG10184	FBgn0039094	0.12947	0.04042	3.2028002	0.0743162
CG5214	FBgn0037891	0.04925	0.09306	-1.8895317	0.0744968
CG1674	FBgn0039897	0.08432	0.03738	2.2558589	0.0751071
Klc	FBgn0010235	0.05102	0.06774	-1.3275794	0.0753256
CG5931	FBgn0036548	0.00401	0.00174	2.3065117	0.0754444

GlcAT-I	FBgn0066114	0.01173	0	Inf	0.0755411
CG5787	FBgn0032454	0.00077	0.00694	-9.0459555	0.075576
RpS9	FBgn0010408	0.3553	0.49786	-1.4012253	0.0756063
l(2)37Cb	FBgn0086444	0.00257	0	Inf	0.0758329
DebB	FBgn0000426	0	0.03488	-Inf	0.0766546
CG11771	FBgn0039252	0	0.00363	-Inf	0.0767308
l(1)G0222	FBgn0028343	0.00323	0.01184	-3.6703771	0.07756
CG6188	FBgn0038074	0.03115	0.07145	-2.29383	0.077637
RpLP1	FBgn0002593	2.20139	1.6272	1.3528673	0.077652
CG5265	FBgn0038486	0	0.0041	-Inf	0.0777721
CG31780	FBgn0051780	0.00507	0	Inf	0.0780884
CG31997	FBgn0051997	0.01591	0	Inf	0.0780884
CG5966	FBgn0029831	0.00436	0	Inf	0.0780884
CG7227	FBgn0031970	0.00455	0	Inf	0.0780884
CG7255	FBgn0036493	0.00307	0	Inf	0.0780884
CG7766	FBgn0030087	0.00189	0	Inf	0.0780884
emp	FBgn0010435	0.00454	0	Inf	0.0780884
Mct1	FBgn0023549	0.00376	0	Inf	0.0780884
nAcRbeta-21C	FBgn0031261	0.0072	0	Inf	0.0780884
Stat92E	FBgn0016917	0.00309	0	Inf	0.0780884
Fdh	FBgn0011768	0.2446	0.27596	-1.1282127	0.0781186
wupA	FBgn0004028	0.05033	0.0206	2.442663	0.0781669
viaf	FBgn0036237	0.01181	0.02984	-2.5264575	0.0782831
Droj2	FBgn0038145	0.08242	0.13182	-1.5992861	0.0783501
CG32662	FBgn0052662	0	0.00264	-Inf	0.0784543
CG4594	FBgn0032161	0	0.011	-Inf	0.0784543
CG17343	FBgn0032751	0	0.03006	-Inf	0.0786324
CG8379	FBgn0037638	0	0.00378	-Inf	0.0786324
ebi	FBgn0023444	0	0.00382	-Inf	0.0786324
poe	FBgn0011230	0.00098	0.00023	4.2072377	0.0788124
Ice	FBgn0019972	0.00621	0.02295	-3.6934607	0.0788319
jbug	FBgn0028371	0	0.00193	-Inf	0.0789004
CG11151	FBgn0030519	0.41315	0.28221	1.4639693	0.0789731
DIP2	FBgn0024806	0	0.00314	-Inf	0.0791612
CG9577	FBgn0031092	0.24514	0.15818	1.5497768	0.0796736
CG11577	FBgn0036847	0	0.014	-Inf	0.0803724
CG17244	FBgn0039031	0	0.01946	-Inf	0.0803724
MTA1-like	FBgn0027951	0	0.00537	-Inf	0.0803724
Lsd-1	FBgn0039114	0.03402	0.00146	23.346591	0.0804576
Cdc37	FBgn0011573	0.02878	0.05631	-1.956401	0.0807487
Pp2A-29B	FBgn0260439	0.2044	0.13409	1.5243498	0.0808497
RpS6	FBgn0004922	0.30631	0.3676	-1.2000949	0.0809193

CG12512	FBgn0031703	0	0.00447	-Inf	0.080968
CG31999	FBgn0051999	0	0.00289	-Inf	0.080968
CG9689	FBgn0030159	0	0.01532	-Inf	0.080968
dpa	FBgn0015929	0	0.0031	-Inf	0.0814167
CG14629	FBgn0040398	0.03376	0.06556	-1.9420063	0.081721
CG1291	FBgn0035401	0.03196	0.01591	2.0093265	0.0820575
T-cp1	FBgn0003676	0.08226	0.14023	-1.7048156	0.0821531
awd	FBgn0000150	1.44303	2.25537	-1.5629366	0.0825545
CG31029	FBgn0051029	0	0.00591	-Inf	0.0827098
CG2118	FBgn0039877	0.00256	0.00943	-3.6759	0.0830093
CG7484	FBgn0036745	0.04208	0.10269	-2.4400166	0.0831631
dod	FBgn0015379	0.09651	0.04419	2.1841587	0.083199
CG3683	FBgn0035046	0.08897	0.0481	1.849421	0.0835786
SC35	FBgn0040286	0.01194	0.05493	-4.6007262	0.0838264
wal	FBgn0010516	0.26394	0.36749	-1.3923262	0.0839514
Nop60B	FBgn0259937	0.02468	0.04576	-1.8539939	0.0839969
CG32230	FBgn0052230	0.0605	0.1408	-2.3274081	0.0842807
CG33205	FBgn0053205	0.01657	0.00345	4.804948	0.0843302
CG3397	FBgn0037975	0.06093	0.01968	3.095874	0.0848488
BicD	FBgn0000183	0.00387	0.01609	-4.1523563	0.0850623
v(2)k05816	FBgn0042627	0.00758	0.01651	-2.1785652	0.0853725
RpS3A	FBgn0017545	0.61417	0.77108	-1.2554759	0.0855841
RpL38	FBgn0040007	0.48376	0.25231	1.9173669	0.0863107
Cog3	FBgn0031536	0.00905	0.0043	2.1038505	0.0864021
Mi-2	FBgn0013591	0.00232	0.00465	-2.0005343	0.0866424
Rrp1	FBgn0004584	0	0.00577	-Inf	0.0868549
Gap69C	FBgn0020655	0.04316	0.07629	-1.7676732	0.0869637
bor	FBgn0040237	0	0.00888	-Inf	0.0869733
l(2)35Bg	FBgn0001977	0.0397	0.06197	-1.5609898	0.0872237
Ard1	FBgn0036064	0.0156	0.06063	-3.8874233	0.0878873
CG4500	FBgn0028519	0.01683	0	Inf	0.0889234
La	FBgn0011638	0.01647	0.0437	-2.6527773	0.0890411
Nedd8	FBgn0032725	0.08547	0.17801	-2.0827231	0.0894748
CG3532	FBgn0037979	0.00525	0.01106	-2.104793	0.0895992
CG14544	FBgn0039407	0	0.00774	-Inf	0.0895992
Muc55B	FBgn0034294	0	0.00649	-Inf	0.0895992
CG12279	FBgn0038080	0.16116	0.21773	-1.351059	0.0897591
CG13084	FBgn0032788	0	0.0086	-Inf	0.0900224
CG3663	FBgn0035044	0	0.01878	-Inf	0.0900224
Dhc16F	FBgn0013809	0	0.00096	-Inf	0.0900224
Alg-2	FBgn0086378	0.01948	0	Inf	0.0902184
CG11486	FBgn0035397	0.00276	0	Inf	0.0902184

CG11874	FBgn0039634	0.00311	0	Inf	0.0902184
CG13865	FBgn0039965	0.00802	0	Inf	0.0902184
CG1518	FBgn0031149	0.00299	0	Inf	0.0902184
CG30120	FBgn0050120	0.00445	0	Inf	0.0902184
CG31370	FBgn0051370	0.00539	0	Inf	0.0902184
CstF-64	FBgn0027841	0.00488	0	Inf	0.0902184
Cyp6d2	FBgn0034756	0.00417	0	Inf	0.0902184
Prp8	FBgn0033688	0.00161	0	Inf	0.0902184
LanB2	FBgn0002528	0.01489	0.02786	-1.8713987	0.0902679
CG10289	FBgn0035688	0.00394	0.00972	-2.4681903	0.0904654
RpL12	FBgn0034968	0.39125	0.54752	-1.3994045	0.0907943
CG32549	FBgn0052549	0.04238	0.01907	2.2222575	0.0915155
Bap	FBgn0010380	0.05829	0.02965	1.9659745	0.0924527
CG4365	FBgn0037024	0.01554	0.04985	-3.2074307	0.092702
CG5377	FBgn0038974	0.00515	0.01175	-2.2828613	0.093065
CG9302	FBgn0032514	0.00281	0.0064	-2.2828613	0.093065
Srp54	FBgn0024285	0.00279	0.00637	-2.2828613	0.093065
CG4538	FBgn0038745	0	0.00516	-Inf	0.0934251
mRpL54	FBgn0034579	0	0.01868	-Inf	0.0934251
O-fut1	FBgn0033901	0	0.00613	-Inf	0.0934251
Ppt2	FBgn0032358	0	0.00856	-Inf	0.0934251
serp	FBgn0260653	0	0.00456	-Inf	0.0934251
spag	FBgn0015544	0	0.00462	-Inf	0.0934251
sra	FBgn0086370	0	0.00844	-Inf	0.0934251
Dpy-30L1	FBgn0032293	0.02805	0.05823	-2.0759387	0.0936763
CG6084	FBgn0086254	0.24586	0.29968	-1.2189348	0.0938016
Tig	FBgn0011722	0.05671	0.03263	1.7378108	0.0949079
CG6020	FBgn0037001	0.01217	0.0446	-3.6637129	0.0950684
CG4764	FBgn0031310	0.03817	0.0738	-1.933544	0.0951388
CG3305	FBgn0032949	0.05284	0.034	1.5542175	0.0955193
RpS24	FBgn0034751	0.74458	0.61169	1.2172505	0.0958222
Dsor1	FBgn0010269	0.00184	0.01612	-8.7623266	0.0960308
PHGPx	FBgn0035438	0.33353	0.24731	1.3486143	0.0962829
CG18591	FBgn0031962	0.02297	0	Inf	0.0963193
CG31935	FBgn0051935	0.00236	0	Inf	0.0963193
Gp150	FBgn0013272	0.00205	0	Inf	0.0963193
Hf	FBgn0014000	0.01009	0	Inf	0.0963193
t	FBgn0086367	0.00558	0	Inf	0.0963193
RpL3	FBgn0020910	0.6739	0.52387	1.2863781	0.0965316
RpL37A	FBgn0028696	0.89101	0.6487	1.3735263	0.0965906
Cda4	FBgn0052499	0	0.0051	-Inf	0.0968071
CG6697	FBgn0027526	0	0.00774	-Inf	0.0968071

CG7967	FBgn0035251	0	0.01567	-Inf	0.0968071
Eps-15	FBgn0035060	0	0.00201	-Inf	0.0968071
kuk	FBgn0038476	0	0.00434	-Inf	0.0968071
mRpL4	FBgn0001995	0	0.00837	-Inf	0.0968071
yellow-c	FBgn0041713	0	0.01998	-Inf	0.0968443
CG3835	FBgn0023507	0.01015	0.02387	-2.3507187	0.0971162
CG9485	FBgn0034618	0.00363	0.00039	9.2847834	0.0973638
CG17173	FBgn0036447	0.00635	0.01565	-2.4654576	0.0981094
Vha68-2	FBgn0020367	0.49185	0.56443	-1.1475556	0.0983508
Tm2	FBgn0004117	0.86	0.45936	1.872175	0.0984457
Dsp1	FBgn0011764	0.00635	0.01926	-3.0311194	0.0985838
CG3884	FBgn0033786	0.02215	0.00211	10.491578	0.0987245
Dref	FBgn0015664	0.01139	0.00346	3.2937513	0.0988434
CG1319	FBgn0035529	0.03054	0.06116	-2.0028528	0.0994752
U2af38	FBgn0017457	0.02538	0.055	-2.1669865	0.0995232
l(2)s5379	FBgn0010704	0.01431	0.04093	-2.8606455	0.0998077
CG18594	FBgn0038973	0.03776	0.0035	10.775578	0.1000441
Stim	FBgn0045073	0.00689	0.01548	-2.247071	0.1003446
Gip	FBgn0011770	0.05463	0.10929	-2.0005353	0.1004123
PPP4R2r	FBgn0030208	0.00364	0.01044	-2.8685178	0.1013147
PGRP-SA	FBgn0030310	0.00346	0.03928	-11.358501	0.1013542
CG41128	FBgn0069923	0	0.05703	-Inf	0.1016278
CG13364	FBgn0026879	0.04735	0.19531	-4.1252071	0.1017092
CG8665	FBgn0032945	0.03175	0.00269	11.818855	0.1030768
Prosbeta3	FBgn0026380	0.27615	0.21199	1.3026932	0.1033478
CG6900	FBgn0030958	0.01932	0.09747	-5.0441715	0.1036435
CG9140	FBgn0031771	0.04053	0.055	-1.3569371	0.1037062
shg	FBgn0003391	0	0.00285	-Inf	0.1037494
Ahcy89E	FBgn0015011	0.00291	0.00669	-2.2997399	0.1039355
DppIII	FBgn0037580	0.13744	0.20695	-1.5057031	0.1043478
betaCop	FBgn0008635	0.23726	0.18574	1.2773783	0.1049282
CG6812	FBgn0036843	0.00215	0.02895	-13.485645	0.1052386
Psa	FBgn0261243	0.03431	0.01422	2.4127836	0.1053267
RpS28b	FBgn0030136	0.56189	0.7976	-1.4194985	0.1055004
Ef1alpha48D	FBgn0000556	2.42256	3.32502	-1.3725249	0.1055453
CG1837	FBgn0030329	0.1118	0.07845	1.4252054	0.1058153
CG9021	FBgn0031747	0	0.01166	-Inf	0.1062323
RnrL	FBgn0011703	0	0.00454	-Inf	0.1062323
CG9466	FBgn0032068	0.00403	0.00146	2.7640068	0.1065429
CG4300	FBgn0036272	0.03074	0.02011	1.5286605	0.1067564
Mlp84B	FBgn0014863	0.09851	0.05451	1.8072358	0.1068793
CG3505	FBgn0038250	0.0641	0.0228	2.81181	0.1068826

CG5191	FBgn0038803	0.00266	0.01872	-7.0394215	0.1074826
spt4	FBgn0028683	0	0.03198	-Inf	0.1076267
DhpD	FBgn0261436	0.01565	0.00542	2.8870909	0.1076512
skpA	FBgn0025637	0.05298	0.03294	1.6085588	0.1076944
flr	FBgn0260049	0.13094	0.11468	1.1417825	0.1078484
Tm1	FBgn0003721	0.34757	0.25385	1.3691673	0.108189
RpL7	FBgn0005593	0.41876	0.33389	1.2541792	0.108771
CG5382	FBgn0038950	0.12648	0.07005	1.805721	0.1091969
regucalcin	FBgn0030362	1.64431	1.18129	1.3919659	0.1092619
scf	FBgn0025682	0.04374	0.02229	1.9626595	0.1096944
beta-Spec	FBgn0250788	0.0455	0.03288	1.3837208	0.1097806
CG6673	FBgn0035906	0	0.03048	-Inf	0.1100796
Arpc3A	FBgn0038369	0	0.01959	-Inf	0.1102312
CG9572	FBgn0031089	0	0.00844	-Inf	0.1102312
woc	FBgn0010328	0	0.0022	-Inf	0.1102312
CG6178	FBgn0039156	0.01134	0	Inf	0.1106039
CG7320	FBgn0036782	0.00536	0	Inf	0.1106039
CG7048	FBgn0038976	0.01687	0.04894	-2.9000091	0.1108797
CG6230	FBgn0027582	0.00206	0	Inf	0.1115932
CG2736	FBgn0035090	0.02815	0.00732	3.8462905	0.1118589
Elongin-C	FBgn0023211	0.0544	0.08766	-1.6114065	0.1118689
CG5703	FBgn0030853	0.02794	0.05333	-1.9086517	0.1119645
CG3415	FBgn0030731	0.14661	0.11532	1.2713981	0.1129843
RFeSP	FBgn0021906	0.01186	0.03565	-3.0060454	0.1132794
Drp1	FBgn0026479	0.01893	0.03007	-1.5880901	0.1135151
Cyp9b2	FBgn0015039	0.01754	0.00244	7.181798	0.11379
CG17754	FBgn0030114	0.00596	0	Inf	0.1151088
CG8765	FBgn0036900	0.00362	0	Inf	0.1151088
vig	FBgn0024183	0.01385	0.02095	-1.5122945	0.1158489
mit(1)15	FBgn0004643	0.01506	0.0034	4.4249784	0.1167316
Sgt	FBgn0032640	0.07622	0.13937	-1.8285539	0.1169549
sds22	FBgn0028992	0.02306	0.01388	1.661754	0.1170958
RpS10b	FBgn0031035	0.75979	1.05349	-1.3865554	0.1178105
CG31012	FBgn0027598	0.00242	0.00699	-2.8894873	0.1185449
Aats-his	FBgn0027087	0.01231	0.02427	-1.9721152	0.118813
mmy	FBgn0259749	0.00665	0.01649	-2.4795877	0.1194784
CG1753	FBgn0031148	0.00134	0.00826	-6.1448777	0.1199184
vir-1	FBgn0043841	0.09611	0.0483	1.9896809	0.1201304
CG1236	FBgn0037370	0.23326	0.16064	1.4521115	0.121187
Rho1	FBgn0014020	0.33322	0.26884	1.2394627	0.1214576
sec23	FBgn0037357	0.28441	0.34022	-1.196245	0.1216973
CG14977	FBgn0035469	0.02525	0.01017	2.4824391	0.1232795

Pka-R2	FBgn0022382	0.03088	0.0223	1.3845933	0.1235025
CG18858	FBgn0042175	0.03426	0.01856	1.8459234	0.1244773
Cyp4d1	FBgn0005670	0.00777	0.00118	6.5921205	0.124971
Nplp2	FBgn0040813	0.65787	0.96351	-1.4645997	0.1261055
CG7694	FBgn0038627	0	0.03246	-Inf	0.1262556
CG9132	FBgn0030791	0.01163	0.04358	-3.7463131	0.1264915
Pep	FBgn0004401	0.03299	0.07166	-2.1723461	0.1274623
CG1924	FBgn0030377	0.02047	0.01107	1.8485557	0.1280357
ERp60	FBgn0033663	1.04522	0.94894	1.1014604	0.1287319
colt	FBgn0019830	0.00531	0.01333	-2.5092796	0.1287962
CG5045	FBgn0032229	0.00854	0.02338	-2.7394102	0.1289328
RpL9	FBgn0015756	0.5369	0.38112	1.4087429	0.1291481
CG5384	FBgn0032216	0.11728	0.14632	-1.2476284	0.1291584
HBS1	FBgn0042712	0	0.00491	-Inf	0.1299421
pUf68	FBgn0028577	0	0.00517	-Inf	0.1299421
Trax	FBgn0038327	0	0.01276	-Inf	0.1299421
smid	FBgn0016983	0.00191	0.00797	-4.1683594	0.1300598
CHORD	FBgn0029503	0.00404	0.01744	-4.3150298	0.1300648
CG2970	FBgn0034936	0.00441	0.01109	-2.5172047	0.1304077
alpha-Est2	FBgn0015570	0.01963	0.0022	8.9106355	0.130706
AGO2	FBgn0087035	0.00425	0.01846	-4.3404745	0.1309096
CG10635	FBgn0035603	0.01017	0.02822	-2.7735286	0.1319731
Sc2	FBgn0035471	0.01585	0.00395	4.0168943	0.1341078
CG14812	FBgn0026090	0.02888	0	Inf	0.1342175
CG3590	FBgn0038467	0.03166	0.02084	1.5195132	0.1344542
CG31048	FBgn0051048	0.0017	0	Inf	0.1347083
alpha-Est7	FBgn0015575	0.06045	0.0222	2.7229041	0.1357372
CG3394	FBgn0034999	0.03225	0.01398	2.3063821	0.1361456
eIF5B	FBgn0026259	0.01756	0.0272	-1.5490246	0.1363145
pic	FBgn0260962	0.01557	0.00788	1.9757093	0.1364164
CG11255	FBgn0036337	0.06462	0.04391	1.4716517	0.1368518
mub	FBgn0014362	0.00793	0.0192	-2.4193379	0.1368907
ade2	FBgn0000052	0.01013	0.00274	3.6940206	0.1369258
Cdlc2	FBgn0026141	0.54344	0.37743	1.4398677	0.1373885
levy	FBgn0034877	0.04712	0.1263	-2.6803774	0.1378665
Adk1	FBgn0022709	0.01665	0	Inf	0.1383511
RpL13A	FBgn0037351	0.15314	0.10709	1.4300172	0.1384771
CG12262	FBgn0035811	0.16762	0.13432	1.2478853	0.1387115
cl	FBgn0000318	0.33745	0.40352	-1.1958091	0.13893
CG9590	FBgn0038360	0.03117	0.01096	2.8432315	0.1393724
CG8207	FBgn0034035	0.04407	0.06303	-1.4304513	0.1394278
yuri	FBgn0045842	0.03071	0.00107	28.681421	0.1396624

CG6638	FBgn0035911	0.02137	0.00733	2.9131229	0.1397252
Ald	FBgn0000064	1.47381	1.28783	1.1444065	0.1398144
CG2200	FBgn0030447	0.0602	0.10902	-1.8108606	0.1400058
CG32473	FBgn0052473	0.00643	0.00259	2.4871053	0.1400937
CG11309	FBgn0037070	0.01611	0.00354	4.5513824	0.1401794
Cp190	FBgn0000283	0.00765	0.00523	1.4634915	0.1405023
RpL27	FBgn0039359	0.56395	0.44666	1.2625817	0.1407072
Nurf-38	FBgn0016687	0.28717	0.41188	-1.4342835	0.1409176
spz	FBgn0003495	0.00224	0.01372	-6.1393933	0.1413409
Rbp1	FBgn0260944	0.03702	0.06249	-1.6877108	0.1422087
CG3699	FBgn0040349	0.03094	0.01066	2.9029385	0.1423714
CG6664	FBgn0036685	0.00157	0.00753	-4.7936039	0.1429579
TRAM	FBgn0040340	0.02294	0.03664	-1.5974243	0.1430146
TfIIS	FBgn0010422	0	0.01375	-Inf	0.1440392
Peritrophin-15a	FBgn0040959	0.04481	0.00885	5.0658273	0.1443609
CG2021	FBgn0035271	0.06379	0.04099	1.5561694	0.144922
vls	FBgn0003978	0.00191	0.009	-4.7052674	0.1451241
CG33491	FBgn0053491	0.00575	0.02687	-4.6685572	0.1455973
CG33498	FBgn0053498	0.0058	0.02709	-4.6685572	0.1455973
Karybeta3	FBgn0087013	0.119	0.08832	1.3473476	0.1463735
comt	FBgn0000346	0.00716	0.00246	2.9042544	0.1470927
pix	FBgn0086706	0.06902	0.11524	-1.669552	0.1474371
CG12224	FBgn0037974	0.02518	0.00411	6.1293106	0.1476773
Smg5	FBgn0019890	0	0.00471	-Inf	0.1480244
Cka	FBgn0044323	0.00289	0.00814	-2.8203086	0.148605
P58IPK	FBgn0037718	0.06539	0.08066	-1.2333996	0.1491737
CG4115	FBgn0038017	0.02129	0.04577	-2.1503889	0.1494565
Prat2	FBgn0041194	0.00692	0.00128	5.3853258	0.1494941
CG11242	FBgn0034451	0.00518	0.01738	-3.3542741	0.1498712
CG17598	FBgn0031194	0.00216	0.00948	-4.3971796	0.1501804
CG1440	FBgn0030038	0.094	0.06326	1.4859489	0.1506402
CG6891	FBgn0030955	0.13718	0.19038	-1.3877622	0.1508686
RpS23	FBgn0033912	1.73588	1.31439	1.3206743	0.1512507
CG7860	FBgn0030653	0.14857	0.09122	1.6286912	0.1523554
CG3376	FBgn0034997	0.00459	0.00087	5.2728063	0.1525966
Muc11A	FBgn0052656	0.00339	0.00064	5.2728063	0.1525966
Reps	FBgn0032341	0	0.00632	-Inf	0.1526292
Trl	FBgn0013263	0.00125	0.00783	-6.2388103	0.1527552
Sgs1	FBgn0003372	0.00401	0.00143	2.8124537	0.1533883
RpS10a	FBgn0027494	0.1062	0.13808	-1.300238	0.1534618
CG3909	FBgn0027524	0.00856	0.02157	-2.5179388	0.1537094
fl(2)d	FBgn0000662	0	0.00572	-Inf	0.1542084

SP1070	FBgn0031879	0	0.00091	-Inf	0.1542084
Su(var)2-10	FBgn0003612	0	0.00556	-Inf	0.1542084
CG6707	FBgn0036058	0.0331	0.01478	2.2397868	0.1549961
gammaSnap	FBgn0028552	0.00762	0.02656	-3.4859924	0.155032
Paf-AHalpha	FBgn0025809	0.01896	0.06518	-3.4378127	0.1555983
Got2	FBgn0001125	0.23562	0.28642	-1.21556	0.1556121
Act42A	FBgn0000043	2.56736	2.77543	-1.0810434	0.1557835
CG9769	FBgn0037270	0.19299	0.13449	1.4349095	0.1560546
serpin-1	FBgn0011710	0.02068	0.03694	-1.786654	0.1575065
CG9547	FBgn0031824	0.00696	0.01951	-2.8038379	0.1575209
eIF-4B	FBgn0020660	0.08137	0.13208	-1.6231873	0.1577533
CG13492	FBgn0034662	0.00238	0.00042	5.7269752	0.1579255
Lcp65Ab1	FBgn0020644	0.07493	0.01386	5.4049703	0.1582651
CG8149	FBgn0037700	0	0.01008	-Inf	0.1588012
Fpps	FBgn0025373	0	0.00817	-Inf	0.1588012
Rme-8	FBgn0015477	0	0.00291	-Inf	0.1588012
ubl	FBgn0022224	0	0.04253	-Inf	0.1588012
CG2846	FBgn0014930	0.00935	0.0253	-2.704911	0.1592181
CaBP1	FBgn0025678	0.18921	0.27756	-1.4669235	0.1594312
br	FBgn0000210	0.00848	0.01325	-1.5621551	0.1594792
CG10399	FBgn0031877	0.00226	0.01202	-5.3262081	0.1597454
CG4752	FBgn0034733	0.00602	0.00095	6.3177654	0.1598728
CG9099	FBgn0030802	0.02643	0.05439	-2.0582513	0.1603749
Uba2	FBgn0029113	0.01379	0.01933	-1.4023257	0.1612777
CG4586	FBgn0029924	0.00534	0	Inf	0.1617957
CSN5	FBgn0027053	0.01802	0.01006	1.7905428	0.1618227
CG9673	FBgn0030775	0.01934	0.00231	8.357062	0.1622638
Past1	FBgn0016693	0.21194	0.26663	-1.2580555	0.1637634
l(2)k09913	FBgn0021979	0.02095	0.00979	2.140181	0.164949
SelD	FBgn0261270	0.10714	0.137	-1.2786334	0.1653117
CG31698	FBgn0051698	0.2079	0.40861	-1.965361	0.1654838
CG7739	FBgn0036509	0.0048	0.00101	4.7387791	0.1664039
Spase12	FBgn0040623	0.0982	0.05458	1.7991801	0.1666947
CG17333	FBgn0030239	0.05379	0.10273	-1.9098966	0.1670625
ctp	FBgn0011760	0.5753	0.3982	1.4447523	0.1676143
Dbp80	FBgn0024804	0.02276	0.00981	2.3204559	0.1678776
CG10664	FBgn0032833	0.02451	0.01009	2.4300202	0.1680694
CG7322	FBgn0030968	0.09848	0.17043	-1.730539	0.1688225
Dip-C	FBgn0000455	0.02005	0.01421	1.4112841	0.1692882
CG10802	FBgn0029664	0.00161	0.00984	-6.1107279	0.1698191
RpL19	FBgn0002607	0.39427	0.52886	-1.3413809	0.1706256
CG6767	FBgn0036030	0.10071	0.05815	1.7317884	0.1707729

Act79B	FBgn0000045	1.76648	1.48123	1.1925753	0.1714584
CG7946	FBgn0039743	0.00832	0.00264	3.1480631	0.1718752
mod	FBgn0002780	0.09706	0.1254	-1.2920101	0.1722335
Cog7	FBgn0051040	0.01486	0.00583	2.5486945	0.1741378
inx3	FBgn0028373	0.00178	0.00777	-4.3718338	0.1752095
CG8891	FBgn0031663	0.02791	0.04492	-1.6092939	0.1754872
Trap1	FBgn0026761	0.01406	0.02108	-1.4989771	0.1756552
Got1	FBgn0001124	0.11239	0.08686	1.2939275	0.1756877
CG13049	FBgn0036592	0.01271	0.08864	-6.9715077	0.176421
CG33322	FBgn0053322	0.0089	0	Inf	0.1770759
CG33111	FBgn0053111	0.00136	0.00598	-4.3878775	0.1771461
CG7675	FBgn0038610	0	0.01163	-Inf	0.1773405
lig	FBgn0020279	0.04159	0.0583	-1.4017247	0.1782362
CG5168	FBgn0032246	0.00976	0.02163	-2.2165303	0.1782836
CG2812	FBgn0034931	0.01009	0.03128	-3.1010438	0.1787451
CG10962	FBgn0030073	0.07723	0.01232	6.2685847	0.1789239
CG15445	FBgn0031161	0.00121	0.00534	-4.4062327	0.1791501
Gmd	FBgn0031661	0.02196	0.00468	4.6916874	0.1800735
Aly	FBgn0010774	0.00939	0.01997	-2.1277048	0.1805189
Gdi	FBgn0004868	0.38533	0.47457	-1.2316162	0.1806677
eIF-2beta	FBgn0004926	0.03022	0.04867	-1.6105147	0.1809915
CG14671	FBgn0037340	0.00447	0.01883	-4.2117112	0.1814062
CG12310	FBgn0036467	0	0.03458	-Inf	0.1818829
RpS26	FBgn0004413	0.53049	0.63871	-1.2039917	0.1822927
CG32479	FBgn0052479	0.00048	0.00203	-4.2271674	0.1833127
Cyt-b5	FBgn0033189	0.11763	0.07949	1.4798921	0.1837828
Thiolase	FBgn0025352	0.11845	0.16836	-1.4214267	0.1838629
Gal	FBgn0001089	0.00885	0.00396	2.232946	0.1840676
CG8613	FBgn0033924	0.00254	0.00782	-3.0749922	0.1841416
p115	FBgn0040087	0.05075	0.03483	1.4571119	0.1848331
Sdic3	FBgn0052823	0.00129	0.00677	-5.2480225	0.1861726
pnut	FBgn0013726	0.00702	0.01409	-2.0058441	0.1867316
ics	FBgn0028546	0.01903	0.01089	1.7480385	0.1867325
Bap60	FBgn0025463	0.00278	0.00675	-2.4295895	0.1869788
Acer	FBgn0016122	0.00258	0.00779	-3.0176967	0.1876508
Hel25E	FBgn0014189	0.20868	0.24206	-1.1599801	0.1877989
CG10418	FBgn0036277	0.05463	0.03452	1.5826001	0.1879001
fax	FBgn0014163	0.10927	0.08008	1.3644972	0.1889702
Mtor	FBgn0013756	0.00074	0.0039	-5.2847327	0.1899607
CG11876	FBgn0039635	0.26348	0.21028	1.2529906	0.1900034
CG2263	FBgn0030007	0.01932	0.03329	-1.7227953	0.1900286
Pros45	FBgn0020369	0.18856	0.14037	1.3432352	0.1907129

emb	FBgn0020497	0.01029	0.00655	1.5704147	0.1907351
RpL13	FBgn0011272	0.59283	0.77131	-1.3010603	0.1912655
fat-spondin	FBgn0026721	0.00505	0.01324	-2.6216114	0.1923914
Trx-2	FBgn0040070	0.05885	0.12378	-2.1033744	0.1926182
CG5290	FBgn0036772	0.0014	0.00744	-5.3007765	0.1928522
ALiX	FBgn0086346	0.02097	0.02871	-1.3689501	0.1931623
CG10166	FBgn0032799	0.12687	0.11216	1.13122	0.1940196
CG12321	FBgn0038577	0.01896	0.02909	-1.5346336	0.1946065
Ef1alpha100E	FBgn0000557	1.03861	1.49362	-1.4380842	0.1948007
Manf	FBgn0027095	0.31575	0.4482	-1.4194744	0.1949572
Aats-arg	FBgn0027093	0.03186	0.05126	-1.6091102	0.1954818
flw	FBgn0000711	0.01522	0.00437	3.482491	0.1959921
Srp54k	FBgn0010747	0.03175	0.05172	-1.6291456	0.1963431
yki	FBgn0034970	0.01258	0.03021	-2.4025629	0.1965358
RpL31	FBgn0025286	0.40809	0.3273	1.2468475	0.1969786
CG6045	FBgn0038349	0.00344	0.0072	-2.0925062	0.1971936
CG1532	FBgn0031143	0.05499	0.09516	-1.7306265	0.1971967
kst	FBgn0004167	0.00477	0.00721	-1.5128337	0.1994242
CG11089	FBgn0039241	0.3751	0.25931	1.4465475	0.2001877
CG17838	FBgn0038826	0.05099	0.03142	1.6226341	0.2002014
eIF2B-delta	FBgn0034858	0.01023	0.01568	-1.5332434	0.2006034
CG32528	FBgn0052528	0.01818	0.00725	2.5066584	0.201755
Pxn	FBgn0011828	0.00415	0.0012	3.4511862	0.2018438
smp-30	FBgn0038257	0.031	0.01294	2.3959408	0.2019724
CG2887	FBgn0030207	0.00624	0.01312	-2.103726	0.2026036
CG5028	FBgn0039358	0.05539	0.07028	-1.2687803	0.20278
CG4095	FBgn0029890	0.00791	0.00243	3.2612633	0.2027825
alpha-Cat	FBgn0010215	0	0.00136	-Inf	0.2031419
betaggt-I	FBgn0015000	0	0.00315	-Inf	0.2031419
cals	FBgn0039928	0	0.00127	-Inf	0.2031419
cg	FBgn0000289	0	0.00245	-Inf	0.2031419
CG10555	FBgn0030034	0	0.00134	-Inf	0.2031419
CG11779	FBgn0038683	0	0.00271	-Inf	0.2031419
CG12567	FBgn0039958	0	0.0073	-Inf	0.2031419
CG1622	FBgn0030468	0	0.00313	-Inf	0.2031419
CG17386	FBgn0033936	0	0.00144	-Inf	0.2031419
CG33470	FBgn0053470	0	0.00929	-Inf	0.2031419
CG3446	FBgn0029868	0	0.00808	-Inf	0.2031419
CG4159	FBgn0038811	0	0.00304	-Inf	0.2031419
CG4844	FBgn0061354	0	0.00438	-Inf	0.2031419
CG6129	FBgn0039152	0	0.00101	-Inf	0.2031419
CG6418	FBgn0036104	0	0.00157	-Inf	0.2031419

CG7265	FBgn0038272	0	0.00265	-Inf	0.2031419
CG9578	FBgn0031094	0	0.00458	-Inf	0.2031419
CG9733	FBgn0039759	0	0.00596	-Inf	0.2031419
Cpr78E	FBgn0037114	0	0.00909	-Inf	0.2031419
drpr	FBgn0027594	0	0.00141	-Inf	0.2031419
eIF2B-alpha	FBgn0039726	0	0.01245	-Inf	0.2031419
fh	FBgn0030092	0	0.00655	-Inf	0.2031419
gek	FBgn0023081	0	0.00077	-Inf	0.2031419
icln	FBgn0029079	0	0.01158	-Inf	0.2031419
Ilp6	FBgn0044047	0	0.01163	-Inf	0.2031419
mats	FBgn0038965	0	0.00568	-Inf	0.2031419
Mcm6	FBgn0025815	0	0.00305	-Inf	0.2031419
mip130	FBgn0023509	0	0.00126	-Inf	0.2031419
Mocs2	FBgn0039280	0	0.00339	-Inf	0.2031419
Pdp	FBgn0029958	0	0.00262	-Inf	0.2031419
Rpp20	FBgn0066304	0	0.00745	-Inf	0.2031419
SPE	FBgn0039102	0	0.00311	-Inf	0.2031419
Ubp64E	FBgn0016756	0	0.0016	-Inf	0.2031419
wuho	FBgn0029857	0	0.00294	-Inf	0.2031419
Aos1	FBgn0029512	0.02207	0.05283	-2.3937695	0.2031454
CG12237	FBgn0031048	0	0.00399	-Inf	0.2031531
CG3566	FBgn0029854	0	0.01043	-Inf	0.2031531
CG6856	FBgn0036819	0	0.00424	-Inf	0.2031531
CG8444	FBgn0037671	0	0.00381	-Inf	0.2031531
ncm	FBgn0086707	0	0.00121	-Inf	0.2031531
Nopp140	FBgn0037137	0	0.00178	-Inf	0.2031531
pch2	FBgn0051453	0	0.0029	-Inf	0.2031531
row	FBgn0033998	0	0.00208	-Inf	0.2031531
Tap42	FBgn0051852	0	0.00321	-Inf	0.2031531
CG10005	FBgn0037972	0	0.00533	-Inf	0.2032571
CG13472	FBgn0036450	0	0.00147	-Inf	0.2032571
CG32214	FBgn0052214	0	0.00874	-Inf	0.2032571
CG3604	FBgn0031562	0	0.00933	-Inf	0.2032571
CG6194	FBgn0038325	0	0.00189	-Inf	0.2032571
CG8243	FBgn0033349	0	0.00238	-Inf	0.2032571
Cht3	FBgn0250907	0	0.00269	-Inf	0.2032571
Cip4	FBgn0035533	0	0.00195	-Inf	0.2032571
hyx	FBgn0037657	0	0.00229	-Inf	0.2032571
Mkk4	FBgn0024326	0	0.00291	-Inf	0.2032571
mRpL18	FBgn0026741	0	0.00662	-Inf	0.2032571
mus301	FBgn0002899	0	0.00117	-Inf	0.2032571
obst-B	FBgn0027600	0	0.00366	-Inf	0.2032571

Pak3	FBgn0044826	0	0.00304	-Inf	0.2032571
pen	FBgn0015527	0	0.00167	-Inf	0.2032571
pum	FBgn0003165	0	0.0008	-Inf	0.2032571
RfC3	FBgn0032244	0	0.00371	-Inf	0.2032571
Rpb7	FBgn0051155	0	0.00712	-Inf	0.2032571
SoxN	FBgn0029123	0	0.00216	-Inf	0.2032571
tacc	FBgn0026620	0	0.00104	-Inf	0.2032571
l(2)tid	FBgn0002174	0	0.00711	-Inf	0.2033499
CG12024	FBgn0035283	0.00325	0.01795	-5.5222494	0.2053426
CG4673	FBgn0039348	0.01407	0.02173	-1.5441232	0.2072272
Prx2540-1	FBgn0033520	0.12404	0.19557	-1.5766826	0.2072519
DNaseII	FBgn0000477	0.02268	0.0398	-1.7552223	0.2078038
SrpRbeta	FBgn0011509	0.08896	0.06047	1.4710427	0.2083199
Dph5	FBgn0024558	0.01009	0.02851	-2.8259542	0.2086838
Rpd3	FBgn0015805	0.00721	0.01225	-1.6983521	0.2087349
fws	FBgn0024689	0.0059	0.00164	3.5948093	0.2090683
CG13674	FBgn0035858	0	0.01052	-Inf	0.2093775
CG31357	FBgn0051357	0	0.00366	-Inf	0.2093775
CG6454	FBgn0039187	0	0.00093	-Inf	0.2093775
CG8578	FBgn0030699	0	0.00364	-Inf	0.2093775
mRpL3	FBgn0030686	0	0.00398	-Inf	0.2093775
CG32335	FBgn0063667	0.01159	0.00574	2.0188755	0.2101736
bchs	FBgn0043362	0	0.00041	-Inf	0.2102617
CG11257	FBgn0034442	0	0.00267	-Inf	0.2102617
CG11882	FBgn0039642	0	0.00544	-Inf	0.2102617
CG12063	FBgn0039851	0	0.00185	-Inf	0.2102617
CG14434	FBgn0029915	0	0.00765	-Inf	0.2102617
CG5919	FBgn0038876	0	0.00559	-Inf	0.2102617
dre4	FBgn0002183	0	0.00132	-Inf	0.2102617
hk	FBgn0001202	0	0.00211	-Inf	0.2102617
psidin	FBgn0243511	0	0.00151	-Inf	0.2102617
Taf6	FBgn0010417	0	0.00236	-Inf	0.2102617
nrv1	FBgn0015776	0.02053	0	Inf	0.2111146
RpL23A	FBgn0026372	0.51395	0.45455	1.1306952	0.2113027
CG17109	FBgn0039051	0	0.00354	-Inf	0.2113612
CG30349	FBgn0050349	0	0.00229	-Inf	0.2113612
CG4702	FBgn0037992	0	0.00496	-Inf	0.2113612
CG7580	FBgn0036728	0	0.04779	-Inf	0.2113612
JhI-26	FBgn0028424	0	0.00323	-Inf	0.2113612
PpV	FBgn0003139	0	0.00468	-Inf	0.2113612
swm	FBgn0002044	0	0.00133	-Inf	0.2113612
Zw	FBgn0004057	0.02033	0.00894	2.2746882	0.2116597

CG15828	FBgn0032136	0.00095	0.00204	-2.1327173	0.211848
membrin	FBgn0260856	0.02378	0.05125	-2.1554719	0.2121793
Arc42	FBgn0038742	0.01101	0.02897	-2.6297546	0.2126612
CG31919	FBgn0031674	0.02737	0.01638	1.6704836	0.2137493
CG3605	FBgn0031493	0.00097	0.00359	-3.6866084	0.2141896
CG3301	FBgn0038878	0.04646	0.07632	-1.6426454	0.2146961
CG2199	FBgn0035213	0	0.00625	-Inf	0.2150107
I-2	FBgn0028429	0.01136	0.02496	-2.1977796	0.2151616
Prx2540-2	FBgn0033518	0.12404	0.18997	-1.531539	0.2156791
Cat	FBgn0000261	0.41989	0.36854	1.139353	0.2161867
AttA	FBgn0012042	0	0.01359	-Inf	0.2165564
AttB	FBgn0041581	0	0.01397	-Inf	0.2165564
CG30022	FBgn0050022	0	0.01113	-Inf	0.2167586
su(Hw)	FBgn0003567	0	0.0033	-Inf	0.2167586
yellow-e	FBgn0041711	0	0.00586	-Inf	0.2167586
CG31300	FBgn0051300	0	0.00479	-Inf	0.2172609
Lectin-galC1	FBgn0016675	0	0.01105	-Inf	0.2172609
san	FBgn0024188	0	0.01099	-Inf	0.2172609
sPLA2	FBgn0033170	0	0.01087	-Inf	0.2172609
CG18815	FBgn0042138	0.08038	0.13428	-1.6705051	0.2172615
CG12338	FBgn0033543	0.0092	0.00184	4.9995638	0.2181217
aPKC	FBgn0022131	0	0.00338	-Inf	0.2187334
CG10830	FBgn0038839	0	0.00898	-Inf	0.2187334
CG9804	FBgn0037251	0	0.00875	-Inf	0.2187334
CG15784	FBgn0029766	0.00962	0.01408	-1.4632949	0.2201437
CG7207	FBgn0027569	0.00513	0.01218	-2.3746652	0.2218725
CG3652	FBgn0031600	0.01654	0.0028	5.9002833	0.2220362
bai	FBgn0045866	0.2212	0.14522	1.5231863	0.2235773
Fmr1	FBgn0028734	0.01439	0.00811	1.7758421	0.2235876
usnp	FBgn0034913	0.01996	0.03832	-1.9195874	0.2241445
CG12079	FBgn0035404	0.09272	0.11726	-1.2647398	0.224393
Ugt	FBgn0014075	0.06154	0.04988	1.2337565	0.2252633
RluA-1	FBgn0051719	0.01079	0.00302	3.5721514	0.2256568
CG6195	FBgn0038723	0.00448	0.01185	-2.6452116	0.2259889
CG31343	FBgn0051343	0.00583	0.00191	3.0515158	0.2264235
Arf102F	FBgn0013749	0.39486	0.25573	1.5440438	0.2270567
Pgd	FBgn0004654	0.214	0.2411	-1.126638	0.2271388
Aldh-III	FBgn0010548	0.04114	0.03261	1.2614932	0.2279844
ppl	FBgn0027945	0.07631	0.04608	1.6560816	0.2300361
RpS16	FBgn0034743	0.54203	0.6087	-1.1230031	0.2303721
RpS15Ab	FBgn0033555	0.19571	0.28307	-1.4464224	0.2308333
eIF-1A	FBgn0026250	0.08321	0.1285	-1.5442078	0.2312699

CG14526	FBgn0027578	0.00213	0.0093	-4.3568658	0.2316976
Rm62	FBgn0003261	0.02673	0.04774	-1.7859786	0.2320327
CG31472	FBgn0051472	0.01942	0.03728	-1.9198049	0.2321873
CG7637	FBgn0033548	0.07012	0.03832	1.8298043	0.2326948
nop5	FBgn0026196	0.01689	0.03021	-1.7892011	0.2342005
SH3PX1	FBgn0040475	0.00665	0.01237	-1.8594355	0.235388
CG6912	FBgn0038290	0.02247	0.01082	2.0771583	0.2359251
CG32631	FBgn0052631	0.00755	0.00198	3.8179835	0.2361525
Timp	FBgn0025879	0.01121	0.00294	3.8179835	0.2361525
Irc	FBgn0038465	0.00439	0.01064	-2.4269441	0.2366809
p16-ARC	FBgn0031437	0.03884	0.01486	2.6132205	0.2373069
Mtch	FBgn0027786	0.00222	0.0293	-13.188922	0.2374577
CAP	FBgn0033504	0.00133	0.00465	-3.4933337	0.2379999
CG31974	FBgn0051974	0.0017	0.00594	-3.4933337	0.2379999
CG13043	FBgn0036600	0	0.0124	-Inf	0.2389415
shi	FBgn0003392	0.00758	0.01386	-1.8282446	0.239321
Unr	FBgn0035895	0.00218	0.00058	3.7314305	0.2396737
Obp83g	FBgn0046875	0	0.0125	-Inf	0.2406943
Pgam5	FBgn0023517	0	0.00621	-Inf	0.2406943
CG32972	FBgn0028905	0	0.001	-Inf	0.2409888
CG33054	FBgn0053054	0	0.01217	-Inf	0.2409888
CG3308	FBgn0038877	0	0.00584	-Inf	0.2409888
CG9372	FBgn0036891	0	0.00456	-Inf	0.2409888
CG9596	FBgn0031832	0	0.00401	-Inf	0.2409888
dalao	FBgn0030093	0	0.00497	-Inf	0.2409888
fs(1)M3	FBgn0005390	0	0.00104	-Inf	0.2409888
Mcm7	FBgn0020633	0	0.0026	-Inf	0.2409888
Mur89F	FBgn0038492	0	0.00088	-Inf	0.2409888
wdb	FBgn0027492	0	0.00355	-Inf	0.2409888
dco	FBgn0002413	0.00535	0.00143	3.7495075	0.2411633
AcCoAS	FBgn0012034	0.02788	0.01823	1.5289667	0.2418541
CG4065	FBgn0034982	0.00502	0.00234	2.1393874	0.2428954
Ero1L	FBgn0261274	0.02375	0.03468	-1.4600706	0.2435981
CG2070	FBgn0033203	0	0.00576	-Inf	0.2445683
Nipped-A	FBgn0053554	0	0.00049	-Inf	0.2445683
Snr1	FBgn0011715	0	0.00506	-Inf	0.2445683
ImpE3	FBgn0001255	0	0.00565	-Inf	0.2448704
Tom40	FBgn0016041	0	0.00534	-Inf	0.2448704
CG3292	FBgn0034710	0.00129	0.00456	-3.5277326	0.2452538
RpL23	FBgn0010078	1.41067	1.23371	1.1434413	0.2457643
nes	FBgn0026630	0.00141	0.00412	-2.9138684	0.2458282
CG10853	FBgn0035478	0.75491	1.05977	-1.4038394	0.2459193

Aprt	FBgn0000109	0	0.01022	-Inf	0.2466934
CG6734	FBgn0032395	0	0.00095	-Inf	0.2466934
nec	FBgn0002930	0	0.00527	-Inf	0.2466934
Trxr-2	FBgn0037170	0	0.0036	-Inf	0.2466934
Vha26	FBgn0015324	0.40384	0.30226	1.3360672	0.2467036
Act5C	FBgn0000042	2.77035	3.00098	-1.0832522	0.2468159
Aats-lys	FBgn0027084	0.07626	0.10616	-1.3920504	0.2468522
CG10420	FBgn0039296	0.0034	0.01143	-3.3653871	0.2474374
CG2107	FBgn0035383	0.00105	0.00352	-3.3653871	0.2474374
CG4646	FBgn0033810	0.0217	0.00378	5.7347957	0.2480908
CG14899	FBgn0038438	0.01171	0.00708	1.653546	0.2482323
Ccp84Ad	FBgn0004780	0	0.02612	-Inf	0.248315
MBD-like	FBgn0027950	0.00207	0.006	-2.8978247	0.2483531
Upf1	FBgn0030354	0.00059	0.00172	-2.8978247	0.2483531
Rpn12	FBgn0028693	0.08532	0.10394	-1.2181771	0.2486249
CG16908	FBgn0037741	0.0033	0.00115	2.8628941	0.2493123
Lcp3	FBgn0002534	0.01452	0.09146	-6.2995474	0.2496762
Pgm	FBgn0003076	0.10243	0.08974	1.1413966	0.2506343
CG1516	FBgn0027580	0.16978	0.12502	1.3580707	0.2506783
CG14527	FBgn0039613	0.00104	0.00352	-3.3830699	0.2512012
Cht6	FBgn0030171	0.00016	0.00055	-3.3830699	0.2512012
Fas2	FBgn0000635	0.00083	0.00282	-3.3830699	0.2512012
CG10623	FBgn0032727	0.04757	0.09893	-2.0794152	0.2527127
CG13059	FBgn0036607	0	0.08296	-Inf	0.2538592
CG11857	FBgn0039303	0.10532	0.07869	1.3383284	0.2542885
CG5537	FBgn0035639	0.00279	0.00949	-3.3985261	0.2544998
PpD6	FBgn0005779	0.00217	0.00737	-3.3985261	0.2544998
epsilonCOP	FBgn0027496	0.31118	0.39388	-1.2657391	0.2547197
Ca-P60A	FBgn0004551	0.11117	0.07409	1.5006061	0.2553712
CG4914	FBgn0036436	0	0.00712	-Inf	0.2558911
CG6512	FBgn0036702	0.00105	0.00295	-2.8248281	0.256192
CG17024	FBgn0032437	0.00589	0.00312	1.8898396	0.2563889
CG2807	FBgn0031266	0.00216	0.00046	4.6830449	0.256685
Rpt3R	FBgn0037742	0.01448	0.02942	-2.0316128	0.2567159
CG4802	FBgn0034215	0.0495	0.03843	1.2883244	0.2578361
CG2025	FBgn0030344	0.00714	0.00463	1.5423725	0.2578681
Nlp	FBgn0016685	0.1641	0.21659	-1.3198637	0.2582925
CG17514	FBgn0039959	0.04761	0.01164	4.0912259	0.2590043
CG15522	FBgn0039723	0.00421	0.01182	-2.8071452	0.2593347
mge	FBgn0035473	0.00597	0.01677	-2.8071452	0.2593347
CSN7	FBgn0028836	0.01039	0.00226	4.5990539	0.2600456
sm	FBgn0003435	0.02292	0.04198	-1.8315483	0.2601817

mor	FBgn0002783	0.00686	0.00328	2.087565	0.2609777
CG6783	FBgn0037913	0.62444	0.52886	1.1807289	0.2613481
scu	FBgn0021765	0.70486	0.56381	1.2501647	0.2614165
CG7920	FBgn0039737	0.02239	0.04729	-2.1124406	0.2619713
CG14722	FBgn0037943	0.00146	0.00409	-2.7916891	0.2619961
RpL8	FBgn0024939	0.95572	0.84187	1.1352336	0.2640523
Roe1	FBgn0014877	0.01014	0.02876	-2.8365436	0.2643205
Eb1	FBgn0027066	0.09404	0.12579	-1.3376642	0.2644476
CG15118	FBgn0034418	0.00817	0.002	4.0922547	0.2646074
CG2004	FBgn0030060	0.04654	0.02659	1.7505345	0.2657701
CG5793	FBgn0038858	0.01033	0.02255	-2.1831237	0.2690452
P5cr	FBgn0015781	0.00691	0.01508	-2.1831237	0.2690452
CG6259	FBgn0036740	0.04246	0.07435	-1.7510358	0.2694073
brm	FBgn0000212	0	0.00138	-Inf	0.2698628
CG11474	FBgn0034688	0.01277	0.00612	2.084556	0.2699886
NHP2	FBgn0029148	0.03332	0.02049	1.6258523	0.2705039
CG17271	FBgn0038829	0.31	0.25291	1.2257427	0.2708148
Hop	FBgn0024352	0.09066	0.12848	-1.4172109	0.2712544
Vps26	FBgn0014411	0.00628	0.01246	-1.9825782	0.2724706
LysX	FBgn0004431	0.02115	0.04583	-2.1670158	0.2733069
CG1091	FBgn0037470	0.00422	0.0012	3.5319843	0.2735219
CG32437	FBgn0052437	0.00137	0.00407	-2.9798339	0.2737583
CG11999	FBgn0037312	0.13017	0.18784	-1.4430356	0.2752382
CG10535	FBgn0037926	0.00058	0.00153	-2.6331888	0.2753952
CG13131	FBgn0032175	0.00053	0.0014	-2.6331888	0.2753952
CG15343	FBgn0030029	0.0033	0.00868	-2.6331888	0.2753952
CG2950	FBgn0031637	0.00108	0.00283	-2.6331888	0.2753952
Ssb-c31a	FBgn0015299	0.00638	0.01681	-2.6331888	0.2753952
CG7182	FBgn0035878	0.00826	0.01725	-2.0875779	0.275396
if	FBgn0001250	0.00283	0.00412	-1.455676	0.2759881
LanB1	FBgn0002527	0.01266	0.01697	-1.3407412	0.277085
dro6	FBgn0052268	0.00975	0.1956	-20.059657	0.2774074
RpL17	FBgn0029897	0.69409	0.77647	-1.1186792	0.2779885
Pcd	FBgn0024841	0.03272	0.01932	1.6932249	0.2783734
bur	FBgn0000239	0.02582	0.01943	1.3289523	0.2786016
CG3226	FBgn0029882	0.02805	0.04899	-1.7464771	0.2787392
CG2145	FBgn0030251	0.03197	0.04662	-1.4582672	0.2790931
CG8993	FBgn0035334	0.06383	0.0895	-1.4021213	0.2793795
CG15404	FBgn0031512	0.22565	0.13265	1.7011268	0.2794732
CG32536	FBgn0052536	0.00974	0.00282	3.458188	0.2801062
CG9062	FBgn0033607	0	0.00365	-Inf	0.2813932
Pdi	FBgn0014002	2.57123	2.84305	-1.1057131	0.2816481

GstD3	FBgn0010039	0.08958	0.16636	-1.8570741	0.282228
Myo61F	FBgn0010246	0.00209	0.0006	3.5014645	0.283293
CG13994	FBgn0031772	0	0.0152	-Inf	0.2836564
Osi14	FBgn0040279	0	0.00925	-Inf	0.2836564
Eig71Ek	FBgn0014851	0.72434	0.65223	1.1105559	0.2850596
sun	FBgn0014391	0.27035	0.35219	-1.3027015	0.2853869
18w	FBgn0004364	0.00051	0	Inf	0.2855909
Aats-leu	FBgn0027085	0.00084	0	Inf	0.2855909
Acox57D-p	FBgn0034628	0.00108	0	Inf	0.2855909
Acp62F	FBgn0020509	0.0061	0	Inf	0.2855909
aralar1	FBgn0028646	0.00105	0	Inf	0.2855909
Ark	FBgn0024252	0.00075	0	Inf	0.2855909
asf1	FBgn0029094	0.00322	0	Inf	0.2855909
Atg2	FBgn0044452	0.00037	0	Inf	0.2855909
Atg9	FBgn0034110	0.00193	0	Inf	0.2855909
bgm	FBgn0027348	0.00135	0	Inf	0.2855909
CaMKI	FBgn0016126	0.02024	0	Inf	0.2855909
Cbp53E	FBgn0004580	0.00226	0	Inf	0.2855909
CecA2	FBgn0000277	0.02229	0	Inf	0.2855909
CecC	FBgn0000279	0.02229	0	Inf	0.2855909
CG10069	FBgn0034611	0.00868	0	Inf	0.2855909
CG10188	FBgn0032796	0.00074	0	Inf	0.2855909
CG10353	FBgn0030349	0.00086	0	Inf	0.2855909
CG10413	FBgn0032689	0.00191	0	Inf	0.2855909
CG10463	FBgn0032819	0.00121	0	Inf	0.2855909
CG10621	FBgn0032726	0.00224	0	Inf	0.2855909
CG10710	FBgn0036377	0.00099	0	Inf	0.2855909
CG10747	FBgn0032845	0.00274	0	Inf	0.2855909
CG10943	FBgn0036320	0.00583	0	Inf	0.2855909
CG10960	FBgn0036316	0.00309	0	Inf	0.2855909
CG11384	FBgn0040363	0.00305	0	Inf	0.2855909
CG11459	FBgn0037396	0.00217	0	Inf	0.2855909
CG12056	FBgn0030099	0.00245	0	Inf	0.2855909
CG12130	FBgn0033466	0.00269	0	Inf	0.2855909
CG12241	FBgn0038304	0.00112	0	Inf	0.2855909
CG12288	FBgn0032620	0.00168	0	Inf	0.2855909
CG12402	FBgn0038202	0.00284	0	Inf	0.2855909
CG1308	FBgn0035507	0.00041	0	Inf	0.2855909
CG13088	FBgn0032047	0.00182	0	Inf	0.2855909
CG13117	FBgn0032140	0.00638	0	Inf	0.2855909
CG13189	FBgn0033665	0.00206	0	Inf	0.2855909
CG13284	FBgn0032614	0.00224	0	Inf	0.2855909

CG13567	FBgn0034963	0.00295	0	Inf	0.2855909
CG14073	FBgn0036814	0.00086	0	Inf	0.2855909
CG14184	FBgn0036932	0.0039	0	Inf	0.2855909
CG14220	FBgn0031036	0.00274	0	Inf	0.2855909
CG1427	FBgn0037347	0.002	0	Inf	0.2855909
CG14273	FBgn0032024	0.00578	0	Inf	0.2855909
CG14285	FBgn0038674	0.00245	0	Inf	0.2855909
CG14935	FBgn0032382	0.00159	0	Inf	0.2855909
CG14946	FBgn0032405	0.00243	0	Inf	0.2855909
CG15012	FBgn0035528	0.00479	0	Inf	0.2855909
CG15168	FBgn0032732	0.00644	0	Inf	0.2855909
CG15210	FBgn0040850	0.01017	0	Inf	0.2855909
CG15309	FBgn0030183	0.00616	0	Inf	0.2855909
CG15438	FBgn0025684	0.0048	0	Inf	0.2855909
CG15630	FBgn0031627	0.00156	0	Inf	0.2855909
CG15735	FBgn0030364	0.00336	0	Inf	0.2855909
CG15829	FBgn0035743	0.00889	0	Inf	0.2855909
CG16732	FBgn0039086	0.00135	0	Inf	0.2855909
CG1681	FBgn0030484	0.00615	0	Inf	0.2855909
CG17124	FBgn0032297	0.00566	0	Inf	0.2855909
CG17129	FBgn0035151	0.00121	0	Inf	0.2855909
CG17184	FBgn0037884	0.00198	0	Inf	0.2855909
CG17186	FBgn0038741	0.00184	0	Inf	0.2855909
CG17294	FBgn0032032	0.00275	0	Inf	0.2855909
CG17565	FBgn0038424	0.00428	0	Inf	0.2855909
CG17646	FBgn0031362	0.00117	0	Inf	0.2855909
CG18765	FBgn0042110	0.00197	0	Inf	0.2855909
CG2010	FBgn0039667	0.00142	0	Inf	0.2855909
CG2082	FBgn0027608	0.00349	0	Inf	0.2855909
CG2246	FBgn0039790	0.00188	0	Inf	0.2855909
CG2277	FBgn0035204	0.00168	0	Inf	0.2855909
CG2818	FBgn0031566	0.00135	0	Inf	0.2855909
CG30035	FBgn0050035	0.00144	0	Inf	0.2855909
CG30193	FBgn0050193	0.00161	0	Inf	0.2855909
CG3040	FBgn0029925	0.00295	0	Inf	0.2855909
CG31004	FBgn0051004	0.00084	0	Inf	0.2855909
CG31076	FBgn0051076	0.0037	0	Inf	0.2855909
CG31183	FBgn0051183	0.0005	0	Inf	0.2855909
CG31551	FBgn0051551	0.00052	0	Inf	0.2855909
CG31612	FBgn0051612	0.00071	0	Inf	0.2855909
CG31636	FBgn0051636	0.00466	0	Inf	0.2855909
CG31689	FBgn0031449	0.00146	0	Inf	0.2855909

CG31729	FBgn0051729	0.00065	0	Inf	0.2855909
CG31769	FBgn0051769	0.00234	0	Inf	0.2855909
CG31778	FBgn0051778	0.0088	0	Inf	0.2855909
CG32069	FBgn0052069	0.00878	0	Inf	0.2855909
CG32195	FBgn0052195	0.00182	0	Inf	0.2855909
CG32226	FBgn0052226	0.00054	0	Inf	0.2855909
CG32352	FBgn0052352	0.00074	0	Inf	0.2855909
CG32444	FBgn0043783	0.00243	0	Inf	0.2855909
CG32633	FBgn0052633	0.0063	0	Inf	0.2855909
CG32758	FBgn0052758	0.00132	0	Inf	0.2855909
CG32795	FBgn0040384	0.00232	0	Inf	0.2855909
CG33214	FBgn0053214	0.00081	0	Inf	0.2855909
CG33285	FBgn0053285	0.0022	0	Inf	0.2855909
CG3338	FBgn0031598	0.00158	0	Inf	0.2855909
CG3353	FBgn0038869	0.00179	0	Inf	0.2855909
CG3363	FBgn0034987	0.00076	0	Inf	0.2855909
CG33651	FBgn0053651	0.00572	0	Inf	0.2855909
CG3408	FBgn0036008	0.0022	0	Inf	0.2855909
CG3573	FBgn0023508	0.00083	0	Inf	0.2855909
CG3775	FBgn0030425	0.00111	0	Inf	0.2855909
CG4041	FBgn0029736	0.00087	0	Inf	0.2855909
CG4293	FBgn0024983	0.00318	0	Inf	0.2855909
CG4570	FBgn0037844	0.00255	0	Inf	0.2855909
CG4650	FBgn0032549	0.00275	0	Inf	0.2855909
CG4669	FBgn0035598	0.00147	0	Inf	0.2855909
CG4928	FBgn0027556	0.00261	0	Inf	0.2855909
CG4972	FBgn0032217	0.00125	0	Inf	0.2855909
CG5114	FBgn0036460	0.00171	0	Inf	0.2855909
CG5161	FBgn0036573	0.00505	0	Inf	0.2855909
CG5189	FBgn0034350	0.00583	0	Inf	0.2855909
CG5322	FBgn0032253	0.00151	0	Inf	0.2855909
CG5385	FBgn0032215	0.02065	0	Inf	0.2855909
CG5594	FBgn0025698	0.00138	0	Inf	0.2855909
CG5618	FBgn0036975	0.00259	0	Inf	0.2855909
CG5641	FBgn0038046	0.00177	0	Inf	0.2855909
CG5789	FBgn0039207	0.00064	0	Inf	0.2855909
CG5946	FBgn0036211	0.00267	0	Inf	0.2855909
CG5978	FBgn0035916	0.00223	0	Inf	0.2855909
CG6199	FBgn0036147	0.00122	0	Inf	0.2855909
CG6241	FBgn0037792	0.00091	0	Inf	0.2855909
CG6903	FBgn0029737	0.00156	0	Inf	0.2855909
CG6983	FBgn0035896	0.0039	0	Inf	0.2855909

CG7024	FBgn0029722	0.00152	0	Inf	0.2855909
CG7218	FBgn0038569	0.00133	0	Inf	0.2855909
CG7272	FBgn0036501	0.00394	0	Inf	0.2855909
CG7289	FBgn0031379	0.0011	0	Inf	0.2855909
CG7328	FBgn0036942	0.00238	0	Inf	0.2855909
CG7376	FBgn0035689	0.00057	0	Inf	0.2855909
CG7447	FBgn0035539	0.00137	0	Inf	0.2855909
CG7504	FBgn0035842	0.0005	0	Inf	0.2855909
CG7627	FBgn0032026	0.00091	0	Inf	0.2855909
CG7634	FBgn0037101	0.00121	0	Inf	0.2855909
CG7813	FBgn0034133	0.00099	0	Inf	0.2855909
CG7900	FBgn0037548	0.00147	0	Inf	0.2855909
CG8129	FBgn0037684	0.00155	0	Inf	0.2855909
CG8184	FBgn0030674	0.00076	0	Inf	0.2855909
CG8234	FBgn0033644	0.00149	0	Inf	0.2855909
CG8366	FBgn0034054	0.00154	0	Inf	0.2855909
CG8475	FBgn0031995	0.00067	0	Inf	0.2855909
CG8611	FBgn0027602	0.00072	0	Inf	0.2855909
CG8745	FBgn0036381	0.00142	0	Inf	0.2855909
CG8774	FBgn0038136	0.00082	0	Inf	0.2855909
CG9133	FBgn0035198	0.00454	0	Inf	0.2855909
CG9270	FBgn0032908	0.00061	0	Inf	0.2855909
CG9346	FBgn0034572	0.00073	0	Inf	0.2855909
CG9360	FBgn0030332	0.00559	0	Inf	0.2855909
CG9389	FBgn0037064	0.00118	0	Inf	0.2855909
CG9416	FBgn0034438	0.00104	0	Inf	0.2855909
CG9486	FBgn0031791	0.00337	0	Inf	0.2855909
CG9536	FBgn0031818	0.00162	0	Inf	0.2855909
CG9706	FBgn0036662	0.00171	0	Inf	0.2855909
CG9853	FBgn0086605	0.00215	0	Inf	0.2855909
CG9917	FBgn0030740	0.00242	0	Inf	0.2855909
Cng	FBgn0014462	0.00317	0	Inf	0.2855909
crl	FBgn0015374	0.01053	0	Inf	0.2855909
croc	FBgn0014143	0.00143	0	Inf	0.2855909
cry	FBgn0025680	0.0013	0	Inf	0.2855909
CSN1b	FBgn0027057	0.00134	0	Inf	0.2855909
Cyp12c1	FBgn0036806	0.00171	0	Inf	0.2855909
cyp33	FBgn0028382	0.00468	0	Inf	0.2855909
Cyp6a21	FBgn0033981	0.00139	0	Inf	0.2855909
Cypl	FBgn0035141	0.00399	0	Inf	0.2855909
Dhc36C	FBgn0013810	0.00018	0	Inf	0.2855909
Dhc98D	FBgn0013813	0.00014	0	Inf	0.2855909

dia	FBgn0011202	0.00064	0	Inf	0.2855909
dik	FBgn0030891	0.00126	0	Inf	0.2855909
dock	FBgn0010583	0.00178	0	Inf	0.2855909
Dp	FBgn0011763	0.00202	0	Inf	0.2855909
Egfr	FBgn0003731	0.00055	0	Inf	0.2855909
Eip63E	FBgn0005640	0.00191	0	Inf	0.2855909
Eip63F-1	FBgn0004910	0.01091	0	Inf	0.2855909
Eip93F	FBgn0013948	0.00063	0	Inf	0.2855909
elav	FBgn0260400	0.00291	0	Inf	0.2855909
Elp3	FBgn0031604	0.00132	0	Inf	0.2855909
etaTry	FBgn0011554	0.00278	0	Inf	0.2855909
fat2	FBgn0036930	0.00015	0	Inf	0.2855909
fbl	FBgn0011205	0.00164	0	Inf	0.2855909
Flo-2	FBgn0024753	0.00205	0	Inf	0.2855909
fne	FBgn0086675	0.00789	0	Inf	0.2855909
fz2	FBgn0016797	0.00105	0	Inf	0.2855909
Gclm	FBgn0046114	0.00256	0	Inf	0.2855909
G-ialpha65A	FBgn0001104	0.00205	0	Inf	0.2855909
gish	FBgn0250823	0.00262	0	Inf	0.2855909
G-oalpha47A	FBgn0001122	0.00206	0	Inf	0.2855909
hang	FBgn0026575	0.00037	0	Inf	0.2855909
Hex-C	FBgn0001187	0.00521	0	Inf	0.2855909
ImpL2	FBgn0001257	0.00273	0	Inf	0.2855909
Iswi	FBgn0011604	0.00068	0	Inf	0.2855909
Jheh1	FBgn0010053	0.00288	0	Inf	0.2855909
KaiRIA	FBgn0028422	0.00099	0	Inf	0.2855909
Klp3A	FBgn0011606	0.00058	0	Inf	0.2855909
l(2)01810	FBgn0010497	0.00181	0	Inf	0.2855909
l(3)04053	FBgn0010830	0.0012	0	Inf	0.2855909
Lip4	FBgn0032264	0.00168	0	Inf	0.2855909
Lis-1	FBgn0015754	0.00171	0	Inf	0.2855909
loj	FBgn0061492	0.00296	0	Inf	0.2855909
LSm3	FBgn0051184	0.00682	0	Inf	0.2855909
Map60	FBgn0010342	0.0016	0	Inf	0.2855909
Mcr	FBgn0020240	0.00041	0	Inf	0.2855909
Mec2	FBgn0030993	0.00625	0	Inf	0.2855909
MESK2	FBgn0043070	0.00552	0	Inf	0.2855909
Mgat1	FBgn0034521	0.0016	0	Inf	0.2855909
Mkrn1	FBgn0029152	0.00189	0	Inf	0.2855909
Mmp2	FBgn0033438	0.00118	0	Inf	0.2855909
mRpL14	FBgn0040389	0.00436	0	Inf	0.2855909
mRpL19	FBgn0037608	0.00229	0	Inf	0.2855909

mRpL24	FBgn0031651	0.00295	0	Inf	0.2855909
mRpL38	FBgn0030552	0.00175	0	Inf	0.2855909
mRpS31	FBgn0036557	0.00239	0	Inf	0.2855909
Muc14A	FBgn0052580	4.3E-05	0	Inf	0.2855909
mus312	FBgn0002909	0.00086	0	Inf	0.2855909
nej	FBgn0015624	0.00023	0	Inf	0.2855909
nimC4	FBgn0260011	0.0058	0	Inf	0.2855909
Noa36	FBgn0026400	0.00223	0	Inf	0.2855909
Nup153	FBgn0061200	0.00074	0	Inf	0.2855909
Nup58	FBgn0038722	0.00133	0	Inf	0.2855909
Nup75	FBgn0034310	0.00105	0	Inf	0.2855909
nvy	FBgn0005636	0.00094	0	Inf	0.2855909
Oatp30B	FBgn0032123	0.00236	0	Inf	0.2855909
Obp99d	FBgn0039684	0.00655	0	Inf	0.2855909
osa	FBgn0003013	0.00026	0	Inf	0.2855909
Papst2	FBgn0036695	0.00368	0	Inf	0.2855909
para	FBgn0260993	0.00034	0	Inf	0.2855909
PEK	FBgn0037327	0.0006	0	Inf	0.2855909
Psf2	FBgn0031599	0.00346	0	Inf	0.2855909
Ptpa	FBgn0016698	0.00176	0	Inf	0.2855909
Pvr	FBgn0032006	0.00048	0	Inf	0.2855909
qm	FBgn0019662	0.00415	0	Inf	0.2855909
Rab-RP4	FBgn0015794	0.0074	0	Inf	0.2855909
Rala	FBgn0015286	0.00363	0	Inf	0.2855909
Rassf	FBgn0039055	0.00087	0	Inf	0.2855909
Rbp9	FBgn0010263	0.00217	0	Inf	0.2855909
Rel	FBgn0014018	0.00092	0	Inf	0.2855909
RhoGAP1A	FBgn0025836	0.00137	0	Inf	0.2855909
Rrp46	FBgn0037815	0.00301	0	Inf	0.2855909
Rtf1	FBgn0034722	0.00094	0	Inf	0.2855909
Sbf	FBgn0025802	0.00041	0	Inf	0.2855909
Scp2	FBgn0020907	0.00736	0	Inf	0.2855909
sec15	FBgn0038856	0.00095	0	Inf	0.2855909
simj	FBgn0010762	0.00077	0	Inf	0.2855909
slik	FBgn0035001	0.00152	0	Inf	0.2855909
slmb	FBgn0023423	0.00138	0	Inf	0.2855909
Smr	FBgn0024308	0.00021	0	Inf	0.2855909
snf	FBgn0003449	0.00325	0	Inf	0.2855909
SNF1A	FBgn0023169	0.00154	0	Inf	0.2855909
snRNP70K	FBgn0016978	0.00163	0	Inf	0.2855909
stan	FBgn0024836	0.00039	0	Inf	0.2855909
Syt1	FBgn0004242	0.00307	0	Inf	0.2855909

Syx18	FBgn0039212	0.00355	0	Inf	0.2855909
Taf2	FBgn0011836	0.00115	0	Inf	0.2855909
Taf4	FBgn0010280	0.00097	0	Inf	0.2855909
Tango5	FBgn0052675	0.00169	0	Inf	0.2855909
TfIIB	FBgn0004915	0.00231	0	Inf	0.2855909
tok	FBgn0004885	0.0005	0	Inf	0.2855909
TpnC4	FBgn0033027	0.00586	0	Inf	0.2855909
trio	FBgn0024277	0.00031	0	Inf	0.2855909
trn	FBgn0010452	0.00099	0	Inf	0.2855909
twe	FBgn0002673	0.00165	0	Inf	0.2855909
UbcD4	FBgn0015321	0.00353	0	Inf	0.2855909
Use1	FBgn0035965	0.00562	0	Inf	0.2855909
wdp	FBgn0034718	0.00108	0	Inf	0.2855909
wntD	FBgn0038134	0.0029	0	Inf	0.2855909
wun	FBgn0016078	0.00192	0	Inf	0.2855909
xl6	FBgn0028554	0.00272	0	Inf	0.2855909
zormin	FBgn0052311	0.00334	0	Inf	0.2855909
CkIIbeta	FBgn0000259	0.02972	0.03399	-1.1436299	0.2868585
crn	FBgn0000377	0	0.0035	-Inf	0.2878406
CG5525	FBgn0032444	0.0929	0.11557	-1.2440664	0.2885007
bif	FBgn0014133	0.00291	0.00167	1.7447067	0.2889478
Rtnl1	FBgn0053113	0.12526	0.0916	1.3674761	0.2909597
CG6766	FBgn0032398	0.01067	0.0064	1.6684377	0.2911175
kdn	FBgn0086133	0.1623	0.18435	-1.1358912	0.2911698
Ddc	FBgn0000422	0.00143	0.01441	-10.085159	0.291199
CG10225	FBgn0039110	0.00831	0.0179	-2.1530251	0.291674
Cbp20	FBgn0022943	0.00473	0.012	-2.5367458	0.2918323
CG1737	FBgn0030293	0.00077	0.00196	-2.5367458	0.2918323
CG5548	FBgn0030605	0.00623	0.0158	-2.5367458	0.2918323
RpL18A	FBgn0010409	0.27787	0.34303	-1.2344658	0.2924587
Hsp26	FBgn0001225	0.08629	0.12171	-1.410433	0.2931758
Gclc	FBgn0040319	0.00196	0.00598	-3.0553639	0.2933241
CG15881	FBgn0036909	0.01032	0.03154	-3.0552394	0.2933624
smt3	FBgn0026170	0.25433	0.21197	1.1998406	0.2942844
His1:CG33807	FBgn0053807	0.13047	0.09219	1.4151829	0.2944013
His1:CG33861	FBgn0053861	0.13047	0.09219	1.4151829	0.2944013
His1:CG33864	FBgn0053864	0.13047	0.09219	1.4151829	0.2944013
Faf	FBgn0025608	0.0078	0.00175	4.4445858	0.296492
CG1240	FBgn0035370	0.02415	0.04378	-1.8132917	0.2968471
opa1-like	FBgn0261276	0.00328	0.00132	2.4781437	0.2968928
Aats-ile	FBgn0027086	0.02922	0.03919	-1.3410942	0.2969905
Ef1beta	FBgn0028737	0.74808	0.86505	-1.1563717	0.2976698

Usp7	FBgn0030366	0.00711	0.0113	-1.589679	0.2982191
CG7280	FBgn0030966	0.00822	0.00359	2.287751	0.2993658
SdhA	FBgn0261439	0.05478	0.07024	-1.2821908	0.2996294
Tim8	FBgn0027359	0.14319	0.07926	1.8065786	0.3002434
CG31294	FBgn0051294	0.06406	0.11039	-1.7232094	0.3005279
Nat1	FBgn0031020	0.00583	0.00946	-1.622442	0.3015153
l(2)09851	FBgn0022288	0.0077	0.01571	-2.0403764	0.3016986
Tudor-SN	FBgn0035121	0.44226	0.52448	-1.1858884	0.3025281
CG12400	FBgn0031505	0.01402	0.03338	-2.3811651	0.3031582
Gapdh2	FBgn0001092	1.60103	1.78258	-1.1133909	0.3034262
chic	FBgn0000308	0.66129	0.7596	-1.1486673	0.3040285
Mms19	FBgn0037301	0.00544	0.00343	1.5852943	0.3043376
RhoGDI	FBgn0036921	0.12838	0.15323	-1.1935334	0.3044533
CG1598	FBgn0033191	0.01695	0.00734	2.3105849	0.3055704
CG2852	FBgn0034753	0.87044	0.77295	1.1261311	0.3063289
Sop2	FBgn0001961	0.02791	0.03596	-1.2885851	0.3076863
atl	FBgn0039213	0.04707	0.03562	1.3217053	0.30843
blw	FBgn0011211	0.48992	0.58367	-1.1913624	0.3111744
HdacX	FBgn0051119	0.02617	0.03251	-1.2422258	0.3118498
SRPK	FBgn0026370	0.00375	0.0016	2.3443756	0.3119127
Rac1	FBgn0010333	0.03258	0.02048	1.5911648	0.3128242
Mlc-c	FBgn0004687	0.80395	0.87946	-1.0939337	0.3134994
bel	FBgn0000171	0.08258	0.09654	-1.1689852	0.3161552
Pp1-13C	FBgn0003132	0.03825	0.02314	1.6531633	0.316162
CG1316	FBgn0035526	0.00382	0.01049	-2.7476673	0.3162432
SmD3	FBgn0023167	0.02601	0.01371	1.8974339	0.3168804
tud	FBgn0003891	0.00029	0.00294	-10.13598	0.3169464
pont	FBgn0040078	0.01606	0.00905	1.7736845	0.3171303
Sgs7	FBgn0003377	6.58235	5.14599	1.2791219	0.3174674
CG14103	FBgn0036908	0.01193	0.00401	2.9727869	0.3180587
Cyt-b5-r	FBgn0000406	0.00823	0.00277	2.9727869	0.3180587
Rlb1	FBgn0014022	0.00196	0.00541	-2.7602204	0.3188151
Est-6	FBgn0000592	0	0.00573	-Inf	0.3188663
CG5103	FBgn0036784	0.00338	0.00722	-2.1357341	0.3191973
capt	FBgn0261458	0.26378	0.217	1.2155692	0.3197013
CG2915	FBgn0033241	0.07507	0.10298	-1.3717221	0.3198234
l(1)G0320	FBgn0028327	0.11743	0.0922	1.2737064	0.3200439
eIF-3p66	FBgn0040227	0.15454	0.18639	-1.2061004	0.3207608
Prx5	FBgn0038570	0.25156	0.2696	-1.0717003	0.3238667
alphaTub85E	FBgn0003886	0.62549	0.5936	1.0537309	0.3251564
mts	FBgn0004177	0.11647	0.08025	1.4514047	0.3255619
CG7945	FBgn0036505	0.00577	0.01247	-2.1620181	0.3284335

sgg	FBgn0003371	0.00273	0.00657	-2.4060267	0.3300552
CG10990	FBgn0030520	0.04007	0.02462	1.6272109	0.331853
CG9527	FBgn0031813	0.00335	0.00116	2.8935106	0.3322931
MED4	FBgn0035754	0.00913	0.00315	2.8935106	0.3322931
nonA	FBgn0004227	0.00873	0.00532	1.6428154	0.3325388
CG5976	FBgn0036999	0.02272	0.00858	2.6488832	0.3330088
CG8331	FBgn0033906	0.05092	0.0324	1.5716105	0.3337714
Cas	FBgn0022213	0.00731	0.01604	-2.1948291	0.3350255
CG2016	FBgn0250839	0.01431	0.02471	-1.7262034	0.3363683
Sclp	FBgn0030357	0.06541	0.03535	1.8506782	0.3388449
Rbcn-3A	FBgn0023458	0.0002	0.00091	-4.4245878	0.3390402
CG7843	FBgn0033062	0.00074	0.00395	-5.3030879	0.3392469
CG6852	FBgn0036820	0.14443	0.11179	1.29202	0.3401007
EndoGI	FBgn0028515	0.15411	0.20157	-1.3079756	0.3412368
Fatp	FBgn0021953	0	0.00616	-Inf	0.3418425
Ykt6	FBgn0260858	0.01902	0.00935	2.0353506	0.3426872
CG6724	FBgn0032298	0.00889	0.00443	2.0066492	0.342983
l(3)01239	FBgn0010741	0.02983	0.0487	-1.6324607	0.3436038
CG15032	FBgn0030626	0.00253	0.01033	-4.0753595	0.3460048
CG9667	FBgn0037550	0.00258	0.01052	-4.0753595	0.3460048
CG5446	FBgn0032429	0.0195	0.04255	-2.1816366	0.3463836
Updo	FBgn0033428	0.04942	0.0808	-1.6348099	0.3465767
Gfat2	FBgn0039580	0.0138	0.02223	-1.6106682	0.3492291
ND42	FBgn0019957	0.03307	0.04843	-1.464202	0.3492887
CG17734	FBgn0037890	0.00944	0.02167	-2.2942735	0.3497602
GstD9	FBgn0038020	0.50394	0.43292	1.1640472	0.350703
CG32441	FBgn0052441	0.00653	0.00243	2.6926629	0.3509702
CG6910	FBgn0036262	0.00577	0.00214	2.6926629	0.3509702
l(1)G0289	FBgn0028331	0.0026	0.00097	2.6926629	0.3509702
mtm	FBgn0025742	0.00263	0.00098	2.6926629	0.3509702
CG14207	FBgn0031037	0.43423	0.3754	1.1567229	0.3514019
Ranbp9	FBgn0037894	0.00581	0.0038	1.5292324	0.3518846
AP-1gamma	FBgn0030089	0.01269	0.00752	1.6878011	0.3521085
Art1	FBgn0037834	0.01328	0.00659	2.0166084	0.3526531
CG17119	FBgn0039045	0.00226	0.00512	-2.2673586	0.357355
RpL40	FBgn0003941	0.51509	0.39856	1.2923797	0.3575188
Ubi-p5E	FBgn0086558	0.12347	0.09553	1.2923797	0.3575188
Ubi-p63E	FBgn0003943	0.06179	0.04781	1.2923797	0.3575188
CG16936	FBgn0027590	0.27574	0.29842	-1.0822361	0.3576725
RpL21	FBgn0032987	0.82168	0.91465	-1.113142	0.3578281
Uba1	FBgn0023143	0.14077	0.16051	-1.1402621	0.3581158
sop	FBgn0004867	0.5038	0.56299	-1.1174852	0.3582922

RanGap	FBgn0003346	0.00753	0.00552	1.3638226	0.3588189
RpS18	FBgn0010411	0.61177	0.677	-1.1066321	0.3593257
RpL11	FBgn0013325	0.36398	0.45445	-1.2485501	0.3602561
Abi	FBgn0020510	0.00338	0.00128	2.6484629	0.3603654
CG9498	FBgn0031801	0.00383	0.00145	2.6364031	0.3613838
jdp	FBgn0027654	0.00834	0.00316	2.6364031	0.3613838
Pp4-19C	FBgn0023177	0.0053	0.00201	2.6364031	0.3613838
CAH1	FBgn0027844	0.01112	0.00461	2.4128348	0.3615185
CG8199	FBgn0037709	0.01061	0.00741	1.4304333	0.3616247
Ahcy13	FBgn0014455	0.17469	0.20447	-1.1704392	0.3628814
CG6950	FBgn0037955	0.02736	0.01869	1.4634177	0.3638716
Hsp67Ba	FBgn0001227	0.00947	0.00141	6.7073294	0.3653529
CG4593	FBgn0029929	0.03142	0.05106	-1.6250964	0.3660185
ldlCp	FBgn0026634	0.01454	0.00953	1.5256245	0.366389
CG6133	FBgn0026079	0.004	0.00824	-2.05992	0.3677777
Tpi	FBgn0086355	0.41813	0.45785	-1.0949908	0.3694828
CG2918	FBgn0023529	0.20603	0.22252	-1.0800072	0.3697719
CG7375	FBgn0035853	0.01178	0.02716	-2.3050259	0.3698087
RpL27A	FBgn0010410	0.7606	0.90808	-1.1938882	0.3701505
CG5840	FBgn0038516	0.00596	0.0023	2.5891189	0.370542
yata	FBgn0260990	0.00247	0.00449	-1.8144959	0.3708556
CG2177	FBgn0039902	0.00796	0.00307	2.5931266	0.3709802
CG1104	FBgn0037467	0.08026	0.09781	-1.2186118	0.3719226
CG15717	FBgn0030451	0.10173	0.08066	1.2611907	0.3727364
CG15293	FBgn0028526	0.01507	0.008	1.8854355	0.3739661
exba	FBgn0250753	0.0363	0.04989	-1.3742803	0.3752301
Sucb	FBgn0029118	0.04031	0.06403	-1.588709	0.3756541
Rack1	FBgn0020618	1.37107	1.5653	-1.1416637	0.376061
eIF-5A	FBgn0034967	0.85641	0.76707	1.1164641	0.3781068
Crc	FBgn0005585	1.26807	1.22293	1.0369171	0.3793544
CG14476	FBgn0027588	0.19205	0.15857	1.211117	0.3793709
betaTub56D	FBgn0003887	1.76729	1.69693	1.0414614	0.3799282
Art8	FBgn0032329	0.00469	0.00184	2.5466186	0.380309
CG10703	FBgn0037881	0.0037	0.00145	2.5466186	0.380309
CG7215	FBgn0038571	0.02891	0.05801	-2.0063742	0.3819526
CG12203	FBgn0031021	0.05963	0.04936	1.2079111	0.3837079
Sec16	FBgn0052654	0.0166	0.01233	1.3467731	0.3838181
Rbcn-3B	FBgn0023510	0.00427	0.00293	1.4562114	0.3839454
CG3529	FBgn0035995	0.04749	0.06667	-1.4037366	0.3846759
lark	FBgn0011640	0.01681	0.01043	1.611271	0.3851844
yps	FBgn0022959	0.02535	0.0326	-1.2861343	0.3861957
His1:CG33801	FBgn0053801	0.12488	0.09219	1.3545598	0.3863359

RpL32	FBgn0002626	0.3801	0.46066	-1.2119497	0.3868721
Grasp65	FBgn0036919	0.15666	0.14828	1.0565207	0.3871388
GstD7	FBgn0010043	0.00964	0.02355	-2.4426326	0.3872548
CanA-14F	FBgn0030758	0.01719	0.02623	-1.5257637	0.3882155
Pp2B-14D	FBgn0011826	0.01743	0.0266	-1.5257637	0.3882155
Aats-val	FBgn0027079	0.0286	0.04222	-1.476163	0.3882204
BM-40-SPARC	FBgn0026562	0.0071	0.00268	2.6536324	0.3896639
Idgf3	FBgn0020414	0.08344	0.10302	-1.234722	0.3912066
CG3714	FBgn0031589	0.00384	0.00589	-1.5314303	0.3915901
stck	FBgn0020249	0.00829	0.01304	-1.5724867	0.3927885
Pglym87	FBgn0011270	0.06507	0.04775	1.3628417	0.3944282
CG4199	FBgn0025628	0.00386	0.006	-1.555349	0.3944388
CG14894	FBgn0038428	0.00949	0.01486	-1.5650221	0.3945267
CG1749	FBgn0030305	0.12035	0.17058	-1.4173242	0.3970715
Sod	FBgn0003462	0.529	0.61581	-1.1640928	0.3997491
14-3-3epsilon	FBgn0020238	0.46021	0.41262	1.1153312	0.4001512
Pros35	FBgn0250843	0.31642	0.34405	-1.0873352	0.400267
CG1309	FBgn0035519	0.00268	0.00588	-2.1939388	0.4003678
krz	FBgn0040206	0.00603	0.0026	2.3225089	0.4011357
eEF1delta	FBgn0032198	0.49266	0.5939	-1.2055016	0.4016826
CG7349	FBgn0030975	0.0111	0.01642	-1.4790026	0.4024133
blue	FBgn0041161	0.00263	0.00448	-1.7026695	0.4039632
Pcmt	FBgn0086768	0.00397	0.00818	-2.0602983	0.405097
RpL29	FBgn0016726	0.20415	0.26649	-1.3053613	0.4061423
Cpr64Ad	FBgn0035513	0.04644	0.07569	-1.629668	0.4073144
CG5389	FBgn0036568	0.20614	0.16741	1.2313093	0.4091572
Gos28	FBgn0044871	0.01222	0.00537	2.2774498	0.4096537
CG5001	FBgn0031322	0.01378	0.00783	1.7591449	0.4103596
Gapdh1	FBgn0001091	1.37278	1.22347	1.122034	0.4115119
CG3902	FBgn0036824	0.24975	0.28821	-1.1539663	0.4121436
CG1486	FBgn0031174	0.09116	0.10922	-1.1981866	0.4121524
CG5126	FBgn0031320	0.00351	0.00859	-2.4440616	0.4121856
CG30152	FBgn0034543	0.00334	0.01222	-3.6556961	0.4122875
CG3961	FBgn0036821	0.01022	0.00245	4.1791906	0.413082
CG7816	FBgn0039714	0.00791	0.00174	4.5532154	0.4138664
PDCD-5	FBgn0036580	0.02111	0.00464	4.5532154	0.4138664
CG9922	FBgn0038196	0.04751	0.03112	1.5267793	0.4155447
CG7770	FBgn0036918	0.01145	0.00483	2.3693896	0.4157019
Ufd1-like	FBgn0036136	0.00453	0.00191	2.3693896	0.4157019
CG1458	FBgn0062442	0.03774	0.06144	-1.6278317	0.4157426
Sodh-2	FBgn0022359	0.20756	0.17962	1.1555443	0.4188634
shep	FBgn0052423	0.03088	0.02123	1.4546673	0.4192095

RpS13	FBgn0010265	0.4661	0.40419	1.153156	0.4198924
sqh	FBgn0003514	0.45563	0.52765	-1.1580696	0.4199599
Sdic4	FBgn0053499	0.00656	0.01133	-1.7256989	0.4207679
sw	FBgn0003654	0.00538	0.00928	-1.7256989	0.4207679
CG30185	FBgn0050185	0.04959	0.03946	1.256795	0.4211982
Hsp83	FBgn0001233	0.52073	0.54902	-1.0543204	0.4216288
Srp68	FBgn0035947	0.06955	0.09048	-1.3010085	0.4220304
fray	FBgn0023083	0.01678	0.00898	1.8688736	0.4220634
CG12547	FBgn0250830	0.00497	0.00741	-1.4906081	0.4220934
Prx5037	FBgn0038519	0.05408	0.03792	1.4260579	0.424222
RpL36	FBgn0002579	0.33302	0.27448	1.213304	0.4244213
CG11284	FBgn0030056	0.00572	0.00247	2.3198842	0.4279249
CG13506	FBgn0034723	0.00284	0.00123	2.3198842	0.4279249
CG16892	FBgn0030122	0.00307	0.00132	2.3198842	0.4279249
Edem2	FBgn0032480	0.00179	0.00077	2.3198842	0.4279249
RpII140	FBgn0003276	0.00122	0.00052	2.3198842	0.4279249
Vps20	FBgn0034744	0.01417	0.00675	2.0994771	0.4285824
CG4572	FBgn0038738	0.02927	0.02128	1.3756277	0.4289567
Nmdmc	FBgn0010222	0.00699	0.01811	-2.5912159	0.4300061
CG9186	FBgn0035206	0.03499	0.02996	1.1681437	0.430391
nimB3	FBgn0054003	0.00735	0.02041	-2.7745821	0.4308647
Coprox	FBgn0021944	0.00554	0.00948	-1.7120659	0.4322452
Snx6	FBgn0032005	0.01619	0.02413	-1.4904048	0.4355957
ab	FBgn0259750	0	0.00067	-Inf	0.4365881
Acox57D-d	FBgn0034629	0	0.00091	-Inf	0.4365881
adp	FBgn0000057	0	0.00203	-Inf	0.4365881
AIF	FBgn0031392	0	0.00082	-Inf	0.4365881
alien	FBgn0013746	0	0.00139	-Inf	0.4365881
alpha-Est4	FBgn0015572	0	0.00112	-Inf	0.4365881
ana1	FBgn0039206	0	0.00058	-Inf	0.4365881
Arf84F	FBgn0004908	0	0.00335	-Inf	0.4365881
arm	FBgn0000117	0	0.00521	-Inf	0.4365881
Arp11	FBgn0031050	0	0.00163	-Inf	0.4365881
Atg5	FBgn0029943	0	0.00224	-Inf	0.4365881
Bap170	FBgn0042085	0	0.00068	-Inf	0.4365881
BEAF-32	FBgn0015602	0	0.00223	-Inf	0.4365881
Bruce	FBgn0037808	0	0.00013	-Inf	0.4365881
cac	FBgn0005563	0	0.00033	-Inf	0.4365881
cact	FBgn0000250	0	0.00121	-Inf	0.4365881
CadN2	FBgn0032655	0	0.00028	-Inf	0.4365881
cana	FBgn0040233	0	0.00031	-Inf	0.4365881
Cap-D3	FBgn0051989	0	0.0005	-Inf	0.4365881

CBP	FBgn0026144	0	0.00272	-Inf	0.4365881
Ccp84Aa	FBgn0004783	0	0.00613	-Inf	0.4365881
Ccp84Ab	FBgn0004782	0	0.00568	-Inf	0.4365881
Cct2	FBgn0035231	0	0.00165	-Inf	0.4365881
cdi	FBgn0004876	0	0.0005	-Inf	0.4365881
Cdk5	FBgn0013762	0	0.0021	-Inf	0.4365881
CG10320	FBgn0034645	0	0.00561	-Inf	0.4365881
CG10375	FBgn0039116	0	0.00238	-Inf	0.4365881
CG10470	FBgn0032746	0	0.00348	-Inf	0.4365881
CG10585	FBgn0037044	0	0.00135	-Inf	0.4365881
CG10625	FBgn0035612	0	0.00119	-Inf	0.4365881
CG10834	FBgn0032972	0	0.00623	-Inf	0.4365881
CG10877	FBgn0038804	0	0.00285	-Inf	0.4365881
CG1092	FBgn0037228	0	0.00392	-Inf	0.4365881
CG10973	FBgn0036306	0	0.00319	-Inf	0.4365881
CG11165	FBgn0033238	0	0.00424	-Inf	0.4365881
CG11251	FBgn0036346	0	0.00179	-Inf	0.4365881
CG11266	FBgn0031883	0	0.00104	-Inf	0.4365881
CG11909	FBgn0039330	0	0.00094	-Inf	0.4365881
CG11982	FBgn0037653	0	0.00165	-Inf	0.4365881
CG12093	FBgn0035372	0	0.00192	-Inf	0.4365881
CG12301	FBgn0036514	0	0.0008	-Inf	0.4365881
CG12343	FBgn0033556	0	0.00273	-Inf	0.4365881
CG12344	FBgn0033558	0	0.00134	-Inf	0.4365881
CG12560	FBgn0031974	0	0.00234	-Inf	0.4365881
CG12582	FBgn0037215	0	0.00136	-Inf	0.4365881
CG12734	FBgn0035411	0	0.00045	-Inf	0.4365881
CG12848	FBgn0040666	0	0.00678	-Inf	0.4365881
CG12868	FBgn0033945	0	0.00515	-Inf	0.4365881
CG12975	FBgn0037061	0	0.00497	-Inf	0.4365881
CG13041	FBgn0036605	0	0.00506	-Inf	0.4365881
CG13060	FBgn0036606	0	0.00479	-Inf	0.4365881
CG13090	FBgn0032054	0	0.00136	-Inf	0.4365881
CG13096	FBgn0032050	0	0.00092	-Inf	0.4365881
CG13097	FBgn0032051	0	0.00095	-Inf	0.4365881
CG13163	FBgn0033712	0	0.00467	-Inf	0.4365881
CG1347	FBgn0037363	0	0.00048	-Inf	0.4365881
CG13827	FBgn0039068	0	0.00259	-Inf	0.4365881
CG13842	FBgn0039009	0	0.00234	-Inf	0.4365881
CG13850	FBgn0038961	0	0.00109	-Inf	0.4365881
CG14137	FBgn0036178	0	0.00599	-Inf	0.4365881
CG14205	FBgn0031034	0	0.00173	-Inf	0.4365881

CG14614	FBgn0031186	0	0.00183	-Inf	0.4365881
CG14641	FBgn0037220	0	0.0015	-Inf	0.4365881
CG14696	FBgn0037853	0	0.00137	-Inf	0.4365881
CG14712	FBgn0037924	0	0.00049	-Inf	0.4365881
CG14854	FBgn0038238	0	0.00335	-Inf	0.4365881
CG14971	FBgn0035449	0	0.00174	-Inf	0.4365881
CG14984	FBgn0035480	0	0.00472	-Inf	0.4365881
CG15080	FBgn0034391	0	0.00054	-Inf	0.4365881
CG1544	FBgn0039827	0	0.00106	-Inf	0.4365881
CG15727	FBgn0030410	0	0.0021	-Inf	0.4365881
CG1582	FBgn0030246	0	0.00049	-Inf	0.4365881
CG15890	FBgn0030576	0	0.00105	-Inf	0.4365881
CG15891	FBgn0029860	0	0.00414	-Inf	0.4365881
CG1597	FBgn0030289	0	0.00068	-Inf	0.4365881
CG1665	FBgn0033451	0	0.00185	-Inf	0.4365881
CG1677	FBgn0029941	0	0.00063	-Inf	0.4365881
CG16941	FBgn0038464	0	0.00077	-Inf	0.4365881
CG16986	FBgn0035356	0	0.00422	-Inf	0.4365881
CG17032	FBgn0036547	0	0.00198	-Inf	0.4365881
CG17134	FBgn0032304	0	0.00161	-Inf	0.4365881
CG17153	FBgn0036248	0	0.00171	-Inf	0.4365881
CG17249	FBgn0035249	0	0.00131	-Inf	0.4365881
CG17278	FBgn0046763	0	0.00785	-Inf	0.4365881
CG17364	FBgn0036391	0	0.00075	-Inf	0.4365881
CG17544	FBgn0032775	0	0.00089	-Inf	0.4365881
CG17633	FBgn0032144	0	0.0014	-Inf	0.4365881
CG17840	FBgn0031611	0	0.0007	-Inf	0.4365881
CG18259	FBgn0030956	0	0.0013	-Inf	0.4365881
CG1832	FBgn0032979	0	0.00266	-Inf	0.4365881
CG18347	FBgn0260743	0	0.00192	-Inf	0.4365881
CG18490	FBgn0036149	0	0.00049	-Inf	0.4365881
CG18616	FBgn0260444	0	0.00099	-Inf	0.4365881
CG1951	FBgn0039623	0	0.00074	-Inf	0.4365881
CG2051	FBgn0037376	0	0.00357	-Inf	0.4365881
CG2091	FBgn0037372	0	0.00161	-Inf	0.4365881
CG2794	FBgn0031265	0	0.00086	-Inf	0.4365881
CG2816	FBgn0031564	0	0.00894	-Inf	0.4365881
CG2837	FBgn0031646	0	0.00242	-Inf	0.4365881
CG3004	FBgn0030142	0	0.00197	-Inf	0.4365881
CG30360	FBgn0050360	0	0.00112	-Inf	0.4365881
CG30372	FBgn0050372	0	0.00111	-Inf	0.4365881
CG3056	FBgn0024987	0	0.00142	-Inf	0.4365881

CG31063	FBgn0051063	0	0.00761	-Inf	0.4365881
CG31120	FBgn0051120	0	0.00115	-Inf	0.4365881
CG31550	FBgn0051550	0	0.00201	-Inf	0.4365881
CG31637	FBgn0051637	0	0.00127	-Inf	0.4365881
CG31704	FBgn0051704	0	0.00924	-Inf	0.4365881
CG31716	FBgn0051716	0	0.00059	-Inf	0.4365881
CG31821	FBgn0051821	0	0.00145	-Inf	0.4365881
CG32176	FBgn0052176	0	0.00212	-Inf	0.4365881
CG32196	FBgn0052196	0	0.00308	-Inf	0.4365881
CG32264	FBgn0052264	0	0.00062	-Inf	0.4365881
CG32355	FBgn0052355	0	0.00091	-Inf	0.4365881
CG32372	FBgn0052372	0	0.001	-Inf	0.4365881
CG32425	FBgn0052425	0	0.00131	-Inf	0.4365881
CG3246	FBgn0031538	0	0.00141	-Inf	0.4365881
CG32573	FBgn0052573	0	0.0016	-Inf	0.4365881
CG32649	FBgn0052649	0	0.00095	-Inf	0.4365881
CG32702	FBgn0052702	0	0.00105	-Inf	0.4365881
CG33096	FBgn0053096	0	0.00257	-Inf	0.4365881
CG33097	FBgn0053097	0	0.0009	-Inf	0.4365881
CG33099	FBgn0053099	0	0.00246	-Inf	0.4365881
CG33331	FBgn0067628	0	0.0018	-Inf	0.4365881
CG3349	FBgn0036459	0	0.00081	-Inf	0.4365881
CG33496	FBgn0053496	0	0.00667	-Inf	0.4365881
CG3362	FBgn0034988	0	0.00193	-Inf	0.4365881
CG33791	FBgn0035240	0	0.00049	-Inf	0.4365881
CG3402	FBgn0035148	0	0.00501	-Inf	0.4365881
CG34022	FBgn0054022	0	0.00391	-Inf	0.4365881
CG3500	FBgn0034849	0	0.00317	-Inf	0.4365881
CG3534	FBgn0038463	0	0.00147	-Inf	0.4365881
CG3588	FBgn0025643	0	0.00111	-Inf	0.4365881
CG3740	FBgn0023530	0	0.00449	-Inf	0.4365881
CG3748	FBgn0032110	0	0.00149	-Inf	0.4365881
CG3781	FBgn0029853	0	0.00279	-Inf	0.4365881
CG3847	FBgn0029867	0	0.00165	-Inf	0.4365881
CG4030	FBgn0034585	0	0.00093	-Inf	0.4365881
CG4045	FBgn0025629	0	0.00236	-Inf	0.4365881
CG4098	FBgn0036648	0	0.00194	-Inf	0.4365881
CG4140	FBgn0028535	0	0.00861	-Inf	0.4365881
CG4338	FBgn0038313	0	0.0022	-Inf	0.4365881
CG4382	FBgn0032132	0	0.00106	-Inf	0.4365881
CG4452	FBgn0035981	0	0.00209	-Inf	0.4365881
CG4589	FBgn0019886	0	0.00062	-Inf	0.4365881

CG4622	FBgn0035021	0	0.00125	-Inf	0.4365881
CG4679	FBgn0033816	0	0.00095	-Inf	0.4365881
CG4980	FBgn0039558	0	0.00226	-Inf	0.4365881
CG5003	FBgn0039554	0	0.00088	-Inf	0.4365881
CG5205	FBgn0038344	0	0.00028	-Inf	0.4365881
CG5342	FBgn0037916	0	0.00077	-Inf	0.4365881
CG5412	FBgn0038806	0	0.0045	-Inf	0.4365881
CG5451	FBgn0038666	0	0.00123	-Inf	0.4365881
CG5543	FBgn0034908	0	0.00094	-Inf	0.4365881
CG5611	FBgn0039531	0	0.00189	-Inf	0.4365881
CG5613	FBgn0030839	0	0.00124	-Inf	0.4365881
CG5639	FBgn0039527	0	0.00041	-Inf	0.4365881
CG5746	FBgn0039186	0	0.00135	-Inf	0.4365881
CG5849	FBgn0038897	0	0.00064	-Inf	0.4365881
CG5953	FBgn0032587	0	0.00176	-Inf	0.4365881
CG6015	FBgn0038927	0	0.00105	-Inf	0.4365881
CG6026	FBgn0038676	0	0.00041	-Inf	0.4365881
CG6040	FBgn0038679	0	0.00034	-Inf	0.4365881
CG6153	FBgn0032445	0	0.00286	-Inf	0.4365881
CG6388	FBgn0032430	0	0.00107	-Inf	0.4365881
CG6409	FBgn0036106	0	0.00168	-Inf	0.4365881
CG6448	FBgn0032976	0	0.00035	-Inf	0.4365881
CG6607	FBgn0039204	0	0.00152	-Inf	0.4365881
CG6687	FBgn0038299	0	0.00191	-Inf	0.4365881
CG6693	FBgn0037878	0	0.00202	-Inf	0.4365881
CG6876	FBgn0036487	0	0.00162	-Inf	0.4365881
CG6938	FBgn0036235	0	0.0005	-Inf	0.4365881
CG6961	FBgn0030959	0	0.0013	-Inf	0.4365881
CG7006	FBgn0039233	0	0.00335	-Inf	0.4365881
CG7277	FBgn0031713	0	0.00129	-Inf	0.4365881
CG7299	FBgn0032282	0	0.00355	-Inf	0.4365881
CG7650	FBgn0036519	0	0.00228	-Inf	0.4365881
CG7927	FBgn0027549	0	0.00089	-Inf	0.4365881
CG7970	FBgn0035252	0	0.00969	-Inf	0.4365881
CG7993	FBgn0038585	0	0.00393	-Inf	0.4365881
CG8065	FBgn0036075	0	0.00159	-Inf	0.4365881
CG8121	FBgn0037680	0	0.00243	-Inf	0.4365881
CG8176	FBgn0037702	0	0.00067	-Inf	0.4365881
CG8239	FBgn0030683	0	0.00318	-Inf	0.4365881
CG8368	FBgn0035707	0	0.00089	-Inf	0.4365881
CG8478	FBgn0037746	0	0.00114	-Inf	0.4365881
CG8545	FBgn0033741	0	0.00465	-Inf	0.4365881

CG8628	FBgn0250836	0	0.00734	-Inf	0.4365881
CG8831	FBgn0033737	0	0.00101	-Inf	0.4365881
CG8838	FBgn0031526	0	0.00256	-Inf	0.4365881
CG8851	FBgn0031546	0	0.00094	-Inf	0.4365881
CG8885	FBgn0031656	0	0.00246	-Inf	0.4365881
CG8920	FBgn0027529	0	0.00601	-Inf	0.4365881
CG8945	FBgn0030815	0	0.00043	-Inf	0.4365881
CG8979	FBgn0033669	0	0.00233	-Inf	0.4365881
CG9173	FBgn0035218	0	0.00139	-Inf	0.4365881
CG9259	FBgn0032913	0	0.00146	-Inf	0.4365881
CG9411	FBgn0030569	0	0.00063	-Inf	0.4365881
CG9468	FBgn0032069	0	0.00184	-Inf	0.4365881
CG9586	FBgn0032101	0	0.00297	-Inf	0.4365881
CG9588	FBgn0038166	0	0.0028	-Inf	0.4365881
CG9684	FBgn0037583	0	0.00094	-Inf	0.4365881
CG9782	FBgn0030763	0	0.00273	-Inf	0.4365881
CG9932	FBgn0032469	0	0.00116	-Inf	0.4365881
CG9948	FBgn0035721	0	0.00288	-Inf	0.4365881
CHIP	FBgn0027052	0	0.00217	-Inf	0.4365881
Chmp1	FBgn0036805	0	0.00928	-Inf	0.4365881
comr	FBgn0034667	0	0.00101	-Inf	0.4365881
Cpr31A	FBgn0053302	0	0.00185	-Inf	0.4365881
Cpr60D	FBgn0050163	0	0.00649	-Inf	0.4365881
Cpr64Ab	FBgn0035511	0	0.00554	-Inf	0.4365881
Cpr65Av	FBgn0052405	0	0.00566	-Inf	0.4365881
CrebB-17A	FBgn0014467	0	0.00175	-Inf	0.4365881
Csl4	FBgn0032346	0	0.00296	-Inf	0.4365881
Cyp6d5	FBgn0038194	0	0.00121	-Inf	0.4365881
D19A	FBgn0022935	0	0.00073	-Inf	0.4365881
dally	FBgn0011577	0	0.00296	-Inf	0.4365881
dbr	FBgn0067779	0	0.00126	-Inf	0.4365881
Ddx1	FBgn0015075	0	0.00112	-Inf	0.4365881
dom	FBgn0020306	0	0.00102	-Inf	0.4365881
Drs-l	FBgn0052274	0	0.00894	-Inf	0.4365881
dyn-p25	FBgn0040228	0	0.00295	-Inf	0.4365881
e(y)2	FBgn0000618	0	0.00611	-Inf	0.4365881
E2f	FBgn0011766	0	0.00078	-Inf	0.4365881
east	FBgn0010110	0	0.00027	-Inf	0.4365881
ecd	FBgn0000543	0	0.0009	-Inf	0.4365881
ECSIT	FBgn0028436	0	0.00154	-Inf	0.4365881
EloA	FBgn0039066	0	0.00096	-Inf	0.4365881
Faa	FBgn0016013	0	0.00148	-Inf	0.4365881

gce	FBgn0030627	0	0.00091	-Inf	0.4365881
gfzf	FBgn0250732	0	0.00078	-Inf	0.4365881
Gld	FBgn0001112	0	0.00097	-Inf	0.4365881
Gld2	FBgn0038934	0	0.0006	-Inf	0.4365881
gogo	FBgn0052227	0	0.00047	-Inf	0.4365881
gp210	FBgn0033039	0	0.00043	-Inf	0.4365881
Gug	FBgn0010825	0	0.00041	-Inf	0.4365881
hay	FBgn0001179	0	0.00077	-Inf	0.4365881
Hlc	FBgn0001565	0	0.00159	-Inf	0.4365881
hop	FBgn0004864	0	0.00069	-Inf	0.4365881
HP1b	FBgn0030082	0	0.00339	-Inf	0.4365881
Hph	FBgn0086689	0	0.00126	-Inf	0.4365881
hpo	FBgn0261456	0	0.00094	-Inf	0.4365881
Hs3st-A	FBgn0053147	0	0.00135	-Inf	0.4365881
Iap2	FBgn0015247	0	0.00124	-Inf	0.4365881
IM18	FBgn0067903	0	0.01737	-Inf	0.4365881
inx2	FBgn0027108	0	0.00168	-Inf	0.4365881
ird1	FBgn0260935	0	0.00046	-Inf	0.4365881
isopeptidase-T-3	FBgn0028372	0	0.00137	-Inf	0.4365881
Jon25Bi	FBgn0020906	0	0.00299	-Inf	0.4365881
Jon99Ciii	FBgn0003357	0	0.00237	-Inf	0.4365881
ken	FBgn0011236	0	0.00103	-Inf	0.4365881
Klp61F	FBgn0004378	0	0.00059	-Inf	0.4365881
l(1)G0193	FBgn0027280	0	0.00093	-Inf	0.4365881
l(1)G0232	FBgn0028341	0	0.00124	-Inf	0.4365881
LBR	FBgn0034657	0	0.00083	-Inf	0.4365881
Lcp65Af	FBgn0020639	0	0.00628	-Inf	0.4365881
Lhr	FBgn0034217	0	0.00185	-Inf	0.4365881
lid	FBgn0031759	0	0.00034	-Inf	0.4365881
loco	FBgn0020278	0	0.00069	-Inf	0.4365881
LysS	FBgn0004430	0	0.00881	-Inf	0.4365881
Mad	FBgn0011648	0	0.00138	-Inf	0.4365881
mago	FBgn0002736	0	0.00411	-Inf	0.4365881
Marf	FBgn0029870	0	0.00075	-Inf	0.4365881
mask	FBgn0043884	0	0.0008	-Inf	0.4365881
Mat89Bb	FBgn0020407	0	0.00115	-Inf	0.4365881
Mcm2	FBgn0014861	0	0.0007	-Inf	0.4365881
MESR3	FBgn0032694	0	0.00216	-Inf	0.4365881
mia	FBgn0014342	0	0.00103	-Inf	0.4365881
mip120	FBgn0033846	0	0.00108	-Inf	0.4365881
Mnf	FBgn0036134	0	0.0009	-Inf	0.4365881

mof	FBgn0014340	0	0.00098	-Inf	0.4365881
mre11	FBgn0020270	0	0.00101	-Inf	0.4365881
MRG15	FBgn0027378	0	0.00148	-Inf	0.4365881
mRpL50	FBgn0028648	0	0.00326	-Inf	0.4365881
mRpL53	FBgn0050481	0	0.0039	-Inf	0.4365881
mRpL9	FBgn0038319	0	0.00243	-Inf	0.4365881
mRpS14	FBgn0044030	0	0.00482	-Inf	0.4365881
mRpS22	FBgn0039555	0	0.0016	-Inf	0.4365881
mRpS23	FBgn0260407	0	0.00326	-Inf	0.4365881
mthl12	FBgn0045442	0	0.00247	-Inf	0.4365881
Myo28B1	FBgn0040299	0	0.00028	-Inf	0.4365881
nAcRalpha-34E	FBgn0028875	0	0.0011	-Inf	0.4365881
NELF-B	FBgn0027553	0	0.00106	-Inf	0.4365881
Nep2	FBgn0027570	0	0.00079	-Inf	0.4365881
Nle	FBgn0021874	0	0.00128	-Inf	0.4365881
Npc2f	FBgn0039154	0	0.00479	-Inf	0.4365881
ns3	FBgn0028274	0	0.00104	-Inf	0.4365881
ns4	FBgn0032882	0	0.00107	-Inf	0.4365881
Nup107	FBgn0027868	0	0.00073	-Inf	0.4365881
obst-E	FBgn0031737	0	0.0051	-Inf	0.4365881
Ote	FBgn0003022	0	0.00145	-Inf	0.4365881
par-6	FBgn0026192	0	0.00176	-Inf	0.4365881
pasha	FBgn0039861	0	0.00096	-Inf	0.4365881
Peritrophin-15b	FBgn0040958	0	0.00663	-Inf	0.4365881
Pi3K21B	FBgn0020622	0	0.00119	-Inf	0.4365881
Pi3K92E	FBgn0015279	0	0.00075	-Inf	0.4365881
pita	FBgn0034878	0	0.00099	-Inf	0.4365881
pk	FBgn0003090	0	0.00063	-Inf	0.4365881
Pka-C3	FBgn0000489	0	0.00108	-Inf	0.4365881
Pkn	FBgn0020621	0	0.00053	-Inf	0.4365881
pod1	FBgn0029903	0	0.01841	-Inf	0.4365881
Pop2	FBgn0036239	0	0.00214	-Inf	0.4365881
Pros28.1A	FBgn0017557	0	0.00248	-Inf	0.4365881
r2d2	FBgn0031951	0	0.00202	-Inf	0.4365881
RacGAP84C	FBgn0045843	0	0.00157	-Inf	0.4365881
Rae1	FBgn0034646	0	0.00171	-Inf	0.4365881
rhi	FBgn0004400	0	0.0015	-Inf	0.4365881
roq	FBgn0036621	0	0.00075	-Inf	0.4365881
RpA-70	FBgn0010173	0	0.00312	-Inf	0.4365881
Rpb4	FBgn0053520	0	0.00543	-Inf	0.4365881
Rpb8	FBgn0037121	0	0.00414	-Inf	0.4365881
RpL37a	FBgn0030616	0	0.04375	-Inf	0.4365881

Rrp4	FBgn0034879	0	0.00207	-Inf	0.4365881
Rrp40	FBgn0260648	0	0.00266	-Inf	0.4365881
SA	FBgn0020616	0	0.00055	-Inf	0.4365881
sas	FBgn0002306	0	0.00036	-Inf	0.4365881
scny	FBgn0260936	0	0.00058	-Inf	0.4365881
Sdic1	FBgn0067861	0	0.01108	-Inf	0.4365881
sdt	FBgn0243505	0	0.00069	-Inf	0.4365881
sec3	FBgn0086475	0	0.00068	-Inf	0.4365881
Sema-1b	FBgn0016059	0	0.00106	-Inf	0.4365881
Sema-2a	FBgn0011260	0	0.00087	-Inf	0.4365881
Sgt1	FBgn0260939	0	0.00381	-Inf	0.4365881
Shab	FBgn0003383	0	0.00063	-Inf	0.4365881
shot	FBgn0013733	0	0.00108	-Inf	0.4365881
Sin3A	FBgn0022764	0	0.0003	-Inf	0.4365881
Smox	FBgn0025800	0	0.0013	-Inf	0.4365881
sol	FBgn0003464	0	0.00038	-Inf	0.4365881
SP1029	FBgn0040282	0	0.00066	-Inf	0.4365881
SP71	FBgn0029128	0	0.00086	-Inf	0.4365881
spen	FBgn0016977	0	0.00011	-Inf	0.4365881
Spn1	FBgn0028988	0	0.00162	-Inf	0.4365881
spn-F	FBgn0086362	0	0.00169	-Inf	0.4365881
Ssdp	FBgn0011481	0	0.00139	-Inf	0.4365881
Ssrp	FBgn0010278	0	0.00261	-Inf	0.4365881
Su(fu)	FBgn0005355	0	0.00132	-Inf	0.4365881
su(s)	FBgn0003575	0	0.00047	-Inf	0.4365881
Sxl	FBgn0003659	0	0.00171	-Inf	0.4365881
Syn2	FBgn0034135	0	0.0012	-Inf	0.4365881
synj	FBgn0034691	0	0.00064	-Inf	0.4365881
Taf5	FBgn0010356	0	0.00116	-Inf	0.4365881
TfIIA-L	FBgn0011289	0	0.00165	-Inf	0.4365881
TfIIFbeta	FBgn0010421	0	0.00223	-Inf	0.4365881
tho2	FBgn0031390	0	0.00086	-Inf	0.4365881
thoc7	FBgn0035110	0	0.00223	-Inf	0.4365881
Tim10	FBgn0027360	0	0.0067	-Inf	0.4365881
Tom70	FBgn0032397	0	0.00105	-Inf	0.4365881
trbd	FBgn0037734	0	0.00081	-Inf	0.4365881
Tsf2	FBgn0036299	0	0.00151	-Inf	0.4365881
TSG101	FBgn0036666	0	0.00243	-Inf	0.4365881
ttm50	FBgn0250874	0	0.00144	-Inf	0.4365881
twin	FBgn0011725	0	0.00175	-Inf	0.4365881
unc-104	FBgn0034155	0	0.00038	-Inf	0.4365881
vas	FBgn0003970	0	0.0019	-Inf	0.4365881

Vps28	FBgn0021814	0	0.00299	-Inf	0.4365881
wgn	FBgn0030941	0	0.00183	-Inf	0.4365881
XNP	FBgn0039338	0	0.00062	-Inf	0.4365881
Yp2	FBgn0005391	0	0.00137	-Inf	0.4365881
zfh2	FBgn0004607	0	0.00021	-Inf	0.4365881
CG31678	FBgn0051678	0.00055	0.00151	-2.7207524	0.4370998
CG5431	FBgn0034888	0.0218	0.00851	2.5619908	0.4377059
CG10688	FBgn0036300	0.06098	0.04523	1.3483201	0.4382117
CG15099	FBgn0034400	0.00066	0.00029	2.2782768	0.4386166
CG4091	FBgn0034894	0.00681	0.00299	2.2782768	0.4386166
Nrt	FBgn0004108	0.00169	0.00074	2.2782768	0.4386166
Ppt1	FBgn0030057	0.00456	0.002	2.2782768	0.4386166
CG6776	FBgn0035904	0.07064	0.08678	-1.2284684	0.4398782
CG6907	FBgn0031711	0.00334	0.01142	-3.4228236	0.4403694
CG3107	FBgn0033005	0.0007	0.00293	-4.1608894	0.4437909
CG10424	FBgn0036848	0.00711	0.01291	-1.8153181	0.4443362
CkIIalpha	FBgn0000258	0.14453	0.12697	1.1383594	0.4446079
CG11015	FBgn0031830	0.11875	0.13183	-1.1101362	0.4450828
CG10131	FBgn0033949	0.00796	0.00416	1.9115064	0.4459341
CG2023	FBgn0037383	0.0283	0.01716	1.6492099	0.4462909
CG3689	FBgn0035987	0.00705	0.02095	-2.9723602	0.4482892
dUTPase	FBgn0250837	0.01435	0.02825	-1.9691978	0.448489
eIF3-S9	FBgn0034237	0.13678	0.15581	-1.1390812	0.4485003
CG8965	FBgn0031745	0.00581	0.00284	2.0453421	0.4487746
Sac1	FBgn0035195	0.00881	0.00552	1.5962224	0.4492048
Stam	FBgn0027363	0.02452	0.01728	1.4189955	0.4495047
granny-smith	FBgn0040493	0.11213	0.10142	1.1055513	0.4500157
CG31694	FBgn0051694	0.03187	0.0212	1.5029451	0.45054
CG3731	FBgn0038271	0.19324	0.18126	1.0660814	0.4524134
CG12030	FBgn0035147	0.74241	0.82861	-1.1161046	0.4525064
CG14291	FBgn0038660	0.00139	0.00466	-3.3477042	0.4545255
CG1950	FBgn0030370	0.01113	0.00721	1.5435448	0.4562702
CG3560	FBgn0030733	0.16547	0.20308	-1.2273023	0.456545
dmt	FBgn0016792	0.00269	0.00144	1.8681729	0.4580205
CSN3	FBgn0027055	0.00561	0.0028	2.0056604	0.4593259
Lcp9	FBgn0025578	0.00763	0.02426	-3.1785043	0.4595533
DnaJ-1	FBgn0015657	0.01562	0.01967	-1.2594361	0.4596346
CG17556	FBgn0038462	0.07799	0.05629	1.3855313	0.4596355
CG3678	FBgn0038461	0.07799	0.05629	1.3855313	0.4596355
Rpn7	FBgn0028688	0.10309	0.08083	1.275456	0.4598627
CG13887	FBgn0035165	0.09966	0.10952	-1.0989963	0.4607896
Prosalpha5	FBgn0016697	0.26283	0.23479	1.1193987	0.4613801

CG31674	FBgn0051674	0.00497	0.01119	-2.2510547	0.463163
lqf	FBgn0028582	0.00108	0.00447	-4.1367668	0.4641431
CG3355	FBgn0031619	0.02505	0.03584	-1.4306364	0.4642909
CG32495	FBgn0052495	0.13067	0.11751	1.1119407	0.464517
CG14688	FBgn0037819	0.01065	0.00649	1.6420994	0.4646814
CG11594	FBgn0035484	0.00862	0.00562	1.5354769	0.4648673
c11.1	FBgn0040236	0.0015	0.00043	3.4877843	0.4652935
AP-50	FBgn0024832	0.02092	0.01788	1.170109	0.4687118
RpL4	FBgn0003279	0.76159	0.69706	1.0925764	0.4711677
Nacalpha	FBgn0086904	0.25036	0.21266	1.1772368	0.4715405
Elongin-B	FBgn0023212	0.12192	0.14424	-1.1830838	0.4729437
CG13630	FBgn0039219	0.00383	0.00659	-1.7230899	0.473045
CG10777	FBgn0029979	0.00151	0.00262	-1.7309621	0.4746027
Npc2a	FBgn0031381	0.22383	0.24186	-1.0805678	0.4749626
CG17493	FBgn0040010	0.00511	0.01111	-2.1767393	0.4755753
CG11009	FBgn0036318	0.018	0.02511	-1.3949658	0.4765647
Tango4	FBgn0030365	0.0259	0.03189	-1.2310941	0.4776609
RpL14	FBgn0017579	0.64809	0.72836	-1.1238585	0.4777019
CG10306	FBgn0034654	0.10451	0.08646	1.2087881	0.4777105
Tsf3	FBgn0034094	0.02059	0.03092	-1.5012162	0.4779642
CG4658	FBgn0032170	0.00133	0.00354	-2.6515439	0.4794488
mRpL44	FBgn0037330	0.0021	0.00557	-2.6515439	0.4794488
UK114	FBgn0086691	0.24668	0.20042	1.2308353	0.4800822
CG14782	FBgn0025381	0.00344	0.00918	-2.6675877	0.4806764
U2A	FBgn0033210	0.00265	0.00707	-2.6675877	0.4806764
CG31459	FBgn0051459	0.00285	0.00746	-2.6148337	0.4821057
RpL24	FBgn0032518	0.42864	0.49235	-1.1486379	0.4821775
lva	FBgn0029688	0.06015	0.07309	-1.2151381	0.4831768
CG4420	FBgn0030753	0.03908	0.03232	1.2090824	0.4834827
CG5642	FBgn0036258	0.10304	0.09737	1.0582009	0.485542
CG6073	FBgn0039417	0.0019	0.00498	-2.6171451	0.4869337
CG5871	FBgn0038870	0.00344	0.0012	2.8758027	0.4870436
Rpt4R	FBgn0036224	0.01987	0.02611	-1.3140287	0.4881205
CG8683	FBgn0031985	0.00255	0.00133	1.9116025	0.4894683
WASp	FBgn0024273	0.00903	0.00659	1.3704605	0.4900576
Rad23	FBgn0026777	0.05943	0.06925	-1.1650977	0.4907043
CG6523	FBgn0032509	0.10482	0.12907	-1.2313662	0.4911401
CG18522	FBgn0038347	0.00057	0.00146	-2.5544286	0.491482
Ssadh	FBgn0039349	0.00143	0.00366	-2.5544286	0.491482
CSN6	FBgn0028837	0.00214	0.00549	-2.5698848	0.4925437
CG7556	FBgn0030990	0.01607	0.01844	-1.1475547	0.4926347
CG1943	FBgn0037468	0.11341	0.09222	1.229798	0.4936863

CG12883	FBgn0039538	0.00894	0.01689	-1.8881624	0.493795
CG14990	FBgn0035496	0.00226	0.0057	-2.5190629	0.4944058
RpS30	FBgn0038834	0.32508	0.37652	-1.1582341	0.494917
Pglym78	FBgn0014869	0.58162	0.54872	1.0599479	0.4963848
CG9344	FBgn0034564	0.00922	0.02354	-2.5522019	0.4965991
CG15202	FBgn0030271	0.07542	0.10332	-1.3699229	0.4984808
CG2014	FBgn0039669	0.00342	0.00863	-2.5212896	0.4990997
CG31249	FBgn0051249	0.00291	0.00735	-2.5212896	0.4990997
CG9172	FBgn0030718	0.0033	0.00831	-2.5212896	0.4990997
mtSSB	FBgn0010438	0.00499	0.01258	-2.5212896	0.4990997
sec24	FBgn0033460	0.0883	0.11009	-1.2468082	0.500142
CG17065	FBgn0031099	0.00935	0.01637	-1.7499705	0.5047224
CG11811	FBgn0036099	0.00999	0.00539	1.8535036	0.5051622
Hira	FBgn0022786	0.00697	0.00466	1.4942304	0.5072602
Spase22-23	FBgn0039172	0.04984	0.0608	-1.2198944	0.5084795
Sodh-1	FBgn0024289	0.10836	0.09276	1.1682098	0.5085966
CG9906	FBgn0030755	0.02616	0.02008	1.3026759	0.5086354
Atx2	FBgn0041188	0.01002	0.01296	-1.2939747	0.5105319
Gl	FBgn0001108	0.00393	0.00614	-1.5636349	0.5118881
Hexo2	FBgn0041629	0.00289	0.00099	2.9096456	0.5119867
Pdsw	FBgn0021967	0.02945	0.04271	-1.4501275	0.5134107
CG4747	FBgn0043456	0.0816	0.10125	-1.240803	0.5154157
CG9779	FBgn0037231	0.01434	0.02216	-1.5450461	0.515439
Pgk	FBgn0250906	0.55116	0.58052	-1.0532632	0.5162778
CG5555	FBgn0038686	0.00384	0.0022	1.7473483	0.5189691
Nup133	FBgn0039004	0.00209	0.0012	1.7473483	0.5189691
ATPCL	FBgn0020236	0.18518	0.20371	-1.100098	0.5192661
CG9175	FBgn0031779	0.00485	0.00277	1.7530384	0.5227683
Prosbeta7	FBgn0250746	0.10603	0.09622	1.1020158	0.5230173
Ubqn	FBgn0031057	0.03707	0.04279	-1.1542406	0.5230374
Fmo-2	FBgn0033079	0.00379	0.0019	1.9980339	0.5236453
sub	FBgn0003545	0.00509	0.00296	1.7182909	0.5248162
CG8552	FBgn0031990	0.0258	0.03044	-1.1797929	0.525951
Prosbeta5	FBgn0029134	0.08924	0.10559	-1.1832319	0.5261883
cpb	FBgn0011570	0.03406	0.02309	1.4753738	0.5266281
CG14109	FBgn0036364	0.02922	0.01861	1.5701151	0.5281574
Trip1	FBgn0015834	0.26983	0.31784	-1.1779306	0.5295418
CG6151	FBgn0036533	0.03948	0.03278	1.2043855	0.5316557
alpha-Spec	FBgn0250789	0.09195	0.10139	-1.1027245	0.5316763
CG9391	FBgn0037063	0.02119	0.01556	1.3621529	0.5321036
Irp-1A	FBgn0024958	0.04823	0.05463	-1.1326342	0.5326633
HP1c	FBgn0039019	0.009	0.00525	1.713448	0.5327542

CG13369	FBgn0025640	0.01228	0.01553	-1.2649531	0.5340731
CG11505	FBgn0035424	0.00166	0.00085	1.9652362	0.5354233
sbr	FBgn0003321	0.00238	0.00121	1.9652362	0.5354233
serpin-2	FBgn0014029	0.01285	0.01662	-1.2934773	0.5386597
CG11444	FBgn0029715	0.02715	0.03629	-1.3362629	0.5404894
Irp-1B	FBgn0024957	0.15022	0.13634	1.1017734	0.5409845
Pen	FBgn0011823	0.0058	0.0051	1.1380962	0.5411522
LanA	FBgn0002526	0.01977	0.02333	-1.1801518	0.5414496
CG9356	FBgn0037688	0.00514	0.00831	-1.6170459	0.543266
CG30291	FBgn0050291	0.0661	0.0765	-1.1573629	0.543547
NUCB1	FBgn0052190	0.13569	0.15096	-1.1125009	0.5438638
pr	FBgn0003141	0.03491	0.04381	-1.2547807	0.5444746
CG17691	FBgn0039993	0.01294	0.00897	1.4418438	0.5458248
Srp9	FBgn0035827	0.14171	0.11746	1.2064068	0.5461544
CoVa	FBgn0019624	0.23884	0.26505	-1.1097192	0.5472567
CG11414	FBgn0035024	0.00165	0.00432	-2.6166908	0.5479805
mst	FBgn0020272	0.00367	0.00142	2.5880371	0.5481991
Cnx99A	FBgn0015622	0.08641	0.07637	1.1314492	0.5503948
RpS14b	FBgn0004404	1.45039	1.57655	-1.0869882	0.5506775
CG14096	FBgn0036871	0.00575	0.01182	-2.0537235	0.5519544
Pgant35A	FBgn0001970	0.00928	0.01201	-1.2943868	0.5529194
CG32210	FBgn0052210	0.0008	0.00142	-1.7638663	0.5533692
CG4789	FBgn0030792	0.00512	0.009	-1.7558444	0.5538521
garz	FBgn0033714	0.00193	0.0034	-1.7558444	0.5538521
GstD4	FBgn0010040	0.44517	0.48198	-1.0826712	0.5553915
CG5110	FBgn0032642	0.02265	0.00993	2.2796066	0.5553973
Idgf2	FBgn0020415	0.04059	0.04891	-1.2048214	0.5554515
CG32412	FBgn0052412	0.00206	0.00421	-2.0376797	0.5562347
eIF3-S10	FBgn0037249	0.09857	0.08608	1.1451107	0.5569037
CG6838	FBgn0037182	0.06644	0.0815	-1.2266414	0.55782
His2B:CG33910	FBgn0053910	0.55348	0.63227	-1.1423616	0.559581
Vinc	FBgn0004397	0.07885	0.08548	-1.0841517	0.5610888
CG4278	FBgn0014092	0.00788	0.00414	1.9055288	0.5619527
CG32164	FBgn0042177	0.00366	0.00631	-1.7210583	0.5623992
RpL35	FBgn0029785	0.13206	0.11333	1.1652078	0.563116
Aac11	FBgn0027885	0.0182	0.02499	-1.3728908	0.5632305
lic	FBgn0261524	0.00862	0.01358	-1.5746778	0.5636948
Fib	FBgn0003062	0.11993	0.11251	1.0659652	0.5646078
Sp7	FBgn0037515	0.02449	0.03431	-1.4009074	0.5667318
CG6841	FBgn0036828	0.00175	0.00265	-1.5162207	0.5689883
Mgstl	FBgn0025814	0.0107	0.01622	-1.5162207	0.5689883

Mmp1	FBgn0035049	0.00812	0.00578	1.4036199	0.5690844
snRNP69D	FBgn0016940	0.06514	0.08578	-1.3167602	0.5694527
nct	FBgn0039234	0.00105	0.00207	-1.9785039	0.5695497
CG30382	FBgn0050382	0.16731	0.14438	1.1588278	0.5712746
l(1)G0230	FBgn0028342	0.4675	0.43527	1.074046	0.5721511
unk	FBgn0004395	0.00243	0.00101	2.4135896	0.5722124
dj-1beta	FBgn0039802	0.04695	0.05508	-1.1731938	0.5770541
CtBP	FBgn0020496	0.03205	0.03625	-1.1309203	0.577156
CG2943	FBgn0037530	0.00861	0.00627	1.373224	0.578064
CG2233	FBgn0029990	0.35728	0.32775	1.0901145	0.5784504
endos	FBgn0061515	0.00612	0.01191	-1.9453649	0.5791314
CG17331	FBgn0032596	0.14235	0.12741	1.117218	0.5807947
CG6762	FBgn0030876	0.02441	0.02906	-1.1907041	0.5810823
Nnp-1	FBgn0022069	0.00212	0.00357	-1.6826935	0.5811617
eIF4E-4	FBgn0035709	0.0142	0.00904	1.5711468	0.5843287
CG1907	FBgn0039674	0.01017	0.01611	-1.5828787	0.5845689
Pros26.4	FBgn0015282	0.11788	0.11042	1.067555	0.5846249
Rpn11	FBgn0028694	0.17867	0.16574	1.0779975	0.5851343
CG7966	FBgn0038115	0.02578	0.03192	-1.2381093	0.5854824
His2A:CG33859	FBgn0053859	1.50839	1.38499	1.089094	0.5855355
His2A:CG33865	FBgn0053865	1.52065	1.39625	1.089094	0.5855355
sec31	FBgn0033339	0.11795	0.1065	1.1074892	0.5856087
atms	FBgn0010750	0.00261	0.00112	2.3251896	0.5858207
CG3295	FBgn0034573	0.00325	0.0014	2.3251896	0.5858207
CG5690	FBgn0035295	0.00219	0.00094	2.3207771	0.5865279
qkr58E-3	FBgn0022984	0.0046	0.00198	2.3207771	0.5865279
Rac2	FBgn0014011	0.01199	0.0172	-1.4353809	0.587454
RpL5	FBgn0064225	0.74478	0.81155	-1.0896465	0.5894981
fbp	FBgn0032820	0.21394	0.22937	-1.0721373	0.5896128
l(2)06496	FBgn0010622	0.02411	0.02028	1.1887641	0.5899489
pug	FBgn0020385	0.0511	0.04392	1.1634449	0.5904166
CG11980	FBgn0037652	0.09955	0.08817	1.1290912	0.5919607
CG14903	FBgn0038446	0.01337	0.00587	2.2766077	0.5937604
Vps45	FBgn0261049	0.00245	0.00107	2.2766077	0.5937604
CG5869	FBgn0028894	0.06904	0.09478	-1.3729027	0.5946391
CG17202	FBgn0038043	0.01581	0.01124	1.406585	0.5953716
Top1	FBgn0004924	0.00589	0.00419	1.406585	0.5953716
Zasp52	FBgn0083919	0.02561	0.02911	-1.1363507	0.5955733
CG32165	FBgn0042178	0.00366	0.00573	-1.5650791	0.5966507
CG33123	FBgn0053123	0.02676	0.03459	-1.2928172	0.5981572

CG5510	FBgn0039160	0.01731	0.02308	-1.3329643	0.5990259
His3.3B	FBgn0004828	0.22314	0.18295	1.2196984	0.5995899
Cp1	FBgn0013770	0.84004	0.78357	1.0720609	0.5998865
Pabp2	FBgn0005648	0.01341	0.00727	1.8452971	0.6001862
CG1578	FBgn0030336	0.00312	0.00139	2.2357765	0.6007031
CG30392	FBgn0050392	0.0063	0.00282	2.2357765	0.6007031
Nup160	FBgn0260937	0.001	0.00045	2.2357765	0.6007031
RpII215	FBgn0003277	0.00074	0.00033	2.2357765	0.6007031
cib	FBgn0026084	0.89651	0.99818	-1.1134116	0.602492
Dlc90F	FBgn0024432	0.02706	0.01676	1.6148306	0.6073671
Dhpr	FBgn0035964	0.23005	0.26324	-1.1442781	0.6083517
CG10221	FBgn0028475	0.0026	0.00399	-1.5321911	0.6100324
ATPsyn-d	FBgn0016120	0.42342	0.40155	1.0544456	0.6109319
Aats-glupro	FBgn0005674	0.03494	0.03863	-1.1054663	0.6214996
CG9338	FBgn0032899	0.00478	0.00847	-1.7730439	0.621954
Cul-4	FBgn0033260	0.00117	0.00207	-1.7730439	0.621954
Madm	FBgn0027497	0.0011	0.00195	-1.7730439	0.621954
nito	FBgn0027548	0.00119	0.00211	-1.7730439	0.621954
Rrp45	FBgn0030789	0.0017	0.00302	-1.7730439	0.621954
Vps36	FBgn0086785	0.00176	0.00312	-1.7730439	0.621954
ATPsyn-b	FBgn0019644	0.12652	0.13224	-1.0452092	0.6232995
Hsc70-4	FBgn0001219	1.18867	1.10709	1.0736929	0.6242975
CG11985	FBgn0040534	0.00826	0.01449	-1.7546887	0.6277608
CG17211	FBgn0032414	0.00052	0.00091	-1.7546887	0.6277608
Zn72D	FBgn0017453	0.00079	0.00139	-1.7546887	0.6277608
CG5706	FBgn0039175	0.03844	0.04286	-1.1149215	0.6281356
CG9205	FBgn0035181	0.00758	0.00433	1.7507323	0.6291569
CG17593	FBgn0031544	0.00454	0.00298	1.5232998	0.6300816
Sgs3	FBgn0003373	0.60081	0.6916	-1.1511238	0.6302957
unc-115	FBgn0260463	0.00772	0.00571	1.3519542	0.6303817
l(1)G0255	FBgn0028336	0.0466	0.0421	1.1068488	0.6307927
CG1637	FBgn0030245	0.00561	0.00729	-1.2995781	0.6309174
RpS12	FBgn0260441	1.41712	1.35295	1.0474296	0.6311726
Arc-p20	FBgn0031781	0.00418	0.00727	-1.738645	0.6328133
Aut1	FBgn0036813	0.00213	0.0037	-1.738645	0.6328133
Def	FBgn0010385	0.00763	0.01327	-1.738645	0.6328133
CG7414	FBgn0037135	0.01482	0.01806	-1.2186708	0.6329272
RpL36A	FBgn0031980	0.1168	0.10287	1.1354529	0.6331102
Pros54	FBgn0015283	0.02947	0.03672	-1.2463109	0.6341009
CG7185	FBgn0035872	0.00882	0.01166	-1.3222658	0.6345486
SelR	FBgn0037847	0.01357	0.02078	-1.5316306	0.6361264
Qm	FBgn0024733	0.61854	0.59693	1.0362012	0.6370556

chb	FBgn0021760	0.00203	0.00288	-1.42	0.6373076
CG9914	FBgn0030737	0.13374	0.11827	1.1308228	0.638086
CG15356	FBgn0031377	0.00071	0.00184	-2.5853409	0.63837
CG12433	FBgn0030811	0.00844	0.01083	-1.2831284	0.6387741
hts	FBgn0004873	0.07661	0.08383	-1.0943282	0.6424469
CG14997	FBgn0035515	0.00159	0.00272	-1.7081045	0.6428022
CG6361	FBgn0030925	0.00193	0.00329	-1.7081045	0.6428022
CG7526	FBgn0035798	0.00088	0.0015	-1.7081045	0.6428022
CG8003	FBgn0036096	0.00179	0.00306	-1.7081045	0.6428022
CG8353	FBgn0032002	0.00429	0.00732	-1.7081045	0.6428022
CG8443	FBgn0034087	0.0005	0.00086	-1.7081045	0.6428022
mRpS5	FBgn0044510	0.00179	0.00306	-1.7081045	0.6428022
Tom20	FBgn0036928	0.00426	0.00728	-1.7081045	0.6428022
lap	FBgn0086372	0.0127	0.00956	1.328314	0.6430182
Kap-alpha1	FBgn0024889	0.01077	0.00738	1.4597681	0.6442019
Ance-4	FBgn0033366	0.00231	0.00403	-1.7478407	0.6451348
CG7324	FBgn0037074	0.00124	0.00206	-1.6657492	0.6469313
Mapmodulin	FBgn0034282	0.02172	0.02833	-1.3042294	0.6470515
Hcf	FBgn0039904	0.00107	0.00166	-1.5566248	0.6477646
CG10340	FBgn0022344	0.00266	0.0045	-1.6904216	0.6488132
RhoL	FBgn0014380	0.00384	0.00648	-1.6904216	0.6488132
w-cup	FBgn0032269	0.00355	0.00601	-1.6904216	0.6488132
CG6180	FBgn0032453	0.08724	0.07559	1.1540737	0.648958
CG7789	FBgn0039698	0.02631	0.03013	-1.1452466	0.6496219
drk	FBgn0004638	0.08284	0.10214	-1.2329869	0.6499469
Gfat1	FBgn0027341	0.00408	0.00714	-1.7484041	0.6507303
tsr	FBgn0011726	1.12273	1.09458	1.0257158	0.6515729
CG30103	FBgn0050103	0.00124	0.00208	-1.6749655	0.654053
CG9248	FBgn0032923	0.00148	0.00247	-1.6749655	0.654053
GstE8	FBgn0063492	0.00328	0.0055	-1.6749655	0.654053
CG2046	FBgn0037378	0.03437	0.02806	1.2250801	0.6564951
Cpr65Ax2	FBgn0042118	0.04042	0.05608	-1.3876234	0.6573216
CG13900	FBgn0035162	0.0035	0.00251	1.3926634	0.6574607
CG9953	FBgn0035726	0.00845	0.00607	1.3926634	0.6574607
CG8209	FBgn0035830	0.09139	0.07723	1.1832918	0.6597185
CG6770	FBgn0032400	0.0407	0.06217	-1.5276197	0.6619684
CG10103	FBgn0035715	0.01076	0.01232	-1.1451763	0.6632826
Tango1	FBgn0031842	0.01009	0.01106	-1.0965352	0.6641196
CG9306	FBgn0032511	0.02592	0.03124	-1.2052493	0.6641212
CG11490	FBgn0031233	0.00098	0.00228	-2.3183594	0.6650288
Gga	FBgn0030141	0.00323	0.0047	-1.455645	0.6679202
Sh3beta	FBgn0035772	0.12395	0.1089	1.13823	0.6681163

CG4810	FBgn0037994	0.00382	0.00222	1.7254816	0.668697
CG6617	FBgn0030944	0.0126	0.01747	-1.3867721	0.6704043
CG9674	FBgn0036663	0.0065	0.00491	1.3245005	0.6704847
MESR6	FBgn0036846	0.01785	0.02134	-1.1958592	0.6719547
nrv2	FBgn0015777	0.00652	0.00381	1.7097049	0.6731154
RpL10Ab	FBgn0036213	0.51632	0.48448	1.065712	0.6734683
CG8417	FBgn0037744	0.01176	0.01295	-1.1013089	0.6741174
Aats-gln	FBgn0027090	0.0392	0.03601	1.0884585	0.6761476
CG14286	FBgn0038673	0.00715	0.00924	-1.2920339	0.6764672
CG3939	FBgn0040396	0.12447	0.13376	-1.0746342	0.6795391
amon	FBgn0023179	0.02929	0.03377	-1.152906	0.6810187
CG18547	FBgn0037973	0.01553	0.0124	1.2527915	0.6810806
CG1885	FBgn0030066	0.00901	0.00667	1.3505009	0.6837278
CG6719	FBgn0037893	0.04155	0.04769	-1.1479583	0.6841016
eff	FBgn0011217	0.10742	0.124	-1.1543574	0.6853332
CG12375	FBgn0031987	0.03195	0.02774	1.1519876	0.6857981
CSN4	FBgn0027054	0.0022	0.00351	-1.5943514	0.6866756
Pak	FBgn0014001	0.00127	0.00203	-1.5943514	0.6866756
CG9149	FBgn0035203	0.02956	0.02563	1.153419	0.6870703
CG30499	FBgn0050499	0.03655	0.02855	1.2802222	0.6874062
CG4390	FBgn0038771	0.15012	0.13741	1.0925317	0.6897719
ATPsyn-Cf6	FBgn0016119	0.17646	0.19163	-1.0859819	0.6904754
CG1983	FBgn0039751	0.00353	0.00558	-1.5799897	0.6926068
Fs(2)Ket	FBgn0000986	0.00549	0.00438	1.2529937	0.6927929
CG32068	FBgn0052068	0.05308	0.06143	-1.1573964	0.693168
l(1)G0156	FBgn0027291	0.14385	0.16068	-1.117015	0.6938366
CG1115	FBgn0037299	0.011	0.01446	-1.313686	0.6938684
GS	FBgn0030882	0.28029	0.26747	1.0479415	0.6942184
CG30115	FBgn0050115	0.00415	0.00307	1.3501001	0.694511
cpa	FBgn0034577	0.11704	0.10238	1.1431428	0.6948412
betaTub97EF	FBgn0003890	0.43481	0.42213	1.0300372	0.6949491
msk	FBgn0026252	0.04567	0.05025	-1.10016	0.6982269
Slh	FBgn0015816	0.0908	0.09972	-1.0982631	0.6987397
Ccp84Ag	FBgn0004777	0.01647	0.02303	-1.3976872	0.7008682
CG9934	FBgn0032467	0.00218	0.00382	-1.7508817	0.7017003
Srp19	FBgn0015298	0.08047	0.09249	-1.1493501	0.706323
CG6453	FBgn0032643	0.04184	0.04779	-1.1423459	0.7078566
Prosalpha7	FBgn0023175	0.15745	0.16515	-1.0488647	0.707977
FK506-bp2	FBgn0013954	0.78262	0.75711	1.0336906	0.7081215
Cortactin	FBgn0025865	0.00638	0.00888	-1.3931162	0.7112924
SsRbeta	FBgn0011016	0.3118	0.32527	-1.0432032	0.7117614
fon	FBgn0032773	0.14052	0.13246	1.0608307	0.7117834

UGP	FBgn0035978	0.23101	0.22392	1.0316931	0.7118586
ck	FBgn0000317	0.00324	0.00401	-1.2354435	0.7120239
CG4169	FBgn0250814	0.27196	0.29403	-1.0811693	0.7122543
Hsp67Bb	FBgn0001228	0.05892	0.0463	1.272671	0.7123896
CG10512	FBgn0037057	0.10261	0.08965	1.1445618	0.7128747
CG7872	FBgn0030658	0.02292	0.02643	-1.1530583	0.7156628
CG10126	FBgn0038088	0.06044	0.05235	1.1545624	0.7184038
Prx6005	FBgn0031479	0.00949	0.00556	1.7074558	0.7185823
sec13	FBgn0024509	0.22552	0.23404	-1.0377869	0.7186282
CG30069	FBgn0050069	0.0093	0.01056	-1.1348826	0.7191078
Adk3	FBgn0042094	0.02661	0.03349	-1.2582327	0.7195638
CG11378	FBgn0040364	0.01213	0.00991	1.2237477	0.7214636
l(2)gl	FBgn0002121	0.00321	0.00264	1.2159841	0.7214993
hoip	FBgn0015393	0.38027	0.35558	1.0694199	0.7238344
RpS7	FBgn0039757	1.22692	1.15054	1.0663876	0.7255753
l(2)44DEa	FBgn0010609	0.02287	0.01982	1.1538394	0.7284665
CG9009	FBgn0027601	0.01244	0.00921	1.3513628	0.7289599
endoA	FBgn0038659	0.00441	0.00334	1.319938	0.7322503
PP2A-B'	FBgn0042693	0.01172	0.01285	-1.0969182	0.732766
RpL28	FBgn0035422	0.72986	0.76012	-1.0414694	0.7347989
CG6488	FBgn0032361	0.00744	0.00573	1.2977971	0.7391377
RpL22	FBgn0015288	0.48583	0.50111	-1.0314466	0.7404744
CG7456	FBgn0032258	0.00759	0.00635	1.1948834	0.742861
CG31546	FBgn0051546	0.00266	0.00476	-1.7890876	0.7429551
CG32521	FBgn0052521	0.00669	0.00882	-1.3176769	0.7469472
CG9977	FBgn0035371	0.03382	0.02954	1.1448997	0.7470768
CG7949	FBgn0036107	0.01025	0.0079	1.2982712	0.7485426
sqd	FBgn0086897	0.14801	0.15428	-1.0423373	0.748803
CG16940	FBgn0035111	0.00067	0.00118	-1.7570001	0.7492326
CG7603	FBgn0036726	0.00575	0.01011	-1.7570001	0.7492326
l(2)gd1	FBgn0250747	0.00086	0.00151	-1.7570001	0.7492326
rg	FBgn0086911	0.0002	0.00034	-1.7570001	0.7492326
Nup98	FBgn0039120	0.00107	0.00073	1.4722628	0.752074
Sgs5	FBgn0003375	4.90043	4.73873	1.0341222	0.7525004
shrb	FBgn0086656	0.07549	0.08355	-1.1067168	0.7529317
CG14542	FBgn0039402	0.00909	0.00799	1.1380336	0.7534159
Fim	FBgn0024238	0.05972	0.05252	1.1370666	0.7537909
Jafrac2	FBgn0040308	0.11512	0.12177	-1.0578392	0.7550317
CG1702	FBgn0031117	0.0032	0.00551	-1.7235606	0.7560232
CG8547	FBgn0033919	0.0053	0.00643	-1.2132066	0.7566569
lolal	FBgn0022238	0.00553	0.00951	-1.7202899	0.7567015
Eig71Ej	FBgn0014850	0.36142	0.38884	-1.0758682	0.7577432

msps	FBgn0027948	0.00078	0.00061	1.2848311	0.7584087
Plap	FBgn0024314	0.01608	0.01434	1.1209259	0.7603282
Ef1gamma	FBgn0029176	0.64057	0.62257	1.0289006	0.761336
wmd	FBgn0034876	0.00222	0.00376	-1.6926483	0.7625375
Hrs	FBgn0031450	0.01956	0.0216	-1.1042445	0.7637502
His3:CG33866	FBgn0053866	0.35547	0.29771	1.1940015	0.7640955
CG17026	FBgn0036550	0.01076	0.00929	1.1586306	0.7640977
Trn	FBgn0024921	0.00494	0.00639	-1.2953225	0.7642323
CG6726	FBgn0039049	0.02343	0.0259	-1.1054855	0.7662613
baf	FBgn0031977	0.13843	0.11678	1.1853668	0.7667554
CG1640	FBgn0030478	0.06724	0.06165	1.0906877	0.7697893
CG2493	FBgn0032864	0.01235	0.01459	-1.1812703	0.7705954
CG4612	FBgn0035016	0.00292	0.00405	-1.3872911	0.7716881
Jupiter	FBgn0051363	0.12616	0.11388	1.1077926	0.7739879
Hrb98DE	FBgn0001215	0.06064	0.06341	-1.0457103	0.7760192
faf	FBgn0005632	0.00129	0.00156	-1.2047037	0.7768533
Rpt4	FBgn0028685	0.11868	0.11498	1.0322136	0.7778178
CG18294	FBgn0036873	0.00636	0.00874	-1.3729294	0.778656
Pros29	FBgn0261394	0.25662	0.24566	1.0446264	0.7788402
Arp53D	FBgn0011743	0.00955	0.00754	1.2662786	0.778922
CG1140	FBgn0035298	0.00749	0.00862	-1.1506925	0.7790513
Ank	FBgn0011747	0.00723	0.00796	-1.1009604	0.7794428
Papss	FBgn0020389	0.03801	0.03497	1.0868614	0.7796768
CG8108	FBgn0027567	0.00725	0.00787	-1.0859187	0.7798337
gammaCop	FBgn0028968	0.36282	0.37137	-1.0235717	0.7822966
CG5346	FBgn0038981	0.00397	0.00612	-1.5425394	0.7838767
v	FBgn0003965	0.00799	0.007	1.1429315	0.7852238
Act88F	FBgn0000047	1.96121	2.00414	-1.0218944	0.7854662
wol	FBgn0261020	0.01807	0.02007	-1.1106936	0.7860183
Pka-C1	FBgn0000273	0.01873	0.02161	-1.1535313	0.7880151
ari-1	FBgn0017418	0.00178	0.0012	1.4858681	0.788446
MRP	FBgn0032456	0.00058	0.00039	1.4858681	0.788446
ppk	FBgn0020258	0.00148	0.001	1.4858681	0.788446
Lasp	FBgn0063485	0.00717	0.0081	-1.1306669	0.7892296
Gmer	FBgn0034794	0.01835	0.01533	1.1976191	0.7894663
CG4552	FBgn0031304	0.01185	0.01037	1.142512	0.7895333
CG17904	FBgn0032597	0.01452	0.01177	1.2333333	0.7899654
CG3493	FBgn0034854	0.00667	0.00758	-1.1365245	0.7955501
CG31352	FBgn0051352	0.00999	0.00895	1.1165915	0.7963536
AP-47	FBgn0024833	0.05549	0.05095	1.0891427	0.7986405
ref(2)P	FBgn0003231	0.00665	0.00825	-1.241889	0.7987683
CG10425	FBgn0039304	0.00267	0.00184	1.4548228	0.7994517

Cul-5	FBgn0039632	0.00141	0.00097	1.4548228	0.7994517
CG5862	FBgn0038868	0.01826	0.01448	1.260843	0.8004207
primo-1	FBgn0040077	0.02442	0.02131	1.1459746	0.8011126
CG32576	FBgn0052576	0.05211	0.04685	1.1124395	0.8018613
Mdr49	FBgn0004512	0.00125	0.00093	1.3463314	0.8026748
Rat1	FBgn0031868	0.00491	0.0057	-1.1603306	0.8065284
CG11526	FBgn0035437	0.00097	0.00068	1.4287304	0.8089499
CG12519	FBgn0036872	0.00685	0.00479	1.4287304	0.8089499
CG6867	FBgn0030887	0.00095	0.00066	1.4287304	0.8089499
ph-d	FBgn0004860	0.00066	0.00046	1.4287304	0.8089499
ph-p	FBgn0004861	0.00056	0.0004	1.4287304	0.8089499
TH1	FBgn0010416	0.00155	0.00109	1.4287304	0.8089499
Fit1	FBgn0035498	0.00864	0.0093	-1.0764368	0.8091646
eIF2B-beta	FBgn0024996	0.00399	0.00532	-1.3337938	0.8094319
Ilk	FBgn0028427	0.0119	0.01324	-1.1123301	0.8106662
Catsup	FBgn0002022	0.00356	0.00412	-1.1558899	0.8130127
CG5362	FBgn0032237	0.44959	0.43551	1.0323304	0.8173906
Ras64B	FBgn0003206	0.01592	0.01816	-1.1409002	0.8197767
Vap-33-1	FBgn0029687	0.15171	0.14508	1.0457013	0.8216406
Ant2	FBgn0025111	0.08778	0.09447	-1.0761884	0.8223441
mRpL12	FBgn0011787	0.02571	0.02058	1.2495494	0.8228885
betaggt-II	FBgn0028970	0.00663	0.00771	-1.1624929	0.8235991
Tequila	FBgn0023479	0.00617	0.00688	-1.1140812	0.8241832
CG17127	FBgn0032299	0.01433	0.01862	-1.299395	0.8251112
CG5515	FBgn0039163	0.00874	0.00667	1.3104174	0.8257649
glo	FBgn0259139	0.00851	0.01036	-1.2168914	0.8277999
me31B	FBgn0004419	0.05146	0.04755	1.0822398	0.828218
UbcD6	FBgn0004436	0.01412	0.01224	1.1537412	0.8294185
for	FBgn0000721	0.00171	0.00132	1.2965633	0.8294392
Phm	FBgn0019948	0.02106	0.02246	-1.0664627	0.834359
Uch	FBgn0010288	0.2718	0.28793	-1.0593594	0.8355296
His2Av	FBgn0001197	0.55715	0.58442	-1.0489518	0.8359686
rumi	FBgn0086253	0.00525	0.00648	-1.2336263	0.8371508
GM130	FBgn0034697	0.06349	0.05825	1.0899425	0.8390985
Rox8	FBgn0005649	0.01206	0.01385	-1.147918	0.8391133
Dcr-2	FBgn0034246	0.00312	0.00333	-1.0673055	0.8398624
CG7546	FBgn0035793	0.00979	0.01113	-1.1364152	0.8413251
CG5174	FBgn0034345	0.21959	0.20987	1.0463174	0.8415665
CG5656	FBgn0037083	0.01089	0.00947	1.1500383	0.8417547
CG2604	FBgn0037298	0.00372	0.00292	1.2733093	0.8420748
Shc	FBgn0015296	0.00439	0.00347	1.2658311	0.8422638
retm	FBgn0031814	0.00217	0.00185	1.1721878	0.8458685

Atg8a	FBgn0052672	0.05824	0.04869	1.1961231	0.846914
CG4038	FBgn0011824	0.05301	0.05616	-1.059386	0.8477588
Jheh2	FBgn0034405	0.00939	0.00793	1.1831264	0.8489866
ben	FBgn0000173	0.1204	0.11502	1.046782	0.8501332
CG5075	FBgn0032464	0.07142	0.07431	-1.0404686	0.8501958
CG6000	FBgn0039145	0.01459	0.01673	-1.1468434	0.8515213
CG5366	FBgn0027568	0.01051	0.00976	1.0772806	0.8545412
Ppat-Dpck	FBgn0035632	0.0027	0.00233	1.16147	0.8549001
ns1	FBgn0038473	0.00613	0.00698	-1.1381506	0.8549983
Sap47	FBgn0013334	0.03732	0.03543	1.0533139	0.8569284
Eip55E	FBgn0000566	0.15206	0.14653	1.0377326	0.8572306
Set	FBgn0014879	0.02775	0.02589	1.0719102	0.8598342
CG32147	FBgn0047178	0.06252	0.05772	1.0831706	0.8601965
Caf1	FBgn0015610	0.08053	0.07533	1.0691086	0.8619741
CG18811	FBgn0042134	0.01962	0.01818	1.079088	0.8644146
CG33052	FBgn0053052	0.00423	0.00368	1.1494461	0.8650749
CG8507	FBgn0037756	0.00755	0.00855	-1.1329914	0.8661502
CG7011	FBgn0036489	0.00955	0.00876	1.0910311	0.8675608
CG10077	FBgn0035720	0.00196	0.00229	-1.17099	0.8691019
LSm7	FBgn0261068	0.07472	0.08032	-1.0748168	0.8700971
alphaTub84B	FBgn0003884	1.07263	1.09064	-1.0167931	0.8705527
alphaTub84D	FBgn0003885	1.07263	1.09064	-1.0167931	0.8705527
Oat	FBgn0022774	0.05465	0.0516	1.0591205	0.8715077
CG1607	FBgn0039844	0.00317	0.00369	-1.1639473	0.8729356
glob1	FBgn0027657	0.24467	0.25772	-1.0533377	0.8734924
CG2976	FBgn0031633	0.03229	0.03412	-1.0563749	0.8760341
CG14005	FBgn0031739	0.00664	0.00774	-1.1644446	0.8762544
Scsalpha	FBgn0004888	0.26053	0.2674	-1.0263709	0.8771328
Atg18	FBgn0035850	0.00848	0.00758	1.118603	0.8781153
CG1648	FBgn0033446	0.02876	0.02648	1.0859515	0.879173
CG33307	FBgn0053307	0.02441	0.02661	-1.0902995	0.879474
GstD5	FBgn0010041	0.01246	0.01033	1.2062862	0.8798372
CG7857	FBgn0026738	0.01142	0.01055	1.0830236	0.8801031
alphaTub67C	FBgn0087040	0.04504	0.04613	-1.0240989	0.8815151
Strn-Mlck	FBgn0013988	0.00381	0.00418	-1.097855	0.8825607
FK506-bp1	FBgn0013269	0.06681	0.06422	1.040281	0.8839604
eIF-3p40	FBgn0022023	0.20791	0.20297	1.024306	0.8845111
CG17121	FBgn0039043	0.00404	0.00341	1.1831368	0.8849427
CG1970	FBgn0039909	0.0311	0.03248	-1.0442601	0.8862695
r	FBgn0003189	0.01255	0.01331	-1.0604055	0.8886722
Drs	FBgn0010381	0.07338	0.0676	1.0853695	0.8893515
Pmm45A	FBgn0033377	0.0067	0.00732	-1.0918863	0.893572

l(1)G0334	FBgn0028325	0.17909	0.18526	-1.0344517	0.8942677
rept	FBgn0040075	0.01552	0.0162	-1.0436661	0.8946875
ND23	FBgn0017567	0.07998	0.07475	1.0699825	0.8966944
Hsc70-3	FBgn0001218	1.86061	1.8803	-1.0105802	0.8991282
aux	FBgn0037218	0.0011	0.00091	1.2067948	0.8994195
bou	FBgn0261284	0.00489	0.00405	1.2067948	0.8994195
CG1344	FBgn0027507	0.00114	0.00094	1.2067948	0.8994195
CG4907	FBgn0039010	0.00079	0.00066	1.2067948	0.8994195
cin	FBgn0000316	0.00216	0.00179	1.2067948	0.8994195
GluRIIA	FBgn0004620	0.0008	0.00067	1.2067948	0.8994195
Mpk2	FBgn0015765	0.00199	0.00165	1.2067948	0.8994195
SCAR	FBgn0041781	0.00119	0.00099	1.2067948	0.8994195
Tango13	FBgn0086674	0.00146	0.00121	1.2067948	0.8994195
Ts	FBgn0024920	0.00227	0.00188	1.2067948	0.8994195
yellow-f	FBgn0041710	0.0017	0.00141	1.2067948	0.8994195
CG11148	FBgn0039936	0.00227	0.00207	1.0986569	0.8995878
Gmap	FBgn0027287	0.01498	0.01427	1.0497024	0.8998242
REG	FBgn0029133	0.03562	0.0336	1.0600189	0.8999941
Hrb27C	FBgn0004838	0.17125	0.1631	1.0499606	0.900244
CG8858	FBgn0033698	0.00134	0.0015	-1.1236754	0.900463
GstS1	FBgn0010226	0.07469	0.07236	1.0322188	0.9014106
snRNP2	FBgn0037434	0.04667	0.04486	1.0403955	0.9021354
Rpt3	FBgn0028686	0.24412	0.25092	-1.0278663	0.9030768
CG4968	FBgn0032214	0.0134	0.01181	1.1347562	0.9032264
rab3-GAP	FBgn0027505	0.00105	0.00091	1.1503211	0.9036179
skap	FBgn0037643	0.08999	0.08707	1.0335645	0.9060532
Pur-alpha	FBgn0022361	0.00582	0.00685	-1.1780327	0.9075682
CG2147	FBgn0030025	0.02687	0.02876	-1.0701243	0.9090922
Clc	FBgn0024814	0.07904	0.0815	-1.0312103	0.9105188
ca	FBgn0000247	0.00037	0.00031	1.1815803	0.9108361
CG12173	FBgn0037305	0.00285	0.00241	1.1815803	0.9108361
CG2254	FBgn0029994	0.00228	0.00193	1.1815803	0.9108361
CG3860	FBgn0034951	0.0016	0.00136	1.1815803	0.9108361
CG6782	FBgn0037912	0.0023	0.00195	1.1815803	0.9108361
CG8042	FBgn0027554	0.00143	0.00121	1.1815803	0.9108361
CG9257	FBgn0032916	0.0021	0.00178	1.1815803	0.9108361
Cul-2	FBgn0032956	0.00097	0.00082	1.1815803	0.9108361
Jarid2	FBgn0036004	0.00031	0.00026	1.1815803	0.9108361
ninaG	FBgn0037896	0.00125	0.00106	1.1815803	0.9108361
RPA2	FBgn0032906	0.00296	0.00251	1.1815803	0.9108361
RpII33	FBgn0026373	0.00623	0.00527	1.1815803	0.9108361
CG11134	FBgn0030518	0.05488	0.05185	1.0585254	0.9113161

p38b	FBgn0024846	0.01814	0.01739	1.0431115	0.9116779
Srp14	FBgn0038808	0.06145	0.05693	1.0793677	0.9141054
CG14407	FBgn0030584	0.01939	0.02062	-1.0634663	0.9145987
CG9662	FBgn0031529	0.04329	0.04518	-1.0435047	0.9166105
Cdep	FBgn0051536	0.00082	0.0007	1.1625948	0.9195888
CG3473	FBgn0028913	0.00465	0.004	1.1625948	0.9195888
hig	FBgn0010114	0.00073	0.00063	1.1625948	0.9195888
Patr-1	FBgn0028470	0.00073	0.00062	1.1625948	0.9195888
Prosalpha3T	FBgn0261395	0.0028	0.00241	1.1625948	0.9195888
Sra-1	FBgn0038320	0.00059	0.00051	1.1625948	0.9195888
wkd	FBgn0037917	0.00193	0.00166	1.1625948	0.9195888
CG1646	FBgn0039600	0.00231	0.00243	-1.0534527	0.919919
Su(var)205	FBgn0003607	0.14545	0.14809	-1.0181174	0.9202872
scb	FBgn0003328	0.00631	0.00607	1.0400289	0.9206019
CG10673	FBgn0035590	0.00325	0.0028	1.1603886	0.9206147
CG11092	FBgn0027537	0.00089	0.00076	1.1603886	0.9206147
CG3592	FBgn0029642	0.00331	0.00285	1.1603886	0.9206147
CG4960	FBgn0039371	0.00419	0.00361	1.1603886	0.9206147
CG5902	FBgn0039136	0.003	0.00258	1.1603886	0.9206147
CG8336	FBgn0036020	0.0019	0.00164	1.1603886	0.9206147
Dcp1	FBgn0034921	0.00188	0.00162	1.1603886	0.9206147
E(bx)	FBgn0000541	0.00027	0.00024	1.1603886	0.9206147
Fis1	FBgn0039969	0.00744	0.00641	1.1603886	0.9206147
HDAC6	FBgn0026428	0.00064	0.00055	1.1603886	0.9206147
MEP-1	FBgn0035357	0.00063	0.00055	1.1603886	0.9206147
Nup214	FBgn0010660	0.00043	0.00037	1.1603886	0.9206147
Phk-3	FBgn0035089	0.00602	0.00519	1.1603886	0.9206147
U2af50	FBgn0005411	0.0035	0.00302	1.1603886	0.9206147
U4-U6-60K	FBgn0036733	0.00132	0.00114	1.1603886	0.9206147
betaTub85D	FBgn0003889	0.91889	0.91141	1.0082113	0.9230142
betaTub60D	FBgn0003888	0.67386	0.68249	-1.0128003	0.9233771
M(2)21AB	FBgn0005278	0.00701	0.00755	-1.0770729	0.9237956
CG10516	FBgn0036549	0.00205	0.00238	-1.1591797	0.9249257
Nrg	FBgn0002968	0.00556	0.00601	-1.0822333	0.9260934
CG4164	FBgn0031256	0.10628	0.10962	-1.0313742	0.9262442
stai	FBgn0051641	0.04884	0.05241	-1.0731762	0.9270158
Rop	FBgn0004574	0.0217	0.02238	-1.0312108	0.9272724
CG8132	FBgn0037687	0.0108	0.01011	1.0683962	0.9283809
Pros26	FBgn0002284	0.23145	0.23391	-1.0106191	0.9309736
AGO1	FBgn0026611	0.00166	0.00145	1.1383038	0.9309834
ash2	FBgn0000139	0.00113	0.00099	1.1383038	0.9309834
CG12068	FBgn0039695	0.0021	0.00184	1.1383038	0.9309834

CG14216	FBgn0031054	0.0072	0.00633	1.1383038	0.9309834
CG1890	FBgn0039869	0.00638	0.00561	1.1383038	0.9309834
CG2034	FBgn0015359	0.00268	0.00235	1.1383038	0.9309834
CG6905	FBgn0035136	0.00086	0.00076	1.1383038	0.9309834
CG7656	FBgn0036516	0.0022	0.00193	1.1383038	0.9309834
CG9286	FBgn0038183	0.00236	0.00208	1.1383038	0.9309834
gbb	FBgn0024234	0.00154	0.00136	1.1383038	0.9309834
hyd	FBgn0002431	0.00024	0.00021	1.1383038	0.9309834
Ide	FBgn0001247	0.00071	0.00062	1.1383038	0.9309834
RpII15	FBgn0004855	0.00544	0.00478	1.1383038	0.9309834
Rya-r44F	FBgn0011286	0.00014	0.00012	1.1383038	0.9309834
Sara	FBgn0026369	0.00052	0.00046	1.1383038	0.9309834
sec71	FBgn0028538	0.00042	0.00037	1.1383038	0.9309834
SF1	FBgn0025571	0.00091	0.0008	1.1383038	0.9309834
SNF4Agamma	FBgn0025803	0.00109	0.00095	1.1383038	0.9309834
Syx16	FBgn0031106	0.00199	0.00175	1.1383038	0.9309834
CG8066	FBgn0038243	0.04503	0.04774	-1.0601678	0.9372221
CG11377	FBgn0031217	0.00188	0.00168	1.1178882	0.94073
CG3756	FBgn0031657	0.00211	0.00189	1.1178882	0.94073
CG5428	FBgn0034887	0.00415	0.00372	1.1178882	0.94073
CG6013	FBgn0038675	0.0033	0.00295	1.1178882	0.94073
CG7203	FBgn0031942	0.00484	0.00433	1.1178882	0.94073
CG7433	FBgn0036927	0.00144	0.00129	1.1178882	0.94073
CG7806	FBgn0032018	0.00047	0.00042	1.1178882	0.94073
iPLA2-VIA	FBgn0036053	0.00182	0.00163	1.1178882	0.94073
MED19	FBgn0036761	0.00208	0.00186	1.1178882	0.94073
Ubc-E2H	FBgn0029996	0.00413	0.00369	1.1178882	0.94073
CG6364	FBgn0039179	0.03431	0.03569	-1.0399891	0.9412758
CG31751	FBgn0086909	0.01622	0.01667	-1.0281024	0.9431295
CG5577	FBgn0036759	0.00231	0.00258	-1.1167236	0.9433996
elm	FBgn0037358	0.00313	0.00349	-1.1167236	0.9433996
Fas1	FBgn0000634	0.00112	0.00125	-1.1167236	0.9433996
Msr-110	FBgn0015766	0.00118	0.00132	-1.1167236	0.9433996
wds	FBgn0040066	0.00202	0.00225	-1.1167236	0.9433996
Vha13	FBgn0026753	0.18435	0.17698	1.0416351	0.9434916
CG18067	FBgn0034512	0.02939	0.03037	-1.0333832	0.9448284
Pfk	FBgn0003071	0.07075	0.06978	1.0139018	0.9465258
CG40045	FBgn0058045	0.03173	0.03293	-1.0378014	0.9470724
Arc-p34	FBgn0032859	0.01296	0.01221	1.0614856	0.9471017
bocksbeutel	FBgn0037719	0.0059	0.00618	-1.0469843	0.9475089
CG11727	FBgn0030299	0.00115	0.00104	1.1025572	0.9481508
CG14299	FBgn0038651	0.00037	0.00034	1.1025572	0.9481508

CG17768	FBgn0032240	0.00583	0.00528	1.1025572	0.9481508
CG8549	FBgn0035714	0.00356	0.00323	1.1025572	0.9481508
Menl-2	FBgn0029153	0.00161	0.00146	1.1025572	0.9481508
polybromo	FBgn0039227	0.00054	0.00049	1.1025572	0.9481508
RpL30	FBgn0086710	0.90211	0.90614	-1.0044638	0.9482698
CG5941	FBgn0029833	0.08232	0.0833	-1.0119339	0.9487533
CG8100	FBgn0036410	0.00375	0.00414	-1.1048551	0.9487564
CG9510	FBgn0032076	0.03268	0.03209	1.0182873	0.949905
Jafrac1	FBgn0040309	0.83796	0.84371	-1.0068672	0.9523597
CG10672	FBgn0035588	0.00743	0.00785	-1.056551	0.9571256
CG11739	FBgn0037239	0.02594	0.02669	-1.0290796	0.9604327
Tcp-1zeta	FBgn0027329	0.11786	0.11934	-1.0125921	0.9611834
GstD2	FBgn0010038	0.01252	0.01319	-1.0533264	0.963666
CG12304	FBgn0036515	0.01328	0.01358	-1.0227793	0.9642064
Rpt6R	FBgn0039788	0.08422	0.08336	1.0103364	0.9667722
CG12404	FBgn0032465	0.01148	0.01172	-1.0208876	0.9680453
Tim9a	FBgn0030480	0.0319	0.03256	-1.0208876	0.9680453
mtacp1	FBgn0011361	0.07658	0.07687	-1.0038046	0.9689871
CG5112	FBgn0039341	0.00982	0.00941	1.0437162	0.9698245
CG9135	FBgn0031769	0.01976	0.01946	1.0154688	0.9712197
eIF6	FBgn0034915	0.04443	0.04503	-1.0134377	0.9720417
CG4389	FBgn0028479	0.15377	0.15449	-1.0046999	0.9739784
Msp-300	FBgn0260952	0.00044	0.00045	-1.0241375	0.9744552
ens	FBgn0035500	0.00215	0.00222	-1.0301492	0.9753976
Clic	FBgn0030529	0.09983	0.10074	-1.0091163	0.9770117
rl	FBgn0003256	0.0156	0.01537	1.0147089	0.9778264
CG9705	FBgn0036661	0.05121	0.05196	-1.014675	0.9803296
tws	FBgn0004889	0.01305	0.01279	1.0205953	0.9806483
CG13779	FBgn0040954	0.03802	0.03871	-1.018169	0.9844477
Nup358	FBgn0039302	0.00757	0.00753	1.0045427	0.9864106
miple2	FBgn0029002	0.00895	0.00884	1.0126534	0.9866308
mod(mdg4)	FBgn0002781	0.0023	0.00235	-1.0188399	0.9869587
torp4a	FBgn0025615	0.00413	0.00421	-1.0188399	0.9869587
CG6567	FBgn0037842	0.0352	0.03498	1.0063145	0.9872199
l(3)03670	FBgn0010808	0.03144	0.03134	1.0033124	0.9913663
CG10343	FBgn0032703	0.00669	0.00662	1.0092574	0.9913852
CG5854	FBgn0039130	0.00937	0.00929	1.0088753	0.9914112
CG5567	FBgn0036760	0.00442	0.00437	1.0108648	0.9924622
CG9911	FBgn0030734	0.52033	0.52014	1.0003683	0.9983507
Dbp73D	FBgn0004556	0.00208	0.00208	1.0001662	0.9998446

Appendix 3: Proteins identified by proteomics in *Drosophila* salivary glands upon ectopic proteasome impairment.

Protein names and FBgn numbers are based on Flybase annotation (http://flybase.org/). The values for peptides mapped to the genes listed are indicated. Protein quantities were determined using the spectral counting method in which spectral counts (spectral peptide matches) for each protein were summed and normalized across runs based on the total spectral counts obtained for each run. The ratio2 values for peptides mapped to the genes listed are indicated (ratio2=average detection value experimental sample divided by average detection value control sample). p values were obtained using the Student's t-test followed by multiple testing adjustment using the Benjamini-Hochberg method (Hochberg and Benjamini, 1990). Inf indicates a numerical value divided by 0. –Inf indicates 0 divided by a numerical value.

symbol	FBgn	fkh-GAL4; UAS-Dts7 AVE	Control UAS-Dts7/+ AVE	ratio2	p_value
CG5946	FBgn0036211	0	0.0086047	-Inf	9.42E-08
for	FBgn0000443	0	0.0030954	-Inf	4.89E-07
CG31357	FBgn0051357	0	0.0073378	-Inf	4.89E-07
CG30349	FBgn0033343	0.0037999	0	Inf	2.20E-06
Catsup	FBgn0002022	0	0.0062959	-Inf	2.32E-06
RhoGDI	FBgn0036921	0.2748285	0.1819593	1.51038459	3.30E-06
CG11880	FBgn0039637	0.0051509	0	Inf	7.48E-06
CG7556	FBgn0030990	0.0141515	0.0363923	-2.5716241	8.29E-06
Cul-4	FBgn0033260	0.0037671	0	Inf	1.05E-05
Irc	FBgn0038465	0.1468319	0.0392597	3.74001367	2.90E-05
CG12715	FBgn0030443	0.0604779	0.175663	-2.9045813	3.38E-05
Aats-val	FBgn0010542	0.0154951	0.0476091	-3.0725184	4.03E-05
RhoGAP68F	FBgn0036257	0	0.0052835	-Inf	4.18E-05
CG3192	FBgn0029888	0.0474585	0.0253745	1.87032148	4.73E-05
kis	FBgn0001309	0	0.0004786	-Inf	5.56E-05

ps	FBgn0026188	0.0100592	0.040024	-3.9788585	6.64E-05
CG3609	FBgn0031418	0.1536892	0.3031725	-1.9726337	6.81E-05
l(3)01239	FBgn0010741	0.0476637	0.0973776	-2.0430128	7.03E-05
Ef1beta	FBgn0025828	0.6236099	1.3236748	-2.1226008	7.16E-05
CG7924	FBgn0036416	0.3372782	0.1594624	2.11509633	7.41E-05
CG14715	FBgn0037930	0.1316531	0.0327773	4.01659352	8.24E-05
raps	FBgn0020384	0.0076554	0	Inf	8.42E-05
CG10126	FBgn0038088	0.2926874	0.0897731	3.2603015	8.51E-05
Hsp23	FBgn0001224	3.8326647	0.9968923	3.8446124	9.57E-05
CG9705	FBgn0036661	0.1297005	0.0182065	7.12384246	9.73E-05
CG7322	FBgn0030968	0.6811168	0.2086471	3.26444489	9.85E-05
CG8552	FBgn0031989	0.0216864	0.0485494	-2.238702	0.0001
Hsp27	FBgn0001226	1.5016946	0.8777615	1.71082294	0.00011
p24-2	FBgn0053105	0.1040149	0.1871231	-1.7990026	0.00013
eca	FBgn0037732	0.1174983	0.2113798	-1.7990026	0.00013
ferrochelatase	FBgn0024891	0.0602054	0.0144429	4.16850403	0.00013
Npc2h	FBgn0039801	0.2148379	0.1283109	1.67435476	0.00014
CG1681	FBgn0030484	0.0645429	0.0038304	16.8503446	0.00019
Timp	FBgn0025879	0.0134879	0.043147	-3.1989294	0.00021
Gp93	FBgn0039562	0.6445413	0.8299947	-1.2877291	0.00021
CG31549	FBgn0037353	0.108659	0.0469559	2.31406565	0.00024
Mmp1	FBgn0022198	0.021256	0	Inf	0.00025
CG10098	FBgn0037472	0.2331772	0.1509615	1.54461362	0.00027
CG7145	FBgn0037138	0.1088413	0.1527112	-1.4030631	0.00028
cana	FBgn0022074	0	0.0017125	-Inf	0.00029
CG3777	FBgn0024989	0.0134788	0.0013708	9.83250396	0.00029
RpLP2	FBgn0003274	1.315648	1.8434536	-1.4011754	0.00031
mfas	FBgn0024211	0.1725203	0.0715977	2.40957834	0.00032
Aats-glupro	FBgn0005674	0.0234513	0.0430424	-1.8353975	0.00033
CG10194	FBgn0032790	0.014472	0	Inf	0.00035
CG1104	FBgn0037467	0.0421589	0.0833181	-1.976286	0.00037
eEF1delta	FBgn0032198	0.4668945	0.6036354	-1.2928733	0.0004
Ect3	FBgn0037977	0.0411775	0.0039985	10.2981902	0.0004
CG1950	FBgn0030370	0.0243932	0.0141485	1.72407796	0.00041
CG10175	FBgn0039084	0.0140787	0.0481818	-3.4223107	0.00044
TepII	FBgn0031931	0.4006197	0.5778542	-1.4424008	0.00046
CG4729	FBgn0036623	0	0.0295779	-Inf	0.00047
CG9336	FBgn0032897	0.1478596	0.0164863	8.96861069	0.00047
CG11876	FBgn0039635	0.2987094	0.2318046	1.28862589	0.00047
Cyp12c1	FBgn0036806	0.020018	0.0013142	15.2322217	0.00048
CG8444	FBgn0037671	0.0152742	0.0082963	1.84107916	0.00053
lva	FBgn0029688	0.0520971	0.0807119	-1.5492588	0.00053

Ef2b	FBgn0000559	0.4867545	0.8405756	-1.7268985	0.00056
beta'Cop	FBgn0025724	0.1212173	0.1697414	-1.4003064	0.0006
CG17259	FBgn0031497	0.4021759	0.5325467	-1.3241637	0.0006
fbp	FBgn0032820	0.1225848	0.2371279	-1.934399	0.00065
CG3415	FBgn0030731	0.2074123	0.1253562	1.65458256	0.00067
CG32521	FBgn0031165	0.0489641	0.013812	3.54504597	0.00068
CG10576	FBgn0035630	0.3417451	0.4593141	-1.3440253	0.00072
Aats-lys	FBgn0027084	0.079459	0.1220731	-1.536302	0.00075
CG1458	FBgn0039653	0.0787635	0.1064756	-1.351839	0.00076
CG12481	FBgn0030542	0.0833484	0.0303426	2.74690961	0.00076
Dbi	FBgn0010387	0.1734616	0.0488335	3.55210589	0.00085
Idh	FBgn0001248	0.5679384	0.3938553	1.44199755	0.00085
CG9917	FBgn0030740	0.0095467	0	Inf	0.00088
Sodh-1	FBgn0024289	0.2058647	0.1450133	1.41962671	0.00092
GstE6	FBgn0034340	0.0212278	0	Inf	0.00098
CG7532	FBgn0026299	0.2583661	0.069665	3.70869313	0.00108
Eig71Ek	FBgn0014851	0.5414133	1.0473169	-1.9344131	0.00112
Dp1	FBgn0027520	0.1462895	0.2165823	-1.4805051	0.00119
UGP	FBgn0035978	0.122604	0.2225955	-1.815565	0.00119
AIF	FBgn0031392	0.0089618	0.0013347	6.71420565	0.00125
CG7906	FBgn0036417	0.2589422	0.1070475	2.41894795	0.00126
zetaCOP	FBgn0036651	0.0215868	0.0656307	-3.0403187	0.00132
Prx2540-2	FBgn0033518	0.1803045	0.0779504	2.31306691	0.00136
CG6643	FBgn0039208	0.0090432	0.0286111	-3.1638254	0.00137
CG3074	FBgn0034709	0.0574181	0.0126553	4.53708962	0.0014
Nep2	FBgn0027570	0.0037162	0	Inf	0.00141
CG3011	FBgn0029823	0.1886309	0.1162104	1.62318373	0.00141
RpLP1	FBgn0002593	1.1098485	1.9625555	-1.7683093	0.00144
CG16713	FBgn0031560	0.4761053	0.3408608	1.39677346	0.00144
sec31	FBgn0033339	0.0771846	0.1156196	-1.4979617	0.00147
eIF-2alpha	FBgn0004925	0.1863456	0.2406708	-1.2915288	0.00147
TepIV	FBgn0032806	0.1128388	0.0354252	3.18526781	0.00148
dro2	FBgn0035433	0.0439479	0	Inf	0.00149
CG3652	FBgn0031600	0.0049686	0.0281691	-5.66939	0.0016
Prx2540-1	FBgn0033520	0.184088	0.0779504	2.36160427	0.00163
CG9977	FBgn0035371	0.043362	0.018987	2.28377037	0.00168
Eig71Eh	FBgn0014848	0.1739187	0.0673436	2.58255702	0.0017
Lcp65Af	FBgn0020639	0.0260597	0	Inf	0.00173
Rpt3R	FBgn0037742	0.0518005	0.01975	2.62281518	0.00173
Edg84A	FBgn0000552	0.0138267	0	Inf	0.00177
Trxr-2	FBgn0037170	0.0154976	0.0063811	2.42867143	0.00177
bai	FBgn0039262	0.0871423	0.1525172	-1.7502072	0.0019

trol	FBgn0001402	0.1267528	0.0842055	1.50527986	0.00191
CG10424	FBgn0036848	0.0113901	0.0258248	-2.2673125	0.00199
NLaz	FBgn0031336	0.3336426	0.1389547	2.40108831	0.00209
Arf102F	FBgn0013749	0.2297542	0.4819655	-2.0977439	0.00215
CG15784	FBgn0029766	0.0281884	0.0029396	9.58910556	0.00216
Gap69C	FBgn0020655	0.0412634	0.0799344	-1.9371732	0.00216
CG13887	FBgn0035165	0.0363771	0.0680286	-1.8700948	0.00218
Srp72	FBgn0038810	0.1773161	0.2382339	-1.3435553	0.00222
CG2918	FBgn0023529	0.3339439	0.41919	-1.2552706	0.00224
Glt	FBgn0001114	0.1688411	0.104852	1.61028012	0.00235
Obp83g	FBgn0046875	0.1225785	0.0409225	2.99538034	0.00236
verm	FBgn0036901	0.1721528	0.086653	1.9866914	0.00238
Dip-B	FBgn0000454	0.2201527	0.1526208	1.44248212	0.00238
Grasp65	FBgn0036919	0.1097262	0.1666298	-1.5185961	0.00242
CG16979	FBgn0036512	0.0102399	0.022355	-2.1831251	0.00242
CG14109	FBgn0036364	0.0126007	0	Inf	0.00245
Aats-thr	FBgn0022209	0.0956746	0.1641125	-1.7153198	0.00248
Vinc	FBgn0004397	0.0874319	0.1124042	-1.2856206	0.0025
Eig71Ej	FBgn0014850	0.3867473	0.8412758	-2.1752595	0.00252
CG14062	FBgn0039592	0.7052202	1.4436732	-2.047124	0.00254
ras	FBgn0003204	0.1078063	0.0545729	1.97545416	0.00255
CG7872	FBgn0030658	0.0051139	0.0340624	-6.6607012	0.00257
lox	FBgn0039848	0.3040828	0.6723413	-2.2110468	0.00258
Csat	FBgn0015871	0.0110923	0.0290663	-2.6203905	0.00261
CG4572	FBgn0038738	0.0181483	0.0037224	4.87550051	0.00261
CG15343	FBgn0030029	0.0215065	0.0450675	-2.0955274	0.00263
CG13393	FBgn0032035	0.0641813	0.0992793	-1.5468567	0.00265
CG18067	FBgn0034512	0.03071	0.0122111	2.51493231	0.00267
Gfat2	FBgn0039580	0.0236974	0.0564961	-2.3840615	0.00274
Aats-tyr	FBgn0025537	0.0776088	0.1100582	-1.4181143	0.0028
CG10627	FBgn0036298	0.0323741	0.0661893	-2.0445124	0.00282
Pdi	FBgn0014002	3.0393565	3.8964405	-1.2819952	0.00284
Srp54k	FBgn0010747	0.06148	0.0977067	-1.5892428	0.00288
Arf79F	FBgn0010348	0.380605	0.7232085	-1.9001552	0.0029
Gapdh1	FBgn0001091	1.2171059	0.9751083	1.24817507	0.00293
CG5174	FBgn0034345	0.2364413	0.1793325	1.31845226	0.00293
lectin-28C	FBgn0031956	0.0277076	0	Inf	0.00307
Pomp	FBgn0032884	0.0281196	0	Inf	0.00311
grass	FBgn0039494	0.0120969	0	Inf	0.00312
CG5745	FBgn0038855	0	0.0068988	-Inf	0.00313
CR18217	FBgn0036646	0.005285	0	Inf	0.00313
CG4098	FBgn0036648	0.0101621	0	Inf	0.00313

Hf	FBgn0014000	0.0145516	0	Inf	0.00313
Kr-h2	FBgn0001326	0.0165405	0.0444997	-2.6903451	0.00323
Vha44	FBgn0020611	0.0331608	0.0583482	-1.7595548	0.00324
CG32412	FBgn0035646	0.0099522	0	Inf	0.00326
CG17127	FBgn0032299	0.1638011	0.0420167	3.89847323	0.00326
CG9629	FBgn0036857	0.0317602	0.0144279	2.20130525	0.00329
Vago	FBgn0030262	0.0248224	0	Inf	0.00331
Argk	FBgn0000116	0.9786687	0.7589738	1.28946315	0.00331
CG9686	FBgn0027688	0.0510974	0.0107586	4.74946767	0.00332
Drs	FBgn0010381	0.2074745	0.0893104	2.32307159	0.00334
Ald	FBgn0000064	1.0485086	1.3387736	-1.2768361	0.00377
pix	FBgn0035946	0.0378002	0.1039619	-2.7503038	0.00379
CG13842	FBgn0039009	0.0092008	0.0067582	1.36142723	0.00391
Moe	FBgn0011661	0.2460443	0.3572417	-1.4519404	0.00406
CG33138	FBgn0033801	0.025042	0.0085989	2.91223021	0.0041
CG31673	FBgn0051673	0.0420331	0.014999	2.80238695	0.00412
sgl	FBgn0002456	0.0090535	0	Inf	0.00412
CG5171	FBgn0031907	0.1211361	0.0544117	2.22628537	0.00414
Act79B	FBgn0000045	1.6675642	1.1249227	1.48238115	0.00443
CG15202	FBgn0030271	0.1672189	0.3943435	-2.3582476	0.00446
LanA	FBgn0002526	0.0300448	0.0173512	1.73157397	0.00446
CG9769	FBgn0037270	0.164983	0.2132829	-1.2927567	0.00447
CG31705	FBgn0028490	0.0345553	0.0069165	4.99604966	0.00453
sec23	FBgn0011441	0.2836285	0.3594845	-1.2674486	0.00456
Spn4	FBgn0028985	0.1160096	0.0403166	2.877465	0.00457
sop	FBgn0004867	0.4864166	0.5853868	-1.2034678	0.00464
Pcd	FBgn0024841	0.0411497	0.0214087	1.92209975	0.0047
Tctp	FBgn0037874	0.315914	0.6068297	-1.9208699	0.00471
CG2915	FBgn0033241	0.0850515	0.1512232	-1.7780194	0.00472
CG9356	FBgn0037688	0.0044841	0.0208799	-4.6564179	0.00476
CG33123	FBgn0025535	0.0122834	0.0298902	-2.4333866	0.00477
Dak1	FBgn0028833	0.2898474	0.3953826	-1.3641063	0.00478
CG11897	FBgn0039644	0.002298	0	Inf	0.0048
Cg25C	FBgn0000299	0.032004	0.0201784	1.58605315	0.00492
Pepck	FBgn0003067	0.0475977	0.011525	4.12994221	0.00502
Act57B	FBgn0000044	2.1247895	1.5259298	1.3924556	0.00505
drpr	FBgn0027594	0.0054242	0	Inf	0.0051
CG9119	FBgn0035189	0.2228399	0.1214113	1.83541245	0.00515
Tango2	FBgn0030503	0.0099693	0	Inf	0.00515
CG5941	FBgn0029833	0.1056823	0.1687639	-1.5968974	0.00515
CG9331	FBgn0032889	0.3311245	0.1945788	1.70174969	0.00524
CG3244	FBgn0031629	0.2989965	0.114518	2.61091292	0.00526

Act87E	FBgn0000046	2.0784622	1.4908343	1.39416041	0.00528
Tsf3	FBgn0034094	0.1030486	0.0478973	2.15144865	0.00533
CG2233	FBgn0029990	0.1036776	0.2777964	-2.6794248	0.00536
Mpk2	FBgn0013952	0.007709	0	Inf	0.00551
Sdic	FBgn0025801	0.0205803	0.0247143	-1.2008715	0.00551
Gld	FBgn0001112	0.0044812	0	Inf	0.00552
Npc2g	FBgn0039800	0.4643026	0.2966582	1.56510922	0.00554
Act88F	FBgn0000047	1.8799308	1.2913549	1.45578168	0.0057
Sec22	FBgn0025617	0.0496842	0.0996523	-2.005714	0.00575
CG9360	FBgn0030332	0.0464015	0.0063603	7.29551735	0.00577
Spn43Ab	FBgn0024293	0.0625463	0.0357255	1.75074496	0.00583
CG32573	FBgn0030767	0.008051	0	Inf	0.00584
His4	FBgn0013981	1.7935312	1.3801444	1.29952428	0.00586
His4r	FBgn0013981	1.7935312	1.3801444	1.29952428	0.00586
His4:CG31611	FBgn0013981	1.7935312	1.3801444	1.29952428	0.00586
CG4164	FBgn0031256	0.0924134	0.1367156	-1.4793912	0.00592
CG10664	FBgn0032833	0.0373961	0.0590272	-1.5784324	0.00598
l(2)gl	FBgn0002121	0.0081786	0.0044	1.85878881	0.00602
Nc	FBgn0025326	0.0123953	0	Inf	0.00614
CG6767	FBgn0036030	0.0991481	0.0589804	1.68103426	0.00614
CG2023	FBgn0037383	0.0254225	0.062721	-2.4671432	0.00622
CG9281	FBgn0030672	0.0348097	0.0988215	-2.8389099	0.00623
ergic53	FBgn0011010	0.0897086	0.1452991	-1.6196788	0.00624
woc	FBgn0010328	0.003006	0.0005378	5.58940807	0.00628
Tango1	FBgn0031842	0.0181112	0.0398094	-2.1980491	0.0063
CG3040	FBgn0029925	0	0.0163071	-Inf	0.00632
CG31751	FBgn0032696	0.0324685	0.0503228	-1.5498982	0.00634
CG17919	FBgn0037433	0.0819868	0.0432359	1.89626658	0.00641
CG8331	FBgn0033906	0.0695358	0.1300409	-1.8701296	0.00641
CG10306	FBgn0034654	0.1780252	0.2662817	-1.4957529	0.00656
CG2976	FBgn0031633	0.0456748	0.0193848	2.35621433	0.00657
beta-Spec	FBgn0003471	0.016778	0.0249891	-1.4893922	0.00659
CG33491	FBgn0053491	0.1026584	0.0418718	2.45173259	0.00667
CG13813	FBgn0036956	0.0106782	0.0336256	-3.1490028	0.00678
ERp60	FBgn0025187	1.1579105	1.4387748	-1.2425613	0.0068
CG9812	FBgn0034860	0.1597554	0.0573667	2.78481332	0.00683
CG6776	FBgn0035904	0.1398867	0.0984562	1.42080099	0.00684
CG10688	FBgn0036300	0.1276379	0.1931291	-1.5131018	0.00692
Peritrophin-15a	FBgn0040959	0.0370787	0	Inf	0.00706
Idgf4	FBgn0026066	0.7291651	0.4933936	1.477857	0.00726

CG11378	FBgn0029561	0.0236756	0.0022072	10.7267316	0.00727
Srp68	FBgn0035947	0.0525966	0.0834266	-1.5861602	0.00728
glob1	FBgn0027657	0.135994	0.2057646	-1.5130413	0.00733
CG11151	FBgn0030519	0.2672911	0.1557709	1.71592489	0.00741
CG2774	FBgn0031534	0.0342384	0.0524819	-1.5328341	0.00742
CG11377	FBgn0031217	0.0062817	0.0106452	-1.6946202	0.00744
Spase12	FBgn0040623	0.0409062	0.0972181	-2.3766101	0.00772
Eip55E	FBgn0000566	0.1721346	0.2299812	-1.3360544	0.00772
rg	FBgn0003244	0.0016844	0.0007977	2.11153041	0.00773
Hsp26	FBgn0001225	0.253515	0.1287751	1.96866415	0.00779
Map205	FBgn0002645	0.0264878	0.0038959	6.79881625	0.00788
Tsf2	FBgn0036299	0.0041619	0	Inf	0.00797
Clic	FBgn0030529	0.0706008	0.1378934	-1.9531428	0.008
FKBP59	FBgn0015990	0.0930344	0.1149138	-1.2351748	0.00806
CG4334	FBgn0038312	0.0045834	0.013534	-2.9527999	0.00811
alpha-Est5	FBgn0015573	0.007708	0	Inf	0.00822
Pax	FBgn0032776	0.1219983	0.0835688	1.45985486	0.00826
yellow-f	FBgn0038104	0.0236349	0.0067095	3.52260753	0.00845
Tig	FBgn0011722	0.0867778	0.0432745	2.00528793	0.00849
UK114	FBgn0028510	0.1445982	0.1062817	1.36051808	0.00853
BicD	FBgn0000183	0.0452673	0.020782	2.17819713	0.00855
Men	FBgn0002719	0.187074	0.1125642	1.66193142	0.00868
Phm	FBgn0019948	0.0206561	0.0466681	-2.2592862	0.00888
CG31315	FBgn0051315	0	0.0533092	-Inf	0.00895
CG1943	FBgn0037468	0.1140326	0.0683679	1.66792708	0.00902
CG15404	FBgn0031512	0.1797049	0.0639764	2.80892293	0.00907
dro5	FBgn0035434	0.0820847	0.0491927	1.66863756	0.00913
Ranbp9	FBgn0037894	0.0028379	0.0112903	-3.9784366	0.00913
Past1	FBgn0016693	0.1554657	0.2282056	-1.4678843	0.00923
Crc	FBgn0005585	0.9093575	1.3930511	-1.5319069	0.0093
Sodh-2	FBgn0022359	0.3336838	0.2384463	1.39940863	0.00943
CG31919	FBgn0031674	0.0601418	0.0214785	2.80009422	0.00955
CG3967	FBgn0035989	0.0076892	0	Inf	0.00961
RpS3	FBgn0002622	0.6589218	0.8227329	-1.2486047	0.00963
TwdlE	FBgn0031957	0.1733276	0.046451	3.73140711	0.00964
CG2145	FBgn0030251	0.1265097	0.038846	3.25670306	0.0097
CG10602	FBgn0032721	0.0870155	0.1279582	-1.4705217	0.00971
CG9362	FBgn0037696	0.0254688	0.0041978	6.06715755	0.00985
if	FBgn0001250	0.0015984	0.0051721	-3.2358699	0.01003
Ppt1	FBgn0030057	0.0107999	0	Inf	0.01009
Spn43Aa	FBgn0024294	0.3110356	0.1903466	1.63404906	0.01011
fon	FBgn0032773	0.2066231	0.112396	1.83834947	0.01021

Ubqn	FBgn0019902	0.02814	0.0659813	-2.3447486	0.01024
Surf4	FBgn0019925	0.0540689	0.0939128	-1.7369113	0.01035
CG6838	FBgn0037182	0.0780177	0.1234262	-1.5820279	0.01048
shrb	FBgn0033385	0.1008844	0.1675935	-1.661243	0.01048
Oat	FBgn0022774	0.1038261	0.070473	1.47327428	0.01048
RpS24	FBgn0034751	0.6512369	1.0523924	-1.6159903	0.01068
CG7603	FBgn0036726	0.0212023	0.0378078	-1.7831912	0.01082
btz	FBgn0016077	0.002827	0.0086597	-3.0631816	0.01083
M(2)21AB	FBgn0005278	0.0096386	0.0177493	-1.8414936	0.01097
VhaSFD	FBgn0027779	0.1186537	0.1656475	-1.3960583	0.01105
Imp	FBgn0025229	0.0376347	0.0139708	2.69380524	0.01106
CG3603	FBgn0029648	0.1198886	0.0559063	2.14445495	0.0111
SsRbeta	FBgn0011016	0.2640657	0.3919335	-1.4842273	0.01113
Zw	FBgn0004057	0.0202104	0.0047504	4.25446483	0.01119
nero	FBgn0011013	0.0038213	0.0163081	-4.2676595	0.01119
CG2263	FBgn0030007	0.0329116	0.0528908	-1.6070564	0.01136
CG9175	FBgn0031779	0.0013872	0.0084076	-6.0607705	0.01137
Fer2LCH	FBgn0010705	0.8291688	0.5666825	1.46319819	0.01152
Spp	FBgn0031260	0.0442324	0.102565	-2.3187755	0.01153
Gs2	FBgn0001145	0.0848326	0.0476901	1.77882849	0.01158
CG1499	FBgn0025950	0.0134303	0.0018169	7.39175366	0.01162
CG11015	FBgn0025316	0.1053807	0.1767158	-1.6769283	0.01162
CG8193	FBgn0033367	0.5016733	0.3643395	1.37693886	0.01177
CG6891	FBgn0030955	0.4469319	0.2563717	1.74329665	0.01187
TRAM	FBgn0029545	0.0172329	0.0580774	-3.3701559	0.01192
Prosbeta3	FBgn0026380	0.3835855	0.2685748	1.42822583	0.01224
vib	FBgn0026158	0.1681776	0.2901951	-1.7255282	0.01229
RpS3A	FBgn0002630	0.7217696	0.9042893	-1.2528781	0.01236
svr	FBgn0000521	0.0130834	0.0040156	3.25810385	0.0126
Gapdh2	FBgn0001092	1.4492779	1.2693505	1.14174763	0.01261
CG6509	FBgn0032363	0.0014692	0	Inf	0.01262
Eig71Ef	FBgn0004593	2.4865797	3.8219076	-1.5370139	0.01275
CG2950	FBgn0031637	0.0044069	0.0079593	-1.8061063	0.01294
Sh3beta	FBgn0035772	0.1132671	0.1794646	-1.5844379	0.01296
RpII140	FBgn0003276	0.0004564	0.0028122	-6.161828	0.01298
CG6084	FBgn0036182	0.3765227	0.2285323	1.64756879	0.013
Ance	FBgn0012037	0.1249389	0.0596626	2.09408883	0.01309
Aats-arg	FBgn0027093	0.0143327	0.0391575	-2.7320333	0.01311
Dhpr	FBgn0035964	0.2781659	0.2135651	1.30248782	0.01314
CG7059	FBgn0038957	0.0502737	0.1067612	-2.1235976	0.01349
Mf	FBgn0038294	0.3464811	0.2289793	1.51315488	0.01353
CG42233	FBgn0039880	0.0008334	0.0046003	-5.5197736	0.01359

CG9149	FBgn0035203	0.0374791	0.0644298	-1.7190835	0.01368
CG9338	FBgn0032899	0.1105856	0	Inf	0.01389
RpL18	FBgn0035753	0.381018	0.5018113	-1.3170277	0.01411
ade5	FBgn0020513	0.0938656	0.0654605	1.43392859	0.01413
CG3604	FBgn0031562	0.0044284	0.037747	-8.5238365	0.01424
CrebB-17A	FBgn0004972	0.0080102	0	Inf	0.01431
CG5642	FBgn0036258	0.0628572	0.0999098	-1.589473	0.01441
CG3909	FBgn0027524	0.0372843	0.0180333	2.0675308	0.01448
CG32679	FBgn0052679	0.0727221	0.1487561	-2.0455405	0.01461
Idgf1	FBgn0020416	0.0264352	0.0067006	3.94518559	0.01464
CG11255	FBgn0036337	0.0553579	0.0316942	1.74662485	0.01467
CG6783	FBgn0025540	0.4653372	0.7318657	-1.5727641	0.01477
CG30185	FBgn0027712	0.0425706	0.0867739	-2.0383538	0.01478
betaCop	FBgn0008635	0.1369926	0.2109902	-1.5401576	0.0149
Stim	FBgn0045073	0.0201555	0.0143241	1.40709819	0.01503
Mov34	FBgn0002787	0.3707142	0.2585167	1.43400501	0.01509
Pfk	FBgn0003071	0.0456652	0.068969	-1.5103198	0.01516
RpS16	FBgn0034743	0.5759677	0.7200803	-1.2502094	0.01537
His3.3B	FBgn0004828	0.2318552	0.0618018	3.75159106	0.01545
His3.3A	FBgn0004828	0.2318552	0.0618018	3.75159106	0.01545
l(2)tid	FBgn0002174	0.0010322	0.0071451	-6.9225138	0.01545
CG1665	FBgn0033451	0.0145459	0.0027015	5.38441399	0.01548
mRpS16	FBgn0033907	0.0581609	0.0323142	1.79985727	0.01549
Prosbeta5	FBgn0029134	0.1521716	0.0826977	1.84009341	0.0156
CG5515	FBgn0039163	0.0088414	0.0245066	-2.7718054	0.01571
CG3321	FBgn0025554	0.2581784	0.1762955	1.46446442	0.01571
CG4658	FBgn0032170	0.0010204	0.0057018	-5.587876	0.01572
CG4069	FBgn0036301	0.001187	0.008203	-6.9104922	0.01592
Idgf2	FBgn0020415	0.1414409	0.0729304	1.93939467	0.01613
CG3473	FBgn0028913	0.0302593	0.0106433	2.84303918	0.01615
Hex-A	FBgn0001186	0.0533608	0.0914112	-1.7130784	0.0162
bocksbeutel	FBgn0037719	0.0015307	0.010331	-6.7491069	0.0163
Trxr-1	FBgn0020653	0.3170936	0.2564516	1.23646572	0.01634
Bj1	FBgn0002638	0.0414956	0.0656746	-1.5826892	0.01638
vkg	FBgn0010477	0.0408942	0.0316671	1.29137686	0.01642
sqd	FBgn0003498	0.1560198	0.2478736	-1.5887318	0.01648
CG4151	FBgn0029770	3.1805094	4.1444161	-1.3030668	0.01649
nimB2	FBgn0027908	0.0944287	0.0336712	2.80443156	0.01666
CG12079	FBgn0035404	0.1757424	0.1164193	1.50956412	0.01673
CG7272	FBgn0036501	0.0251051	0.0397717	-1.5842082	0.01677
CG1578	FBgn0030336	0.0054035	0.0010432	5.17976412	0.01686
Eig71Eb	FBgn0004589	1.0603557	1.471534	-1.3877739	0.01698

SdhB	FBgn0014028	0.121268	0.0759073	1.59757935	0.01699
CG1236	FBgn0037370	0.1461093	0.1688199	-1.1554356	0.01699
eIF-2beta	FBgn0004926	0.0739574	0.107371	-1.4517947	0.01726
CG17224	FBgn0031489	0.0179215	0	Inf	0.01731
CG32016	FBgn0039933	0.0006161	0.0043886	-7.123331	0.01731
Ahcy13	FBgn0014455	0.1401804	0.2094678	-1.4942731	0.01737
CG12321	FBgn0038577	0.08524	0.0566537	1.50457823	0.01755
CG33498	FBgn0053498	0.0661686	0.0393722	1.68058876	0.01756
fau	FBgn0020439	0.016911	0.0074688	2.2642211	0.01761
eRF1	FBgn0010710	0.2908291	0.3823222	-1.3145942	0.01769
Osbp	FBgn0020626	0.0232079	0.0323436	-1.3936428	0.01774
miple2	FBgn0029002	0.0153238	0	Inf	0.01784
Amun	FBgn0030328	0.0302381	0.0145317	2.08082886	0.01791
CG11854	FBgn0039299	0.0598868	0.0212904	2.81285275	0.01798
CG10853	FBgn0035478	0.7977119	1.2866833	-1.6129674	0.01802
Sop2	FBgn0001961	0.0542638	0.0361178	1.5024086	0.0183
CG6523	FBgn0032509	0.1306362	0.1773867	-1.3578675	0.01904
CG4764	FBgn0031310	0.0995063	0.071593	1.38988987	0.01904
Dph5	FBgn0024558	0.0267572	0.0049003	5.46033313	0.01909
Tudor-SN	FBgn0035121	0.4425416	0.512739	-1.1586234	0.01913
dco	FBgn0002413	0.0023673	0.0093522	-3.9505274	0.01914
CG12119	FBgn0030102	0.0016169	0.0160291	-9.9133853	0.01918
Nsf2	FBgn0013998	0.0322768	0.0521861	-1.6168327	0.01918
CG7054	FBgn0038972	0.0208744	0	Inf	0.01921
Tim10	FBgn0027360	0.0058339	0.0295945	-5.0728207	0.01924
Trip1	FBgn0015834	0.190449	0.2188515	-1.1491342	0.01947
yrt	FBgn0000466	0.0038737	0.0009446	4.10072652	0.0197
dp	FBgn0000488	0.0001616	0	Inf	0.0198
CG9021	FBgn0031747	0.0343618	0.0082183	4.18115415	0.01991
CG10420	FBgn0039296	0.0091492	0.025283	-2.7634198	0.02
CD98hc	FBgn0037533	0.0142599	0.0368504	-2.5842011	0.02002
cyp33	FBgn0028382	0.002014	0.0100895	-5.0096544	0.02003
Gal	FBgn0001089	0.0185577	0.0070882	2.61811008	0.02052
SmB	FBgn0010083	0.1433398	0.0821858	1.74409446	0.02062
Arp66B	FBgn0011744	0.1313764	0.0568199	2.31215568	0.02074
CG11009	FBgn0036318	0.0160182	0.0258969	-1.6167156	0.02085
Int6	FBgn0010945	0.175063	0.245977	-1.4050771	0.02091
CAH1	FBgn0027844	0.057991	0.0130999	4.4268266	0.02097
CG30291	FBgn0034571	0.0734957	0.1074695	-1.4622569	0.02132
Cortactin	FBgn0025865	0.0163194	0.0076817	2.12444939	0.0214
zf30C	FBgn0019699	0.0006957	0.0034168	-4.9110759	0.02153
CG8636	FBgn0029629	0.1679118	0.2367224	-1.4098025	0.02198

eIF4G	FBgn0023213	0.0392641	0.0828633	-2.1104076	0.0223
Act42A	FBgn0000043	2.7736297	2.1201603	1.30821696	0.02245
CG8243	FBgn0033349	0.0065646	0.0134254	-2.0451339	0.02258
RpL9	FBgn0015756	0.4778586	0.632372	-1.3233456	0.02278
CG10635	FBgn0035603	0.0042359	0.0276057	-6.5171353	0.0229
RpL23	FBgn0010078	1.0319153	1.4239069	-1.3798679	0.02317
CG12224	FBgn0037974	0.014642	0.0105413	1.38901613	0.02351
CaBP1	FBgn0025678	0.2956177	0.4519591	-1.5288637	0.02355
Chd64	FBgn0025973	1.500983	1.2040168	1.24664622	0.02356
CG13059	FBgn0036607	0.022355	0	Inf	0.02364
Hsp67Bb	FBgn0001228	0.0863325	0.0331895	2.60119929	0.0237
MP1	FBgn0027930	0.0618685	0.0370286	1.67083086	0.02373
CG2034	FBgn0015359	0.0169066	0.0034649	4.87943613	0.0238
GalNAc-T2	FBgn0030930	0.0513131	0.0867969	-1.6915146	0.02388
Gip	FBgn0011770	0.1897306	0.1252762	1.51449879	0.02389
CG12171	FBgn0037354	0.3042666	0.2369562	1.28406281	0.02411
fog	FBgn0000719	0.0008367	0.0040583	-4.8506771	0.02416
Sod2	FBgn0010213	0.2905887	0.2033101	1.4292877	0.02432
Act5C	FBgn0000042	2.8957664	2.2053774	1.31304796	0.02435
pgant5	FBgn0031681	0.018135	0.0343268	-1.8928502	0.02444
levy	FBgn0034877	0.1898898	0.1022552	1.85701863	0.02446
MAPk-Ak2	FBgn0013987	0.0142238	0.021292	-1.4969291	0.02476
Klp10A	FBgn0030268	0.0106449	0.003164	3.36433455	0.0248
Nup214	FBgn0010660	0.0003368	0.001631	-4.8426479	0.02493
RpS15Aa	FBgn0010198	0.4727971	0.6900145	-1.4594304	0.025
scb	FBgn0003328	0.0138835	0.0042208	3.28933724	0.02505
CG5976	FBgn0036999	0.0191517	0.0388349	-2.0277548	0.02513
CG1486	FBgn0031174	0.0565984	0.0888793	-1.5703509	0.02532
Hsp83	FBgn0001233	0.6736434	0.8119748	-1.2053482	0.02551
Est-6	FBgn0000592	0.0167118	0.008592	1.9450351	0.02556
Rab2	FBgn0014009	0.0287647	0.0627324	-2.1808813	0.0256
CG6900	FBgn0030958	0.3049765	0.131499	2.31923094	0.02561
LanB2	FBgn0002528	0.0347162	0.0251067	1.38274902	0.02572
Eb1	FBgn0010578	0.1680249	0.2220885	-1.3217595	0.02586
Idgf5	FBgn0034333	0.0265851	0.0019384	13.7149934	0.02587
Sec61alpha	FBgn0019697	0.11458	0.1385197	-1.208934	0.02624
exba	FBgn0010791	0.0708211	0.0943647	-1.3324368	0.02645
CG9186	FBgn0035206	0.0134729	0.0317122	-2.3537784	0.02649
lap	FBgn0011467	0.0055536	0.0151148	-2.7216173	0.02656
Rab8	FBgn0015796	0.0799281	0.0877348	-1.0976718	0.02669
Top2	FBgn0003732	0.0069347	0.0146274	-2.1092867	0.02675
Got2	FBgn0001125	0.3619674	0.3045753	1.18843313	0.02702

CG6463	FBgn0036100	0.1850309	0.1077581	1.71709611	0.02726
CG2846	FBgn0014930	0.0387723	0.0213801	1.81347718	0.02729
Aats-ala	FBgn0027094	0.0786313	0.13062	-1.66117	0.02735
da	FBgn0000413	0.0043413	0.0009699	4.4760057	0.02738
Ccp84Ab	FBgn0004782	0.0191574	0.003116	6.14809114	0.02747
Ccp84Aa	FBgn0004783	0.0206526	0.0033592	6.14809114	0.02747
slgA	FBgn0003423	0.0079939	0.0158281	-1.980014	0.02749
wibg	FBgn0027071	0.0029822	0.0139841	-4.6892015	0.02751
CG11980	FBgn0037652	0.0856182	0.1130802	-1.3207498	0.0276
Ance-4	FBgn0033366	0.0173495	0	Inf	0.02765
CG6950	FBgn0037955	0.0200984	0.0394306	-1.9618808	0.02773
pen	FBgn0015527	0.0007283	0.0035966	-4.9386448	0.02781
CdsA	FBgn0010350	0.0112392	0.0020309	5.5342034	0.02797
Npc2a	FBgn0031381	0.1774176	0.264313	-1.4897787	0.02811
Rab6	FBgn0010648	0.0626282	0.1015355	-1.6212412	0.02824
Eig71Eg	FBgn0004594	1.1726083	1.973689	-1.6831614	0.02835
Spase22-23	FBgn0039172	0.0943294	0.1533415	-1.6255956	0.02845
La	FBgn0011638	0.0599175	0.0941677	-1.5716226	0.02846
CG5276	FBgn0037900	0.001442	0.0076708	-5.3195464	0.02847
Lsd-2	FBgn0030608	0.0703806	0.0385332	1.82649106	0.02859
Edem2	FBgn0032480	0.0014255	0.0053152	-3.728655	0.02861
Mtch	FBgn0027786	0.0345961	0.0592242	-1.7118756	0.02887
TfIIFbeta	FBgn0010421	0.0021812	0.0100612	-4.6126177	0.02914
wol	FBgn0032012	0.0289908	0.0447837	-1.5447575	0.02935
CG31698	FBgn0051698	0.6834394	0.2509088	2.72385574	0.02937
CG9536	FBgn0031818	0.0011927	0.0056601	-4.7455724	0.02952
CG7580	FBgn0036728	0.0615283	0.1327275	-2.1571769	0.0298
CG5325	FBgn0032407	0.0302732	0.0625213	-2.0652335	0.03011
CG17024	FBgn0032437	0.0108682	0.0044771	2.42753008	0.03059
Plap	FBgn0024314	0.0183393	0.0303423	-1.6544943	0.03076
CG5149	FBgn0031904	0.003703	0.0097126	-2.6229034	0.03085
CG17896	FBgn0023537	0.2562068	0.3192299	-1.2459852	0.03086
RpL10Ab	FBgn0026276	0.3496665	0.5137713	-1.4693183	0.03111
nop5	FBgn0022271	0.0218764	0.0460343	-2.1042835	0.03138
Aldh-III	FBgn0010548	0.05695	0.0727078	-1.2766956	0.03148
CCS	FBgn0010531	0.0393571	0.0207479	1.89692251	0.03169
me31B	FBgn0004419	0.0270389	0.0621417	-2.2982362	0.03176
Mdh	FBgn0027671	0.0134	0.0225254	-1.681002	0.03222
Lcp1	FBgn0002531	0.0569675	0.0423819	1.34414773	0.03248
Rpt3	FBgn0026699	0.276956	0.246027	1.12571375	0.03294
nec	FBgn0002930	0.012874	0	Inf	0.03331
CG5869	FBgn0028894	0.1055489	0.0610859	1.72787755	0.0335

Eig71Ei	FBgn0014849	0.3138849	0.1599279	1.96266477	0.03377
CG7300	FBgn0032286	0.0232361	0	Inf	0.03412
CG12163	FBgn0037303	0.027009	0.0146757	1.84039496	0.03418
RpS13	FBgn0010265	0.372753	0.461428	-1.237892	0.03455
CG3397	FBgn0037975	0.0291386	0.0115783	2.51665066	0.03459
Lis-1	FBgn0015754	0.0014021	0.0065275	-4.6556345	0.03495
CG6236	FBgn0038318	0.0059087	0	Inf	0.03502
Rad23	FBgn0026777	0.0799029	0.1217599	-1.5238472	0.03506
CG17278	FBgn0040577	0.0398815	0	Inf	0.03533
CG4752	FBgn0034733	0.0050642	0.0025611	1.97735351	0.03535
Hsc70-2	FBgn0001217	0.084534	0.1076248	-1.2731543	0.03553
CG10623	FBgn0032727	0.1954337	0.1573497	1.24203367	0.03555
torp4a	FBgn0025615	0.0160689	0.0027015	5.94820869	0.03562
LysB	FBgn0004425	0.0142129	0.0337678	-2.3758586	0.03589
LysC	FBgn0002575	0.0142129	0.0337678	-2.3758586	0.03589
LysA	FBgn0002575	0.0142129	0.0337678	-2.3758586	0.03589
CG15743	FBgn0030465	0.0081208	0.0193516	-2.382965	0.03594
CG11893	FBgn0039316	0.0464472	0	Inf	0.036
Aats-ile	FBgn0010728	0.0098661	0.0220616	-2.2361039	0.03615
Trx-2	FBgn0032134	0.3083916	0.1645218	1.87447264	0.03626
Mo25	FBgn0010713	0.1332678	0.0981004	1.35848347	0.03646
CG7215	FBgn0038571	0.0881164	0.0347944	2.53249038	0.03709
CG1832	FBgn0032979	0.004457	0.0012167	3.66328276	0.03711
CG30120	FBgn0050120	0.0013061	0.0056766	-4.3460532	0.03716
Rab1	FBgn0016700	0.1522388	0.2114432	-1.3888913	0.03719
serp	FBgn0036902	0.0581614	0.0398955	1.45784387	0.03729
CG31997	FBgn0043807	0.10015	0.0391635	2.5572298	0.03738
CG1316	FBgn0035526	0.0052779	0.0141731	-2.6853718	0.03749
AnnX	FBgn0000084	0.1986311	0.1371738	1.44802537	0.03762
CG10881	FBgn0038796	0.0542077	0.0712284	-1.3139905	0.03765
CG7967	FBgn0035251	0.0190531	0.0101033	1.88581878	0.03785
CG31352	FBgn0037733	0.0204743	0.0105206	1.94611309	0.03786
unc-115	FBgn0037733	0.0204743	0.0105206	1.94611309	0.03786
Rpd3	FBgn0003632	0.0075086	0.0121175	-1.6138089	0.03788
His2B	FBgn0053868	0.5197369	0.7760122	-1.4930866	0.03819
His2B:CG17949	FBgn0053868	0.5197369	0.7760122	-1.4930866	0.03819
EndoGI	FBgn0027856	0.163885	0.2298902	-1.4027528	0.03828
CG4802	FBgn0034215	0.0330294	0.0535438	-1.6210967	0.03838
CG32479	FBgn0035172	0.0052125	0.0094892	-1.8204583	0.03842
MESR6	FBgn0036846	0.0523042	0.0389613	1.34246399	0.03873
CG9231	FBgn0036887	0.0138562	0.04011	-2.8947266	0.03875

WASp	FBgn0024273	0.0068579	0.0104488	-1.5236117	0.03897
CLIP-190	FBgn0020503	0.0115315	0.0050925	2.26442481	0.03923
CG18135	FBgn0036837	0.0106501	0.0029259	3.63992732	0.0398
Hsc70Cb	FBgn0010707	0.3172823	0.2551987	1.24327523	0.03983
Thiolase	FBgn0010464	0.2294575	0.1992372	1.15167981	0.04007
Chc	FBgn0000319	0.1730756	0.1352128	1.28002355	0.04022
mal	FBgn0002641	0.0035717	0.0008817	4.05076325	0.04034
CG10467	FBgn0035679	0.0764639	0.055638	1.37430961	0.04044
CG17737	FBgn0025534	0.2252457	0.3854581	-1.7112785	0.04119
CG12279	FBgn0038080	0.2437014	0.1745318	1.39631554	0.04123
Adk1	FBgn0022709	0.0201429	0.0041045	4.90756523	0.04143
Spn27A	FBgn0028990	0.0393472	0.0129361	3.04164518	0.04169
ND23	FBgn0017567	0.1478596	0.120125	1.23088114	0.04181
CG7564	FBgn0036734	0.0144589	0.0032792	4.40927408	0.04189
RpL13	FBgn0011272	0.4547812	0.5787856	-1.2726683	0.04214
Fer1HCH	FBgn0010717	0.7618739	0.4877683	1.56195858	0.04232
CG14876	FBgn0038368	0.0015433	0.0097305	-6.3050524	0.04244
CG17273	FBgn0027493	0.1102689	0.1466763	-1.3301692	0.04307
CG5028	FBgn0039358	0.0635311	0.0827328	-1.3022407	0.04308
GS	FBgn0030882	0.168735	0.120151	1.40435846	0.0431
Lcp65Ag2	FBgn0002539	0.1216613	0.0613178	1.9841118	0.04315
Lcp65Ag1	FBgn0002539	0.1216613	0.0613178	1.9841118	0.04315
Gel	FBgn0010225	0.2140856	0.1480371	1.44616209	0.04318
Neurochondrin	FBgn0037447	0.0106423	0.0042217	2.52085968	0.0434
CG2021	FBgn0035271	0.1064774	0.0271814	3.91728736	0.04363
CG16704	FBgn0031558	0.10216	0.0669819	1.52518872	0.04365
Adk3	FBgn0037854	0.0450644	0.018633	2.41852888	0.04373
Acer	FBgn0016122	0.0099746	0.0040089	2.4880879	0.04393
und	FBgn0025117	0.0234699	0.0392606	-1.6728104	0.04397
eIF-5A	FBgn0010483	0.7686709	0.881809	-1.1471866	0.04411
AGO1	FBgn0010586	0.0014025	0.005265	-3.7539024	0.04421
Gdh	FBgn0001098	0.2866567	0.3649959	-1.2732861	0.04427
Abi	FBgn0020510	0.0047866	0.0014559	3.28772559	0.04438
Bap	FBgn0010380	0.0318216	0.0469866	-1.4765651	0.04452
Cda4	FBgn0031198	0.0415503	0.0143537	2.89473685	0.04461
Lcp9	FBgn0025578	0.0427627	0	Inf	0.04483
MESR3	FBgn0032694	0.0113799	0.0214848	-1.887967	0.04507
Aly	FBgn0010774	0.0352522	0.0525243	-1.4899584	0.04513
CG9603	FBgn0040529	0.3024818	0.1931048	1.56641264	0.04529
Cpr49Ac	FBgn0033725	0.0997095	0.0745688	1.33714757	0.04569
Adk2	FBgn0022708	0.127725	0.188735	-1.4776662	0.0457

PH4alphaSG2	FBgn0039779	0.2102237	0.0948861	2.21553655	0.04575
PGRP-SB2	FBgn0036657	1.4601348	2.2211518	-1.5211964	0.04583
CG30022	FBgn0033632	0.0063553	0.0164941	-2.5953367	0.04599
l(1)G0222	FBgn0028328	0.0023263	0.0065779	-2.8275463	0.04608
CG1837	FBgn0027709	0.1884489	0.1442608	1.30630777	0.04669
CG10932	FBgn0029969	0.2230988	0.2962509	-1.3278911	0.04678
CG9099	FBgn0030802	0.0347501	0.075593	-2.1753287	0.04696
Gtp-bp	FBgn0010391	0.0839851	0.1239338	-1.475665	0.04769
Ice	FBgn0019972	0.0145969	0.0054821	2.66267088	0.04777
Actn	FBgn0000667	0.2257236	0.2549734	-1.1295828	0.0478
CG9588	FBgn0038166	0.010522	0.0199879	-1.8996318	0.04807
Osi7	FBgn0037414	0.0041216	0.0190072	-4.6116551	0.04816
CG14526	FBgn0027578	0.0343889	0.0138487	2.48319174	0.04818
Spn5	FBgn0028984	0.0328656	0.0092486	3.55356461	0.04849
CG6151	FBgn0036533	0.0132602	0.0321929	-2.4277804	0.04904
Jafrac1	FBgn0030472	0.4154262	0.3723704	1.11562632	0.04956
bnb	FBgn0001090	0.1566558	0.0685084	2.28666612	0.04968
CG12065	FBgn0030052	0.0083964	0.001611	5.21188368	0.04982
CG8042	FBgn0027554	0.0021919	0.006222	-2.8386777	0.05011
Eig71Ed	FBgn0004591	2.0407558	3.0256988	-1.4826364	0.05015
Vps20	FBgn0027684	0.0101015	0.0285317	-2.8244836	0.05023
CG6255	FBgn0038708	0.0362909	0.0215552	1.68362372	0.05061
Cht5	FBgn0038180	0.0888742	0.0540801	1.64338303	0.05067
CG6412	FBgn0032646	0.031572	0.0130276	2.42347768	0.05088
Hel25E	FBgn0001929	0.2444483	0.3056586	-1.2504018	0.05097
Atox1	FBgn0037112	0.1310055	0.2072277	-1.5818249	0.05102
CG7375	FBgn0035853	0.0316294	0.0583465	-1.8446948	0.05127
U2A	FBgn0004136	0.0021745	0.0131584	-6.0511588	0.0513
CG10672	FBgn0035588	0.0136927	0.0032576	4.20329575	0.05161
CG5862	FBgn0038868	0.0214784	0.0330606	-1.539249	0.05169
CG32230	FBgn0047088	0.4932323	0.3500749	1.40893358	0.05171
CG11883	FBgn0033538	0.0025043	0	Inf	0.05234
PNUTS	FBgn0031291	0.0028446	0	Inf	0.05239
Dhc36C	FBgn0013810	0.001136	0.0020763	-1.8276609	0.05239
Rat1	FBgn0031868	0.0051984	0	Inf	0.05245
CG31688	FBgn0032861	0.002759	0	Inf	0.05256
CG8939	FBgn0030720	0.0020777	0	Inf	0.05262
CG31678	FBgn0032874	0.0010599	0	Inf	0.05295
CG3626	FBgn0029706	0.0018376	0	Inf	0.05296
CG13847	FBgn0038967	0.0022674	0	Inf	0.05296
dlg1	FBgn0001624	0.0245231	0.0101401	2.41844049	0.05312
CG7470	FBgn0037146	0.0238442	0.0076911	3.10021537	0.05318

CG6026	FBgn0038676	0.001091	0	Inf	0.05319
hpo	FBgn0034453	0.0025988	0	Inf	0.05323
CG18522	FBgn0038347	0.004906	0.0007384	6.64458629	0.05331
CG3402	FBgn0035148	0.013221	0	Inf	0.05336
Adgf-A	FBgn0036752	0.005065	0.0012453	4.06740525	0.05339
CG32354	FBgn0035893	0.0026263	0	Inf	0.05345
Cpr31A	FBgn0032177	0.0101421	0	Inf	0.0535
CG11137	FBgn0037199	0.010642	0	Inf	0.05352
CG5991	FBgn0026576	0.00399	0	Inf	0.05352
dj-1beta	FBgn0039802	0.0929273	0.0570107	1.62999771	0.0537
Nop60B	FBgn0022178	0.0253256	0.0491124	-1.939244	0.05375
RpS25	FBgn0010413	0.7500604	0.647051	1.15919825	0.05385
CG3756	FBgn0031657	0.0049424	0	Inf	0.05402
CG15201	FBgn0030272	0.0149881	0	Inf	0.05405
CG5001	FBgn0031322	0.0069777	0	Inf	0.05405
Rpn2	FBgn0028692	0.1130425	0.0919497	1.22939467	0.05417
CG6912	FBgn0038290	0.0038161	0	Inf	0.05428
CG14291	FBgn0038660	0.0032964	0	Inf	0.05465
SamDC	FBgn0014220	0.0048048	0	Inf	0.05491
CG1951	FBgn0039623	0.0019967	0	Inf	0.05491
loj	FBgn0010829	0.0070349	0	Inf	0.05491
CG3987	FBgn0038292	0.0068984	0.0017045	4.04709109	0.05519
Tim9a	FBgn0030480	0.0723716	0.0535002	1.35273504	0.05533
GstD2	FBgn0010038	0.2001383	0.0086438	23.1539151	0.05574
CG11334	FBgn0039849	0.0631515	0.0390439	1.61744933	0.05583
Aats-gln	FBgn0010867	0.0488221	0.0644839	-1.3207925	0.05684
Scsalpha	FBgn0004888	0.4186888	0.3437103	1.21814441	0.05722
NTPase	FBgn0024947	0.0297012	0.0577811	-1.94541	0.05743
Pak	FBgn0014001	0.0053457	0.0014669	3.6443497	0.05743
CG8891	FBgn0031663	0.041309	0.0213151	1.93801413	0.05751
snRNP2	FBgn0037434	0.08456	0.0610712	1.38461518	0.05755
CG7946	FBgn0039743	0.0102866	0.0163119	-1.5857435	0.05778
CG18417	FBgn0035780	0.0082554	0.0020508	4.02552504	0.05798
CG14199	FBgn0040890	0.0081649	0.0459636	-5.6294384	0.05827
Peritrophin-A	FBgn0022770	0.0086164	0	Inf	0.05875
CG6188	FBgn0038074	0.0155794	0.037781	-2.425059	0.05914
Uch-L3	FBgn0011327	0.102307	0.0739733	1.38302626	0.0594
CG31639	FBgn0011327	0.102307	0.0739733	1.38302626	0.0594
CG15118	FBgn0025243	0.0054972	0.0013926	3.94731787	0.05942
snRNP69D	FBgn0016940	0.0464735	0.1032536	-2.2217748	0.0595
Pbgs	FBgn0036271	0.011436	0.0231789	-2.0268365	0.05996
nonA-l	FBgn0015520	0.0017666	0.0046968	-2.6586117	0.06045

obst-E	FBgn0031737	0.0164338	0.0040759	4.03191385	0.06046
caz	FBgn0003059	0.0142945	0.0267543	-1.8716516	0.06066
Mp20	FBgn0002789	0.6572333	0.4307983	1.52561712	0.06077
CG11423	FBgn0034251	0.0027855	0	Inf	0.06082
CG31313	FBgn0047056	0.1701228	0.1006059	1.69098192	0.06092
TwdlBeta	FBgn0033658	0.0360019	0.0152553	2.35995122	0.0611
gammaCop	FBgn0028968	0.2378923	0.3161552	-1.3289844	0.0617
chic	FBgn0000308	0.831248	0.6986145	1.18985226	0.06191
CG7265	FBgn0038272	0.0041787	0	Inf	0.06199
eIF2B-beta	FBgn0024996	0.009874	0.0024877	3.96910452	0.06206
ebi	FBgn0021820	0.0049652	0.001251	3.96908961	0.06217
CG10882	FBgn0031408	0.1350232	0.1919318	-1.4214728	0.06228
CHORD	FBgn0029503	0.0153843	0.0224932	-1.4620875	0.06234
Nhe1	FBgn0026787	0	0.002814	-Inf	0.06236
Aats-leu	FBgn0027085	0	0.0019981	-Inf	0.06237
Cyp6d2	FBgn0034756	0	0.0033913	-Inf	0.06237
Trn	FBgn0024921	0.0097006	0.0041656	2.32873248	0.0624
TpnC4	FBgn0033027	0	0.0117266	-Inf	0.06251
CG16837	FBgn0035009	0	0.0138013	-Inf	0.06251
Cpr60D	FBgn0035045	0.05738	0.0192922	2.97425885	0.06296
a10	FBgn0010402	0	0.0127263	-Inf	0.06296
Orct	FBgn0019952	0	0.0035996	-Inf	0.06296
Nup107	FBgn0027868	0	0.0023344	-Inf	0.06296
Cypl	FBgn0035141	0	0.0112079	-Inf	0.06296
CG13457	FBgn0036482	0	0.0019282	-Inf	0.06296
CG14609	FBgn0037483	0	0.0033042	-Inf	0.06296
nemy	FBgn0033765	0.0027583	0	Inf	0.06297
CG16892	FBgn0030122	0	0.0042793	-Inf	0.06326
CG5265	FBgn0038486	0	0.0031014	-Inf	0.06326
Grip163	FBgn0026432	0	0.0014442	-Inf	0.0633
CG31824	FBgn0032574	0	0.00539	-Inf	0.0633
CG1702	FBgn0031117	0	0.0081669	-Inf	0.06333
Rrp4	FBgn0034879	0	0.0062485	-Inf	0.06333
CG11915	FBgn0036673	0	0.0026831	-Inf	0.06333
LanB1	FBgn0002527	0.0195225	0.0118911	1.64177356	0.06338
ogre	FBgn0000265	0	0.0053604	-Inf	0.0635
capt	FBgn0010632	0.3382097	0.29491	1.14682351	0.0636
RpS17	FBgn0002217	1.1557601	1.4689085	-1.2709458	0.06372
CG5177	FBgn0031908	0.3756612	0.2666243	1.40895358	0.06378
Tg	FBgn0031975	0.0040134	0.0085599	-2.132812	0.06381
regucalcin	FBgn0030362	1.1539867	0.9460171	1.21983714	0.06386
Su(var)205	FBgn0003607	0.1020672	0.0605237	1.68640041	0.06397

CG10069	FBgn0034611	0	0.0033716	-Inf	0.06423
CG4973	FBgn0038772	0	0.0053455	-Inf	0.06423
Roe1	FBgn0014877	0.0377304	0.0571225	-1.5139646	0.06426
TwdlT	FBgn0029170	0.0345597	0.0148271	2.33085051	0.06452
CG7802	FBgn0039704	0.0082712	0.0012345	6.69980723	0.06464
CG7427	FBgn0036510	0	0.0067011	-Inf	0.06472
CG15100	FBgn0025966	0.0280972	0.0429582	-1.5289168	0.06486
CG7456	FBgn0032258	0	0.0024677	-Inf	0.06518
NUCB1	FBgn0023185	0.12518	0.1866067	-1.4907068	0.06534
Ccp84Ag	FBgn0004777	0.0902088	0.0211659	4.26198925	0.0654
Fbp2	FBgn0000640	0.3667361	0.2500779	1.46648742	0.06577
Hexo1	FBgn0035527	0.013088	0.0032197	4.06493312	0.06581
CG6443	FBgn0032290	0	0.0052318	-Inf	0.06632
alphaCop	FBgn0025725	0.1942819	0.2885874	-1.4854055	0.06645
CG10962	FBgn0030072	0.0193813	0.0048392	4.00504463	0.06672
CG31012	FBgn0027598	0.0088468	0.0047853	1.84874897	0.06685
Sry-delta	FBgn0003512	0.0106483	0.0037611	2.83116699	0.06711
Lcp4	FBgn0002535	0.2388976	0.0921449	2.59262936	0.06714
CG33111	FBgn0039121	0.0046657	0	Inf	0.06754
CG30392	FBgn0034613	0.0079512	0.0168886	-2.1240255	0.06757
CG8709	FBgn0033269	0.0019329	0	Inf	0.06783
Pis	FBgn0030670	0	0.0071747	-Inf	0.06803
CG5757	FBgn0034299	0	0.0093985	-Inf	0.06803
CG13872	FBgn0034477	0	0.0026218	-Inf	0.06803
CG1607	FBgn0039844	0	0.0122682	-Inf	0.06803
CG9953	FBgn0035726	0.0079562	0.0020328	3.91391618	0.0681
wds	FBgn0001403	0.0079533	0.0019076	4.16933452	0.06877
Taf2	FBgn0011836	0	0.0013338	-Inf	0.06896
CG12404	FBgn0032465	0	0.0061688	-Inf	0.06896
CG9133	FBgn0035198	0	0.0052704	-Inf	0.06896
CG11885	FBgn0031253	0.025667	0.0048839	5.25540736	0.06914
GstD5	FBgn0010041	0.0772588	0.0086038	8.9796145	0.06924
lic	FBgn0015763	0.0050229	0.0166025	-3.3053585	0.06935
Gdi	FBgn0004868	0.4883456	0.5433126	-1.1125575	0.0694
CG1342	FBgn0039795	0.1444181	0.0976822	1.47844866	0.07003
Rab7	FBgn0015795	0.0758715	0.0991559	-1.3068926	0.07061
AP-47	FBgn0024833	0.0318743	0.058135	-1.823887	0.07085
ScpX	FBgn0015808	0.1178039	0.0907398	1.29826056	0.07086
Nelf-E	FBgn0017430	0	0.0059822	-Inf	0.07113
Pde8	FBgn0034886	0	0.0018326	-Inf	0.07113
wbl	FBgn0004003	0.0953264	0.1351706	-1.417976	0.0713
l(2)efl	FBgn0011296	0.1985774	0.0983832	2.01840811	0.0713

CSN6	FBgn0028837	0.0232617	0.0131573	1.76797732	0.07167
CG6227	FBgn0030631	0.0037858	0	Inf	0.07178
CG17255	FBgn0030205	0.004994	0.0084284	-1.6877087	0.07197
Uch	FBgn0010288	0.4252743	0.2882048	1.47559727	0.072
Ca-P60A	FBgn0004119	0.0473565	0.0680532	-1.4370392	0.07201
Lhr	FBgn0034217	0.0123571	0.0020618	5.99342822	0.07205
Nc73EF	FBgn0010352	0.0947472	0.0741456	1.27785303	0.07206
B52	FBgn0004424	0.0754348	0.0967123	-1.2820649	0.07215
Nup358	FBgn0039302	0.0040047	0.0102997	-2.5718853	0.07217
Fis1	FBgn0039969	0.0255318	0.0452015	-1.7704009	0.07235
JhI-1	FBgn0028426	0.0026641	0	Inf	0.07269
stai	FBgn0026568	0.0185892	0.014479	1.2838731	0.07293
CG6015	FBgn0038927	0	0.0039857	-Inf	0.07345
825-Oak	FBgn0052208	0.0178305	0	Inf	0.07356
CG32214	FBgn0052214	0.0194745	0	Inf	0.07356
Sas-4	FBgn0011020	0.0031668	0	Inf	0.0737
TM9SF4	FBgn0027852	0.0090138	0.0186359	-2.0674758	0.07456
CG1344	FBgn0027507	0	0.002719	-Inf	0.07458
Tsp42Ea	FBgn0029508	0	0.0077462	-Inf	0.07458
CG16721	FBgn0029820	0	0.0035281	-Inf	0.07458
CG15814	FBgn0030873	0	0.0057903	-Inf	0.07458
CG1440	FBgn0030038	0.1334768	0.1036284	1.28803267	0.0746
CG8207	FBgn0034035	0.0843633	0.0984723	-1.1672407	0.07484
CG5885	FBgn0025700	0.0449372	0.0863138	-1.9207672	0.07489
CG4998	FBgn0036612	0.0046509	0.0007729	6.01761188	0.07508
CAP	FBgn0033503	0.0071441	0.002585	2.76366356	0.07513
Amy-d	FBgn0000079	0.0087104	0.0196543	-2.2564212	0.07559
Amy-p	FBgn0000078	0.0087104	0.0196543	-2.2564212	0.07559
CG6719	FBgn0037893	0.0135372	0.0279182	-2.0623323	0.07612
how	FBgn0011379	0.0027385	0.0069798	-2.5487476	0.07684
CG17026	FBgn0036550	0.0072579	0.0161532	-2.2256172	0.07702
CG31637	FBgn0031827	0.0047528	0	Inf	0.07767
CG16936	FBgn0027590	0.1998705	0.240204	-1.201798	0.07777
CG30104	FBgn0034226	0.0284212	0.0511167	-1.7985416	0.07821
viaf	FBgn0036237	0.032818	0.0173083	1.89608394	0.07888
Sucb	FBgn0029118	0.0964368	0.0753283	1.28022085	0.07949
drk	FBgn0004638	0.1145711	0.0832322	1.37652297	0.07974
pug	FBgn0020385	0.0315075	0.0140981	2.23488257	0.0798
Ccp84Ad	FBgn0004780	0.0412684	0.0134814	3.06112626	0.07993
CG6415	FBgn0024715	0.038974	0.0247844	1.57252208	0.08007
CG11739	FBgn0037239	0.0290689	0.0120252	2.41733734	0.08011
Pros45	FBgn0020369	0.2243013	0.1834695	1.22255395	0.08037

Arp11	FBgn0031050	0.0044729	0.01353	-3.024869	0.0804
sls	FBgn0002186	0.0047468	0.0027943	1.69872192	0.08047
CG3061	FBgn0038195	0.0089055	0.0196413	-2.205528	0.08056
CG7299	FBgn0032282	0.0274319	0.0123805	2.21574307	0.08084
CG9312	FBgn0038179	0.0137807	0	Inf	0.08086
pnr	FBgn0003117	0	0.0051556	-Inf	0.08088
CG5567	FBgn0036760	0.0081123	0	Inf	0.08123
GstS1	FBgn0010226	0.1024517	0.054756	1.87105767	0.08131
Smn	FBgn0036641	0.0100977	0	Inf	0.08135
CG11882	FBgn0039642	0.0085949	0	Inf	0.08188
CG3223	FBgn0037538	0.0237417	0.012497	1.89979145	0.08211
CG4747	FBgn0026572	0.0635311	0.0857574	-1.3498507	0.08212
Ubp64E	FBgn0013225	0.0024389	0.0039447	-1.6173839	0.08238
RpS15Ab	FBgn0033555	0.3811522	0.5362415	-1.4068959	0.08262
CG4860	FBgn0037999	0.0067914	0	Inf	0.08302
simj	FBgn0010762	0.0024788	0	Inf	0.08309
CG16712	FBgn0031561	0.7866589	0.5021001	1.5667373	0.0834
eIF2B-alpha	FBgn0039726	0.0148379	0	Inf	0.08377
Pros26.4	FBgn0015282	0.1797317	0.1611899	1.1150313	0.08393
Msp-300	FBgn0001926	0.0028514	0.006763	-2.3717967	0.08434
Spn1	FBgn0028988	0.0074082	0.0023136	3.20204269	0.08476
CG13044	FBgn0036599	0.0553363	0.0269615	2.05241869	0.0849
CG1640	FBgn0030478	0.0789114	0.1042281	-1.3208238	0.08513
SmG	FBgn0030765	0.0346841	0	Inf	0.08552
CG5290	FBgn0036772	0.0033894	0	Inf	0.08621
Chit	FBgn0013763	0.5033764	0.3617405	1.39154005	0.08682
CG15828	FBgn0032136	0.0030034	0.0017713	1.6955731	0.08694
Ect4	FBgn0035834	0.0034524	0.0006911	4.99532201	0.087
Ugt	FBgn0014075	0.0497458	0.0643351	-1.293277	0.08702
Paf-AHalpha	FBgn0025809	0.1286744	0.0783904	1.6414556	0.08714
CG6859	FBgn0036484	0.0136136	0.0024414	5.57627456	0.0872
Idgf3	FBgn0020414	0.1526055	0.1066995	1.43023695	0.08753
Eig71Ea	FBgn0004588	0.8343909	1.1705814	-1.4029173	0.08819
l(1)G0334	FBgn0028325	0.1634632	0.1340103	1.21978092	0.08857
spn-E	FBgn0003483	0.0015417	0	Inf	0.08927
LamC	FBgn0010037	0.1848115	0.1425821	1.29617623	0.0896
CG4844	FBgn0022342	0.0099873	0	Inf	0.08962
CG10211	FBgn0032685	0.0062257	0.000988	6.30128363	0.08998
CG9684	FBgn0037583	0.0046836	0	Inf	0.09032
Art4	FBgn0037770	0.0041431	0	Inf	0.09049
CG32495	FBgn0052495	0.1178148	0.0806954	1.45999443	0.09058
Fs(2)Ket	FBgn0000984	0.0079913	0.0137978	-1.7265961	0.09107

GM130	FBgn0034697	0.0691275	0.089193	-1.2902673	0.09115
wdp	FBgn0034718	0.0055297	0.0017799	3.10683437	0.09163
CG15209	FBgn0027706	0.0159833	0	Inf	0.09211
DNaseII	FBgn0000477	0.0675952	0.0524834	1.28793387	0.09303
Lsd-1	FBgn0039114	0.0085765	0.0027957	3.06769055	0.0931
Vha55	FBgn0002345	0.6815945	0.7902026	-1.1593442	0.09323
CG11811	FBgn0036099	0.0195956	0.0281135	-1.4346873	0.0935
CG9932	FBgn0032469	0.0039682	0.0023562	1.68417768	0.09357
OstStt3	FBgn0011336	0.0060007	0.0102249	-1.7039526	0.09393
Cpr	FBgn0015623	0.0666662	0.0493356	1.35128021	0.09399
cib	FBgn0026084	0.906902	0.6595393	1.3750538	0.09405
Ama	FBgn0000071	0.1787733	0.1134382	1.57595342	0.09413
ImpE3	FBgn0001255	0.0070769	0	Inf	0.09426
GstD7	FBgn0010043	0.0531535	0.0228512	2.32607234	0.09442
CG5023	FBgn0038774	0.3655675	0.2951191	1.23871197	0.09516
CG5377	FBgn0038974	0.0613056	0.0233286	2.62791916	0.09531
Obp56d	FBgn0034470	0.4225978	0.2024536	2.08738073	0.09585
CG6905	FBgn0035136	0.0029369	0	Inf	0.09639
sn	FBgn0003447	0.0295312	0.0116164	2.5421956	0.0966
CG2150	FBgn0003065	0.0195877	0.0095775	2.04517928	0.09674
obst-B	FBgn0027600	0.0263832	0.0148487	1.77680283	0.09691
PH4alphaNE1	FBgn0039780	0.0517994	0.0326684	1.58561319	0.0974
Adh	FBgn0000055	1.4906126	1.2360246	1.2059732	0.09761
CG32762	FBgn0052762	2.5129517	3.6083346	-1.4358949	0.09776
14-3-3zeta	FBgn0004907	0.5011724	0.624836	-1.2467484	0.09806
CG4757	FBgn0027584	0.1109173	0.0356374	3.11238822	0.09823
Eig71Ee	FBgn0004592	0.0106657	0	Inf	0.09826
CG9782	FBgn0030763	0.0365256	0.0160454	2.27639064	0.09843
CG30410	FBgn0034848	0.0901717	0.0799396	1.12799743	0.09902
CG17271	FBgn0038829	0.1473248	0.2257565	-1.5323731	0.09916
Kif19A	FBgn0038205	0.0047965	0	Inf	0.09946
ph-d	FBgn0004860	0.001686	0	Inf	0.09955
ph-p	FBgn0003077	0.001442	0	Inf	0.09955
Nmt	FBgn0011313	0.0135645	0.0252414	-1.8608428	0.09968
CG1969	FBgn0039690	0.6561514	0.8094956	-1.2337025	0.09969
mRpS23	FBgn0051842	0.0152967	0.0046332	3.30156103	0.10028
Obp99b	FBgn0039685	5.5718159	3.6171006	1.54040942	0.10107
Arp53D	FBgn0011743	0.0368876	0.0237443	1.55353705	0.10118
bsf	FBgn0032679	0.0049658	0.0099209	-1.9978543	0.10155
Cat	FBgn0000261	0.3027696	0.2685245	1.12753072	0.1017
rin	FBgn0015778	0.0695603	0.0512663	1.35684216	0.10291
CG42232	FBgn0038434	0.0050279	0.0015835	3.1751702	0.1034

CG3847	FBgn0029867	0.0116475	0.0036244	3.21364216	0.10352
CG1907	FBgn0039674	0.0609214	0.0377829	1.61240479	0.1042
CG3505	FBgn0038250	0.0160899	0.0067542	2.38219776	0.10471
CG7834	FBgn0039697	0.2580213	0.3146598	-1.2195107	0.1048
RpS4	FBgn0011284	0.8671229	0.9940407	-1.1463666	0.10483
CG2911	FBgn0037350	0.0151472	0	Inf	0.1049
CG1753	FBgn0031148	0.0049655	0.0079372	-1.5984651	0.10502
CG8547	FBgn0033919	0.0048955	0.0096676	-1.9748076	0.10508
CG7519	FBgn0037087	0.0254713	0.0449276	-1.7638548	0.1051
CG32267	FBgn0052267	0.0232841	0.0548356	-2.3550636	0.10545
CG17244	FBgn0039031	0.0328997	0.0066305	4.96186476	0.10595
Rpt6R	FBgn0039788	0.1341718	0.1078538	1.24401574	0.10604
NELF-A	FBgn0038872	0.0018563	0.0007	2.65198305	0.10675
CG7196	FBgn0031944	0.0053234	0	Inf	0.10695
Stam	FBgn0027363	0.0307906	0.01847	1.66705934	0.1079
CG42388	FBgn0030076	0.0357894	0.0179794	1.99057201	0.10804
CG6020	FBgn0037001	0.0771259	0.0626458	1.2311416	0.10828
CG10565	FBgn0037051	0.0058457	0.011055	-1.8911509	0.10897
p115	FBgn0026701	0.0286411	0.0455849	-1.591593	0.10927
ana1	FBgn0039206	0.0033582	0.0008434	3.98154456	0.10986
His3	FBgn0051613	0.3277889	0.0558495	5.86914907	0.11053
PGRP-SA	FBgn0030310	0.0409329	0	Inf	0.1107
primo-1	FBgn0038174	0.0319793	0.0196953	1.6237031	0.11071
CG17202	FBgn0038043	0.0143747	0.0200346	-1.3937391	0.11072
CG30069	FBgn0033909	0.0249585	0.0184783	1.35069039	0.11103
path	FBgn0036007	0	0.0059383	-Inf	0.11111
Nurf-38	FBgn0016687	0.3237243	0.3527729	-1.0897326	0.11164
CG9257	FBgn0032916	0.0078863	0.014143	-1.7933495	0.11185
CG4300	FBgn0036272	0.0123357	0.0192919	-1.5639169	0.11238
PR2	FBgn0013955	0	0.0026929	-Inf	0.1125
CG18815	FBgn0027720	0.1636612	0.1285541	1.27309138	0.11259
CG12262	FBgn0035811	0.1228295	0.1004449	1.22285378	0.11266
CG6904	FBgn0038293	0.010635	0.0041938	2.53587883	0.11318
fh	FBgn0030092	0.0122557	0	Inf	0.11336
ftz-f1	FBgn0001078	0.0011303	0.0048261	-4.269829	0.11341
epsilonCOP	FBgn0027496	0.2547974	0.2966363	-1.1642046	0.1135
Crk	FBgn0024811	0.0284469	0.0216803	1.31210666	0.11386
bl	FBgn0010589	0.0472601	0.0293061	1.61263373	0.11438
Uev1A	FBgn0035601	0.0990065	0.1389805	-1.4037506	0.11443
PRL-1	FBgn0024734	0.0252127	0.0365867	-1.4511192	0.11503
CG5590	FBgn0039537	0.0671238	0.0507037	1.3238456	0.11584
RpL7A	FBgn0014026	0.7331665	0.6372209	1.15056887	0.11622

14-3-3epsilon	FBgn0011329	0.6276672	0.7259543	-1.1565911	0.1163
Gl	FBgn0001108	0.0072287	0.0056998	1.26825114	0.11635
CG6287	FBgn0032350	0.1937007	0.1768056	1.09555733	0.11654
CG9689	FBgn0030159	0.0372319	0.0090422	4.11755705	0.1166
Drp1	FBgn0005566	0.0374657	0.0521077	-1.3908094	0.11702
Akap200	FBgn0027932	0.1197225	0.1001987	1.19485059	0.11733
gammaSnap	FBgn0028552	0.015076	0.0236367	-1.5678394	0.11798
Sgs3	FBgn0003373	0.2500245	0.351177	-1.4045704	0.11816
t	FBgn0030106	0.006653	0.0023734	2.80316171	0.1184
dally	FBgn0010889	0.003639	0.0013988	2.60146351	0.11867
CG31367	FBgn0037438	0.0057381	0.0022057	2.60146351	0.11867
Srp14	FBgn0038808	0.0653395	0.0507003	1.2887413	0.11879
GNBP3	FBgn0035939	0.0401653	0.0216545	1.85482807	0.11949
CG32638	FBgn0052638	0.0594541	0.023069	2.57723393	0.11961
CG17065	FBgn0031099	0.0095979	0.0033028	2.90599835	0.12025
CG4042	FBgn0037018	0.0180398	0.0094611	1.90673594	0.12167
ImpE1	FBgn0001253	0.0108513	0.0060353	1.79795545	0.12196
CG15239	FBgn0029681	0.0203737	0.0068396	2.97877866	0.12222
Vha100-2	FBgn0027516	0.006764	0.0031217	2.1667534	0.12229
comt	FBgn0000346	0.004526	0.0095727	-2.1150206	0.12329
CkIalpha	FBgn0015024	0.0035858	0.0123366	-3.4404523	0.12382
l(1)G0255	FBgn0027231	0.0903742	0.0645493	1.40008016	0.12394
Qm	FBgn0024733	0.6151363	0.7893182	-1.2831598	0.12395
Pros28.1	FBgn0004066	0.2302884	0.2130196	1.0810666	0.12439
sec63	FBgn0035771	0.0140302	0.0266157	-1.897034	0.12449
CG14419	FBgn0029639	0.0309975	0.0088272	3.51160848	0.12504
glo	FBgn0037954	0.0127095	0.0078627	1.61643222	0.12515
CG7048	FBgn0038976	0.0369716	0.0538494	-1.4565075	0.12527
RpL35A	FBgn0026272	0.1594234	0.1271726	1.25359818	0.12534
CG8003	FBgn0036096	0.0142492	0.0074478	1.91320476	0.12553
lolal	FBgn0022238	0.0354438	0.0074009	4.78909491	0.12563
Klc	FBgn0010235	0.1223844	0.1049227	1.16642501	0.12567
CG17272	FBgn0038830	0.0077271	0.0180054	-2.3301681	0.12598
LysE	FBgn0004428	0.0142129	0.0267993	-1.8855676	0.1264
Vha16	FBgn0004145	0.0265973	0.0095189	2.79416653	0.12674
heph	FBgn0010798	0.0094463	0	Inf	0.12699
CG7587	FBgn0038523	1.6768047	1.1200592	1.49706792	0.12761
TotA	FBgn0028396	0.4064493	0.304865	1.33321084	0.12782
Mcm3	FBgn0020632	0.0047329	0.0031973	1.4802844	0.12811
ref(2)P	FBgn0003231	0.0054286	0.0143886	-2.6505037	0.1284
Prosbeta7	FBgn0037314	0.1121813	0.0909309	1.2336982	0.12879
Bin1	FBgn0024491	0.0222303	0.0045909	4.84225674	0.12888

CG4789	FBgn0030792	0.0139113	0.0025133	5.53517093	0.12916
l(2)37Cc	FBgn0002031	0.3029152	0.2832789	1.06931778	0.12947
stv	FBgn0036370	0.0047362	0.0091232	-1.92628	0.12977
Zn72D	FBgn0017453	0.0024764	0.0052634	-2.1254408	0.12979
Mkk4	FBgn0024326	0.0102115	0.0150499	-1.4738179	0.12985
betaTub97EF	FBgn0003890	0.422298	0.3508101	1.2037795	0.13053
Yp2	FBgn0000847	0	0.0083094	-Inf	0.13053
CG12030	FBgn0035147	0.8435736	0.9399726	-1.1142745	0.13061
Hsc70-3	FBgn0001218	1.7421754	2.0274261	-1.1637325	0.13075
Rbp1-like	FBgn0030479	0.0930018	0.0675638	1.37650306	0.13075
Oscillin	FBgn0031717	0.0992351	0.1379281	-1.3899127	0.13091
CG8602	FBgn0035763	0.0110977	0.0047799	2.32176075	0.13094
Lcp2	FBgn0002533	0.1150787	0.0752399	1.52949103	0.13097
PGRP-SB1	FBgn0036658	0.0387183	0.0108717	3.56140298	0.13099
CG17597	FBgn0032715	0.1440953	0.1122139	1.2841127	0.13162
CG2789	FBgn0025550	0.1020221	0.0728681	1.40009322	0.13225
CG11560	FBgn0036249	0.0075673	0.0164692	-2.1763667	0.13332
CG9140	FBgn0031771	0.0331624	0.024628	1.34653248	0.13333
gro	FBgn0001139	0.007984	0.0039705	2.01081957	0.13369
Hira	FBgn0022786	0.0155211	0.013385	1.15958991	0.13398
RpII33	FBgn0001964	0.0064109	0.0141514	-2.2074021	0.13401
CG31694	FBgn0031475	0.0247543	0.015959	1.55111861	0.13428
PpD3	FBgn0005777	0.0077044	0.015389	-1.9974446	0.13436
CG3560	FBgn0025544	0.386424	0.3216562	1.20135724	0.13473
Cam	FBgn0000253	0.4212444	0.5494918	-1.3044487	0.13488
Dpy-30L1	FBgn0032293	0.0623811	0.0245173	2.5443746	0.13504
hkl	FBgn0032745	0.0122136	0.0081943	1.49050941	0.13576
Uba1	FBgn0023143	0.1349868	0.1547046	-1.1460721	0.13737
RpS5b	FBgn0038277	0.1874156	0.242104	-1.2918027	0.13793
RpL32	FBgn0002626	0.4958777	0.5631331	-1.1356291	0.13949
CG9232	FBgn0031845	0.009079	0.01604	-1.7667056	0.1398
CG4702	FBgn0037992	0.0116995	0.0030093	3.88782685	0.1402
Vap-33-1	FBgn0025953	0.1262928	0.1571316	-1.2441854	0.14034
CG17331	FBgn0032596	0.2215791	0.1863629	1.18896574	0.14043
CG14207	FBgn0031037	0.2793038	0.3568274	-1.2775599	0.14056
CG5010	FBgn0030821	0.0868585	0.0508509	1.70810243	0.14073
Cys	FBgn0004121	0.6421427	0.4070719	1.57746728	0.14101
R	FBgn0003190	0.0398705	0.0244436	1.63112386	0.14138
Sgs1	FBgn0003372	0.0020104	0.0028198	-1.4025778	0.1415
mats	FBgn0038965	0.0077635	0.0132013	-1.7004237	0.14246
CG16908	FBgn0037741	0.002949	0.0060107	-2.0382254	0.14254
CSN8	FBgn0028835	0.0149411	0.0302728	-2.0261434	0.14286

Dlc90F	FBgn0010833	0.0589364	0.0951292	-1.6140986	0.14287
CG4365	FBgn0037024	0.0361868	0.0548243	-1.5150348	0.143
CG7789	FBgn0039698	0.0204194	0.0270433	-1.3243926	0.14357
CG12264	FBgn0032393	0.015919	0.0094397	1.68637851	0.14379
Rrp46	FBgn0037815	0.0070918	0.0121146	-1.7082532	0.14402
CG6422	FBgn0039261	0.0077558	0.003844	2.01763411	0.1445
CG9086	FBgn0030809	0.0015754	0.0008752	1.79999087	0.14472
GalNAc-T1	FBgn0034025	0.0624624	0.0789398	-1.2637974	0.14528
CG9674	FBgn0036663	0.0046705	0.0072643	-1.5553652	0.14668
SH3PX1	FBgn0036033	0.0294106	0.0378065	-1.2854703	0.14695
CG3529	FBgn0035995	0.0855134	0.0562121	1.52126226	0.14706
Rab10	FBgn0015789	0.0756516	0.0865427	-1.1439638	0.14814
mtacp1	FBgn0011361	0.1417413	0.1072643	1.32142066	0.14833
CG13994	FBgn0031772	0.0101155	0.0212842	-2.1041106	0.1493
Pgm	FBgn0003076	0.069715	0.0539896	1.2912666	0.14963
CG33487	FBgn0053487	0.0699037	0.0375478	1.86172374	0.14992
CG33496	FBgn0053487	0.0699037	0.0375478	1.86172374	0.14992
mRpL54	FBgn0034579	0.0087427	0.0193234	-2.2102262	0.14992
CG3246	FBgn0031538	0.0082941	0.003095	2.67984982	0.15
CG8036	FBgn0037607	0.4671185	0.3972425	1.17590258	0.15087
CG1910	FBgn0022349	0.1164179	0.1569059	-1.3477816	0.1519
stck	FBgn0020249	0.0200003	0.0075428	2.6515703	0.15206
CG10131	FBgn0033949	0.0351383	0.0122845	2.860391	0.15227
Taf4	FBgn0005542	0.0039397	0.0022591	1.7439369	0.15452
LysX	FBgn0004431	0.0100993	0.0227097	-2.2486458	0.1549
CG9577	FBgn0031092	0.172001	0.108207	1.58955576	0.15511
RpS20	FBgn0019936	0.3768036	0.324388	1.16158304	0.1556
Lsp2	FBgn0002565	1.5574825	1.3164609	1.18308298	0.15563
CG6455	FBgn0019960	0.0804256	0.0650924	1.23556066	0.15609
CG2016	FBgn0037289	0.0149486	0.0058057	2.57480016	0.15675
Dhod	FBgn0000447	0.0137047	0.0077155	1.77625581	0.15752
boca	FBgn0004132	0.1272845	0.15587	-1.2245794	0.15798
usnp	FBgn0034913	0.0188778	0.0286586	-1.5181143	0.15826
CG3542	FBgn0031492	0.0051238	0.0077198	-1.5066381	0.15833
GstD3	FBgn0010039	0.2018841	0.114769	1.75904765	0.15865
CG3884	FBgn0033786	0.010952	0	Inf	0.16086
CG4452	FBgn0035981	0.0072178	0.0027032	2.67008599	0.16098
cpb	FBgn0011570	0.0548855	0.0453695	1.20974265	0.1613
CG14990	FBgn0035496	0.0473905	0.0054127	8.75545262	0.16169
Oscp	FBgn0016691	0.4290702	0.4744745	-1.1058204	0.16191
RpL31	FBgn0025286	0.5946477	0.7857102	-1.3213035	0.16219
CG7993	FBgn0038585	0.0055615	0.0161399	-2.902071	0.16288

Cog3	FBgn0031536	0.0046786	0.0078346	-1.6745583	0.16328
CG13993	FBgn0027693	0.0295757	0.0202435	1.46099812	0.1637
Cpr65Ax2	FBgn0042118	0.033714	0.0164217	2.05301823	0.16371
Spase25	FBgn0030306	0.3679554	0.4468198	-1.2143314	0.1646
CG30463	FBgn0034148	0.0286753	0.0367135	-1.2803174	0.16476
Ahcy89E	FBgn0015011	0.0071164	0.0017493	4.06818801	0.16545
Sdc	FBgn0010415	0.0034221	0.007425	-2.1697167	0.16572
Gclm	FBgn0039001	0.0097812	0.0036991	2.64419607	0.16591
l(2)35Bg	FBgn0001977	0.1085618	0.0854068	1.27111409	0.16638
fax	FBgn0014163	0.1343868	0.0947829	1.41783789	0.16689
CG8858	FBgn0033698	0.0018199	0.0009493	1.91714042	0.16712
Hrs	FBgn0013527	0.0276435	0.0199778	1.38371616	0.16766
Cas	FBgn0022213	0.007891	0.0146504	-1.8566077	0.16767
l(1)G0320	FBgn0028327	0.1039785	0.1227995	-1.1810087	0.16787
Fit2	FBgn0036688	0.005274	0.0036623	1.44008143	0.1686
Cka	FBgn0010608	0.0125848	0.0091844	1.37023847	0.16862
yki	FBgn0034970	0.0104027	0.017622	-1.6939792	0.16917
Art1	FBgn0037834	0.0131191	0.0195105	-1.4871821	0.16923
CG10590	FBgn0035622	0.0133244	0.0252854	-1.8976695	0.16987
Gmer	FBgn0034794	0.0175409	0.0251086	-1.4314297	0.17039
Pros29	FBgn0003150	0.3766788	0.317359	1.18691698	0.17143
Nmdmc	FBgn0010222	0.0138407	0.0195708	-1.4140088	0.17163
RpL22	FBgn0015288	0.3187366	0.3908907	-1.2263754	0.17241
swm	FBgn0002044	0.001523	0.0034288	-2.2513952	0.17343
SpdS	FBgn0037723	0.0314507	0.0404274	-1.2854203	0.17367
mRpS30	FBgn0030692	0.0009705	0.004983	-5.1344051	0.17405
Pros28.1A	FBgn0017555	0.0296998	0.0242618	1.22413724	0.17424
ubl	FBgn0022224	0.0903123	0.064324	1.40402156	0.17425
l(3)neo18	FBgn0011455	0.0458246	0.0372783	1.22925482	0.17442
mts	FBgn0004177	0.1088335	0.1170142	-1.0751673	0.17448
Sap-r	FBgn0000416	0.1304462	0.1528594	-1.1718195	0.17516
CG5871	FBgn0038870	0.0034439	0.0009014	3.82070284	0.17564
VhaAC39	FBgn0025327	0.0301121	0.0217168	1.38658031	0.17621
pAbp	FBgn0003031	0.5452541	0.6471671	-1.1869091	0.17632
Ero1L	FBgn0028736	0.0241321	0.0353081	-1.4631188	0.17655
Prosbeta1	FBgn0010590	0.317979	0.2803144	1.13436573	0.17723
Tal	FBgn0023477	0.0439907	0.0552776	-1.2565741	0.17824
Chmp1	FBgn0036805	0.0206157	0.0117515	1.7543087	0.17872
vig2	FBgn0039279	0.0680612	0.0881408	-1.2950234	0.17915
v(2)k05816	FBgn0031502	0.0079406	0.0033687	2.35719053	0.17949
CG18437	FBgn0039536	0.0028502	0.0013662	2.08613125	0.18
RpL27A	FBgn0010410	0.5483823	0.4471922	1.22627884	0.18098

CG4769	FBgn0027754	0.0801041	0.0949523	-1.1853612	0.1815
atl	FBgn0039213	0.0175064	0.0322189	-1.8404031	0.18163
CG9471	FBgn0037749	0.0181866	0.008795	2.0678366	0.18177
CG4278	FBgn0014092	0.024662	0.0151118	1.63196953	0.18194
CG13049	FBgn0036592	0.1494512	0.0528709	2.82671781	0.18219
Spase18-21	FBgn0026567	0.1885508	0.2372713	-1.2583945	0.18251
CG6812	FBgn0036843	0.0218216	0.0161479	1.35135494	0.18254
RpL13A	FBgn0025276	0.094432	0.1172853	-1.2420072	0.18321
CG5346	FBgn0038981	0.0217743	0.0160132	1.35977605	0.18372
CG10103	FBgn0035715	0.0240607	0.0329801	-1.3707028	0.18428
tmod	FBgn0010731	0.0309917	0.0225586	1.37383078	0.18432
tws	FBgn0004889	0.0226802	0.0155342	1.46001248	0.1862
CG6639	FBgn0032638	0.0160077	0.0060413	2.64970645	0.18684
KdelR	FBgn0022268	0.1058914	0.1439425	-1.3593414	0.18686
CG9485	FBgn0034618	0.00093	0.0019189	-2.063288	0.18697
CG4038	FBgn0011824	0.0745603	0.1014809	-1.3610571	0.18847
CG9318	FBgn0032880	0.0098412	0.0166724	-1.6941406	0.18867
RpS5a	FBgn0002590	0.3669375	0.5042497	-1.3742114	0.18896
CG6697	FBgn0027526	0.0186495	0.0117364	1.58902667	0.18965
CG30122	FBgn0034369	0.0187548	0.0221821	-1.1827443	0.18965
CG9662	FBgn0031529	0.0271784	0.0461992	-1.6998495	0.19015
CG3353	FBgn0038869	0.0050807	0.0100751	-1.9830059	0.19028
CG13822	FBgn0039098	0.0074545	0.0222667	-2.9870257	0.19082
Aats-asp	FBgn0002069	0.1569775	0.1787318	-1.1385822	0.19112
Inos	FBgn0025885	0.0273223	0.0153	1.78577604	0.19125
CG11384	FBgn0029562	0.006659	0.0023423	2.84293013	0.19152
CG3740	FBgn0023530	0.0036065	0.0208307	-5.775908	0.19197
CG17556	FBgn0038461	0.0652964	0.0346566	1.88409685	0.19222
CG3621	FBgn0014087	0.0934341	0.1085486	-1.1617664	0.19242
CG17293	FBgn0032030	0.0100957	0.0051374	1.96514724	0.19256
CG2004	FBgn0030060	0.0415551	0.0550076	-1.3237262	0.19257
RpL35	FBgn0025262	0.2218095	0.2445371	-1.1024642	0.19328
r-l	FBgn0003257	0.0075067	0.0129871	-1.73006	0.19331
Bet3	FBgn0035992	0.0433723	0.0282538	1.53509585	0.19358
fat-spondin	FBgn0026721	0.0158659	0.0072669	2.18331646	0.19379
Mical	FBgn0037774	0.001044	0.0004496	2.32195389	0.19413
alpha-Spec	FBgn0003470	0.1272581	0.1160583	1.09650144	0.19416
CG32631	FBgn0030496	0.0253733	0.0135093	1.87821243	0.1942
nudC	FBgn0021768	0.1214107	0.0730641	1.66169978	0.19452
Rtf1	FBgn0034722	0.0044524	0.0020185	2.20586216	0.19485
Cip4	FBgn0035533	0.0117104	0.0069866	1.67612396	0.19584
RpS10a	FBgn0027494	0.1062057	0.1211896	-1.1410837	0.19612

CG6617	FBgn0027737	0.0280481	0.0158147	1.77354792	0.1967
Elf	FBgn0020443	0.1651294	0.1781455	-1.0788236	0.19672
CstF-64	FBgn0027841	0.0064225	0.0095545	-1.4876643	0.19745
CG10359	FBgn0035452	0.0070802	0	Inf	0.19779
CG4306	FBgn0036787	0.0423271	0.0223365	1.89497159	0.19791
CG7332	FBgn0030973	0.0047432	0.0012297	3.85721255	0.19885
CG13077	FBgn0032810	0.0019953	0.0131804	-6.6058666	0.19907
Cul-3	FBgn0001980	0.0050781	0.0012159	4.17629672	0.19941
Rrp40	FBgn0051938	0.0119595	0.0029683	4.02914965	0.19983
CG4408	FBgn0039073	0.0365595	0.0493484	-1.3498115	0.20055
CG13962	FBgn0032824	0.0490173	0.0148956	3.29071917	0.2008
CG6512	FBgn0036702	0.0101148	0.0053676	1.88443535	0.20108
CG17032	FBgn0036547	0.0144719	0.0055862	2.5906696	0.20118
CG9706	FBgn0036662	0.0049424	0.0083573	-1.6909387	0.20218
Tbp-1	FBgn0010835	0.2697777	0.3027368	-1.1221715	0.20262
lqf	FBgn0022808	0.0161441	0.0088197	1.83045226	0.20299
Mcm5	FBgn0017577	0.001652	0	Inf	0.20311
Muc11A	FBgn0030371	0.0011245	0	Inf	0.20312
Gnf1	FBgn0004913	0.0012606	0	Inf	0.20313
abs	FBgn0010723	0.002008	0	Inf	0.20313
CG14275	FBgn0032022	0.0083983	0	Inf	0.20313
CG7573	FBgn0036153	0.0026058	0	Inf	0.20313
CG31778	FBgn0031565	0.0121858	0	Inf	0.20313
CG33054	FBgn0037056	0.0077202	0	Inf	0.20313
CG6409	FBgn0036106	0.0032244	0	Inf	0.20313
CG31728	FBgn0032496	0.0024033	0	Inf	0.20313
yip2	FBgn0032158	0.1655866	0.2173	-1.3123042	0.20318
MBD-like	FBgn0027950	0.00526	0	Inf	0.20321
CG10492	FBgn0005567	0.0015183	0	Inf	0.20323
CG17746	FBgn0035425	0.0033149	0	Inf	0.20323
CG8607	FBgn0035760	0.0044722	0	Inf	0.20323
CG6272	FBgn0036126	0.0108836	0	Inf	0.20323
Npc2e	FBgn0040540	0.0133678	0	Inf	0.20323
Ac13E	FBgn0022710	0.0006911	0	Inf	0.20332
CG3077	FBgn0031457	0.003621	0	Inf	0.20332
CG15145	FBgn0032649	0.0013475	0	Inf	0.20332
Jhebp29	FBgn0022215	0.0044884	0	Inf	0.20332
mRpL39	FBgn0036462	0.0035449	0	Inf	0.20332
dyn-p25	FBgn0001976	0.0057583	0	Inf	0.20332
fliI	FBgn0000709	0.0009569	0	Inf	0.20339
CG3108	FBgn0029807	0.0010617	0	Inf	0.20339
CG8353	FBgn0032002	0.0070698	0	Inf	0.20339

CG14232	FBgn0019900	0.0024729	0	Inf	0.20343
aru	FBgn0029095	0.001294	0	Inf	0.20347
CG6687	FBgn0038299	0.0024451	0	Inf	0.20347
mRpL55	FBgn0038678	0.0097349	0	Inf	0.20347
Cpr100A	FBgn0039805	0.0043221	0	Inf	0.20347
Cpr65Av	FBgn0035684	0.0093841	0	Inf	0.20347
Nedd4	FBgn0036736	0.0010344	0	Inf	0.20347
CG3295	FBgn0034573	0.0027629	0	Inf	0.20356
modSP	FBgn0013291	0.0019006	0	Inf	0.20356
Nca	FBgn0013303	0.0058887	0	Inf	0.20359
SNF4Agamma	FBgn0025803	0.0017202	0	Inf	0.20359
CG16791	FBgn0038881	0.0010045	0	Inf	0.20359
Dat	FBgn0000418	0.004688	0	Inf	0.20369
CG9344	FBgn0034564	0.0142421	0	Inf	0.20369
Prat	FBgn0004901	0.0010554	0.0054659	-5.1790147	0.2037
pcx	FBgn0000752	0.0003501	0	Inf	0.20375
CG4594	FBgn0032161	0.0042925	0	Inf	0.20375
CG12038	FBgn0035179	0.002953	0	Inf	0.20375
CG14969	FBgn0035440	0.0038155	0	Inf	0.20375
CG13041	FBgn0036605	0.0096927	0	Inf	0.20375
CG13060	FBgn0036606	0.0091747	0	Inf	0.20375
CG31974	FBgn0031223	0.0029101	0	Inf	0.20375
CG32195	FBgn0052195	0.0029972	0	Inf	0.20375
Nak	FBgn0015772	0.0016064	0	Inf	0.2038
CG6361	FBgn0030925	0.0029663	0	Inf	0.2038
PGRP-SD	FBgn0035806	0.0060283	0	Inf	0.2038
Msr-110	FBgn0015766	0.0018829	0	Inf	0.20429
CG10754	FBgn0036314	0.0043363	0	Inf	0.20429
CG18769	FBgn0035705	0.0040199	0	Inf	0.20432
pot	FBgn0030355	0.0011897	0	Inf	0.20432
CG11417	FBgn0024364	0.0014798	0	Inf	0.20444
CG7791	FBgn0033038	0.0016322	0	Inf	0.20444
CG15080	FBgn0034391	0.0009802	0	Inf	0.20444
CG6018	FBgn0034736	0.0020158	0	Inf	0.20444
CG6480	FBgn0036964	0.0043547	0	Inf	0.20444
aux	FBgn0037218	0.0017183	0	Inf	0.20444
CG31999	FBgn0039894	0.0043898	0.000751	5.84561492	0.20446
Ssb-c31a	FBgn0015299	0.0178627	0	Inf	0.20468
CG6745	FBgn0035901	0.0015633	0	Inf	0.20469
Aats-gly	FBgn0027088	0.2539566	0.2891196	-1.1384607	0.2049
tomosyn	FBgn0030412	0.001549	0	Inf	0.20496

Ncc69	FBgn0025706	0.0009855	0	Inf	0.20496
CG12519	FBgn0036872	0.0089024	0	Inf	0.20513
CG18294	FBgn0036873	0.0082711	0	Inf	0.20513
CG3097	FBgn0029804	0.0024482	0	Inf	0.20514
Rrp45	FBgn0030789	0.0026443	0	Inf	0.20514
CG10433	FBgn0034638	0.0085784	0	Inf	0.20514
CG5532	FBgn0034902	0.0097273	0	Inf	0.20514
mRpL17	FBgn0035122	0.0061901	0	Inf	0.20514
Cpr66D	FBgn0035919	0.004035	0	Inf	0.20514
bun	FBgn0010460	0.0009034	0	Inf	0.20514
RpS23	FBgn0026271	1.3504763	1.8323364	-1.3568075	0.20531
CG4669	FBgn0035598	0.0019024	0	Inf	0.20533
CG6933	FBgn0036952	0.0033116	0	Inf	0.20533
Fdh	FBgn0002986	0.2321682	0.2191448	1.05942857	0.20566
CG15735	FBgn0030364	0.0168034	0.012695	1.32361877	0.20588
CG33129	FBgn0032319	0.0392732	0.0552923	-1.4078885	0.20596
CG4960	FBgn0039371	0.0181256	0.0047492	3.81655541	0.20614
raptor	FBgn0029840	0.0006829	0	Inf	0.20615
CG8486	FBgn0025998	0.0004078	0	Inf	0.20615
Csl4	FBgn0032346	0.0054368	0	Inf	0.20615
CG14695	FBgn0037850	0.0038377	0	Inf	0.20615
CG11905	FBgn0036678	0.0027543	0	Inf	0.2062
CG1308	FBgn0035507	0.0006502	0	Inf	0.20652
Or82a	FBgn0041621	0.0028978	0	Inf	0.20652
CG12360	FBgn0038111	0.0071605	0.0105729	-1.4765667	0.20661
shi	FBgn0003392	0.0110514	0.0074284	1.48772192	0.20679
Src42A	FBgn0004603	0.0047754	0	Inf	0.20691
dob	FBgn0030607	0.002338	0	Inf	0.20691
CG5162	FBgn0030828	0.0027305	0	Inf	0.20691
Slh	FBgn0015816	0.0586059	0.084513	-1.4420564	0.20696
CG7182	FBgn0035878	0.0055592	0.0081463	-1.465369	0.20715
BEAF-32	FBgn0013752	0.004009	0	Inf	0.20743
ninaG	FBgn0037896	0.0019459	0	Inf	0.20743
cpa	FBgn0034577	0.1343125	0.1139661	1.17853064	0.20765
ldlCp	FBgn0026634	0.0008695	0.0038559	-4.4348886	0.20799
Hop	FBgn0022263	0.1635133	0.1380897	1.18410923	0.2081
inx3	FBgn0028373	0.0062222	0.0017434	3.56905815	0.20857
CG4406	FBgn0023545	0.0062736	0.0019398	3.2341293	0.20948
qkr58E-1	FBgn0022986	0.0055213	0.0126262	-2.2868441	0.21041
CG7716	FBgn0035800	0.0031307	0.0014185	2.20707471	0.21081
Papst2	FBgn0036695	0.0027205	0.0116231	-4.2724742	0.21097
CG32667	FBgn0052667	0.5432201	0.4118512	1.31897165	0.2111

Nop56	FBgn0038964	0.0122795	0.0205824	-1.6761643	0.21177
CG12159	FBgn0033232	0.0072782	0	Inf	0.21225
CG11752	FBgn0027728	0.0049594	0.019146	-3.8605215	0.21248
mbo	FBgn0010853	0.0007646	0.0031886	-4.1705066	0.21272
emc	FBgn0000575	0.007	0	Inf	0.21281
CG4500	FBgn0019862	0.0020753	0	Inf	0.21429
CG12582	FBgn0037215	0.0028152	0	Inf	0.21429
Hexo2	FBgn0030059	0.0031527	0	Inf	0.21463
rump	FBgn0037701	0.0322646	0.0413773	-1.2824352	0.21474
CG32626	FBgn0030531	0.0238029	0.0178747	1.33165337	0.2148
Hrb27C	FBgn0004838	0.1106992	0.1288843	-1.1642749	0.2155
Vps45	FBgn0037711	0.0096407	0.0047371	2.03516985	0.21572
ATPsyn-d	FBgn0016120	0.4651633	0.5225118	-1.1232868	0.21588
CG11857	FBgn0039303	0.0677043	0.0972813	-1.4368542	0.21599
Rbp1	FBgn0010252	0.1201862	0.0925694	1.29833586	0.21603
eIF5	FBgn0025193	0.0467522	0.0552269	-1.1812691	0.21665
Kaz1-ORFB	FBgn0026414	0.0130571	0	Inf	0.21731
sw	FBgn0003654	0.0225313	0.02696	-1.1965598	0.21857
CG4593	FBgn0029929	0.0247782	0.0435654	-1.758214	0.21905
CG10616	FBgn0036286	0.0222836	0.0329692	-1.4795227	0.21911
baf	FBgn0031977	0.0954018	0.0566307	1.68463054	0.21926
CG8578	FBgn0030699	0.0078255	0.0045469	1.7210731	0.21949
CG14629	FBgn0029556	0.1069544	0.0705077	1.51691815	0.21951
CG6766	FBgn0032398	0.0233317	0.0155391	1.50148595	0.22005
CG12082	FBgn0035402	0.0540457	0.0608237	-1.1254116	0.22057
Vps28	FBgn0021814	0.0171685	0.0243526	-1.4184476	0.22099
CG4877	FBgn0036624	0.0044545	0.0007312	6.09181101	0.22109
Rpn11	FBgn0028694	0.1331753	0.1104554	1.20569272	0.2212
CG2444	FBgn0030326	0.3535017	0.2681375	1.31835955	0.2216
ApepP	FBgn0026150	0.0662829	0.059588	1.11235395	0.22176
CG9922	FBgn0038196	0.0500182	0.0791139	-1.5817037	0.22272
CG12121	FBgn0030109	0.0017796	0	Inf	0.22283
CG6656	FBgn0038912	0.003325	0	Inf	0.22283
CG31683	FBgn0027612	0.0056327	0.0094313	-1.6743956	0.22305
Fbp1	FBgn0000639	2.2542453	1.6566136	1.36075509	0.22306
l(3)03670	FBgn0010808	0.0319733	0.0121904	2.62281421	0.22319
eIF2B-epsilon	FBgn0023512	0.0079415	0.0038127	2.08291123	0.22376
Fas2	FBgn0000635	0.0049323	0.0027949	1.76471882	0.22435
CG7998	FBgn0038587	0.8314116	0.7722269	1.07664162	0.22467
CG17565	FBgn0038424	0.0038677	0	Inf	0.2254
Hph	FBgn0010773	0.0051725	0	Inf	0.22573
CG10585	FBgn0037044	0.0036027	0	Inf	0.2263

Dlic	FBgn0027319	0.0166183	0.023633	-1.4221133	0.22633
Irp-1B	FBgn0024957	0.1035794	0.0887691	1.16684086	0.22672
CG12164	FBgn0033158	0.0097684	0.0026616	3.67010618	0.22683
Pros26	FBgn0002284	0.0415463	0.0702193	-1.6901447	0.22696
lola	FBgn0005630	0.0046256	0.0021947	2.10763699	0.22764
CG3663	FBgn0035044	0.0238599	0.0135702	1.75825692	0.22777
Mgstl	FBgn0025814	0.012964	0.0218031	-1.681825	0.22814
CG7714	FBgn0026298	0.0293973	0.0182487	1.61092591	0.22814
Acp53Ea	FBgn0015584	0.0141591	0	Inf	0.22852
MRP	FBgn0032456	0.0010976	0	Inf	0.22852
crl	FBgn0015374	0.0057239	0.0170341	-2.9759583	0.22871
nct	FBgn0039234	0.0025601	0	Inf	0.22879
CG14095	FBgn0036870	0.0101888	0	Inf	0.22912
CG7806	FBgn0032018	0.001137	0	Inf	0.22968
CG33056	FBgn0053056	0.0296781	0.0093947	3.15901802	0.22979
CG8979	FBgn0033669	0.0062871	0	Inf	0.23023
CG31343	FBgn0038898	0.0017664	0	Inf	0.23023
Ppn	FBgn0003137	0.0311373	0.0248237	1.25433982	0.23058
spz	FBgn0003495	0.0254415	0.0201015	1.265652	0.23086
CG9914	FBgn0030737	0.0810039	0.0626072	1.29384325	0.23091
cype	FBgn0010553	0.1032864	0.063159	1.6353401	0.23108
CG14688	FBgn0037819	0.0058721	0	Inf	0.23201
asf1	FBgn0029094	0.0077266	0	Inf	0.23214
CG1962	FBgn0032876	0.0021321	0	Inf	0.23214
ird1	FBgn0037663	0.0020667	0	Inf	0.23214
Pcaf	FBgn0020388	0.0044588	0.0011561	3.8567543	0.23316
CG31717	FBgn0051717	0.006982	0	Inf	0.23381
Nup98	FBgn0021781	0.0003083	0.0011552	-3.7473222	0.23385
CG5288	FBgn0035950	0.1393708	0.1672912	-1.2003318	0.23447
Shc	FBgn0015296	0.0040538	0	Inf	0.23459
l(3)05822	FBgn0010877	0.0029636	0	Inf	0.23488
ben	FBgn0000173	0.1474672	0.1827653	-1.2393625	0.23489
CG31368	FBgn0037959	0.0011271	0	Inf	0.23517
mRpL20	FBgn0036335	0.1045041	0.0720578	1.45028098	0.23525
CG10943	FBgn0036320	0.0054081	0	Inf	0.23525
CG30499	FBgn0033193	0.0219524	0.0285666	-1.301296	0.23592
CG1703	FBgn0030321	0.0424039	0.0529353	-1.2483595	0.23599
128up	FBgn0010196	0.0652393	0.0890609	-1.3651429	0.23606
Nipsnap	FBgn0030724	0.1661941	0.1357437	1.22432267	0.2361
Top3beta	FBgn0026015	0.0006134	0.0022056	-3.595757	0.2362
retn	FBgn0004795	0.0018183	0	Inf	0.23651
Doa	FBgn0000480	0.0019909	0	Inf	0.23651

ab	FBgn0000011	0.0018323	0	Inf	0.23651
CG8306	FBgn0034142	0.0147879	0.0092323	1.60175952	0.23687
CG3107	FBgn0033005	0.0066693	0.0101238	-1.5179706	0.23688
CG11444	FBgn0029715	0.0465412	0.0604977	-1.2998754	0.23715
Mcm2	FBgn0011511	0.0007053	0.0026124	-3.7037014	0.23722
RpS6	FBgn0004371	0.3535285	0.3979259	-1.1255838	0.23729
Pglym87	FBgn0011270	0.1566125	0.1168986	1.33972955	0.23756
yellow-c	FBgn0026296	0.054659	0.0370214	1.47641435	0.23781
CG5888	FBgn0028523	0.0038628	0	Inf	0.23802
Nrt	FBgn0004108	0.0020765	0	Inf	0.23816
CG4968	FBgn0032214	0.0183761	0.0122104	1.5049484	0.23894
MED15	FBgn0027592	0.0007166	0.0025478	-3.5555338	0.23904
Cyp4ad1	FBgn0033292	0.0039756	0.006744	-1.6963449	0.23918
ATPCL	FBgn0027531	0.0005784	0.0020635	-3.5677659	0.23923
CG18858	FBgn0042175	0.0138144	0.0086135	1.60381073	0.23933
Rpt4R	FBgn0036224	0.0253063	0.018431	1.3730271	0.23942
Lcp65Ac	FBgn0020642	0.0691673	0.0373828	1.85024541	0.24043
Neb-cGP	FBgn0040943	0.3751915	0.1463018	2.5645031	0.24097
CG11267	FBgn0036334	0.3843974	0.3191501	1.20444107	0.24108
CG30197	FBgn0050197	0.0378953	0.0461212	-1.21707	0.24232
CG6522	FBgn0034223	0.0030025	0	Inf	0.24262
CG6218	FBgn0038321	0.0046574	0	Inf	0.24268
CG7671	FBgn0038609	0.0065354	0	Inf	0.24268
Sclp	FBgn0030357	0.0333569	0.0136398	2.4455557	0.24351
ATPsyn-gamma	FBgn0020235	0.258395	0.2871177	-1.1111583	0.24401
lectin-22C	FBgn0031385	0.0013509	0	Inf	0.24419
CG2107	FBgn0035383	0.0077947	0.0045204	1.72434738	0.24437
mRpL36	FBgn0042112	0.0305986	0.0139333	2.19606882	0.24455
CG14235	FBgn0031066	0.3508251	0.2917549	1.20246516	0.24467
dnc	FBgn0000479	0.0069807	0.004516	1.54576499	0.24478
CG8176	FBgn0037702	0.0005333	0.0018419	-3.4540112	0.24593
CG6136	FBgn0038332	0.0068173	0	Inf	0.24607
CG11459	FBgn0037396	0.0152623	0.0078565	1.94262477	0.24608
tral	FBgn0027756	0.0273963	0.0390002	-1.4235569	0.24632
colt	FBgn0019830	0.011175	0.0088977	1.25593811	0.24635
CG10512	FBgn0037057	0.0825863	0.1142134	-1.3829576	0.24655
ALiX	FBgn0039541	0.018753	0.0255254	-1.3611396	0.24798
CHOp24	FBgn0029709	0.1730547	0.2251878	-1.3012523	0.24807
CG30103	FBgn0050103	0.0039349	0.0058938	-1.4978422	0.24827
mus209	FBgn0002895	0.0306183	0.044849	-1.4647799	0.24872
Gs1l	FBgn0019982	0.0068619	0	Inf	0.24956

GstE7	FBgn0034341	0.0782778	0.0544357	1.43798539	0.24961
mRpL4	FBgn0001995	0.0061178	0	Inf	0.24972
Pglym78	FBgn0014869	0.5712521	0.5226318	1.09302961	0.24994
CG11590	FBgn0030545	0.0105335	0.003478	3.02865403	0.25053
CG9989	FBgn0039593	0.0049393	0	Inf	0.2511
Use1	FBgn0035965	0.0023382	0.0079767	-3.4114701	0.25125
CG3493	FBgn0034854	0.0134195	0.0166338	-1.2395262	0.25195
CG14544	FBgn0039407	0.0143267	0.0081474	1.75843581	0.25209
Gmd	FBgn0031661	0.0229049	0.0281611	-1.2294778	0.25234
alpha-Adaptin	FBgn0010623	0.0081256	0.005331	1.52423215	0.25357
Reps	FBgn0032341	0.0054467	0.0036423	1.49540382	0.25361
CG6680	FBgn0036968	0.0093261	0.0026777	3.48288654	0.25367
CG10990	FBgn0030520	0.0293467	0.0316429	-1.0782442	0.25376
Cap-D3	FBgn0031712	0.0004548	0.00154	-3.3859728	0.25385
CSN7	FBgn0028836	0.0251727	0.0168765	1.49158468	0.25542
CG3731	FBgn0038271	0.2208285	0.2417895	-1.09492	0.25608
mbf1	FBgn0026208	0.0255328	0.0362387	-1.4193034	0.25616
CG5390	FBgn0032213	0.1498468	0.1225186	1.22305354	0.25684
Tsf1	FBgn0022355	0.2157803	0.1621884	1.33042986	0.25686
CG8613	FBgn0033924	0.0076352	0.0112122	-1.4684903	0.25696
U4-U6-60K	FBgn0036733	0.0057346	0.0032173	1.78244409	0.25762
CG8790	FBgn0027610	0.0059786	0	Inf	0.25782
CG9934	FBgn0032467	0.0017347	0	Inf	0.25782
Synd	FBgn0038831	0.0132825	0.0167297	-1.2595324	0.25782
CG8436	FBgn0037670	0.0047687	0.0131514	-2.7578275	0.25797
Obp99c	FBgn0039682	0.3347161	0.2699539	1.23990082	0.25809
CG1749	FBgn0030305	0.1213594	0.1371861	-1.130412	0.25829
mge	FBgn0016009	0.0491449	0.0283475	1.73365925	0.25834
CG17633	FBgn0032144	0.0041582	0	Inf	0.25854
Droj2	FBgn0038145	0.1413451	0.1549632	-1.0963459	0.25865
yellow-d	FBgn0034855	0.001642	0.0054808	-3.3378961	0.25881
CG5758	FBgn0032666	0.003838	0.0011018	3.48336302	0.25885
Faf	FBgn0025608	0.0075683	0.0021258	3.56018954	0.25928
MstProx	FBgn0015770	0.0007549	0.0025023	-3.3148411	0.2604
Cnx99A	FBgn0015622	0.1256236	0.1400887	-1.1151469	0.26222
Psi	FBgn0014870	0.0066623	0.0041136	1.61959958	0.2625
CG3704	FBgn0029546	0.0031634	0.0132232	-4.180131	0.26276
CG5362	FBgn0032237	0.3777957	0.3351844	1.12712795	0.26297
CG2118	FBgn0039877	0.0104671	0.0139909	-1.3366445	0.26423
CG5987	FBgn0039501	0.0080478	0	Inf	0.26481
alien	FBgn0013746	0.0049309	0.001551	3.17919443	0.26505
Jhe	FBgn0010052	0.0030596	0	Inf	0.26505

TfIIB	FBgn0004915	0.0033068	0.0099053	-2.9954526	0.26535
RpL37A	FBgn0028696	0.8282856	0.9997087	-1.2069613	0.26623
Sgt	FBgn0032640	0.1144005	0.1001644	1.1421274	0.26637
CG1600	FBgn0033188	0.0196442	0.0119594	1.64257272	0.26647
CG5198	FBgn0032250	0.0073593	0.0021587	3.40906841	0.26681
CG11577	FBgn0036847	0.0128708	0.0156973	-1.2196075	0.26683
Rassf	FBgn0039055	0.0029333	0.0008544	3.43325207	0.2674
CG10877	FBgn0038804	0.0139836	0.0090608	1.54329953	0.26762
CG30259	FBgn0034765	0.0013304	0.0054432	-4.0913296	0.26765
CG7739	FBgn0036509	0.0046936	0.0011554	4.0621948	0.26778
betaggt-II	FBgn0028970	0.0061895	0	Inf	0.26832
Gasp	FBgn0026077	0.1324261	0.1019984	1.29831517	0.26857
Sgt1	FBgn0037568	0.0414863	0.0270678	1.53268025	0.26871
tnc	FBgn0039257	0.0041297	0.0026333	1.56826472	0.26881
Khc	FBgn0001308	0.1165604	0.1062716	1.09681647	0.26881
Ef1alpha100E	FBgn0000557	1.4492839	1.1597518	1.24965006	0.27011
l(2)s5379	FBgn0010704	0.0061731	0.0199417	-3.2303993	0.27057
CG9527	FBgn0031813	0.0009196	0.0029698	-3.2293334	0.27074
CG11790	FBgn0039265	0.0416726	0.0514659	-1.2350049	0.27149
SF2	FBgn0038417	0.1021556	0.0883982	1.15562994	0.27186
endos	FBgn0026212	0.0791234	0.0545877	1.44947336	0.27216
RpL34b	FBgn0025253	0.1272344	0.1085099	1.17255977	0.27283
CG11266	FBgn0031883	0.0077156	0	Inf	0.27287
T48	FBgn0004359	0.0054841	0.0016435	3.33683406	0.27288
CG6907	FBgn0031711	0.0162766	0.0227055	-1.394976	0.27328
sds22	FBgn0028992	0.040382	0.0255266	1.5819612	0.27371
mRpL24	FBgn0031651	0.0113097	0.0037186	3.04136952	0.27384
Prosalpha3T	FBgn0039819	0.0024594	0.0078589	-3.1954273	0.27426
CG5706	FBgn0039175	0.0378739	0.0453395	-1.1971189	0.2747
CG5902	FBgn0039136	0.0025134	0.0080295	-3.1946636	0.27478
Sec61gamma	FBgn0031049	0.0085963	0.0273297	-3.1792391	0.27545
CG8860	FBgn0033691	0.0085963	0.0273297	-3.1792391	0.27545
Snap	FBgn0011712	0.2550622	0.28434	-1.1147868	0.27599
Bap60	FBgn0025463	0.0068136	0.0041232	1.65249556	0.27667
alc	FBgn0033383	0.0161688	0.0080787	2.00142073	0.27676
bt	FBgn0000232	0.0066741	0.0105157	-1.5755968	0.2769
mop	FBgn0036448	0.0026421	0.0021152	1.24907652	0.27748
Vps4	FBgn0027605	0.0629453	0.048954	1.28580492	0.27768
Dbp73D	FBgn0004556	0.0049264	0.0074503	-1.5123317	0.27782
Rpn7	FBgn0028688	0.0887077	0.0769056	1.15346206	0.27833
CG18624	FBgn0029971	0.0090162	0.0290813	-3.2254497	0.27834
CG16985	FBgn0035355	0.0113927	0.021954	-1.9270324	0.27858

Fst	FBgn0037724	0.0022206	0.0070186	-3.1607304	0.27885
CSN5	FBgn0016027	0.0317115	0.0198758	1.59548505	0.27892
CG15630	FBgn0031627	0.003997	0.0015303	2.61192264	0.27916
CG4389	FBgn0028479	0.2053226	0.1788033	1.14831525	0.27916
Ssadh	FBgn0039349	0.0194412	0.0099015	1.96344685	0.27933
Dref	FBgn0010077	0.0063915	0.0099874	-1.5626077	0.28029
Prx5	FBgn0038570	0.3525825	0.3941641	-1.1179343	0.28051
bor	FBgn0038409	0.0459165	0.0338625	1.35596973	0.28085
Syx18	FBgn0039212	0.002637	0.007265	-2.7549755	0.28088
vir-1	FBgn0032426	0.0344412	0.0297242	1.15869051	0.28126
nes	FBgn0026630	0.0121943	0.0204103	-1.6737535	0.28174
CG10217	FBgn0039113	0.0027314	0.0051682	-1.8921305	0.28191
CG6013	FBgn0038675	0.0023705	0.0075452	-3.1830282	0.28211
Fatp	FBgn0021953	0.0094639	0.0051746	1.82890547	0.28241
ImpL1	FBgn0001256	0.1707709	0.2109499	-1.2352797	0.28271
Kap-alpha1	FBgn0024889	0.0172837	0.014521	1.19025624	0.28334
Hsc70-1	FBgn0001216	0.1430655	0.1581071	-1.1051378	0.28335
fw	FBgn0001083	0	0.0010127	-Inf	0.28559
Hsf	FBgn0001222	0	0.0014944	-Inf	0.28559
klar	FBgn0001316	0	0.0003044	-Inf	0.28559
crp	FBgn0001994	0	0.0023151	-Inf	0.28559
mus205	FBgn0002891	0	0.0006609	-Inf	0.28559
px	FBgn0003175	0	0.0008826	-Inf	0.28559
ry	FBgn0003308	0	0.0006559	-Inf	0.28559
sl	FBgn0003416	0	0.0008396	-Inf	0.28559
Yp3	FBgn0000781	0	0.0065577	-Inf	0.28559
Klp98A	FBgn0004387	0	0.0007236	-Inf	0.28559
LysP	FBgn0004429	0	0.0097679	-Inf	0.28559
Ggamma1	FBgn0004921	0	0.0150607	-Inf	0.28559
bys	FBgn0010292	0	0.0015794	-Inf	0.28559
Taf5	FBgn0010356	0	0.0013351	-Inf	0.28559
RNaseX25	FBgn0010406	0	0.0028921	-Inf	0.28559
Sema-1a	FBgn0011259	0	0.0012149	-Inf	0.28559
Iswi	FBgn0010436	0	0.0006705	-Inf	0.28559
Mvl	FBgn0011672	0	0.001577	-Inf	0.28559
Nmda1	FBgn0013305	0	0.0027711	-Inf	0.28559
Cyp4e2	FBgn0014469	0	0.0013092	-Inf	0.28559
betaggt-I	FBgn0015000	0	0.0017434	-Inf	0.28559
Cyp9b2	FBgn0015039	0	0.0018612	-Inf	0.28559
dare	FBgn0015582	0	0.0014778	-Inf	0.28559
Lectin-galC1	FBgn0016675	0	0.0049606	-Inf	0.28559
smi35A	FBgn0016930	0	0.0014602	-Inf	0.28559

Rga	FBgn0010819	0	0.0011772	-Inf	0.28559
Max	FBgn0017578	0	0.0064141	-Inf	0.28559
Dredd	FBgn0013388	0	0.0013346	-Inf	0.28559
Nup154	FBgn0010493	0	0.0006886	-Inf	0.28559
D19A	FBgn0022935	0	0.0010363	-Inf	0.28559
Rbcn-3A	FBgn0015656	0	0.0005107	-Inf	0.28559
CG3573	FBgn0023508	0	0.0008102	-Inf	0.28559
Hr4	FBgn0023546	0	0.0006192	-Inf	0.28559
E2f2	FBgn0024371	0	0.002791	-Inf	0.28559
kin17	FBgn0024887	0	0.0028223	-Inf	0.28559
CG2685	FBgn0024998	0	0.0012475	-Inf	0.28559
CG13367	FBgn0013389	0	0.0021463	-Inf	0.28559
mtm	FBgn0025742	0	0.0016683	-Inf	0.28559
Smox	FBgn0024186	0	0.0014169	-Inf	0.28559
bonsai	FBgn0026261	0	0.0033569	-Inf	0.28559
5-Sep	FBgn0026361	0	0.0020751	-Inf	0.28559
Yippee	FBgn0026749	0	0.0082527	-Inf	0.28559
l(1)G0020	FBgn0027330	0	0.0010245	-Inf	0.28559
Pfrx	FBgn0027621	0	0.0013127	-Inf	0.28559
NP15.6	FBgn0027785	0	0.0070283	-Inf	0.28559
ns3	FBgn0027792	0	0.001445	-Inf	0.28559
CG10839	FBgn0028858	0	0.0115852	-Inf	0.28559
Ir7a	FBgn0029961	0	0.0011216	-Inf	0.28559
CG10555	FBgn0030034	0	0.0007437	-Inf	0.28559
Gga	FBgn0030141	0	0.0020876	-Inf	0.28559
Or10a	FBgn0030298	0	0.0025967	-Inf	0.28559
mRpL38	FBgn0030552	0	0.0024824	-Inf	0.28559
mRNA-capping-enzyme	FBgn0030556	0	0.0010611	-Inf	0.28559
CG8974	FBgn0030693	0	0.002486	-Inf	0.28559
CG7288	FBgn0030969	0	0.0017726	-Inf	0.28559
CG15618	FBgn0031077	0	0.0004733	-Inf	0.28559
CG5397	FBgn0031327	0	0.0012942	-Inf	0.28559
CG7289	FBgn0031379	0	0.001655	-Inf	0.28559
CG8851	FBgn0031546	0	0.0014595	-Inf	0.28559
r2d2	FBgn0031951	0	0.0027674	-Inf	0.28559
CG12560	FBgn0031974	0	0.0052169	-Inf	0.28559
CG13097	FBgn0032051	0	0.0010402	-Inf	0.28559
CG9465	FBgn0032067	0	0.0010962	-Inf	0.28559
CG9468	FBgn0032069	0	0.0010469	-Inf	0.28559
CG6750	FBgn0032292	0	0.0038053	-Inf	0.28559

Samuel	FBgn0032330	0	0.0007114	-Inf	0.28559
dgt2	FBgn0032390	0	0.0039762	-Inf	0.28559
CG6108	FBgn0032498	0	0.0012395	-Inf	0.28559
CG8738	FBgn0033321	0	0.0017596	-Inf	0.28559
CG13189	FBgn0033665	0	0.0027564	-Inf	0.28559
garz	FBgn0033714	0	0.0012504	-Inf	0.28559
Dyb	FBgn0033739	0	0.0014262	-Inf	0.28559
CG13337	FBgn0033863	0	0.0037644	-Inf	0.28559
CG13343	FBgn0033882	0	0.0020411	-Inf	0.28559
CG10915	FBgn0034308	0	0.0011308	-Inf	0.28559
CG9752	FBgn0034614	0	0.005106	-Inf	0.28559
LBR	FBgn0034657	0	0.0011817	-Inf	0.28559
Grx-1	FBgn0034658	0	0.0089023	-Inf	0.28559
osm-1	FBgn0035317	0	0.0005183	-Inf	0.28559
CG1146	FBgn0035346	0	0.0032783	-Inf	0.28559
CG14971	FBgn0035449	0	0.0025692	-Inf	0.28559
CG13720	FBgn0035555	0	0.001414	-Inf	0.28559
CG8629	FBgn0035742	0	0.008198	-Inf	0.28559
MED4	FBgn0035754	0	0.0033941	-Inf	0.28559
Atg18	FBgn0035850	0	0.0024363	-Inf	0.28559
CG18490	FBgn0036149	0	0.0007102	-Inf	0.28559
PCID2	FBgn0036184	0	0.0045964	-Inf	0.28559
CG14125	FBgn0036232	0	0.00269	-Inf	0.28559
CG14110	FBgn0036352	0	0.0029674	-Inf	0.28559
CG6854	FBgn0036478	0	0.0014991	-Inf	0.28559
CG17027	FBgn0036553	0	0.0035856	-Inf	0.28559
CG9669	FBgn0036667	0	0.013516	-Inf	0.28559
CG3961	FBgn0036821	0	0.0009966	-Inf	0.28559
CG6841	FBgn0036828	0	0.0010096	-Inf	0.28559
CG14183	FBgn0036931	0	0.0023685	-Inf	0.28559
CG5665	FBgn0036977	0	0.0061288	-Inf	0.28559
mRpL15	FBgn0036990	0	0.0024078	-Inf	0.28559
CG7634	FBgn0037101	0	0.0011894	-Inf	0.28559
Syn1	FBgn0037130	0	0.0016837	-Inf	0.28559
CG10298	FBgn0037432	0	0.0073651	-Inf	0.28559
CG8420	FBgn0037664	0	0.0017701	-Inf	0.28559
mtTFB2	FBgn0037778	0	0.0015235	-Inf	0.28559
CG6208	FBgn0037789	0	0.0024333	-Inf	0.28559
CG5608	FBgn0038058	0	0.0012746	-Inf	0.28559
CG7091	FBgn0038099	0	0.0013218	-Inf	0.28559
CG5205	FBgn0038344	0	0.0004011	-Inf	0.28559
CG4159	FBgn0038811	0	0.0025713	-Inf	0.28559

CG10830	FBgn0038839	0	0.0046239	-Inf	0.28559
CG5630	FBgn0038842	0	0.0018266	-Inf	0.28559
CG7044	FBgn0038854	0	0.0012731	-Inf	0.28559
CG6738	FBgn0039053	0	0.0026291	-Inf	0.28559
CG13827	FBgn0039068	0	0.0039421	-Inf	0.28559
SPE	FBgn0039102	0	0.0017216	-Inf	0.28559
CG13603	FBgn0039135	0	0.004034	-Inf	0.28559
CG13614	FBgn0039194	0	0.0033682	-Inf	0.28559
Rpb10	FBgn0039218	0	0.0102781	-Inf	0.28559
CG18410	FBgn0039226	0	0.0019398	-Inf	0.28559
CG11875	FBgn0039301	0	0.0027365	-Inf	0.28559
jigr1	FBgn0039350	0	0.0027336	-Inf	0.28559
Moca-cyp	FBgn0039581	0	0.000938	-Inf	0.28559
Trc8	FBgn0039668	0	0.0012765	-Inf	0.28559
CG15533	FBgn0039768	0	0.0009951	-Inf	0.28559
kat80	FBgn0030730	0	0.0010692	-Inf	0.28559
CG32795	FBgn0029634	0	0.0023457	-Inf	0.28559
CG8620	FBgn0040837	0	0.0088452	-Inf	0.28559
asparagine-synthetase	FBgn0041607	0	0.0024682	-Inf	0.28559
CG18766	FBgn0039499	0	0.0030517	-Inf	0.28559
bchs	FBgn0031748	0	0.0001974	-Inf	0.28559
CG30020	FBgn0033567	0	0.0018726	-Inf	0.28559
Cyp12d1-p	FBgn0033576	0	0.0013218	-Inf	0.28559
CG31493	FBgn0037474	0	0.0085712	-Inf	0.28559
CG31636	FBgn0031843	0	0.0022001	-Inf	0.28559
CG31704	FBgn0051704	0	0.0128775	-Inf	0.28559
CG31855	FBgn0051855	0	0.009474	-Inf	0.28559
eap	FBgn0052099	0	0.0047492	-Inf	0.28559
CG32581	FBgn0052581	0	0.0030743	-Inf	0.28559
CG32649	FBgn0030430	0	0.001422	-Inf	0.28559
Tango5	FBgn0030229	0	0.001609	-Inf	0.28559
CG33099	FBgn0038982	0	0.0031851	-Inf	0.28559
Cyp12d1-d	FBgn0033577	0	0.0013218	-Inf	0.28559
HSPC300	FBgn0050173	0	0.0129786	-Inf	0.28559
As	FBgn0036148	0	0.0009	-Inf	0.28559
GstE8	FBgn0034342	0	0.0041374	-Inf	0.28559
CG34349	FBgn0039268	0	0.000962	-Inf	0.28559
Pvf3	FBgn0031889	0	0.0022383	-Inf	0.28559
spn-F	FBgn0039837	0	0.0025822	-Inf	0.28559
mib2	FBgn0032742	0	0.0006565	-Inf	0.28559
Vps36	FBgn0036375	0	0.002302	-Inf	0.28559

e(y)3	FBgn0026680	0	0.0005148	-Inf	0.28559
CG4567	FBgn0031898	0	0.0016174	-Inf	0.28559
l(2)gd1	FBgn0032342	0	0.001292	-Inf	0.28559
Ten-a	FBgn0004446	0	0.0003058	-Inf	0.28559
wisp	FBgn0030353	0	0.0006268	-Inf	0.28559
Bet5	FBgn0039753	0	0.0071218	-Inf	0.28559
Mtor	FBgn0013756	0.0087959	0.0074237	1.18483581	0.28599
CG5355	FBgn0032242	0.2059864	0.2198099	-1.067109	0.2872
CG6453	FBgn0032643	0.0925605	0.1089512	-1.1770807	0.28824
TSG101	FBgn0036666	0.0024792	0.007664	-3.0913504	0.28869
Nap1	FBgn0015268	0.1469478	0.1640077	-1.1160955	0.28889
CG4829	FBgn0030796	0.0030162	0	Inf	0.28899
CG4810	FBgn0037994	0.0076026	0.0098909	-1.3009957	0.28906
RpS28b	FBgn0030136	0.5396062	0.6596291	-1.2224268	0.29031
sun	FBgn0014391	0.290883	0.3178009	-1.0925385	0.29196
Cp190	FBgn0000283	0.0056577	0.0073215	-1.2940694	0.29206
RpS19a	FBgn0010412	1.0281929	0.9736096	1.0560628	0.29346
CG4589	FBgn0019886	0.0077513	0.0060765	1.27563331	0.29411
inx2	FBgn0026672	0.0130185	0.0182981	-1.405537	0.29429
up	FBgn0001267	0.153707	0.1214015	1.26610456	0.29468
Eip63F-1	FBgn0004910	0.0225689	0.0356641	-1.5802303	0.2947
Rpn5	FBgn0028690	0.1334693	0.1199908	1.11232976	0.29513
Gclc	FBgn0029998	0.0086942	0.005668	1.53391249	0.29549
Hsp67Ba	FBgn0001227	0.0107332	0.0057719	1.85956876	0.2957
Cpr64Ad	FBgn0035513	0.0592685	0.0226272	2.61934787	0.29575
mRpL1	FBgn0037566	0.0049113	0.0019453	2.52472708	0.29585
nrv2	FBgn0014867	0.0080945	0.00291	2.78164235	0.29713
CG1105	FBgn0037465	0.0111622	0.0178343	-1.5977465	0.29819
mod	FBgn0002780	0.139953	0.1508703	-1.0780074	0.29835
ade3	FBgn0000053	0.0120832	0.0084673	1.42704418	0.29855
Clc	FBgn0024814	0.1585315	0.1784218	-1.1254659	0.29889
RpS10b	FBgn0031035	0.7120033	0.80416	-1.129433	0.29927
CG15881	FBgn0036909	0.0443321	0.0256535	1.72811005	0.29995
vas	FBgn0003970	0.0042523	0.0069144	-1.6260269	0.30278
CG2025	FBgn0030344	0.0098065	0.0061961	1.58267684	0.30315
Tom34	FBgn0010812	0.0281407	0.0238628	1.17927095	0.30342
lark	FBgn0011640	0.0408002	0.0285308	1.43004159	0.30406
Prosalpha5	FBgn0016697	0.2522408	0.2247224	1.12245475	0.3052
chb	FBgn0021760	0.0011874	0.0017538	-1.4770115	0.30593
CG18547	FBgn0037973	0.0136832	0.0087555	1.56281601	0.30787
CG5656	FBgn0037083	0.0329431	0.0241006	1.3668999	0.30808
Rpn12	FBgn0028693	0.1484352	0.1218171	1.21850904	0.30931

CG9330	FBgn0036888	0.0136622	0.0098606	1.38553182	0.31001
CG3226	FBgn0029882	0.0933851	0.1185017	-1.2689574	0.31034
mRpL33	FBgn0040907	0.747735	0.8310729	-1.1114539	0.31091
CG3683	FBgn0035046	0.0808218	0.0613888	1.31655453	0.31106
CG9510	FBgn0032076	0.0143938	0.0068007	2.116511	0.31158
aralar1	FBgn0028646	0.0115551	0.0089646	1.28897027	0.312
CG12512	FBgn0031703	0.0053276	0.0032545	1.63698533	0.3129
pzg	FBgn0037066	0.0410167	0.0353486	1.16034794	0.31308
smp-30	FBgn0038257	0.1308804	0.1018822	1.28462445	0.31326
Rab14	FBgn0014431	0.0367476	0.0330515	1.11182882	0.31353
CG5045	FBgn0032229	0.0303492	0.0374286	-1.2332652	0.31595
CG10673	FBgn0035590	0.0182104	0.0105064	1.73327524	0.31718
Sgs5	FBgn0003375	2.2864863	2.6608994	-1.1637504	0.31724
Aats-asn	FBgn0027092	0.0559544	0.0676768	-1.2094999	0.318
CG9836	FBgn0037637	0.0035103	0.0101578	-2.8937632	0.31882
gce	FBgn0030627	0.0016926	0.0042271	-2.4973884	0.31993
RpL36	FBgn0002579	0.291645	0.3199457	-1.0970382	0.32004
CG14103	FBgn0036908	0.0111509	0.005197	2.14562175	0.32222
Vha26	FBgn0015324	0.3965559	0.4344396	-1.0955317	0.32277
Pdsw	FBgn0021967	0.0903069	0.104113	-1.1528805	0.32332
ligatin	FBgn0041588	0.0040615	0.004467	-1.099858	0.32347
CG7860	FBgn0030653	0.0686585	0.0785264	-1.1437258	0.32389
CG13369	FBgn0025640	0.0088625	0.0137824	-1.5551343	0.32456
DebB	FBgn0000426	0.0474054	0.0293501	1.61517004	0.32475
CG5787	FBgn0032454	0.0135648	0.0110549	1.22703476	0.32488
CG31249	FBgn0038537	0.0094985	0.0035027	2.71176922	0.32729
CG10225	FBgn0039110	0.0273144	0.0234479	1.16489677	0.32835
Rack1	FBgn0020618	1.4298167	1.5694728	-1.0976741	0.3285
AnnIX	FBgn0000083	0.3172328	0.3468122	-1.0932418	0.32869
CG17904	FBgn0032597	0.0183775	0.0161359	1.13891767	0.3291
CG32783	FBgn0052783	0.0006706	0.0019344	-2.8846156	0.3297
CG32786	FBgn0052786	0.0006706	0.0019344	-2.8846156	0.3297
sgg	FBgn0003371	0.0071165	0.0093561	-1.3147063	0.32977
SCAR	FBgn0021868	0.0056029	0.0042717	1.31162107	0.32988
blw	FBgn0010487	0.4863176	0.5133043	-1.0554919	0.3308
qkr58E-3	FBgn0022984	0.0108951	0.0136926	-1.256763	0.33148
Hsc70-4	FBgn0001219	1.0939118	1.0451676	1.04663767	0.33176
Phk-3	FBgn0035089	0.0845351	0.0613608	1.37767326	0.33177
CG9018	FBgn0035318	0.0068048	0.002568	2.64988958	0.33281
Pros54	FBgn0015283	0.0712676	0.056073	1.27097932	0.33292
Akt1	FBgn0010379	0.0245999	0.0157632	1.56058849	0.33382
Hsp60	FBgn0001483	0.3465131	0.3719533	-1.0734178	0.3344

CG10639	FBgn0032729	0.0084138	0.0035418	2.3755988	0.33446
car	FBgn0000257	0.0033576	0.0014192	2.36579301	0.33502
Reg-2	FBgn0016715	0.0495571	0.0360885	1.37321186	0.33598
tud	FBgn0003891	0.0022257	0.0035843	-1.6104281	0.33704
pUf68	FBgn0028577	0.0201097	0.0237664	-1.1818399	0.33726
RpS12	FBgn0011809	1.2771437	1.200421	1.06391314	0.3382
Ufd1-like	FBgn0036136	0.0062715	0.0090342	-1.4405322	0.33827
dalao	FBgn0024493	0.0037021	0.0014075	2.63018493	0.33844
CG7830	FBgn0032015	0.0360721	0.0513867	-1.4245557	0.33917
CG14894	FBgn0038428	0.0089238	0.013747	-1.5404972	0.34017
CG1890	FBgn0039869	0.0213418	0.0079607	2.68091309	0.34209
CG31300	FBgn0039314	0.0152845	0.0093501	1.63468769	0.34271
CG1319	FBgn0035529	0.0379948	0.0247958	1.53231241	0.34272
SdhC	FBgn0037873	0.0136189	0.0153132	-1.1244119	0.34317
CG4390	FBgn0038771	0.0604978	0.0456302	1.32582833	0.34493
Def	FBgn0010385	0.1336763	0	Inf	0.34502
Prat2	FBgn0035717	0.0050381	0.0016792	3.00036723	0.34556
tsu	FBgn0033378	0.0397814	0.0278942	1.4261536	0.34632
CG3689	FBgn0035987	0.0439145	0.0303781	1.44559928	0.34642
Vha68-2	FBgn0010494	0.5611802	0.5933356	-1.0572996	0.34756
Arc-p34	FBgn0032859	0.0236092	0.0151339	1.56001721	0.34804
RpS27	FBgn0025532	0.4050655	0.4349253	-1.0737159	0.34822
CG13492	FBgn0034662	0.0009522	0.0003323	2.86505212	0.34909
tsr	FBgn0011567	0.9534397	0.8523298	1.11862766	0.3505
CG8310	FBgn0029623	0.0559493	0.0434781	1.28683798	0.35139
RpL34a	FBgn0039406	0.1282629	0.1125288	1.13982292	0.35149
CG1648	FBgn0033446	0.0467405	0.0399917	1.16875563	0.35161
CG31472	FBgn0037522	0.0574864	0.0391841	1.4670866	0.35167
sub	FBgn0003545	0.0035203	0.0014967	2.35204582	0.35231
CG5168	FBgn0032246	0.0148973	0.0098137	1.51800322	0.35252
RpS26	FBgn0003280	0.5098832	0.5503932	-1.0794496	0.35358
f	FBgn0000630	0.0004291	0.0011566	-2.6953878	0.35448
Rlc1	FBgn0014023	0.0022295	0.0060094	-2.6953878	0.35448
msk	FBgn0024487	0.0236343	0.0312624	-1.3227586	0.35484
CG2970	FBgn0034936	0.0140439	0.0184404	-1.3130539	0.35628
SelD	FBgn0020615	0.1497883	0.130415	1.14855067	0.35645
Tpi	FBgn0003738	0.3972012	0.4292185	-1.0806073	0.35699
Tango4	FBgn0030365	0.0349704	0.0326996	1.06944199	0.35944
Art8	FBgn0032329	0.0017718	0.004713	-2.6599378	0.35991
CG8360	FBgn0032001	0.0684959	0.044022	1.55594785	0.36057
CG11284	FBgn0030056	0.0024204	0.0064285	-2.6560042	0.36063
CG8507	FBgn0037756	0.0173003	0.0113563	1.52341987	0.36093

Kap-alpha3	FBgn0024888	0.1660861	0.1489679	1.11491175	0.36106
CG31739	FBgn0032611	0.0009627	0.0021119	-2.1937385	0.36188
Ank	FBgn0011747	0.0080368	0.006376	1.26047394	0.36232
Nat1	FBgn0027223	0.0178371	0.0215037	-1.2055561	0.36263
APP-BP1	FBgn0036127	0.0050015	0.0072696	-1.4534831	0.36312
CG13551	FBgn0040660	0.4225693	0.371126	1.13861416	0.36379
Aats-his	FBgn0027087	0.0638271	0.0794285	-1.2444321	0.36514
CG6607	FBgn0039204	0.0130029	0.0062735	2.07265423	0.36539
CG6195	FBgn0038723	0.008487	0.0127184	-1.4985839	0.36632
CG7484	FBgn0036745	0.1214606	0.1019878	1.19093295	0.36938
CG14407	FBgn0030584	0.0317982	0.0186739	1.70281656	0.37115
CG11414	FBgn0035024	0.0023332	0.0010594	2.20236365	0.37158
CG34422	FBgn0030967	0.0004105	0.0010627	-2.5890519	0.3716
didum	FBgn0015933	0.0003372	0.0008729	-2.5890519	0.3716
lid	FBgn0010658	0.0012185	0.0017799	-1.4606883	0.37191
CG7207	FBgn0027569	0.0076112	0.010685	-1.403847	0.37206
Vha13	FBgn0010857	0.1762758	0.0975089	1.80779228	0.37292
CG12433	FBgn0030811	0.0112943	0.00797	1.41709198	0.37424
betaTub60D	FBgn0003888	0.8949924	0.7894748	1.13365555	0.37429
Cyp1	FBgn0004432	1.0166634	0.9915037	1.02537532	0.37442
Rheb	FBgn0037343	0.0241937	0.0171691	1.40914038	0.37483
CG18418	FBgn0035568	0.0053262	0.0091928	-1.725964	0.37526
CG31063	FBgn0039496	0.0320402	0.0378196	-1.1803806	0.37621
galectin	FBgn0031213	0.0085825	0.0130894	-1.5251299	0.37632
CG1677	FBgn0029941	0.0032456	0.0015643	2.07480122	0.3766
Irp-1A	FBgn0024958	0.0456512	0.054077	-1.1845697	0.37689
CG2091	FBgn0037372	0.0054675	0.0076443	-1.3981227	0.37702
CG10516	FBgn0036549	0.0017858	0.004574	-2.5612561	0.37716
CG11858	FBgn0039305	0.0046981	0.0120331	-2.5612561	0.37716
CG30359	FBgn0033295	0.0242675	0.0172753	1.40474763	0.37737
CG4858	FBgn0037011	0.023142	0.0171773	1.34724381	0.37744
CG32972	FBgn0028905	0.003137	0.00194	1.61703137	0.37802
CG4019	FBgn0034885	0.0257005	0.0188274	1.3650561	0.37835
CG6726	FBgn0039049	0.0149104	0.020488	-1.3740786	0.37907
CG13364	FBgn0026879	0.140913	0.1059992	1.32937842	0.37926
CG31674	FBgn0032890	0.0188439	0.0129878	1.45088765	0.37984
CG9466	FBgn0032068	0.0032172	0.003788	-1.1774158	0.38043
CG9132	FBgn0030791	0.0786366	0.0601738	1.30682515	0.38067
Rab11	FBgn0004235	0.1079142	0.1176619	-1.0903283	0.38118
Acon	FBgn0010100	0.2586898	0.2724881	-1.0533392	0.38126
CG8223	FBgn0037624	0.1951048	0.2211361	-1.1334224	0.38142
CG5886	FBgn0039379	0.0044724	0.0085389	-1.9092447	0.3821

l(2)k09913	FBgn0021979	0.0036997	0.0098739	-2.668855	0.38242
Sec16	FBgn0030404	0.0031496	0.0079812	-2.5340509	0.38272
CG6418	FBgn0036104	0.0013656	0.0035469	-2.5973085	0.38357
CG12811	FBgn0037779	0.0502355	0.0275785	1.8215428	0.3838
Tps1	FBgn0001908	0.0055488	0.0037155	1.49343877	0.3842
Vha16-3	FBgn0028667	0.0373953	0.0124858	2.99502741	0.38454
CG2046	FBgn0037378	0.0523719	0.0456118	1.14820943	0.38515
TfIIFalpha	FBgn0010281	0.0073796	0.0055332	1.33370053	0.38902
CG10237	FBgn0032783	0.0081907	0.0120997	-1.477252	0.38924
Tcp-1eta	FBgn0037632	0.116771	0.1306242	-1.1186355	0.39044
CG8460	FBgn0031996	0.0416144	0.0299389	1.38997647	0.39119
CG32372	FBgn0019866	0.0034891	0.0022747	1.53388217	0.3932
Srp19	FBgn0015298	0.1323358	0.1454311	-1.0989551	0.39334
Df31	FBgn0015041	0.2764249	0.3333139	-1.2058025	0.39348
CG5384	FBgn0032216	0.1342377	0.153187	-1.1411621	0.39433
CG7324	FBgn0037074	0.003044	0.00177	1.71979103	0.39442
CG9548	FBgn0031822	0.0111978	0.0244385	-2.1824388	0.39475
CG6234	FBgn0038071	0.0038256	0.0016874	2.26719453	0.39586
Srp9	FBgn0035827	0.0413813	0.0529185	-1.2788011	0.3979
CG8498	FBgn0031992	0.3268673	0.3652809	-1.1175205	0.39927
Ag5r	FBgn0015010	0.1726419	0.2022652	-1.1715875	0.40014
CG31961	FBgn0031587	0.0076046	0.0029089	2.61423545	0.40082
CG14722	FBgn0037943	0.0046347	0.0090832	-1.9598314	0.40157
RpL4	FBgn0003279	0.6784187	0.7390479	-1.0893684	0.40207
CG6259	FBgn0023102	0.078451	0.08947	-1.1404566	0.40378
Snx6	FBgn0032005	0.0327788	0.0366931	-1.1194172	0.4038
CG4557	FBgn0029912	0.0058364	0.0074159	-1.2706256	0.4052
CG13900	FBgn0035162	0.0039069	0.006089	-1.5585131	0.4052
CG6206	FBgn0027611	0.0607563	0.0540608	1.12385187	0.40595
Atpalpha	FBgn0002921	0.0170152	0.0223428	-1.3131065	0.40676
spag	FBgn0015544	0.0101758	0.0057087	1.78251993	0.40724
l(2)09851	FBgn0022053	0.0120334	0.0090945	1.32314068	0.40746
CG4115	FBgn0038017	0.1774563	0.1462195	1.21362982	0.4076
Ddc	FBgn0000422	0.014113	0.0064785	2.17843047	0.4077
eIF-4a	FBgn0001942	0.8031651	0.8770531	-1.091996	0.40778
Rrp1	FBgn0004584	0.0048671	0.0081887	-1.68245	0.41
Hsp70Ab	FBgn0001231	0.1274206	0.135606	-1.0642397	0.41017
Trp1	FBgn0011584	0.0359166	0.0507134	-1.4119783	0.41029
CG13890	FBgn0035169	0.0171275	0.0135084	1.26791643	0.41223
Lcp3	FBgn0002534	0.0303724	0.0368348	-1.2127718	0.41232
Tom20	FBgn0036928	0.0303428	0.0376788	-1.2417728	0.41327
CG7787	FBgn0032020	0.0356355	0.0259954	1.37083671	0.41363

mmy	FBgn0027501	0.0165122	0.0144555	1.14227906	0.4153
CG18347	FBgn0037969	0.0130905	0.0171781	-1.3122588	0.41557
CG31948	FBgn0031427	0.005983	0.002834	2.11113518	0.41638
Gie	FBgn0037551	0.0536683	0.0646803	-1.2051872	0.41782
CG11134	FBgn0030518	0.052543	0.0423166	1.24166397	0.41794
Vha36	FBgn0022097	0.1286288	0.1130264	1.13804152	0.41857
Scamp	FBgn0030637	0.0046213	0.0078216	-1.6925141	0.41898
lig	FBgn0020279	0.0526132	0.0490171	1.07336434	0.42006
Ccp84Ae	FBgn0004779	0.0313457	0.0123484	2.5384323	0.42045
CG5873	FBgn0038511	0.002663	0.0054035	-2.0290848	0.42083
CG2493	FBgn0032864	0.0291302	0.024483	1.1898139	0.42094
CG3305	FBgn0032949	0.0330697	0.038555	-1.1658694	0.42202
cg	FBgn0000289	0.0056047	0.0027068	2.07059327	0.42205
mys	FBgn0001448	0.0157315	0.0123397	1.27486587	0.42242
T-cp1	FBgn0003676	0.11908	0.1273263	-1.0692503	0.42383
row	FBgn0033998	0.0035663	0.0078184	-2.1923232	0.4246
CG3800	FBgn0025228	0.3271953	0.3642786	-1.1133371	0.42461
Tap42	FBgn0032510	0.0053702	0.007439	-1.3852381	0.42605
RpA-70	FBgn0010173	0.0090813	0.0049843	1.82197829	0.42645
nvy	FBgn0005636	0.0023111	0.0011583	1.99520715	0.4268
CG10777	FBgn0029979	0.0038297	0.0049081	-1.2816061	0.42811
bcn92	FBgn0013432	0.027986	0.032202	-1.1506498	0.42856
r	FBgn0003189	0.0059297	0.0051492	1.15158655	0.42932
Rac1	FBgn0010333	0.0510723	0.0395894	1.29005094	0.4295
CG1309	FBgn0035519	0.0075933	0.0085302	-1.1233759	0.43027
CG1532	FBgn0031143	0.0883343	0.0968767	-1.0967053	0.43042
alpha-Est1	FBgn0015568	0.0031439	0.0015835	1.98543066	0.43043
Rab-RP4	FBgn0015794	0.0092345	0.0046624	1.98062309	0.43125
CPTI	FBgn0027842	0.0108584	0.0062712	1.73146145	0.43149
CG7770	FBgn0036918	0.0704287	0.0838816	-1.1910135	0.43149
Dgp-1	FBgn0027836	0.0023694	0.0049922	-2.1069974	0.4325
Tom40	FBgn0016041	0.0413286	0.0329099	1.25580969	0.43251
CG7181	FBgn0037097	0.1669598	0.0948381	1.7604713	0.43332
rok	FBgn0026181	0.0028387	0.0021577	1.3156605	0.43495
CG7358	FBgn0030974	0.00179	0.000898	1.99343307	0.43506
san	FBgn0024188	0.0526736	0.0418222	1.25946682	0.43526
Vha14	FBgn0010426	0.1176863	0.1296726	-1.1018498	0.43565
CecA1	FBgn0000276	0.1496788	0	Inf	0.43659
CecA2	FBgn0000276	0.1496788	0	Inf	0.43659
CecC	FBgn0000279	0.1496788	0	Inf	0.43659
chif	FBgn0000307	0.0002951	0	Inf	0.43659
cni	FBgn0000339	0.0075013	0	Inf	0.43659

dor	FBgn0000482	0.001078	0	Inf	0.43659
Hsp22	FBgn0001223	0.0046463	0	Inf	0.43659
l(1)10Bb	FBgn0001491	0.0040594	0	Inf	0.43659
l(2)35Df	FBgn0001986	0.0005087	0	Inf	0.43659
hyd	FBgn0002317	0.0001997	0	Inf	0.43659
sti	FBgn0002466	0.0004321	0	Inf	0.43659
mor	FBgn0002783	0.0162451	0	Inf	0.43659
MtnA	FBgn0002868	0.0270048	0	Inf	0.43659
Pu	FBgn0003162	0.0016566	0	Inf	0.43659
rb	FBgn0003210	0.0004353	0	Inf	0.43659
RpII215	FBgn0001616	0.0002844	0	Inf	0.43659
RpI135	FBgn0003278	0.0009568	0	Inf	0.43659
snf	FBgn0003449	0.0024848	0	Inf	0.43659
su(s)	FBgn0003575	0.0004722	0	Inf	0.43659
Su(var)2-10	FBgn0003612	0.0010551	0	Inf	0.43659
CG16778	FBgn0003715	0.0005902	0	Inf	0.43659
tor	FBgn0003733	0.0005815	0	Inf	0.43659
ttk	FBgn0003870	0.0009601	0	Inf	0.43659
vir	FBgn0003977	0.0003153	0	Inf	0.43659
cdc2	FBgn0004106	0.003637	0	Inf	0.43659
fwd	FBgn0004373	0.0004676	0	Inf	0.43659
fs(1)N	FBgn0000750	0.0002534	0	Inf	0.43659
fs(1)h	FBgn0000809	0.0002634	0	Inf	0.43659
RpII15	FBgn0004855	0.0041905	0	Inf	0.43659
tok	FBgn0004885	0.0003692	0	Inf	0.43659
east	FBgn0010110	0.0002683	0	Inf	0.43659
Myo61F	FBgn0010246	0.0004878	0	Inf	0.43659
Taf1	FBgn0004775	0.0002838	0	Inf	0.43659
sbb	FBgn0010575	0.0005603	0	Inf	0.43659
dock	FBgn0010583	0.0013091	0	Inf	0.43659
ox	FBgn0011227	0.0104773	0	Inf	0.43659
Sema-2a	FBgn0011260	0.001492	0	Inf	0.43659
thetaTry	FBgn0011555	0.0022311	0	Inf	0.43659
mas	FBgn0011653	0.0005126	0	Inf	0.43659
twin	FBgn0011725	0.0016877	0	Inf	0.43659
Gp150	FBgn0013272	0.0005749	0	Inf	0.43659
TfIIA-S	FBgn0010326	0.0058237	0	Inf	0.43659
Bgb	FBgn0013753	0.0028366	0	Inf	0.43659
Cdk5	FBgn0013762	0.0020551	0	Inf	0.43659
Ela	FBgn0013949	0.001634	0	Inf	0.43659
Ptp69D	FBgn0014007	0.0004133	0	Inf	0.43659
CG13397	FBgn0014417	0.0013884	0	Inf	0.43659

alpha-Est3	FBgn0015571	0.0009865	0	Inf	0.43659
rtGEF	FBgn0015803	0.0008808	0	Inf	0.43659
Faa	FBgn0016013	0.0015003	0	Inf	0.43659
ari-1	FBgn0014203	0.0012012	0	Inf	0.43659
Smg5	FBgn0019890	0.0006546	0	Inf	0.43659
Khc-73	FBgn0019968	0.0003257	0	Inf	0.43659
Mcr	FBgn0014086	0.0003274	0	Inf	0.43659
mst	FBgn0001566	0.0009351	0	Inf	0.43659
dbe	FBgn0020305	0.0015557	0	Inf	0.43659
crol	FBgn0010573	0.000599	0	Inf	0.43659
Pkn	FBgn0004459	0.0009097	0	Inf	0.43659
Scp2	FBgn0020907	0.0058759	0	Inf	0.43659
Dgkepsilon	FBgn0020930	0.0011315	0	Inf	0.43659
Nle	FBgn0021874	0.0021997	0	Inf	0.43659
ytr	FBgn0021895	0.0031144	0	Inf	0.43659
Rs1	FBgn0021995	0.000976	0	Inf	0.43659
Thor	FBgn0017459	0.0051641	0	Inf	0.43659
CG10340	FBgn0022344	0.0022051	0	Inf	0.43659
Sin3A	FBgn0010646	0.0006092	0	Inf	0.43659
Dmau\CecA1	FBgn0000276	0.1496788	0	Inf	0.43659
slmb	FBgn0016060	0.0011847	0	Inf	0.43659
Tequila	FBgn0023479	0.0016328	0	Inf	0.43659
CG14815	FBgn0023516	0.000984	0	Inf	0.43659
mRpL16	FBgn0019893	0.0019878	0	Inf	0.43659
trio	FBgn0015758	0.000267	0	Inf	0.43659
Flo-2	FBgn0024753	0.0013156	0	Inf	0.43659
CG4585	FBgn0025335	0.001596	0	Inf	0.43659
CG4882	FBgn0025336	0.0014882	0	Inf	0.43659
bab2	FBgn0012044	0.0005663	0	Inf	0.43659
unc-119	FBgn0025549	0.0020254	0	Inf	0.43659
CG4061	FBgn0025630	0.0017331	0	Inf	0.43659
CG3588	FBgn0025643	0.0019857	0	Inf	0.43659
CG3164	FBgn0025683	0.0022613	0	Inf	0.43659
CG15438	FBgn0025684	0.0024606	0	Inf	0.43659
CG5594	FBgn0025698	0.0006086	0	Inf	0.43659
plexB	FBgn0024198	0.000301	0	Inf	0.43659
plexA	FBgn0025741	0.0003106	0	Inf	0.43659
Rap2l	FBgn0025806	0.0058981	0	Inf	0.43659
Mhcl	FBgn0026059	0.0006354	0	Inf	0.43659
TXBP181-like	FBgn0026326	0.0006917	0	Inf	0.43659
Rhp	FBgn0026374	0.0008714	0	Inf	0.43659

HDAC6	FBgn0026428	0.0005182	0	Inf	0.43659
ear	FBgn0026441	0.0011615	0	Inf	0.43659
mRpL18	FBgn0026741	0.0028856	0	Inf	0.43659
l(1)G0193	FBgn0027280	0.0009685	0	Inf	0.43659
Tim9b	FBgn0027358	0.0045874	0	Inf	0.43659
CG7261	FBgn0027509	0.0004246	0	Inf	0.43659
morgue	FBgn0027609	0.0015453	0	Inf	0.43659
YT521-B	FBgn0027616	0.0007465	0	Inf	0.43659
Cpsf100	FBgn0027873	0.0009099	0	Inf	0.43659
CG11070	FBgn0028467	0.0005405	0	Inf	0.43659
CG9063	FBgn0028500	0.0004228	0	Inf	0.43659
CG18477	FBgn0028864	0.0012419	0	Inf	0.43659
Tsp42Ee	FBgn0029506	0.0035459	0	Inf	0.43659
CG15896	FBgn0029858	0.0009866	0	Inf	0.43659
CG15891	FBgn0029860	0.0036022	0	Inf	0.43659
CG15894	FBgn0029864	0.0003916	0	Inf	0.43659
CG3842	FBgn0029866	0.0014398	0	Inf	0.43659
CG2254	FBgn0029994	0.0018881	0	Inf	0.43659
sni	FBgn0030026	0.0024462	0	Inf	0.43659
CG1387	FBgn0030033	0.0005287	0	Inf	0.43659
CG11190	FBgn0030035	0.0009103	0	Inf	0.43659
CG3004	FBgn0030142	0.0018411	0	Inf	0.43659
CG15203	FBgn0030261	0.0045668	0	Inf	0.43659
CG2076	FBgn0030263	0.0018103	0	Inf	0.43659
ATP7	FBgn0030343	0.0004403	0	Inf	0.43659
CG1622	FBgn0030468	0.001551	0	Inf	0.43659
CG15756	FBgn0030493	0.0026612	0	Inf	0.43659
CG11063	FBgn0030530	0.0017667	0	Inf	0.43659
mRpS25	FBgn0030572	0.003618	0	Inf	0.43659
CG15032	FBgn0030626	0.0021812	0	Inf	0.43659
CG9673	FBgn0030775	0.0020564	0	Inf	0.43659
CG10597	FBgn0030832	0.0050051	0	Inf	0.43659
CG8173	FBgn0030864	0.001572	0	Inf	0.43659
CG7772	FBgn0030883	0.0070274	0	Inf	0.43659
Mur18B	FBgn0030999	0.0011158	0	Inf	0.43659
Tao-1	FBgn0031030	0.0011444	0	Inf	0.43659
CG9581	FBgn0031093	0.0009264	0	Inf	0.43659
CG15452	FBgn0031130	0.0050109	0	Inf	0.43659
r-cup	FBgn0031142	0.0009036	0	Inf	0.43659
CG10918	FBgn0031178	0.0058658	0	Inf	0.43659
CG14614	FBgn0031186	0.0070601	0	Inf	0.43659
CG3709	FBgn0031227	0.0011525	0	Inf	0.43659

tho2	FBgn0031390	0.0003682	0	Inf	0.43659
CG7082	FBgn0031401	0.0009318	0	Inf	0.43659
CG15435	FBgn0031608	0.0011456	0	Inf	0.43659
CG5828	FBgn0031682	0.0015027	0	Inf	0.43659
CG7382	FBgn0031708	0.0045771	0	Inf	0.43659
CG7371	FBgn0031710	0.0009451	0	Inf	0.43659
CG14005	FBgn0031739	0.0015928	0	Inf	0.43659
CG11034	FBgn0031741	0.0008398	0	Inf	0.43659
CG9498	FBgn0031801	0.001425	0	Inf	0.43659
CG11050	FBgn0031836	0.0013833	0	Inf	0.43659
neuroligin	FBgn0031866	0.0004684	0	Inf	0.43659
CG10158	FBgn0031871	0.0017039	0	Inf	0.43659
CG3430	FBgn0031875	0.0009525	0	Inf	0.43659
CG5181	FBgn0031909	0.002631	0	Inf	0.43659
CG7231	FBgn0031968	0.0019292	0	Inf	0.43659
Wwox	FBgn0025543	0.0014292	0	Inf	0.43659
Spn28D	FBgn0031973	0.0010751	0	Inf	0.43659
PrBP	FBgn0032059	0.0040013	0	Inf	0.43659
CG9463	FBgn0032066	0.0005672	0	Inf	0.43659
CG4382	FBgn0032132	0.0009857	0	Inf	0.43659
CG4036	FBgn0032149	0.0019913	0	Inf	0.43659
RluA-2	FBgn0032256	0.0019748	0	Inf	0.43659
CG17134	FBgn0032304	0.0034404	0	Inf	0.43659
Ced-12	FBgn0032409	0.0011167	0	Inf	0.43659
CG17211	FBgn0032414	0.0003964	0	Inf	0.43659
CG6388	FBgn0032430	0.0010567	0	Inf	0.43659
CG5780	FBgn0032446	0.0025094	0	Inf	0.43659
spict	FBgn0032451	0.0013941	0	Inf	0.43659
CG9928	FBgn0032472	0.0050634	0	Inf	0.43659
Pect	FBgn0032482	0.0016155	0	Inf	0.43659
Tpr2	FBgn0032586	0.0010565	0	Inf	0.43659
CG5131	FBgn0032644	0.0020655	0	Inf	0.43659
kon	FBgn0032683	0.0002144	0	Inf	0.43659
Irk3	FBgn0032706	0.002831	0	Inf	0.43659
mRpL13	FBgn0025194	0.0034681	0	Inf	0.43659
CG17549	FBgn0032774	0.0020078	0	Inf	0.43659
CG9987	FBgn0032781	0.0021214	0	Inf	0.43659
CG13084	FBgn0032788	0.0012876	0	Inf	0.43659
CG10631	FBgn0032817	0.0001524	0	Inf	0.43659
mRpS18B	FBgn0032849	0.0029939	0	Inf	0.43659
CG10949	FBgn0032858	0.0013163	0	Inf	0.43659
CG2614	FBgn0032873	0.0007975	0	Inf	0.43659

CG12926	FBgn0033437	0.0017148	0	Inf	0.43659
CG12130	FBgn0033466	0.0009333	0	Inf	0.43659
CG13188	FBgn0033668	0.0011233	0	Inf	0.43659
Rcd1	FBgn0033897	0.0005869	0	Inf	0.43659
CG10253	FBgn0033983	0.0009783	0	Inf	0.43659
CG7639	FBgn0033989	0.0014123	0	Inf	0.43659
alphaPS4	FBgn0034005	0.0006082	0	Inf	0.43659
CG12964	FBgn0034022	0.0009568	0	Inf	0.43659
Atg9	FBgn0034110	0.0006451	0	Inf	0.43659
CG15611	FBgn0034194	0.0013022	0	Inf	0.43659
CG10914	FBgn0034307	0.0009893	0	Inf	0.43659
Nup75	FBgn0034310	0.0008035	0	Inf	0.43659
IM23	FBgn0034328	0.0161135	0	Inf	0.43659
CG15067	FBgn0027666	0.0034852	0	Inf	0.43659
CG5335	FBgn0034365	0.0015729	0	Inf	0.43659
CG8929	FBgn0034504	0.0008318	0	Inf	0.43659
CG4030	FBgn0034585	0.0009035	0	Inf	0.43659
CG15666	FBgn0034622	0.0006399	0	Inf	0.43659
CG4386	FBgn0034661	0.0013573	0	Inf	0.43659
CG9308	FBgn0034681	0.003082	0	Inf	0.43659
CG11298	FBgn0034721	0.0035311	0	Inf	0.43659
PIP5K59B	FBgn0034789	0.0007905	0	Inf	0.43659
CG13539	FBgn0034833	0.0024063	0	Inf	0.43659
mRpL43	FBgn0034893	0.0031469	0	Inf	0.43659
CG5602	FBgn0034922	0.0008176	0	Inf	0.43659
CG5591	FBgn0034926	0.0004165	0	Inf	0.43659
CG3163	FBgn0034961	0.0014585	0	Inf	0.43659
Fcp1	FBgn0035026	0.000599	0	Inf	0.43659
spz6	FBgn0035056	0.0029653	0	Inf	0.43659
CG3829	FBgn0035091	0.0019305	0	Inf	0.43659
CG9205	FBgn0035181	0.0017716	0	Inf	0.43659
CG9129	FBgn0035196	0.0020116	0	Inf	0.43659
CG9134	FBgn0035199	0.0028549	0	Inf	0.43659
CG2277	FBgn0035204	0.0011315	0	Inf	0.43659
CG9153	FBgn0035207	0.0005711	0	Inf	0.43659
CG12099	FBgn0035232	0.0008719	0	Inf	0.43659
CG13926	FBgn0035243	0.0029673	0	Inf	0.43659
CG7970	FBgn0035252	0.0030605	0	Inf	0.43659
Mfap1	FBgn0035294	0.0011229	0	Inf	0.43659
CG1275	FBgn0035321	0.0044452	0	Inf	0.43659
CG16758	FBgn0035348	0.0017952	0	Inf	0.43659
CG11537	FBgn0035400	0.0012821	0	Inf	0.43659

CG14997	FBgn0035515	0.0011744	0	Inf	0.43659
CG7465	FBgn0035551	0.001821	0	Inf	0.43659
CG10630	FBgn0035608	0.0034401	0	Inf	0.43659
CG8270	FBgn0035703	0.0009249	0	Inf	0.43659
CG10144	FBgn0035704	0.0004916	0	Inf	0.43659
CG8549	FBgn0035714	0.0020036	0	Inf	0.43659
CG7550	FBgn0035839	0.0025721	0	Inf	0.43659
CG6683	FBgn0035902	0.002563	0	Inf	0.43659
CG4447	FBgn0035980	0.0022687	0	Inf	0.43659
CG8336	FBgn0036020	0.0015262	0	Inf	0.43659
CG18179	FBgn0036023	0.0020027	0	Inf	0.43659
CG7394	FBgn0036173	0.0045485	0	Inf	0.43659
Pop2	FBgn0036239	0.001995	0	Inf	0.43659
CG10646	FBgn0036292	0.0016118	0	Inf	0.43659
CG10732	FBgn0036365	0.0007631	0	Inf	0.43659
CG6661	FBgn0036403	0.0009918	0	Inf	0.43659
CG13472	FBgn0036450	0.0009671	0	Inf	0.43659
CG6876	FBgn0025957	0.001206	0	Inf	0.43659
CG7650	FBgn0036519	0.0021891	0	Inf	0.43659
CG17029	FBgn0036551	0.0020412	0	Inf	0.43659
CG13047	FBgn0036594	0.0034952	0	Inf	0.43659
CG4893	FBgn0036616	0.0032152	0	Inf	0.43659
CG13026	FBgn0036656	0.0043623	0	Inf	0.43659
CG13028	FBgn0036676	0.0033368	0	Inf	0.43659
CG13023	FBgn0036677	0.0029401	0	Inf	0.43659
Cad74A	FBgn0036715	0.0003212	0	Inf	0.43659
Edc3	FBgn0036735	0.0015885	0	Inf	0.43659
CG5577	FBgn0036759	0.0055671	0	Inf	0.43659
MED19	FBgn0036761	0.0014982	0	Inf	0.43659
CG7408	FBgn0036765	0.0009175	0	Inf	0.43659
CG14353	FBgn0036771	0.0013464	0	Inf	0.43659
mRpS26	FBgn0036774	0.0027436	0	Inf	0.43659
CG3893	FBgn0036826	0.003618	0	Inf	0.43659
trpml	FBgn0036904	0.0008232	0	Inf	0.43659
CG7757	FBgn0036915	0.0011443	0	Inf	0.43659
CG8004	FBgn0036920	0.0022461	0	Inf	0.43659
CG5847	FBgn0036985	0.0002649	0	Inf	0.43659
CG3698	FBgn0037023	0.0018401	0	Inf	0.43659
CG3680	FBgn0037027	0.0006666	0	Inf	0.43659
CG7177	FBgn0037098	0.0004564	0	Inf	0.43659
CG14636	FBgn0037217	0.0027595	0	Inf	0.43659
CG14647	FBgn0037244	0.00171	0	Inf	0.43659

CG9775	FBgn0037261	0.0014861	0	Inf	0.43659
CG12162	FBgn0037329	0.0011715	0	Inf	0.43659
Hcs	FBgn0037332	0.0005156	0	Inf	0.43659
Pi4KIIalpha	FBgn0037339	0.0011113	0	Inf	0.43659
CG10092	FBgn0037526	0.00085	0	Inf	0.43659
CG10435	FBgn0037539	0.0011641	0	Inf	0.43659
CG9667	FBgn0037550	0.0022213	0	Inf	0.43659
CG11694	FBgn0037571	0.0022079	0	Inf	0.43659
CG9837	FBgn0037635	0.0024392	0	Inf	0.43659
RagA	FBgn0037647	0.0020117	0	Inf	0.43659
CG8866	FBgn0037679	0.000971	0	Inf	0.43659
RnpS1	FBgn0037707	0.0016155	0	Inf	0.43659
Pnn	FBgn0037737	0.0016664	0	Inf	0.43659
CG12948	FBgn0037739	0.0024236	0	Inf	0.43659
CG11722	FBgn0037777	0.0028387	0	Inf	0.43659
CG11870	FBgn0037804	0.0004548	0	Inf	0.43659
mRpL40	FBgn0037892	0.0030827	0	Inf	0.43659
CG10898	FBgn0037911	0.0016949	0	Inf	0.43659
CG14712	FBgn0037924	0.000424	0	Inf	0.43659
CG6908	FBgn0037936	0.0014559	0	Inf	0.43659
ssp5	FBgn0037985	0.0008682	0	Inf	0.43659
CG8449	FBgn0038129	0.0009239	0	Inf	0.43659
omd	FBgn0038168	0.0006144	0	Inf	0.43659
Npc2b	FBgn0038198	0.0033756	0	Inf	0.43659
mRpL11	FBgn0038234	0.0025761	0	Inf	0.43659
CG3817	FBgn0038275	0.0019446	0	Inf	0.43659
Art3	FBgn0038306	0.0012747	0	Inf	0.43659
CG5404	FBgn0038354	0.000856	0	Inf	0.43659
mRpS11	FBgn0038474	0.003037	0	Inf	0.43659
CG5840	FBgn0038516	0.0022612	0	Inf	0.43659
CG7685	FBgn0038619	0.0028366	0	Inf	0.43659
CG7705	FBgn0038639	0.0025821	0	Inf	0.43659
CG14299	FBgn0038651	0.0002603	0	Inf	0.43659
CG5451	FBgn0038666	0.0011321	0	Inf	0.43659
CG5555	FBgn0038686	0.0010383	0	Inf	0.43659
CG4733	FBgn0038744	0.0006384	0	Inf	0.43659
CG4538	FBgn0038745	0.0008686	0	Inf	0.43659
CG4783	FBgn0038756	0.006241	0	Inf	0.43659
CG10889	FBgn0038769	0.0011586	0	Inf	0.43659
CG17199	FBgn0038775	0.0013106	0	Inf	0.43659
CG5077	FBgn0038786	0.0006709	0	Inf	0.43659
CG5191	FBgn0038803	0.0010914	0	Inf	0.43659

CG16953	FBgn0038809	0.0009367	0	Inf	0.43659
Fancd2	FBgn0038827	0.0035782	0	Inf	0.43659
CG3308	FBgn0038877	0.0016825	0	Inf	0.43659
Dcr-1	FBgn0039016	0.0004803	0	Inf	0.43659
CG13836	FBgn0039060	0.0046393	0	Inf	0.43659
CG10214	FBgn0039115	0.0028635	0	Inf	0.43659
tst	FBgn0039117	0.0005227	0	Inf	0.43659
AP-1sigma	FBgn0039132	0.0034186	0	Inf	0.43659
CG5933	FBgn0039139	0.0008828	0	Inf	0.43659
Npc2f	FBgn0039154	0.00297	0	Inf	0.43659
CG13634	FBgn0039224	0.0013078	0	Inf	0.43659
XNP	FBgn0039338	0.0008239	0	Inf	0.43659
CG6073	FBgn0039417	0.0016955	0	Inf	0.43659
CG6330	FBgn0039464	0.0017438	0	Inf	0.43659
TwdlC	FBgn0039469	0.0027556	0	Inf	0.43659
CG5882	FBgn0039490	0.0006198	0	Inf	0.43659
CG5934	FBgn0039505	0.0039757	0	Inf	0.43659
CG5639	FBgn0039527	0.0007749	0	Inf	0.43659
mRpS22	FBgn0039555	0.0014874	0	Inf	0.43659
CG14528	FBgn0039611	0.0007403	0	Inf	0.43659
Cul-5	FBgn0039632	0.0009191	0	Inf	0.43659
CG31033	FBgn0039705	0.0009678	0	Inf	0.43659
CG15523	FBgn0039727	0.0001439	0	Inf	0.43659
CG7896	FBgn0039728	0.0004435	0	Inf	0.43659
CG11498	FBgn0039749	0.001121	0	Inf	0.43659
PH4alphaEFB	FBgn0039775	0.000918	0	Inf	0.43659
CG11337	FBgn0039846	0.0007848	0	Inf	0.43659
CstF-50	FBgn0039867	0.0013591	0	Inf	0.43659
CG2135	FBgn0039874	0.0015746	0	Inf	0.43659
RecQ4	FBgn0035846	0.0004035	0	Inf	0.43659
MED22	FBgn0025972	0.0043169	0	Inf	0.43659
kappaB-Ras	FBgn0033172	0.0026703	0	Inf	0.43659
CG15386	FBgn0040715	0.0075915	0	Inf	0.43659
dpr	FBgn0040726	0.0016821	0	Inf	0.43659
CG14933	FBgn0040968	0.0075915	0	Inf	0.43659
CG6115	FBgn0040985	0.0071082	0	Inf	0.43659
TepIII	FBgn0031933	0.0003979	0	Inf	0.43659
yellow-e	FBgn0038152	0.0011647	0	Inf	0.43659
CG5180	FBgn0038802	0.0014021	0	Inf	0.43659
mRpS14	FBgn0031019	0.0039446	0	Inf	0.43659
Atg2	FBgn0035373	0.0002866	0	Inf	0.43659
TotC	FBgn0044812	0.0045314	0	Inf	0.43659

CG1109	FBgn0037361	0.0007498	0	Inf	0.43659
Liprin-alpha	FBgn0024747	0.0004204	0	Inf	0.43659
Obp83ef	FBgn0037401	0.0043814	0	Inf	0.43659
CG30193	FBgn0034799	0.0012338	0	Inf	0.43659
PH4alphaPV	FBgn0039793	0.0009617	0	Inf	0.43659
CG31195	FBgn0051195	0.0007537	0	Inf	0.43659
CG31327	FBgn0051327	0.0008509	0	Inf	0.43659
CG31436	FBgn0039320	0.0025719	0	Inf	0.43659
CG31547	FBgn0037335	0.0005394	0	Inf	0.43659
CG31716	FBgn0032238	0.0005771	0	Inf	0.43659
CG31780	FBgn0028864	0.0012419	0	Inf	0.43659
CG31789	FBgn0051789	0.0052762	0	Inf	0.43659
CG31907	FBgn0045995	0.001425	0	Inf	0.43659
CG32086	FBgn0036175	0.0011905	0	Inf	0.43659
CG32113	FBgn0036307	0.0001608	0	Inf	0.43659
CG32163	FBgn0052163	0.004271	0	Inf	0.43659
Drs-l	FBgn0035441	0.0083507	0	Inf	0.43659
CG32368	FBgn0052368	0.0068659	0	Inf	0.43659
Cpr65Aw	FBgn0052404	0.0092324	0	Inf	0.43659
CG32407	FBgn0035650	0.0023911	0	Inf	0.43659
CG32529	FBgn0031075	0.0002389	0	Inf	0.43659
Twdlalpha	FBgn0030785	0.0014852	0	Inf	0.43659
CG32662	FBgn0025954	0.0010926	0	Inf	0.43659
CG32685	FBgn0030175	0.0003661	0	Inf	0.43659
CG32694	FBgn0030168	0.0030815	0	Inf	0.43659
CG32732	FBgn0029921	0.0009402	0	Inf	0.43659
CG32758	FBgn0029794	0.0009509	0	Inf	0.43659
CG33493	FBgn0053493	0.0056495	0	Inf	0.43659
dbr	FBgn0028472	0.0012204	0	Inf	0.43659
Patj	FBgn0002177	0.0006162	0	Inf	0.43659
CG34126	FBgn0051653	0.0007199	0	Inf	0.43659
sra	FBgn0020250	0.0020692	0	Inf	0.43659
l(3)L1231	FBgn0026578	0.0004802	0	Inf	0.43659
Bre1	FBgn0035637	0.0005787	0	Inf	0.43659
Cenp-C	FBgn0037598	0.0004119	0	Inf	0.43659
bbg	FBgn0036424	0.0005688	0	Inf	0.43659
Vrp1	FBgn0034695	0.0007053	0	Inf	0.43659
CG8628	FBgn0035744	0.0128594	0	Inf	0.43659
CG34434	FBgn0029777	0.006794	0	Inf	0.43659
cno	FBgn0000340	0.0002835	0	Inf	0.43659
CG42345	FBgn0033022	0.0007322	0	Inf	0.43659
mRpS34	FBgn0036613	0.0026857	0	Inf	0.43659

CG42542	FBgn0038297	0.0015632	0	Inf	0.43659
Tango9	FBgn0037971	0.0014087	0	Inf	0.43659
Vti1	FBgn0035156	0.0050109	0	Inf	0.43659
exo84	FBgn0039401	0.0007987	0	Inf	0.43659
CG42593	FBgn0029985	0.0003651	0	Inf	0.43659
Rbsn-5	FBgn0031991	0.0010628	0	Inf	0.43659
bou	FBgn0029927	0.0041431	0	Inf	0.43659
sxc	FBgn0027591	0.0004994	0	Inf	0.43659
haf	FBgn0031349	0.0004379	0	Inf	0.43659
CG10320	FBgn0027667	0.0254657	0.0125206	2.03389711	0.43772
Pka-C1	FBgn0000273	0.0088925	0.0107923	-1.2136365	0.43795
CG1140	FBgn0027933	0.0220364	0.0186787	1.17976572	0.4383
CG17119	FBgn0039045	0.0100681	0.0073907	1.36227638	0.43965
Arp14D	FBgn0011742	0.0167652	0.0144297	1.16185984	0.44014
CG8289	FBgn0030854	0.0204453	0.0229643	-1.1232071	0.44032
CG1291	FBgn0035401	0.0361325	0.0218046	1.65710638	0.44137
RpLP0	FBgn0000100	1.0798901	1.1658232	-1.0795758	0.44178
CG33214	FBgn0037088	0.0016075	0.000823	1.95321514	0.44186
AP-50	FBgn0024832	0.0085103	0.0112222	-1.318656	0.44361
CG32069	FBgn0036119	0.0504327	0.0732727	-1.452882	0.44391
CG11779	FBgn0038683	0.0100333	0.0130583	-1.3015001	0.44487
CG32473	FBgn0038137	0.0038593	0.0047637	-1.2343504	0.44571
shot	FBgn0013733	0.0047374	0.0059992	-1.266362	0.4467
su(r)	FBgn0016718	0.001759	0.0034054	-1.9360139	0.44692
CG15014	FBgn0035532	0.0068262	0.0093421	-1.3685689	0.44724
mRpL12	FBgn0011362	0.0953547	0.1135117	-1.1904143	0.44766
GstD10	FBgn0038019	0.0150964	0.0193309	-1.2804969	0.45021
Prm	FBgn0003149	0.2731096	0.237724	1.14885198	0.45077
CG17734	FBgn0037890	0.0336098	0.0271874	1.23622508	0.45093
CG16733	FBgn0037665	0.0015978	0.0059489	-3.7231371	0.45097
CG14782	FBgn0025381	0.0135938	0.0214813	-1.5802208	0.45117
Osi14	FBgn0037423	0.0102459	0.0051409	1.99302279	0.45137
Atg4	FBgn0031298	0.0274254	0.0236182	1.16120063	0.45345
CG7077	FBgn0038946	0.0099889	0.0138849	-1.39004	0.45348
Ras64B	FBgn0003206	0.0186403	0.0260626	-1.3981872	0.45527
Eip63E	FBgn0005640	0.0019955	0.0036684	-1.8383686	0.4559
CG9009	FBgn0027601	0.0088538	0.0068508	1.29237326	0.45607
CG2767	FBgn0037537	0.1915109	0.2034988	-1.0625966	0.45678
Obp56a	FBgn0034468	0.1756122	0.1349043	1.30175359	0.45679
Aats-trp	FBgn0010803	0.1798158	0.2008361	-1.1168991	0.45691
Dsp1	FBgn0011764	0.0073368	0.0052942	1.3858148	0.45715
Nopp140	FBgn0037137	0.0121797	0.0076453	1.59309591	0.45798

Acph-1	FBgn0000032	0.0198932	0.024068	-1.2098609	0.45827
CG11999	FBgn0037312	0.1610247	0.1828247	-1.1353829	0.45921
CG15293	FBgn0027904	0.0114289	0.0041359	2.76332159	0.45963
nonA	FBgn0000188	0.0100662	0.0122675	-1.2186913	0.45973
emb	FBgn0020497	0.0039184	0.006502	-1.659347	0.45999
eIF4E-4	FBgn0035709	0.025245	0.0336716	-1.3337925	0.46022
Pcmt	FBgn0015276	0.0073773	0.0038747	1.90399076	0.46102
Nlp	FBgn0016133	0.2049803	0.1860759	1.10159516	0.46117
Cyp4d8	FBgn0015033	0.0011592	0.0041142	-3.5490924	0.46135
Got1	FBgn0001124	0.0984149	0.1052897	-1.0698554	0.46247
G-salpha60A	FBgn0001123	0.0045158	0.0023857	1.89285094	0.46321
CG5112	FBgn0039341	0.0034028	0.0017972	1.89343531	0.46348
CG5103	FBgn0036784	0.0189816	0.0129473	1.46606735	0.4653
Madm	FBgn0027497	0.0071388	0.0041677	1.71288875	0.46584
Cbp20	FBgn0022943	0.011448	0.0185658	-1.6217549	0.46641
Tsp66E	FBgn0035936	0.0064805	0.0034401	1.8838146	0.4666
CG7011	FBgn0036489	0.0089637	0.0072036	1.24433116	0.46911
CG11490	FBgn0031233	0.0024016	0.0042039	-1.7504491	0.46916
dUTPase	FBgn0013349	0.0623746	0.0572703	1.08912676	0.46935
CG2604	FBgn0037298	0.0049188	0.008443	-1.7164842	0.46952
Rac2	FBgn0014011	0.0351079	0.027819	1.26201138	0.46969
ttm3	FBgn0032971	0.0033888	0.0060843	-1.7954059	0.46998
Ubi-p63E	FBgn0003941	0.8355076	0.9165333	-1.0969778	0.47034
Gos28	FBgn0038637	0.0127616	0.0172869	-1.3545983	0.47191
CG8993	FBgn0035334	0.0945839	0.1168043	-1.2349285	0.47283
Ilp6	FBgn0029612	0.0216846	0.0232038	-1.0700572	0.47467
CG42533	FBgn0031921	0.0003113	0.0010418	-3.3465964	0.47501
RpL37a	FBgn0030616	0.2833244	0.4177532	-1.4744693	0.47579
DnaJ-1	FBgn0015657	0.0618702	0.0506816	1.22076254	0.47605
Eig71Ec	FBgn0004590	0.7658184	0.8473031	-1.1064022	0.47699
CG31150	FBgn0038372	0.0062735	0.004075	1.53950424	0.4773
TpnC73F	FBgn0010424	0.1443116	0.1183859	1.21899274	0.47748
Fim	FBgn0024238	0.0672861	0.0742061	-1.1028435	0.47778
CG12413	FBgn0039588	0.0025113	0.0013505	1.85958685	0.4779
CG6782	FBgn0037912	0.0169361	0.0120852	1.40139515	0.47801
CG5446	FBgn0032429	0.0432281	0.0684292	-1.5829789	0.47855
Pep	FBgn0004401	0.0618976	0.0695622	-1.1238274	0.47858
Hsp60C	FBgn0031728	0.0441006	0.0420848	1.04789925	0.48049
CG5432	FBgn0039425	0.002993	0.005302	-1.771455	0.48245
Spt5	FBgn0034445	0.0174166	0.0157101	1.10862875	0.48258
Pros25	FBgn0010405	0.2942907	0.2679465	1.09831887	0.48274
alph	FBgn0039672	0.0220209	0.0158774	1.3869354	0.4829

CG14567	FBgn0037126	0.011847	0.0072488	1.63434102	0.48471
mRpL30	FBgn0029718	0.0098323	0.0038257	2.57003402	0.48531
Noa36	FBgn0026400	0.0056503	0.0021861	2.58461761	0.48549
CG10343	FBgn0032703	0.0048674	0.0085341	-1.7533069	0.48635
CG17294	FBgn0032032	0.0065383	0.00356	1.83661439	0.48672
CG6055	FBgn0031918	0.0640988	0.0461749	1.38817551	0.48674
Nplp2	FBgn0040813	1.3629764	1.1580247	1.17698388	0.48818
Nrg	FBgn0002968	0.0053004	0.0042153	1.2574191	0.48842
snRNP70K	FBgn0003458	0.0063468	0.0034918	1.81766436	0.48965
CG4706	FBgn0037862	0.0318159	0.0342626	-1.0769022	0.4919
SmD3	FBgn0023167	0.0289924	0.0225252	1.28710937	0.4939
Ant2	FBgn0025111	0.171433	0.2030852	-1.1846329	0.49402
Arp87C	FBgn0011745	0.1049647	0.0955326	1.09873192	0.49408
CG3301	FBgn0038878	0.0238023	0.0335731	-1.4105008	0.49448
CG8184	FBgn0030674	0.000223	0.0003875	-1.7378709	0.49463
CkIIalpha	FBgn0000258	0.1275859	0.1151384	1.10810924	0.49509
CG9906	FBgn0030755	0.0409309	0.0360016	1.13691808	0.496
CG3887	FBgn0031670	0.0532683	0.0413795	1.28731176	0.49621
RpL3	FBgn0020910	0.3455613	0.3707657	-1.0729377	0.49622
Eno	FBgn0000579	0.7030245	0.7522344	-1.0699975	0.49649
CG12975	FBgn0037061	0.0084002	0.0145207	-1.7286066	0.49759
vari	FBgn0032885	0.002221	0.0038392	-1.7286066	0.49759
wdb	FBgn0026590	0.0058591	0.0033953	1.7256335	0.49764
Tango11	FBgn0025252	0.007509	0.0031613	2.3753021	0.4982
IM10	FBgn0033835	0.0191012	0.0025695	7.4337151	0.49916
CG17660	FBgn0031356	0.0011517	0.0035072	-3.0451914	0.49923
S6k	FBgn0010455	0.0041624	0.0046508	-1.1173372	0.49956
Rpb7	FBgn0038305	0.0097899	0.0054331	1.80191587	0.49983
mRpL46	FBgn0035272	0.0065025	0.0026691	2.43619294	0.49985
DptB	FBgn0034407	0.0580085	0.0079436	7.30258433	0.50037
Lsp1alpha	FBgn0002562	0.7119398	0.6551485	1.08668462	0.50147
nrv1	FBgn0015776	0.0057324	0.0022286	2.57221512	0.50192
CG8492	FBgn0035813	0.002097	0.0037358	-1.7814731	0.50216
RnrL	FBgn0011703	0.0069899	0.009888	-1.4146123	0.50328
Fas3	FBgn0000636	0.0032398	0.0018081	1.79186522	0.50398
CG12063	FBgn0039851	0.0065835	0.0029123	2.26059386	0.50539
His1	FBgn0051617	0.0679695	0.0593864	1.14452966	0.50629
His1:CG31617	FBgn0051617	0.0679695	0.0593864	1.14452966	0.50629
Rab39	FBgn0029959	0.032464	0.0290088	1.11910886	0.50654
Obp99a	FBgn0039678	0.0163793	0.0295452	-1.8038173	0.5068
alpha-Est7	FBgn0004945	0.029369	0.0359601	-1.2244223	0.50716

l(1)G0156	FBgn0027291	0.1893033	0.2026573	-1.0705429	0.50839
CG11242	FBgn0034451	0.0317476	0.0287228	1.10531061	0.50844
CG32068	FBgn0052068	0.0340101	0.0301029	1.129796	0.50845
Rel	FBgn0011469	0.0030197	0.0018037	1.67422829	0.51015
CG10221	FBgn0028475	0.003485	0.0051941	-1.4904158	0.51036
CG18594	FBgn0038973	0.0115948	0.0293419	-2.5306092	0.51073
CG33307	FBgn0028921	0.1207316	0.1076905	1.1210972	0.51104
Pur-alpha	FBgn0022361	0.0054889	0.0099003	-1.8036836	0.51185
CG6751	FBgn0033562	0.0025109	0.0052052	-2.073039	0.51196
Arf72A	FBgn0000115	0.0539959	0.0618814	-1.1460388	0.51268
RpS18	FBgn0010411	1.0583956	1.1220464	-1.0601389	0.51321
Mmp2	FBgn0010512	0.0019841	0.0052052	-2.6234051	0.51335
CG9302	FBgn0032514	0.0233433	0.0285659	-1.2237322	0.51373
CG8066	FBgn0038243	0.0357284	0.0269769	1.32440666	0.51562
RpL30	FBgn0015745	0.7302762	0.7655032	-1.048238	0.51591
CG11523	FBgn0037156	0.0160492	0.0174356	-1.0863822	0.51628
CG7430	FBgn0036762	0.2674362	0.2823428	-1.055739	0.51652
ImpE2	FBgn0001254	0.1611478	0.128714	1.2519835	0.51867
Aprt	FBgn0000109	0.0390156	0.0466091	-1.1946278	0.51936
CG9248	FBgn0032923	0.0060456	0.003863	1.56499795	0.51942
26-29-p	FBgn0024586	0.0631145	0.0688968	-1.0916149	0.5202
Bx42	FBgn0004856	0.0031974	0.0049122	-1.5362939	0.52067
mRpL9	FBgn0038319	0.0072826	0.004164	1.74896433	0.52087
scu	FBgn0001550	0.7315871	0.7665955	-1.0478527	0.52127
CG1091	FBgn0037470	0.0044109	0.0070249	-1.5926479	0.52266
CG17593	FBgn0031544	0.0126489	0.0160466	-1.2686181	0.52282
pgant4	FBgn0031541	0.0016889	0.0028201	-1.6697831	0.52378
CG5510	FBgn0039160	0.0090001	0.0111436	-1.2381683	0.52488
Jafrac2	FBgn0035389	0.1773475	0.1550949	1.14347731	0.52519
Dpt	FBgn0004240	0.0610157	0.0113676	5.3675094	0.52566
bic	FBgn0000181	0.2501861	0.2630652	-1.051478	0.52585
CG3338	FBgn0031598	0.004566	0.0028881	1.58094628	0.5265
sesB	FBgn0001474	0.5628669	0.6213026	-1.103818	0.52659
Mlp60A	FBgn0011643	0.2969081	0.2501079	1.18712026	0.52757
U2af38	FBgn0010626	0.0248839	0.029365	-1.180081	0.52771
CG4199	FBgn0025628	0.0085786	0.0063611	1.34860519	0.5293
PGRP-SC2	FBgn0033328	0.0204807	0.0040271	5.08571034	0.53108
CG3999	FBgn0037801	0.0086721	0.0062341	1.39106103	0.53115
CG4140	FBgn0027870	0.0021394	0.0058359	-2.7277623	0.53132
l(2)k14505	FBgn0021856	0.004231	0.0069934	-1.6528993	0.53268
CG8132	FBgn0037687	0.0060158	0.0106213	-1.7655754	0.53281
alt	FBgn0038535	0.0859327	0.0921319	-1.0721399	0.5333

CG9411	FBgn0030569	0.0057921	0.0046451	1.24693635	0.53357
CG32441	FBgn0037103	0.0137094	0.0113361	1.20935535	0.53431
Usp7	FBgn0030366	0.0094814	0.0112279	-1.1841922	0.53444
mub	FBgn0010834	0.031215	0.0282494	1.10497764	0.53478
CG8831	FBgn0033737	0.0025985	0.0011289	2.30180481	0.53507
AttA	FBgn0012042	0.0070462	0.0030743	2.29200504	0.53616
c11.1	FBgn0030123	0.0011218	0.0004894	2.29200504	0.53616
Rpn3	FBgn0000486	0.0581187	0.0517167	1.12378995	0.53654
CG3566	FBgn0029854	0.0635113	0.0718892	-1.1319127	0.53672
CG5214	FBgn0037891	0.1193238	0.1276933	-1.0701414	0.53709
HP1b	FBgn0030082	0.0073768	0.0043028	1.7144218	0.53716
ATPsyn-beta	FBgn0010217	0.9372849	0.9669443	-1.031644	0.53726
Arc42	FBgn0038742	0.0205236	0.0242045	-1.1793517	0.5379
CG2064	FBgn0033205	0.097512	0.106419	-1.0913418	0.53829
HmgZ	FBgn0010228	0.3634923	0.406259	-1.117655	0.53927
Pp2A-29B	FBgn0005776	0.2609987	0.2512571	1.03877133	0.5402
Mapmodulin	FBgn0025202	0.0554024	0.0466341	1.18802554	0.5407
Sxl	FBgn0000823	0.0028526	0.0055425	-1.9429769	0.54131
Rpt4	FBgn0027213	0.1602998	0.1706296	-1.0644403	0.54192
CG10077	FBgn0035720	0.0048517	0.0060212	-1.2410535	0.54262
CG12093	FBgn0035372	0.0036774	0.0060122	-1.6349056	0.54292
sta	FBgn0003517	1.1436445	1.0951615	1.04427016	0.54352
CG9894	FBgn0025946	0.1719181	0.1628345	1.05578384	0.54378
Pdp	FBgn0029958	0.0068547	0.0036692	1.86816495	0.54424
Rpn1	FBgn0027517	0.1241846	0.1390413	-1.1196341	0.54836
obst-A	FBgn0031097	0.1722234	0.1546138	1.11389386	0.54863
cin	FBgn0000316	0.0081308	0.0057366	1.41735645	0.54865
CG5690	FBgn0027777	0.0026202	0.0015529	1.68732869	0.54946
CG12203	FBgn0031021	0.0822033	0.0746414	1.10131036	0.54969
GlcAT-I	FBgn0047321	0.0038848	0.0090049	-2.3179853	0.54976
CG6364	FBgn0039179	0.0518861	0.0583182	-1.1239668	0.55004
CG9784	FBgn0030761	0.0119799	0.0151689	-1.2661946	0.5505
CG7433	FBgn0036927	0.0045881	0.0078538	-1.7117943	0.55096
CoRest	FBgn0031025	0.0021466	0.0010481	2.04803509	0.55294
DhpD	FBgn0037219	0.02011	0.0172706	1.16440826	0.55308
Dap160	FBgn0023388	0.0015562	0.0026883	-1.7274986	0.55309
CG5903	FBgn0027665	0.0469382	0.037906	1.23827977	0.55415
Dek	FBgn0010567	0.0196905	0.0221136	-1.1230619	0.55488
CG6852	FBgn0036820	0.1828583	0.151534	1.2067149	0.55532
kst	FBgn0004167	0.0037696	0.0024018	1.56947867	0.55566
Pgi	FBgn0003074	0.1954566	0.1889177	1.03461214	0.55693
Ost48	FBgn0014868	0.1678448	0.1639675	1.02364632	0.55775

CG8798	FBgn0036892	0.0085102	0.0066825	1.27350451	0.55863
CG7945	FBgn0036505	0.0276803	0.0357433	-1.2912902	0.56024
mfrn	FBgn0025206	0.002961	0.004734	-1.5987685	0.56067
Sgs7	FBgn0003377	3.5112337	3.2149357	1.09216296	0.56119
CG10992	FBgn0026294	0.2609365	0.2478494	1.05280264	0.5613
CG10413	FBgn0032689	0.0018476	0.0029725	-1.6088577	0.5617
atms	FBgn0010750	0.0060771	0.0033946	1.7902314	0.56402
CG14805	FBgn0023514	0.0021199	0.0033685	-1.5889394	0.56414
ppl	FBgn0013569	0.0493186	0.0433481	1.13773338	0.56441
jdp	FBgn0027654	0.0104314	0.0061793	1.68812227	0.56534
CG7675	FBgn0038610	0.0429188	0.0365215	1.17516672	0.566
ric8a	FBgn0028292	0.0030155	0.0015282	1.97319607	0.56754
CG9796	FBgn0038149	0.0382484	0.0307383	1.24432535	0.56808
Hsc70-5	FBgn0001220	0.1057372	0.1132085	-1.0706594	0.56901
deltaCOP	FBgn0015013	0.3390807	0.3619976	-1.0675855	0.56924
flfl	FBgn0024555	0.0069918	0.0097947	-1.4008699	0.56934
Gbeta13F	FBgn0001105	0.0695412	0.0602075	1.15502495	0.56975
Pgd	FBgn0001395	0.1452406	0.1649898	-1.1359756	0.56986
CG3902	FBgn0036823	0.2661246	0.2347663	1.13357238	0.57009
Cpr11A	FBgn0030394	0.008285	0.0065894	1.25730652	0.5702
eIF2B-gamma	FBgn0034029	0.0116346	0.0155389	-1.3355806	0.57025
CG3835	FBgn0023507	0.0133561	0.0104843	1.27391169	0.57296
CG1924	FBgn0030377	0.0258472	0.0230034	1.12362642	0.57397
CG32663	FBgn0052663	0.0165716	0.0192885	-1.163946	0.57446
CG12024	FBgn0035283	0.0147122	0.0183	-1.2438665	0.57531
Upf1	FBgn0030354	0.0028312	0.0016445	1.72167322	0.5755
CG6439	FBgn0038922	0.1319488	0.1252815	1.05321866	0.57556
CG8801	FBgn0028473	0.0008838	0.0021124	-2.3900561	0.57573
CRMP	FBgn0023023	0.0008572	0.0020458	-2.3865068	0.57627
mod(mdg4)	FBgn0002781	0.006565	0.0049276	1.33229316	0.57629
scf	FBgn0025546	0.0705319	0.0646814	1.09045107	0.57661
vimar	FBgn0021806	0.0062628	0.0089164	-1.4237086	0.57762
Prosalpha7	FBgn0023175	0.1873342	0.1727231	1.08459237	0.57893
eIF-1A	FBgn0025531	0.0871795	0.115942	-1.3299233	0.57971
Papss	FBgn0020389	0.1007596	0.1084846	-1.0766674	0.58059
CG5389	FBgn0036568	0.1668331	0.1552122	1.0748712	0.58157
Ide	FBgn0001247	0.0028899	0.0017404	1.66043097	0.58309
dpr18	FBgn0030723	0.0032886	0.0020313	1.61894088	0.58387
CG11188	FBgn0031851	0.0133265	0.0142657	-1.0704801	0.58406
par-6	FBgn0026192	0.0023033	0.0053557	-2.3252172	0.58582
csw	FBgn0000382	0.0027383	0.0016296	1.68039985	0.58691
CG11594	FBgn0035484	0.0071884	0.0093165	-1.2960516	0.5875

wmd	FBgn0034876	0.0158584	0.0177813	-1.1212512	0.5878
Eps-15	FBgn0035060	0.0042792	0.0027948	1.53114929	0.58861
CG6762	FBgn0030876	0.0158933	0.0215153	-1.3537324	0.58941
U2af50	FBgn0005411	0.0021571	0.0049661	-2.3021749	0.58954
CG6724	FBgn0032298	0.0063519	0.0095827	-1.5086258	0.59038
CG10470	FBgn0005568	0.0228153	0.0176758	1.29076518	0.59124
ran	FBgn0020255	0.7225894	0.6793407	1.0636627	0.59142
CG10005	FBgn0037972	0.0072625	0.0037258	1.94928045	0.59184
RpL7	FBgn0005593	0.3987242	0.4220892	-1.0585993	0.59188
Ptpa	FBgn0016698	0.0125008	0.0074971	1.66743214	0.59304
CG6345	FBgn0037816	0.0019233	0.0029895	-1.5543831	0.59353
CG6180	FBgn0032453	0.1462983	0.159102	-1.0875177	0.59432
His2Av	FBgn0001197	0.9075153	0.8382381	1.08264623	0.59436
Uba2	FBgn0029113	0.0279967	0.0308693	-1.1026052	0.59455
CG10527	FBgn0034583	0.3723174	0.3902165	-1.0480746	0.59487
oho23B	FBgn0010545	0.823938	0.9339304	-1.1334959	0.59575
sals	FBgn0037904	0.0017602	0.0011045	1.59377304	0.59643
CG17544	FBgn0032775	0.0024352	0.0012636	1.92717891	0.59679
fray	FBgn0010922	0.0284765	0.0255562	1.1142706	0.5977
FK506-bp2	FBgn0013954	0.5534742	0.6037101	-1.0907646	0.59882
pr	FBgn0003141	0.0768701	0.0678533	1.13288677	0.60004
CG6707	FBgn0036058	0.0158852	0.0181374	-1.1417841	0.60028
wupA	FBgn0004028	0.0289693	0.036776	-1.2694846	0.60038
CG8209	FBgn0035830	0.0840013	0.0800761	1.04901915	0.60105
CG30152	FBgn0034543	0.0169961	0.0154343	1.10119165	0.60432
Aac11	FBgn0022116	0.0282884	0.031751	-1.1224026	0.60531
CG7112	FBgn0035879	0.0016181	0.0010275	1.5747434	0.60588
CG2147	FBgn0030025	0.0136146	0.0171323	-1.2583777	0.60589
CG9691	FBgn0030160	0.2010004	0.1682584	1.1945935	0.60738
CG1218	FBgn0037377	0.0051323	0.003484	1.47312256	0.60855
CG31075	FBgn0039468	0.5187398	0.5687361	-1.0963803	0.60916
CG10535	FBgn0037926	0.002323	0.0034655	-1.491836	0.61031
Prosbeta2	FBgn0002419	0.152607	0.1421221	1.07377351	0.61154
CG14812	FBgn0026090	0.0311799	0.0242495	1.28579199	0.6119
p38b	FBgn0014421	0.016486	0.018024	-1.0932883	0.61382
CG3214	FBgn0025287	0.0221838	0.024572	-1.1076543	0.61444
CG6638	FBgn0035911	0.0277721	0.023179	1.19816016	0.61466
Set	FBgn0014879	0.0522428	0.0545398	-1.0439669	0.61521
spas	FBgn0039141	0.0013742	0.0020637	-1.5017864	0.61547
RPA2	FBgn0032906	0.0116026	0.0073194	1.58518313	0.61719
Nacalpha	FBgn0017565	0.1986031	0.2198705	-1.1070852	0.61787
Stat92E	FBgn0010885	0.0016161	0.0009049	1.7859146	0.61805

CG9797	FBgn0037621	0.0029422	0.0016475	1.7859146	0.61805
Sirt2	FBgn0038788	0.0069557	0.0024667	2.81984296	0.6194
CG10641	FBgn0032731	0.0101183	0.0063469	1.5942191	0.62105
Lerp	FBgn0039455	0.0051204	0.0057123	-1.1156021	0.62227
gammaTub23C	FBgn0004176	0.0033898	0.0055128	-1.6262642	0.62251
CG30427	FBgn0035081	0.0039543	0.0063216	-1.5986778	0.62315
CG6000	FBgn0039145	0.0350208	0.0383915	-1.0962482	0.62529
Updo	FBgn0033428	0.0689605	0.0763041	-1.10649	0.62562
Trl	FBgn0005691	0.0177191	0.0153116	1.15723578	0.62593
dpa	FBgn0004127	0.005866	0.0044406	1.32098863	0.62668
CG6178	FBgn0039156	0.0041361	0.0052554	-1.2706317	0.62716
elm	FBgn0037358	0.0074055	0.0101444	-1.3698539	0.62741
GstD9	FBgn0038020	0.6575213	0.6082864	1.08094035	0.62764
REG	FBgn0029133	0.0388356	0.0448449	-1.1547374	0.62791
CG3699	FBgn0029549	0.00198	0.0041343	-2.0880089	0.62808
CG5802	FBgn0025240	0.0014938	0.0031191	-2.0880089	0.62808
CG11241	FBgn0037186	0.0023659	0.0013556	1.74528627	0.63083
CG33205	FBgn0036049	0.0031783	0.0059562	-1.8740127	0.63116
cl	FBgn0000318	0.4658946	0.4346942	1.07177546	0.63132
Atac1	FBgn0031876	0.0049331	0.0026402	1.86844595	0.63279
Sgs8	FBgn0003378	2.1503913	2.3686071	-1.1014773	0.63291
Gyk	FBgn0025592	0.0066219	0.0048886	1.35457317	0.63385
CG17843	FBgn0038919	0.0044733	0.0017028	2.6270927	0.63472
CG3792	FBgn0027670	0.0047364	0.0027327	1.73323359	0.6348
CG13298	FBgn0035692	0.0098642	0.0056912	1.73323359	0.6348
Sply	FBgn0010591	0.0125015	0.0151721	-1.213617	0.63612
CG8885	FBgn0031656	0.0020116	0.0041142	-2.0452513	0.63671
CG14985	FBgn0035482	0.0020951	0.0042849	-2.0452513	0.63671
rumi	FBgn0039021	0.002237	0.0045738	-2.0446059	0.63684
CG4021	FBgn0034659	0.0070088	0.0037773	1.85549599	0.63843
CG3008	FBgn0031643	0.0026287	0.0014522	1.81015395	0.63871
Cht12	FBgn0045113	0.0033726	0.0018631	1.81015395	0.63871
dre4	FBgn0002182	0.001006	0.0014741	-1.4653451	0.63877
CG31120	FBgn0039247	0.0020326	0.0029784	-1.4653451	0.63877
Mlc-c	FBgn0004687	0.8855846	0.9285436	-1.0485092	0.63922
CG15715	FBgn0036538	0.0767869	0.0685774	1.1197105	0.64031
Tm2	FBgn0002442	0.4005072	0.3662487	1.09353905	0.6408
CG16941	FBgn0038464	0.0015057	0.0008784	1.71419005	0.64089
ens	FBgn0035500	0.005684	0.007261	-1.2774445	0.64093
CG7911	FBgn0039735	0.2639334	0.2795457	-1.0591525	0.64261
Strn-Mlck	FBgn0013988	0.0035928	0.0046845	-1.3038814	0.64334

PDCD-5	FBgn0036580	0.0325776	0.0284795	1.14389749	0.64435
Prx5037	FBgn0038519	0.0844141	0.0778048	1.08494609	0.6444
Rab3	FBgn0005586	0.0308404	0.0287451	1.07289154	0.64441
chrw	FBgn0015372	0.0259957	0.0242296	1.07289154	0.64441
Rab-RP3	FBgn0015793	0.0309812	0.0288763	1.07289154	0.64441
Rab35	FBgn0031090	0.0461556	0.0430199	1.07289154	0.64441
Rab30	FBgn0031882	0.0304255	0.0283584	1.07289154	0.64441
RabX4	FBgn0039231	0.0318539	0.0296898	1.07289154	0.64441
CG3500	FBgn0034849	0.0057954	0.0084597	-1.4597298	0.64461
growl	FBgn0037245	0.1977609	0.2092042	-1.057864	0.64518
Mcm7	FBgn0020633	0.0027541	0.0038132	-1.3845771	0.64523
CG7706	FBgn0038640	0.0206454	0.0172425	1.19735372	0.6458
CG7277	FBgn0031713	0.0023527	0.0034142	-1.4511872	0.64919
Roc1a	FBgn0025527	0.0107481	0.0063762	1.68565355	0.65037
Zasp66	FBgn0035917	0.0113931	0.0103998	1.09551005	0.65073
sec5	FBgn0031537	0.0013002	0.0007703	1.68792665	0.6508
ttm50	FBgn0024978	0.0086648	0.0101559	-1.1720899	0.65252
CG11158	FBgn0030511	0.0015602	0.0030647	-1.9642398	0.65404
CG9879	FBgn0031444	0.0034865	0.0020805	1.67583482	0.65473
CG1968	FBgn0033401	0.0046778	0.0053237	-1.1380884	0.65675
CG6357	FBgn0033875	0.0058415	0.00749	-1.282198	0.65718
Ate1	FBgn0021941	0.0037044	0.0021336	1.73623899	0.65773
TfIIS	FBgn0000474	0.0108468	0.0082515	1.31452093	0.65807
MTA1-like	FBgn0027951	0.0029676	0.0024351	1.21864119	0.65811
I-2	FBgn0028429	0.0141292	0.0181663	-1.2857325	0.65831
Ef1alpha48D	FBgn0000556	2.4345885	2.3386011	1.04104481	0.66041
Pp1-13C	FBgn0003132	0.0347613	0.0303471	1.14545544	0.66104
osa	FBgn0003013	0.0004464	0.0002694	1.65679127	0.66108
ns4	FBgn0032882	0.0019842	0.0011976	1.65679127	0.66108
CG7083	FBgn0035877	0.0026048	0.0015722	1.65679127	0.66108
HP1c	FBgn0039019	0.004814	0.0029056	1.65679127	0.66108
Tango13	FBgn0030497	0.0022864	0.00138	1.65679127	0.66108
Gpdh	FBgn0001128	0.4566599	0.4446033	1.02711757	0.66143
RpS30	FBgn0025548	0.4998213	0.5437985	-1.0879858	0.66164
Fmr1	FBgn0028734	0.0296449	0.0269939	1.09820769	0.66179
CG9921	FBgn0030743	0.0178351	0.0103358	1.72556316	0.6621
CG5537	FBgn0025533	0.0248087	0.0190077	1.30518882	0.66231
CG5382	FBgn0038950	0.0511329	0.0575769	-1.1260241	0.66256
Su(P)	FBgn0004465	0.0056674	0.004144	1.36761636	0.66262
CG4119	FBgn0028474	0.0011432	0.0016318	-1.4274008	0.66278
eas	FBgn0000536	0.0010381	0.0019974	-1.9240166	0.66314
CG17219	FBgn0031494	0.0026836	0.0051633	-1.9240166	0.66314

poe	FBgn0010161	0.0005544	0.0003291	1.68463117	0.66522
RhoL	FBgn0014380	0.010537	0.0142209	-1.3496205	0.66719
CG2082	FBgn0027608	0.0031317	0.0019076	1.64172671	0.66797
Elongin-C	FBgn0023211	0.0489412	0.0551582	-1.1270292	0.66973
yata	FBgn0039692	0.0056685	0.0071171	-1.2555597	0.66984
rut	FBgn0003301	0.0005029	0.0007102	-1.4120841	0.67288
icln	FBgn0029079	0.0053676	0.0075747	-1.4111804	0.6733
SC35	FBgn0032432	0.0207868	0.0244168	-1.1746317	0.67336
Mms19	FBgn0037301	0.0023546	0.0014362	1.63950512	0.67354
mRpS18A	FBgn0037596	0.0069503	0.0118516	-1.7051898	0.67437
RpL26	FBgn0036825	0.6002169	0.5565236	1.07851125	0.6744
CalpB	FBgn0025866	0.0030817	0.0024816	1.24183087	0.67495
Pdk	FBgn0017558	0.0026948	0.0016674	1.6162021	0.67528
Dis3	FBgn0039183	0.0011334	0.0007013	1.6162021	0.67528
CG7006	FBgn0039233	0.0061832	0.0038257	1.6162021	0.67528
CG31550	FBgn0037333	0.0025704	0.0015904	1.6162021	0.67528
Hrb98DE	FBgn0001215	0.0843261	0.0863842	-1.0244065	0.67535
CG9572	FBgn0031089	0.0170918	0.0140789	1.21400581	0.67729
smt3	FBgn0010577	0.3760364	0.3628746	1.03627095	0.67762
PyK	FBgn0003178	0.4781228	0.4628467	1.03300452	0.67766
robo3	FBgn0031328	0.0003762	0.0007004	-1.8615685	0.67798
CG7280	FBgn0030966	0.0019372	0.0012018	1.61189077	0.67818
CG9643	FBgn0031485	0.0050644	0.0031444	1.61059133	0.67863
Syb	FBgn0003660	0.0617877	0.073722	-1.1931508	0.67956
smid	FBgn0011034	0.0115342	0.0098426	1.1718575	0.68071
ics	FBgn0028546	0.0174893	0.0202164	-1.1559278	0.68133
Pka-R1	FBgn0000275	0.0076019	0.0054929	1.38394914	0.68158
CG31548	FBgn0051548	0.1851123	0.1967896	-1.0630824	0.68374
Anxb11	FBgn0030749	0.0615414	0.0686918	-1.1161894	0.68441
Spn	FBgn0010905	0.0011677	0.0008765	1.33225546	0.68591
imd	FBgn0013983	0.0071606	0.0053748	1.33225546	0.68591
scrib	FBgn0039433	0.0055277	0.0037032	1.49268155	0.6861
RpL8	FBgn0024939	0.6766035	0.7012159	-1.0363764	0.68742
flw	FBgn0000711	0.0169386	0.0152718	1.10914487	0.68745
HmgD	FBgn0004362	0.0825622	0.0892912	-1.0815013	0.68795
SdhA	FBgn0017539	0.106296	0.1103105	-1.0377674	0.6885
mRpS9	FBgn0037529	0.0012782	0.0023253	-1.8191471	0.68857
CG4552	FBgn0031304	0.0096805	0.0082462	1.17393408	0.6888
Hsp68	FBgn0001230	0.1627852	0.1566397	1.0392333	0.6891
CG3719	FBgn0024986	0.0180619	0.0232929	-1.2896165	0.69178
CG11089	FBgn0039241	0.2341523	0.2214791	1.05722103	0.69222
Dhc16F	FBgn0013809	0.0001432	0.0002583	-1.8035296	0.69258

Ddx1	FBgn0013790	0.0008041	0.0014501	-1.8035296	0.69258
p16-ARC	FBgn0031437	0.0467861	0.0452997	1.03281202	0.69278
CG9306	FBgn0032511	0.0239624	0.0292388	-1.220196	0.69474
CG11178	FBgn0030499	0.0271383	0.0258192	1.05109099	0.69537
BM-40-SPARC	FBgn0026562	0.0095745	0.0074478	1.28555098	0.69541
CG7889	FBgn0031003	0.0018064	0.0032372	-1.7920423	0.69556
Bap170	FBgn0027541	0.0004847	0.0008685	-1.7920423	0.69556
alpha-Man-I	FBgn0010338	0.0038129	0.0028184	1.35288464	0.69581
CG3446	FBgn0029868	0.0299299	0.0353317	-1.1804834	0.69605
CG1572	FBgn0030309	0.0105064	0.0065891	1.59451447	0.69685
CG5412	FBgn0038806	0.0071502	0.0091419	-1.2785618	0.69706
CG2246	FBgn0039790	0.0037153	0.0023795	1.56134698	0.69879
CG32603	FBgn0052603	0.0167098	0.020806	-1.2451328	0.6988
TpnC25D	FBgn0025551	0.0174218	0.0224109	-1.2863757	0.69968
CG9027	FBgn0033631	0.006696	0.0041307	1.62105728	0.69987
Su(fu)	FBgn0003562	0.0030185	0.0019397	1.55614056	0.70161
NHP2	FBgn0029148	0.0197217	0.0246191	-1.2483273	0.70165
CG3534	FBgn0038463	0.0112557	0.009923	1.13430098	0.70213
CG14215	FBgn0031052	0.0002769	0.0004892	-1.7665975	0.70229
CG6230	FBgn0027582	0.0041024	0.0045299	-1.1042081	0.70245
RpL18A	FBgn0010409	0.2473586	0.2664746	-1.0772807	0.70258
Ykt6	FBgn0026664	0.0081106	0.0051893	1.56296449	0.7059
Cctgamma	FBgn0015019	0.1946609	0.1854116	1.04988525	0.70635
PpV	FBgn0003139	0.0017714	0.003102	-1.7512219	0.70644
pum	FBgn0003165	0.0003501	0.0006131	-1.7512219	0.70644
dia	FBgn0011202	0.000492	0.0008615	-1.7512219	0.70644
FucT6	FBgn0025708	0.0008671	0.0015184	-1.7512219	0.70644
SP1070	FBgn0031879	0.000346	0.000606	-1.7512219	0.70644
CG17121	FBgn0039043	0.0014868	0.0026037	-1.7512219	0.70644
Dys	FBgn0024242	0.0001535	0.0002688	-1.7512219	0.70644
CG30344	FBgn0033386	0.0025905	0.0035388	-1.3660882	0.70666
CG14216	FBgn0029511	0.0059181	0.0080221	-1.3555078	0.70854
CG14527	FBgn0039613	0.0069969	0.0064618	1.08281571	0.70872
Pgam5	FBgn0023517	0.0057083	0.0036479	1.56480115	0.70951
CG8997	FBgn0028920	0.0020791	0.0036151	-1.7387304	0.70985
CG2794	FBgn0031265	0.0007723	0.0013427	-1.7387304	0.70985
Snap24	FBgn0028401	0.0023816	0.0041305	-1.7343211	0.71107
CG1518	FBgn0031149	0.0007081	0.0012282	-1.7343211	0.71107
CG11131	FBgn0037204	0.0103527	0.0137822	-1.331271	0.71168
Aos1	FBgn0029512	0.0693135	0.0640601	1.08200836	0.71206
Mlc2	FBgn0002773	0.6142842	0.5709036	1.07598588	0.71244

Rop	FBgn0004574	0.0359422	0.0379736	-1.0565177	0.71257
Elongin-B	FBgn0023212	0.1256159	0.1143935	1.09810272	0.7126
CG9547	FBgn0031824	0.0178971	0.0186894	-1.0442676	0.71272
RpS7	FBgn0039757	0.7389626	0.753109	-1.0191436	0.71329
CG10347	FBgn0030342	0.0038116	0.0050717	-1.3305904	0.71376
CG13510	FBgn0034758	0.0199015	0.020829	-1.0466082	0.7139
CG12400	FBgn0031505	0.1643136	0.1761057	-1.0717661	0.71434
CG11816	FBgn0030495	0.0041559	0.0056392	-1.3569086	0.71454
yps	FBgn0022959	0.0405258	0.037338	1.08537772	0.71576
Pi3K21B	FBgn0020262	0.0020586	0.0013609	1.51260338	0.71584
CG10625	FBgn0035612	0.0038867	0.0025695	1.51260338	0.71584
Prp19	FBgn0013969	0.0119728	0.0079153	1.51260338	0.71584
CG10333	FBgn0032690	0.0034795	0.0029874	1.16474979	0.71633
CG5110	FBgn0032642	0.023404	0.0185143	1.26410397	0.71693
pyd	FBgn0003177	0.000551	0.000943	-1.711315	0.71749
santa-maria	FBgn0025697	0.0010146	0.0017363	-1.711315	0.71749
CG10908	FBgn0031376	0.0021907	0.003749	-1.711315	0.71749
Ntf-2r	FBgn0032680	0.0041286	0.0070654	-1.711315	0.71749
l(2)37Ce	FBgn0032761	0.0029012	0.0049649	-1.711315	0.71749
RpL29	FBgn0016726	0.2026251	0.2149306	-1.0607303	0.71788
Dhc93AB	FBgn0013812	0.0001344	0.0002297	-1.7091401	0.71811
CG17768	FBgn0032240	0.0039234	0.0067056	-1.7091401	0.71811
Cul-2	FBgn0010507	0.0008024	0.0013714	-1.7091401	0.71811
CG18507	FBgn0028527	0.001201	0.0020511	-1.7078036	0.71848
CG6693	FBgn0037878	0.0020646	0.0035259	-1.7078036	0.71848
CG3394	FBgn0034999	0.0382253	0.0416802	-1.0903822	0.71877
Cdc42	FBgn0010341	0.0673608	0.0578269	1.16487134	0.71917
eIF-4E	FBgn0002202	0.168989	0.1642488	1.02885947	0.71928
CG5021	FBgn0035944	0.0208073	0.0226475	-1.0884391	0.72069
Cyp9f2	FBgn0027751	0.0046423	0.0036016	1.28895795	0.72171
Mlp84B	FBgn0011644	0.0685553	0.0611577	1.12095946	0.72176
CG10289	FBgn0035688	0.0033483	0.0025155	1.33106699	0.72278
endoA	FBgn0038659	0.0014545	0.0024602	-1.6913695	0.72317
Nup153	FBgn0030762	0.0007578	0.0012812	-1.690791	0.72334
Prx6005	FBgn0031479	0.018118	0.0163536	1.10789047	0.72349
tacc	FBgn0026620	0.0085685	0.0118878	-1.3873873	0.72366
CG17107	FBgn0032281	0.0065171	0.0109818	-1.6850739	0.72499
CG14107	FBgn0036351	0.0058312	0.007848	-1.3458453	0.72629
CG1041	FBgn0037440	0.0634746	0.0670006	-1.0555489	0.72743
CG32703	FBgn0030118	0.0006739	0.0011274	-1.6728317	0.72855
P5cr	FBgn0015781	0.0122168	0.0101723	1.20097914	0.72917
CG5126	FBgn0031320	0.0098204	0.0076244	1.28801817	0.73136

Mtp	FBgn0032904	0.0050208	0.0043567	1.15241664	0.73195
UbcD4	FBgn0015321	0.0578654	0.0610651	-1.0552957	0.73205
CG13779	FBgn0040954	0.1642735	0.1819931	-1.1078665	0.73214
CG8031	FBgn0038110	0.1219523	0.1165871	1.04601935	0.7329
brm	FBgn0000212	0.0007287	0.0011084	-1.5211524	0.73306
Surf6	FBgn0038746	0.0036636	0.0048281	-1.3178579	0.73434
CG5913	FBgn0039385	0.001375	0.0022696	-1.6505674	0.73514
MESK2	FBgn0010491	0.0015297	0.0025248	-1.6505674	0.73514
AttC	FBgn0033833	0.0078367	0.0042849	1.82891358	0.73547
CG31098	FBgn0039317	0.0026417	0.0034762	-1.3159257	0.73564
RpL21	FBgn0026278	1.007393	1.0454319	-1.0377598	0.73655
CG32210	FBgn0036883	0.0007816	0.0010307	-1.3186868	0.73854
stops	FBgn0039822	0.0013578	0.0022166	-1.6325322	0.74058
Ubc-E2H	FBgn0029996	0.0119378	0.0095797	1.24614664	0.74068
kay	FBgn0000468	0.0007434	0.0012128	-1.6315172	0.74089
vls	FBgn0003978	0.0014625	0.002386	-1.6315172	0.74089
CG12703	FBgn0031069	0.0008071	0.0013168	-1.6315172	0.74089
CG31088	FBgn0051088	0.0040355	0.006584	-1.6315172	0.74089
CG32425	FBgn0037002	0.0010535	0.0017183	-1.6311001	0.74102
Sptr	FBgn0014032	0.0212578	0.0182496	1.16483213	0.74111
RpS27A	FBgn0002728	0.2427846	0.2330222	1.04189496	0.74214
RpL6	FBgn0039857	0.5054833	0.4776366	1.05830108	0.74224
Spt6	FBgn0026691	0.0002952	0.0004782	-1.6198796	0.74445
pgant6	FBgn0035375	0.0142653	0.0119407	1.19467762	0.74699
CG11771	FBgn0027773	0.0045477	0.0050017	-1.0998195	0.74741
CG5548	FBgn0030605	0.0187912	0.0152064	1.23573899	0.74776
CG8605	FBgn0035762	0.0008074	0.0012982	-1.6079404	0.74815
CG2070	FBgn0033203	0.0191473	0.0165888	1.15422632	0.74833
Pen	FBgn0011823	0.0127247	0.0148238	-1.1649635	0.74879
ND42	FBgn0019957	0.0674317	0.0639029	1.05522215	0.74922
CG32226	FBgn0036965	0.0003976	0.0006375	-1.6035261	0.74953
CG17931	FBgn0038421	0.0244812	0.0268391	-1.0963129	0.74978
Ras85D	FBgn0003205	0.0200339	0.0170067	1.17799982	0.74989
Dsor1	FBgn0010269	0.0102436	0.011116	-1.0851664	0.75028
Ard1	FBgn0036064	0.0632804	0.0586938	1.07814471	0.75104
SF1	FBgn0025571	0.0065752	0.007158	-1.0886437	0.75106
CG3499	FBgn0034792	0.0008387	0.0013402	-1.5978512	0.75131
CSN1b	FBgn0027057	0.0044375	0.0051792	-1.167147	0.75305
CG2943	FBgn0037530	0.0087268	0.0107356	-1.2301788	0.75429
Rox8	FBgn0005649	0.0306747	0.0290277	1.05674013	0.75452
betaTub56D	FBgn0003887	1.8846534	1.9362547	-1.0273797	0.7547
pnut	FBgn0010304	0.0250061	0.0265993	-1.0637131	0.75493

Lam	FBgn0001930	0.0652145	0.0687834	-1.0547256	0.75763
CG2862	FBgn0031459	0.228674	0.2138575	1.06928182	0.75812
CG13043	FBgn0036600	0.0153172	0.0125814	1.2174507	0.75842
CG32528	FBgn0031067	0.0098517	0.0120819	-1.2263817	0.75862
CG18516	FBgn0038350	0.0017221	0.0013876	1.24098888	0.75924
Rm62	FBgn0003261	0.0483195	0.0448551	1.07723574	0.75961
Rcp	FBgn0030801	0.0026331	0.0041374	-1.5712987	0.75976
CG3605	FBgn0031493	0.0007804	0.0012263	-1.5712987	0.75976
CG2926	FBgn0037344	0.0003926	0.0006169	-1.5712987	0.75976
CG4598	FBgn0032160	0.1319679	0.1360945	-1.0312696	0.76009
l(2)01289	FBgn0010482	0.0022827	0.0027532	-1.2061096	0.76118
TFAM	FBgn0038805	0.0386109	0.035986	1.07294012	0.76134
LSm7	FBgn0032599	0.08162	0.0712877	1.14493849	0.76241
Fib	FBgn0003062	0.1288978	0.136159	-1.0563328	0.7632
CG8149	FBgn0037700	0.016591	0.0181085	-1.091471	0.7635
Rab9Db	FBgn0030221	0.0403682	0.0412051	-1.0207318	0.7641
Rab9Fa	FBgn0030253	0.0403682	0.0412051	-1.0207318	0.7641
Rab9E	FBgn0046863	0.0403682	0.0412051	-1.0207318	0.7641
Rab9D	FBgn0046864	0.0403682	0.0412051	-1.0207318	0.7641
Golgin84	FBgn0039188	0.0055805	0.0051992	1.0733299	0.76456
CG32549	FBgn0030916	0.0132273	0.0155905	-1.1786543	0.76466
mRpL50	FBgn0028648	0.0031968	0.0049731	-1.5556433	0.76485
kuk	FBgn0038476	0.00106	0.001649	-1.5556433	0.76485
RanGap	FBgn0003346	0.0146489	0.0133315	1.09881821	0.76567
CG6488	FBgn0032361	0.0075219	0.0084646	-1.1253384	0.76685
krz	FBgn0028053	0.0229999	0.0206358	1.11456295	0.76724
su(Hw)	FBgn0003567	0.001307	0.0016624	-1.2719574	0.76799
CG32026	FBgn0047312	0.0027907	0.0033818	-1.2118349	0.76854
Rala	FBgn0015286	0.011074	0.0090861	1.21878678	0.77021
Coprox	FBgn0021932	0.03019	0.0278219	1.08511452	0.7707
CG1646	FBgn0039600	0.0021345	0.0026251	-1.2298632	0.77082
Srp54	FBgn0024285	0.0067247	0.0063558	1.05804669	0.77151
bur	FBgn0000239	0.0140539	0.0124955	1.12471899	0.77168
CG6448	FBgn0032976	0.0006952	0.0005033	1.38122525	0.77463
CG5284	FBgn0036566	0.000751	0.0011435	-1.5225957	0.77583
dl	FBgn0000462	0.0006179	0.0009409	-1.5225957	0.77583
CG14681	FBgn0037820	0.0030198	0.0025161	1.20020072	0.77643
CG32536	FBgn0031009	0.0027589	0.0041941	-1.5201933	0.77664
CG4420	FBgn0030753	0.0287602	0.0313271	-1.08925	0.77665
CG16833	FBgn0026147	0.000696	0.0010576	-1.5196063	0.77684
CG8239	FBgn0030683	0.0014852	0.0022569	-1.5196063	0.77684
CG32228	FBgn0052228	0.0006298	0.000957	-1.5196063	0.77684

Mpcp	FBgn0010721	0.0450993	0.0418509	1.07761755	0.77708
noi	FBgn0011357	0.0024711	0.00311	-1.2585373	0.77813
CHIP	FBgn0027052	0.0075912	0.0054523	1.39227662	0.77851
CG6304	FBgn0032624	0.002848	0.0020751	1.37250423	0.77891
jar	FBgn0004452	0.0040864	0.0045693	-1.1181824	0.77942
dod	FBgn0015379	0.0811719	0.0852692	-1.0504774	0.77977
Bub3	FBgn0025457	0.0018477	0.0027761	-1.5024753	0.78269
Map60	FBgn0010342	0.0014219	0.0021362	-1.502331	0.78274
Plip	FBgn0039111	0.0031282	0.0046996	-1.502331	0.78274
usp	FBgn0003964	0.0011507	0.0017238	-1.4980297	0.78422
CG8199	FBgn0037709	0.010756	0.0122396	-1.1379368	0.78485
CG4165	FBgn0029763	0.0012874	0.0009363	1.37498478	0.78526
Pabp2	FBgn0005648	0.0190875	0.0207066	-1.0848241	0.78649
CG18259	FBgn0030956	0.0012885	0.0019152	-1.4863449	0.78828
CG6961	FBgn0030959	0.0012885	0.0019152	-1.4863449	0.78828
Trap1	FBgn0026761	0.0265139	0.0281994	-1.0635692	0.78951
Sod	FBgn0003462	0.5557875	0.5695864	-1.0248275	0.78985
CG9911	FBgn0030734	0.4937057	0.5049405	-1.0227561	0.79022
TBPH	FBgn0025790	0.0022248	0.0016491	1.34907185	0.79044
egl	FBgn0000562	0.0010888	0.0006935	1.57000215	0.79086
Arf84F	FBgn0004908	0.0064155	0.0047591	1.34804996	0.79094
CG12310	FBgn0036467	0.0463111	0.0386445	1.19838712	0.79113
blp	FBgn0010754	0.0260897	0.0225719	1.15584847	0.79117
RhoGEF4	FBgn0035761	0.005672	0.0071053	-1.2526915	0.79154
Sap47	FBgn0013334	0.0437337	0.0456365	-1.0435095	0.79205
GlyP	FBgn0004507	0.179244	0.1753501	1.02220692	0.79302
CBP	FBgn0026144	0.0036022	0.0023109	1.55880332	0.79366
CG4914	FBgn0036436	0.0016728	0.0024559	-1.4680959	0.79471
CG3408	FBgn0036008	0.0036733	0.0027426	1.33934541	0.79526
Lsp1beta	FBgn0002563	1.0995049	1.0694864	1.02806815	0.79551
PP2A-B'	FBgn0038572	0.0028932	0.0024499	1.1809303	0.7956
2-Sep	FBgn0014029	0.0201124	0.0208799	-1.0381573	0.79595
CG4692	FBgn0027681	0.1156758	0.1103616	1.04815242	0.79603
sqh	FBgn0003514	0.3465699	0.366332	-1.0570218	0.79729
CG12009	FBgn0035430	0.0015616	0.0011649	1.34052639	0.79783
CG10375	FBgn0039116	0.0045176	0.0033884	1.33327348	0.79877
mRpL2	FBgn0036135	0.0076945	0.0064909	1.18542838	0.79878
Myo31DF	FBgn0011673	0.0022376	0.0025193	-1.1259224	0.7988
Cht6	FBgn0030171	0.0018484	0.0016908	1.09321997	0.79999
CkIIbeta	FBgn0000259	0.0445009	0.0470891	-1.0581622	0.80028
Hcf	FBgn0039904	0.0010677	0.0008033	1.32907557	0.80048
alphaTub85E	FBgn0003886	0.5930711	0.5847715	1.01419286	0.80064

Rab5	FBgn0014010	0.0319302	0.0351675	-1.1013875	0.80096
mip130	FBgn0023509	0.0022803	0.0026852	-1.1775573	0.801
l(2)06496	FBgn0010622	0.0238933	0.0217658	1.09774709	0.80127
Ote	FBgn0003022	0.001425	0.0020653	-1.4493073	0.80144
CG9776	FBgn0027866	0.0004795	0.000695	-1.4493073	0.80144
CG12883	FBgn0039538	0.0038484	0.0055775	-1.4493073	0.80144
CG8680	FBgn0031684	0.107678	0.1015413	1.06043513	0.80189
Mbs	FBgn0005536	0.0005285	0.0007648	-1.4471641	0.80222
ATPsyn-Cf6	FBgn0016119	0.2892148	0.2991763	-1.0344433	0.80313
CG15445	FBgn0031161	0.0081193	0.0069562	1.16719458	0.80319
CG7518	FBgn0038108	0.0018375	0.0017761	1.0345488	0.80428
CG5044	FBgn0038326	0.0698932	0.0657331	1.06328775	0.8046
RpL17	FBgn0026274	0.7998222	0.7702684	1.03836817	0.80535
RpS14a	FBgn0002584	1.2791307	1.2519143	1.02173981	0.80587
RpS14b	FBgn0002584	1.2791307	1.2519143	1.02173981	0.80587
TpnC47D	FBgn0010423	0.1636925	0.1542598	1.06114832	0.80623
CG3781	FBgn0029853	0.0052219	0.0039623	1.31788716	0.80671
Marf	FBgn0029870	0.0014247	0.0010811	1.31788716	0.80671
Dcr-2	FBgn0034246	0.0025814	0.0020424	1.26392926	0.80725
CG10463	FBgn0032819	0.0037783	0.0032127	1.1760536	0.80733
gw	FBgn0027730	0.0029643	0.0031514	-1.0631458	0.80779
RpS8	FBgn0025277	0.6242157	0.6351588	-1.017531	0.8085
CG31048	FBgn0039605	0.0014452	0.0012967	1.11453491	0.80886
qkr58E-2	FBgn0022985	0.007869	0.0070357	1.11845099	0.8099
Cdc37	FBgn0004640	0.0593885	0.0574752	1.03328977	0.81319
DIP2	FBgn0024806	0.0017119	0.0013129	1.30393309	0.81383
CG5599	FBgn0030612	0.0065977	0.007767	-1.1772344	0.81522
Ntf-2	FBgn0027201	0.3468511	0.3589072	-1.0347589	0.81546
CG5958	FBgn0031913	0.0266575	0.0234606	1.13626823	0.8159
Aut1	FBgn0036813	0.0076307	0.009043	-1.1850705	0.81633
CG9427	FBgn0037721	0.0608784	0.0564818	1.07784138	0.81683
hk	FBgn0001202	0.0037696	0.0043314	-1.1490146	0.81723
mtSSB	FBgn0010438	0.0489978	0.046851	1.04582061	0.81812
Rho1	FBgn0014020	0.380148	0.3624814	1.04873797	0.81819
CanA1	FBgn0004466	0.0027077	0.0033222	-1.2269251	0.81931
Fas1	FBgn0000634	0.0033907	0.0029052	1.16712825	0.81961
Prosbeta2R1	FBgn0029812	0.0308666	0.0329829	-1.0685609	0.82044
synj	FBgn0034691	0.0006437	0.0008974	-1.3941819	0.82188
LSm3	FBgn0039138	0.0059933	0.0083558	-1.3941819	0.82188
CG13641	FBgn0039239	0.0079234	0.0061667	1.28487333	0.82372
CaMKII	FBgn0004624	0.0037573	0.0029232	1.28534385	0.82388
CG14476	FBgn0027588	0.2084554	0.2047904	1.01789665	0.82426

CG3523	FBgn0027571	0.0680521	0.0646473	1.05266818	0.82694
Rbp2	FBgn0010256	0.060985	0.0633185	-1.0382634	0.82819
asrij	FBgn0034793	0.0064075	0.0080385	-1.2545517	0.82964
CG9804	FBgn0037251	0.0047563	0.0037422	1.27099161	0.83118
SMC1	FBgn0039146	0.000899	0.0007073	1.27099161	0.83118
Mlc1	FBgn0002772	0.3211326	0.3071813	1.04541728	0.83119
Tim8	FBgn0027359	0.1206984	0.1154325	1.0456187	0.83128
Dhc64C	FBgn0001059	0.0040524	0.0038958	1.04020183	0.8313
CG14841	FBgn0038218	0.0099828	0.0104191	-1.0437004	0.83281
Ssrp	FBgn0005644	0.0039141	0.0040976	-1.0468963	0.83347
mRpL22	FBgn0030786	0.002167	0.0029555	-1.3638811	0.83357
Elp3	FBgn0031604	0.0009147	0.0012475	-1.3638811	0.83357
CG7777	FBgn0033635	0.001884	0.0025695	-1.3638811	0.83357
Nup58	FBgn0038722	0.0009247	0.0012612	-1.3638811	0.83357
CSN4	FBgn0022061	0.0078417	0.0071128	1.10247369	0.83399
wkd	FBgn0037917	0.0030554	0.0024123	1.26657927	0.83415
CG11964	FBgn0037644	0.0020006	0.0015809	1.26550038	0.83455
Sc2	FBgn0002196	0.010198	0.010691	-1.0483397	0.83469
sar1	FBgn0010874	0.5315267	0.5459743	-1.0271812	0.83495
Pros35	FBgn0003151	0.3281417	0.3209839	1.02229947	0.83548
Mhc	FBgn0002741	0.3069718	0.3172954	-1.0336305	0.83663
CG10638	FBgn0036290	0.139008	0.1366067	1.01757759	0.83734
CG10096	FBgn0038032	0.0081304	0.0069649	1.16733426	0.83761
CG3590	FBgn0038467	0.0204561	0.0195017	1.04894116	0.83785
Fpps	FBgn0022145	0.0038421	0.0045865	-1.1937631	0.83822
CG5854	FBgn0039130	0.0160613	0.0143926	1.11594166	0.83873
Pka-R2	FBgn0022382	0.0289214	0.0305406	-1.0559857	0.83877
CG4095	FBgn0029890	0.0100216	0.0109089	-1.0885361	0.83917
CG5703	FBgn0030853	0.073435	0.0753705	-1.0263573	0.8397
l(1)G0289	FBgn0028331	0.0070607	0.0061929	1.14012333	0.8399
janA	FBgn0001280	0.0208986	0.0198726	1.05162592	0.84064
RpL23A	FBgn0014878	0.4089145	0.4166146	-1.0188308	0.8411
dy	FBgn0000525	0.0032033	0.0040456	-1.2629421	0.84276
CG14899	FBgn0038438	0.0088691	0.0101559	-1.1450909	0.84304
Su(var)3-9	FBgn0003600	0.0358077	0.037241	-1.0400276	0.84531
CG7298	FBgn0026283	0.0077335	0.0069813	1.10775333	0.84537
RpL14	FBgn0017579	0.8849942	0.8734708	1.01319266	0.84584
CG18591	FBgn0031962	0.0511194	0.0543819	-1.0638224	0.84999
CG4169	FBgn0025538	0.3591307	0.3613937	-1.0063014	0.85021
MSBP	FBgn0030703	0.0892998	0.0859458	1.03902421	0.85028
faf	FBgn0005632	0.0013792	0.0012434	1.10919248	0.8505
pod1	FBgn0029903	0.0173487	0.0140287	1.23666214	0.8505

CG7506	FBgn0035805	0.0049186	0.0039827	1.23499674	0.85101
Pp1-87B	FBgn0002338	0.076116	0.0798264	-1.0487454	0.85105
l(2)35Di	FBgn0001989	0.0292486	0.0265144	1.10311948	0.85134
p24-1	FBgn0025988	0.0835372	0.08832	-1.0572535	0.8518
CG4857	FBgn0026082	0.0017202	0.0021536	-1.2519447	0.85216
CG8108	FBgn0027567	0.0115426	0.0125198	-1.084664	0.85218
wal	FBgn0010516	0.3371821	0.3325105	1.01404962	0.85335
Lasp	FBgn0016776	0.0060692	0.0063225	-1.041735	0.85401
l(1)G0230	FBgn0028342	0.4335386	0.423196	1.02443926	0.85426
CG9135	FBgn0031769	0.0360556	0.0374938	-1.0398882	0.8548
CG3875	FBgn0034740	0.0049973	0.0040508	1.23366416	0.85662
CR33317	FBgn0032903	0.0146473	0.011873	1.23366416	0.85662
CG7441	FBgn0036763	0.0044226	0.0048116	-1.087969	0.85753
pic	FBgn0027049	0.0050013	0.0051794	-1.0356169	0.85794
CG14434	FBgn0029915	0.0123426	0.0105486	1.17007674	0.85851
CG31122	FBgn0038620	0.0034037	0.0028884	1.17841513	0.85972
CG4848	FBgn0037998	0.0025828	0.0029151	-1.1286504	0.85995
CG14423	FBgn0029646	0.0093463	0.0097134	-1.0392804	0.85996
bif	FBgn0014133	0.0015273	0.0012441	1.22761824	0.86013
His2A	FBgn0045839	2.0605311	2.0143874	1.02290702	0.86041
His2A:CG31618	FBgn0045839	2.0605311	2.0143874	1.02290702	0.86041
CG7857	FBgn0026738	0.0120893	0.0107367	1.12598217	0.86211
CG5554	FBgn0034914	0.2045687	0.2135753	-1.0440272	0.86333
CREG	FBgn0025456	0.1518399	0.1487818	1.02055443	0.86428
CG5525	FBgn0032444	0.1422701	0.1382507	1.02907308	0.86434
shg	FBgn0003391	0.0048207	0.0044415	1.08538444	0.86444
CG7414	FBgn0037135	0.0222575	0.0232595	-1.0450192	0.86583
spt4	FBgn0022179	0.0249055	0.0225738	1.10329456	0.86625
crn	FBgn0000377	0.0007646	0.000981	-1.2830355	0.86633
kkv	FBgn0001311	0.0003323	0.0004264	-1.2830355	0.86633
mRpL51	FBgn0032053	0.0030846	0.0039577	-1.2830355	0.86633
CG3262	FBgn0032986	0.0018071	0.0023186	-1.2830355	0.86633
Jheh2	FBgn0034405	0.0011592	0.0014873	-1.2830355	0.86633
CG3376	FBgn0034997	0.0007581	0.0009726	-1.2830355	0.86633
mRpS35	FBgn0035374	0.0016464	0.0021124	-1.2830355	0.86633
CG5919	FBgn0038876	0.0020966	0.00269	-1.2830355	0.86633
Nup133	FBgn0039004	0.0005262	0.0006751	-1.2830355	0.86633
polybromo	FBgn0039227	0.0003245	0.0004163	-1.2830355	0.86633
CG2177	FBgn0039902	0.0026703	0.003426	-1.2830355	0.86633
cals	FBgn0039928	0.0005488	0.0007041	-1.2830355	0.86633
CG31935	FBgn0031348	0.0005859	0.0007518	-1.2830355	0.86633

CG1542	FBgn0039828	0.0034966	0.0044853	-1.2827672	0.86645
Ppox	FBgn0020018	0.0045109	0.0053171	-1.1787173	0.86663
Zpr1	FBgn0030096	0.0102382	0.0112799	-1.1017487	0.86703
CG10418	FBgn0036277	0.0755035	0.0717772	1.05191481	0.86805
CG9733	FBgn0039759	0.0040249	0.0044547	-1.1067836	0.86826
CG12007	FBgn0037293	0.0039435	0.0043868	-1.1124285	0.86827
CG17471	FBgn0039924	0.0103321	0.0095187	1.08545323	0.8684
Cpr78E	FBgn0037114	0.0821872	0.0781483	1.05168222	0.86902
CG7337	FBgn0031374	0.000457	0.0005821	-1.2738836	0.87019
CG4645	FBgn0030435	0.0104905	0.0107814	-1.0277233	0.8709
CG5844	FBgn0038049	0.0830404	0.0816562	1.01695183	0.87228
mRpL44	FBgn0037330	0.0109585	0.0116868	-1.0664626	0.87248
CG6567	FBgn0037842	0.0280962	0.0300022	-1.0678393	0.87284
vig	FBgn0024183	0.0231909	0.0223793	1.03626565	0.87323
CG1115	FBgn0037299	0.011784	0.0105801	1.11378877	0.87563
CG7668	FBgn0036929	0.0028263	0.0033923	-1.2002547	0.87566
br	FBgn0000801	0.007755	0.0080521	-1.0383134	0.87786
CG11943	FBgn0027698	0.0023123	0.0027041	-1.1694465	0.87882
Snr1	FBgn0010744	0.0080185	0.0086288	-1.0761056	0.87885
CG11148	FBgn0039936	0.0022713	0.0020515	1.10713183	0.87941
Cyt-c-p	FBgn0000409	0.3889741	0.3952488	-1.0161315	0.88028
CG17598	FBgn0031194	0.0122537	0.0119083	1.02900991	0.88155
CG13630	FBgn0039219	0.0073342	0.008048	-1.0973115	0.88158
coil	FBgn0033265	0.0017038	0.0021224	-1.2457325	0.88225
CG10973	FBgn0036306	0.00353	0.0043975	-1.2457325	0.88225
CG14641	FBgn0037220	0.0026534	0.0022486	1.18000229	0.88338
CG4612	FBgn0035016	0.0065436	0.0071866	-1.0982614	0.88373
Syx5	FBgn0001996	0.0038393	0.0033497	1.14616309	0.8863
Hn	FBgn0001208	0.0075831	0.0082059	-1.0821329	0.88771
Rae1	FBgn0034646	0.007357	0.0066956	1.09877777	0.88803
Hmu	FBgn0010259	0.0865423	0.0885577	-1.0232887	0.88818
eIF6	FBgn0021890	0.0616065	0.0583063	1.05660035	0.88856
RpL24	FBgn0026273	0.46059	0.4529554	1.0168549	0.88858
Rep	FBgn0026378	0.0034925	0.0030613	1.1408573	0.8903
tex	FBgn0037569	0.0076805	0.008183	-1.065418	0.89088
CG32164	FBgn0036647	0.003154	0.0034044	-1.0793993	0.89125
CG32165	FBgn0014929	0.003151	0.0034012	-1.0793993	0.89125
CG7637	FBgn0033548	0.0756885	0.0783551	-1.0352318	0.89195
Top1	FBgn0004924	0.0155576	0.0153339	1.01459233	0.89292
rept	FBgn0010908	0.0214887	0.0204694	1.04979809	0.89472
CG8417	FBgn0037744	0.013213	0.0140323	-1.0620108	0.89517
CG16817	FBgn0037728	0.247733	0.2415678	1.02552145	0.89535

mRpL28	FBgn0031660	0.0054498	0.0062246	-1.1421835	0.89615
CG10703	FBgn0037881	0.0023681	0.0027048	-1.1421835	0.89615
gbb	FBgn0004788	0.0037244	0.003438	1.08330168	0.89617
Pak3	FBgn0038430	0.008063	0.0088549	-1.0982102	0.89768
CG9425	FBgn0036451	0.000548	0.0004469	1.22616633	0.89785
CG14542	FBgn0039402	0.0132998	0.0128592	1.0342684	0.89785
CG32147	FBgn0047178	0.0189783	0.0197744	-1.0419458	0.8981
CG18508	FBgn0028746	0.0229186	0.0210799	1.0872236	0.89895
Ilk	FBgn0013568	0.0059749	0.0054846	1.08940503	0.89977
CG10738	FBgn0036368	0.0009332	0.0008118	1.1494617	0.90148
1-Sep	FBgn0005665	0.0207063	0.0211565	-1.0217419	0.90273
zfh2	FBgn0004607	0.0003585	0.0003128	1.14616215	0.90347
Cap	FBgn0015615	0.0004681	0.0005594	-1.1950281	0.90472
CSN3	FBgn0027055	0.0012949	0.0015475	-1.1950281	0.90472
CG10184	FBgn0039094	0.0783527	0.0800302	-1.0214097	0.90504
CG5793	FBgn0038858	0.0175448	0.0166604	1.05308305	0.90512
opa1-like	FBgn0033914	0.001764	0.0018954	-1.0744999	0.90622
dro6	FBgn0035442	0.0709591	0.0737751	-1.0396856	0.90674
Ts	FBgn0024920	0.0070439	0.0063373	1.11150539	0.90676
Mcm6	FBgn0000821	0.0048373	0.0045048	1.07382396	0.90686
Rbcn-3B	FBgn0023510	0.0017038	0.001578	1.07971799	0.90756
Ank2	FBgn0017645	0.0005048	0.0005983	-1.1852231	0.90917
CG31715	FBgn0051715	0.1006925	0.0983607	1.02370695	0.90936
Prosalpha1	FBgn0026781	0.226506	0.221048	1.02469182	0.90964
hoip	FBgn0015393	0.3825313	0.376889	1.01497082	0.9097
Arc-p20	FBgn0025530	0.0216832	0.0231644	-1.0683112	0.91036
FK506-bp1	FBgn0013269	0.0772849	0.0785318	-1.0161336	0.91071
wuho	FBgn0029857	0.0152162	0.0156007	-1.0252725	0.91185
Tm1	FBgn0003721	0.4379461	0.430773	1.01665177	0.91195
CG8369	FBgn0027745	0.104167	0.1008525	1.03286454	0.91241
CG3056	FBgn0024987	0.0012053	0.0014199	-1.1780601	0.91245
CG13676	FBgn0035844	0.000662	0.0007799	-1.1780601	0.91245
Pp4-19C	FBgn0005784	0.0051632	0.0056772	-1.0995423	0.9172
CG9779	FBgn0037231	0.0051923	0.0046308	1.12126879	0.91918
Vps26	FBgn0014411	0.0016913	0.0019664	-1.1626086	0.91958
Pp1alpha-96A	FBgn0003134	0.0607395	0.0626213	-1.0309805	0.91967
CG3501	FBgn0034791	0.0498533	0.0488973	1.01955059	0.92028
CG13506	FBgn0034723	0.0024024	0.002053	1.17017909	0.92031
CG7526	FBgn0035798	0.0019353	0.0016554	1.16910249	0.92076
xl6	FBgn0028554	0.0087944	0.0080051	1.09858825	0.92363
RpL19	FBgn0002607	0.3955716	0.4002366	-1.011793	0.92615
CG6983	FBgn0035896	0.0057868	0.0052218	1.10821127	0.92735

CG18749	FBgn0037557	0.0021214	0.0019143	1.10821127	0.92735
skpA	FBgn0025637	0.0933967	0.0950327	-1.0175159	0.92742
Pgk	FBgn0003075	0.6857505	0.6915605	-1.0084724	0.92761
eff	FBgn0004831	0.1847784	0.1861892	-1.007635	0.9277
CG8300	FBgn0029937	0.0042867	0.0037223	1.15160194	0.92815
Glycogenin	FBgn0034603	0.0884936	0.085434	1.03581188	0.92824
ade2	FBgn0000052	0.0056727	0.0054913	1.03302834	0.92861
CG3702	FBgn0031590	0.0016852	0.0014663	1.14923954	0.92916
Ho	FBgn0037933	0.0036493	0.0031754	1.14923954	0.92916
CG18012	FBgn0038552	0.002422	0.0021074	1.14923954	0.92916
CG4338	FBgn0038313	0.0022051	0.0025133	-1.1397445	0.9303
CG32486	FBgn0035394	0.0014665	0.0016714	-1.1397445	0.9303
Mob3	FBgn0032203	0.0027464	0.0031302	-1.1397445	0.9303
CG9391	FBgn0037063	0.0281899	0.0271746	1.03736382	0.93035
CG7630	FBgn0027722	0.1959514	0.1994343	-1.0177744	0.93036
Hml	FBgn0029167	0.0052532	0.0050029	1.0500411	0.93151
Bsg	FBgn0010613	0.0280092	0.0288991	-1.0317733	0.93181
CG9853	FBgn0037243	0.004996	0.0047408	1.05383605	0.93222
CG9596	FBgn0031832	0.0024177	0.0021169	1.14205973	0.93225
Lsp1gamma	FBgn0002564	1.1215769	1.1278498	-1.0055929	0.93388
CG15168	FBgn0032732	0.0154974	0.0143514	1.07985329	0.93515
mRpL3	FBgn0030686	0.0053294	0.0049739	1.07145582	0.93589
MRG15	FBgn0024526	0.0014405	0.0016241	-1.1275084	0.93612
Lmpt	FBgn0036672	0.0160569	0.0165418	-1.0301954	0.93616
loqs	FBgn0032515	0.0030132	0.0027526	1.09465025	0.93619
ns1	FBgn0038473	0.0034458	0.0032846	1.04909336	0.93843
CG6995	FBgn0039229	0.0057669	0.0060671	-1.0520436	0.93896
nuf	FBgn0013718	0.0033105	0.0034719	-1.0487623	0.93957
Sac1	FBgn0035195	0.0086881	0.0088754	-1.0215559	0.93969
CG15717	FBgn0030451	0.0623089	0.063443	-1.0182014	0.93969
mago	FBgn0002095	0.0114355	0.0122053	-1.0673125	0.94067
CG10802	FBgn0027766	0.0126786	0.0121679	1.0419707	0.94082
CanB2	FBgn0015614	0.0333278	0.0320705	1.03920282	0.94141
twf	FBgn0038206	0.0713793	0.0704213	1.01360464	0.94184
sec71	FBgn0027855	0.0003825	0.0004267	-1.1155321	0.94186
Tom70	FBgn0032397	0.0010481	0.0011692	-1.1155321	0.94186
CG12946	FBgn0037750	0.001201	0.0013398	-1.1155321	0.94186
Reg-5	FBgn0015801	0.0097867	0.010399	-1.0625642	0.94263
bsk	FBgn0000229	0.0129597	0.012458	1.04027124	0.94292
ctp	FBgn0011760	0.3944374	0.3974438	-1.0076222	0.94322
Cdlc2	FBgn0026141	0.3944374	0.3974438	-1.0076222	0.94322
CG1416	FBgn0032961	0.0683993	0.0688953	-1.0072525	0.94343

Lcp65Ad	FBgn0020641	0.1425126	0.1442073	-1.0118919	0.94518
CG1885	FBgn0030066	0.0145957	0.0141672	1.03024315	0.94565
betaTub85D	FBgn0003889	1.084828	1.0764524	1.00778074	0.94616
CG9286	FBgn0038183	0.0057687	0.0054112	1.06606353	0.94703
RpL11	FBgn0013325	0.4164299	0.4150444	1.00333825	0.94849
CG5167	FBgn0038038	0.0138192	0.0136087	1.01546798	0.94957
CG17333	FBgn0030239	0.0754103	0.0766727	-1.0167409	0.94965
Lac	FBgn0010238	0.0030894	0.0028765	1.07402701	0.94971
CG30115	FBgn0034358	0.002314	0.0022216	1.04156034	0.95051
CG17184	FBgn0037884	0.006148	0.0058194	1.05646489	0.95615
CG11474	FBgn0034688	0.0036766	0.003921	-1.0664635	0.95683
D1	FBgn0000412	0.0589352	0.0580031	1.01606933	0.95739
GckIII	FBgn0038477	0.0012593	0.001364	-1.0831385	0.95767
Dip-C	FBgn0000455	0.0202914	0.0208488	-1.0274721	0.95781
CG1674	FBgn0039897	0.0185455	0.0188561	-1.0167461	0.95861
l(3)04053	FBgn0010830	0.0028744	0.0027839	1.0325117	0.95862
Caf1	FBgn0015610	0.0539149	0.0547998	-1.0164125	0.95872
Gmap	FBgn0027287	0.0239193	0.0236595	1.01098246	0.95899
Fit1	FBgn0035498	0.0104415	0.0103154	1.01222026	0.95942
alphaTub84B	FBgn0003884	1.0053108	1.0082289	-1.0029027	0.96024
alphaTub84D	FBgn0003885	1.0053108	1.0082289	-1.0029027	0.96024
CG6770	FBgn0032400	0.0785943	0.0797973	-1.0153069	0.9609
Pp2B-14D	FBgn0005782	0.025439	0.0258856	-1.0175581	0.96135
hts	FBgn0004873	0.0831629	0.0828313	1.00400247	0.96191
Lcp6	FBgn0002536	0.0817191	0.080416	1.01620477	0.96241
Mi-2	FBgn0010735	0.0034469	0.0033989	1.01413317	0.96266
CG1637	FBgn0030245	0.0081943	0.0083138	-1.0145827	0.96336
CtBP	FBgn0002353	0.0400565	0.0396974	1.00904772	0.96402
CG1240	FBgn0035370	0.0799215	0.0792842	1.00803885	0.96495
CG1970	FBgn0039909	0.0326639	0.0323285	1.01037451	0.96519
CG31546	FBgn0037355	0.0172056	0.0173501	-1.0084022	0.96529
alphaTub67C	FBgn0001067	0.0170555	0.0168019	1.01509732	0.96628
awd	FBgn0000150	1.3130508	1.3087759	1.00326637	0.96637
IM18	FBgn0034881	0.0455945	0.0484872	-1.0634461	0.96747
RpS9	FBgn0010408	0.5678308	0.5650803	1.00486743	0.96755
CG7504	FBgn0035842	0.0046768	0.0046983	-1.0046054	0.96786
P58IPK	FBgn0037718	0.1117178	0.111204	1.00462046	0.96803
CG34133	FBgn0051035	0.0025167	0.0025673	-1.0200828	0.96858
CG17109	FBgn0039051	0.004768	0.0046176	1.03257132	0.96999
CG7185	FBgn0035872	0.0083771	0.0084624	-1.0101818	0.97001
CG5611	FBgn0039531	0.0062343	0.0063823	-1.0237412	0.97125
Atg8a	FBgn0052672	0.0589485	0.0584801	1.00801026	0.97159

CG5075	FBgn0032464	0.1228543	0.1232668	-1.0033574	0.97181
eIF4AIII	FBgn0004221	0.1221649	0.1226808	-1.0042228	0.97205
l(2)06225	FBgn0010612	0.0500326	0.0509059	-1.0174535	0.97239
UbcD6	FBgn0004436	0.0393133	0.0396	-1.0072938	0.9733
CG4972	FBgn0032217	0.0070817	0.0072341	-1.0215119	0.97418
CG3267	FBgn0042083	0.0095749	0.0094507	1.0131391	0.97433
CanB	FBgn0010014	0.0315507	0.0320705	-1.0164752	0.97576
Txl	FBgn0035631	0.1578856	0.1575653	1.00203332	0.97643
CG6597	FBgn0036967	0.0043556	0.004164	1.04602705	0.97661
RpL27	FBgn0039359	0.5838417	0.5863139	-1.0042344	0.97664
Hrb87F	FBgn0004237	0.1223488	0.12206	1.00236577	0.97724
CG8100	FBgn0036410	0.0029144	0.0029895	-1.0257783	0.97725
CG7349	FBgn0030975	0.0209487	0.0207755	1.0083365	0.97849
larp	FBgn0039578	0.0073653	0.0073329	1.00442217	0.97874
skap	FBgn0037643	0.138516	0.1380547	1.00334106	0.98031
TppII	FBgn0020370	0.1400381	0.1402634	-1.001609	0.98096
CG1983	FBgn0039751	0.0132213	0.0133488	-1.0096424	0.9835
Vha68-1	FBgn0020368	0.2486153	0.2483869	1.0009195	0.98791
Pmm45A	FBgn0033377	0.0112531	0.0112818	-1.0025553	0.98812
CG7039	FBgn0030088	0.011443	0.0115845	-1.0123683	0.98851
CG10166	FBgn0032799	0.0987579	0.0989786	-1.0022346	0.98873
Tcp-1zeta	FBgn0026695	0.1551075	0.1553116	-1.0013157	0.98919
l(2)37Bb	FBgn0002021	0.0034433	0.0034838	-1.0117717	0.98962
Manf	FBgn0026289	0.3458023	0.3450646	1.00213794	0.99083
CG18081	FBgn0036537	0.0811225	0.0809703	1.00187912	0.99143
CG18811	FBgn0042134	0.0338782	0.0338282	1.00147803	0.9941
Fkbp13	FBgn0010470	0.1769582	0.1771575	-1.0011259	0.99411
GstD1	FBgn0001149	2.5626658	2.566038	-1.0013159	0.99441
nito	FBgn0027548	0.0065841	0.0066077	-1.0035837	0.99445
Osi6	FBgn0027527	0.083431	0.0832905	1.00168619	0.9961
CG7920	FBgn0039737	0.0362502	0.036213	1.0010267	0.99733
CG9172	FBgn0030718	0.0126097	0.012627	-1.0013704	0.99781
sec13	FBgn0024509	0.2123071	0.2122505	1.00026693	0.99784
CG18178	FBgn0036035	0.008025	0.0080072	1.00221714	0.99814

Appendix 4: *Drosophila* salivary gland proteins identified by proteomics that have positive ratio2 values following ectopic proteasome impairment as well as between 6h and 13h after puparium formation during Wild-type salivary gland cell death.

Protein names and FBgn numbers are based on Flybase annotation (http://flybase.org/). The values for peptides mapped to the genes listed are indicated. Protein quantities were determined using the spectral counting method in which spectral counts (spectral peptide matches) for each protein were summed and normalized across runs based on the total spectral counts obtained for each run. The ratio2 values for peptides mapped to the genes listed are indicated (ratio2=average detection value experimental sample divided by average detection value control sample). p values were obtained using the Student's t-test followed by multiple testing adjustment using the Benjamini-Hochberg method (Hochberg and Benjamini, 1990). Inf indicates a numerical value divided by 0.

symbol	FBgn	ratio2	p value	ratio2	p value
CG11880	FBgn0039637	Inf	7.48E-06	Inf	0.06648
CG10126	FBgn0038088	3.2603	8.51E-05	1.15456	0.7184
Hsp23	FBgn0001224	3.8446	9.57E-05	1.21622	0.03231
CG1681	FBgn0030484	16.85	0.00019	Inf	0.28559
Mmp1	FBgn0022198	Inf	0.00025	1.40362	0.56908
Ect3	FBgn0037977	10.298	0.0004	28.0652	0.00094
CG1950	FBgn0030370	1.7241	0.00041	1.54354	0.45627
CG9336	FBgn0032897	8.9686	0.00047	Inf	0.06533
CG11876	FBgn0039635	1.2886	0.00047	1.25299	0.19
Cyp12c1	FBgn0036806	15.232	0.00048	Inf	0.28559
CG3415	FBgn0030731	1.6546	0.00067	1.2714	0.11298
Dbi	FBgn0010387	3.5521	0.00085	Inf	0.00075
Idh	FBgn0001248	1.442	0.00085	1.56947	0.00038

CG9917	FBgn0030740	Inf	0.00088	Inf	0.28559
Sodh-1	FBgn0024289	1.4196	0.00092	1.16821	0.5086
CG3074	FBgn0034709	4.5371	0.0014	3.39126	0.05425
CG3011	FBgn0029823	1.6232	0.00141	1.6894	0.05042
dro2	FBgn0035433	Inf	0.00149	Inf	0.06533
CG9977	FBgn0035371	2.2838	0.00168	1.1449	0.74708
Edg84A	FBgn0000552	Inf	0.00177	Inf	0.00137
trol	FBgn0001402	1.5053	0.00191	1.90776	0.00881
Glt	FBgn0001114	1.6103	0.00235	1.36426	0.02728
CG14109	FBgn0036364	Inf	0.00245	1.57012	0.52816
CG4572	FBgn0038738	4.8755	0.00261	1.37563	0.42896
Gapdh1	FBgn0001091	1.2482	0.00293	1.12203	0.41151
CG5174	FBgn0034345	1.3185	0.00293	1.04632	0.84157
lectin-28C	FBgn0031956	Inf	0.00307	Inf	0.02297
Hf	FBgn0014000	Inf	0.00313	Inf	0.09632
CG9629	FBgn0036857	2.2013	0.00329	6.34414	0.00771
Vago	FBgn0030262	Inf	0.00331	8.9802	0.01286
Argk	FBgn0000116	1.2895	0.00331	1.71154	0.01955
Drs	FBgn0010381	2.3231	0.00334	1.08537	0.88935
CG33138	FBgn0033801	2.9122	0.0041	2.95768	0.01495
CG31673	FBgn0051673	2.8024	0.00412	Inf	2.49E-05
CG5171	FBgn0031907	2.2263	0.00414	5.77677	0.00061
Act79B	FBgn0000045	1.4824	0.00443	1.19258	0.17146
Pcd	FBgn0024841	1.9221	0.0047	1.69322	0.27837
Cg25C	FBgn0000299	1.5861	0.00492	1.77659	0.00259
Pepck	FBgn0003067	4.1299	0.00502	5.65681	0.0209
Act57B	FBgn0000044	1.3925	0.00505	1.35679	0.02551
Act87E	FBgn0000046	1.3942	0.00528	1.34342	0.03147
Mpk2	FBgn0013952	Inf	0.00551	1.20679	0.89942
CG9360	FBgn0030332	7.2955	0.00577	Inf	0.28559
l(2)gl	FBgn0002121	1.8588	0.00602	1.21598	0.7215
CG6767	FBgn0036030	1.681	0.00614	1.73179	0.17077
Peritrophin-15a	FBgn0040959	Inf	0.00706	5.06583	0.14436
CG11378	FBgn0029561	10.727	0.00727	1.22375	0.72146
CG11151	FBgn0030519	1.7159	0.00741	1.46397	0.07897
Map205	FBgn0002645	6.7988	0.00788	Inf	1.15E-09
Pax	FBgn0032776	1.4599	0.00826	1.72259	0.00046
yellow-f	FBgn0038104	3.5226	0.00845	1.20679	0.89942
Tig	FBgn0011722	2.0053	0.00849	1.73781	0.09491
UK114	FBgn0028510	1.3605	0.00853	1.23084	0.48008
Men	FBgn0002719	1.6619	0.00868	1.55933	0.00189
CG1943	FBgn0037468	1.6679	0.00902	1.2298	0.49369

CG15404	FBgn0031512	2.8089	0.00907	1.70113	0.27947
Sodh-2	FBgn0022359	1.3994	0.00943	1.15554	0.41886
CG31919	FBgn0031674	2.8001	0.00955	1.67048	0.21375
Ppt1	FBgn0030057	Inf	0.01009	2.27828	0.43862
fon	FBgn0032773	1.8383	0.01021	1.06083	0.71178
Oat	FBgn0022774	1.4733	0.01048	1.05912	0.87151
Imp	FBgn0025229	2.6938	0.01106	1.80042	0.07317
Zw	FBgn0004057	4.2545	0.01119	2.27469	0.21166
Gs2	FBgn0001145	1.7788	0.01158	15.0392	1.65E-07
Prosbeta3	FBgn0026380	1.4282	0.01224	1.30269	0.10335
svr	FBgn0000268	3.2581	0.0126	2.77957	0.04916
Mf	FBgn0038294	1.5132	0.01353	3.26568	0.0029
ade5	FBgn0020513	1.4339	0.01413	2.71211	0.00696
Idgf1	FBgn0020416	3.9452	0.01464	2.73772	0.07139
CG11255	FBgn0036337	1.7466	0.01467	1.47165	0.13685
His3.3B	FBgn0004828	3.7516	0.01545	1.2197	0.59959
CG3473	FBgn0028913	2.843	0.01615	1.16259	0.91959
vkg	FBgn0010477	1.2914	0.01642	1.7625	0.01905
CG1578	FBgn0030336	5.1798	0.01686	2.23578	0.6007
fau	FBgn0020439	2.2642	0.01761	8.42063	0.00249
miple2	FBgn0029002	Inf	0.01784	1.01265	0.98663
yrt	FBgn0000466	4.1007	0.0197	Inf	0.06245
Gal	FBgn0001089	2.6181	0.02052	2.23295	0.18407
CAH1	FBgn0027844	4.4268	0.02097	2.41283	0.36152
CG12224	FBgn0037974	1.389	0.02351	6.12931	0.14768
Hsp67Bb	FBgn0001228	2.6012	0.0237	1.27267	0.71239
CG2034	FBgn0015359	4.8794	0.0238	1.1383	0.93098
scb	FBgn0003328	3.2893	0.02505	1.04003	0.9206
CdsA	FBgn0010350	5.5342	0.02797	Inf	0.01602
Lsd-2	FBgn0030608	1.8265	0.02859	2.08086	0.02137
CG17024	FBgn0032437	2.4275	0.03059	1.88984	0.25639
CG12163	FBgn0037303	1.8404	0.03418	3.07675	0.00353
CG3397	FBgn0037975	2.5167	0.03459	3.09587	0.08485
CG4752	FBgn0034733	1.9774	0.03535	6.31777	0.15987
CG31997	FBgn0043807	2.5572	0.03738	Inf	0.07809
unc-115	FBgn0037733	1.9461	0.03786	1.35195	0.63038
CG31352	FBgn0037733	1.9461	0.03786	1.11659	0.79635
CG18135	FBgn0036837	3.6399	0.0398	5.1994	0.03062
Chc	FBgn0000319	1.28	0.04022	2.2288	0.00063
Adk1	FBgn0022709	4.9076	0.04143	Inf	0.13835
ND23	FBgn0017567	1.2309	0.04181	1.06998	0.89669
CG7564	FBgn0036734	4.4093	0.04189	Inf	0.06533

GS	FBgn0030882	1.4044	0.0431	1.04794	0.69422
Neurochondrin	FBgn0037447	2.5209	0.0434	4.18934	0.05505
CG2021	FBgn0035271	3.9173	0.04363	1.55617	0.14492
Abi	FBgn0020510	3.2877	0.04438	2.64846	0.36037
CG1837	FBgn0027709	1.3063	0.04669	1.42521	0.10582
CG7470	FBgn0037146	3.1002	0.05318	12.9317	0.00426
Adgf-A	FBgn0036752	4.0674	0.05339	7.10317	0.02066
CG3756	FBgn0031657	Inf	0.05402	1.11789	0.94073
CG5001	FBgn0031322	Inf	0.05405	1.75914	0.41036
Rpn2	FBgn0028692	1.2294	0.05417	1.38489	0.01105
CG6912	FBgn0038290	Inf	0.05428	2.07716	0.23593
loj	FBgn0010829	Inf	0.05491	Inf	0.28559
CG3987	FBgn0038292	4.0471	0.05519	Inf	0.00127
CG11334	FBgn0039849	1.6174	0.05583	4.11531	0.00027
snRNP2	FBgn0037434	1.3846	0.05755	1.0404	0.90214
CG15118	FBgn0025243	3.9473	0.05942	4.09225	0.26461
Mp20	FBgn0002789	1.5256	0.06077	1.80574	0.03548
capt	FBgn0010632	1.1468	0.0636	1.21557	0.3197
CG5177	FBgn0031908	1.409	0.06378	2.4146	0.01442
regucalcin	FBgn0030362	1.2198	0.06386	1.39197	0.10926
Fbp2	FBgn0000640	1.4665	0.06577	2.1806	0.02373
CG10962	FBgn0030072	4.005	0.06672	6.26858	0.17892
CG8709	FBgn0033269	Inf	0.06783	1.85538	0.06902
CG9953	FBgn0035726	3.9139	0.0681	1.39266	0.65746
GstD5	FBgn0010041	8.9796	0.06924	1.20629	0.87984
ScpX	FBgn0015808	1.2983	0.07086	1.8675	0.05388
l(2)efl	FBgn0011296	2.0184	0.0713	3.89286	0.03121
CG1440	FBgn0030038	1.288	0.0746	1.48595	0.15064
pug	FBgn0020385	2.2349	0.0798	1.16344	0.59042
CG6415	FBgn0024715	1.5725	0.08007	2.57666	0.01526
Pros45	FBgn0020369	1.2226	0.08037	1.34324	0.19071
sls	FBgn0002186	1.6987	0.08047	7.14149	0.01302
CG5567	FBgn0036760	Inf	0.08123	1.01086	0.99246
GstS1	FBgn0010226	1.8711	0.08131	1.03222	0.90141
simj	FBgn0010762	Inf	0.08309	Inf	0.28559
Pros26.4	FBgn0015282	1.115	0.08393	1.06756	0.58462
SmG	FBgn0030765	Inf	0.08552	Inf	0.06533
LamC	FBgn0010037	1.2962	0.0896	1.34374	0.05975
CG32495	FBgn0052495	1.46	0.09058	1.11194	0.46452
wdp	FBgn0034718	3.1068	0.09163	Inf	0.28559
Lsd-1	FBgn0039114	3.0677	0.0931	23.3466	0.08046
Cpr	FBgn0015623	1.3513	0.09399	1.78304	0.00746

CG5023	FBgn0038774	1.2387	0.09516	2.77367	0.02268
CG6905	FBgn0035136	Inf	0.09639	1.1383	0.93098
Adh	FBgn0000055	1.206	0.09761	1.54779	0.0133
CG30410	FBgn0034848	1.128	0.09902	1.64314	0.03316
ph-d	FBgn0004860	Inf	0.09955	1.42873	0.80895
ph-p	FBgn0003077	Inf	0.09955	1.42873	0.80895
Arp53D	FBgn0011743	1.5535	0.10118	1.26628	0.77892
Cat	FBgn0000261	1.1275	0.1017	1.13935	0.21619
CG3505	FBgn0038250	2.3822	0.10471	2.81181	0.10688
Rpt6R	FBgn0039788	1.244	0.10604	1.01034	0.96677
Stam	FBgn0027363	1.6671	0.1079	1.419	0.4495
primo-1	FBgn0038174	1.6237	0.11071	1.14597	0.80111
CG12262	FBgn0035811	1.2229	0.11266	1.24789	0.13871
CG6904	FBgn0038293	2.5359	0.11318	6.22854	0.01716
RpL7A	FBgn0014026	1.1506	0.11622	1.48222	0.00146
CG6287	FBgn0032350	1.0956	0.11654	1.60962	0.00064
t	FBgn0030106	2.8032	0.1184	Inf	0.09632
Srp14	FBgn0038808	1.2887	0.11879	1.07937	0.91411
CG32638	FBgn0052638	2.5772	0.11961	9.92563	0.00619
CG15239	FBgn0029681	2.9788	0.12222	4.8674	0.04846
Vha100-2	FBgn0027516	2.1668	0.12229	11.3275	0.00112
l(1)G0255	FBgn0027231	1.4001	0.12394	1.10685	0.63079
Vha16	FBgn0004145	2.7942	0.12674	Inf	0.00975
TotA	FBgn0028396	1.3332	0.12782	1.94628	0.0283
Prosbeta7	FBgn0037314	1.2337	0.12879	1.10202	0.52302
betaTub97EF	FBgn0003890	1.2038	0.13053	1.03004	0.69495
CG8602	FBgn0035763	2.3218	0.13094	5.01785	0.0396
CG17597	FBgn0032715	1.2841	0.13162	1.74043	0.06258
Hira	FBgn0022786	1.1596	0.13398	1.49423	0.50726
CG31694	FBgn0031475	1.5511	0.13428	1.50295	0.45054
CG17331	FBgn0032596	1.189	0.14043	1.11722	0.58079
R	FBgn0003190	1.6311	0.14138	4.41158	0.00908
CG9086	FBgn0030809	1.8	0.14472	5.94278	0.06517
Pgm	FBgn0003076	1.2913	0.14963	1.1414	0.25063
CG8036	FBgn0037607	1.1759	0.15087	1.37001	0.012
CG10131	FBgn0033949	2.8604	0.15227	1.91151	0.44593
Taf4	FBgn0005542	1.7439	0.15452	Inf	0.28559
CG9577	FBgn0031092	1.5896	0.15511	1.54978	0.07967
CG3884	FBgn0033786	Inf	0.16086	10.4916	0.09872
cpb	FBgn0011570	1.2097	0.1613	1.47537	0.52663
Gclm	FBgn0039001	2.6442	0.16591	Inf	0.28559
fax	FBgn0014163	1.4178	0.16689	1.3645	0.18897

Pros29	FBgn0003150	1.1869	0.17143	1.04463	0.77884
CG5871	FBgn0038870	3.8207	0.17564	2.8758	0.48704
VhaAC39	FBgn0025327	1.3866	0.17621	34.4624	0.00013
Prosbeta1	FBgn0010590	1.1344	0.17723	1.26021	0.00649
CG4278	FBgn0014092	1.632	0.18194	1.90553	0.56195
tmod	FBgn0010731	1.3738	0.18432	3.34017	0.00455
tws	FBgn0004889	1.46	0.1862	1.0206	0.98065
CG11384	FBgn0029562	2.8429	0.19152	Inf	0.28559
CG17556	FBgn0038461	1.8841	0.19222	1.38553	0.45964
Mical	FBgn0037774	2.322	0.19413	55.2128	0.0078
CG32631	FBgn0030496	1.8782	0.1942	3.81798	0.23615
Rtf1	FBgn0034722	2.2059	0.19485	Inf	0.28559
CG10359	FBgn0035452	Inf	0.19779	Inf	0.06245
CG13962	FBgn0032824	3.2907	0.2008	Inf	0.01602
Muc11A	FBgn0030371	Inf	0.20312	5.27281	0.1526
CG31778	FBgn0031565	Inf	0.20313	Inf	0.28559
CG17746	FBgn0035425	Inf	0.20323	Inf	0.00192
CG3295	FBgn0034573	Inf	0.20356	2.32519	0.58582
SNF4Agamma	FBgn0025803	Inf	0.20359	1.1383	0.93098
CG32195	FBgn0052195	Inf	0.20375	Inf	0.28559
aux	FBgn0037218	Inf	0.20444	1.20679	0.89942
CG12519	FBgn0036872	Inf	0.20513	1.42873	0.80895
CG10433	FBgn0034638	Inf	0.20514	Inf	0.00192
CG4669	FBgn0035598	Inf	0.20533	Inf	0.28559
CG15735	FBgn0030364	1.3236	0.20588	Inf	0.28559
CG4960	FBgn0039371	3.8166	0.20614	1.16039	0.92061
Or82a	FBgn0041621	Inf	0.20652	Inf	0.06533
CG1308	FBgn0035507	Inf	0.20652	Inf	0.28559
ninaG	FBgn0037896	Inf	0.20743	1.18158	0.91084
cpa	FBgn0034577	1.1785	0.20765	1.14314	0.69484
CG4500	FBgn0019862	Inf	0.21429	Inf	0.08892
Hexo2	FBgn0030059	Inf	0.21463	2.90965	0.51199
CG32626	FBgn0030531	1.3317	0.2148	2.19613	0.01595
Vps45	FBgn0037711	2.0352	0.21572	2.27661	0.59376
baf	FBgn0031977	1.6846	0.21926	1.18537	0.76676
CG6766	FBgn0032398	1.5015	0.22005	1.66844	0.29112
Rpn11	FBgn0028694	1.2057	0.2212	1.078	0.58513
Fbp1	FBgn0000639	1.3608	0.22306	2.7233	0.00606
l(3)03670	FBgn0010808	2.6228	0.22319	1.00331	0.99137
CG17565	FBgn0038424	Inf	0.2254	Inf	0.28559
Irp-1B	FBgn0024957	1.1668	0.22672	1.10177	0.54098
MRP	FBgn0032456	Inf	0.22852	1.48587	0.78845

CG7806	FBgn0032018	Inf	0.22968	1.11789	0.94073
CG31343	FBgn0038898	Inf	0.23023	3.05152	0.22642
CG9914	FBgn0030737	1.2938	0.23091	1.13082	0.63809
CG14688	FBgn0037819	Inf	0.23201	1.6421	0.46468
asf1	FBgn0029094	Inf	0.23214	Inf	0.28559
Shc	FBgn0015296	Inf	0.23459	1.26583	0.84226
CG10943	FBgn0036320	Inf	0.23525	Inf	0.28559
CG8306	FBgn0034142	1.6018	0.23687	3.92679	0.00385
Pglym87	FBgn0011270	1.3397	0.23756	1.36284	0.39443
Nrt	FBgn0004108	Inf	0.23816	2.27828	0.43862
CG4968	FBgn0032214	1.5049	0.23894	1.13476	0.90323
CG18858	FBgn0042175	1.6038	0.23933	1.84592	0.12448
Lcp65Ac	FBgn0020642	1.8502	0.24043	1.71176	0.06744
Sclp	FBgn0030357	2.4456	0.24351	1.85068	0.33884
CG14235	FBgn0031066	1.2025	0.24467	2.55005	0.00562
dnc	FBgn0000479	1.5458	0.24478	7.26212	0.01786
CG11459	FBgn0037396	1.9426	0.24608	Inf	0.28559
Pglym78	FBgn0014869	1.093	0.24994	1.05995	0.49638
alpha-Adaptin	FBgn0010623	1.5242	0.25357	4.48746	0.0007
CSN7	FBgn0028836	1.4916	0.25542	4.59905	0.26005
U4-U6-60K	FBgn0036733	1.7824	0.25762	1.16039	0.92061
Faf	FBgn0025608	3.5602	0.25928	4.44459	0.29649
CG5362	FBgn0032237	1.1271	0.26297	1.03233	0.81739
CG1600	FBgn0033188	1.6426	0.26647	9.66607	8.38E-06
Rassf	FBgn0039055	3.4333	0.2674	Inf	0.28559
CG7739	FBgn0036509	4.0622	0.26778	4.73878	0.1664
RpL34b	FBgn0025253	1.1726	0.27283	2.01167	0.00567
sds22	FBgn0028992	1.582	0.27371	1.66175	0.1171
mRpL24	FBgn0031651	3.0414	0.27384	Inf	0.28559
Rpn7	FBgn0028688	1.1535	0.27833	1.27546	0.45986
CSN5	FBgn0016027	1.5955	0.27892	1.79054	0.16182
CG15630	FBgn0031627	2.6119	0.27916	Inf	0.28559
vir-1	FBgn0032426	1.1587	0.28126	1.98968	0.12013
Kap-alpha1	FBgn0024889	1.1903	0.28334	1.45977	0.6442
up	FBgn0001267	1.2661	0.29468	2.97917	0.01232
Rpn5	FBgn0028690	1.1123	0.29513	1.50355	0.05448
Hsp67Ba	FBgn0001227	1.8596	0.2957	6.70733	0.36535
nrv2	FBgn0014867	2.7816	0.29713	1.7097	0.67312
ade3	FBgn0000053	1.427	0.29855	3.85156	0.04381
CG2025	FBgn0030344	1.5827	0.30315	1.54237	0.25787
lark	FBgn0011640	1.43	0.30406	1.61127	0.38518
Prosalpha5	FBgn0016697	1.1225	0.3052	1.1194	0.46138

CG18547	FBgn0037973	1.5628	0.30787	1.25279	0.68108
CG5656	FBgn0037083	1.3669	0.30808	1.15004	0.84175
CG3683	FBgn0035046	1.3166	0.31106	1.84942	0.08358
CG9510	FBgn0032076	2.1165	0.31158	1.01829	0.94991
aralar1	FBgn0028646	1.289	0.312	Inf	0.28559
smp-30	FBgn0038257	1.2846	0.31326	2.39594	0.20197
Rab14	FBgn0014431	1.1118	0.31353	2.51209	0.01033
CG10673	FBgn0035590	1.7333	0.31718	1.16039	0.92061
CG14103	FBgn0036908	2.1456	0.32222	2.97279	0.31806
CG17904	FBgn0032597	1.1389	0.3291	1.23333	0.78997
SCAR	FBgn0021868	1.3116	0.32988	1.20679	0.89942
Hsc70-4	FBgn0001219	1.0466	0.33176	1.07369	0.6243
Phk-3	FBgn0035089	1.3777	0.33177	1.16039	0.92061
Reg-2	FBgn0016715	1.3732	0.33598	4.56696	0.0038
RpS12	FBgn0011809	1.0639	0.3382	1.04743	0.63117
CG1890	FBgn0039869	2.6809	0.34209	1.1383	0.93098
CG4390	FBgn0038771	1.3258	0.34493	1.09253	0.68977
Prat2	FBgn0035717	3.0004	0.34556	5.38533	0.14949
Arc-p34	FBgn0032859	1.56	0.34804	1.06149	0.9471
CG13492	FBgn0034662	2.8651	0.34909	5.72698	0.15793
tsr	FBgn0011567	1.1186	0.3505	1.02572	0.65157
RpL34a	FBgn0039406	1.1398	0.35149	2.39984	0.00374
CG1648	FBgn0033446	1.1688	0.35161	1.08595	0.87917
sub	FBgn0003545	2.352	0.35231	1.71829	0.52482
Vha13	FBgn0010857	1.8078	0.37292	1.04164	0.94349
Rheb	FBgn0037343	1.4091	0.37483	Inf	0.07155
CG30359	FBgn0033295	1.4047	0.37737	3.85976	0.01381
CG4858	FBgn0037011	1.3472	0.37744	5.34113	0.07185
CG4019	FBgn0034885	1.3651	0.37835	4.30317	0.02151
Tps1	FBgn0001908	1.4934	0.3842	8.69156	0.02352
Vha16-3	FBgn0028667	2.995	0.38454	Inf	0.0018
CG2046	FBgn0037378	1.1482	0.38515	1.22508	0.6565
CG13890	FBgn0035169	1.2679	0.41223	27.1636	0.01652
CG7787	FBgn0032020	1.3708	0.41363	5.94278	0.06517
CG11134	FBgn0030518	1.2417	0.41794	1.05853	0.91132
Ccp84Ae	FBgn0004779	2.5384	0.42045	8.4894	0.03802
mys	FBgn0001448	1.2749	0.42242	4.91948	0.0147
nvy	FBgn0005636	1.9952	0.4268	Inf	0.28559
Rac1	FBgn0010333	1.2901	0.4295	1.59116	0.31282
Rab-RP4	FBgn0015794	1.9806	0.43125	Inf	0.28559
CPTI	FBgn0027842	1.7315	0.43149	Inf	0.0013
Thor	FBgn0017459	Inf	0.43659	Inf	1.72E-05

Tango9	FBgn0037971	Inf	0.43659	Inf	2.25E-05
CG3164	FBgn0025683	Inf	0.43659	Inf	0.00174
CG16758	FBgn0035348	Inf	0.43659	11.4107	0.03806
Spn28D	FBgn0031973	Inf	0.43659	Inf	0.06245
Tsp42Ee	FBgn0029506	Inf	0.43659	Inf	0.06245
RpI135	FBgn0003278	Inf	0.43659	3.85526	0.0648
CG31780	FBgn0028864	Inf	0.43659	Inf	0.07809
Gp150	FBgn0013272	Inf	0.43659	Inf	0.09632
CG9673	FBgn0030775	Inf	0.43659	8.35706	0.16226
mor	FBgn0002783	Inf	0.43659	2.08757	0.26098
Myo61F	FBgn0010246	Inf	0.43659	3.50146	0.28329
Atg2	FBgn0035373	Inf	0.43659	Inf	0.28559
Atg9	FBgn0034110	Inf	0.43659	Inf	0.28559
CecA2	FBgn0000276	Inf	0.43659	Inf	0.28559
CecC	FBgn0000279	Inf	0.43659	Inf	0.28559
CG12130	FBgn0033466	Inf	0.43659	Inf	0.28559
CG15438	FBgn0025684	Inf	0.43659	Inf	0.28559
CG2277	FBgn0035204	Inf	0.43659	Inf	0.28559
CG30193	FBgn0034799	Inf	0.43659	Inf	0.28559
CG32758	FBgn0029794	Inf	0.43659	Inf	0.28559
CG5594	FBgn0025698	Inf	0.43659	Inf	0.28559
dock	FBgn0010583	Inf	0.43659	Inf	0.28559
Flo-2	FBgn0024753	Inf	0.43659	Inf	0.28559
Mcr	FBgn0014086	Inf	0.43659	Inf	0.28559
Nup75	FBgn0034310	Inf	0.43659	Inf	0.28559
Scp2	FBgn0020907	Inf	0.43659	Inf	0.28559
slmb	FBgn0016060	Inf	0.43659	Inf	0.28559
snf	FBgn0003449	Inf	0.43659	Inf	0.28559
tok	FBgn0004885	Inf	0.43659	Inf	0.28559
trio	FBgn0015758	Inf	0.43659	Inf	0.28559
CG9498	FBgn0031801	Inf	0.43659	2.6364	0.36138
CG5840	FBgn0038516	Inf	0.43659	2.58912	0.37054
CG5555	FBgn0038686	Inf	0.43659	1.74735	0.51897
mst	FBgn0001566	Inf	0.43659	2.58804	0.5482
RpII215	FBgn0001616	Inf	0.43659	2.23578	0.6007
CG9205	FBgn0035181	Inf	0.43659	1.75073	0.62916
ari-1	FBgn0014203	Inf	0.43659	1.48587	0.78845
Cul-5	FBgn0039632	Inf	0.43659	1.45482	0.79945
bou	FBgn0029927	Inf	0.43659	1.20679	0.89942
CG2254	FBgn0029994	Inf	0.43659	1.18158	0.91084
CG8336	FBgn0036020	Inf	0.43659	1.16039	0.92061
HDAC6	FBgn0026428	Inf	0.43659	1.16039	0.92061

hyd	FBgn0002317	Inf	0.43659	1.1383	0.93098
RpII15	FBgn0004855	Inf	0.43659	1.1383	0.93098
MED19	FBgn0036761	Inf	0.43659	1.11789	0.94073
CG14299	FBgn0038651	Inf	0.43659	1.10256	0.94815
CG8549	FBgn0035714	Inf	0.43659	1.10256	0.94815
CG1291	FBgn0035401	1.6571	0.44137	2.00933	0.08206
CG33214	FBgn0037088	1.9532	0.44186	Inf	0.28559
Prm	FBgn0003149	1.1489	0.45077	3.16159	0.00022
CG9009	FBgn0027601	1.2924	0.45607	1.35136	0.72896
CG15293	FBgn0027904	2.7633	0.45963	1.88544	0.37397
CG5112	FBgn0039341	1.8934	0.46348	1.04372	0.96982
CG7011	FBgn0036489	1.2443	0.46911	1.09103	0.86756
TpnC73F	FBgn0010424	1.219	0.47748	5.4633	0.00598
CG6782	FBgn0037912	1.4014	0.47801	1.18158	0.91084
Pros25	FBgn0010405	1.0983	0.48274	1.50463	0.01363
alph	FBgn0039672	1.3869	0.4829	4.95629	0.04608
Noa36	FBgn0026400	2.5846	0.48549	Inf	0.28559
CG17294	FBgn0032032	1.8366	0.48672	Inf	0.28559
snRNP70K	FBgn0003458	1.8177	0.48965	Inf	0.28559
SmD3	FBgn0023167	1.2871	0.4939	1.89743	0.31688
CkIIalpha	FBgn0000258	1.1081	0.49509	1.13836	0.44461
CG9906	FBgn0030755	1.1369	0.496	1.30268	0.50864
CG3887	FBgn0031670	1.2873	0.49621	4.00925	0.02097
Lsp1alpha	FBgn0002562	1.0867	0.50147	3.55609	1.44E-05
nrv1	FBgn0015776	2.5722	0.50192	Inf	0.21111
Rab39	FBgn0029959	1.1191	0.50654	2.23236	0.01598
Rel	FBgn0011469	1.6742	0.51015	Inf	0.28559
CG3338	FBgn0031598	1.5809	0.5265	Inf	0.28559
CG3999	FBgn0037801	1.3911	0.53115	6.33734	0.01129
CG32441	FBgn0037103	1.2094	0.53431	2.69266	0.35097
c11.1	FBgn0030123	2.292	0.53616	3.48778	0.46529
Pp2A-29B	FBgn0005776	1.0388	0.5402	1.52435	0.08085
cin	FBgn0000316	1.4174	0.54865	1.20679	0.89942
CG5690	FBgn0027777	1.6873	0.54946	2.32078	0.58653
CG12203	FBgn0031021	1.1013	0.54969	1.20791	0.38371
DhpD	FBgn0037219	1.1644	0.55308	2.88709	0.10765
CG6852	FBgn0036820	1.2067	0.55532	1.29202	0.3401
Pgi	FBgn0003074	1.0346	0.55693	1.7871	0.00366
Ost48	FBgn0014868	1.0236	0.55775	1.81796	0.00196
Sgs7	FBgn0003377	1.0922	0.56119	1.27912	0.31747
CG10992	FBgn0026294	1.0528	0.5613	1.6281	0.01628
atms	FBgn0010750	1.7902	0.56402	2.32519	0.58582

ppl	FBgn0013569	1.1377	0.56441	1.65608	0.23004
jdp	FBgn0027654	1.6881	0.56534	2.6364	0.36138
Gbeta13F	FBgn0001105	1.155	0.56975	1.68923	0.02951
CG1924	FBgn0030377	1.1236	0.57397	1.84856	0.12804
scf	FBgn0025546	1.0905	0.57661	1.96266	0.10969
CG5389	FBgn0036568	1.0749	0.58157	1.23131	0.40916
Ide	FBgn0001247	1.6604	0.58309	1.1383	0.93098
Ptpa	FBgn0016698	1.6674	0.59304	Inf	0.28559
sals	FBgn0037904	1.5938	0.59643	Inf	0.00039
fray	FBgn0010922	1.1143	0.5977	1.86887	0.42206
CG8209	FBgn0035830	1.049	0.60105	1.18329	0.65972
CG14812	FBgn0026090	1.2858	0.6119	Inf	0.13422
CG6638	FBgn0035911	1.1982	0.61466	2.91312	0.13973
RPA2	FBgn0032906	1.5852	0.61719	1.18158	0.91084
Stat92E	FBgn0010885	1.7859	0.61805	Inf	0.07809
GstD9	FBgn0038020	1.0809	0.62764	1.16405	0.3507
Tm2	FBgn0002442	1.0935	0.6408	1.87218	0.09845
PDCD-5	FBgn0036580	1.1439	0.64435	4.55322	0.41387
Prx5037	FBgn0038519	1.0849	0.6444	1.42606	0.42422
Rab35	FBgn0031090	1.0729	0.64441	2.30766	0.00868
chrw	FBgn0015372	1.0729	0.64441	2.23236	0.01598
Rab3	FBgn0005586	1.0729	0.64441	2.23236	0.01598
Rab30	FBgn0031882	1.0729	0.64441	2.23236	0.01598
Rab-RP3	FBgn0015793	1.0729	0.64441	2.23236	0.01598
RabX4	FBgn0039231	1.0729	0.64441	2.23236	0.01598
Zasp66	FBgn0035917	1.0955	0.65073	2.39817	0.00214
Pp1-13C	FBgn0003132	1.1455	0.66104	1.65316	0.31616
CG7083	FBgn0035877	1.6568	0.66108	Inf	0.06245
osa	FBgn0003013	1.6568	0.66108	Inf	0.28559
HP1c	FBgn0039019	1.6568	0.66108	1.71345	0.53275
Tango13	FBgn0030497	1.6568	0.66108	1.20679	0.89942
Gpdh	FBgn0001128	1.0271	0.66143	1.22577	0.00242
Fmr1	FBgn0028734	1.0982	0.66179	1.77584	0.22359
poe	FBgn0010161	1.6846	0.66522	4.20724	0.07881
CG2082	FBgn0027608	1.6417	0.66797	Inf	0.28559
Mms19	FBgn0037301	1.6395	0.67354	1.58529	0.30434
CalpB	FBgn0025866	1.2418	0.67495	9.38145	0.02152
smt3	FBgn0010577	1.0363	0.67762	1.19984	0.29428
PyK	FBgn0003178	1.033	0.67766	1.25868	0.07243
CG7280	FBgn0030966	1.6119	0.67818	2.28775	0.29937
flw	FBgn0000711	1.1091	0.68745	3.48249	0.19599
CG4552	FBgn0031304	1.1739	0.6888	1.14251	0.78953

CG11089	FBgn0039241	1.0572	0.69222	1.44655	0.20019
p16-ARC	FBgn0031437	1.0328	0.69278	2.61322	0.23731
BM-40-SPARC	FBgn0026562	1.2856	0.69541	2.65363	0.38966
CG2246	FBgn0039790	1.5613	0.69879	Inf	0.28559
CG9027	FBgn0033631	1.6211	0.69987	Inf	0.00299
Ykt6	FBgn0026664	1.563	0.7059	2.03535	0.34269
Mlc2	FBgn0002773	1.076	0.71244	3.26998	0.00681
Prp19	FBgn0013969	1.5126	0.71584	7.14567	0.02349
CG5110	FBgn0032642	1.2641	0.71693	2.27961	0.5554
Cdc42	FBgn0010341	1.1649	0.71917	2.29734	0.03808
Mlp84B	FBgn0011644	1.121	0.72176	1.80724	0.10688
Prx6005	FBgn0031479	1.1079	0.72349	1.70746	0.71858
Mtp	FBgn0032904	1.1524	0.73195	8.56606	0.02981
Ubc-E2H	FBgn0029996	1.2461	0.74068	1.11789	0.94073
RpL6	FBgn0039857	1.0583	0.74224	1.80916	0.00766
pgant6	FBgn0035375	1.1947	0.74699	18.3772	0.00792
Ras85D	FBgn0003205	1.178	0.74989	Inf	0.06245
RanGap	FBgn0003346	1.0988	0.76567	1.36382	0.35882
krz	FBgn0028053	1.1146	0.76724	2.32251	0.40114
Rala	FBgn0015286	1.2188	0.77021	Inf	0.28559
bur	FBgn0000239	1.1247	0.77168	1.32895	0.2786
GlyP	FBgn0004507	1.0222	0.79302	2.08149	0.00041
CG3408	FBgn0036008	1.3393	0.79526	Inf	0.28559
Lsp1beta	FBgn0002563	1.0281	0.79551	2.66077	0.00027
alphaTub85E	FBgn0003886	1.0142	0.80064	1.05373	0.32516
l(2)06496	FBgn0010622	1.0977	0.80127	1.18876	0.58995
TpnC47D	FBgn0010423	1.0611	0.80623	3.16503	0.00113
CG10463	FBgn0032819	1.1761	0.80733	Inf	0.28559
CG31048	FBgn0039605	1.1145	0.80886	Inf	0.13471
CG5958	FBgn0031913	1.1363	0.8159	6.78025	0.00656
Rho1	FBgn0014020	1.0487	0.81819	1.23946	0.12146
CaMKII	FBgn0004624	1.2853	0.82388	5.9255	0.07193
CG14476	FBgn0027588	1.0179	0.82426	1.21112	0.37937
CG3523	FBgn0027571	1.0527	0.82694	1.41064	0.02044
Mlc1	FBgn0002772	1.0454	0.83119	4.86871	0.00172
Tim8	FBgn0027359	1.0456	0.83128	1.80658	0.30024
Dhc64C	FBgn0001059	1.0402	0.8313	2.39031	0.05565
wkd	FBgn0037917	1.2666	0.83415	1.16259	0.91959
CG3590	FBgn0038467	1.0489	0.83785	1.51951	0.13445
CG5854	FBgn0039130	1.1159	0.83873	1.00888	0.99141
l(1)G0289	FBgn0028331	1.1401	0.8399	2.69266	0.35097
MSBP	FBgn0030703	1.039	0.85028	2.5392	0.02911

l(1)G0230	FBgn0028342	1.0244	0.85426	1.07405	0.57215
bif	FBgn0014133	1.2276	0.86013	1.74471	0.28895
CG7857	FBgn0026738	1.126	0.86211	1.08302	0.8801
CREG	FBgn0025456	1.0206	0.86428	2.05017	0.01161
CG10418	FBgn0036277	1.0519	0.86805	1.5826	0.1879
CG17471	FBgn0039924	1.0855	0.8684	3.77471	0.07022
CG11148	FBgn0039936	1.1071	0.87941	1.09866	0.89959
Syx5	FBgn0001996	1.1462	0.8863	Inf	0.00192
Top1	FBgn0004924	1.0146	0.89292	1.40659	0.59537
CG16817	FBgn0037728	1.0255	0.89535	1.71603	0.01429
gbb	FBgn0004788	1.0833	0.89617	1.1383	0.93098
CG14542	FBgn0039402	1.0343	0.89785	1.13803	0.75342
Ts	FBgn0024920	1.1115	0.90676	1.20679	0.89942
Rbcn-3B	FBgn0023510	1.0797	0.90756	1.45621	0.38395
hoip	FBgn0015393	1.015	0.9097	1.06942	0.72383
Tm1	FBgn0003721	1.0167	0.91195	1.36917	0.10819
CG13506	FBgn0034723	1.1702	0.92031	2.31988	0.42792
xl6	FBgn0028554	1.0986	0.92363	Inf	0.28559
CG6983	FBgn0035896	1.1082	0.92735	Inf	0.28559
Glycogenin	FBgn0034603	1.0358	0.92824	3.76238	6.37E-05
ade2	FBgn0000052	1.033	0.92861	3.69402	0.13693
CG3702	FBgn0031590	1.1492	0.92916	Inf	0.06533
Ho	FBgn0037933	1.1492	0.92916	Inf	0.06533
CG9391	FBgn0037063	1.0374	0.93035	1.36215	0.5321
CG9853	FBgn0037243	1.0538	0.93222	Inf	0.28559
CG15168	FBgn0032732	1.0799	0.93515	Inf	0.28559
CanB2	FBgn0015614	1.0392	0.94141	4.02844	0.03759
CG1885	FBgn0030066	1.0302	0.94565	1.3505	0.68373
betaTub85D	FBgn0003889	1.0078	0.94616	1.00821	0.92301
CG9286	FBgn0038183	1.0661	0.94703	1.1383	0.93098
CG5167	FBgn0038038	1.0155	0.94957	3.8204	0.01956
CG30115	FBgn0034358	1.0416	0.95051	1.3501	0.69451
CG17184	FBgn0037884	1.0565	0.95615	Inf	0.28559
l(3)04053	FBgn0010830	1.0325	0.95862	Inf	0.28559
Gmap	FBgn0027287	1.011	0.95899	1.0497	0.89982
Atg8a	FBgn0052672	1.008	0.97159	1.19612	0.84691
skap	FBgn0037643	1.0033	0.98031	1.03356	0.90605
CG18811	FBgn0042134	1.0015	0.9941	1.07909	0.86441

References

Abrams J.M. (1999) An emerging blueprint for apoptosis in *Drosophila*. Trends Cell Biol. 9:435-440.

Adams J. (2004) The development of proteasome inhibitors as anticancer drugs. Cancer Cell 5:417-21.

Adrain C., Creagh E.M., Cullen S.P., Martin S.J. (2004) Caspase-dependent inactivation of proteasome function during programmed cell death in Drosophila and man. J. Biol. Chem. 279:36923-30.

Aebersold R., Mann M. (2003) Mass spectrometry-based proteomics. Nature 422:198-207.

Akdemir F., Farkas R., Chen P., Juhasz G., Medved'ova L., Sass M., Wang L., Wang X., Chittaranjan S., Gorski S.M., Rodriguez A., Abrams J.M. (2006) Autophagy occurs upstream or parallel to the apoptosome during histolytic cell death. Development 133:1457-1465.

Andrade R.M., Wessendarp M., Gubbels M.J., Striepen B., Subauste C.S. (2006) CD40 induces macrophage anti-Toxoplasma gondii activity by triggering autophagy-dependent fusion of pathogen-containing vacuoles and lysosomes. J. Clin. Invest. 116:2366-77.

Aravind L., Dixit V.M., Koonin E.V. (2001) Apoptotic molecular machinery: vastly increased complexity in vertebrates revealed by genome comparisons. Science 291:1279-1284.

Arsham A.M., Neufeld T.P. (2006) Thinking globally and acting locally with TOR. Curr. Opin. Cell Biol. 18:589-97.

Awasaki T., Tatsumi R., Takahashi K., Arai K., Nakanishi Y., Ueda R., Ito K. (2006) Essential role of the apoptotic cell engulfment genes draper and ced-6 in programmed axon pruning during Drosophila metamorphosis. Neuron 50:855-67.

Axe E.L., Walker S.A., Manifava M., Chandra P., Roderick H.L., Habermann A., Griffiths G., Ktistakis N.T. (2008) Autophagosome formation from membrane compartments enriched in phosphatidylinositol 3-phosphate and dynamically connected to the endoplasmic reticulum. J. Cell Biol. 182:685-701.

Backer J.M. (2008) The regulation and function of Class III PI3Ks: novel roles for Vps34. Biochem J 410:1-17.

Baehrecke E.H. (2000) Steroid regulation of programmed cell death during *Drosophila* development. Cell Death & Differ. 7:1057-1062.

Baehrecke E.H. (2002) How death shapes life during development. Nature Reviews Mol. Cell Biol. 3:779-787.

Baehrecke E.H. (2003) Autophagic programmed cell death in *Drosophila*. Cell Death & Differ. 10:940-945.

Barrow A.D., Trowsdale J. (2006) You say ITAM and I say ITIM, let's call the whole thing off: the ambiguity of immunoreceptor signalling. Eur. J. Immunol. 36:1646-53.
Belote J.M., Fortier E. (2002) Targeted expression of dominant negative proteasome mutants in Drosophila melanogaster. Genesis 34:80-2.
Bence N.F., Bennett E.J., Kopito R.R. (2005) Application and analysis of the GFPu family of ubiquitin-proteasome system reporters. Methods Enzymol. 399:481-90.
Bennett E.J., Harper J.W. (2008) DNA damage: ubiquitin marks the spot. Nat Struct Mol Biol 15:20-2.
Bernards A., Hariharan I.K. (2001) Of flies and men--studying human disease in *Drosophila*. Curr. Opin. Genet. Dev. 11:274-278.
Berry D.L., Baehrecke E.H. (2007) Growth arrest and autophagy are required for salivary gland cell degradation in *Drosophila*. Cell 131:1137-1148.
Bjorkoy G., Lamark T., Brech A., Outzen H., Perander M., Overvatn A., Stenmark H., Johansen T. (2005) p62/SQSTM1 forms protein aggregates degraded by autophagy and has a protective effect on huntingtin-induced cell death. J. Cell Biol. 171:603-14.
Blommaart E.F., Luiken J.J., Blommaart P.J., van Woerkom G.M., Meijer A.J. (1995) Phosphorylation of ribosomal protein S6 is inhibitory for autophagy in isolated rat hepatocytes. J. Biol. Chem. 270:2320-6.
Bosu D.R., Kipreos E.T. (2008) Cullin-RING ubiquitin ligases: global regulation and activation cycles. Cell Div 3:7.
Brand A.H., Perrimon N. (1993) Targeted gene expression as a means of altering cell fates and generating dominant phenotypes. Development 118:401-415.
Busch S., Schwier E.U., Nahlik K., Bayram O., Helmstaedt K., Draht O.W., Krappmann S., Valerius O., Lipscomb W.N., Braus G.H. (2007) An eight-subunit COP9 signalosome with an intact JAMM motif is required for fungal fruit body formation. Proc Natl Acad Sci U S A 104:8089-94.
Byfield M.P., Murray J.T., Backer J.M. (2005) hVps34 is a nutrient-regulated lipid kinase required for activation of p70 S6 kinase. J. Biol. Chem 280:33076-82.
Cadwell K., Liu J.Y., Brown S.L., Miyoshi H., Loh J., Lennerz J.K., Kishi C., Kc W., Carrero J.A., Hunt S., Stone C.D., Brunt E.M., Xavier R.J., Sleckman B.P., Li E., Mizushima N., Stappenbeck T.S., Virgin H.W.t. (2008) A key role for autophagy and the autophagy gene Atg16l1 in mouse and human intestinal Paneth cells. Nature 456:259-63.
Cecconi F., Levine B. (2008) The role of autophagy in mammalian development: cell makeover rather than cell death. Dev. Cell 15:344-57.
Chamovitz D.A., Wei N., Osterlund M.T., von Arnim A.G., Staub J.M., Matsui M., Deng X.W. (1996) The COP9 complex, a novel multisubunit nuclear regulator involved in light control of a plant developmental switch. Cell 86:115-21.
Chan J., Tian Y., Tanaka K.E., Tsang M.S., Yu K., Salgame P., Carroll D., Kress Y., Teitelbaum R., Bloom B.R. (1996) Effects of protein calorie malnutrition on tuberculosis in mice. Proc. Natl. Acad. Sci. U S A 93:14857-61.
Chandra R.K. (1996) Nutrition, immunity and infection: from basic knowledge of dietary manipulation of immune responses to practical application of

ameliorating suffering and improving survival. Proc. Natl. Acad. Sci. U S A 93:14304-7.
Chen J., Balgley B.M., DeVoe D.L., Lee C.S. (2003) Capillary isoelectric focusing-based multidimensional concentration/separation platform for proteome analysis. Anal. Chem. 75:3145-3152.
Chen N., Karantza-Wadsworth V. (2009) Role and regulation of autophagy in cancer. Biochim Biophys Acta 1793:1516-23.
Chen P., Nordstrom W., Gish B., Abrams J.M. (1996) *grim*, a novel cell death gene in *Drosophila*. Genes & Dev. 10:1773-1782.
Chen P., Rodriguez A., Erskine R., Thach T., Abrams J.M. (1998) *Dredd*, a novel effector of the apoptosis activators *Reaper*, *Grim*, and *Hid* in *Drosophila*. Dev. Biol. 201:202-216.
Cheong H., Yorimitsu T., Reggiori F., Legakis J.E., Wang C.W., Klionsky D.J. (2005) Atg17 regulates the magnitude of the autophagic response. Mol Biol Cell 16:3438-53.
Christich A., Kauppila S., Chen P., Sogame N., Ho S.I., Abrams J.M. (2002) Damage-responsive *Drosophila* gene *sickle* encodes a novel IAP binding protein similar to but distinct from *reaper, grim*, and *hid*. Curr. Biol. 12:137-140.
Ciechanover A. (2005) Proteolysis: from the lysosome to ubiquitin and the proteasome. Nat Rev Mol Cell Biol 6:79-87.
Ciechanover A., Heller H., Katz-Etzion R., Hershko A. (1981) Activation of the heat-stable polypeptide of the ATP-dependent proteolytic system. Proc Natl Acad Sci U S A 78:761-5.
Ciechanover A., Elias S., Heller H., Ferber S., Hershko A. (1980) Characterization of the heat-stable polypeptide of the ATP-dependent proteolytic system from reticulocytes. J. Biol. Chem. 255:7525-8.
Clarke P.G.H. (1990) Developmental cell death: morphological diversity and multiple mechanisms. Anat. Embryol. 181:195-213.
Colombani J., Bianchini L., Layalle S., Pondeville E., Dauphin-Villemant C., Antoniewski C., Carre C., Noselli S., Leopold P. (2005) Antagonistic actions of ecdysone and insulins determine final size in Drosophila. Science 310:667-670.
Conlon I., Raff M. (1999) Size control in animal development. Cell 96:235-244.
Conradt B., Horvitz H.R. (1998) The C. elegans protein EGL-1 is required for programmed cell death and interacts with the Bcl-2-like protein CED-9. Cell 93:519-529.
Cope G.A., Suh G.S., Aravind L., Schwarz S.E., Zipursky S.L., Koonin E.V., Deshaies R.J. (2002) Role of predicted metalloprotease motif of Jab1/Csn5 in cleavage of Nedd8 from Cul1. Science 298:608-11.
Cronin S.J., Nehme N.T., Limmer S., Liegeois S., Pospisilik J.A., Schramek D., Leibbrandt A., Simoes Rde M., Gruber S., Puc U., Ebersberger I., Zoranovic T., Neely G.G., von Haeseler A., Ferrandon D., Penninger J.M. (2009) Genome-wide RNAi screen identifies genes involved in intestinal pathogenic bacterial infection. Science 325:340-3.
Cryns V., Yuan J. (1998) Proteases to die for. Genes & Dev. 12:1551-1570.

Cuervo A.M. (2008) Autophagy and aging: keeping that old broom working. Trends. Genet. 24:604-12.
Cuervo A.M., Dice J.F. (2000) Age-related decline in chaperone-mediated autophagy. J. Biol. Chem. 275:31505-13.
Daffre S., Kylsten P., Samakovlis C., Hultmark D. (1994) The lysozyme locus in Drosophila melanogaster: an expanded gene family adapted for expression in the digestive tract. Mol Gen Genet 242:152-62.
Danial N.N., Korsmeyer S.J. (2004) Cell death: critical control points. Cell 116:205-19.
Dantuma N.P., Lindsten K., Glas R., Jellne M., Masucci M.G. (2000) Short-lived green fluorescent proteins for quantifying ubiquitin/proteasome-dependent proteolysis in living cells. Nat. Biotechnol. 18:538-43.
Dawson S.P., Arnold J.E., Mayer N.J., Reynolds S.E., Billett M.A., Gordon C., Colleaux L., Kloetzel P.M., Tanaka K., Mayer R.J. (1995) Developmental changes of the 26 S proteasome in abdominal intersegmental muscles of Manduca sexta during programmed cell death. J. Biol. Chem. 270:1850-8.
Debnath J., Mills K.R., Collins N.L., Reginato M.J., Muthuswamy S.K., Brugge J.S. (2002) The role of apoptosis in creating and maintaining luminal space within normal and oncogene-expressing mammary acini. Cell 111:29-40.
del Peso L., Gonzalez V.M., Nunez G. (1998) Caenorhabditis elegans EGL-1 disrupts the interaction of CED-9 with CED-4 and promotes CED-3 activation. J. Biol. Chem. 273:33495-500.
Denton D., Shravage B., Simin R., Mills K., Berry D.L., Baehrecke E.H., Kumar S. (2009) Autophagy, not apoptosis, is essential for midgut cell death in Drosophila. Curr Biol 19:1741-6.
Deveraux Q., Ustrell V., Pickart C., Rechsteiner M. (1994) A 26 S protease subunit that binds ubiquitin conjugates. J. Biol. Chem. 269:7059-61.
Ditzel M., Wilson R., Tenev T., Zachariou A., Paul A., Deas E., Meier P. (2003) Degradation of DIAP1 by the N-end rule pathway is essential for regulating apoptosis. Nat. Cell Biol. 5:467-73.
Domon B., Aebersold R. (2006) Mass spectrometry and protein analysis. Science 312:212-7.
Dorstyn L., Read S.H., Quinn L.M., Richardson H., Kumar S. (1999a) DECAY, a novel *Drosophila* caspase related to mammalian caspase-3 and caspase-7. J. Biol. Chem. 274:30778-30783.
Dorstyn L., Colussi P.A., Quinn L.M., Richardson H., Kumar S. (1999b) DRONC, an ecdysone-inducible *Drosophila* caspase. Proc. Natl. Acad. Sci. USA 96:4307-4312.
Drexler H.C. (1997) Activation of the cell death program by inhibition of proteasome function. Proc. Natl. Acad. Sci. U. S. A. 94:855-60.
Drexler H.C. (1998) Programmed cell death and the proteasome. Apoptosis 3:1-7. DOI: 172964 [pii].
Dunn W.A.J. (1990) Studies on the mechanisms of autophagy: formation of the autophagic vacuole. J. Cell Biol. 110:1923-1933.

Dutta S., Baehrecke E.H. (2008) Warts Is Required for PI3K-Regulated Growth Arrest, Autophagy, and Autophagic Cell Death in Drosophila. Curr. Biol. 18:1466-1475.
Edgar B.A. (2006) From cell structure to transcription: Hippo forges a new path. Cell 124:267-73.
Ellis R.E., Horvitz R.H. (1986) Genetic control of programmed cell death in the nematode C. elegans. Cell 44:817-829.
Ellis R.E., Jacobson D., Horvitz R.H. (1991) Genes required for the engulfment of cell corpses during programmed cell death in *Caenorhabditis elegans*. Genetics 129:79-94.
Faggioni R., Moser A., Feingold K.R., Grunfeld C. (2000) Reduced leptin levels in starvation increase susceptibility to endotoxic shock. Am. J. Pathol. 156:1781-7.
Fang X., Balgley B.M., Lee C.S. (2009) Recent advances in capillary electrophoresis-based proteomic techniques for biomarker discovery. Electrophoresis 30:3998-4007.
Ferrandon D., Imler J.L., Hetru C., Hoffmann J.A. (2007) The Drosophila systemic immune response: sensing and signalling during bacterial and fungal infections. Nat. Rev. Immunol. 7:862-74.
Filimonenko M., Stuffers S., Raiborg C., Yamamoto A., Malerod L., Fisher E.M., Isaacs A., Brech A., Stenmark H., Simonsen A. (2007) Functional multivesicular bodies are required for autophagic clearance of protein aggregates associated with neurodegenerative disease. J. Cell Biol. 179:485-500.
Fimia G.M., Stoykova A., Romagnoli A., Giunta L., Di Bartolomeo S., Nardacci R., Corazzari M., Fuoco C., Ucar A., Schwartz P., Gruss P., Piacentini M., Chowdhury K., Cecconi F. (2007) Ambra1 regulates autophagy and development of the nervous system. Nature 447:1121-5.
Finley K.D., Edeen P.T., Cumming R.C., Mardahl-Dumesnil M.D., Taylor B.J., Rodriguez M.H., Hwang C.E., Benedetti M., McKeown M. (2003) blue cheese mutations define a novel, conserved gene involved in progressive neural degeneration. J. Neurosci. 23:1254-64.
Fodor S., Jakus Z., Mocsai A. (2006) ITAM-based signaling beyond the adaptive immune response. Immunol. Lett. 104:29-37.
Franc N.C., Heitzler P., Ezekowitz A.B., White K. (1999) Requirement for Croquemort in phagocytosis of apoptotic cells in *Drosophila*. Science 284:1991-1994.
Fraser A.G., Evan G.I. (1997) Identification of a Drosophila melanogaster ICE/CED-3-relatedprotease, drICE. EMBO J 16:2805-2813.
Freeman M.R., Delrow J., Kim J., ., Johnson E., Doe C.Q. (2003) Unwrapping glial biology: Gcm target genes regulating glial development, diversification, and function. Neuron 38:567-580.
Gao M.X., Liao E.H., Yu B., Wang Y., Zhen M., Derry W.B. (2008) The SCF FSN-1 ubiquitin ligase controls germline apoptosis through CEP-1/p53 in C. elegans. Cell Death Differ 15:1054-62.

Geer L.Y., Markey S.P., Kowalak J.A., Wagner L., Xu M., Maynard D.M., Yang X., Shi W., Bryant S.H. (2004) Open mass spectrometry search algorithm. J Proteome Res 3:958-64.

Goldknopf I.L., Busch H. (1977) Isopeptide linkage between nonhistone and histone 2A polypeptides of chromosomal conjugate-protein A24. Proc. Natl. Acad. Sci. U. S. A. 74:864-8.

Goldstein G., Scheid M., Hammerling U., Schlesinger D.H., Niall H.D., Boyse E.A. (1975) Isolation of a polypeptide that has lymphocyte-differentiating properties and is probably represented universally in living cells. Proc. Natl. Acad. Sci. U. S. A. 72:11-5.

Grether M.E., Abrams J.M., Agapite J., White K., Steller H. (1995) The *head involution defective* gene of *Drosophila melanogaster* functions in programmed cell death. Genes & Dev. 9:1694-1708.

Gu H., Chen X., Gao G., Dong H. (2008) Caspase-2 functions upstream of mitochondria in endoplasmic reticulum stress-induced apoptosis by bortezomib in human myeloma cells. Mol Cancer Ther 7:2298-307.

Gumienny T.L., Brugnera E., Tosello-Trampont A.C., Kinchen J.M., Haney L.B., Nishiwaki K., Walk S.F., Nemergut M.E., Macara I.G., Francis R., Schedl T., Qin Y., Van Aelst L., Hengartner M.O., Ravichandran K.S. (2001) CED-12/ELMO, a novel member of the CrkII/Dock180/Rac pathway, is required for phagocytosis and cell migration. Cell 107:27-41.

Gusmaroli G., Figueroa P., Serino G., Deng X.W. (2007) Role of the MPN subunits in COP9 signalosome assembly and activity, and their regulatory interaction with Arabidopsis Cullin3-based E3 ligases. Plant Cell 19:564-81.

Gutierrez M.G., Master S.S., Singh S.B., Taylor G.A., Colombo M.I., Deretic V. (2004) Autophagy is a defense mechanism inhibiting BCG and Mycobacterium tuberculosis survival in infected macrophages. Cell 119:753-66.

Haas A.L., Rose I.A. (1982) The mechanism of ubiquitin activating enzyme. A kinetic and equilibrium analysis. J Biol Chem 257:10329-37.

Hadari T., Warms J.V., Rose I.A., Hershko A. (1992) A ubiquitin C-terminal isopeptidase that acts on polyubiquitin chains. Role in protein degradation. J. Biol. Chem. 267:719-27.

Haglund K., Dikic I. (2005) Ubiquitylation and cell signaling. EMBO J 24:3353-9.

Hara T., Takamura A., Kishi C., Iemura S., Natsume T., Guan J.L., Mizushima N. (2008) FIP200, a ULK-interacting protein, is required for autophagosome formation in mammalian cells. J Cell Biol 181:497-510.

Hara T., Nakamura K., Matsui M., Yamamoto A., Nakahara Y., Suzuki-Migishima R., Yokoyama M., Mishima K., Saito I., Okano H., Mizushima N. (2006) Suppression of basal autophagy in neural cells causes neurodegenerative disease in mice. Nature 441:885-889.

Harding T.M., Morano K.A., Scott S.V., Klionsky D.J. (1995) Isolation and characterization of yeast mutants in the cytoplasm to vacuole protein targeting pathway. J. Cell Bio. 131:591-602.

Harding T.M., Hefner-Gravink A., Thumm M., Klionsky D.J. (1996) Genetic and phenotypic overlap between autophagy and the cytoplasm to vacuole protein. J. Biol. Chem. 271:17621-17624.
Hariharan I.K., Haber D.A. (2003) Yeast, flies, worms, and fish in the study of human disease. N. Engl. J. Med. 348:2457-63.
Haupt Y., Maya R., Kazaz A., Oren M. (1997) Mdm2 promotes the rapid degradation of p53. Nature 387:296-9.
Hay B.A., Wolff T., Rubin G.M. (1994) Expression of baculovirus P35 prevents cell death in *Drosophila*. Development 120:2121-2129.
Hay B.A., Wassarman D.A., Rubin G.M. (1995) *Drosophila* homologs of baculovirus inhibitor of apoptosis proteins function to block cell death. Cell 83:1253-1262.
Hay B.A., Huh J.R., Guo M. (2004) The genetics of cell death: approaches, insights and opportunities in Drosophila. Nat. Rev. Genet. 5:911-922.
Henderson C.J., Aleo E., Fontanini A., Maestro R., Paroni G., Brancolini C. (2005) Caspase activation and apoptosis in response to proteasome inhibitors. Cell Death Differ. 12:1240-54.
Hengartner M.O., Horvitz H.R. (1994) C. elegans cell survival gene *ced-9* encodes a functional homolog of the mammalian proto-oncogene *bcl-2*. Cell 76:665-676.
Hershko A., Ciechanover A. (1998) The ubiquitin system. Annu. Rev. Biochem. 67:425-79.
Hershko A., Heller H., Elias S., Ciechanover A. (1983) Components of ubiquitin-protein ligase system. Resolution, affinity purification, and role in protein breakdown. J Biol Chem 258:8206-14.
Hershko A., Heller H., Eytan E., Reiss Y. (1986) The protein substrate binding site of the ubiquitin-protein ligase system. J Biol Chem 261:11992-9.
Hershko A., Ciechanover A., Heller H., Haas A.L., Rose I.A. (1980) Proposed role of ATP in protein breakdown: conjugation of protein with multiple chains of the polypeptide of ATP-dependent proteolysis. Proc. Natl. Acad. Sci. U. S. A. 77:1783-6.
Hetfeld B.K., Helfrich A., Kapelari B., Scheel H., Hofmann K., Guterman A., Glickman M., Schade R., Kloetzel P.M., Dubiel W. (2005) The zinc finger of the CSN-associated deubiquitinating enzyme USP15 is essential to rescue the E3 ligase Rbx1. Curr Biol 15:1217-21.
Hochberg Y., Benjamini Y. (1990) More powerful procedures for multiple significance testing. Stat Med 9:811-8.
Hoeller D., Dikic I. (2009) Targeting the ubiquitin system in cancer therapy. Nature 458:438-44.
Hoopfer E.D., McLaughlin T., Watts R.J., Schuldiner O., O'Leary D.D., Luo L. (2006) Wlds protection distinguishes axon degeneration following injury from naturally occurring developmental pruning. Neuron 50:883-95.
Hotton S.K., Callis J. (2008) Regulation of cullin RING ligases. Annu Rev Plant Biol 59:467-89.
Hou Y.C., Chittaranjan S., Barbosa S.G., McCall K., Gorski S.M. (2008) Effector caspase Dcp-1 and IAP protein Bruce regulate starvation-induced autophagy during Drosophila melanogaster oogenesis. J. Cell Biol. 182:1127-39.

Hough R., Pratt G., Rechsteiner M. (1986) Ubiquitin-lysozyme conjugates. Identification and characterization of an ATP-dependent protease from rabbit reticulocyte lysates. J. Biol. Chem. 261:2400-8.
Hoyer-Hansen M., Bastholm L., Szyniarowski P., Campanella M., Szabadkai G., Farkas T., Bianchi K., Fehrenbacher N., Elling F., Rizzuto R., Mathiasen I.S., Jaattela M. (2007) Control of macroautophagy by calcium, calmodulin-dependent kinase kinase-beta, and Bcl-2. Mol. Cell 25:193-205.
Huang J., Klionsky D.J. (2007) Autophagy and human disease. Cell Cycle 6:1837-49.
Huang W.P., Scott S.V., Kim J., Klionsky D.J. (2000) The itinerary of a vesicle component, Aut7p/Cvt5p, terminates in the yeast vacuole via the autophagy/Cvt pathways. J. Biol. Chem. 275:5845-51.
Huang X., Hetfeld B.K., Seifert U., Kahne T., Kloetzel P.M., Naumann M., Bech-Otschir D., Dubiel W. (2005) Consequences of COP9 signalosome and 26S proteasome interaction. FEBS J 272:3909-17.
Ichimura Y., Kirisako T., Takao T., Satomi Y., Shimonishi Y., Ishihara N., Mizushima N., Tanida I., Kominami E., Ohsumi M., Noda T., Ohsumi Y. (2000) A ubiquitin-like system mediates protein lipidation. Nature 408:488-492.
Inohara N., Koseki T., Hu Y., Chen S., Nunez G. (1997) CLARP, a death effector domain-containing protein interacts with caspase-8 and regulates apoptosis. Proc Natl Acad Sci U S A 94:10717-10722.
Itakura E., Kishi C., Inoue K., Mizushima N. (2008) Beclin 1 Forms Two Distinct Phosphatidylinositol 3-Kinase Complexes with Mammalian Atg14 and UVRAG. Mol. Biol. Cell 12:5360-72.
Iwata J., Ezaki J., Komatsu M., Yokota S., Ueno T., Tanida I., Chiba T., Tanaka K., Kominami E. (2006) Excess peroxisomes are degraded by autophagic machinery in mammals. J. Biol. Chem. 281:4035-41.
Jiang C., Baehrecke E.H., Thummel C.S. (1997) Steroid regulated programmed cell death during *Drosophila* metamorphosis. Development 124:4673-4683.
Jones M.E., Haire M.F., Kloetzel P.M., Mykles D.L., Schwartz L.M. (1995) Changes in the structure and function of the multicatalytic proteinase (proteasome) during programmed cell death in the intersegmental muscles of the hawkmoth, Manduca sexta. Dev. Biol. 169:436-47.
Joubert P.E., Meiffren G., Gregoire I.P., Pontini G., Richetta C., Flacher M., Azocar O., Vidalain P.O., Vidal M., Lotteau V., Codogno P., Rabourdin-Combe C., Faure M. (2009) Autophagy induction by the pathogen receptor CD46. Cell Host Microbe 6:354-66.
Jounai N., Takeshita F., Kobiyama K., Sawano A., Miyawaki A., Xin K.Q., Ishii K.J., Kawai T., Akira S., Suzuki K., Okuda K. (2007) The Atg5 Atg12 conjugate associates with innate antiviral immune responses. Proc. Natl. Acad. Sci. U S A 104:14050-5.
Juhasz G., Neufeld T.P. (2006) Autophagy: a forty-year search for a missing membrane source. PLoS Biol. 4:e36.
Juhász G., Erdi B., Sass M., Neufeld T.P. (2007) Atg7-dependent autophagy promotes neuronal health, stress tolerance, and longevity but is dispensable for metamorphosis in Drosophila. Genes Dev. 21:3061-3066.

Juhász G., Hill J.H., Yan Y., Sass M., Baehrecke E.H., Backer J.M., Neufeld T.P. (2008) The class III PI(3)K Vps34 promotes autophagy and endocytosis but not TOR signaling in Drosophila. J. Cell Biol. 181:655-666.

Kabeya Y., Mizushima N., Ueno T., Yamamoto A., Kirisako T., Noda T., Kominami E., Ohsumi Y., Yoshimori T. (2000) LC3, a mammalian homologue of yeast Apg8p, is localized in autophagosome membranes after processing. EMBO J. 19:5720-5728.

Kamada Y., Funakoshi T., Shintani T., Nagano K., Ohsumi M., Ohsumi Y. (2000) Tor-mediated induction of autophagy via an Apg1 protein kinase complex. J. Cell Biol. 150:1507-1513.

Kamada Y., Yoshino K., Kondo C., Kawamata T., Oshiro N., Yonezawa K., Ohsumi Y. (2010) Tor directly controls the Atg1 kinase complex to regulate autophagy. Mol Cell Biol 30:1049-58.

Kametaka S., Okano T., Ohsumi M., Ohsumi Y. (1998) Apg14p and Apg6/Vps30p form a protein complex essential for autophagy in the yeast, Saccharomyces cerevisiae. J. Biol. Chem. 273:22284-91.

Kanuka H., Sawamoto K., Inohara N., Matsuno K., Okano H., Miura M. (1999) Control of the cell death pathway by Dapaf-1, a *Drosophila* Apaf-1/CED-4-related caspase activator. Mol. Cell 4:757-769.

Karniol B., Malec P., Chamovitz D.A. (1999) Arabidopsis FUSCA5 encodes a novel phosphoprotein that is a component of the COP9 complex. Plant Cell 11:839-48.

Katzmann D.J., Odorizzi G., Emr S.D. (2002) Receptor downregulation and multivesicular-body sorting. Nat Rev Mol Cell Biol 3:893-905.

Kawaguchi Y., Kovacs J.J., McLaurin A., Vance J.M., Ito A., Yao T.P. (2003) The deacetylase HDAC6 regulates aggresome formation and cell viability in response to misfolded protein stress. Cell 115:727-38.

Kerr J.F., Wyllie A.H., Currie A.R. (1972) Apoptosis: a basic biological phenomenon with wide-ranging implications in tissue kinetics. Br. J. Cancer 26:239-257.

Kiffin R., Christian C., Knecht E., Cuervo A.M. (2004) Activation of chaperone-mediated autophagy during oxidative stress. Mol. Biol. Cell 15:4829-40.

Kiffin R., Kaushik S., Zeng M., Bandyopadhyay U., Zhang C., Massey A.C., Martinez-Vicente M., Cuervo A.M. (2007) Altered dynamics of the lysosomal receptor for chaperone-mediated autophagy with age. J. Cell Sci. 120:782-91.

Kihara A., Noda T., Ishihara N., Ohsumi Y. (2001) Two distinct Vps34 phosphatidylinositol 3-kinase complexes function in autophagy and carboxypeptidase Y sorting in Saccharomyces cerevisiae. J. Cell Biol. 152:519-30.

Kim E., Goraksha-Hicks P., Li L., Neufeld T.P., Guan K.L. (2008) Regulation of TORC1 by Rag GTPases in nutrient response. Nat. Cell Biol. 10:935-45.

Kinchen J.M., Cabello J., Klingele D., Wong K., Feichtinger R., Schnabel H., Schnabel R., Hengartner M.O. (2005) Two pathways converge at CED-10 to mediate actin rearrangement and corpse removal in C. elegans. Nature 434:93-9.

King-Jones K., Thummel C.S. (2005) Developmental biology. Less steroids make bigger flies. Science 310:630-1.

Kirisako T., Baba M., Ishihara N., Miyazawa K., Ohsumi M., Yoshimori T., Noda T., Ohsumi Y. (1999) Formation process of autophagosome is traced with Apg8/Aut7p in yeast. J. Cell Biol. 147:435-46.

Kirisako T., Ichimura Y., Okada H., Kabeya Y., Mizushima N., Yoshimori T., Ohsumi M., Takao T., Noda T., Ohsumi Y. (2000) The reversible modification regulates the membrane-binding state of Apg8/Aut7 essential for autophagy and the cytoplasm to vacuole targeting pathway. J. Cell Biol. 151:263-276.

Kirkegaard K., Taylor M.P., Jackson W.T. (2004) Cellular autophagy: surrender, avoidance and subversion by microorganisms. Nat. Rev. Microbiol. 2:301-14.

Klionsky D.J. (2005) The molecular machinery of autophagy: unanswered questions. J. Cell Sci. 118:7-18.

Klionsky D.J., Abeliovich H., Agostinis P., Agrawal D.K., Aliev G., Askew D.S., Baba M., Baehrecke E.H., Bahr B.A., Ballabio A., Bamber B.A., Bassham D.C., Bergamini E., Bi X., Biard-Piechaczyk M., Blum J.S., Bredesen D.E., Brodsky J.L., Brumell J.H., Brunk U.T., Bursch W., Camougrand N., Cebollero E., Cecconi F., Chen Y., Chin L.S., Choi A., Chu C.T., Chung J., Clarke P.G., Clark R.S., Clarke S.G., Clavé C., Cleveland J.L., Codogno P., Colombo M.I., Coto-Montes A., Cregg J.M., Cuervo A.M., Debnath J., Demarchi F., Dennis P.B., Dennis P.A., Deretic V., Devenish R.J., Di Sano F., Dice J.F., Difiglia M., Dinesh-Kumar S., Distelhorst C.W., Djavaheri-Mergny M., Dorsey F.C., Dröge W., Dron M., Dunn W.A.J., Duszenko M., Eissa N.T., Elazar Z., Esclatine A., Eskelinen E.L., Fésüs L., Finley K.D., Fuentes J.M., Fueyo J., Fujisaki K., Galliot B., Gao F.B., Gewirtz D.A., Gibson S.B., Gohla A., Goldberg A.L., Gonzalez R., González-Estévez C., Gorski S., Gottlieb R.A., Häussinger D., He Y.W., Heidenreich K., Hill J.A., Høyer-Hansen M., Hu X., Huang W.P., Iwasaki A., Jäättelä M., Jackson W.T., Jiang X., Jin S., Johansen T., Jung J.U., Kadowaki M., Kang C., Kelekar A., Kessel D.H., Kiel J.A., Kim H.P., Kimchi A., Kinsella T.J., Kiselyov K., Kitamoto K., Knecht E*., et al.* (2008) Guidelines for the use and interpretation of assays for monitoring autophagy in higher eukaryotes. Autophagy 4:151-175.

Knowles A., Koh K., Wu J.T., Chien C.T., Chamovitz D.A., Blau J. (2009) The COP9 signalosome is required for light-dependent timeless degradation and Drosophila clock resetting. J Neurosci 29:1152-62.

Komander D. (2009) The emerging complexity of protein ubiquitination. Biochem Soc Trans 37:937-53.

Komatsu M., Waguri S., Chiba T., Murata S., Iwata J., Tanida I., Ueno T., Koike M., Uchiyama Y., Kominami E., Tanaka K. (2006) Loss of autophagy in the central nervous system causes neurodegeneration in mice. Nature 441:880-884.

Komatsu M., Waguri S., Ueno T., Iwata J., Murata S., Tanida I., Ezaki J., Mizushima N., Ohsumi Y., Uchiyama Y., Kominami E., Tanaka K., Chiba T. (2005) Impairment of starvation-induced and constitutive autophagy in Atg7-deficient mice. J. Cell Biol. 169:425-34.

Komatsu M., Waguri S., Koike M., Sou Y.S., Ueno T., Hara T., Mizushima N., Iwata J., Ezaki J., Murata S., Hamazaki J., Nishito Y., Iemura S., Natsume T.,

Yanagawa T., Uwayama J., Warabi E., Yoshida H., Ishii T., Kobayashi A., Yamamoto M., Yue Z., Uchiyama Y., Kominami E., Tanaka K. (2007) Homeostatic levels of p62 control cytoplasmic inclusion body formation in autophagy-deficient mice. Cell 131:1149-63.

Kubbutat M.H., Jones S.N., Vousden K.H. (1997) Regulation of p53 stability by Mdm2. Nature 387:299-303.

Kuma A., Mizushima N., Ishihara N., Ohsumi Y. (2002) Formation of the approximately 350-kDa Apg12-Apg5.Apg16 multimeric complex, mediated by Apg16 oligomerization, is essential for autophagy in yeast. J. Biol. Chem. 277:18619-25.

Kuma A., Hatano M., Matsui M., Yamamoto A., Nakaya H., Yoshimori T., Ohsumi Y., Tokuhisa T., Mizushima N. (2004) The role of autophagy during the early neonatal starvation period. Nature 432:1032-6.

Kuraishi T., Nakagawa Y., Nagaosa K., Hashimoto Y., Ishimoto T., Moki T., Fujita Y., Nakayama H., Dohmae N., Shiratsuchi A., Yamamoto N., Ueda K., Yamaguchi M., Awasaki T., Nakanishi Y. (2009) Pretaporter, a Drosophila protein serving as a ligand for Draper in the phagocytosis of apoptotic cells. EMBO J 28:3868-78.

Kurant E., Axelrod S., Leaman D., Gaul U. (2008) Six-microns-under acts upstream of Draper in the glial phagocytosis of apoptotic neurons. Cell 133:498-509.

Kwok S.F., Piekos B., Misera S., Deng X.W. (1996) A complement of ten essential and pleiotropic arabidopsis COP/DET/FUS genes is necessary for repression of photomorphogenesis in darkness. Plant Physiol 110:731-42.

Lang T., Schaeffeler E., Bernreuther D., Bredschneider M., Wolf D.H., Thumm M. (1998) Aut2p and Aut7p, two novel microtubule-associated proteins are essential for delivery of autophagic vesicles to the vacuole. Embo J. 17:3597-607.

Layalle S., Arquier N., Leopold P. (2008) The TOR pathway couples nutrition and developmental timing in Drosophila. Dev. Cell 15:568-77.

Lee C.-Y., Baehrecke E.H. (2001) Steroid regulation of autophagic programmed cell death during development. Development 128:1443-1455.

Lee C.-Y., Cooksey B.A.K., Baehrecke E.H. (2002) Steroid regulation of midgut cell death during *Drosophila* development. Dev. Biol. 250:101-111.

Lee C.-Y., Clough E.A., Yellon P., Teslovich T.M., Stephan D.A., Baehrecke E.H. (2003) Genome-wide analyses of steroid- and radiation-triggered programmed cell death in *Drosophila*. Curr. Biol. 13:350-357.

Lee C.Y., Wendel D.P., Reid P., Lam G., Thummel C.S., Baehrecke E.H. (2000) E93 directs steroid-triggered programmed cell death in Drosophila. Mol Cell 6:433-43.

Lee J.A., Beigneux A., Ahmad S.T., Young S.G., Gao F.B. (2007) ESCRT-III dysfunction causes autophagosome accumulation and neurodegeneration. Curr. Biol. 17:1561-7.

Lee Y.S., Carthew R.W. (2003) Making a better RNAi vector for Drosophila: use of intron spacers. Methods 30:322-9.

Levine B., Klionsky D.J. (2004) Development by self-digestion: molecular mechanisms and biological functions of autophagy. Dev. Cell 6:463-477.

Liang C., Feng P., Ku B., Dotan I., Canaani D., Oh B.H., Jung J.U. (2006) Autophagic and tumour suppressor activity of a novel Beclin1-binding protein UVRAG. Nat. Cell Biol. 8:688-99.

Liang J., Shao S.H., Xu Z.X., Hennessy B., Ding Z., Larrea M., Kondo S., Dumont D.J., Gutterman J.U., Walker C.L., Slingerland J.M., Mills G.B. (2007) The energy sensing LKB1-AMPK pathway regulates p27(kip1) phosphorylation mediating the decision to enter autophagy or apoptosis. Nat. Cell Biol. 9:218-24.

Lindmo K., Stenmark H. (2006) Regulation of membrane traffic by phosphoinositide 3-kinases. J Cell Sci 119:605-14.

Lindmo K., Brech A., Finley K.D., Gaumer S., Contamine D., Rusten T.E., Stenmark H. (2008) The PI 3-kinase regulator Vps15 is required for autophagic clearance of protein aggregates. Autophagy 4:500-6.

Lindner J.R., Hillman P.R., Barrett A.L., Jackson M.C., Perry T.L., Park Y., Datta S. (2007) The Drosophila Perlecan gene trol regulates multiple signaling pathways in different developmental contexts. BMC Dev Biol 7:121.

Ling Y.H., Liebes L., Jiang J.D., Holland J.F., Elliott P.J., Adams J., Muggia F.M., Perez-Soler R. (2003) Mechanisms of proteasome inhibitor PS-341-induced G(2)-M-phase arrest and apoptosis in human non-small cell lung cancer cell lines. Clin Cancer Res 9:1145-54.

Ling Y.M., Shaw M.H., Ayala C., Coppens I., Taylor G.A., Ferguson D.J., Yap G.S. (2006) Vacuolar and plasma membrane stripping and autophagic elimination of Toxoplasma gondii in primed effector macrophages. J. Exp. Med. 203:2063-71.

Lippai M., Csikos G., Maroy P., Lukacsovich T., Juhasz G., Sass M. (2008) SNF4Agamma, the Drosophila AMPK gamma subunit is required for regulation of developmental and stress-induced autophagy. Autophagy 4:476-86.

Liu Q.A., Hengartner M.O. (1998) Candidate adaptor protein CED-6 promotes the engulfment of apoptotic cells in C. elegans. Cell 93:961-72.

Lockshin R.A., Williams C.M. (1965) Programmed cell death-I. Cytology of degeneration in the intersegmental muscles of the pernyi silkmoth. J. Insect Physiol. 11:123-133.

Lum J.J., DeBerardinis R.J., Thompson C.B. (2005) Autophagy in metazoans: cell survival in the land of plenty. Nat. Rev. Mol. Cell Biol. 6:439-448.

Lyapina S., Cope G., Shevchenko A., Serino G., Tsuge T., Zhou C., Wolf D.A., Wei N., Deshaies R.J. (2001) Promotion of NEDD-CUL1 conjugate cleavage by COP9 signalosome. Science 292:1382-5.

MacDonald J.M., Beach M.G., Porpiglia E., Sheehan A.E., Watts R.J., Freeman M.R. (2006) The Drosophila cell corpse engulfment receptor Draper mediates glial clearance of severed axons. Neuron 50:869-881.

Martin D.N., Baehrecke E.H. (2004) Caspases function in autophagic cell death in *Drosophila*. Development 131:275-284.

Martin D.N., Balgley B., Dutta S., Chen J., Rudnick P., Cranford J., Kantartzis S., DeVoe D.L., Lee C., Baehrecke E.H. (2007) Proteomic analysis of steroid-

triggered autophagic programmed cell death during Drosophila development. Cell Death Differ. 14:916-923.
Massey A.C., Kaushik S., Sovak G., Kiffin R., Cuervo A.M. (2006) Consequences of the selective blockage of chaperone-mediated autophagy. Proc. Natl. Acad. Sci. U S A 103:5805-10.
Mathew R., Karantza-Wadsworth V., White E. (2007a) Role of autophagy in cancer. Nat. Rev. Cancer 7:961-967.
Mathew R., Kongara S., Beaudoin B., Karp C.M., Bray K., Degenhardt K., Chen G., Jin S., White E. (2007b) Autophagy suppresses tumor progression by limiting chromosomal instability. Genes Dev. 21:1367-1381.
Mathew R., Karp C.M., Beaudoin B., Vuong N., Chen G., Chen H.Y., Bray K., Reddy A., Bhanot G., Gelinas C., Dipaola R.S., Karantza-Wadsworth V., White E. (2009) Autophagy suppresses tumorigenesis through elimination of p62. Cell 137:1062-75.
Meister S., Schubert U., Neubert K., Herrmann K., Burger R., Gramatzki M., Hahn S., Schreiber S., Wilhelm S., Herrmann M., Jack H.M., Voll R.E. (2007) Extensive immunoglobulin production sensitizes myeloma cells for proteasome inhibition. Cancer Res 67:1783-92.
Meléndez A., Neufeld T.P. (2008) The cell biology of autophagy in metazoans: a developing story. Development 135:2347-2360.
Mellen M.A., de la Rosa E.J., Boya P. (2008) The autophagic machinery is necessary for removal of cell corpses from the developing retinal neuroepithelium. Cell Death Differ. 15:1279-90.
Mills K.R., Reginato M., Debnath J., Queenan B., Brugge J.S. (2004) Tumor necrosis factor-related apoptosis-inducing ligand (TRAIL) is required for induction of autophagy during lumen formation in vitro. Proc. Natl. Acad. Sci. USA 101:3438-3443.
Mizushima N. (2007) Autophagy: process and function. Genes Dev. 21:2861-73.
Mizushima N., Noda T., Ohsumi Y. (1999) Apg16p is required for the function of the Apg12p-Apg5p conjugate in the yeast autophagy pathway. Embo J. 18:3888-96.
Mizushima N., Levine B., Cuervo A.M., Klionsky D.J. (2008) Autophagy fights disease through cellular self-digestion. Nature 451:1069-1075.
Mizushima N., Noda T., Yoshimori T., Tanaka Y., Ishii T., George M.D., Klionsky D.J., Ohsumi M., Ohsumi Y. (1998) A protein conjugation system essential for autophagy. Nature 395:395-398.
Mohseni N., McMillan S.C., Chaudhary R., Mok J., Reed B.H. (2009) Autophagy promotes caspase-dependent cell death during Drosophila development. Autophagy 5.
Monroe J.G. (2006) ITAM-mediated tonic signalling through pre-BCR and BCR complexes. Nat. Rev. Immunol. 6:283-94.
Mpakou V.E., Nezis I.P., Stravopodis D.J., Margaritis L.H., Papassideri I.S. (2006) Programmed cell death of the ovarian nurse cells during oogenesis of the silkmoth Bombyx mori. Dev. Growth Differ. 48:419-28.
Mukhopadhyay D., Riezman H. (2007) Proteasome-independent functions of ubiquitin in endocytosis and signaling. Science 315:201-5.

Muro I., Hay B.A., Clem R.J. (2002) The Drosophila DIAP1 protein is required to prevent accumulation of a continuously generated, processed form of the apical caspase DRONC. J. Biol. Chem. 277:49644-50.
Muro I., Monser K., Clem R.J. (2004) Mechanism of Dronc activation in Drosophila cells. J. Cell Sci. 117:5035-41.
Muro I., Berry D.L., Huh J.R., Chen C.H., Huang H., Yoo S.J., Guo M., Baehrecke E.H., Hay B.A. (2006) The Drosophila caspase Ice is important for many apoptotic cell deaths and for spermatid individualization, a nonapoptotic process. Development 133:3305-3315.
Nakagawa I., Amano A., Mizushima N., Yamamoto A., Yamaguchi H., Kamimoto T., Nara A., Funao J., Nakata M., Tsuda K., Hamada S., Yoshimori T. (2004) Autophagy defends cells against invading group A Streptococcus. Science 306:1037-40.
Nakatogawa H., Ichimura Y., Ohsumi Y. (2007) Atg8, a ubiquitin-like protein required for autophagosome formation, mediates membrane tethering and hemifusion. Cell 130:165-78.
Nedelsky N.B., Todd P.K., Taylor J.P. (2008) Autophagy and the ubiquitin-proteasome system: Collaborators in neuroprotection. Biochim. Biophys. Acta 12:691-9.
Nedjic J., Aichinger M., Emmerich J., Mizushima N., Klein L. (2008) Autophagy in thymic epithelium shapes the T-cell repertoire and is essential for tolerance. Nature 455:396-400.
Neufeld T.P., Baehrecke E.H. (2008) Eating on the fly: function and regulation of autophagy during cell growth, survival and death in Drosophila. Autophagy 4:557-62.
Nezis I.P., Stravopodis D.J., Margaritis L.H., Papassideri I.S. (2006a) Programmed cell death of follicular epithelium during the late developmental stages of oogenesis in the fruit flies Bactrocera oleae and Ceratitis capitata (Diptera, Tephritidae) is mediated by autophagy. Dev. Growth Differ. 48:189-98.
Nezis I.P., Stravopodis D.J., Margaritis L.H., Papassideri I.S. (2006b) Autophagy is required for the degeneration of the ovarian follicular epithelium in higher Diptera. Autophagy 2:297-8.
Nezis I.P., Simonsen A., Sagona A.P., Finley K., Gaumer S., Contamine D., Rusten T.E., Stenmark H., Brech A. (2008) Ref(2)P, the Drosophila melanogaster homologue of mammalian p62, is required for the formation of protein aggregates in adult brain. J. Cell Biol. 180:1065-71.
Nezis I.P., Lamark T., Velentzas A.D., Rusten T.E., Bjorkoy G., Johansen T., Papassideri I.S., Stravopodis D.J., Margaritis L.H., Stenmark H., Brech A. (2009) Cell death during Drosophila melanogaster early oogenesis is mediated through autophagy. Autophagy 5.
Nobukuni T., Joaquin M., Roccio M., Dann S.G., Kim S.Y., Gulati P., Byfield M.P., Backer J.M., Natt F., Bos J.L., Zwartkruis F.J., Thomas G. (2005) Amino acids mediate mTOR/raptor signaling through activation of class 3 phosphatidylinositol 3OH-kinase. Proc. Natl. Acad. Sci. U S A 102:14238-43.
Ogawa M., Yoshimori T., Suzuki T., Sagara H., Mizushima N., Sasakawa C. (2005) Escape of intracellular Shigella from autophagy. Science 307:727-31.

Ohsumi Y. (2001) Molecular dissection of autophagy: two ubiquitin-like systems. Nature Reviews Mol. Cell Biol. 2:211-216.
Paglin S., Hollister T., Delohery T., Hackett N., McMahill M., Sphicas E., Domingo D., Yahalom J. (2001) A novel response of cancer cells to radiation involves autophagy and formation of acidic vesicles. Cancer Res. 61:439-444.
Panattoni M., Sanvito F., Basso V., Doglioni C., Casorati G., Montini E., Bender J.R., Mondino A., Pardi R. (2008) Targeted inactivation of the COP9 signalosome impairs multiple stages of T cell development. J Exp Med 205:465-77.
Pandey U.B., Nie Z., Batlevi Y., McCray B.A., Ritson G.P., Nedelsky N.B., Schwartz S.L., DiProspero N.A., Knight M.A., Schuldiner O., Padmanabhan R., Hild M., Berry D.L., Garza D., Hubbert C.C., Yao T.P., Baehrecke E.H., Taylor J.P. (2007) HDAC6 rescues neurodegeneration and provides an essential link between autophagy and the UPS. Nature 447:859-863.
Park Y., Ng C., Datta S. (2003) Induction of string rescues the neuroblast proliferation defect in trol mutant animals. Genesis 36:187-95.
Parkinson N., Ince P.G., Smith M.O., Highley R., Skibinski G., Andersen P.M., Morrison K.E., Pall H.S., Hardiman O., Collinge J., Shaw P.J., Fisher E.M. (2006) ALS phenotypes with mutations in CHMP2B (charged multivesicular body protein 2B). Neurology 67:1074-7.
Pattingre S., Espert L., Biard-Piechaczyk M., Codogno P. (2007) Regulation of macroautophagy by mTOR and Beclin 1 complexes. Biochimie 2:313-23.
Peng Z., Serino G., Deng X.W. (2001) A role of Arabidopsis COP9 signalosome in multifaceted developmental processes revealed by the characterization of its subunit 3. Development 128:4277-88.
Qu X., Zou Z., Sun Q., Luby-Phelps K., Cheng P., Hogan R.N., Gilpin C., Levine B. (2007) Autophagy gene-dependent clearance of apoptotic cells during embryonic development. Cell 128:931-946.
Ravikumar B., Imarisio S., Sarkar S., O'Kane C.J., Rubinsztein D.C. (2008) Rab5 modulates aggregation and toxicity of mutant huntingtin through macroautophagy in cell and fly models of Huntington disease. J. Cell Sci. 121:1649-60.
Ravikumar B., Vacher C., Berger Z., Davies J.E., Luo S., Oroz L.G., Scaravilli F., Easton D.F., Duden R., O'Kane C.J., Rubinsztein D.C. (2004) Inhibition of mTOR induces autophagy and reduces toxicity of polyglutamine expansions in fly and mouse models of Huntington disease. Nat. Genetics 36:585-595.
Rechsteiner M., Hoffman L., Dubiel W. (1993) The multicatalytic and 26 S proteases. J. Biol. Chem. 268:6065-8.
Reddien P.W., Horvitz H.R. (2000) CED-2/CrkII and CED-10/Rac control phagocytosis and cell migration in *Caenorhabditis elegans*. Nature Cell Biol. 2:131-136.
Regel R., Matioli S.R., Terra W.R. (1998) Molecular adaptation of Drosophila melanogaster lysozymes to a digestive function. Insect Biochem Mol Biol 28:309-19.
Reggiori F., Klionsky D.J. (2002) Autophagy in the eukaryotic cell. Eukaryot. Cell 1:11-21.

Rodriguez A., Oliver H., Zou H., Chen P., Wang X., Abrams J.M. (1999) Dark is a *Drosophila* homologue of Apaf-1/CED-4 and functions in an evolutionarily conserved death pathway. Nat. Cell Biol. 1:272-279.

Rubin G.M.e.a. (2000) Comparative genomics of the eukaryotes. Science 287:2204-2215.

Rusten T.E., Lindmo K., Juhasz G., Sass M., Seglen P.O., Brech A., Stenmark H. (2004) Programmed autophagy in the Drosophila fat body is induced by ecdysone through regulation of the PI3K pathway. Dev. Cell 7:179-192.

Rusten T.E., Vaccari T., Lindmo K., Rodahl L.M., Nezis I.P., Sem-Jacobsen C., Wendler F., Vincent J.P., Brech A., Bilder D., Stenmark H. (2007) ESCRTs and Fab1 regulate distinct steps of autophagy. Curr. Biol. 17:1817-1825.

Ryoo H.D., Bergmann A., Gonen H., Ciechanover A., Steller H. (2002) Regulation of *Drosophila* IAP1 degradation and apoptosis by *reaper* and *ubcD1*. Nature Cell Biol. 4:432-438.

Saitoh T., Fujita N., Jang M.H., Uematsu S., Yang B.G., Satoh T., Omori H., Noda T., Yamamoto N., Komatsu M., Tanaka K., Kawai T., Tsujimura T., Takeuchi O., Yoshimori T., Akira S. (2008) Loss of the autophagy protein Atg16L1 enhances endotoxin-induced IL-1beta production. Nature 456:264-8.

Sancak Y., Peterson T.R., Shaul Y.D., Lindquist R.A., Thoreen C.C., Bar-Peled L., Sabatini D.M. (2008) The Rag GTPases bind raptor and mediate amino acid signaling to mTORC1. Science 320:1496-501.

Sanjuan M.A., Dillon C.P., Tait S.W., Moshiach S., Dorsey F., Connell S., Komatsu M., Tanaka K., Cleveland J.L., Withoff S., Green D.R. (2007) Toll-like receptor signalling in macrophages links the autophagy pathway to phagocytosis. Nature 450:1253-1257.

Sarkar S., Rubinsztein D.C. (2008) Small molecule enhancers of autophagy for neurodegenerative diseases. Mol Biosyst 4:895-901.

Schwartz A.L., Ciechanover A. (1999) The ubiquitin-proteasome pathway and pathogenesis of human diseases. Annu Rev Med 50:57-74.

Schwartz L.M., Myer A., Kosz L., Engelstein M., Maier C. (1990) Activation of polyubiquitin gene expression during developmentally programmed cell death. Neuron 5:411-9.

Schwechheimer C., Serino G., Callis J., Crosby W.L., Lyapina S., Deshaies R.J., Gray W.M., Estelle M., Deng X.W. (2001) Interactions of the COP9 signalosome with the E3 ubiquitin ligase SCFTIRI in mediating auxin response. Science 292:1379-82.

Schweichel J.-U., Merker H.-J. (1973) The morphology of various types of cell death in prenatal tissues. Teratology 7:253-266.

Scott R.C., Schuldiner O., TP. N. (2004) Role and regulation of starvation-induced autophagy in the Drosophila fat body. Dev. Cell 7:167-178.

Scott R.C., Juhász G., Neufeld T.P. (2007) Direct induction of autophagy by Atg1 inhibits cell growth and induces apoptotic cell death. Curr. Biol. 17:1-11.

Serino G., Deng X.W. (2003) The COP9 signalosome: regulating plant development through the control of proteolysis. Annu Rev Plant Biol 54:165-82.

Serino G., Tsuge T., Kwok S., Matsui M., Wei N., Deng X.W. (1999) Arabidopsis cop8 and fus4 mutations define the same gene that encodes subunit 4 of the COP9 signalosome. Plant Cell 11:1967-80.
Serino G., Su H., Peng Z., Tsuge T., Wei N., Gu H., Deng X.W. (2003) Characterization of the last subunit of the Arabidopsis COP9 signalosome: implications for the overall structure and origin of the complex. Plant Cell 15:719-31.
Shinohara K., Tomioka M., Nakano H., Tone S., Ito H., Kawashima S. (1996) Apoptosis induction resulting from proteasome inhibition. Biochem. J. 317 (Pt 2):385-8.
Shintani T., Mizushima N., Ogawa Y., Matsuura A., Noda T., Ohsumi Y. (1999) Apg10p, a novel protein-conjugating enzyme essential for autophagy in yeast. EMBO J. 18:5234-5241.
Simonsen A., Cumming R.C., Brech A., Isakson P., Schubert D.R., Finley K.D. (2008) Promoting basal levels of autophagy in the nervous system enhances longevity and oxidant resistance in adult Drosophila. Autophagy 4:176-84.
Simonsen A., Birkeland H.C., Gillooly D.J., Mizushima N., Kuma A., Yoshimori T., Slagsvold T., Brech A., Stenmark H. (2004) Alfy, a novel FYVE-domain-containing protein associated with protein granules and autophagic membranes. J. Cell Sci. 117:4239-51.
Singh S.B., Davis A.S., Taylor G.A., Deretic V. (2006) Human IRGM induces autophagy to eliminate intracellular mycobacteria. Science 313:1438-41.
Skibinski G., Parkinson N.J., Brown J.M., Chakrabarti L., Lloyd S.L., Hummerich H., Nielsen J.E., Hodges J.R., Spillantini M.G., Thusgaard T., Brandner S., Brun A., Rossor M.N., Gade A., Johannsen P., Sorensen S.A., Gydesen S., Fisher E.M., Collinge J. (2005) Mutations in the endosomal ESCRTIII-complex subunit CHMP2B in frontotemporal dementia. Nat. Genet. 37:806-8.
Song Z., McCall K., Steller H. (1997) DCP-1, a *Drosophila* cell death protease essential for development. Science 275:536-540.
Srinivasula S.M., Datta P., Kobayashi M., Wu J.W., Fujioka M., Hegde R., Zhang Z., Mukattash R., Fernandes-Alnemri T., Shi Y., Jaynes J., Alnemri E.S. (2002) *sickle*, a novel *Drosophila* death gene in the *reaper/hid/grim* region, encodes an IAP-inhibitory protein. Curr. Biol. 12:125-130.
Staub J.M., Wei N., Deng X.W. (1996) Evidence for FUS6 as a component of the nuclear-localized COP9 complex in Arabidopsis. Plant Cell 8:2047-56.
Stephan J.S., Yeh Y.Y., Ramachandran V., Deminoff S.J., Herman P.K. (2009) The Tor and PKA signaling pathways independently target the Atg1/Atg13 protein kinase complex to control autophagy. Proc Natl Acad Sci U S A 106:17049-54.
Su H., Huang W., Wang X. (2009) The COP9 signalosome negatively regulates proteasome proteolytic function and is essential to transcription. Int J Biochem Cell Biol 41:615-24.
Su H.P., Nakada-Tsukui K., Tosello-Trampont A.C., Li Y., Bu G., Henson P.M., Ravichandran K.S. (2002) Interaction of CED-6/GULP, an adapter protein involved in engulfment of apoptotic cells with CED-1 and CD91/low density lipoprotein receptor-related protein (LRP). J Biol Chem 277:11772-9.

Sun Q., Fan W., Chen K., Ding X., Chen S., Zhong Q. (2008) Identification of Barkor as a mammalian autophagy-specific factor for Beclin 1 and class III phosphatidylinositol 3-kinase, Proc. Natl. Acad. Sci. U. S. A. pp. 19211-6.
Sun X.M., Butterworth M., MacFarlane M., Dubiel W., Ciechanover A., Cohen G.M. (2004) Caspase activation inhibits proteasome function during apoptosis. Mol. Cell 14:81-93.
Suzuki K., Kirisako T., Kamada Y., Mizushima N., Noda T., Y. O. (2001) The pre-autophagosomal structure organized by concerted functions of APG genes is essential for autophagosome formation. EMBO J. 20:5971-5981.
Takahashi Y., Coppola D., Matsushita N., Cualing H.D., Sun M., Sato Y., Liang C., Jung J.U., Cheng J.Q., Mul J.J., Pledger W.J., Wang H.G. (2007) Bif-1 interacts with Beclin 1 through UVRAG and regulates autophagy and tumorigenesis. Nat. Cell Biol. 9:1142-51.
Takayanagi K., Dawson S., Reynolds S.E., Mayer R.J. (1996) Specific developmental changes in the regulatory subunits of the 26 S proteasome in intersegmental muscles preceding eclosion in Manduca sexta. Biochem. Biophys. Res. Commun. 228:517-23.
Tanida I., Mizushima N., Kiyooka M., Ohsumi M., Ueno T., Ohsumi Y., Kominami E. (1999) Apg7p/Cvt2p: A novel protein-activating enzyme essential for autophagy. Mol. Biol. Cell 10:1367-1379.
Terlecky S.R., Koepke J.I., Walton P.A. (2006) Peroxisomes and aging. Biochim. Biophys. Acta 1763:1749-54.
Thompson C.B. (1995) Apoptosis in the pathogenesis and treatment of disease. Science 267:1456-1462.
Thumm M., Egner R., Koch B., Schlumpberger M., Straub M., Veenhuis M., Wolf D.H. (1994) Isolation of autophagocytosis mutants of *Saccharomyces cerevisiae*. FEBS Lett. 349:275-280.
Tobinai K. (2007) Proteasome inhibitor, bortezomib, for myeloma and lymphoma. Int J Clin Oncol 12:318-26.
Tomoda K., Yoneda-Kato N., Fukumoto A., Yamanaka S., Kato J.Y. (2004) Multiple functions of Jab1 are required for early embryonic development and growth potential in mice. J Biol Chem 279:43013-8.
Tsukada M., Ohsumi Y. (1993) Isolation and characterization of autophagy-defective mutants of *Saccharomyces cerevisiae*. FEBS Lett. 1-2:169-174.
Underhill D.M., Goodridge H.S. (2007) The many faces of ITAMs. Trends Immunol. 28:66-73.
Vaux D.L., Weissman I.L., Kim S.K. (1992) Prevention of programmed cell death in Caenorhabditis elegans by human bcl-2. Science 258:1955-1957.
Velentzas A.D., Nezis I.P., Stravopodis D.J., Papassideri I.S., Margaritis L.H. (2007a) Stage-specific regulation of programmed cell death during oogenesis of the medfly Ceratitis capitata (Diptera, Tephritidae). Int. J. Dev. Biol. 51:57-66.
Velentzas A.D., Nezis I.P., Stravopodis D.J., Papassideri I.S., Margaritis L.H. (2007b) Mechanisms of programmed cell death during oogenesis in Drosophila virilis. Cell Tissue Res. 327:399-414.
Velentzas A.D., Nezis I.P., Stravopodis D.J., Papassideri I.S., Margaritis L.H. (2007c) Apoptosis and autophagy function cooperatively for the efficacious execution

of programmed nurse cell death during Drosophila virilis oogenesis. Autophagy 3:130-2.
Vernooy S.Y., Copeland J., Ghaboosi N., Griffin E.E., Yoo S.J., Hay B.A. (2000) Cell death regulation in *Drosophila*: conservation of mechanism and unique insights. J. Cell Biol. 150:F69-F75.
Voigt A., Pflanz R., Schafer U., Jackle H. (2002) Perlecan participates in proliferation activation of quiescent Drosophila neuroblasts. Dev Dyn 224:403-12.
Vyas J.M., Van der Veen A.G., Ploegh H.L. (2008) The known unknowns of antigen processing and presentation. Nat. Rev. Immunol. 8:607-18.
Wang J., Maldonado M.A. (2006) The ubiquitin-proteasome system and its role in inflammatory and autoimmune diseases. Cell Mol Immunol 3:255-61.
Wang S.L., Hawkins C.J., Yoo S.J., Müller H.-A.J., Hay B.A. (1999) The *Drosophila* caspase inhibitor DIAP1 is essential for cell survival and is negatively regulated by HID. Cell 98:453-463.
Wee S., Geyer R.K., Toda T., Wolf D.A. (2005) CSN facilitates Cullin-RING ubiquitin ligase function by counteracting autocatalytic adapter instability. Nat Cell Biol 7:387-91.
Wei N., Deng X.W. (1992) COP9: a new genetic locus involved in light-regulated development and gene expression in arabidopsis. Plant Cell 4:1507-18.
Wei N., Chamovitz D.A., Deng X.W. (1994) Arabidopsis COP9 is a component of a novel signaling complex mediating light control of development. Cell 78:117-24.
Wei N., Serino G., Deng X.W. (2008) The COP9 signalosome: more than a protease. Trends Biochem Sci 33:592-600.
White K., Grether M.E., Abrams J.M., Young L., Farrell K., Steller H. (1994) Genetic control of programmed cell death in *Drosophila*. Science 264:677-683.
Wilkinson K.D., Tashayev V.L., O'Connor L.B., Larsen C.N., Kasperek E., Pickart C.M. (1995) Metabolism of the polyubiquitin degradation signal: structure, mechanism, and role of isopeptidase T. Biochemistry 34:14535-46.
Williams D.W., Kondo S., Krzyzanowska A., Hiromi Y., Truman J.W. (2006) Local caspase activity directs engulfment of dendrites during pruning. Nat Neurosci 9:1234-6.
Wilson R., Goyal L., Ditzel M., Zachariou A., Baker D.A., Agapite J., Steller H., Meier P. (2002) The DIAP1 RING finger mediates ubiquitination of Dronc and is indispensable for regulating apoptosis. Nat. Cell Biol. 4:445-50.
Wing J.P., Karres J.S., Ogdahl J.L., Zhou L., Schwartz L.M., Nambu J.R. (2002) *Drosophila sickle* is a novel grim-reaper cell death activator. Curr. Biol. 12:131-135.
Wu J., Randle K.E., Wu L.P. (2007) ird1 is a Vps15 homologue important for antibacterial immune responses in Drosophila. Cell Microbiol. 9:1073-85.
Wu J.T., Lin H.C., Hu Y.C., Chien C.T. (2005) Neddylation and deneddylation regulate Cul1 and Cul3 protein accumulation. Nat Cell Biol 7:1014-20.
Wu Y.-C., Horvitz H.R. (1998) *C. elegans* phagocytosis and cell-migration protein CED-5 is similar to human DOCK180. Nature 392:501-504.
Wullschleger S., Loewith R., Hall M.N. (2006) TOR signaling in growth and metabolism. Cell 124:471-484.

Xie Z., Klionsky D.J. (2007) Autophagosome formation: core machinery and adaptations. Nat. Cell Biol. 9:1102-1109.
Yan N., Huh J.R., Schirf V., Demeler B., Hay B.A., Shi Y. (2006) Structure and activation mechanism of the Drosophila initiator caspase Dronc. J. Biol. Chem. 281:8667-74.
Yano T., Mita S., Ohmori H., Oshima Y., Fujimoto Y., Ueda R., Takada H., Goldman W.E., Fukase K., Silverman N., Yoshimori T., Kurata S. (2008) Autophagic control of listeria through intracellular innate immune recognition in drosophila. Nat. Immunol. 9:908-16.
Yao T.-P., Forman B.M., Jiang Z., Cherbas L., Chen J.D., McKeown M., Cherbas P., Evans R.M. (1993) Functional ecdysone receptor is the product of *EcR* and *ultraspiracle* genes. Nature 366:476-479.
Yoo S.J., Huh J.R., Muro I., Yu H., Wang L., Wang S.L., Feldman R.M., Clem R.J., Muller H.A., Hay B.A. (2002) Hid, Rpr and Grim negatively regulate DIAP1 levels through distinct mechanisms. Nat. Cell Biol. 4:416-424.
Yu L., Wan F., Dutta S., Welsh S., Liu Z., Freundt E., Baehrecke E.H., Lenardo M.J. (2006a) Autophagic programmed cell death by selective catalase degradation. Proc. Natl. Acad. Sci. USA 103:4952-4957.
Yu X., Odera S., Chuang C.H., Lu N., Zhou Z. (2006b) C. elegans Dynamin mediates the signaling of phagocytic receptor CED-1 for the engulfment and degradation of apoptotic cells. Dev Cell 10:743-57.
Zhang C., Cuervo A.M. (2008) Restoration of chaperone-mediated autophagy in aging liver improves cellular maintenance and hepatic function. Nat. Med. 14:959-65.
Zhou C., Wee S., Rhee E., Naumann M., Dubiel W., Wolf D.A. (2003) Fission yeast COP9/signalosome suppresses cullin activity through recruitment of the deubiquitylating enzyme Ubp12p. Mol Cell 11:927-38.
Zhou L., Song Z., Tittel J., Steller H. (1999) HAC-1, a *Drosophila* homolog of APAF-1 and CED-4, functions in developmental and radiation-induced apoptosis. Mol. Cell 4:745-755.
Zhou Z., Hartwieg E., Horvitz H.R. (2001) CED-1 is a transmembrane receptor that mediates cell corpse engulfment in *C. elegans*. Cell 104:43-56.
Ziegenfuss J.S., Biswas R., Avery M.A., Sheehan A.E., Hog K., Yeung Y.-G., Stanley E.R., Freeman M.R. (2008) Draper-dependent glial phagocytic activity is mediated by Src and Syk family kinase signaling. Nature:in press.
Zinke I., Schütz C.S., Katzenberger J.D., Bauer M., Pankratz M.J. (2002) Nutrient control of gene expression in Drosophila: microarray analysis of starvation and sugar-dependent response. EMBO J. 21:6162-6173.
Zou H., Henzel W.J., Liu X., Lutschg A., Wang X. (1997) Apaf-1, a human protein homologous to C. elegans CED-4, participates in cytochrome c-dependent activation of caspase-3. Cell 90:405-413.